

https://dspace.org/

Co-gasification of Coal and Solid Waste to Hydrogen Enriched-Syngas in a Fixed Bed Gasifier

Ozonoh, Maxwell

2020-10
University of the Witwatersrand, Johannesburg
https://hdl.handle.net/10539/44822
Ozonoh, Maxwell. (2020). Co-gasification of Coal and Solid Waste to Hydrogen Enriched-Syngas in a Fixed Bed Gasifier. [PhD thesis, University of the Witwatersrand, Johannesburg]. WIReDSpace. https://hdl.handle.net/10539/44822

Downloaded from a DSpace repository. https://dspace.org/



UNIVERSITY OF THE
WITWATERSRAND,
JOHANNESBURG

Co-gasification of Coal and Solid Waste to Hydrogen Enriched-Syngas in a Fixed Bed Gasifier

Maxwell Ozonoh (1655617)

Thesis presented for the degree of Doctor of Philosophy (PhD) in Engineering (Chemical Engineering) in the School of Chemical and Metallurgical Engineering, Faculty of Engineering and the Built Environment, University of the Witwatersrand, Johannesburg 2050 South Africa

Supervisor: Prof. M.O. Daramola
Co-Supervisor: Prof. B.O. Oboirien

October, 2020

Declaration

I hereby declare that the content of this thesis is my own original work, and that no part of the work or the entire work had been submitted at any university or institution for award of degree.

_____
Signature

_____
Full Name

_____/_____ / _____
Date

Copyright © University of Witwatersrand
All rights reserved

Abstract

The economic growth of every nation around the globe is centred on energy. Energy can be harnessed from different sources using different conversion systems, but such systems should be sustainable. Liquid fuels such as petroleum and solid fuels (e.g. coal & biomass) are largely used for energy production. Energy recovery from these fuels is usually carried out using thermal chemical processes such as combustion, pyrolysis, and gasification systems. Out of the three technologies, gasification is considered the most attractive based on its efficiency and other qualities. In the gasification process, syngas is produced. It is necessary to produce syngas of high quality such as hydrogen-enriched syngas. Hydrogen-enriched syngas can be used in fuel cells, gas turbines and engines for electricity production. This type of gas burns with little gaseous emissions to the atmosphere, but its production is dependent on the type of fuel and process conditions, and energy conversion system employed.

In South Africa, around 95 % of electric power production comes from coal, and the current reserve is projected to last not more than a century [8]. Secondly, the coal is fast depleting and generates a lot of gaseous emissions (e.g. CO_2, NO_X & SO_X) that pose a huge threat to the environment. The emission of the aforementioned gases is a **very serious** issue in South Africa. Presently, some Carbon Capture and Storage (CCS) projects are on-going in the country, although the CCS is not the fuse of this study. **The gasification of biomass waste and coal could assist in gaseous emission reduction.** Similarly, large amounts of agricultural wastes (e.g. sugarcane bagasse, corn cob & pine saw dust) and other solid waste such as tyre are in abundance in SA. It is detailed in chapter 2. Majority of the wastes are disposed indiscriminately, hence resulting in environmental pollution. Importantly, the solitary gasification of biomass is very expensive considering the prices of biomass. Besides that, biomass produces large amount of tar hence, resulting in operational difficulties in the gasifier and end user facilities. In this study, co-gasification of coal and solid wastes is considered as a crucial alternative to addressing the aforementioned problems.

Particularly, the feedstocks used for this study were coal, biomass (corn cob (CC), pine sawdust (PSD), sugarcane bagasse (SCB)) and waste tyre (WT) and were pre-treated by drying, milling, sieving, and torrefaction (coal was not torrefied). The fuel samples were blended with coal at different ratios as detailed in the thesis and used for the study. For the torrefaction process, the most viable torrefaction process conditions and feedstock were determined, while the torrefaction process model for the feedstocks were developed, using Response Surface Methodology (RSM) and Artificial Neural Network (ANN), respectively.

The Performance efficiency of gasification systems was evaluated using experimental data obtained from a few gasifiers (e.g. entrained, fluidised, and fixed bed) operated at varied experimental conditions using blends of feedstocks (e.g. biomass, coal, waste tyre etc.). A backpropagation Levenberg Marquardt (L-M) and Bayesian Regularisation (BR) algorithms of ANN model with Multiple Input- Multiple Output (MIMO) and Multiple Input-Single Output (MISO) layer networks were considered. The results of the MIMO and MISO layer networks obtained from the L-M algorithm were better than that of BR algorithm which is in affirmation with some of the results found in the literature. For model result improvement, Input Variables Representation Technique-by-Visual Inspection Method (IVRT-VIM) and Output Variables Representation Technique-by-Visual Inspection Method (OVRT-VIM) were developed from the study.

Estimation of the gaseous emissions and profits from biomass, tyre, and coal fired co-gasification CHP Plant using Artificial Neural Network (ANN) was carried out for 20-year-investment period using South Africa (SA) and Nigeria as cases studies via Artificial Neural Network (ANN). Higher profits were obtained from South African feedstocks than that of Nigerian feedstocks due to cheaper price of SA coal WFO and WOFC, but the gaseous emissions (CO, NO_X, & SO_2) from the Nigerian fuels were lower than that of SA because of differences in compositions of the fuels.

The potentials of biomass torrefaction in terms of profitability in a co-gasification CHP plant for a 20-year-investment period was carried out using blends of Coal + SCB, Coal + CC, and Coal + PSD with coal-to-biomass ratio of 50:50, 71:29, and 80:20, respectively. The two financial cases mentioned earlier were considered. Four investment terms including: (A) 1^{st} – 5^{th}, (B) 5^{th} – 10^{th}, (C) 10^{th} – 15^{th} & (D) 15^{th} – 20^{th} and two operational cost models; with feedstock costing (WFC) and without feedstock costing (WOFC) were employed. An estimated profit of between USD5.9 million - USD6.5 million and USD7.8 - USD7.9 million was earned at the end of investment plan using WFC and WOFC, respectively. The Internal Rate of Return (IRR) was 5 ± 1 %/yr. and 7 ± 4 %/yr. based on South African electricity price of 0.14 $/c kWh, respectively.

The parametric effect of process variables during torrefaction of coal/biomass/waste tyre blends using ANN and RSM models were studied. The variables considered were Higher Heating Value (HHV), Enhancement Factor (EF), and Sold Yield (SY). The most effective operating process conditions (in terms of blending ratio, temperature and torrefaction time: input variables) is of the order: 50:50 at 300 ^{O}C and 45 min > 50:50 at 250 ^{O}C and 30 min >

50:50 at 200 ^{O}C and 45 min. Similarly, the most viable fuel follows the order of Coal + Torrefied PSD > Coal + Torrefied SCB > Coal + Torrefied CC and > Coal + Torrefied WT. Coal + Torrefied PSD has HHV of 28.27 % and an EF of 1.41. This corresponded to around 10 % increase in the HHV of the torrefied fuel when compared to the raw fuel and about 25.23 % higher than the EF of Coal + Torrefied WT of 1.03. Based on the result of the EF of Coal +Torrefied waste tyre, upgrading of the fuel quality via torrefaction is not recommended.

Furthermore, a comprehensive study on tar treatment techniques was carried out using tars produced from biomass and blends of biomass and coal employing biochar based and Ni-biochar based catalysts. Box Behnken Design of Experiment (DoE) method was used. A full quadratic regression model was used to develop a mathematical model for tar treatment based on the feedstocks studied. The Pine Sawdust-Biochar Catalyst (PSD-BC) and Nickel Pine Sawdust-Biochar Catalyst (Ni-PSD-BC) were the most effective in terms of tar treatment and with an average percentage amount of tar conversion of 89.76 and 96.73 %, respectively. Ni-PSD-BC was more efficient for tar cracking than PSD-BC, but PSD-BC (waste base) may be more attractive if sustainability and cost effectiveness of precursors are considered.

Co-gasification of coal and pine sawdust (PSD) to hydrogen enriched syngas in a fixed bed gasifier was carried out with catalyst (WCAT) at 900 ^{O}C and without catalyst (WOCAT), at 700, 800, and 900 ^{O}C, respectively. Coal-to-PSD ratio of 1:1 was used, while Nickel-pine sawdust-biochar (Ni-PSD-BC) and pine sawdust-biochar (PSD-BC) were employed as catalysts. The gases produced at 700, 800 & 900 ^{O}C using WOCAT cannot be used in fuel cells and gas turbines due to poor quality, while others produced at 900 ^{O}C WCAT, can be used in internal combustion engines and gas turbines, but unfortunately, have lower quality to be employed in fuel cells for electricity production. However, the study provides a method of beneficiation of the high ash content South African coal for energy production. The outcome of this study is also instrumental to energy security, efficiency and sustainability as well as waste management in South Africa, Nigeria and other parts of the globe.

An assessment of the economic, energy and environmental viability of a 5 MW co- gasification power plant was carried out, using blends of coal and biomass, and two financial cases were considered namely: with feedstock costing (WFC) and without feedstock costing (WOFC). Feedstock profitability in the plant for energy production was evaluated. Equipment consisting was not considered. The power plant used 20,473,451.41 kg, 20,986,049.96 kg, 18,251,806.49 kg, and 15,276,277.85 kg of Coal + SCB, Coal + CC, Coal + PSD, and Coal + WT to produce the 5 MW and 5.56 MW electric and thermal power, annually. Coal + Torrefied PSD was the most profitable of the fuels studied. The use of Coal-to-PSD ratio of 4:1 for the power

generation as against Coal-to-PSD blend ratio of 1:1 resulted to an annual loss of about ZAR6, 461,301.77 ($90,458,224.70) and ZAR123,782.47 ($1,732954.58) WFC and WOFC, respectively.

List of published and submitted papers related to this work

1. **M. Ozonoh**, T.C. Aniokete, B.O. Oboirien, M.O. Daramola. Techno-economic analysis of electricity and heat production by co-gasification of coal, biomass and waste tyre in South Africa. Journal of Cleaner Production 201, (2018), 192-204.
2. **M. Ozonoh**, T.C. Aniokete, B.O. Oboirien, M.O. Daramola. Dataset on the assessment of the environmental, economic and energy parameters of 5 MW CHP co- gasification plant using South African coal, biomass and waste-tyre. Data in Brief 21, (2018), 2598-2608.
3. **M. Ozonoh,** B.O. Oboirien, A. Higginson, M.O. Daramola. Performance evaluation of gasification system efficiency using artificial neural network. Renewable Energy 45, (2020), 2253-2270.
4. **M. Ozonoh,** T.C. Aniokete, B. O. Oboirien, B.C. Udeh, K.O. Yoro and M.O. Daramola. Prediction of Emission and Profits from Biomass, Tyre, and Coal Fired Co-gasification CHP Plant Using Artificial Neural Network: Nigerian and South African Perspectives. Journal of Physics: Conference Series, Volume 1378, Issue 2: A paper Presented at international Conference of Engineering and Sustainable World, Canaan University, Nigeria (2019): IOP Indexed.
5. **M. Ozonoh**, B.O. Oboirien, M.O. Daramola. Maximisation of profit in a co-gasification CHP plant through biomass torrefaction. Presented & Published in proceedings of the 27th European Biomass Conference held at Lisbon, Portugal (2019) – Peer reviewed for publication in Biomass & Bioenergy.
6. **M. Ozonoh**, B.O. Oboirien, M.O. Daramola. Optimisation of process variables during torrefaction of coal/biomass/waste tyre blends: Application of Artificial Neural Network & Response Surface Methodology. Biomass and Bioenergy 143 (2020) 105808.
7. **M. Ozonoh**, T.C. Aniokete, B.O. Oboirien, M.O. Daramola. Biochar and Ni-biochar based Catalysts: A sustainable Catalyst for Treatment of tar obtained from Co-gasification of Coal and Biomass in a Fluidised Bed Gasifier. In proceedings of the 36th International Pittsburgh coal conference, Pennsylvania, USA September 3-6 2019.
8. **M. Ozonoh**, B. O. Oboirien, A. Higginson, M.O. Daramola. Dataset from Estimation of Gasification System Efficiency using Artificial Neural Network Technique. Chemical Data Collections 25 (2020) 100321.
9. **M. Ozonoh**, T.C. Aniokete, B.O. Oboirien, M.O. Daramola. Co-gasification of coal

and biomass to hydrogen enriched syngas in a fixed bed gasifier with catalyst (WCAT) and without catalysts (WOCAT). Under review.

Dedication

This work is dedicated to the following people:

My wife: Mrs. Angela Nwuka, Ozonoh

My brother: Mr. Nonye Ude, Ozonoh

My mother: Mrs. Marcellina, Ozonoh (Nneonoh Nwaozoalor)

My son: Mr. Charles Obioma, Ozonoh and others: Izuchukwu, Ugochukwu, Madonna & Chijindu and Oluchi that helps Angela to look after them are equally thanked for their efforts.

It is also dedicated in memory of:

My late father: Mr. Charles Nnadi, Ozonoh

My late grandmother: Maria Uzo-nwa-ude Nwa-onoh, Nwa-ozoudeani (Neohe). My late Uncle: Engr. Elias Onyekaonwu, Ozoalor.

Acknowledgement

This work would not have been a success without the contributions of certain individuals, but most importantly to the Almighty God. I will like to thank my supervisors: Prof. Michael Daramola and Prof. Bilainu Oboirien for their dedicated supervisions throughout the programme. I also thank the Enugu State University of Science and Technology (ESUT) and Tertiary Education Trust Fund (TETFund) for funding the study. My special acknowledgment also goes to Mr. Motlatsi Phali that assisted me in different Laboratory analysis tassociated with my work.

In addition, I wish to give a warm thanks to my wife and mother for their moral support, and most importantly to Mr. Nonye Ozonoh for his incessant financial support all through the studies. I also thank every member of the Ozonoh family including Theo, Anthony, Nonye, Fr. Afam, Uchenna 9my brothers), and Chigolu, Chinelo, Tochukwu, Stella & Theresa (my sisters), & all the kids in Ozonoh's family & Ndimulu be-Ozonoh. My sincere thanks also go to the aforementioned persons for their daily prayers for my success. I also thank Chinedu Nwokor, Devine, Uju & Nicho, bro. Chinedu & the entire members of our prayer team in Ngwo, Awhum Monastery, Upper-Room, & Ugwu-Dinso Eke for their support. I sincerely wish to thank my friends: Mr. Aniokete Thomas Chinedu & Uzo Enweremhuzo, Antony Higgison, and Ude Benson for their contributions. I also wish to thank our wives: Ogechukwu, Rose-Mary, & Isioma Ozonoh for their contributions. May God bless all of you.

Finally, I acknowledge the reviewers that committed their time in reviewing this thesis to a better quality. May the good Lord bless all of you in a special way – Amen.

Table of Content

Declaration..... 2

Abstract ... 3

List of published and submitted papers related to this work ... 7

Dedication ... 9

Acknowledgement ... 10

List of Tables ... 19

List of Figures ... 24

Nomenclature ... 30

Chapter 1: Motivation for the study and research objective ... 1

1.1. Motivation ... 1

1.2. Thesis layout ... 5

1.3. Thesis chapters ... 5

1.3.1. Research benefits and scientific contributions ... 6

Chapter 2: Literature review and state-of-the-art ... 8

2.1. Feasibility of feedstocks for energy production: South African context ... 8

2.1.1. Biomass ... 8

2.1.1.1. South African corn cob (CC) ... 8

2.1.1.2. South African Sugarcane bagasse (SCB) ... 9

2.1.1.3. South African waste-tyre (WT) ... 10

2.1.1.4. South African pine sawdust (PSD) ... 11

2.1.1.5. South African coal ... 11

2.2. Heating value of fuel ... 14

2.3. Techno-economic analysis of feedstock for energy generation in a Combined Heat and Power (CHP) Plant ... 15

2.4. Thermochemical Energy conversion ... 17

2.4.1. Types of gasifiers ... 18

2.4.1.1. Updraft and Downdraft Gasifiers ... 19

2.4.1.2. Entrained bed gasifier ... 19

2.4.1.3. Fluidised bed gasifier (FBG) ... 19

2.5. Biomass gasification reactions ... 20

2.5.1. Factors affecting gasification/co-gasification Process ... 21

2.5.2. Assessment of gasification and co-gasification systems efficiency 22
2.5.3. Effects of gasification operating variables on gasification efficiency 23
2.5.4. Effect of tar yield on gasification efficiency 24
2.5.4.1. Tar formation and treatment processes 24
2.5.4.1. Tar measurement 26
2.5.4.2. Previous studies on tar treatment 26
2.5.5. Gasification of South African coal 29
2.5.5.1. Hydrogen enriched syngas production from coal and co-gasification 30
2.5.5.2. Previous studies on co-gasification of coal and other solid fuels 32
2.5.6. Biomass & coal gasification process models 32
2.5.6.1. Kinetic Models in gasification 33
2.5.6.3. Kinetic model analysis 33
2.5.6.4. Friedman method 34
2.5.6.5. Coats and Redfern method 35
2.6. Thermodynamic Equilibrium Models (TEM) 37
2.6.1. Application of TEM in biomass gasification and co-gasification 38
2.7. Computational Fluid Dynamics (CFD) in gasification process 43
2.7.1. CFD model governing equations 43
2.8. Artificial Neural Networks (ANN) 48
2.9. Concluding remarks 54
Chapter 3: Research Procedure and Methodology 56
3. Introduction 56
3.1. Feedstock collection & pre-treatment 56
3.2. Biomass torrefaction: Experimental 58
3.3. Characterisation of the feedstocks 59
3.3.1. CHNS-O Analysers 59
3.3.2. X-ray diffraction (XRD) analysis 61
3.3.3. Brunauer–Emmett–Teller (BET) analysis 61
3.3.4. Temperature programmed reduction (TPR) analysis 61

3.3.5. Transmission Electron Microscopy (TEM) 62

3.4. Prediction of performance of gasification systems efficiency using ANN model 62

3.5. Emissions prediction and profits assessment of co-gasification of biomass, tyre, and coal fired in CHP plant using Artificial Neural Network: a comparative study of Nigeria and South Africa 63

3.5.1. ANN model training 63

3.6. Maximization of Profit in a co-gasification CHP plant via biomass torrefaction 64

3.7. Investigation of Effect of process variables of biomass torrefaction using Response Surface Methodology (RSM) and Artificial Neural Network (ANN) technique 64

3.8. Development of effective tar treatment technique for production of high quality syngas from blends of coal and biomass 65

3.8.1. Effect of tar treatment conditions on tar yield 66

3.8.2. Tar treatment and analysis 67

3.9. Co-gasification of coal and biomass to hydrogen enriched syngas in a fixed bed gasifier 68

3.11. Concluding remarks 69

Chapter 4: Evaluation of performance efficiency of gasification systems using Artificial Neural Network 71

4. Introduction 71

4.1. Experimental Data 73

4.1.1. Multiple Input-Multiple Output (MIMO) and Multiple Input-Single Output (MISO) Layer 75

4.1.2. ANN Model Development and applications 77

4.2. Gasification Performance Evaluation 78

4.2.1. Cold gas efficiency (CGE) 78

4.2.2. Carbon Conversion Efficiency (CCE) 79

4.2.3. Gas Yield (η_{Gas}) 79

4.2.4. Lower heating value of gas (LHV_{Gas}) 79

4.2.5. Product Gas Composition 80

4.3. Uncertainty Analysis 80

4.4. Results and Discussion 82

4.4.1. Model solutions 82

4.4.2. Bayesian Regularization (BR) algorithm: MIMO layer network 82

4.4.3. Model solutions: Levenberg-Marquardt (L-M) MISO layer network 84

4.5. Prediction of the CGE [%] 84

4.5.1. Prediction of the Gas Yield [kg/Nm^3]: MISO layer network 87

4.5.2. Prediction of the LHV of gas [KJ/Nm^3]: MISO layer network 89

4.5.3. Prediction using proximate analysis data: MISO layer network 90

Input variables 93

Number of neurons 93

Regression Coefficient (R^2) 93

Output variables 93

Training 93

Validation 93

Testing 93

All* 93

Ash, MC, VM 93

21 93

0.75 93

0.76 93

0.71 93

0.76 93

CGE 93

Ash, MC, VM 93

21 93

0.76 93

0.80 93

0.77 93

0.79 93

Gas Yield 93

Ash, MC, VM 93

21 93

0.93 93

0.81 93

0.69 93

0.89 93

LHV_{Gas} 93

4.5.4. Prediction using Ultimate, Proximate & Process condition data: Input Variables Representation Technique with Visual Inspection Method (IVRT-VIM): MISO model 93

4.5.5. Prediction using L-M algorithm without CCE (WOCCE): Output Variables Representation Technique with Visual Inspection Method (OVRT-VIM): MIMO network layer 95

4.6. Sensitivity analysis 98

4.7. Concluding remarks 104

Chapter 5: Comparative study of emission and profit prediction from co-gasification of biomass, tyre, and coal fired CHP plant using Artificial Neural Network in Nigeria and South Africa 106

5.1. Introduction 106

5.2. Material & Method 108

5.2.1. Emission and Profit Estimation 108

5.2.2. Artificial Neural Network (ANN) 108

5.2.3. Gaseous Emission estimation 109

5.2.4. Profit estimation 109

5.3. Results and Discussion 110

5.3.1. ANN modelling of South African feedstock: Profit model 111

5.3.2. ANN modelling of Nigerian feedstock: Profit Model 114

5.3.3. Comparison of South African and Nigerian feedstock: Profit prediction 115

5.3.4. Modelling of South African fuel: Gaseous Emission model 116

5.3.5. ANN Modelling of Nigerian Feedstock: Gaseous emission model 119

5.3.6. Comparison of South African and Nigerian feedstock: Gaseous emission prediction 120

5.4. Results of this study compared with literature 121

5.5. Concluding remarks 122

Chapter 6: Maximization of profit in a co-gasification CHP plant through biomass torrefaction . 124

6.1. Introduction 124

6.2. Experimental Procedure 126

6.2.1. Profitability evaluation 126

6.3. Results and Discussion 126

6.3.1. Most viable process & profit estimations 127

6.4. Effect of time value of money on profit 131

6.5. Effect of blend ratio on profit 132

6.6. Sensitivity analysis 133

6.7. Comparism of this work and literature 136

6.8. Concluding remarks 138

Chapter 7: Investigation of parametric effect of process variables during torrefaction of coal/biomass/waste tyre blends: Comparative study of ANN & RSM 139

7.1. Introduction 139

7.2. Model formulation 141

7.3. Model formulation: Artificial Neural Network 142

7.4. Torrefaction variables 144

7.5. Response Surface Methodology (RSM) 145

7.5.1. Artificial Neural Network (ANN) 146

7.6. Model solutions and analysis 147

7.6.1. Response Surface Methodology 147

7.6.2. Artificial Neural Network 148

7.6. Results and discussion 149

7.7. Regression model result: RSM 154

7.7.1. Response Surface Methodology: Effect of variables & optimization of the fuels 155

7.8. Artificial Neural Network: Effect of variables & optimization of the fuels 162

7.9. Sensitivity and Comparative analysis: ANN & RSM models 166

7.9.1. Comparative analysis: Based on HHV & EF of Coal + PSD & Coal + WT 168

7 .9.2. Comparative analysis based on model performance: ANN & RSM Models 170

7.10. Our results compared with the literature 175

7.11. Concluding remarks 178

Chapter 8: Development of effective tar treatment technique for production of high-quality syngas from blends of coal and biomass. 180

8.1. Introduction 180

8.2. Materials & Method 182

8.2.1. Bio-char production 182

8.2.2. Catalyst synthesis 183

8.2.3. Tar generation and treatment 183

8.2.4. Tar treatment experimental setup 184

8.2.5. Feedstock characterisation 185

8.2.6. Development of tar treatment model 185

8.3. Tar treatment and analysis 186

8.4. Results and Discussion 187

8.4.1. Characterisation of catalysts 187

8.4.1.1. Brunauer, Emmett, Teller (BET) characterisation result of catalysts 187

8.4.1.2. Temperature programmed reduction (TPR) of the Ni-based catalysts 191

8.4.1.3. X-ray diffractometer (XRD) analysis 192

8.4.1.4. Transmission Electron Microscopy (TEM) analysis 194

8.4.2. Tar treatment: Thermal & catalytic techniques 196

8.4.3. Effect of time on tar conversion 198

8.4.4. Effect of temperature on tar conversion 201

8.4.5. Catalyst activity: Biochar and Ni-biochar based catalyst 202

8.4.6. Evaluation of biochar and Ni-biochar based catalysts for tar treatment 205

8.4.7. Development of tar treatment model 206

8.4.8. Analysis of coal + biomass & biomass-based tars 209

8.4.9. Quantitative analysis of blends of coal + biomass and biomass-based tars 228

8.4.19. Tar reduction assessment: Coal + biomass & biomass based tar species 230

8.5. Concluding remarks 231

Chapter 9: Co-gasification of coal and biomass to hydrogen enriched syngas in a fixed bed gasifier with catalyst (WCAT) and without catalysts (WOCAT) 233

9.1. Introduction 233

9.2. Materials & methods 234

9.2.1. Materials 234

9.2.2. Method 234

9.2.3. Feedstock characterisation 236

9.3. Results and Discussion 236

9.3.1. Estimation of gasification systems efficiency 237

9.4. Effect of catalyst on gas composition 238

9.3.1.1. Effect of temperature on gas composition 239

9.3.1.2. Effect of temperature on gas yield 240

9.4. Tar in the product gases 243

9.6. Concluding remarks 244

Chapter 10: Environmental, economic and energy assessment in the co-gasification plant via proximate and ultimate analysis 246

10.1. Introduction 246

10.3. Method 248

10.3.1. Blending of feedstock and cost estimation 248

10.3.2. Estimation of the LHV and annual feed rate of the feedstocks 249

10.3.3. Estimation of fuel requirement for the CHP plant 250

10.3.4. Economic Analysis of a co-gasification Power Plant 250

10.3.4.1. Net Present Value (NPV) 250

10.3.4.2. Internal Rate of Return (IRR) 251

10.3.4.3. Payback Period (PBP) 252

10.4. Emissions reduction by displaced energy 252

10.4.1. Emissions from the transportation of biomass, tyres and coals 254

10.4.2. Effective Emissions Reduction: Biomass Power Plant 256

10.5. Results and Discussion 256

10.5.1. Physio-chemical characterization of the feedstocks 256

10.5.2. Energy analysis of Feedstocks and their blends 257

10.5.3. Feedstocks requirements for the different blends 259

10.6. Relationship between the amount of feedstocks, expenditure and profit for an electric power generating co-gasification plant with 5 MW production capacity 262

10.6.1. Economic evaluation of coal gasification 263

10.6.2. Co-gasification of the feedstocks 264
10.6.3. Effect of Feedstocks blend ratio 264
10.6.4. Effect of Feedstocks on the Economic Parameters: Percentage basis 267
10.7. Profitability analysis using NPV, IRR and PBP 269
10.7.1. Effect of elongation of business period on the business viability 271
10.7.2. Effect of business period elongation on the venture from 11 – 17 years 271
10.7.3. Effect of power production period on the investment viability from 2017 – 2035 273
10.8. Environmental Impact Assessment of the 5 MW co-gasification power plant 273
10.9. Results compared with literature 277
10.9.1. Sulphur and CO_2 capture 280
10.10. Sensitivity of the NPV and impact of uncertainty 281
10.11. Concluding remarks 286
Chapter 11: General conclusion and recommendation 288
11.1. Conclusions 288
11.2. Recommendations 291
References 293

List of Tables

Table 2. 1: Production of corn in South Africa [27]……9

Table 2. 2: Summary of SA Waste Tyre Management and Recycling end of July 2018 [31] ……...10

Table 2. 3: Typical properties of coal with reference to MC, CC & CV (Adapted from Council for Geoscience South Africa; Applied Geoscience Solutions [35] ……..…..……13

Table 2.4: Biomass gasification reactions: reduction zone [69] ……..……..21

Table 2. 5: Allowable tar limits for different facilities [56]…… ….25

Table 2. 6: Typical compositions of tar [102] ……..…..….....26

Table 2.7: Tar concentrations in syngas based on gasifiers & process conditions (Adapted from Rios et al. [101] ……..……27

Table 2.8: Gasification and co-gasification Kinetic Model (KM)…….36

Table 2.9: Gasification and co-gasification Thermodynamic Equilibrium Model (TEM).....39

Table 2.10: Gasification and co-gasification Computational Fluid Dynamic (CFD…….……46

Table 2.11: Gasification and co-gasification Artificial Neural Networks (ANNs) Model……48

Table 4. 1: Input and output variables employed in ANN…….……73

Table 4. 2: L-M MISO layer network: R^2 for the CGE using C, H, & N as the inputs…….85

Table 4. 3: L-M MISO layer network: R^2 for the Gas Yield using C, H, & N as the inputs…….....87

Table 4. 4: Convergence characteristics and R^2 for the LHV of Gas using C, H, & N as the inputs: L-M MISO layer network……88

Table 4. 5: L-M MISO layer network: R^2 for the CGE, Gas Yield, & LHV of Gas using Ash, MC, & VM as input…….....90

Table 4. 6: R^2 result from ultimate, proximate & operating parameters: Input parameters……93

Table 4. 7: Model improvement using OVRT-VIM: MIMO L-M algorithm, WOCCE…….....94

Table 4. 8: BR & L-M algorithm MIMO network results: OVRT-VIM model improvement… 95

Table 4. 9: Results compared with literature……. …98

Table 5. 1: Feedstock Characterization: LHV and MC…….....…...… 105

Table 5.2 presents the calculated input and output variables used for the prediction of profits in the plant ……106

Table 5. 3: ANN model result on profits: 10 MW CHP co-gasification power plant Feedstock ……...…...……107

Table 5. 4: Predicted profits from the CHP plant using MISO layer network….....….....111

Table 5. 5: Input and Output variables used in the ANN: Emission Prediction…….……..112

Table 5. 6: ANN model results on emissions: 10 MW CHP Co-gasification power plant …….....113

Table 5. 7: Predicted emissions from the CHP plant using MIMO layer network …….115

Table 6. 1: Characterisation and torrefaction experimental results: Sever temperature regime ….121

Table 6. 2: Profit earning for term A – term D using WFC: 50:50 …….....122

Table 6. 3: Profit earning for term A – term D using WOFC: 50:50 …….....122

Table 6. 4: Profit evaluation at the end of the 20th Year (Term D): WFC & WOFC ……..123

Table 6. 5: Sensitivity analysis at 20th year, WFC ……..…126

Table 6. 6: Mean NPV and RSE of the investment parameters at 20th Year using WFC ……...127

Table 6. 7: Comparison of this work and literature ……....129

7. 1: Experimental range and levels of the process variables: Box Behnken Design …….……133

Table 7. 2: Ultimate and Proximate analysis: blend of coal and biomass (Raw fuel) ……141

Table 7. 4: Light Torrefaction at temperature of 200 ^{O}C …….…….....142

Table 7. 5: Mild Torrefaction at temperature of 250 ^{O} C ……...143

Table 7. 6: Severe Torrefaction temperature regime (300 ^{O}C)…….….144

Table 7. 7: Analysis of Variance (ANOVA) for response surface quadratic model: HHV of Coal + Torrefied PSD: RSM ……...……...….148

Table 7.8: Analysis of Variance (ANOVA) for response surface quadratic model: EF of Coal + Torrefied PSD: RSM …….149

Table 7. 9: Analysis of Variance (ANOVA) for response surface quadratic model: SY of Coal + Torrefied PSD: RSM …….....150

Table 7. 10: Correlation coefficient, epoch and MSE of EF, SY & HHV predictions: MISO model ……..……155

Table 7. 11: RSM regression analysis for Coal + Torrefied SCB and Coal + Torrefied CC: Response Y_3: Enhancement Factor …….…157

Table 7. 12: RSM regression analysis for Coal + Torrefied WT: Response Y_3: Enhancement Factor …….…….159

Table 7. 13: Sensitivity analysis of the RSM Box-Behnken Design and Artificial Neural Network (ANN) models: HHV: (Response Variable Y_1)……..…...…..161

Table 7.14: Sensitivity analysis of the RSM-Box-Behnken Design and ANN models: EF: (Response Variable Y_2)……...……...162

Table 7.15: Sensitivity analysis of the RSM Box-Behnken Design and ANN Models: SY: (Response Variable Y_3)……..…..…163

Table 7. 16: Summary: Optimization analysis of the optimum fuel: ANN and RSM models ….165

Table 7.17: Summary: Optimization analysis of the other fuels: ANN and RSM model ….……165

Table 7. 18: Comparison of the present work with previous studies ……..…166

Table 8. 1: Experimental range and levels of the process variables: Box Behnken Design……...176

Table 8. 2: Summary of the GC operating process conditions: Tar analysis ……. ...176

Figure 8. 1: Pore Diameter-Pore volume relationship of the Ni-biochar & biochar based catalysts …….…….179

Table 8.4: Elemental composition of the Ni-biochar & biochar based catalysts ……....183

Table 8.5: Tar cracking temperature of 900 ^{O} C: Biochar based catalyst ……..…….…...184

Table 8. 6: Tar cracking temperature of 900 ^{O} C: Ni-based catalyst ……..…….....185

Table 8. 7: Variation in tar conversion of Ni-biochar and biochar based catalysts …….....191

Table 8. 8: Experimental range and levels of the process variables: Box Behnken Design ……...193

Table 8. 9: Compositional tar analysis result of Coal + CC tar (CCC-T) …….….197

Table 8. 10: Compositional tar analysis result of Coal + SCB tar (CSCB-T) …….……...…198

Table 8. 11: Compositional tar analysis result of Coal + PSD tar (CPSD-T) ……..…….200

Table 8. 12: Compositional analysis result of raw CC tar (CC-T) …….....202

Table 8. 13: Compositional tar analysis result of raw SCB tar (SCB-T) ……..204

Table 8. 14: Compositional analysis result of raw PSD tar (PSD-T) ……...205

Table 8. 15: Comparison of compounds in tar samples: Coal + biomass & biomass based tar…...207

Table 8. 16: Properties of tar compounds used for assessment …….……..….208

Table 9.1: Features and experimental conditions of the gasifier …….....214

Table 9. 2: Results of feedstock characterisation: Coal + PSD …….....215

Table 9. 3: Results of performance of gasification system efficiency & amount of tar in the product gas: Bench scale FBG …….....216

Table 10. 1: Feedstock blends and their ratio …….……226

Table 10. 2: Emission factors of fossil fuels [350] …….….230

Table 10. 3: Life cycle emission: renewable energy sources [351] ……....231

Table 10. 4: Heavy-duty diesel classification [352] …….....…….....232

Table 10. 5: Characterization of feedstocks ……...……..234

Table 10. 6: LHV and MC of feedstocks at different blend ratios ……... 235

Table 10.6 (b): Data and economic assumption used for the techno-economic analysis … 235

Table 10. 7: Cost of feedstocks in South Africa and some parts of the globe ……..... 242

Table 10. 8: Variation in feedstocks economic parameters [Coal + Solid Wastes] at WOFC 244

Table 10. 9: Variation in feedstocks economic parameter: Percentage basis ….....245

Table 10. 10: Investment evaluation at 17th Year using WFC ……248

Table 10. 11: Estimated emission reduction from the plant at different blend ratio …….. 250

Table 10. 11: Estimated emission reduction from the plant at different blend ratio ……..…...251

Table 10. 12: Comparison of the present work with previous studies …….....253

Table 10. 13: Sensitivity Analysis of 10th Year using WFC …….....258

Table 10.14: Mean NPV and RSE of Variables (10th Year) using WFC ……..... 260

Table 10.15: Mean NPV and RSE of Variables (10th Year) using WOFC …….…....261

List of Figures

Figure1.1 International Electricity Delivered Table, 2014: US NUS Consulting Electricity & Natural Gas Survey (Adapted from [18])....2
Figure 1. 2: Schematic representation of the thesis structure/study....5
Figure 2. 1: SA Sugarcane Production (SA Canegrowers) [29] 10
Figure 2. 2: SA sugarcane yield & sugarcane/Sugar ratio: Adapted from SA Canegrowers [29] 10
Figure 2. 3: Different types of coal found around the globe [33] 11
Figure 2. 4: Coal production sites in South Africa (adapted from Mineral Council of South Africa) [33]. 12
Figure 2. 5: Coal production sites in South Africa (adapted from Mineral Council of South Africa) [33]. 12
Figure 2. 6: (a) Coal power stations in South Africa (b) Coal consumption in South Africa (Adapted from Mintek reports) [34]. 13
Figure 2. 7: Coal quality assessment in terms of type, grade and rank (Adapted from Council for Geoscience South Africa; Applied Geoscience Solutions) [35]. 13
Figure 2. 8: (a) Schematic diagram of biomass CHP system based on Organic Rankine Cycle (ORC), (b) Schematic diagram of biomass CHP system based on a downdraft gasifier (DDG) (Adapted from Y. Huang et al. [45] with copy write permission). 16
Figure 2. 9: Biomass steam turbine (BST) co-generation system (Adapted from Rincon, et al. [46]. 17
Figure 2. 10: Biomass integrated combined cycle (BIGC) co-generation system (Adapted from Rincon, et al. [46]. 17
Figure 2. 11: Different choices of gasifiers (Adapted from Sikarwar et al. [56]. 19
Figure 2. 12: Schematic diagram of the MIMO ANN Model; a single hidden layer [192] 52
Figure 2. 13: Schematic diagram of the MIMO ANN Model; a double hidden layer [192] …. 52
Figure 3. 1: Overview of the research methodology 56
Figure 3. 2: Photo image of the size reduction & sieving equipment: (a) Biomass cutting machine (b) Milling machine. 57
Figure 3. 3: Photo image of the Pre-treated (dried, milled & sieved) feedstocks: 57
Figure 3. 4: Photo image of blends of coal and solid waste (raw feedstock): Ratio: 50:50 58
Figure 3. 5: Photo image of the torrefied biomass materials and waste tyre 59
Figure 3. 6: (a) Oxygen bomb calorimeter (b) Thermo-gravimetric Analyzer (TGA) 60
Figure 4. 1: Schematic diagram of some gasification systems (Adapted from (Sikarwar et al. [56].74
Figure 4. 2: Architectural design of Multiple Input-Multiple Output (MIMO) layer of the neural

network. 74
Figure 4. 3: Architectural design of the Multiple Input-Single Output (MISO) layer of the neural network. 75
Figure 4. 4: ANN network training flow-sheet 75
Figure 4. 5: Model equation development for the estimation of y_{2i} (output variables) 77
Figure 4. 6: Feedforward neural network (FFNN): 3, 21, 1 architecture 77
Figure 4. 7: Convergence characteristics of the MIMO model, using all the output variables (23 neurons) 83
Figure 4. 8: Convergence characteristics of the MIMO model, using all the output variables, except CCE (23 neurons) 83
Figure 4. 9: Convergence characteristics of the MISO model, CGE prediction using C, H, & N as the input variables (20 Neurons) 84
Figure 4. 10: Convergence characteristics of the MISO model: CGE prediction: C, H, & N as the input variables: 21 Neurons 84
Figure 4. 11: Convergence characteristics of the MISO model: CGE prediction: C, H, & N as the input variables: 22 Neurons 85
Figure 4. 12: Convergence characteristics of the MISO model: Gas Yield prediction: C, H, & N as the input variables: 20 Neurons 86
Figure 4. 13: Convergence characteristics of the MISO model: Gas Yield prediction: C, H, & N as the input variables: 21 Neurons 86
Figure 4. 14: Convergence characteristics of the MISO model: Gas Yield prediction: C, H, & N as the input variables: 22 Neurons 87
Figure 4. 15: CGE prediction using ash, MC, & VM: 21 Neurons 89
Figure 4. 16: Gas Yield prediction using ash, MC, & VM: 21 Neurons 89
Figure 4. 17: LHV of gas prediction using ash, MC, & VM: 21 Neurons 90
Figure 4. 18: CGE prediction: Using C, VM, & T as the input variables: 21 Neurons 92
Figure 4. 19: Gas Yield prediction: Using C, VM, & T as the input variables: 21 Neurons. 92
Figure 4. 20: LHV of gas prediction: Using C, VM, & T as the input variables: 21 Neurons 92
Figure 4. 21: Convergence characteristics of the MIMO L-M model, WOCCE (10 neurons) 94
Figure 4. 22: Convergence characteristics of the MIMO L-M model, WOCCE (23 neurons) 94
Figure 4. 23: Relative effect of each input variable on the output variable: CGE [%]: MISO layer network: 21 hidden layer neurons 96
Figure 4. 24: Relative effect of each input variable on the output variable: Gas Yield [kg/Nm^3]: MISO layer network: 21 hidden layer neurons 97

Figure 4. 25: Relative effect of each input variable on the output variable: LHV of Gas [KJ/Nm^3]: MISO layer network: 21 hidden layer neurons 97
Figure 5. 1: ANN Model Equation development: Feedforward network (MISO layer). 104
Figure 5. 2: Convergence characteristics for SA Coal + SCB: MISO network: Profit.....108
Figure 5. 3: Convergence characteristics for SA Coal + CC: MISO network: Profit.....109
Figure 5. 4: Convergence characteristics for SA Coal + PSD: MISO network: Profit.....109
Figure 5. 5: Convergence characteristics for SA Coal + WT: MISO network: Profit.....109
Figure 5. 6: Convergence characteristics for Nigerian Coal + SCB: MISO network: Profit.....110
Figure 5. 7: Convergence characteristics for Nigerian Coal + SCB: MISO network: Profit.....110
Figure 6. 1: Profit reduction profile for Coal + PSD: 1st – 5th through 15th – 20th Year 124
Figure 6. 2: Profit reduction profile for Coal + CC: 1st –5th through 15th – 20th Year 125
Figure 6. 3: Influence of blend ratio on profit earning: Blend ratio: [71:29].....125
Figure 6. 4: Influence of blend ratio on profit earning: Blend ratio: [80:20].....126
Figure 7. 1: Characteristics of raw and torrefied biomass.....135
Figure 7. 2: Artificial Neural Networks Architectural Design (3, 5, 1): MISO 136
Figure 7. 3: Artificial Neural Networks Architectural Design (3, 5,3): MIMO.....136
Figure 7. 4: An illustration of the RSM torrefaction process modelling.....140
Figure 7. 5: Model equation development for the estimation of y_{2i}: HHV, EF, & SY 141
Figure 7. 6: Feedforward neural network (FFNN): 3, 5, 1 architecture.....141
Figure 7. 7: Correlation of Predicted and Experimental HHV: Coal + Torrefied PSD 147
Figure 7. 8: Correlation of Predicted and Experimental EF: Coal + Torrefied PSD.....148
Figure 7. 9: Correlation of Predicted and Experimental SY: Coal + Torrefied PSD 148
Figure 7. 10: (a) Interactive effects between torrefaction temperature and time on the HHV of Coal + Torrefied PSD for RSM response (3-D) contour plot (b) Interactive effects between torrefaction blending ratio and time on the HHV of the Coal + Torrefied PSD for RSM response (3-D) contour plot (c) Interactive effects between blending ratio and temperature on the HHV of Coal + Torrefied PSD for RSM response (3-D) contour plot. 152
Figure 7. 11: (a) Interactive effects between torrefaction temperature and time on the EF of Coal + Torrefied PSD for RSM response (3-D) contour plot (b) Interactive effects between torrefaction time and blending ratio on the EF of Coal + Torrefied PSD for RSM response (3-D) contour plot (c) Interactive effects between torrefaction temperature and blending ratio on the EF of Coal + Torrefied PSD for RSM response (3-D) contour plot. 153
Figure 7. 12: (a) Interactive effects between torrefaction blending ratio and time on the EF of Coal + Torrefied PSD for RSM response (3-D) and contour plot (b) Interactive effects between torrefaction

temperature and time on the EF of Coal + Torrefied PSD for RSM response (3-D) contour plot (c) Interactive effects between torrefaction blending ratio and temperature on the EF of Coal + Torrefied PSD for RSM response (3-D) and Contour plot. 154
Figure 7. 13: Convergence characteristics of the MISO model for the Coal + Torrefied PSD: EF [with 6 neurons in the hidden layer] 155
Figure 7. 14: Convergence characteristics of the MISO model for the Coal + Torrefied PSD: SY [with 6 neurons in the hidden layer] 155
Figure 7. 15: Convergence characteristics of the MISO model for the Coal +Torrefied PSD: HHV: [with 5 neurons in the hidden layer].....155
Figure 7. 16: Convergence characteristics of the MISO model for the Coal + Torrefied SCB: EF [with 6 neurons in the hidden layer] 157
Figure 7. 17: Convergence characteristics of the MISO model for the Coal + Torrefied CC: EF [with 6 neurons in the hidden layer**]** 157
Figure 7. 18: Convergence characteristics of the MISO model for the Coal + Torrefied WT: EF [with 6 neurons in the hidden layer] 157
Figure 7. 19: Relationship between enhancement factor, raw Coal + WT and Coal + Torrefied WT 160
Figure 7. 20: Relationship between enhancement factor, raw Coal + WT and Torrefied Coal + PSD 161
Figure 8. 1: Tar treatment facility 112
Figure 8. 2: Adsorption-Desorption isotherm plot of the Ni-biochar based catalysts.....115
Figure 8. 3: Adsorption-Desorption isotherm plot of the biochar based catalysts 116
Figure 8. 4: Pore Diameter-Pore volume relationship of the Ni-biochar & biochar based catalysts 117
Figure 8. 5: Temperature Programmed Reduction Profile for Nickel biochar based catalysts.....118
Figure 8. 6: Crystalline phases of the catalysts (a) Biochar based (b) Ni-biochar based:.....120
Figure 8. 7: TEM-EDX of the catalysts (a) Nickel-Corn cob-Biochar catalyst (b) Nickel-Pine sawdust-Biochar catalyst (c) Nickel-Sugarcane Bagasse-Biochar catalyst (d) Corn cob- Biochar catalyst (e) Pine sawdust-Biochar catalyst (f) Sugarcane bagasse-Biochar catalyst.....122
Figure 8. 8: Coal + biomass blend tar: Conversion using biochar based catalyst at 700 ^{O}C 125
Figure 8. 9: Coal + biomass blend tar: Conversion using Ni-biochar based catalyst at 700 ^{O}C.....125
Figure 8. 10: Coal + biomass blend tar: Conversion using biochar based catalyst at 800 ^{O}C 126
Figure 8. 11: Coal + biomass blend tar: Conversion using biochar based catalyst at 800 ^{O}C 126
Figure 8. 12: Coal + biomass blend tar: Conversion using biochar based catalyst at 900 ^{O}C 126

Figure 8. 13: Coal + biomass blend tar: Conversion using Ni-biochar based catalyst at 900 ^{O}C....127
Figure 8. 14: Influence of temperature on tar conversion at 20 minutes: Biochar based catalysts..128
Figure 8. 15: Influence of temperature on tar conversion at 20 minutes: Ni-biochar based catalysts 128
Figure 8. 16: Optimum catalyst evaluation using biochar based catalyst: 900 ^{O}C 130
Figure 8. 17: Optimum catalyst evaluation using Ni-biochar based catalyst: 900....130
Figure 8. 18: Influence of tar conversion temperature and time on tar conversion (PTC) 132
Figure 8. 19: Influence of tar conversion temperature and blend ratio on tar conversion (PTC) 132
Figure 8. 20: Influence of tar conversion time and blend ratio on tar conversion (PTC) 132
Figure 8. 21: Photo images of blends of coal and biomass tar....134
Figure 8. 22: Photo images of analysed tar samples: Blends of coal + biomass & biomass tars.....134
Figure 8. 23: Percentage concentration and tar reduction or changes profile for tar compounds and species 148
Figure 9. 1: Bench-scale fixed bed gasifier (Located at the FT-Lab, School of Chemical & Metallurgical Engineering, University of the Witwatersrand, Johannesburg).....152
Figure 9. 2: Influence of catalyst on product gas composition: At 700 ^{O}C & steam as oxidant.....155
Figure 9. 3: Influence of gasification temperature on product gas composition: At temperature range of 700 – 900 ^{O}C, & steam as oxidant 156
Figure 9. 4: Influence of gasification temperature on product gas yield....157
Figure 9. 5: Influence of gasification temperature on product gas yield....157
Figure 10. 1: Schematic illustration of a co-gasification process plant: Electric and Thermal Power Generation 175
Figure 10. 2: Schematic diagram of the proposed co-gasification plant [13]. 175
Figure 10. 3: Relationship between the amount of fuel and expenditure & profit (Matla coal + PSD: 1:1) using WFC 176
Figure 10. 4: Relationship between the amount of fuel and expenditure & profit (Matla coal + PSD: 1:1) using WOFC 177
Figure 10. 5: 100 % Matla coal economic analysis: 5 MW & 5.56 MW electric & thermal power generations 177
Figure 10. 6: Influence of feedstocks on the economic parameters using WFC....178
Figure 10. 7: Influence of feedstocks on the economic parameters using WOFC....179
Figure 10. 8: Effect of the amount of feedstocks blending ratio on expenditure and profit (Matla Coal + PSD: 4:1) using WFC 181
Figure 10. 9: Economic assessment at the 10th year using WFC at coal to biomass/waste ratio of 1:1

.....184
Figure 10. 10: Economic assessment at the 10th year using WOFC at coal to biomass/waste ratio of 1:1. Figure 10.12 presents similar assessment using Coal-Solid waste blend ratio of 4:1 at WFC. 184
Figure 10. 11: Economic assessment at the 10th year using WFC at coal to biomass/waste ratio of 4:1 185
Figure 10. 12: Economic assessment from 2017 – 2035 (I.e. the 18th year) using WFC at coal to biomass/waste ratio of 1:1.....187

Nomenclature

CFD	Computational fluid dynamics
MSE	Mean square error
Ea	Activation energy
f (α)	Conversion factor
β	Heating value
A	Pre-exponential factor
K	Reaction rate constant
$\frac{Ea}{RT}$	Slope
Mo	Initial mass [% wt.]
M	$Biomass\ weight$ [% $wt.$]
$M\alpha$	$Final\ biomass\ weight$ [% wt]
t	$time$ [min]
T	$Reaction\ temperature$ [K]
R	$Universal\ gas\ constant$ [8.314 KJ/mol/ K
CCS	$Carbon\ capture\ and\ storage$
SA	$South\ Africa$
CC	$Corn\ cob$
PSD	$Pine\ sawdust$
SCB	$Sugarcane\ basggas$
WT	$Waste\ tyre$
MW	$Mega\ watt$
WFC	$With\ feedstock\ costing$
$WOFC$	$Without\ feedstock\ costing$

CHP	Combined heat and power
NPV	$Net\ present\ valuue$
IRR	$Inernal\ rate\ of\ return$
PBP	Payback period
ANN	$Artifical\ neural\ network$
SA	$South\ Africa$
BR	Bayesian Regularisation
$L-M$	$Levenberg\ Marquardt$
MISO	Multiple input single output
$MIMO$	$Multiple\ input\ multiple\ output$
MSE	$Mean\ square\ error$
$IVRT-VIM$	$Input\ variable\ representation\ techniques$
$OVRT-VIM$	$Out\ variable\ representation\ techniques$
$R\&D$	$Research\ and\ development$
USD	$United\ States\ Dollars$
TVM	$Time\ value\ of\ money$
DoE	$Design\ of\ experiemnt$
$Response$	$surface\ methodology$
BBD	$Box\ Behnken\ Design$
GHG	$Greenhouse\ gases$
GA	$Genetic\ algorithm$

BPNN	Backpropagation neural network
FBG	Fixed bed gasifier
MMT	$Million\ metric\ tonne$
MMe	$Maga\ watt\ electricity$
ORC	$Organic\ Rankine\ Cycle$
$BIGC$	$Biomass\ integrated\ gasification\ combined\ cycle$
BFB	Bubbling fluidised bed
CFB	$Circulatin\ fluidised\ bed$
$IFGI$	$Indirect\ fixed\ gasification$
ICE	$Internal\ combustion\ engine$
SCWS	Supper critical water system
LHV	$Lower\ heating\ value\ [MJ/kg]$
HHV	$Higher\ heating\ value\ [MJ/kg]$
μ_s	$Shear\ viscosity$
$\lambda_{s\ Colli}$	$Collisional\ shear\ viscosity$
$\lambda_{s\ Fric}$	$Frictional\ shear\ viscosity$
$\lambda_{s\ Kin}$	$Kinematic\ shear\ viscosity$
ϕ_{gs}	$Energy\ exchange\ betweenn\ gas\ and\ particles$
$I-A$	$Index\ of\ agreement$
λ_s	$Bulk\ Viscosity$

SVR $Support\ vector\ regression$

PaD $Partial\ derivative$

SSD $Sum\ of\ squares\ of\ partial\ derivative$

F_1F_2 Activation function

Wkj $Weight\ between\ output\ neuron\ k\ and\ hidden\ neuron\ j$

P $Pattern\ number$

∂x_i^P $Input\ values\ from\ the\ pattern$

∂ox_i^P $Output\ value\ from\ the\ pattern$ ($Predicted\ variable\ from\ ANN$

Chapter 1: Motivation for the study and research objective

In this chapter, the motivation for the study and the specific research objectives are clearly explained. Secondly, the siginificance of the research to academia and industry are equally described here.

1.1. Motivation

Energy production is one of the most critical aspects of sustainable economic growth around the globe. This is because energy is required for different domestic and industrial activities to drive the economy. Institutions such as the health, agriculture, education, finance, security, military, communication, information, and other allied industries are sustained by the energy sector. If all or some of the aforementioned institutions energy supplies are threatend, it could progressively undermine the world economy.

There are different thermo-chemical energy production systems such as combustion, pyrolysis, and gasification, but out of the three conversion systems, gasification is considered the most attractive [1]. Secondly, different sources of fuels are available for energy production (e.g. biomass, coal, tyre, petroleum, etc.), but the physio-chemical properties are most considered for the choice of fuel for this purpose. The physio-chemical composition of the fuel determines the product yield (e.g. gases, tar, etc.) as well as the efficiency of the conversion system, while fuel availability promotes sustainability in energy production.

In energy production, emission is a very big challenge, especially when coal and petroleum are used as fuels. They are the major sources of fuel for energy production around the world [2], but the greenhouse gases emitted from them, pose huge environmental threats (e.g. global warming and climate change) [3,4].

Emphatically, the total global CO_2 emission in 1970 was around 16 Gton, but it increased to about 36.25 Gton in 2015 [5]. From the 36.25 Gton CO_2 emissions in 2015, around 11 Gton was contributed via coal-based heat and power generation plants. At present and based on the international energy output report, the world CO_2 emissions is expected to rise to about 43.2 billion metric tons in 2035; a situation currently causing sizzles global concern [6].

South Africa is one of the countries in the African continent that has a large deposit of coal of around 32 million metric tons, and the 4^{th} largest coal producer in the world [7]. The country is largely dependent on coal for power production to the extent that about 95 % of electric power generation comes from coal [8]. The fuel (coal) is fast depleting, and on this account,

the current reserve is estimated to last not more than the next century [9]. The electricity generated from coal in South Africa is equally transmitted to other neighbouring countries such as Botswana, Mozambique, Namibia, Swaziland, and Zimbabwe [10]. The process of conversion of coal into energy produces dangerous emissions such CO_2, NO_X, & SO_X, and South Africa is a major contributor based on per capita emissions of CO_2 on the global scale [11]. It emits around 440 Mt. CO_2 annually, and is responsible for over 40 % of CO_2 emitted in the African continent and 1 % global emission, hence; ranking 1st and 12th highest CO_2 emitter in the Africa and world [12-14,11,15]. The amount of emission in the country may be reduced if diversification in energy production is considered, but the cost of electricity supplies may increase due to the fuel source (e.g. biomass).

In 2017 for example, the South African electricity tariff was about $0.1408 c/kWh (SA Power Networks, 2017) [16], but presently (2019), the residential tariff (pre-paid) has been increased by National Energy Regulator of South Africa (NERSA) for <3001 kWh energy (summer/winter) to $0.1549 c/kWh (NERSA, 2019) [17]. It was reported as shown in Figure 1 that South Africa is one of the nations with the lowest electricity tariff around the globe ([18]. This could be attributed to the low price of coal in the country. However, the aforementioned reasons could have contributed to the fast depletion of coal and an increase in emissions in the country.

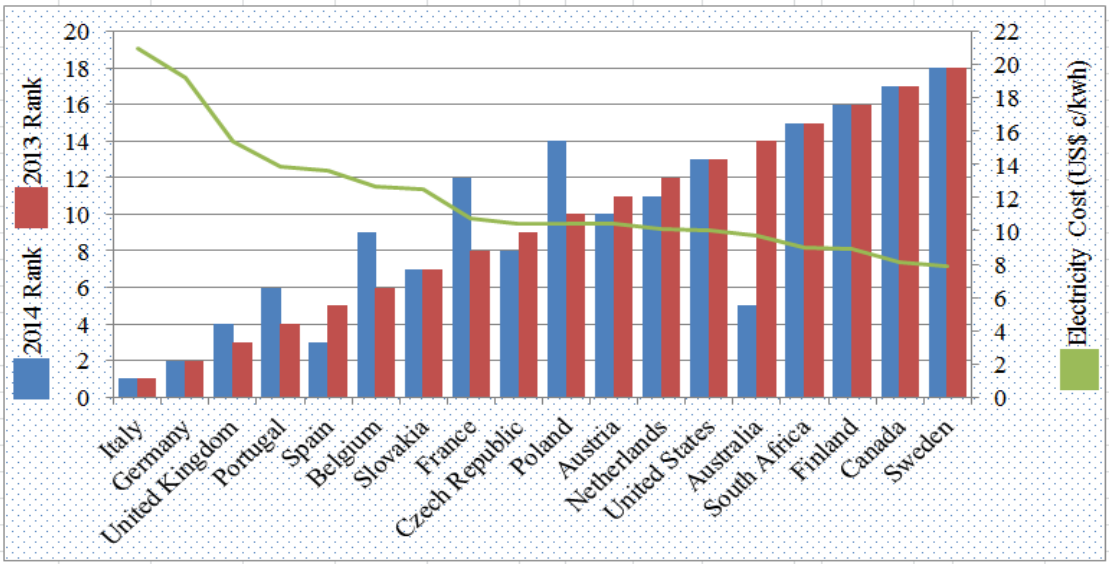


Figure1.1 International Electricity Delivered Table, 2014: US NUS Consulting Electricity & Natural Gas Survey (Adapted from [18])

The CO_2 emissions from thermal power production plants in South Africa are problematic to the government and the entire public in terms of environmental threats. It is therefore very

important to elaborate why it is necessary to proffer solutions to addressing it via this study. For instance, the South African Synthetic Oil Limited (SASOL) operating a power plant at Secunda in Mpumalanga region is the largest Coal-to-Liquid-Fuel producing plant in the world. This plant generates huge amount of CO_2 in the region, and as a result, has been described and categorised as one of the provinces with the highest point of greenhouse gas (GHG) emissions around the globe [19]. Furthermore, in 2012, Carbon Tracker Analysis was carried out by the Carbon Tracker Initiative. It was reported that emissions from South Africa coal processing plants exceeded its allowable CO_2 emissions limit ($GtCO_2e$) by 16.4 Gt CO_2e. This figure is higher than what other industrial sectors may produce from 2010 – 2050 [19].

Recently, Carbon Capture and Storage (CCS) have been demonstrated as a potential strategic option for climate change and mitigation [20]. It have been also reported by White et al. [21] and Subramoney et al. [11] that geological storage of CO_2 in deep un-minable/unprofitable coal seams is one of the feasible geographical sequestration techniques for capturing CO_2 with the synergy for enhanced coal-bed methane production In this regard; South African government has embarked on the project to addressing CO_2 emission issues. It was a good idea, but unfortunately, the CCS project may not independently, solve CO_2 emission problem in the country. Therefore, it will be important to consider some other emission abatement options to compliment the current initiatives. One of the options is to produce hydrogen-enriched syngas that can replace liquid fuels used in some of the South African power plants using blends of biomass and coal. By so doing, the amounts of CO_2, NO_X & SO_X emissions in the country could be considerably reduced due to lower of the emission of these gases biomass than coal.

Biomass materials such as agro-wastes (e.g. sugarcane bagasse, corn cob, pine sawdust, etc.) are in abundance in South Africa. They can be gasified solitary or blended with other solid fuels to produce energy. Presently, the disposal of these agro-wastes in landfills and through incineration contaminates the land and water resources, and pollutes the air quality. Secondly, the indiscriminate dumping of the solid waste (agro-wastes & tyre) harbours pathogens and could also promote fire outbreak. Tyre incineration for example, produces air pollutants. Above all, solid waste disposal and waste management are capital intensive. It will also be necessary to point out that biomass gasification is expensive because of the cost of feedstock (assume agro-waste is not used) [22**]** and besides that, it generates a huge amounts of tar.

The production of tar during biomass gasification process contributes to operational

difficulties, and the presence of tar in the produced gas degrades the quality of the gas and affects the end user facilities. In these facilities, valves, pipes, condensers, etc. are blocked when tar is condensed. To reduce the production of tar and emission generation, co-gasification of coal and biomass is employed **[22]**. Aslo the use of catalyst such as alkaline, transition metal & bimetallic catalysts) in biomass gasification and biomass gasification can also improve the quality of the product gases [4].

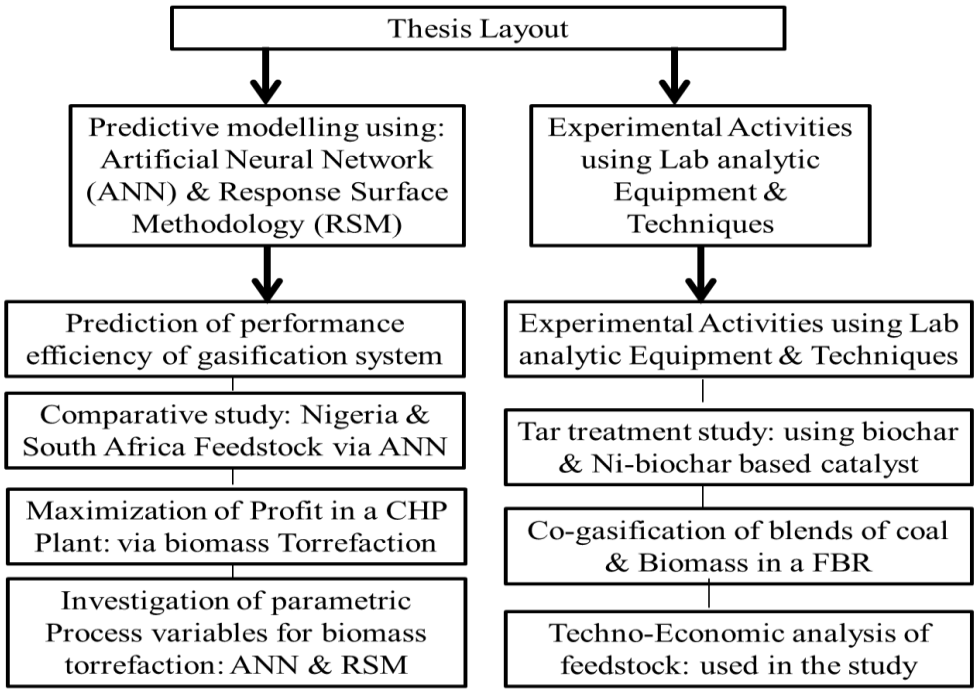
Essentially, the process could be instrumental to augmenting the fast- depletion coal reserves, improving sustainable energy development, and providing an economical means of waste disposal and management in South Africa. The principles adopted in South Africa can be extended to other African countries (e.g. Nigeria) to address energy and emission issues. It involves understanding the optimum experimental process conditions, feedstocks, and catalysts (for tar cracking) to enhance the efficiency of the gasification system and achieve high quality syngas for power production. Finally, the hydrogen enriched syngas can be used in energy conversion devices such as fuel cells, gas turbines, and engines to produce electricity. Having discussed motivations necessitating this study, the research was aimed at co- gasification of coal and solid waste in a fixed bed gasifier (FBG) to produce H_2 enriched syngas. Different objectives are considered to facilitate the achievement of this aim, and are specified in the following section:

1.2. Specific Objectives

1. To carry out economic-environmental impact and energy assessment of a co-gasification plant using the results of the ultimate analysis of the some selected feedstocks such as sugar bagasse, corn cob, waste tyre, and coal in South Africa.
2. To investigate the use of Artificial Neural Networks (ANNs or other existing commercial predictive modelling tool such as Aspen Plus, Genetic Algorithm (GA), etc. in predicting gasification efficiencies, Gas composition, Gas yield, and reactor performance of co-gasification of feedstocks from (1) using a Fixed Bed Gasifier (FBG).
3. To investigate the development of an effective comprehensive tar conversion technique for the production of high-quality syngas using feedstocks in (1) over synthesised heterogeneous catalyst.
4. To carry out co-gasification of coal and biomass to hydrogen enriched syngas in a fixed bed gasifier with catalyst (WCAT) and without catalyst (WOCAT).

1.2. Thesis layout

In this research, activities carried out are broadly classified into two namely; modelling and experimental works as shown in Figure 1. Each of the class has different activities reported as chapters in the thesis and described in section 1.3.1. For the modelling work, information obtained from the experiments were used for model validation, while information from the models were applied in the experiments to enhance effective operations and accuracy of results. Therefore, both classes were dependent on the other.



1. 2: **Schematic representation of the thesis structure/study**

1.3. Thesis chapters

Chapter 1 discusses the motivation, specific objective, and benefits of the study to the scientific and industrial communities around the world.

Chapter 2 is a review of literature describing the different feedstocks used in this study and their availabilities. The chapter further covered the relevance of co-gasification of coal and biomass and coal. An extensive review on previous works on formation of tar and treatment processes, H_2 enriched syngas production, gasification and co-gasification systems efficiency, coal, biomass, and co-gasification of coal and biomass process models were carried out.

Chapter 3 dwells on the research methodology used to accomplish each of the tasks carried out in the entire study.

Chapter 4 dealt with the evaluation of performance efficiency of gasification systems

employing Artificial Neural Network. In this case, different performance efficiency indicators were considered.

Chapter 5 considered the comparative study of emissions and profit prediction from co-gasification of biomass, tyre, and coal fired CHP plant using Artificial Neural Network in Nigeria and South African.

Chapter 6 focused on the maximization of profit in a co-gasification CHP plant through biomass torrefaction. Blends of coal and torrefied biomass materials were used to estimate the profits in the plant.

Chapter 7 is on the investigation of parametric effect of process variables during torrefaction of coal/biomass, waste tyre blends: comparative study of ANN and RSM.

Chapter 8 centered on the development of an effective tar treatment technique for production of **high-quality** syngas from blends of coal and biomass. In this chapter, tar treatment models were developed.

Chapter 9 elaborated the co-gasification of coal and biomass to hydrogen enriched syngas in a fixed bed gasifier. The co-gasification test was carried out using the optimum feedstock (Coal + PSD) obtained from the optimisation process, techno-economic analysis, and process model development of chapter 4 - 5 through chapter 9, respectively. The co-gasification test was based on the improvement of gasification system efficiency (e.g. syngas composition, yield, etc.) with catalyst (WCAT) and without catalyst (WOCAT).

Chapter 10 focused on the techno-economic analysis of the feedstocks to determine their viabilities for heat and power production in a CHP co-gasification plant. Precisely, an assessment of the energy, economic and environmental parameters of the energy plant were considered. Material/equipment costing was not considered.

Chapter 11 highlighted the conclusion, recommendations and future work from the overall study, and which were drawn from the different chapters of this thesis.

1.3.1. Research benefits and scientific contributions

Co-gasification of coal and solid waste to hydrogen enriched syngas is not a new research in the energy development sector, but there some few areas in the process that has not been fully exploited. Some of them were considered in this study, and the following scientific contributions were made:

- Data on comprehensive techno-economic analysis of some selected South African feedstocks used for energy generation was provided in this report. It highlighted the optimum feedstock in terms of profitability that was evaluated via energy, economic and environmental parameters in a co-gasification combined heat and power (CHP) plant. No report on this has been found in the literature, hence; it will serve as a working guide for potential investors and instrumental for further R&D in this area.
- Information on the most viable process variables for biomass torrefaction is provided. It consists of the detailed model development and uncertainty analysis that will be useful for construction of torrefaction process plants and in decision making by stakeholders in this area.
- An ANN model for the assessment of performance efficiency of gasification systems that employs different blends of coal, biomass/waste tyre, and experimental process conditions has been developed. The model is reliable and has the potentials to save time and cost of experimentation for building new gasifiers that can convert different kinds of fuels for energy production.
- An ANN model capable of predicting emissions and profitability in a co-gasification CHP plant using feedstocks from different geographical location has been developed.
- A comprehensive tar treatment method for the production of high quality syngas that can be used in gas turbines and internal combustion engines for heat and electricity generation has been developed. It also contains a tar treatment process model that can effectively estimate amount of tar converted from the feedstocks studied, and also has the capacity to predict amount of tar for other feedstocks similar to those investigated.
- Experimental process conditions for co-gasification of high ash content South African coal and pine sawdust (PSD) to syngas have been developed. Based on the tar content, the quality of the syngas produced is suitable for use in internal combustion and gas turbines for electric power generation.

Chapter 2: Literature review and state-of-the-art

In this chapter, a general overview of the literature covering the entire chapters of this thesis is presented, but a critical review describing the actual investigations carried out based in the research specific objectives are presented in each of the subsequent chapters.

2.1. Feasibility of feedstocks for energy production: South African context

To produce energy via solid fuels, different kinds of feedstocks are employed. In thermo-chemical energy conversion process for example, solid fuels such biomass; coal, tyre, and others are considered. The feedstocks may be used as a stand-alone fuel or blended with other fuels to promote synergetic effects of the fuel on energy production.

2.1.1. Biomass

Biomass is a renewable energy source obtained from plants and animal materials. It includes agricultural crop residues, domestic and industrial food wastes, etc. The major composition of the aforementioned fuels is cellulose, hemicellulose, and lignin [23]. The energy produced from the fuel materials is called biomass energy, and are considered environmentally friendly. Biomass can be found everywhere across the globe when compared to other renewable sources of fuels [24]. It has been projected to contribute a quarter or third of the world primary energy supply by 2050 [25]. A report from Saidur et al. [26] revealed the order of most relevant energy sources as coal, petroleum natural gas, and biomass. Presently, biomass is estimated to provide about 10 % world energy needs, and the fuel can be converted into energy with low gaseous emissions [24] such as CO, SO_X, NO_X, particulates and others. South Africa has abundant amounts of agricultural waste such as corn cob, sugar cane bagasse, pine sawdust, that can be co-gasified with coal to produce syngas. The different agro-waste are discussed in the following sections.

2.1.1.1. South African corn cob (CC)

South Africa is the largest producer of corn in Africa [27]. The implication is that it produces more cobs than any other country in the continent. The Free State, Mpumalanga and North West provinces are the three largest producers in South Africa. They produce about 4.0 tons/hectare, 5.6 tons/hectare, 2.7 tons/hectare, respectively [28]. The total corn production for the 2016/2017 marketing year in South Africa is around 14.6 million tons, obtained from 3.0 million Cultivated hectares of farm land. The production such quantity of corn may be attributed to the quest for

provision of food to the citizens by the government and private industries. Table 2.1 presents a detailed record of the corn production in South Africa for the 2015/2016 to 2017/2018 marketing year.

Table 2. 2: Production of corn in South Africa [27]

Sales Year	2015- 2016			2016 - 2017			2017 - 2018		
Variables	Area, 1000 [ha]	Yield, [t/ha]	Pro. 1000 [t]	Area, 1000 [ha]	Yield, [t/ha]	Pro 1000 [t]	Area, 1000 [ha]	Yield, [t/ha]	Pro 1000 [t]
				Commercial Corn					
White	1,015	3.4	3,409	1,643	5.1	8.313	1,400	4.2	5,950
Yellow	932	4.7	4,370	986	5.7	6.606	100	5.3	5,350
Sub-total	1,947	4.0	7,779	2,629	5.3	13.918	2,400	4.6	11,300
				Subsistence corn					
White	191	1.5	286	300	1.6	500	300	1.6	500
Yellow	75	2.0	150	100	2.0	200	100	2.0	200
Sub-total	266	1.6	436	400	1.7	700	400	1.7	700
Total	2,312	3.7	8,2156	3,029	4.8	14,618	2,800	4.2	12,000

ha: hectare; t: ton; Pro: Production

2.1.1.2. South African Sugarcane bagasse (SCB)

Sugarcane bagasse is obtained from the processing of sugarcane to produce sugar. In South Africa, there are about 42,300 registered sugar cane growers operating mostly in the Kwazulu-Natal, Mpumalanga, and Eastern Cape. According to the USDA Foreign Agricultural Service, about 14.7 MMT was produced in 2015/16 and a forecast of 14.4 MMT made for 2016/17 marketing year [29]. Mbohwa, [30] have reported that crushing around 21.2 MT of sugarcane produced about 2.5 million tons of sugar and 5.9 MMT of sugarcane bagasse annually. The South African sugar cane production is shown in Figure 2.1, while sugarcane yield/sugar ratio (from which sugarcane bagasse (SCB) for the 2015/2016 to 2017/2018 marketing year are shown in Figure 2.2. Figure 2.2 highlights the sugarcane ratio as a function of sugarcane yield, respectively.

For clarity, the two-line graphs in Fig 2.1 represents the amount of sugarcane crushed and produced respectively

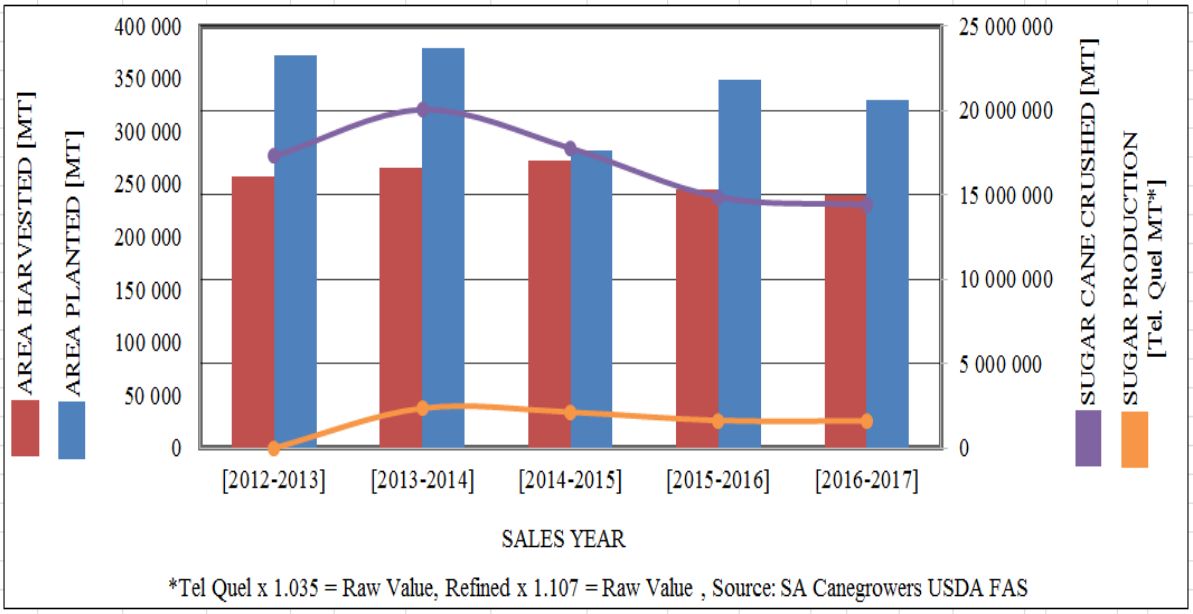


Figure 2. 3: SA Sugarcane Production (SA Canegrowers) [29]

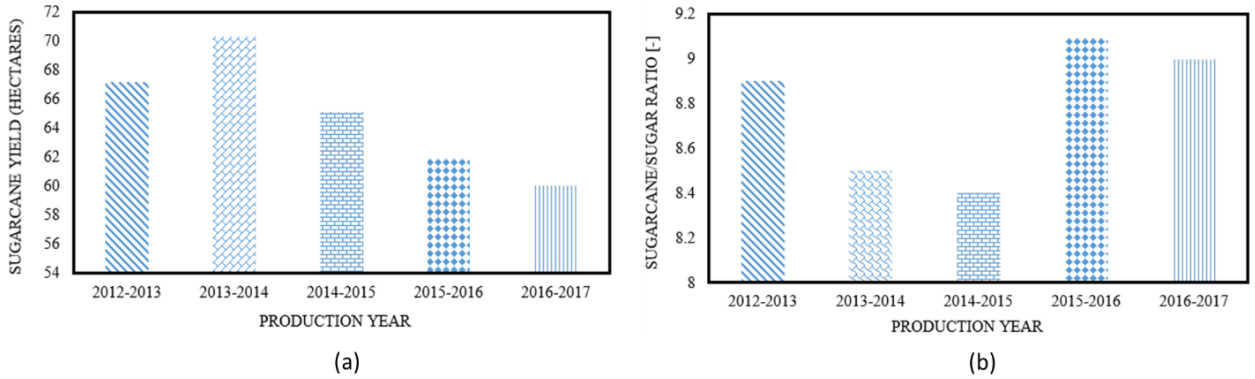


Figure 2. 4: SA sugarcane yield & sugarcane/Sugar ratio: Adapted from SA Canegrowers [29]

2.1.1.3. South African waste-tyre (WT)

Tyre is another solid waste that is in abundance in South Africa [31]. In South Africa, the energy value of tyre is tapped mainly through incineration, and the process promotes environmental pollution. Alternative energy conversion process is needed to address the environmental threats posed by using tyre for energy production. Table 2.2 presents the summary of the statistical data of South Africa waste tyre management and recycling at the end of July 2018.

Table 2. 2: Summary of SA Waste Tyre Management and Recycling end of July 2018 [31]

S/N	Province	Tonnes collected	Tonnes processed	Job created	Number of deports	Number of recycling plants
1	Kwazulu Natal	13,848	10,350	165	8	1
2	Mpumalanga	7,525	6,009	58	2	-
3	Western Cape	10,175	5,850	315	3	1
4	Gauteng	25,571	9,441	1,995	6	5
5	Limpopo	2,987	-	30	3	-
6	Northern Cape	584	354	31	2	-
7	Eastern Cape	7,676	1,898	45	2	-
8	Free State	3,521	1,365	15	3	-
9	North West	2,068	1,970	32	2	-

S/N: Serial number; REDISA: Recycling and Economic Development Initiative of South Africa

2.1.1.4. South African pine sawdust (PSD)

Pine saw dust is one of the abundant agro-waste materials in South Africa. The waste is mainly generated from the wood industries engaged in different wood processing activities used for different domestic and industrial applications. The available commercial timber plantation area in South Africa is covered by about 50.6% pine, while eucalyptus covered around 41.8 % [32]. It implies that pine logs are in abundance for pine sawdust production.

2.1.1.5. South African coal

There are different types of coal around the world for energy production. It includes anthracite, bituminous, sub-bituminous, and lignite (Figure 2.3), but the types typically found in South African coalfields are the anthracite and bituminous coal.



Figure 2. 5: Different types of coal found around the globe [33]

South Africa is one of the largest producers of coal around the world and with about 300 million reserves. According to the South African coal report, around 143.239 TOE mn of coal was produced in South Africa in 2018. Figure 2.4 reveals the amounts of coal produced in SA from 2007 through 2018.

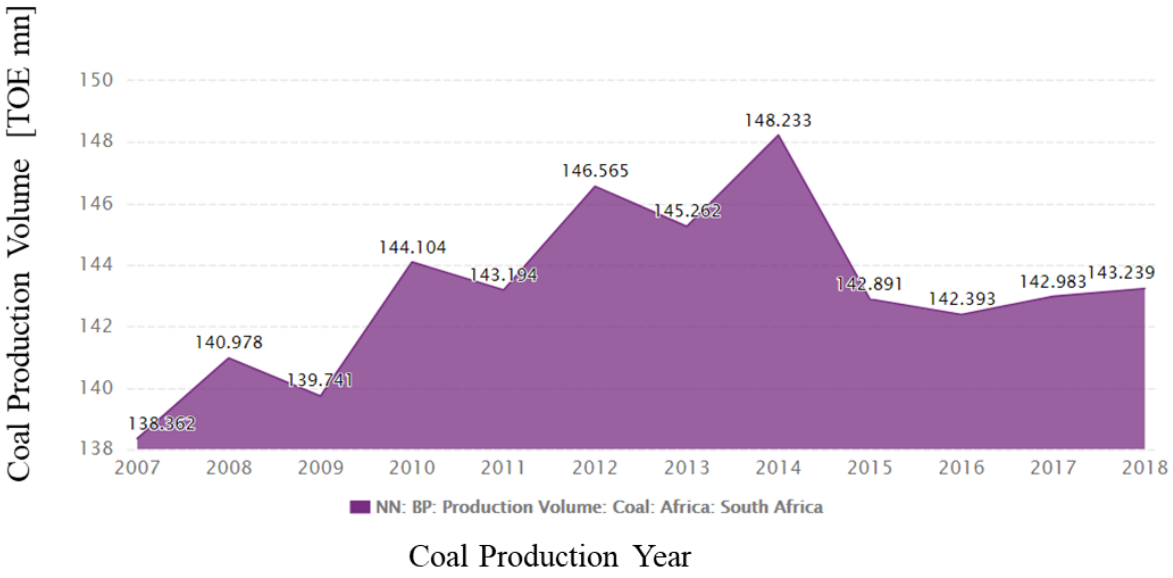


Figure 2. 6: Coal production sites in South Africa (adapted from Mineral Council of South Africa) [33].

South African coal is produced from Free State, Gauteng, Limpopo, and Mpumalanga, but the majority of the coal production is carried out at Mpumalanga as indicated in Figure 2.5.

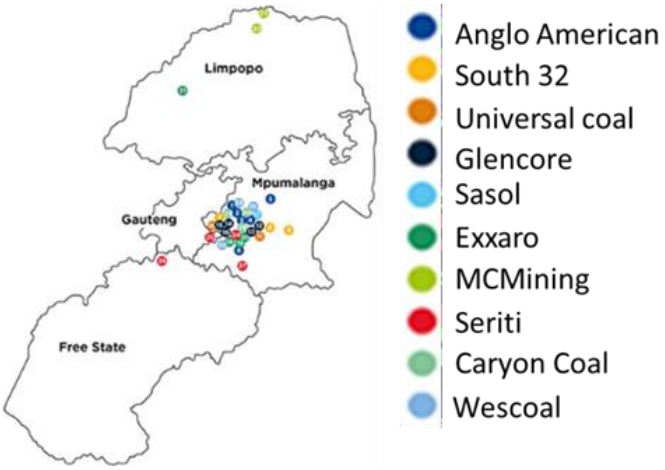


Figure 2. 7: Coal production sites in South Africa (adapted from Mineral Council of South Africa) [33].

Secondly, the majority of the coal produced in South Africa is consumed by Eskom, Sasol, industries, metallurgical, and Merchants & residential as shown in Figure 2.6.

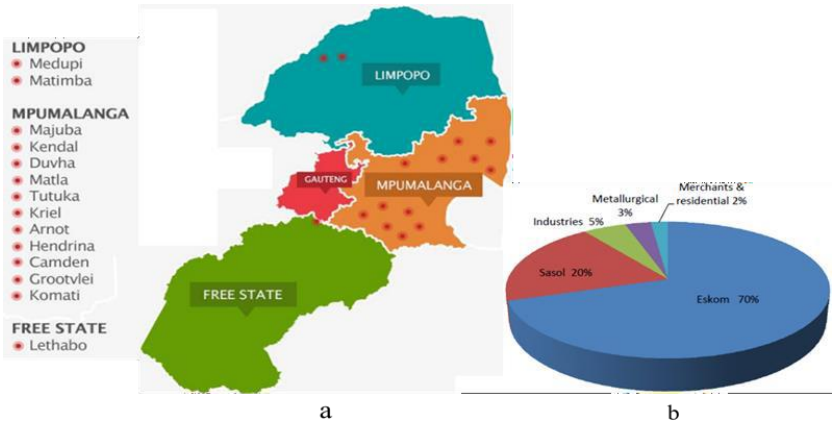


Figure 2. 8: (a) Coal power stations in South Africa (b) Coal consumption in South Africa (Adapted from Mintek reports) [34].

Figure 2.6 also depicts the site locations of coal fired power plants in South Africa, and it can be observed that the amount of coal used by Eskom and Sasol is around 90 % of total coal produced in the country, and this accounts for the high environmental emissions in SA. The basic coal quality assessment in terms of type grade and rank is presented in Figure 2.7, and according to the Council for Geoscience of South Africa, the typical characteristics of coal based on the moisture content, carbon content and calorific value is shown in Figure 2.7

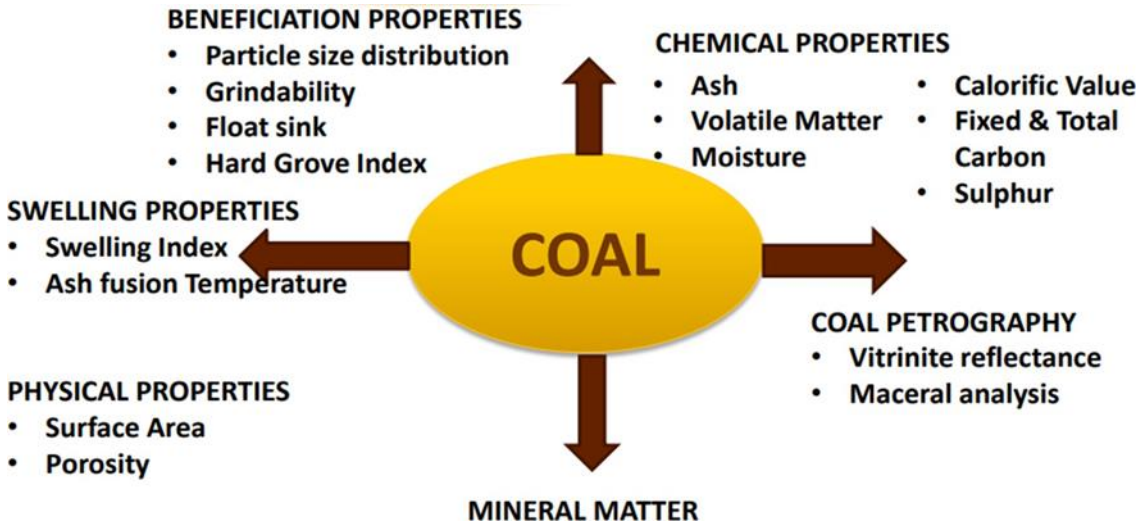


Figure 2. 9: Coal quality assessment in terms of type, grade and rank (Adapted from Council for Geoscience South Africa; Applied Geoscience Solutions) [35].

The typical characteristics of coal based on the MC, CC, & CV is depicted in Table 2.3.

Table 2. 3: Typical properties of coal with reference to MC, CC & CV (Adapted from Council for Geoscience South Africa; Applied Geoscience Solutions [35].

S/N	Coal type	MC [%]	CC [%]	CV [MJ/kg
1	Anthracite	0 - 5	85 - 95	32 - 36
2	Bituminous	8 - 10	45 - 85	23 - 33
3	Sub-bituminous	10	35 - 45	19 - 26
4	Lignite	35	25 - 35	9 21
5	Peat	90	-	-

MC: Moisture content; CC: Carbon content; CV: Calorific value

2.2. Heating value of fuel

The calorific value of fuel is a critical parameter in energy production. According to Shi et al [36], there are two types of Heating Values. It includes the Gross Heating Value (GHV) commonly known as the higher heating value (HHV), and Net Heating Value (NHV) also referred to as the Lower Heating Value (LHV). The HHV describes the amount of energy present in a fuel and it could be regarded as the total energy released by a kilogram of that fuel at complete combustion. Similarly, the LHV is regarded as the amount of heat released by a fuel on the account that the product water was passing through a vapour phase without actually any recovery of the latent heat of vaporization [37]. Both heating values are employed to evaluating the energy content of fuels. In order to determine the heating value of a fuel, bomb calorimeter is used. Bomb calorimeter requires special carefulness to understand its operational techniques to ensure accuracy of results especially when many samples are involved. It is not cost effective measuring the heating value of fuels using the tool when compared to empirical or mathematical techniques. Mathematic methods save time and the experimental costs. [38,39]. Many authors have investigated the use of either modern facilities or mathematical methods to estimate the energy parameters of fuels. The works of Sheng & Azevedo [40], Posom & Sirisomboon [37], Posom & Sirisomboon [41]; Fegan et al. [42] & Andres & Bona [43], the evaluation of the energy parameters of some fuels were reported.

However, there is a scarcity of report in the literature describing the use of the ultimate analysis of South Africa coal and other solid wastes such as sugar bagasse, corn cobs, and waste tyre for

the assessment of the energy parameters (HHV and LHV) of South Africa co- gasification plant. In the light of this, empirical correlations and/or any suitable existing commercial predictive package such as Artificial Neural Networks (ANNs) will be used to perform the assessment.

2.3. Techno-economic analysis of feedstock for energy generation in a Combined Heat and Power (CHP) Plant

Researchers have carried out many studies on the techno-economic analysis of feedstocks used for energy generation using different kinds of energy conversion systems. It is therefore important to critically review some of these works. For example, Y. Huang et al. [45] evaluated the techno-economic analysis of a 150 MWe biomass fueled CHP for commercial buildings using Organic Rankine Cycle (ORC) and biomass gasification system displayed in Figure 2.8. The performance of the two systems was compared in terms of heat and electricity production using willow chips and Miscanthus via ECLIPSE modelling and simulation tool, respectively.

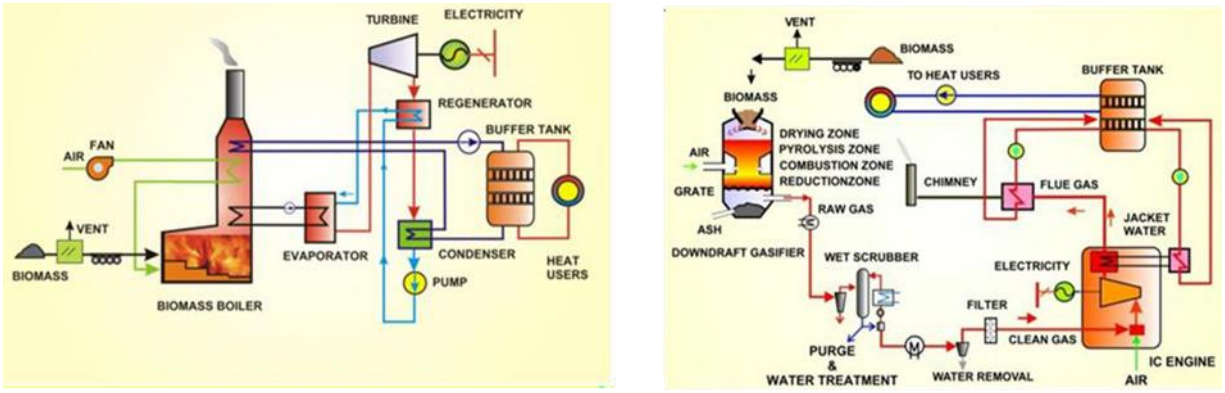
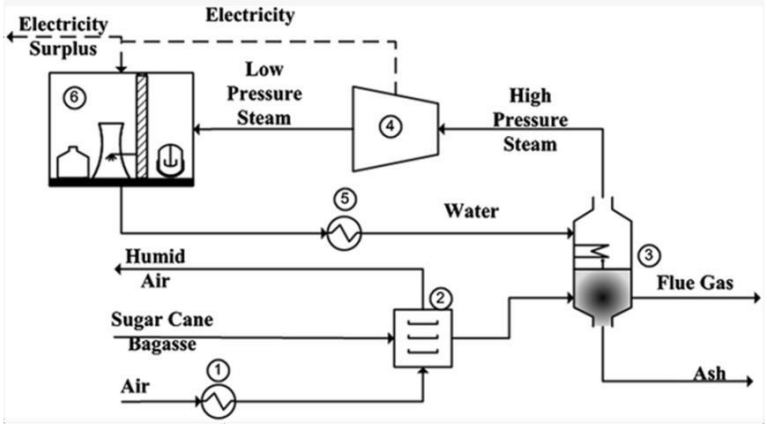


Figure 2. 10: (a) Schematic diagram of biomass CHP system based on Organic Rankine Cycle (ORC), (b) Schematic diagram of biomass CHP system based on a downdraft gasifier (DDG) (Adapted from Y. Huang et al. [45] with copy write permission).

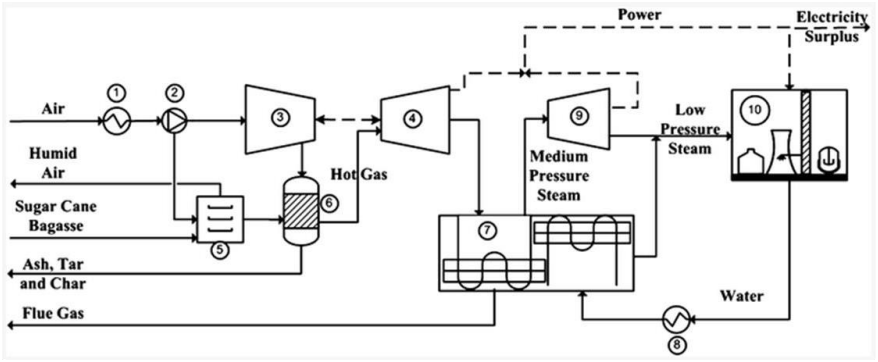
For the biomass gasification-based CHP plant, the efficiency of the CHP plant was 58 % (willow chips) and 64 % (miscanthus), while 76 % (willow chips) and 81 % (miscanthus) was obtained from the ORC based CHP plant. A profit of around 87 – 97 £/MW/h and 40 – 50 £/MW/h was obtained from ORC and biomass-based gasification CHP plants, respectively. It can be seen that the efficiency of the ORC based CHP plant was higher than that of biomass gasification-based CHP system, but Huang and his co-workers concluded that application of low cost agricultural/forestry wastes will favour profitability in both plants. Rincon, et al. [46] assessed the techno-economic of supplying heat and electricity to a sugar/alcohol production plants in South Eastern and Mid- Western Regions of Mexico using sugarcane bagasse (SCB). In this case, a biomass steam turbine and biomass gasification CHP plant shown in Figure 2.9 and figure 2.10

were employed as against ORC & biomass-based CHP system studied by Huang et al. [45]. Agro-waste material (SCB) obtained from each of the regions were used, contrary to fast growing energy crops (willow chips & miscanthus studied by Huang et al. [45].



1. Heater, 2: Dryer, 3: Furnace, 4: Steam turbine, 5: Water condenser, 6: Chemical process

Figure 2. 11: Biomass steam turbine (BST) co-generation system (Adapted from Rincon, et al. [46].



1: Heater, 2 :Divisor, 3: Compressor, 4: Primary gas turbine, 5: Dryer, 6: Integrated gasification and combustion system, 7: Heat recovery steam generator (HRSG), 8: Water condenser, 9: Secondary steam turbine, 10: Chemical process

Figure 2. 12: Biomass integrated combined cycle (BIGC) co-generation system (Adapted from Rincon, et al. [46].

It was observed that the biomass CHP plant was more viable than that of biomass steam turbine. This may be related to the use of biomass waste as against the findings from Huang and his co-workers that used two fast growing energy crops (willow & miscanthus). It was concluded that the BIGC plant is more attractive than the biomass steam turbine by reducing around 18 % cost of producing ethanol.

The viability of a small-scale biomass-fueled CHP plant for community housing was evaluated by Wood & Rowley [47] for 15-year project live using net present value (NPV) model. In this

case, thermal storage, daily and seasonal load impact variations of the different systems that convert the biomass (wood chips) material into fuel was examined. The systems considered were gasifier & internal combustion engine (ICE), Organic Rankine Cycle (ORC), Stirling engine system, indirect fired gas turbine (IFGT), and vegetable oil-fired ICE. The biomass CHP plant demonstrated positive NPV without the need for capital subsidies, hence was more promising than other systems tested. A 5.6 MW & 52.3 CHP plant using corn Stover as fuel for heat and power supplies to an ethanol production plant was studied by Sokhansanj et al. [48]. The analysis was based on the logistic for delivering square bales, dry chops and pellets of corn Stover with emphasis on biomass cost, energy impact and carbon emissions for biomass logistic options (e.g. collection, pre-treatment, transportation, & on-site storage). From the Integrated Biomass Supply Analysis (IBSAL) simulation model result, the delivery cost of square bales corn Stover was 73 \$ mg^{-1} while dry chops and pellets were 88 \$ mg^{-1} and 86 \$ mg^{-1}, respectively. It implies that the square bale is more profitable than the others.

Furthermore, the profitability of simultaneous production of sugar, fuel ethanol, and electricity was compared to that of feedstock distribution, technology for sugar, fuel ethanol, Poly-3-hydroxybutirate (PHB) anthocyanins & electricity production (i.e. Columbian base case) [49]. From the Aspen Plus model result, fuel ethanol and PHB production from combined use of sugarcane bagasse (SCB) and molasses was more promising than the other option. From all the aforementioned studies, it can be seen that blends of coal and biomass/tyre were not considered. The amount of emissions generated from the power plants, and the optimum feedstocks in terms of specified project life were not reported. It will be necessary to carry out studies in this area.

2.4. Thermochemical Energy conversion

Public concern on pollution and climate change arising from desperate need for energy has heightened the interest of researchers on the search for attractive system and sources of energy generation. One of the methods identified by researchers is the thermochemical energy conversion. It involves pyrolysis, gasification, and combustion. Combustion involves direct burning and it is widely known for producing gaseous emissions, whereas pyrolysis which is the degradation of the volatile content of the feedstock produces large amount of bio-chars [50]. Gasification is more attractive than the two systems as already explained in section 1.1.1. Gasification is a process in which solid or liquid carbonaceous materials, such as biomass, react with air, oxygen, steam or mixture of them to produce fuel gas containing H_2, CO, CO_2, CH_4, and tars [50,51]. For example, it is self-sufficient (auto-thermal) in terms of the energy balance. The energy that was invested in the process can be recovered, and its operating efficiency is more

controlled than that of combustion and pyrolysis [52]. However, the product composition from the process depends on several factors including but not limited to the type of feedstocks, and gasifier in use.

2.4.1. Types of gasifiers

In order to design or select a gasifier for biomass or other solid fuels gasification or co-gasification process, it is important to consider the availability of the feedstock and its characteristics, and above all where the facility will be applied [53,54]. Although those gasifiers may be available with regards to the size and design as specified by users, it is in overall classified either as a fixed bed or fluidized bed gasifiers [55] or with reference to the pressure, oxidant and cleaning system in use. The various kinds of gasifiers include;

1. Up-draft gasifier
2. Downdraft gasifier
3. Fluidised bed gasifier, and
4. Entrained bed gasifier

In terms of tar production for example, the updraft, downdraft, fluidised bed and entrained bed gasifiers will produce around 50.0 g Nm^{-3}, 1.0 Nm^{-3}, 10.0 Nm^{-3} and 0.4 Nm^{-3} of tar respectively [56], and for a CFB gasifiers, cold gas efficiency of around 50 70 % can be achieved. According to Probstien & Hicks [57], the Cold gas efficiency of fixed bed (moving bed) such as the Lurgi gasifiers used in Lurgi –process is between 80 – 90 % [57]. However, the various conventional gasification systems are shown in figure 2.11

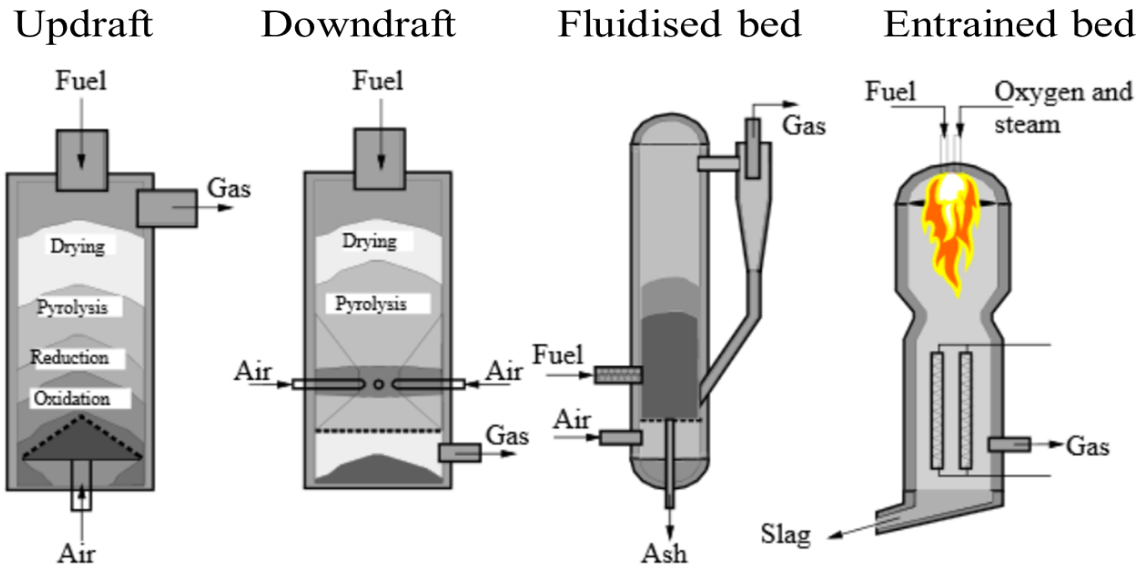


Figure 2. 13: Different choices of gasifiers (Adapted from Sikarwar et al. [56].

2.4.1.1. Updraft and Downdraft Gasifiers

The updraft and downdraft gasifiers are the oldest and simplest forms of gasifiers and they are referred to as fixed bed gasifier. In updraft, feedstock is introduced from the top whereas; the pre-heated gasifying agent is passed through the grip in the bottom section into the reactor. The product gases produced during the thermochemical reactions, exit from the top of the gasifier. The gasification system is not suitable for advanced scale applications because, the product gases generated from it contains large amount of tar [58]. Gas cleaning may be required unless effective primary tar treatment is used, and the cost of gas cleaning process (outside the gasifier: secondary treatment) is quite expensive. Similarly, in the downdraft gasifier, the feedstock and oxidant are introduced from the top of the system into the reactor [59]. Gases produced in the process also exits from the top section of the gasifier The fixed bed gasifier provides low and non-uniform heat and mass transfer within the system, though is of low cost, because of its design concept.

2.4.1.2. Entrained bed gasifier

This type of gasifier is widely used for commercial scale gasification process. It is operated at a high temperature (1300 ^{o}C – 1500 ^{O}C) and pressure (20 – 70 bars) using feedstock of particle diameter of around 0.075 mm. The gasifying agent is usually oxygen, and the systems operating temperature is always far above the melting point of ash, and as such, creates a room for total cracking or destruction of tar. Hence it is more advantageous in dealing with tar problems.

2.4.1.3. Fluidised bed gasifier (FBG)

Fluidised bed gasifier is categorised based upon the fluid dynamic and modes of heat transfer. The fluidising agent can be oxygen, air, steam or a mixture of them. Ashes produced from the reactor are removed as fluidising dry ashes or heavy agglomerates. For dry ash gasifiers, the gasification temperature is relatively low and it favour low grade biomass materials, while for the agglomerates gasifiers which accommodates high grade biomass, high gasification temperatures are employed [60**].** In terms of the reactor capacity, the fluidised bed is higher than fixed bed, but of low capacity when compared to an entrained flow gasifier. Secondly the conversion efficiency of a fluidised bed is low because of entrainment of solid materials into the product gases, but these solids can be recycled to enhance the conversion rate of the system. It is suited for processing high corrosive ash fuels (e.g. biomass) [60]. Basically, there are two types; including bubbling fluidised bed (BFB) and circulating fluidised bed (CFB) gasifiers. The BFB gasifier uses fine inert particles of sand or alumina as the bed material or heat carrier and any of the aforementioned oxidants. Fluidisation in the system is achieved once the weight of the upward moving oxidant counterbalances the weight of the solid material. The particles remain in the reactor but assuming

a boiling state. The velocity at which this process occurs is called the minimum fluidisation velocity, and the gases that are produced during feedstocks thermochemical reactions, exit the gasifier from the top unit. Complete char conversion is not achieved in the system because of back-mixing of solids (high solid mixing), thus; causing the evenly distribution of temperature in the system. One of the problems of the BFB system is the slow diffusion of oxygen from the bubbles to the emulsion phase, and this amounts to poor gasification efficiencies [61].

In a CFB gasifier, the gas velocity is maintained above the minimum fluidisation velocity, thus; originating the entrainment of the solid particles in the gas stream, and the particles are separated in the cyclone as the gas exits the gasifier [62]. Unconverted chars are returned back to the system through the return leg until complete conversion is achieved. Feedstocks of low particle diameter are used hence; providing higher conversion efficiency compared to the BFB gasifier [63,64]. Karatas, & Akgun [65] reported that a BFB gasifier is attractive for medium scale electric power capacities production compared to a CFB gasifier. FBG accommodates wide range of feedstocks, provides good mixing and gas-solid contact that enhances the rate of reaction, supports low tar content in the producer gas because of the use of bed material as heat carrier and catalyst, and enhances the production of high-quality gaseous product [66]. Agglomeration and loss of fluidizability are serious concern in FBG because; the gasifier's operating temperature is within the range of the melting point of the feedstocks ash [67]. Generally, the FBG produces fuel gas with heating value of 4 – 6 MJ/m^3 with H_2 content of 8 – 14 vol. % if air is used as the gasifying agent, and 10.16 MJ/m^3 with H_2 content of 30 – 60 vol. % if steam is used as gasifying agent, whereas, oxygen-enriched air (which is not cost effective) produces gas with medium heating value [68].

2.5. Biomass gasification reactions

The reactions shown in Table 2.4 are typical reaction associated with the biomass gasification process but may be applicable to co-gasification processes such as coal and solid waste. All the reactions are very important, but the Water-Gas-Shift (WGS) reaction that is represented by the equation 2.1 seems to be more important than others. This is because it is in the reaction ($CO + H_2O \leftrightarrow CO_2 + H_2$) that the H_2-enriched syngas is produced. It is therefore very pertinent to apply the necessary operating conditions that will allow the reaction occur in favour of the hydrogen production. Table 2.4 presents the main reactions occurring in the reduction zone during biomass gasification.

Table 2.4: Biomass gasification reactions: reduction zone [69]

Type of reaction	Reaction	Equation
Water–gas reaction:	$C + H_2O \rightarrow CO + H_2$ ΔH=131.4 kJ/mol	2.1
Boudouard reaction:	$C + CO_2 \rightarrow 2CO$ ΔH=172.6 kJ/mol	2.2
Shift reaction:	$CO_2+H_2 \rightarrow CO+H_2O$ ΔH=42 kJ/mol	2.3
Methane reaction:	$C+2H_2 \rightarrow CH_4$ ΔH=75 kJ/mol	2.4

2.5.1. Factors affecting gasification/co-gasification Process

There are several factors that are considered in gasification and/or co-gasification process. It includes; reaction (gasification) temperatures, equivalence ratio (ER), type/size of feedstock (particle size), gasifying agent (oxidant), steam/biomass ratio (S/B), catalyst, etc. Wang et al. [70] investigated H_2-enriched gas production by co-gasification of biomass and coal in a fluidized bed gasifier. The influence of temperature on H_2 concentration was examined. The result revealed that the H_2 content and yield were raised from 28.7 % and 25.63 g/kg at 875 ^{o} C to 46.3 % and 57.88 g/kg at 975^{O}c, respectively. The result was attributed to the enhancement of the water gas reaction (equation 2.6) that was favoured by the increase in the temperature. Wei et al. [71] reported also that the tar, char, CO, and CH_4 in the gaseous product decreased with an increase in the temperature, whereas gas yield and H_2 content increased, as well.

Similarly, the application of steam as oxidant during gasification process affects the gas quality and product yield. Low S/B ratio promotes high char and CH_4 production (Methanation - equation 11), whereas high S/B ratio promotes the product gas yield, calorific value of the gas and decrease in tar production. Sharma et al. [72], identified a limit upon which injection of steam (increase in the S/B ratio) could amount to excess steam which could lower the net temperature of the reactor, tar cracking process and hence; reduce the overall efficiency of the gasifier. Nipattummakul et al. [69] investigated the gasification of sewage sludge using steam as the gasifying agent and observed that hydrogen yield increased about three times as compared to air gasification of the same feedstock. Other authors including [73,74,75,1,76,78] Campoy et al. [73] Chang et al. [74] Corella et al. [75], Udomsirichakorn & Salam [1], Udomsirichakorn et al. [76], & Wang & Chen [78] also carried out biomass gasification with different feedstocks and using steam as the oxidant. The authors observed a similar trend.

Furthermore, if the equivalence ratio (ER) is increased, the H_2 and CO yield will decrease, whereas the CO_2 content will increase. Under this context, the calorific value of the gas will reduce [79]. Tar cracking is also enhanced by the increase of the ER because, sufficient O_2 is provided for the reaction of the volatile fractions, but at the expense of the increase in NH_3 due to surplus nitrogen from the air. On the other hand, the ER increases linearly with the temperature of the system, if there is constant feeding rate. Generally, for fluidized bed gasifier, an optimum ER of around 0.2 – 0.3 is desired. Operating with ER below 0.2 may cause incomplete gasification, whereas operating above 0.3 may move the process from gasification to combustion [80]. As stated earlier, the type of feedstock and its size also play a major role in the gasification efficiency. The composition of the feedstock (cellulose, hemicellulose, and lignin) determines the product gas yield, whereas its size affects heat and mass transfer [56]. The gasification process is better controlled at uniform bed temperature. Poor heat transfer due to large particle size can promote high char production [81], whereas the carbon conversion and H_2 yield increases at reduced particle size, and for fluidized bed systems, the optimum fuel particle size is around < 6.0 mm [82] Particle size above 6.0 mm may cause blockages and very small size could also amount to feeding difficulties.

Meanwhile, the use of catalyst has also been reported to influence the gasification process. Wei et al. [83] have tested the effects of dolomite, limestone, and olivine on the tar cracking and H_2 production. The result indicated that dolomite was more attractive than both limestone and olivine for tar destruction and higher product gas yield. In the light of the foregoing, the next section presents a comprehensive description of some of the previous studies that were carried out by researchers to generate enriched H_2 gas.

2.5.2. Assessment of gasification and co-gasification systems efficiency

It is agreeable that during biomass gasification, the products distribution and the yield of hydrogen-rich gas is dependent on different factors. The factors include the type of feedstock (fuel), reactor configuration, experimental operating conditions (e.g. gas-solid residence time, gasification temperature and pressure, equivalence ratio, oxidant (air, steam, air/steam, CO_2, O_2, etc.) catalyst, and others) [84,85].

Understanding the efficiency of a gasifier is very relevant in gasification or co-gasification process. Some examples of parameters that can be used to evaluate the performance efficiency of a gasification unit are:

- Cold Gas Efficiency (CGE)

- Carbon Conversion Efficiency (CCE)
- Lower heating value of gas
- Gas yield, and
- Product gas composition (e.g. CO, CO_2, CH_4, H_2).

The gasification efficiency indicators can be measured (in the case of product gas composition), estimated from empirical model equations and using data obtained from experimental analysis, simulation and predictive modelling tools such as Artificial Neural Networks (ANNs), Genetic Algorithm (GA), Aspen-Plus or other similar software.

2.5.3. Effects of gasification operating variables on gasification efficiency

The oxidant (steam or steam-oxygen), temperature and catalyst that crack tars and some other operating process condition have strong effects on gasification systems efficiency. Kumabe et al. [86] studied the influence of feedstock blending ratios on the efficiency to understand the efficiency characteristic of a downdraft fixed bed gasifier woody biomass and coal. It was observed that low biomass ratio generated a gas suitable for methanol synthesis, whereas, high biomass ratio gave a gas suitable for Di-Methyl Ether (DME). A different type of gasifier (moving bed) was used by Straka & Bucko [87] to determine the heating value of product using blend of lignite (coal) and waste tyre (WT). The LHV of the gas was increased by 3 %, while H_2S and CH_3SH production were decreased by using blends of coal and WT as against solitary gasification of the coal. Syngas composition and LHV of the gas was studied by Kumabe et al. [86] and Straka & Bucko [87] but Ali et al. [88] investigated the cold gas efficiency (CGE) of the gasifier using blends of biomass and coal. The CGE increased around 82.38 % when blends of the feedstock were used as against coal gasification that produced a CGE of about 79.61 %. In a different study carried out by Kumabe et al. [86] to estimate the CGE of a gasifier using mixture of coal and woody biomass, the CGE increased from 65 % to 85 % contrary to lower efficiency observed during solitary gasification of coal. Several researchers including Aigner et al. [89], Mcllveen, et al. [90] Andre et al. [91], Pinto et al. [92], Kumabe et al. [86], Pinto et al. [93], Alzate et al. [94], Fermoso et al. [95] & de Joug et al. [96] have reported similar trends of results for the CGE and syngas composition, respectively.

Understanding the gasification systems efficiency is very important in the energy production sector. It is considered as one of the factors that drives energy sustainability. Information on evaluation of performance efficiency of gasifiers using the aforementioned tools based on different feedstocks (blends of coal, biomass/tyre), and experimental process condition are required. It will assist stakeholders in designing gasifiers that will process different kinds of fuels and hence; establishing a platform for decision making.

2.5.4. Effect of tar yield on gasification efficiency

During gasification process, tar is produced. The presence of tar in the gasify will reduces the efficiency of the gasifier. This is because tar can easily block the pipings, valves and the feeding system, thereby leading to poor efficiency in terms ofd operating the gasifier.

2.5.4.1. Tar formation and treatment processes

Tar is a complex mixture of aromatics containing a significant fraction of polycyclic aromatic hydrocarbons (PAH) [97]. They exist also as oxygenates and aromatic derivatives of benzene. Normally, at typical reaction temperatures during biomass, coal or their blends gasification, tar formation is practically inevitable. An effective operating process is usually deterred in the presence of tar, both in the gasifier during energy conversion, and at the end use facilities because of its capacity for condensation and solidification. As part of the remedy, the gasifier could be equipped with a condensation and scrubbing unit with suitable solvent to trap or reduce the amount of tar in the product gas [98]. Alternatively, by reacting the produced gas over a tar-cracking catalyst at high temperature may reduce or eliminate unwanted organics and hence; protecting downstream catalyst beds from contamination (Anis & Zainal [99]. It is essentially, on the account that the quality of the produced gas will be degraded.

For an end user facility, there is a specific amount of tar in syngas it can allow for the gas to be used as fuel for electricty production. According to Iversen and Gobel [100], the allowable tar limits for application devices such as gas engines, gas turbines, and fuel cells are 50, 5, and 1 mg/Nm^3 respectively, while Sikarwar et al. [56] reported that the tar limit was as shown in Table 2.5.

Table 2. 5: Allowable tar limits for different facilities [56].

S/N	Facility	Tar Limit (g Nm^{-3})
1	Fuel Cells (SOFC)	1.0
2	Gas Turbines	0.05 – 5.0
3	IC Engines	100.0
4	Compressors	500.0
5	Boilers	No tar limit as long as the tar does not cool below its due point

SOFCs: Sulphur Oxide Fuel Cells; IC: Internal Combustion Engines

To achieve these tar levels in the product gas, effective tar elimination or reduction techniques are required. Generally, there are two main methods of reducing or eliminating tars during biomass gasification. It includes primary and secondary tar treatments. The primary treatment is an internal process (inside the gasifier), whereas the secondary approach is done outside the gasifier. The primary method is meant to prevent tar formation, whereas secondary method is for removal of tar formed and contained in the product gases (Rios et al., 2018) [101]. The two methods are effective, but it is also dependent on the composition of the tar. An overview of a typical tar composition is presented in table 2.6.

Table 2. 6: Typical compositions of tar [102]

S/N	Tar Components	Percentage composition (%)
1	1-Ring Aromatic Hydrocarbon	22
2	2- Ring Aromatic Hydrocarbon	13
3	3-Ring Aromatic Hydrocarbon	6
4	4-Ring Aromatic Hydrocarbon	1
5	Naphthalene	15
6	Heterocyclic Compound	10
7	Phenolic Compound	7
8	Toluene	24
9	Others	2

S/N: Serial number

For effective tar treatment, thermal, mechanical, and catalytic approaches are used. A comprehensive treatment method is required to clearly describe the most attractive technique. This is because different fuels have different physio-chemical properties and may need special treatment method. Extensive works have been carried out by researchers to understand the efficient method of treating tar. On this note, a comprehensive tar treatment model has to be developed to account for the treatment of tar produced from blends of biomass and coal during co-gasification process.

2.5.4.1. Tar measurement

Different analytical techniques are available for analysing and measuring of tars. Thermogravimetric Analysis (TGA), TG-MS, Near Infrared (NIR), Spectroscopy, and TG- MS Thermogravimetric Analysis coupled with Differential Thermogravimetric Analysis (DTG) and GC-MS are among of such measurement equipment [56]. Also, a GC-MS-FID can equally be used for the above-mentioned techniques are considered very beneficial because of their cost effectiveness, precision, and measurement speed.

2.5.4.2. Previous studies on tar treatment

A comprehensive review of tar treatment was carried out as shown in Table 2.7. It can be seen that the content of tar in the produced gas varied based on the process conditions employed. In the case of reaction temperature, there was a reduction in the content of tar when the temperature was increased and Vis versa. In terms of using steam as the gasifying agent, the content of tar in the gas increased by an increase in steam injection. It was attributed to the steam lowering the gasification temperature via steam saturation hence; resulting to poor tar cracking. According to the study carried out by De Sales et al. [103] using oxygen as oxidant produced tar concentration in the range of 59 – 64 mg/Nm^3 as against air-steam that generated tar in the range of 91 – 92 mg/Nm^3. Generally, for air gasification, steam gasification, & Steam-Oxygen gasification, the equivalence ratio (ER), steam-to-biomass ratio (S/B), & steam-to-Oxygen ratio (S/O) are the crucial parameters considered. In this case, the ER was considered as the most influencing parameter influencing the content of tar in the syngas [102]. The concentration of tar in syngas with respect to the gasifier and process condition used for gasification is presented in Table 2.7.

Table 2.7: Tar concentrations in syngas based on gasifiers & process conditions (Adapted from Rios et al. [101].

TG	Feedstock	GA	BM	GT (°C)	T C	Ref
Fixed Bed						
Updraft	Wood	n.a	n.a	1,000	1.0	[104]
Updraft	Straw	Air	n.a	400–500	50.0	[105]
Updraft	Sawdust	Air	n.a	n.a	8.6	[106]
Updraft	Wood pellet	Air/Steam	n.a	650	90.3	[107]
Updraft	Pine pellet	Air	n.a	1,000	132.4	[108]
Downdraft	Wood	n.a	n.a	1,000–1,400	1.0	[104]
Downdraft	Wood chip	n.a	n.a	n.a	0.5	[105]
Downdraft	Pine pellet	Air	n.a	900	32.3	[108]
Downdraft	Hazelnut shell	Air	n.a	821–1,206	3.3	[109]
Downdraft	Pine wood	Steam/O_2	n.a	774–934	2.9	[110]
Downdraft	Pine wood	Air	n.a	870–1,108	12.3	[110]
Downdraft	Pine wood	Steam/O_2	n.a	910–1,090	14.4	[110]
Downdraft	Pine wood	Air	n.a	798–910	1.9	[110]
Downdraft	Eucalyptus wood	Air	n.a	550–700	0.236	[111]
Downdraft	eucalyptus spp	Air/Steam	n.a	500–700	0.0915	[112]
Downdraft	eucalyptus spp	Steam/O_2	n.a	501–700	0.060	[112]
Fluidized Bed						
BFB	Pine wood chips	Air	Silica Sand	780–830	18.0	[113]
BFB	Pine wood chips	Steam	Silica Sand	750–780	53.0	[113]
BFB	Pine wood chips	Steam/O_2	Silica Sand	785–830	24.0	[113]
BFB	Coal/Biomass	Air	Sand	700–900	2.0	[104]
BFB	forestry residues	Air	n.a	700–900	3.0	[114]

BFB	Pine wood chips	Air	Silica Sand + dolomite	700–850	2.0	[115]
BFB	Pine wood chips	Steam/O_2	Silica Sand	780–890	5.0	[116]
BFB	Spruce wood pellet	Air/Steam	Quartz, olivine, dolomite	780	7.6	[116]
BFB	Radiata pine	Steam	Co/MgO	600	8.4	[117]
BFB	Pine wood chips	Steam/O_2	Calcined dolomite	795–835	2.5	[118]
BFB	Pine sawdust	Air	Calcined dolomite	800	13.9	[119]
BFB	Bagasse	Air	n.a	800	14.8	[120]
BFB	Wood sawdust	Air	Silica Sand	750	0.010	[120]
BFB	Almond shell	Steam	Olivine, sand, dolomite	700	6.5	[121]
BFB	Almond shell	Steam	Olivine, sand, dolomite	820	1.3	[121]
BFB	Pine sawdust	Air	Silica Sand	790–810	10.0	[122]
BFB	Pine sawdust	Steam	Silica sand + CaO, MgO	750	180.0	[123]
BFB	Pine sawdust	Steam	Silica sand + CaO, MgO	780	40.0	[123]
BFB	Sawdust	Air	n.a	780	2.0	[105]
BFB	Sawdust	Air	n.a	857	0.3	[105]
BFB	Rice husk	Air	n.a	750	6.0	[105]
BFB	Rice husk	Air	n.a	940	0.8	[105]

CFB	Wood pellet	Steam	Olivine	841	3.5	[124]
CFB	Wood pellet	Steam	Calcite	645	1.4	[124]
CFB	Woody biomass	Air	Silica Sand	800–860	0.270	[125]
CFB	Sawdust	Air	Ni-alumina	700–850	2.4	[126]
CFB	Coal/Biomass	Air	Sand	800	0.7	[104]
Entrained bed						
–	Sawdust wastes	Air	n.a	750	0.001	[127]
–	Sawdust	Air	n.a	700–1,000	0.001	[128]
–	Coconut coir dust	Air	n.a	976	23.6	[129]
–	Coconut coir dust	Air	n.a	1,100	4.8	[129]

TG: type of gasifier; GA: gasification agent; BM: bed material; GT: gasification temperature; TC: tar content; *: g/Nm^3

From Table 2.7, it can be observed that the feedstocks used are mostly, biomass materials. Coal and blends of biomass and coal were not studied except the study carried out by [104]. Using a bubbling and circulating fluidized bed gasifiers respectively and tar treatment models were not considered. It will be necessary that comprehensive study is carried out in the area of tar treatment to ensure improvements in the gasification systems efficiency.

2.5.5. Gasification of South African coal

The critical factors that drives the reactivity of coal during gasification are (1) maceral- and microlithotype composition [130] concentration of active sites or reaction surface area (micropore surface area) [131] accessibility of the particular reactant gas to the active sites (porosity) [132] the catalytic effect of the inorganic constituents (the presence of catalytically active species such as Ca-, K-, Na- and Mg bearing species present in the ash) [133]. The aforementioned factors play a crucial role when coal is co-gasified with other solid fuels such as biomass or tyre. Typically, when a blend of coal and biomass is gasified, gasification efficiency is improved, while emission

and tar formation are considerably reduced. According to (Pinto et al. [134] co-gasification of low grade coal and biomass such as pine and olive oil bagasse has the potentials of improving the gasification efficiency (e.g. syngas quality) and a feasible opportunity of using low grade coal. Mastellone et al. [135] studied co-gasification of low grade South African coal, wood and plastic in a bubbling fluidised bed (BFB) gasifier. It was observed that mixture of coal and wood biomass enhanced the syngas yield and reduced tar production, but the lower heating value of the product gas was low. A mixture of South African Eucalyptus and coal was gasified in a downdraft gasifier by (Gaqa et al. [136] to produce syngas for electricity generation. Gaqa and her co-workers inferred that gasification difficulties (tar formation) was reduced when coal and biomass was tested than solitary gasification of coal or biomass. Zhang et al. [137] affirmed that ash formation in gasifier was minimised by using blends of coal and biomass to produce syngas. Importantly, none of the aforementioned authors reported about standard operating process conditions (optimum condition) for tar reduction or to achieving high quality syngas (H_2-enriched) for electricity production employing blend of coal and biomass/tyre.

2.5.5.1. Hydrogen enriched syngas production from coal and co-gasification

Of all the fuels and energy carriers, hydrogen has the highest energy density with around 122 KJ/kg which is about 2.75 times higher than other hydrocrabons [138]. It has the potentials of replacing gasoline because about 9.5 kg of hydrogen is enough to yield energy equivalent of 25 kg of gasoline [139]. Importantly, it can be used as a liquid or gaseous fuel, liberating water as the by-product during burning, and with no emission irrespective of form it is used [140]. According to Xiao et al. [141], hydrogen rich gas can be produced from steam co-gasification of coal in a dual loop gasification system with olivine as tar destructive catalyst. This could be achieved around temperature of 800 – 920 ^{O}C. As reported by researchers, a slight difference in the content of H_2 in the produced gas of around 48 – 55 vol. % [142], 35 – 45 vol. % [143] 34.6 – 56.0 vol. % [144], 37.5 – 47.9 vol. % [86], and 30 – 60 vol. % [145] could be achieved during hydrogen enriched syngas production. From the works that were carried out by few researchers using steam and catalysts, the H_2/CO ratio obtained were in the range of 1.3 – 2.0 [144], and 1.1–3.3 [146], but Rosas et al. [147] reported H_2-to-CO ratio of 1.6.

Essentially, production of hydrogen enriched syngas that is characterised with a high H_2/CO ratio may be achieved by operating at a higher steam-fuel ratio or by use of catalysts in catalyst assisted gasification of biomass [147], coal, and coal-biomass blends [148]. The syngas obtained from the gasification process can be used in a gas turbine. Hydrogen enriched syngas production has been studied in the past using biomass, coal and blends of coal and biomass. Recently, Zribi et al.

[149] used pellets and powdered blends of Olive mill solid wastes and pine sawdust for the production of hydrogen enriched syngas. The effect of steam and temperature were considered, and both parameters were found to have significant effects on the hydrogen enriched syngas production, with the powdered blends providing higher hydrogen enriched syngas than the pellets. A bench scale fixed bed gasifier was used by Kordoghli et al. [150] to investigate the production of hydrogen enriched syngas from waste tyre (WT). Effects of different catalysts and temperature on syngas composition were evaluated. The hydrogen content in the produced gas responded positively to an increase in temperature and with catalysts (WCAT). The concentration of H_2 and CO in the producer gas from the test conducted by Ziao et al. [151] were 38.5 and 18.0 vol. %, respectively, while around 56 % hydrogen content in the produced gas was obtained from the work carried out by Orazio et al. [152] during steam gasification of biomass using different ceramic filter candles (non- catalytic, catalytic, catalytic with foam). The syngas was more enriched in hydrogen by using foam supported catalytic filter. The production of hydrogen enriched syngas from co-gasification of coal and biomass was also investigated to understand the influence of some critical parameters (e.g. oxidant, catalysts, temperature and others) on syngas composition. In this context, Fermoso et al. [153] tested the effect of blending different rank of coals and biomass on H_2/CO ratio. Around 0.8 – 1.2 and 1.9 – 2.3 H_2-to-CO ratio was obtained in solitary gasification of coal and gasification of blend of coal and biomass respectively. Howaniec & Smolinski [154] carried out a similar study using coal and different biomass materials. The effects of biomass types and steam on hydrogen enriched syngas production were assessed. At the optimum operating temperature (i.e. 900 ^{O}C), more hydrogen enriched syngas production was obtained from coal and biomass gasification than that of coal gasification with steam as the gasifying agent [154]. A contrary result was obtained from the same research group [154] when coal and sewage sludge blend was gasified in different configurations of fixed bed gasifier. The content of hydrogen in the producer gas was found to be higher in coal gasification than that of coal and biomass gasification, hence; confirming the effect of reactor configuration on gasification system efficiency (syngas composition). The majority of the aforementioned studies could not use waste material such as biochar as catalysts or catalysts support to examine the performance on hydrogen enriched syngas production. Moreover, comprehensive study on coal-to-biomass ratio is required to understand the trends of the content of hydrogen in the product gas from co-gasification process.

2.5.5.2. Previous studies on co-gasification of coal and other solid fuels

The blending of coal with biomass will minimize the setbacks related to sulfur and ash contents of coal, and above all reduce the CO_2 emissions. Biomass such as agro-waste materials is naturally very low in sulfur and ash contents [155-157]. Co-gasification of biomass and coal will balance the few negative characteristics of each of the samples during gasification. Several researchers have carried out studies to understand how co-gasification of coal and biomass works, and their findings are discussed below:

Pinto et al. [92] blended biomass and coal at a ratio of 20 % and 80 % respectively to study the gaseous product generation. The H_2 production was found to decrease from 33 % to 29 %. Similarly, Mila coal was co-gasified with 40 % Japanese cedar by Kumabe et al. [86] using atmospheric downdraft fixed bed. The blending ratio tested was from 0 to 1. The authors reported that the H_2 production decreased from 47 % to 37.5 % with an increase in the biomass ratio. In a comparative analysis of coal, wood and their mixtures conducted by (Aigner et al. [89], the amount of H_2 generation decreased from 55 % to 43 % with reference to biomass to coal blending ratio of 0 to 100 %. Other researchers have equally reported a different scenario in terms of H_2 production during the co-gasification process. Their findings revealed that the amount of H_2 generated increased with an increase in the biomass blending ratio. Fermoso et al. [153], de Jong et al. [158] studied the production of H_2-enriched syngas production in a fixed bed reactor using almond shell, olive stones, eucalyptus, olive pulp and pine sawdust at different blending ratios whereas, Li et al. [159], used blend of biomass and coal. There was a significant increase in the quality of syngas produced when blends of coal were used when compared to that of blends of biomass. The quality of syngas was also evaluated using coal samples from different geographical [93]. It was observed that variation in the physio-chemical properties of the fuel has effect on the syngas composition. There was also an increase in the concentrations of syngas [94] in using different ratios of polyethylene and sugarcane bagasse (SCB) as against the report from Alzate et al. [95] during the gasification of biomass and coal. Alzate and his co-workers inferred that biomass gasification was better than co-gasification of biomass and coal in terms of the quality of syngas produced for the feedstocks studied.

2.5.6. Biomass & coal gasification process models

The modeling of gasification process is an important approach for eliminating the huge cost and time associated with laboratory experimental work, and a measure for the validation of experimental data. Besides that, mathematical models have been identified as an efficient approach for providing qualitative guidance on the effect of design, feedstock, and operating

parameters on the gasifier performance [160]. Modelling and simulation also provides effective means of optimising the gasification process and importantly, assists in addressing the factors mitigating on the understanding of co-gasification process. There are different models that can be used to accomplish the task. It includes; the kinetic model, thermodynamic equilibrium model (TEM), Computational Fluid Dynamic (CFD), and Artificial Neural Networks (ANNs). These models are very promising, although each of them has its own merits and demerits as discussed in each of the sections of the model.

2.5.6.1. Kinetic Models in gasification

This model evaluates both the potential and kinetic reactions occurring in the reactor and the hydrodynamics of the reactor. It influences accurately the prediction of the product gas yield and compositions [161]. It is used in modelling low-temperature gasification systems. It uses Arrhenius equation for example, for the description of the kinetic parameters used for the modeling operations. Certain laws including the law of conservation of energy, mass, and momentum are also applied to the model to enhance better predictions.

Chemical kinetics describes how fast reactants are consumed and products are formed, the response of a catalyst to the reaction, and identification of the rate determining step in the overall reaction. Understanding the condition of the reaction, allows for the estimation of the rate of the equilibrium reaction. Factors such as pressure, temperature, and catalyst are considered to achieve this, and the rate depends on them, but could be optimised by choosing a suitable reaction condition. Some variables like rate constant, reaction order, and kinetic parameters (e.g. activation energy and pre-exponential factor) are very essential in chemical kinetics study. This is because they enhance accurate predictions of biomass gasification using the kinetic models.

2.5.6.3. Kinetic model analysis

Thermal degradation of biomass is one of the major processes that lead to biomass gasification. The apparent activation energy and pre-exponential factor are extensively studied to understand the thermogravimetric conditions involved in the process. The Friedman method which is a differential non-isothermal technique and Coats and Redfern method; an integral method that incorporates the thermal degradation mechanism can be used. Originally, Arrhenius law is used to describe the reaction rate constant as shown in equation (2.16).

$$K = [\exp(-E_a/RT)] \quad (2.5)$$

2.5.6.4. Friedman method

The expression found in Equation (2.6) (Friedman [162] is used to describe the Friedman method. It is based on the inter-comparison ($d\alpha/dt$), for a given fraction of conversion versus the reciprocal of temperature ($(1/T)$ at linear heating rate (Greenhalf et al. [163], and

E_a and A are obtained from the plot.

$$\ln\left(\frac{d\alpha}{dt}\right) = InA + nIn(1-\alpha) - \frac{-E_a}{RT} \quad (2.6)$$

$$\frac{d\alpha}{dt}\ Kf(\alpha) \quad (2.7)$$

$$K = A\ exp\left(\frac{-E_a}{RT}\right) \quad (2.8)$$

$$\frac{d\alpha}{dt} = \beta\left(\frac{d\alpha}{dT}\right) \quad (2.9)$$

$$\text{while, } \beta = \left(\frac{dT}{dt}\right) \quad (2.10)$$

Combining Equation (2.9) and (2.10) and taking the logarithm gives

$$\ln\left(\frac{d\alpha}{dt}\right) = In\beta\left(\frac{d\alpha}{dT}\right) = In[Af(\alpha)] - \frac{E_a}{RT} \quad (2.11)$$

$f(\alpha)$, the conversion factor is assumed to be constant, and implying that the biomass degradation is independent of temperature, but depends on the rate of mass loss. A slope corresponding to $\frac{-E_a}{RT}$ is obtained from a plot of $\ln\left(\frac{d\alpha}{dt}\right)$ versus $\frac{1}{T}$ which gives a straight line, and from which A is determined from the intercept ($In(A(1-\alpha)^n$ at zero for 1st or 2nd order reaction.

$\alpha = \frac{M_o - M}{M_o - M_\alpha}$, where M_o is the initial biomass sample weight, M is the biomass sample weight at time t and M_α is the final sample weight at final pyrolysis temperature, while, E_a and A are the activation energy (KJ/mol) and pre-exponential factor (s^{-1}). R is the universal gas constant (8.314 KJ/mol. K),

T is the reaction temperature (K) and β is the heating rate (K/min). The iso-conversional kinetics accounts only for the thermal decomposition process as a single unit. For non-isothermal thermogravimetric process, the temperature is a function of time and it increases with constant heating rate. Reliable result is required assuming summation technique involving all main reaction is incorporated.

2.5.6.5. Coats and Redfern method

The biomass reaction temperature (T) can be expressed as presented in Equation (2.12).

$$T = T_O + \beta t \quad (2.12)$$

Or

$$T = \beta t + T_O \quad (2.13)$$

T_O is regarded as the initial temperature (K).

Similarly,

$$\frac{d\alpha}{dt} = \frac{A}{\beta} f(\alpha) \exp\left(\frac{-Ea}{RT}\right) \quad (2.14)$$

Where the conversion factor $f(\alpha)$ is expressed in Equation (2.15), and n is the reaction order.

$$f(\alpha) = (1-\alpha)^n \quad (2.15)$$

If Equation (2.14) and Equation (2.15) are combined following integration, Equation (2.16) is obtained

$$\int_0^{\alpha} \frac{d\alpha}{(1-\alpha)^n T^2} = \frac{AR}{\beta E_a}\left[exp\left(\frac{-E_a}{RT}\right)\right] - exp\left(\frac{-E_a}{RT_O}\right) \quad (2.16)$$

Equation (2.162.27) is reduced in accordance with the expression displayed in Equation (2.17) on the basis that $1 << \exp\left(\frac{-E_a}{RT}\right)$ from the tested temperature ranges during biomass degradation as reported by (Jayaraman & Gokalp [164]:

$$\int_0^{\alpha} \frac{d\alpha}{(1-\alpha)^n T^2} = In\frac{AR}{\beta E_a} - \frac{Ea}{RT} \quad (2.17)$$

A plot of the left-hand side of Equation (2.17) versus ((1/T) will produce a straight line with $\frac{Ea}{RT}$ as the slope, and reaction order of 1.0. However, other methods available for the estimation of the biomass Ea are the Kissinger–Akahira–Sunose (KAS) and Ozawa–Flynn–Wall, but the Coats and Redfern method is more attractive than the two methods because, it can be used to calculate both the pre-exponential factor (A) and reaction order (n) [165].

A summary of some studied carried out on kinetic model for gasification and co-gasification process is depicted in Table 2.8. Shao et al. [166] examined the impact of oxygen-steam ratio and air-steam ratio as the input variables in the prediction of the gas composition and cold gas efficiency (CGE) in a Fluidized Bed Gasifier (FBG) using kinetic based Chem-kin model, and with wood chips as fuel. A reliable result was obtained, but several kinetic constants and reaction coefficients was required for better applications. Inayat et al. [167] on the other hand reported that hydrogen production is directly proportional to both the reaction temperature and steam-biomass ratio, but the production efficiency reduced by an increase in the steam- biomass ratio at a certain range. Gordillo & Belghit [168] used a downdraft solar packed bed gasifier to investigate temperature and species concentration profile under steady and dynamic states. The kinetic model offered a result that agreed with literature results. An FBG was used by Sreejith et al. [169] to determine gasification system efficiency using wood biomass and CaO as a sorbent for in-situ Co_2 capture. The model yielded some better results

The works reported by Sreejith et al. [169], Gordillo & Belghit [168] & Inayat et al. [167] employing kinetic modelling considered hydrogen gas yield and production efficiency, while Khonde and co-authors constructed a Single Reaction Model (SRM) and Distribution Activation Energy Model (DAEM) to study gasification of rice husk in a double stage biomass gasifier [170]. The aforementioned authors affirmed the effectiveness of kinetic model in estimating gasification performance and tar yield, but Khonde & Chaurasia [170] concluded that DAEM was more efficient than the SER for predicting tar degradation over a wide range of conditions.

Table 2.8: Gasification and co-gasification Kinetic Model (KM)

Type of Model	Type of Gasifier	Type of biomass	Degree of Prediction	Reference
Kinetic Model (KM)	FBG	Wood biomass	Product gas composition and cold gas efficiency (CGE)	[166]
	FBG	Oil palm empty fruit	H_2 production efficiency	[167]
	Fixed bed (Downdraft)	Bio-char	Amount of H_2-enriched syngas	[168]
	FBG	Wood biomass	LHV of the product gas, and H_2 yield.	[169]
	FBG	Rice husks	Gasification kinetic and tar production and degradation	[170]
	Prediction Reliability: Correlating the reactor design and the final product gas composition distinguishes the KM from the other models studied, and this correlation quality positively influences its prediction reliability.			

The major setbacks in using the kinetic model are the difficulties associated with the understanding of the kinetic pathways and reaction rate constants involved in the operation, which is necessary for effective model performance. Establishing an optimum thermal degradation condition (e.g. pressure, temperature, concentration, and catalyst) will enhance effective determination of the rate constant. This promotes the efficiency of the model. However, second order reaction model is not efficient in providing results that agree with experimental data.

2.6. Thermodynamic Equilibrium Models (TEM)

This model takes care of the characteristics of the gaseous product generated from the gasifier under certain operating conditions. The model allows for the assumption of the various reactions occurring at the infinite period of time [160]. It further identifies the thermodynamic boundaries that guide the variables chosen for the gasification process. In this kind of model, a gap is usually created between the findings achieved from the package and the actual experimental conditions or data. On that note, efforts are geared towards developing a reliable model for explaining the gasification operation.

In TEM, two methods are considered. It includes Stoichiometric and Non-stoichiometric TEM.

The stoichiometric method incorporates the thermodynamic and chemical equilibrium of chemical reactions and the accompanied species. Global gasification reaction (single step Stoichiometric) or sub-model gasification process (drying, devolatilization, oxidation, and reduction) can be used. Sub-stoichiometric model appears more interesting than the global or single step stoichiometric equilibrium model because at different zones of the gasification process, the composition and temperature of the process can be evaluated and improved to impact on the next zone. Similarly, the non-stoichiometric (i.e. Gibbs free energy minimisation approach) method, account for the direct minimization of the Gibbs free energy of the reaction. The Lagrange procedure is adopted. It has the capacity of handling complex reaction pathways without the need of identifying the independent set of the reaction. The technique allows also, for the application of different algorithms for solving and obtaining solutions from the equilibrium model equations. The model is particularly suitable for modelling fuels like biomass with distinct known chemical formula [160].

2.6.1. Application of TEM in biomass gasification and co-gasification

TEM has been applied by many researchers to study gasification and co-gasification processes as shown in Table 2.9. The TEM has the potentials for high accuracy of reaction prediction and generality for vast operating conditions in a fluidized bed (FB) gasifiers, only that it is deficient in the accurate prediction on the volume fraction of the four core components of the gaseous product from the FB system including; H_2, CO, CO_2, and CH_4 [171]. Gagliano et al [172] have applied the TEM in Aspen Plus simulation environment to predict the chemical composition, heating value (LHV) of syngas, char and tar yield produced from a downdraft gasifier (fixed bed) [172]. Mansaray et al. [173] have equally used chemical equilibrium relations and balances in Aspen Plus environment to simulate rice husk gasification, whereas; Nikoo & Mahinpey [174] predicted (via Aspen-Plus) the steady-state performance of an atmospheric FBG, and applying hydrodynamic and reaction kinetics approach of the TEM, in the simulation process. Both Nikoo & Mahinpey and Mansaray and their co-workers affirmed that the steady state performance of the gasifier could be predicted with the TEM. The works of Liu et al. [175] and Li et al. [176] indicated some reliability of the TEM in predicting gasification system efficiency (gas composition, carbon conversion, and Cold Gas Efficiency (CGE)), but Li et al. [176] also, tested Particle Swarm Optimization (PSO); ANN (BPNN-PSO) as a means for the improvement of model result.

If the equilibrium temperature is restricted to the temperature lower than the operating temperature, and steam is one or the only oxidant used in gasification process, then, significant prediction inaccuracies will occur. Most importantly, the prediction is only correct if the reactor's

temperature is approximately 800 ^{O}C. Besides that, light hydrocarbons (HC) and tar with exception of CH_4 is predicted. Trial and error technique only, is applied to identify the equilibrium temperature. Similarly, the concentration of CH_4, solid carbon, and tar are required as the input in the outlet stream of the gasifier. This therefore, demands for an estimation of the species in the reactor, but such measurements are carried out experimentally, which has to be conducted on the same plant where the model should be applied [176]. On this account, the Pseudo-TEM becomes very sensitive to the estimation, and leads to poor prediction accuracy. Other drawback of the model is that CO and CO_2, are not efficiently predicted [176].

The TEM calculation is not dependent on the design of the gasifier in producing reliable results. This makes it more feasible for wider development in biomass gasification processes. The model provides gasifier designers enough information to achieve the accurate prediction of the maximum amount of yield for any desired product, under equilibrium condition. The TEM requires a lot of kinetic constants and coefficient for better for efficiency, but such factors are difficult to be provided. Similarly, it does not predict the influence of hydrodynamics or geometric parameters such as fluidizing velocity or design variables (e.g. gasifier's weight or height). It does not consider the rate of reaction unlike the kinetic model [176].

To upgrade the efficiency of the TEM, the empirical correlation is incorporated into its equilibrium calculations. This allows solid carbon, CH_4, and char to be contained in the outlet gas stream, while the corresponding amounts of carbon and hydrogen are discounted from the input fuels. The residual fuel components are used as fluidizing agent and their reaction enables equilibrium to be reached. But the composition of the exiting gases is obtained by the summation of the composition of the gaseous product from the equilibrium reaction and carbon, CH_4, and tar initially discounted. The multiplication factors coupled into the empirical correlation had equally been reported by Costa et al. [177] as a very promising technique. The reaction mechanism for gasification of sugarcane via the model was also reported by Ahmed & Gupta [178]. The application of TEM in biomass gasification via kinetic, hydrodynamic, and QET model equations tried to accounts for the variation in data when a gasifier different from the one used for the modelling process is considered. The limitation of the model unfortunately, is that few aspects of gasification process are not well accounted for. Example, the CO and CO_2, are not efficiently predicted and both the CO and CO_2 are serious environmental pollutants from biomass gasification therefore, further study is required in this area to close the gap.

Table 2.9: Gasification and co-gasification Thermodynamic Equilibrium Model (TEM

Type of Model	Type of Gasifier	Type of biomass	Degree of Prediction	Reference
Thermodynamic Equilibrium Model (TEM)	FBG	Wood chips	Major product gas composition e.g. CO, CO_2, CH_4 & H_2	[171]
	Fixed bed (Downdraft)	-	Chemical composition, LHV of Syngas, char production and tar yield	[17]
	FBG	Rice husks	Estimation of gasification process	[173]
	FBG	-	Producer gas composition using ER,S/B, steam, air as input variables	[179]
	Fixed bed (Downdraft)	Birch wood	Syngas yield, LHV, CGE of the syngas with biomass particle size and ER as the input variable	[180]
	FBG	Coal + Birch wood Saw-dust	Product gas composition and yield, gas heating value and biomass gasification performance in the gasifier	[181]

	FBG	Miscanthus (Portuguese origin)	Gasification products and concentration of species evaluation with ER, temperature, S/B ratio. Parameters has indicated positive and negative effects on the system performance	[182]
	Dual fluidised bed gasifier (DFBG)	-	Efficient route of enhancing the solid circulation rate using particle diameter, solid inventory, steam supply to the gasifier and air supply.	[183]
	FBG	Coal + Rice husks	Prediction of CGE and syngas composition. Reliable for the predictions	[184]

	Entrained Fluidized Bed (EFB)	Coal + Biomass	Effect of coal-to-biomass ratio, density, and size variations on the syngas composition, fixed carbon conversion and hydrogen gas production	[185]
	FBG (Spouted)	Coal + biomass	Evaluation of the gasifiers hydrodynamics information	[186]
	FBG	Biomass : Rice husks	Steady state performance of the system	[174]
	FBG Ash agglomeration Fluidised bed (AFB)	-	Syngas composition, carbon conversion efficiency (CCE), and Cold gas efficiency (CGE)	[175]
		-	Product gas composition, carbon	[176]

			conversion efficiency (CCE), and Cold gas efficiency (CGE)	
	Prediction Reliability: It cannot predict the influence of fluid dynamic or geometric parameters such as fluidisation velocity and design variation (e.g., gasifier height). The model lacks the ability to employ the design parameters to simulate the composition of the gasification product (e.g., gases).			

BFB: bubbling fluidised bed; CFB: circulating fluidised bed; FBG: fluidised bed gasifier DFBG: dual fluidised bed gasifier; EFB: entrained fluidised bed.

2.7. Computational Fluid Dynamics (CFD) in gasification process

CFD model is a kind of model used in studying the hydrodynamics occurring during gasification process. There are two methods used for its operation. They are the Eulerian-Lagrange and Eulerian-Eulerian approaches. In the Eulerian-Lagrange technique, Navier-Stokes equation is applied to describe the gas phase, while the solid phase is treated as a discrete phase. Newton's laws of motion are used to estimate the trajectory of individual particles, and the collisions between these particles are described by the soft-sphere or hard- sphere model.

For the Eulerian-Lagrange approach, the solid phase is treated as a continuum. This leads to minimal computational requirement in the tool. The transport properties of the solid phase using this approach are estimated by the kinetic theory of the granular flows. Generally, the model considers several processes including flow transfer, heat and mass transfer, product gas yield, temperature distributions, etc. A mathematical expression is applied a lot to describe the process and interpret the model. It offers more accurate results compared to the thermodynamic equilibrium and kinetic models. It is reliable for providing accurate predictions for some chemical processes [178].

2.7.1. CFD model governing equations

The gas mixture phase of the CFD model using Eulerian-Eulerian two-fluid model for example, is considered as the primary continuous phase, while the solid phases are considered as the secondary dispersal phases. Both phases are treated numerically as interacting and

interpenetrating continua with one pressure shared by them. Secondly, each of the phases is associated with constitutive relations developed by the application of conservation of mass, momentum, energy, and species governing equations using FLUENT 15 user guide; 2006 [72].

The gas and solid phases of the equations are presented in Equation (2.18) and Equation (2.19) respectively.

$$\frac{d(\alpha_g p_g)}{dt} + \nabla.\left(\alpha_g p_g \overrightarrow{V_g}\right) = S_g \tag{2.18}$$

$$\frac{d(\alpha_{sn} p_{sn})}{dt} + \nabla.\left(\alpha_{sn} p_g \overrightarrow{V_{sn}}\right) = sn \tag{2.19}$$

The gas phase is represented by Equation (2.20), while the solid phase is shown in Equation (2.21)

$$\frac{d(\alpha_g P_g \overrightarrow{V_g})}{dt} + \nabla.\left(\alpha_g P_g \overrightarrow{V_g}\overrightarrow{V_g}\right) = -\alpha_g \nabla_P + \nabla.\bar{\bar{\tau}}_g + \alpha_g P_g \vec{g} + \sum_{S=1}^{n}\left(R_{gs} + \overrightarrow{V_{sg}} m'_{sg} - \overrightarrow{V_{gs}}\, m'_{gs}\right) \tag{2.20}$$

$$\frac{d(\alpha_{sn} P_{sn} \overrightarrow{V_g})}{dt} + \nabla.\left(\alpha_{sn} P_{sn} \overrightarrow{V_{sn}}\overrightarrow{V_{sn}}\right) = -\alpha_{sn} \nabla_P + \nabla.\bar{\bar{\tau}}_{sn} + \alpha_{sn} P_{sn} \vec{g} + \sum_{i=1}^{n}\left(R_{1n} + \overrightarrow{V_{sg}} m'_{sg} - \overrightarrow{V_{gs}}\, m'_{gs}\right) \tag{2.21}$$

where the stress tensors ($\overline{\overline{\tau_{sn}}}$, $\bar{\bar{\tau}}_g$) for the solid and gas phase are shown in Equations (2.22) and (2.23), respectively.

$$\bar{\bar{\tau}}_g = \alpha_g \mu_g \left(\nabla \overrightarrow{V_g} + \nabla \overrightarrow{V_g}^{T}\right) - \frac{2}{3}\alpha_g \mu_g \nabla.\overrightarrow{V_g}\, I \tag{2.22}$$

$$\overline{\overline{\tau_{sn}}} = \alpha_{sn} \mu_s \left(\nabla \overrightarrow{V_s} + \nabla \overrightarrow{V_s}^{T}\right) - \alpha_s \left(\lambda_s - \frac{2}{3}\mu_g\right) \nabla.\overrightarrow{V_g}\, I \tag{2.23}$$

Understanding the transport behaviour of the solid phase as a function of both the granular temperature and radial distribution function is very important. For example, the solid phase bulk viscosity and solid phase shear viscosity are presented in Equations (2.24) and (2.25), and they are parameters very useful in model calculations to achieve better predictions.

$$\lambda_s = \frac{2}{3}\alpha_s P_s d_s P\text{go ss}(1 + e_{ss})\sqrt{\frac{\theta_s}{\pi}} \tag{2.24}$$

$$\mu_s = \mu_{s,col} + \mu_{s,fr} + \mu_{s,kin}\alpha \quad (2.25)$$

The solid phase shear viscosity has collisional, frictional, and kinetic, viscosity as the major component variables, and is expressed in Equations (2.26), (2.27), and (2.28), respectively.

$$\mu_{s,col} = \frac{4}{5}\alpha_s{}^2 P_s d_s go\ ss(1+e_{ss})\sqrt{\frac{\theta_s}{\pi}} \quad (2.26)$$

$$\mu_{s,}fr = \frac{P_s \sin(\theta)}{2\sqrt{I2D}} \quad (2.27)$$

$$\mu_{s,kin} = \frac{\alpha_s P_s d_s \sqrt{\theta_s \pi}}{6(3-e_{ss})\left[1+\frac{2}{3}\right](1+e_{ss})(3e_{ss}-1)\alpha_s\, g_{o\ ss}} \quad (2.28)$$

In a situation where there is multiple phases, the solid pressure with N number of phases can be presented as shown in Equation (2.29) and its radial distribution as in Equation (2.30).

$$p_l = \alpha_l \rho_l \theta_l + 2\sum_{l=1}^{N} \frac{d_{ls}^3}{d_l^3}(1+e_{ls}) g_{o\ ls}\alpha_l \alpha_s \rho_l \theta_l \quad (2.29)$$

$$g_{o,ss} = \left[1-\left(\frac{\alpha_s}{\alpha_{s,max}}\right)^{1/3}\right]^{-1} + \frac{1}{2} d_s \sum_{n=1}^{N} \frac{\alpha_n}{d_n} \quad (2.30)$$

The kinetic fluctuating energy when granular temperature for an nth solid phase is considered is given in Equation (2.31). Anil et al. [179] have applied the equations and approach to study the performance evaluation of fluidized bed biomass gasifier using CFD. The result obtained was very promising.

$$\frac{3}{2}\left[\frac{\partial}{\partial t}(\alpha_s \rho_s \theta_s) + \nabla.(\alpha_s \rho_s v_s \theta_s)\right] = (-\rho_s \bar{\bar{I}} + \bar{\bar{\tau}}_s) : \nabla v_s + \nabla.(k_{\theta s}) - \gamma_{\theta s} + \phi_{gs} \quad (2.31)$$

From Equation (2.31), the energy production by solid stress tensor is $(-\rho_s \bar{\bar{I}} + \bar{\bar{\tau}}_s) : \nabla v_s$, $k_{\theta s}$ is the

diffusion coefficient, $\gamma_{\theta s}$ is the collisional energy dissipation, and ϕ_{gs} is the energy exchange between the gas and particle.

The governing equation for the gas and solid phases transport are represented in Equations (2.32) and (2.33).

$$\frac{\partial(\alpha_g \rho_g x_g)}{\partial t} + \nabla.(\alpha_g \rho_g x_{g,i} \overrightarrow{V_g}) = -\nabla.(\alpha_g \rho_g D_{g,i} \nabla X_{g,i} \overrightarrow{V_g}) + S_{g,i} \quad (2.32)$$

$$\frac{\partial(\alpha_{sn} \rho_{sn} x_{sn,i})}{\partial t} + \nabla.(\alpha_{sn} \rho_{sn} x_{sn,i} \overrightarrow{V_{sn}}) = -\nabla.(\alpha_{sn} \rho_{sn} D_{sn,i} \nabla X_{sn,i} \overrightarrow{V_{sn}}) + S_{sn,i} \quad (2.33)$$

To account for the energy generation for the gas and solid phase, the energy equation is written as expressed in Equation (2.34) and Equation (2.35), respectively.

$$\frac{\partial(\alpha_g \rho_g h_g)}{\partial t} + \nabla.(\alpha_g \rho_g \overrightarrow{V_g} h_g) = -\nabla.\overrightarrow{q_g} + \Delta h_{rg} + \sum_{s=1}^{n} h_{sg} \quad (2.34)$$

$$\frac{\partial(\alpha_{sn} \rho_{sn} h_{sn})}{\partial t} + \nabla.(\alpha_{sn} \rho_{sn} h_{sn} \overrightarrow{V_{sn}}) = -\nabla.\overrightarrow{q_{sn}} + \Delta h_{rsn} + \sum_{s=1}^{n} h_{gs} \quad (2.35)$$

The application of CFD in gasification and co-gasification processes as reported by some authors can be found in Table 2.10. [180] investigated the effect of oxygen-enriched air during the gasification of coffee husks in a biomass gasification system. They applied a Eulerian-Eulerian approach of 2-D CFD model in the study. The CFD has the capacity for the enhancement of the structure of gasifiers, but the process modelling consumes a lot of time and has complex simulation process. The same tool was used by Gao et al. [181] to examine the performance characteristics of catalytic filters located inside biomass fluidized bed gasifier (e.g. BFB, CFB, and FBG). Reliable results were obtained, but extensive computation was involved. The model especially the 3-D type is quite efficient in predicting the biomass gasification characteristics. The operating parameters and geometrical requirements of the gasifier are easily estimated by the tool, and are easily realised compared to other models. The technique involved in the CFD tool allows for stage wise modeling including vaporization, de-volatilization, char reactivity or oxidation, etc., but Monteiro et al. [182] argued that a stage wise modelling approach using CFD model poses more problems in terms of result accuracy

than TEM and Kinetic models. For the identification of the optimal design at any scale, the model seems to be a cost-effective option. One of the drawbacks of the model is that enormous amount of time, lengthy and complex computations are required to achieve better results. The model also, is not promising for the simulation of large-scale fluidized bed systems that has millions of particles. A 2-D CFD model equally, lacks the capacity of describing the hydrodynamics of gasifiers efficiently due to the non-axisymmetric structure of the gasifier.

Table 2.10: Gasification and co-gasification Computational Fluid Dynamic (CFD) Model

Type of Model	Type of Gasifier	Type of biomass	Degree of Prediction	Reference
Computational Fluid Dynamics (CFD)	FBG	Coffee husks	Gas composition and temperature distribution in the gasifier	[180]
	FBG	-	Performance characteristics of catalytic filter, filtration velocity, temperature performance and degradation of tar compounds	[181]
	FBG	Coal	Temperature & velocity distribution in the gasifier and species concentration.	[182]

A 3-D CFD model has received some improvements that allow it to out-perform the 2-D CFD models. Estimation of the temperature and gas concentration by the energy and mass transfer equations of the particles and on the basis that each particle on the system is tracked, improves the accuracy of the model. However, the cold gas efficiency predicted via the CFD model most times disagrees with the experimental data. It could be related to the inability of the model collecting microscopic information from the gasifier. Importantly, different approaches of the CFD modelling were applied by the different authors highlighted in Table 2.10, the summary of the reports have shown that a CFD model is very efficient in estimating biomass gasification

processes, but regrettably, time and extensive calculation are very big setbacks. More investigation is needed to identify a corrective measure to address the gaps.

2.8. Artificial Neural Networks (ANN)

The ANN is a biological simulated computational science that attempts to imitate the operations of a human brain and the nervous system [190]. It is a representation of the best model of brain at a microscopic level. In terms of a broad concept, it is a complex system with large number of identical elements that responds to signal with respect to each other [191]. According to Puig-Arnavat et al. [51], an ANN has the ability to evaluate the linear and non-linear relations between the input and output variables. This is an essential characteristic of the model during the learning process, since it has the properties and fundamental learning techniques similar to the human brain [51]. ANNs had been applied in speech recognition, which is very difficult to resolve by mere rule- based programming. Besides, the system is very useful in artificial intelligence operations, image, and visual recognition issues. In overall, the package plays a major role in applications where predictive accuracy forms the principal focus. Puig-Arnavat et al. [51] reported the application of the tool in several sectors of research, including; signal processing, weather prediction, functions approximation and process simulation. Table 2.11 summarizes some of the works carried out by few researchers in this area

Table 2.11: Gasification and co-gasification Artificial Neural Networks (ANNs) Model

Type of Model	Type of Gasifier	Type of biomass	Degree of Prediction	Reference
Artificial Neural Networks (ANN)	MSW	-	LHV of syngas, LHV_P of the product gas, and the syngas yield.	[192]
	Updraft & FBG	-	Upgrading of ANN model efficiency	[193]
	FBG	-	Determination of the characteristics of gasification	[194]

			product, temperature distributions, and heat content in the gasification system.	
	FBG (Ash Agglomeration Fluidized Bed (AFB) system.	Coal + Biomass	Gas composition, gas yield, LHV of the syngas, and gasification temperature	[176]
	FBG	-	CO_2-Oil minimum miscibility pressure in pure and impure CO_2 streams, demand estimation of oil in Iran, CO_2-Oil molecular diffusion. High accuracy of predication was achieved from the point of view of the correlation	[195]

			coefficient of the lowest MSE & MAPE	
	FBG	MSW (Origin: Fars Province in Iran)	MSW generation rate and the evaluation of the ANN model performance. Higher accuracy prediction compared to MLR from the point of view of: MAE, MAPA, RMSE & correlation coefficient (R).	[196]
	FBG	Biomass residues	Prediction of Higher Heating Value (HHV). Model was very reliable.	[197]
	-	Rubber Seed Oil (RSO)	Optimal oil yield. Model very accurate compared to RSM and with	[198]

		respect to the Lower Relative Error and the Absolute Average Deviation (AAD)	
Fixed Bed: Downdraft	24 biomass samples	Gas composition and the concentration of the major gaseous content: CO, CO_2, CH_4 & H_2. Accurate prediction from the point of view of Absolute fraction of variance (R^2) result.	[199]
Prediction Reliability: Very reliable especially in the prediction of temperature and gas yield in the reactor if the hydrodynamics of the reactor is well known. Most importantly, the tool has the capacity of addressing issues relative to the reactor designs unlike the TEM, but it lacks non-equilibrium, non-mechanistic, and non-analytic behaviour, thus leading to its limitations in dynamic modelling.			

Typically, a Multiple Input and Multi Output (MIMO) variables or Multiple Input and Single Output variables (MISO) are used. Establishing the number of neurons and number of hidden layer are challenging task in operating the model, but Azadi & Karimi-Jashni [196], Azadi &

Sepaskhah [200], Puig-Arnavat et al. [51] has reported that trial and error technique could be used, but applied, but to determine the optimum layer and/or the hidden node in the network was uncertain. Trial and error method may subject the model result to poor accuracy. The training involves developing the ANN weight/bias term tuning process. Getting trapped in the local minima of the ANNs is a set-back, and should be avoided. This can be achieved by applying several independent runs. The output with the lowest training error is targeted,

and the Levenberg-Marquardt (LM) back-propagation algorithm [192] could be used [193] has applied the LM back-propagation algorithm to evaluate the upgrade of the model's efficiency, and a reliable result was obtained. A representation of the schematic diagram of single- and double-layer model are presented in Figure 2.12 and Figure 2.13, respectively.

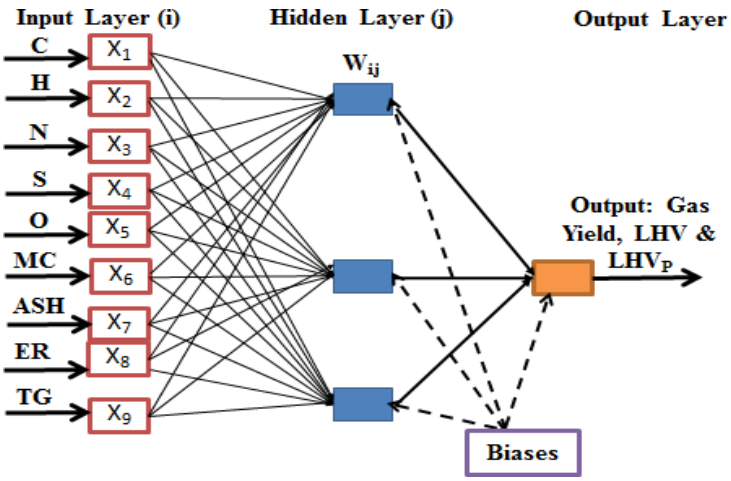


Figure 2. 12: Schematic diagram of the MIMO ANN Model; a single hidden layer [192]

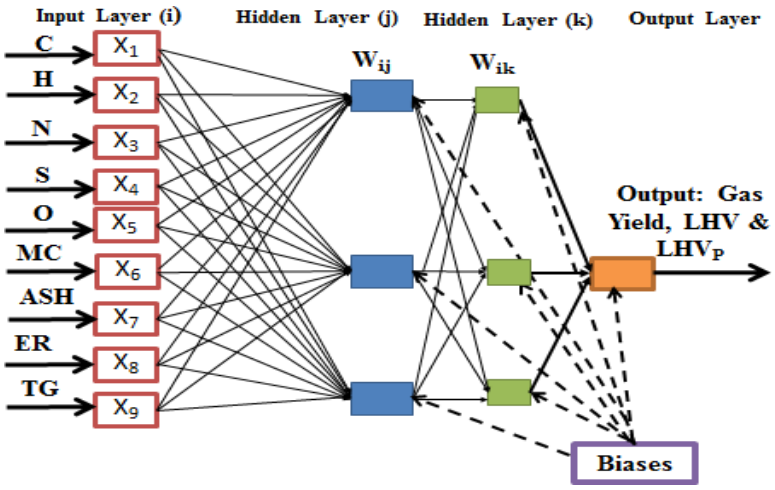


Figure 2. 13: Schematic diagram of the MIMO ANN Model; a double hidden layer [192]

Pandey et al. [192] have modeled the gasification of MSW in an FBG using ANN and applying the LM back-propagation algorithm method for training the MISO and MIMO models. The parameters studied were the heating value of gas (LHV), the heating value of gasification products (LHVp) and the syngas yield (gaseous product) using MSE and R^2 as the evaluation models. The results obtained were promising. When the optimum architecture is chosen in neural networks operation, the prediction accuracy of the model is improved, though the task consumes a lot of time, but achieving better result is desirable. The number of neuron can be selected by varying the number of hidden layers, transfer function and number of neurons in each of the hidden layer. Understanding the performance efficiency of ANNs is very essential because it paves way for the improvement of the tool. Statistical error models such as Mean-Absolute Error (MAE) and Root-Mean-Square Error (RMSE) can be used for the assessment.

The package requires huge amount of data to offer effective prediction, and acquiring such information may at times be a big problem. Determining the number of neuron and hidden layer to create the optimum layer and the model architecture are difficult and consumes a lot of time. Gasifiers that are quite different from the one used for its dataset training, may not perform effectively. The deficiency is attributed to the condition of the dataset, and not the modeling tool [51] The Back Propagation Neural Network (BPNN) relatively displays satisfying prediction results for different gasification processes, but local minima and over- fitting are the two remarkable problems associated with it [194]

The ANNs is used to solve problems instead of the human brain. Another important feature of the package is that it operates in situations outside the training process it encountered. The tool can solve problem without the use of existing solutions such as sequence of steps as obtained in computer algorithms [192], but it may suffer low prediction accuracy which can be attributed to poor data supply. It does not require the formulation of complex numerical equations like in TEM and CFD model to offer better results. The CFD, TEM, kinetic models may not demand large amount of data for accurate predictions compared to the ANNs.

Recently, Particle Swarm Optimisation (PSO) had been used together with BPNN as BPNN- PSO to enhance the performance of the neural network, and many researchers including; Ali et al. [176] and Sreejith et al. [194] and they made huge successes with the application. Genetic Algorithms (GA) and Adaptive Neuro-fuzzy Inference System was also tested by the aforementioned researchers and it demonstrated an efficient approach as predictive model. The BPNN-PSO has

the capacity of displaying high prediction accuracy and do not require extensive information regarding the process, but its efficiency is highly dependent on the quality and quantity of data-set available for the model [195-197], [199-201].

Presently, an evaluation of the performance of gasification systems efficiency (e.g. cold gas efficiency, Carbon conversion efficiency, syngas yield, LHV of gas, and gas composition using dataset obtained from different gasifiers (e.g. fixed bed and FBG), blends of coal/biomass, and tyre, and experimental process conditions is necessary. It is also important using the model to optimise the process variables for biomass gasification processes and biomass torrefaction, and ultimately, develop an alternative method of improving the model result. This is because torrefaction is expected to improve the quality of fuel for syngas production. Furthermore, ANN is yet to be employed in the prediction of emissions and profits in a co-gasification CHP plant using South African feedstocks (e.g. blends of coal and biomass/tyre). Extending biomass gasification research in these areas and finding a standard method of determining the number of neurons in the hidden layer will make the neural network more attractive than the other models. The major drawbacks about ANN as a modelling tool is that it is dependent on the dataset used for its training for effective prediction, and establishing the number of neuron to be used in the hidden layer consumes a lot of training time.

2.9. Concluding remarks

A review on co-gasification of coal and solid waste to hydrogen-enriched syngas in a bench scale fixed bed gasifier was carried out. It considered the feasibilities of some selected South African feedstock for energy production. The feedstocks are coal, tyre and biomass materials including sugarcane bagasse (SCB), corn cob (CC), and pine sawdust (PSD). A critical review on the techno-economic analysis of the aforementioned feedstocks and their blends were carried out. Thermo-chemical energy conversion process, biomass gasification reactions, and relevance of co-gasification of biomass and coal were reviewed. An assessment of gasification systems efficiency, tar treatment methods, gasification and co- gasification processes, and a comprehensive biomass and coal gasification process models were reviewed. From this chapter, the following conclusions were drawn:

- Solid waste materials (e.g. sugarcane bagasse, corn cob, pine saw dust & tyre) that can be co-gasified with coal to produce syngas are in abundant in South Africa. Using the waste materials will reduce the cost of feedstock for energy production and enhance energy sustainability.

- Emissions arising from the use of coal for electricity generation in South Africa are very high, but it could be reduced via co-gasification of coal and solid waste.
- Tar formation during gasification process could be minimized using thermal and catalytic cracking methods, but effective tar treatment model is required for it to be achieved.
- Models describing the evaluation of gasification systems efficiency for biomass, coal, and their blends are necessary and should be pursued through this study.
- Production of high-quality syngas that can be used in gas turbines, engines, and fuel cells is necessary, but needed efficient gasifier and experimental process conditions for it to be realised. Thus, the identified gaps in the review formed the basis of the objectives of this study.

Chapter 3: Research Procedure and Methodology

3. Introduction

This chapter reports on the different methods used to achieve different tasks carried out in this study. A schematic representation of the methodology is depicted in Figure 3.1. It is grouped into eleven (11) major activities with activities 4, 8, 9, & 10 representing the specific research objectives. Typically, Figure 3.1 shows an overview of the tasks/research methodology, but a detailed description of the method(s) used in each of the activity is explained in the appropriate sections of this chapter.

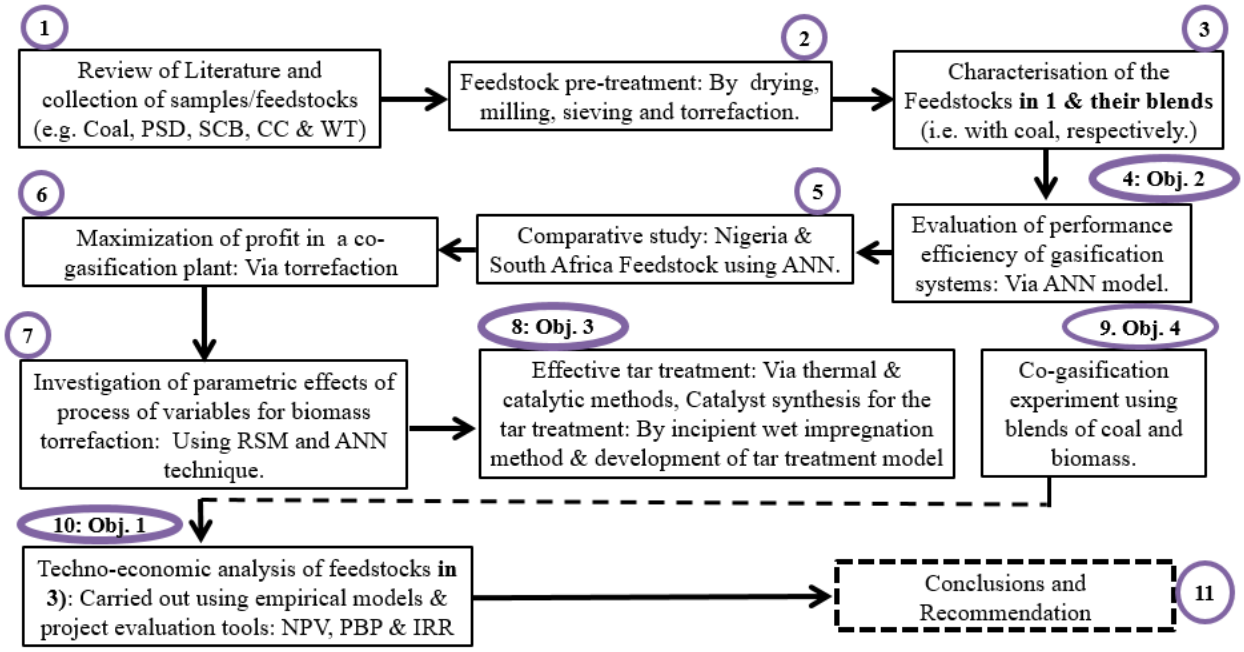


Figure 3. 1: Overview of the research methodology

3.1. Feedstock collection & pre-treatment

In this study, biomass, coal, and waste tyre (WT) were the feedstocks investigated. The biomass materials are comprised of corn cob (CC), sugarcane bagasse (SCB), and pine sawdust (PSD). The PSD were obtained from the Pine tree at the premises of University of the Witwatersrand, while the CC and SCB were collected from Hill-brow market Berea, Johannesburg. The coal sample was obtained from Matla mine, while the WT was collected from a waste tyre recycling plant in Johannesburg, South Africa. Furthermore, The Nigerian coal that was studied alongside South African feedstocks in chapter 8 was obtained from Onyeama mine, in Enugu state, while the biomass and WT were collected at Enugu-Ogbete Main market and mechanic village 9th mile corner Ngwo, respectively. The feedstock pre-treatment process followed the procedure described in the next section and elsewhere [13].

The pre-treatment given to the feedstock includes; drying, milling, sieving, and torrefaction. The feedstocks were dried in the sun (i.e. biomass), milled, and sieved to the required particle sizes, prior to subjecting it (biomass materials) to torrefaction. The essence of drying, particle size reduction and sieving were to ensure an effective heat and mass transfer during the compositional analysis of the fuel and co-gasification test, while biomass torrefaction was performed to upgrade the quality.

The biomass materials were size reduced from 6.0 – 10.0 mm to 0.5 – 2.0 mm using Retsch biomass cutting machine (SM 200 Rostire). Similarly, the coal (from Matla mine) was milled to 0.2 – 2.0 mm employing the milling machine located at the coal analysis Lab of the Richard Ward Building at the University of the Witwatersrand, Johannesburg, South Africa. The waste tyre with original size of around 4.0 – 6.0 mm was shredded to 0.5 – 3.0 mm, and the re-enforced materials removed. The milling and sieving machines used in the study are shown in Figure 3.2, while the pre-treated feedstocks were presented in Figure 3.3.



a b

Figure 3. 2: Photo image of the size reduction & sieving equipment: (a) Biomass cutting machine (b) Milling machine.

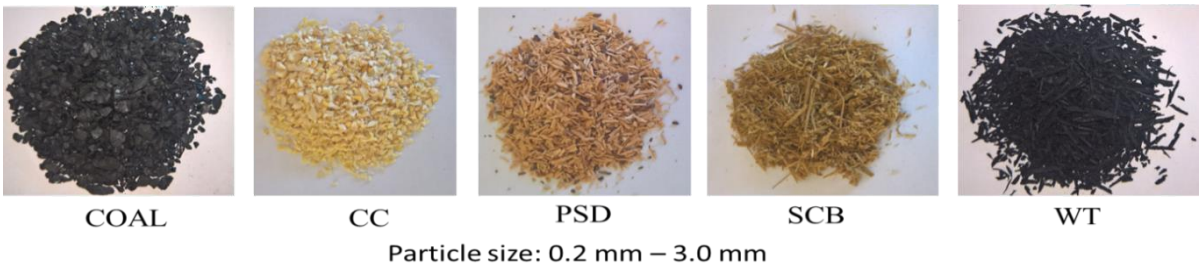


Figure 3. 3: Photo image of the Pre-treated (dried, milled & sieved) feedstocks:

Thereafter, they were blended (torrefied biomass samples) with coal (for example at a coal- to-solid waste ratio of 50:50) as shown in Figure 3.4.

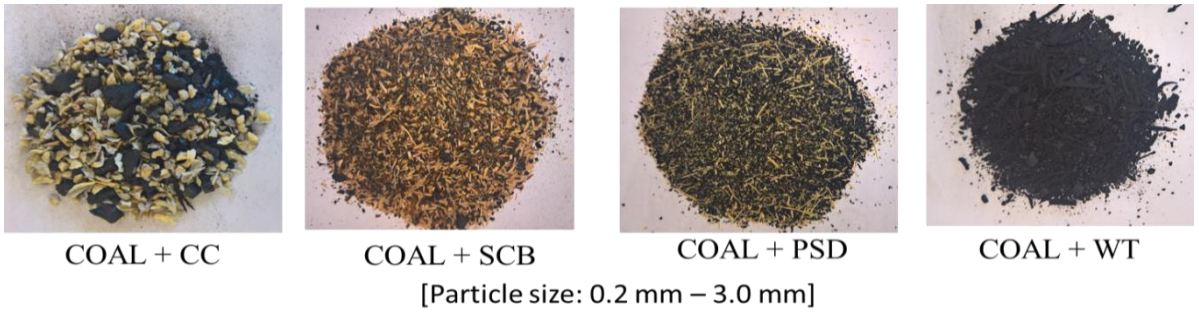


Figure 3. 4: Photo image of blends of coal and solid waste (raw feedstock): Ratio: 50:50

The biomass materials pre-treated by drying, grinding, and sieving, were subjected to torrefaction.

3.2. Biomass torrefaction: Experimental

The biomass materials (SCB, CC, and PSD) and waste tyre (WT) pre-treated as described in section 3.1 were torrefied using a quartz tubular reactor. In this study, three torrefaction temperature regimes including light (200 ^{O}C) mild (250 ^{O}C), and severe (300 ^{O}C), and torrefaction times of 30, 45, and 60 min time, and Coal-to-biomass, and WT blending ratios of 50:50, 71:29, and 80:20 under nitrogen atmosphere with flow rate of 350 mL^{-1} were used to carry out the process, respectively. The torrefaction process was carried out using the results obtained from the Design of experiment (DoE) under Box Behnken Design (BBD) method. The weights of the samples before and after torrefaction were measured and the mass loss was determined. The determination of the mass loss was necessary because the value plays a critical role for the estimation of the mass percentage yield. At the end of each of the experimental run involving different fuel sample, nitrogen and air were used to flush the reactor to prevent contamination. Thereafter, the temperature of the reactor was raised to around 650 ^{o}C to ensure that the residual tars retained in the reactor were burnt and flushed out of the reactor completely. The torrefied fuels were labeled, secured in air tight plastic containers, and later, blended with raw coal using the blend ratios earlier mentioned. The overall process (torrefaction) was aimed to achieving fuel materials with improved physio-chemical quality and the photo image of the torrefied samples are shown in Figure 3.5.

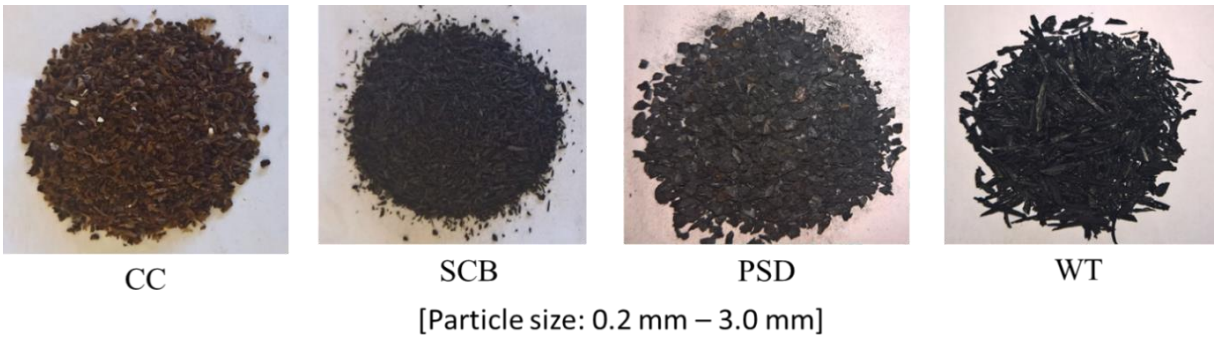


Figure 3. 5: Photo image of the torrefied biomass materials and waste tyre

Generally, the pre-treatment process was carried out to ensure that the physio-chemical qualities of the fuel were enhanced, while the characterisation process was performed to confirm those qualities. The schematic diagram of biomass undergoing torrefaction and expressions describing the torrefaction variables considered in this study are shown in chapter 4. An optimisation of the process variables of the torrefaction of the fuel samples was carried out, and extensively discussed to provide important information to enhance profitability and torrefaction plant development. The essence of drying, particle size reduction and sieving were to ensure an effective heat and mass transfer during the co-gasification test, while biomass torrefaction was performed to upgrade the quality.

3.3. Characterisation of the feedstocks

In this study, different characterisation techniques were employed. It includes: CHNS-O Analysers, Brunauer–Emmett–Teller (BET), temperature programmed reduction (TPR), transmission electron microscope (TEM), and X- ray diffraction (XRD). There analytical techniques using the different samples are described in the following sections.

3.3.1. CHNS-O Analysers

The organic elemental analysis (Ultimate analysis) was carried out using the CHNS-O Organic Elemental Analyzers (FLASH 2000). All the fuel samples (e.g. raw biomass, coal, tyre, blends of raw coal and biomass, blends of coal and torrefied biomass, and biochar displayed in Figures 1, 2 & 3 were analysed with the instrument. The elemental micro- analysis was used to determine the presence of carbon (C), hydrogen (H), nitrogen (N), Sulphur (S) and oxygen (O); by calculation in the fuel materials. It involved weighing in micro-balance around 0.5 mg of the solid sample and combusting it in the CHNS-O Analyser. Upon combustion, uniform

compound gases of the aforementioned elements were produced. A gas chromatography (GC) was used to measure the combustion products (e.g. CO_2, H_2O, NO_2, etc.). In this case, C, H, N, & were simultaneously measured, but O was determined by subtracting the percentage weights of C, H, N, S from 100 %. Secondly, the proximate analysis followed the standard procedure of the American Society for Testing and Materials (ASTM E870-82), while the heating value was measured using a bomb calorimeter (203M 1241). The limitations of the oxygen bomb calorimeter is that it takes only one sample at a time, hence making the test to be time in-effective. The analytic instruments used for the measurement of the heating value & proximate analysis) are displayed in Figures 3.6, and the results obtained from them, were used for different estimations carried out in different chapters of this study.



a b

Figure 3. 6: (a) Oxygen bomb calorimeter (b) Thermo-gravimetric Analyzer (TGA)

In this chapter, some of the characterisation results were reported, while others were presented in different sections of other chapters of this thesis (e.g. techno-economic analysis (chapter four), evaluation of gasification systems efficiency (chapter five), profit maximization assessment (chapter six), profits and emissions prediction analysis (chapter seven), tar treatment technique and model development (chapter eight), etc. Secondly, analytic techniques such as X-ray diffraction (XRD), and Brunauer–Emmett–Teller (BET) of the feedstocks (raw & torrefied) and catalysts were conducted. Furthermore, the temperature programmed reduction (TPR) of the synthesised catalysts was equally carried out, but the results were reported in chapter 9.

3.3.2. X-ray diffraction (XRD) analysis

The Powder XRD is used to determine the crystal phases of solid particles, and in this study, it was employed to identify the crystallinity of the fuel samples and catalysts used for the energy production and tar treatment, respectively. The samples (catalyst & fuels) were run 2u within the range of 5 – 708 with step size of 0.18 and time step of 1.0 s to evaluate the crystallinity of the fuel and catalyst loading. Finally, the XRD phases contained in both the catalyst and fuel samples were identified via JCPDS powder data files. The results obtained are discussed in chapter 9 of this thesis.

3.3.3. Brunauer–Emmett–Teller (BET) analysis

The BET analytic equipment was used to determine the structure (e.g. surface area, pore-size, and pore-volume) of different solid samples (Ni-biochar & biochar-based catalysts). The experiment involved the adsorption of nitrogen at $179^{O}C$ using Micromeretics Gemini surface area instrument. Firstly, around 0.05 – 0.1 g of the sample (e.g Ni-PSD-BC) was degassed at 150 ^{O}C for about 2 h using helium as the carrier gas. In this case, the adsorption isotherm of nitrogen was collected at 197 ^{O} C under relative pressure range of 0.05 – 0.99. The specific surface area, pore volume, and pore size of the solid sample was determined. The same procedure was used for the Ni-SCB & Ni-CC-BC, and the biochar-based catalyst samples, respectively. The results generated from this equipment can be found in the results and discussion section of chapter 9 of this thesis.

3.3.4. Temperature programmed reduction (TPR) analysis

A Micromeretics Autochem II 2920 V4.01 was used for the H_2-TPR analysis. Typically, around 50 mg of the sample (e.g. Ni-PSD-BC, Ni-SCB-BC, Ni-CC-BC catalysts) were analysed. It involved a step-wise increase in temperature from 50 – 900 ^{O}C. A mixture of H_2 and Ar flowing at a rate of 50 ml min^{-1} were used as the reducing gas (about 10 vol. % H_2 in Ar), to reduce the catalyst with a steady temperature ramp. Thereafter, the system's temperature was maintained at 900 ^{O}C until a signal indicating that hydrogen consumption has returned to its initial values. In this case, the amount of H_2 consumed by the catalyst (mmol g^{-1}) was allocated a temperature range that was estimated via integration of the corresponding thermal conductivity detector (TCD) signal intensities. See Chapter 9 of this thesis for the results generated using this equipment.

3.3.5. Transmission Electron Microscopy (TEM)

Transmission electron microscopy coupled to energy dispersive X-ray Spectroscopy (EDS) were carried on FEI Tecnai T12 Spirit TEM that was attached with an Oxford X-ray detector which was operated at an accelerating voltage of 120 KV. The preparation of the samples was performed by dispersing of the powder materials in methanol that served as a solvent. The sample was ultrasonified for about 10 minutes. Thereafter, the processed sample was loaded in a carbon coated copper where it was then analysed by the microscope.

3.4. Prediction of performance of gasification systems efficiency using ANN model

In this study Artificial Neural Network (ANN) was used for the evaluation of performance of gasification systems efficiency. Levenberg Marquardt (L-M) and Bayesian Regularisation (BR) algorithms were used. 315 fuel samples used in this study included biomass, coal, and blends of biomass and coal. Information about their proximate, ultimate, process condition data, and performance indicators were obtained from the literature. The proximate analysis data used were ash, moisture content (MC), and volatile matter (VM), while the ultimate analysis data includes Carbon (C), hydrogen (H), nitrogen (N), oxygen (O), and Sulphur (S), and LHV_{Fuel}. The experimental variables considered in this study were equivalence ratio (ER) and reaction temperature (T). The gasification performance efficiency parameters were cold gas efficiency (CGE), carbon conversion efficiency (CCE), gas yield, lower heating value (LHV) of gas, and gas composition (e.g. CO, CO_2, CH_4, H_2). The dataset was grouped into input and output variables as shown in chapter 5. It was then saved in an excel document for use in the training of the models. For the Bayesian regularization (BR) training algorithm, a MIMO layer networks were employed. The use of the techniques needs a lot of training time, but it is efficient for generalization of difficult and noisy data-sets. In this case, 11 input variables comprising C, H, N, S, O, ash, MC, VM, T, ER, and $LHV_{biomass}$; and 8 output variables comprising gas composition (CO CO_2, H_2, CH_4), gas yield, LHV of gas, CGE, and CCE were used.

The 315 input-output patterns used for the study were divided into three namely: 70 % (221 datasets) for training; 15 % (47 datasets) for validation; 15 % (47 dataset) for testing the model. Further, the input datasets were randomised for each of the iterations, while simulations were carried out by varying the number of neurons in the hidden layer using tansigmoid transfer function. Similar approach was used for the Levenberg-Marquardt (LM) back-propagation algorithm. The networks were evaluated based on the Mean Square Error (MSE) and coefficient of determination (R^2) obtained, and the architecture with the lowest MSE and

highest R^2 were considered as the best candidate model. However, some information on the theories, equations, and working principles of the network are described in chapter 4 & chapter 5 of this thesis, respectively.

3.5. Emissions prediction and profits assessment of co-gasification of biomass, tyre, and coal fired in CHP plant using Artificial Neural Network: a comparative study of Nigeria and South Africa.

Coal, biomass (e.g. Sugarcane bagasse (SCB), Corn cob (CC), Pine sawdust (PSD)) and Waste-tyre (WT) were the feedstocks used in the study. The collection sites for all the South African fuel samples and pre-treatment methods have been described in the earlier section. The Nigerian coal was obtained from Onyeama mine, in Enugu state, while the biomass and WT were collected at Enugu-Ogbete Main market and mechanic village at 9th mile corner Ngwo, respectively. The feedstock pre-treatment process followed the procedure described earlier in this chapter and elsewhere [13].

The annual feedstock and feed-rate needed to operate the 10 MW electric power plant were determined from an empirical equation employing the aforementioned feedstocks using coal-to-solid waste ratios of 1:1, 3:2, and 4:1, respectively. Further estimations such as those carried out using the project management and evaluation tool (e.g. NPV) were conducted using different model equations described comprehensively in chapter 8. The overall equations were used to determine the profitability of the feedstocks for power generation relative to their economic (profits) and environmental (emissions) viabilities.

3.5.1. ANN model training

In this study, Levenberg-Marquardt (L-M) algorithm with Multiple Input-Single Output (MISO) layer networks were employed to model the profits and emissions from the Nigerian and South African feedstocks for a period of 20 years, respectively. The model was developed from the twenty calculated datasets for South African and Nigerian feedstocks in a MATLAB environment using the neural network toolbox (*nn*tool), and 80 %, 10%, and 10 % of the dataset were employed for the training, validation and testing. The ranges of the input and output variables used for the evaluation (emissions and profits), as well as the architectural design of the networks used for the training were shown in chapter 8, respectively. It is crucial to point out that the learning programme carried out using the network explained in this section and applied in Chapter 5, involved a MISO layer network, but in chapter 4 and Chapter 7, a MIMO and MISO layer networks were studied.

3.6. Maximization of Profit in a co-gasification CHP plant via biomass torrefaction

Based on the understanding gained from studying the techno-economic analysis of the feedstock and performance efficiency of the gasification system. From the results obtained from biomass torrefaction, it was evidenced that the use of torrefied biomass could be attractive to maximizing profit in the energy plant.

In this study, corn cob (CC), sugar cane bagasse (SCB), and pine saw dust (PSD) were torrefied and blended with coal using coal-to-biomass ratios of 50:50, 71:29, & 80:20. The results of the physio-chemical properties and biomass pre-treatment were reported in details in chapter three. The heating value (LHV) and moisture content (MC) of the fuels were used to estimate the feed-rate and annual feedstock requirement of the plant. An estimation of the earned profit from a typical CHP plant for a 20-year-investment period divided into four terms: A, B, C, & D was carried out using the Net Present Value (NPV) and Payback Period (PBP) models as described in section 2.2. The operating cost models considered were with feedstock costing (WFC) and without feedstock costing (WOFC). The details of the analysis can be found in chapter 6.

3.7. Investigation of Effect of process variables of biomass torrefaction using Response Surface Methodology (RSM) and Artificial Neural Network (ANN) technique

The process variables of biomass torrefaction were studied using RSM and ANN models, respectively. The RSM Box-Behnken Design (BBD) method and ANN Levenberg-Marquardt (L-M) algorithm for Multiple Input- Single Output (MISO) & Multiple Input-Multiple Output (MIMO) layer networks were studied. It should be recalled that the procedure used for the biomass torrefaction has been explained earlier in section 3.2.1 (Experimental procedure of biomass torrefaction) of this chapter. It is crucial to mention that the results obtained from the feedstock characterizations (proximate & ultimate analysis) were used to determine the enhancement factor (EF) and solid yield (SY) & higher heating value (HHV) of each of the feedstocks studied. The EF, SY, & HHV were the response variables studied, and the results were used alongside the RSM and ANN model results for the overall optimization study. The information containing the Design of Experiment (DoE) used, theoretical background of the RSM & ANN, and calculations carried out are detailed in Chapter 7 of this thesis.

3.8. Development of effective tar treatment technique for production of high quality syngas from blends of coal and biomass

For effective tar treatment technique, five stages of process were involved. Five stages are involved in the development of an effective tar treatment process and they include bio- char production, catalyst synthesis, tar generation and treatment, model development, and tar analysis. In this study, three categories of biomass were used to produce biochar used as catalyst, and catalyst support. The biomasses are woody and herbaceous biomass materials represented by pine sawdust (PSD) and sugarcane bagasse & corn cob (CC), respectively. Both feedstock was chosen based on their availability. For the biochar production, 100 g of PSD, SCB, and CC were measured using a weighing balance, and fed into a quartz tubular reactor using a rectangular ceramic plate, respectively. The process was carried out under nitrogen atmosphere at a flow rate of 350 m/L and reactor temperature of around 500 ^{O}C at a heating rate of 5^{O}C/min. After every experimental run with each of the biomass material, the temperature of the reactor was increased to around 700 ^{O}C to burn-out the residual components of the biomass, while nitrogen and air were used to flush the reactor to prevent contamination. The reactor was allowed to cool, after which, the synthesized biochar was packaged in an air-tight plastic container and stored for compositional analysis and other uses (e.g. as catalyst and catalyst support).

The biochar materials is prepared as described in section 3.9.2 were used as catalysts as well as catalyst support in nickel-biochar catalyst synthesis. The synthesis process involves dissolution of about 15 g of Ni nitrate in a 100 ml of de-ionised water and loading the solution into around 10 g of biochar via incipient wet impregnation method. For the ageing process (i.e allowing the extraction of the precurrsors from the feedstock to form a slurry), the solution was transferred into a 200 ml wide-neck glass reactor containing a magnetic rod and stirrer. The reactor was placed in a hot-plate operated at 250 rpm at 40 ^{O}C for 4h. Thereafter, the solution was poured into a glass container with cover and kept till the next day. After the ageing process, it was dried in an oven at 105 ^{O}C for 12 h following calcination in an air-flow electric furnace at 900 ^{O}C for 1 hr. The same procedure of synthesis was adopted for the three different biochar materials in synthesising the Nickel-biochar based catalysts. The catalysts were thus; denoted as Ni-PSD-BC-C, Ni-SCB-BC-C, and Ni-CC-BC- C, respectively.

Essentially, nickel catalyst may lose its activity because of sintering therefore, it is important to load it with other support material which prevent this occurrence, and as well, ensure product gas enhancement [180]. The tars used in this study were obtained from blends of coal and

biomass materials (Coal + CC, Coal + SCB, & Coal + PSD and raw CC, SCB, & PSD. The last three are biomass tars. The experimental design result was employed for the production of tars and their catalytic conversion experiments. For experimental control, biomass tars (CC, SCB, & PSD) were equally treated with the optimum catalyst, but only to compare the compounds present on them, with that of coal blends (i.e. Coal + CC, Coal + SCB, & Coal + PSD). The tar experimental setup for the tar treatment is presented in chapter 9, while the procedure followed is described in this section.

For the tar production, the precursor (blend of Coal and biomass) and biomass materials (without coal blend: as control) were pyrolysed in reactor A, respectively. Reactor A was pre-heated to temperature of around 450 – 500 ^{O}C using an electric tubular furnace prior to introducing the fuel into it. The volatile materials and gases produced in the unit (reactor A) flows through reactor B that is connected to the product gas line. It is necessary to state that during the process of producing the tar, no catalyst was introduced in reactor B. However, the gases produced flowed into the gas line to the gaseous product exit line that was connected to two condensate bottles containing ethanol, and both bottles were immersed in an ice-water bath. This cooling unit facilitates the condensation of tar that were mixed with aerosols (e.g. dust, fine liquid and solid particle), while the ethanol dissolved the condensing tar, hence; making its collection easier. The tar produced was then separated from other liquids and impurities by decantation and drying in an oven at 60 ^{O}C for about 40 min. It was labelled and kept in tar vial for further analysis as depicted in Figure 8.20 as can be seen later in Chapter 8, while the gases generated leave the system via the product gas exit. Coal + PSD, Coal + SCB, & Coal + CC and PSD, SCB, & CC were used in the process, and the tars generated are referred to as CPSD-T, CSCB-T, & CCC-T, and PSD-T, SCB-T, & CC-T, respectively.

3.8.1. Effect of tar treatment conditions on tar yield

For the tar treatment process, the Box Behnken Design (BBD) method was employed to design the experiment. The design comprised 3 input variables (tar cracking temperature (TCT), tar conversion time (TCVT), and Coal/Biomass blend ratio, and 1 input variable (Percentage tar conversion (PTC). The tar cracking temperature and tar conversion time considered were in the range of 700 – 900 ^{O}C and 10 – 20 minutes respectively, and the coal- to-biomass blend ratio was 1 - 4. Six different tar samples (CPSD-T, CSCB-T, & CCC-T and CC-T, SCB-T, PSD-T) and six different catalysts; Ni-PSD-BC-C, Ni-SCB-BC-C, Ni-CC- BC-C and PSD-BC, SCB-BC, CC-BC) were studied. In this case, Coal + PSD, Coal + SCB, and Coal + CC

and CC, SCB, & PSD initially introduced and used in reactor A for tar generation, were replaced with CPSD-T, CSCB-T, and CCC-T, to carry out the tar treatment, respectively. Each of the tar fed in reactor A was decomposed by heat, and the gases produced passed into reactor B which has a catalyst bed (for tar cracking) supported with a silicon wool filter for trapping the particulates. From reactor B, gases flow through the adjoining gas line into the condensate bottles and finally to the product gas exit. The cracked tar was mixed with other liquid aerosols in the bottles, but it was separated from the liquids via decantation, dried in an ovum at 60 ^{O}C for 40 min, measured, and labelled in tar vial for further analysis, while the gases generated leave the system via the product gas exit. Subsequent experimental runs were performed using different tars and catalysts based on the Design of experiment (DoE) results. At the end of each experimental run, N_2 and air were used to flush the reactors to ensure no contamination of products from the previous tests.

3.8.2. Tar treatment and analysis

Proper treatment of tar during gasification/co-gasification process will enhance the production of high-quality syngas. To achieve this will require the understanding of the different compounds present in a sample of tar. The quality of gas generated will determine the type of energy conversion system (e.g. fuel cells, gas engines, turbines, etc.) it could be fed as fuel to produce electricity.

The tar collected was analysed using a pre-calibrated GC-MS/FID equipped with flame ionization detector (FID). The column has length, thickness, and diameter of 30 m, 0.25 μm, and 0.25 mm respectively. The sample was extracted with 2-propanol (Iso-propanol); solvent. The analytic equipment (GC) was configured and coupled with the MS and FID and were positioned in parallel to each other to enhance simultaneous qualitative and quantitative analysis. Details of modern GC practices and principles as well as applications of MS can be found elsewhere [202,203], while Mclafferty & Turecek [204], described the methods of interpreting the mass spectra. The analysis involves elusion and splitting into two of the sample from the GC into the MS and FID, respectively.

To ensure the resolution of the peaks, the GC oven temperature was programmed to accommodate the condensed tar sample. Secondly, to ensure that the majority of the injected solvent passed through the system prior to turning on the filament, a configuration accounting for the solvent delay/filament start delay was made. Solvent delay promotes the life of the filament by preventing rapid cooling from the solvent; else rapid degradation of the filament

could occur [205,206]. It is usually set (solvent delay) from the beginning of the analysis till the completion of the solvent peak. To identify the compounds in the sample, compound identification method via match number was applied with the match factor set at 80 %. A description of the compound identification process can be found in reports of Stein et al. [207] and Ausloos et al. [208], respectively. The operating process conditions used for the analysis and the photo images of the tars used for the study are shown in Chapter 8, respectively.

3.9. Co-gasification of coal and biomass to hydrogen enriched syngas in a fixed bed gasifier

Coal and Pine sawdust (Coal + PSD) were the feedstock used for the gasification test. Details of their origin, pre-treatment, and characterisations were reported earlier in this chapter (in the feedstock characterisation section). From the techno-economic analysis of the feedstock that was reported in chapter 10, coal-to-biomass ratio of 1:1 was established as the most viable blend ratio, hence; is used in this chapter for the gasification experiment. A schematic of the experimental setup used in this study for the co-gasification test is presented in chapter 10, while the experimental procedure used is described in this section. The gasification experiment was carried out with catalyst (WICAT) and without catalyst (WOCAT) to determine the effect of catalyst on the gasification products and system efficiency. About 20 g of blend of coal and pine sawdust (Coal + PSD) was loaded in a stainless-steel sheet basket, and fed into the reactor that was heated to a temperature of 700, 800, and 900 ^{O}C, respectively. The temperature of the reactor was allowed for around 12 min to stabilize, before the fuel was introduced. Air and steam were used as the gasification agents, and both were introduced at the flowrates of 200 ml min^{-1} and 0.2 g min^{-1}, respectively. Volatiles of tar and gases were released at the temperatures, and they passed through the gas line via the condenser where tar and other liquids droplets and impurities (oil, water & particulates) were condensed in an ice-water bath and then collected using the condensate bottles. The flow rate of the product gases was measured using a gas flow meter while the produced gases were collected at the gas collection port located along the gas sampling/exit line using gas-syringe (contained in the appendix). The product gas was sent to the GC for compositional analysis.

Thereafter, the reactor was cleaned by flushing it with N_2 and air to prevent contamination of the next experiment. Subsequently, other co-gasification runs were carried out using the same feedstock, but mixed with 2 g of PSD-BC and Ni-PSD-BC catalysts (10 % of Coal + PSD) respectively, and employing the same experimental procedure. In this case, the test was carried out with catalyst (WCAT), while the previous tests were conducted without catalyst

(WOCAT). To ensure an effective catalyst activity, the steel basket containing blend of the feedstock and catalyst was introduced into the reactor when the gasification temperature (900 ^{O}C) was stabilized. Co-gasification occurred at this temperature and residence time of around 15 - 20 minutes was used for the conversion process. The condensates and product gases were collected as earlier explained. Furthermore, the residual char contained in the basket after the co-gasification process was collected, measured and packaged for analysis. Finally, the co-gasification performance efficiency indicators were estimated employing the results obtained from the gas analysis.

The results of feedstock characterisation used for the co-gasification test includes; proximate and ultimate analysis results as well as the calorific values. The lower heating value (LHV) was calculated from the higher heating value (HHV) that was determined experimentally using an oxygen bomb calorimeter. The characterisation equipment and methods used were explained in the feedstock characterisation section of this chapter. The characterisation results were presented and used in the result and discussion sections of the appropriate chapters of this thesis.

3.10. Economic assessment of the feedstocks used in the study for energy production

The techno-economic analysis of the feedstocks (coal, Coal + PSD, Coal + SCB, Coal + CC) used for the energy production were carried out. It was based on the energy, economic and environmental parameters of the feedstock for energy generation using a CHP plant as a reference case. Some empirical model equations and project evaluation tools such as the lower heating value (LHV), net present value (NPV), payback period (PBP), and internal rate of return (IRR) were employed, and the details of the model equations, calculations, and analysis carried out are shown in chapter 10 of this thesis.

3.11. Concluding remarks

In this Chapter, procedures employed in this study: collection and pre-treatment of samples; characterisation of feedstocks; predicting of performance efficiency of gasification systems; estimation of profit in a co-gasification CHP plant; comparative study of emission and profit prediction from co-gasification of biomass, tyre, and coal fired CHP plant using Artificial Neural Network in Nigeria and South Africa; Maximization of profit in a co-gasification CHP plant through biomass torrefaction; evaluation of process variables during biomass

torrefaction; development of an effective tar treatment method; co-gasification of coal and solid waste (pine sawdust (PSD) to hydrogen enriched syngas in a fixed bed gasifier (FBG); and techno-economic analysis of selected South African feedstock for energy production in a co- gasification CHP plant are detailed.

Chapter 4: Evaluation of performance efficiency of gasification systems using Artificial Neural Network

4. Introduction

Understanding the performance efficiency of gasification systems is critical in energy conversion process. This chapter therefore examined and discussed comprehensively, the performance efficiency of the gasifier using different indicators such as carbon conversion efficiency (CCE), cold gas efficiency (CGE), gas yield, product gas composition (CH_4, CO, CO, & H_2) and lower heating value (LHV) of gas. Importantly, a part of the information contained in this chapter has been communicated to the global scientific and industrial community via peer-reviewed journal article publication [13] in Renewable Energy Journal. Another paper from this chapter was also published in Chemical Data Collection (see the details in the list of publications (item number 8).

The efficiency of gasification systems is driven majorly, by two critical factors which include the fuel quality and experimental operating conditions. The efficiency varies relative to the fuel quality and operating conditions employed. Typically, solid fuels such as coal, biomass, waste tyre, and others are used in the gasifier to generate product gases used as fuel in different energy conversion devices to produce electricity or liquid fuels. Presently, concerns about energy security and environmental apprehensions have compelled stakeholders and policymakers in the energy sector to consider renewable and sustainable energy options to meet the increasing energy demands of the world. On the environmental regulations point of view and fuel cost savings, biomass and coal can be co-gasified, and the efficiency of the gasifier also maintained, but it requires several experiments to establish the process conditions for better efficiency. To achieve this, a lot of time and money are required.

Alternatively, developing a model that has the capacity of predicting the efficiency parameters irrespective of the type of gasifier, solid fuel, and process condition could be instrumental to reducing costs and saving time. Secondly, a dependable model could equally ensure effective process control and optimisation of the experimental process. Some examples of the modelling tools that can be used to estimate the efficiency of the gasifier include the artificial neural network (ANN), genetic programming [192] and others. The ANN model has the ability of offering high prediction accuracy [192]. It has been used to study some of the processes occurring in the gasification system and prediction of the lower heating value (LHV) of fuels used in the gasifier [209,210]. In view of understanding the performance of a gasifier, several researchers have carried out studies to this effect. Tiwary et al. [211] investigated the performance efficiency of a co-gasification fluidised bed gasifier (FBG) using blends of biomass and coal as fuel, employing

ANN, genetic programming (GA), and support vector regression (SVR) models. The authors used eleven (11) input variables including the gasification temperature, air/fuel ratio, steam/fuel ratio, C, H, O, reaction rate constant, biomass feed rate, coal feed rate, FC, VM, ash, and total gas yield, CCE, CGE, and LHV of gas as the output variables. The findings reported by the authors were comparable with other results reported in the literature in terms of the effectiveness of the models in predicting the gasification performance parameters. However, the experimental dataset used by the authors was obtained from only one type of gasifier operated at the same process conditions (e.g. gasifying agent)

Similarly, Pandey et al. [192] used a Multiple Input-Multiple Output (MIMO) and Multiple Input-Single Output (MISO) ANN layer networks to predict the syngas yield, LHV of gas, and LHV of the gasification products (char and tar) from municipal solid waste in a fluidised bed gasifier (FBG). Additionally, [6] employed MIMO layer network to evaluate product gas composition (CO, CO_2, CH_4, & H_2) in a bubbling fluidised bed (BFB) gasifier. It is noteworthy to state that the works of George et al. [212] & Pandey et al. [192] are very attractive based on the reliability of the models to evaluate performance of the gasifier, but the studies considered a type of gasifier and few experimental conditions. In a study carried out by Baruah et al. [213] to predict the concentrations of the four major product gas compositions from gasification process, the proximate analysis results and experimental process conditions data were the input parameters used in the ANN model. The model result agreed with experimental data, but the data employed in the study comprised only those obtained from biomass and a type of gasifier as inputs and without data from blends of biomass and coal.

In the same vein, the efficiency of the two main fluidised bed gasifiers (bubbling fluidised bed (BFB) and circulating fluidised bed (CFB) gasifiers were evaluated by Puig-Arnavat et al. [51] employing the proximate analysis and operating condition data from biomass gasification as the inputs in an ANN model. With the input variables, Puig-Arnavat and co- workers was able to predict the producer gas composition and gas yield. The results obtained have high agreement with published experimental data, but the study was dwelled on only the MIMO layer networks using Levenberg-Marquardt algorithm, and did not consider the MISO layer networks and Bayesian Regularization algorithm. In addition, the dataset used was obtained only from biomass gasification experiment, and without using data from fixed bed systems.

With regard to the sensitivity analysis performed to estimate the effect of the input variables on the outputs by the aforementioned authors, connection weights method was mainly used. The partial derivatives (PaD) method was not considered, but Montaño & Palmer [214], (Wang et al.

[215] & (Gevrey et al. [216] reported that the PaD is more effective than the step wise, Perturbe, and connection weight methods. In this study, experimental data obtained from a few gasifiers (e.g. entrained, fluidised, and fixed bed) operated at varied experimental conditions using fuels and blends of feedstock (e.g. biomass, coal, waste tyre etc.) were employed in a backpropagation L-M and BR algorithms of ANN model with MIMO and MISO layer networks to study the performance of a gasification unit. The ANN is preferred to other models for this work because it can solve problems that are difficult to be resolved by human brain; it is self-manipulated and can provide nonlinear relations without seeking for external assistance. It does not need the formulation of complex numerical equations to provide solutions, and most importantly, is very reliable in terms of accuracy of results [197].

It is expected that this study will: (i) promote understanding of performance of a gasifier via modelling approach without carrying out actual gasification tests; thereby saving time and reducing cost of experimentation; (ii) allow for the prediction of the efficiency of gasifiers operated at different process conditions and using different fuels (e.g. biomass, coal, and their blends); (iii) provide information that could assist stake-holders to develop gasifiers that has the capacity of converting different solid fuel materials into energy. Importantly, this information could be instrumental to decision making as well and could serve as a platform for further research & development in this field.

4.1. Experimental Data

The materials, methods and experimental data used in this study were described in section 1 of chapter 3 (methodology), but the input and output variables data ranges are displayed in Table 4.1

Table 4. 1: Input and output variables employed in ANN

Input variables	Data range	Output variables	Data range
C (wt.% dry basis)	12.10 – 99.00	CGE (%)	3.98 – 174.43
H (wt. % dry basis)	0.62 – 13.86	CCE (%)	6.10 – 138.85
N (wt. % dry basis)	0.04 – 5.50	Gas Yield (kg/Nm^3)	0.17 – 7.50
S (wt. % dry basis)	0.00 – 2.15	LHV of gas (MJ/Nm^3)	0.62 – 15.31
O (wt.% dry basis)	13.90 – 54.00	Gas composition (Vol.%):	
MC (wt.% dry basis)	0.02 – 15.00	CO	2.74 – 42.68
Ash (wt. % dry basis)	0.15 – 79.16	CO_2	0.12 – 54.15
T (^oC)	600.00 – 1200.00	CH_4	0.00 – 70.10
VM (%)	5.40 – 99.81	H_2	2.50 – 55.55
ER (-)	0.10 – 1.00		
LHV_{Fuel}^{*}	5.5 – 38.04		

η_{Gas}: Gas yield; CGE: Cold Gas Efficiency; CCE: Carbon Conversion Efficiency; T: Gasification Temperature; ER: Equivalence Ratio; VM: Volatile Matter; LHV: Lower Heating Value*****: Biomass, coal, & coal + biomass.

The gasification experiments from which the dataset used in this study were obtained were performed using different types of gasifiers namely; updraft, downdraft, fluidised bed and entrained bed, and they are illustrated in Figure 4.1. The system efficiencies varied based on the mechanisms and the capacity of the gasifiers. For instance, a circulating fluidised bed (CFB) gasifier is known for excellent heat and mass transfer efficiencies and accommodating of a wide range of feedstocks. However, amongst the key factors that affect the efficiency of the gasifiers is the quality of the feedstock and process conditions. In this study, the fuel properties evaluated includes C, H, N, S, O, ash, MC, VM, and LHV, while the process parameter were ER and T. These parameters were used to develop the ANN Model. Hence our model is capable of predicting the gasification efficiency of any of the four gasifiers based on 8 output variables comprised of

gas composition (CO CO_2, H_2, CH_4), gas yield, LHV of gas, CGE, and CCE.

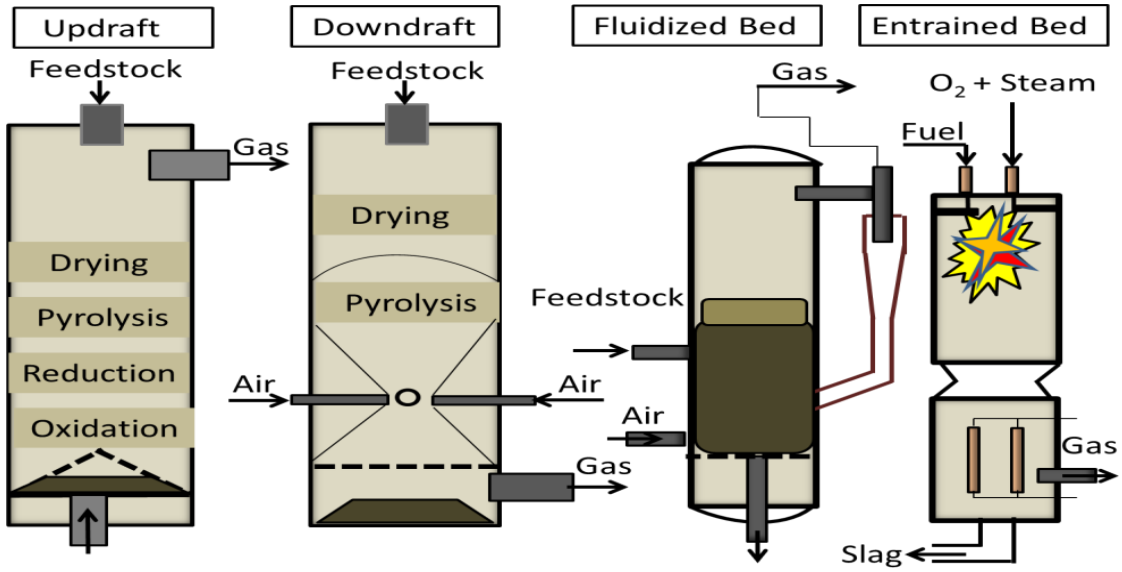


Figure 4. 1: Schematic diagram of some gasification systems (Adapted from (Sikarwar et al. [56]

4.1.1. Multiple Input-Multiple Output (MIMO) and Multiple Input-Single Output (MISO) Layer

The MIMO and MISO layer networks will be studied using the input and output data characteristics shown earlier in Table 4.1, and the architectures are presented in Figure 4.2 and Figure 6.3. The number of neurons in the hidden layer varies, and it is usually determined by trial and error [192].

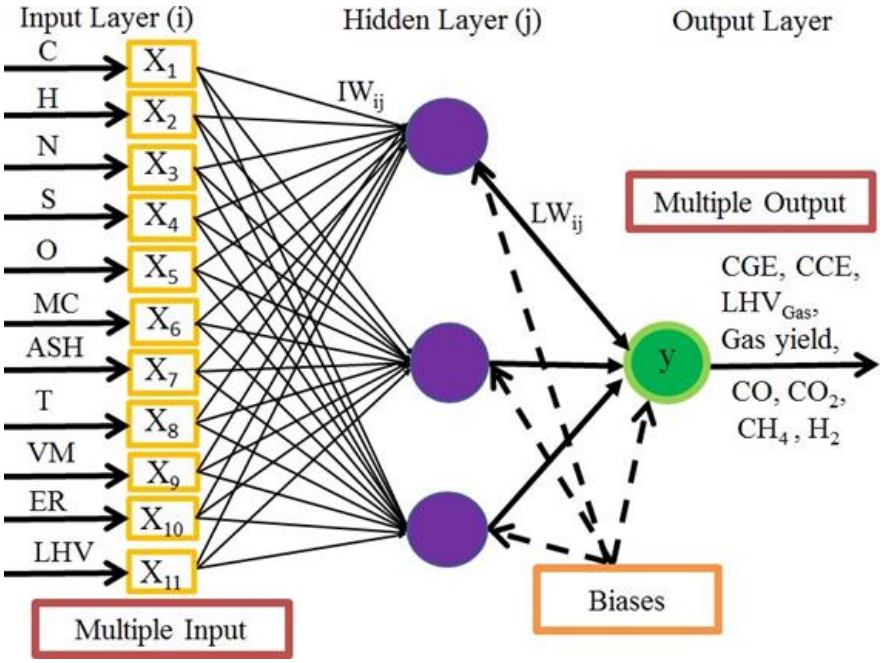


Figure 4. 2: Architectural design of Multiple Input-Multiple Output (MIMO) layer of the neural network.

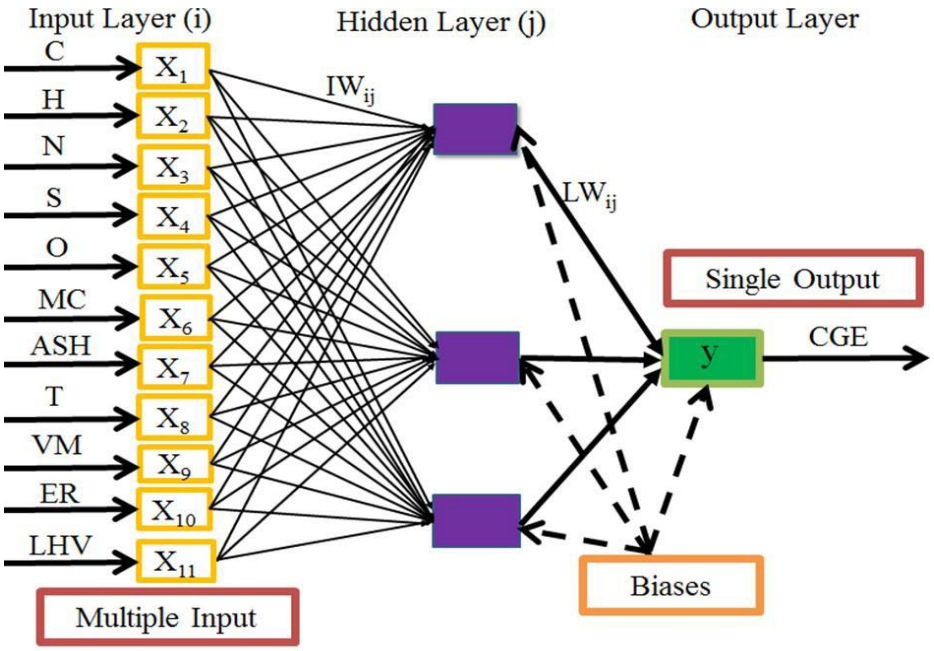


Figure 4. 3: Architectural design of the Multiple Input-Single Output (MISO) layer of the neural network.

The detailed procedure used for the training of the network has been explained in the methodology (chapter 3), but the step-wise technique employed is shown in Figure 4.4.

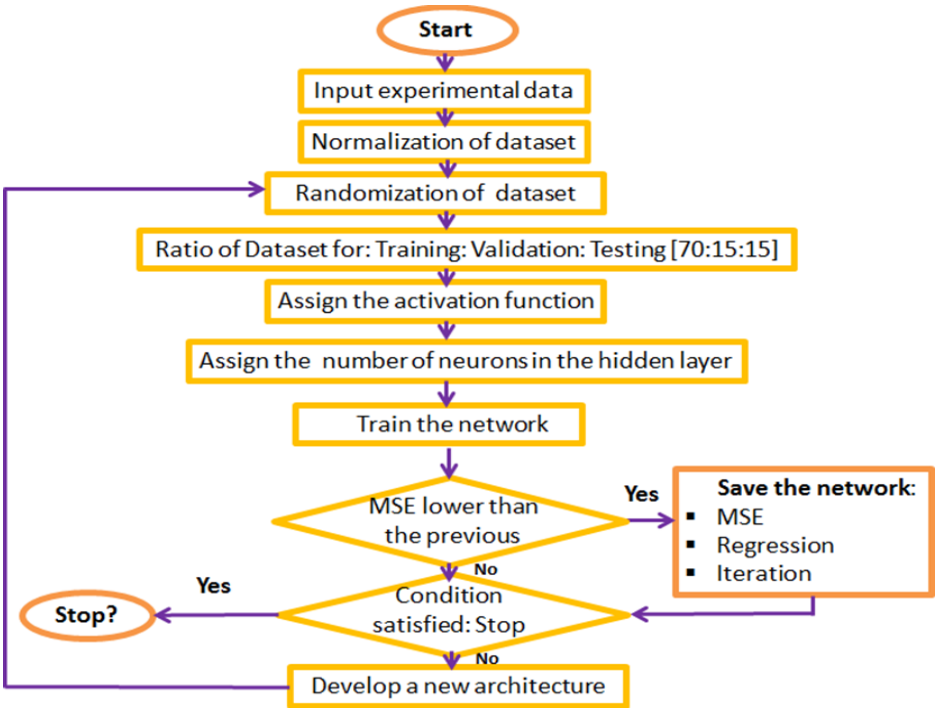


Figure 4. 4: ANN network training flow-sheet

The details of the Levenberg-Marquardt (L-M) training/learning of the ANN model can be found in (Pandey et al. [192].

4.1.2. ANN Model Development and applications

The ANN model was developed from the 315 dataset using the neural network toolbox (nntool) under MATLAB environment. A backpropagation L-M and BR algorithms using a Multiple Input-Multiple Output (MIMO) and Multiple Input-Single Output (MISO) layer networks were employed to study the performance indicators. For the MIMO layer network, C, H, N, S, O, MC, Ash, VM, T, ER, and $LHV_{biomass}$ were used as the input variables, while CGE, CCE, gas yield, LHV of gas, and product gas composition (CO, CO_2, CH4, and H_2) were used as the output variables. The ER and T represents the operating conditions of the gasifier, while C, H, N, S, O, MC, Ash, VM, and $LHV_{biomass}$ represents the fuel characteristics in the input layer. The output layer is represented by the gasifier performance indicators which considerably are influenced by the properties of the fuels and operating condition. In the MISO layer networks, the performance indicators (output parameters) are considered independently, unlike the Multiple Output (MO) of the MIMO layer that jointly examines the output variables. In this case, a single architecture of the neural network was designed for the MIMO network, while one architecture was developed for the each of the performance indicators, and thus; referred to as a MISO layer network. The MIMO and MISO layer architectures for the networks have been shown in Figure 4.2 and Figure 4.3, respectively, but Figure 4.5 describes the computational frame-work and equations that were used for the estimation of the value of y_{2i}; the output variables, while Figure 4.6 shows the actual topography used to train the network. In this case, C, VM, and T are the inputs, whereas CGE, gas yield, and LHV of gas are the outputs. It is important to point out that the three output variables which are shown in Figure 4.5 are trained separately in the network, hence; making it a MISO layer network, but a similar network accounting for the 11 inputs and 8 outputs (MIMO layer network).

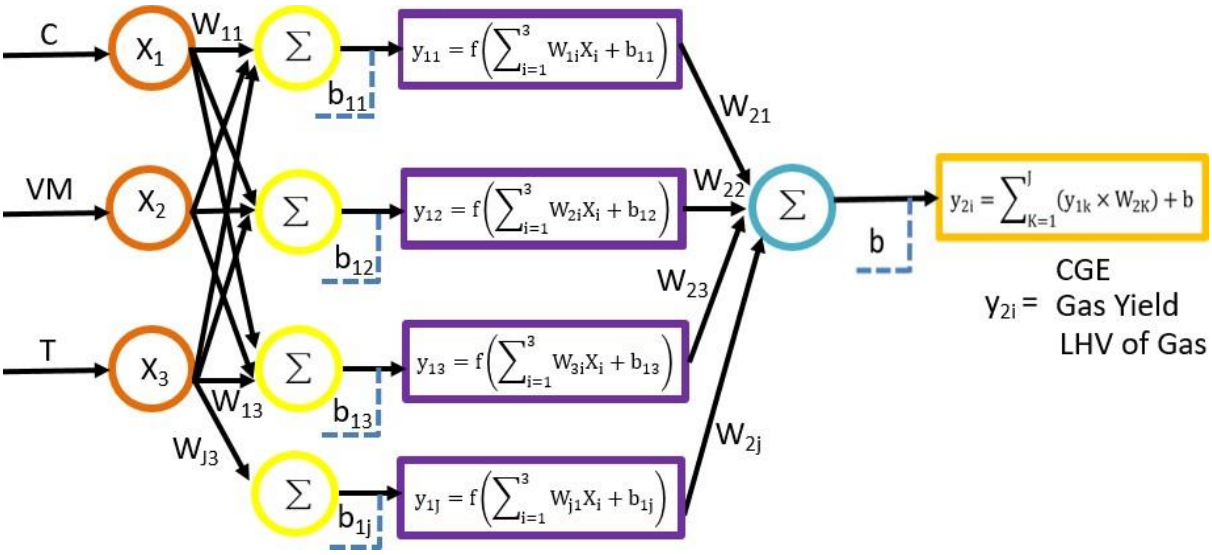


Figure 4. 5: Model equation development for the estimation of y_{2i} (output variables)

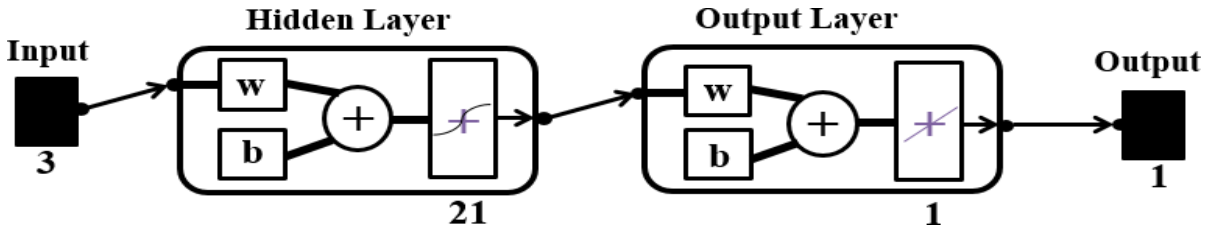


Figure 4. 6: Feedforward neural network (FFNN): 3, 21, 1 architecture

4.2. Gasification Performance Evaluation

The efficiency of a gasifier for biomass and coal gasification or co-gasification of biomass and coal can be evaluated using the gasification performance indicators such as Cold Gas. Efficiency (CGE), Carbon Conversion Efficiency (CCE), product gas yield, LHV of gas, and gas composition (e.g. CO, CO_2, CH_4, & H_2).

4.2.1. Cold gas efficiency (CGE)

The CGE is a measure of the gasification performance. It is the ratio of the syngas yield and lower heating value (LHV) of the syngas to the LHV of the feedstock (biomass or coal). Mathematically, the CGE is expressed in Equation (4.5) [217]:

$$CGE = \frac{[Gas\ Yield(\eta_{Gas})]\times[LHV_{Syngas}]}{[LHV_{Biomass}]} \times 100 \qquad (4.5)$$

4.2.2. Carbon Conversion Efficiency (CCE)

The CCE describes the percentage of the total carbon in the gasifier feedstock, and converted to product gases that contained carbon such as CO, CO_2, and CH_4. The CCE is presented in Equation (4.1) [218,219]. If the gas analysis contains C_2H_4 and C_2H_6 alongside the CO, CO_2, and CH_4, it can be expressed as shown in Equation (4.2) [220,69]:

$$\mathrm{CCE} = \frac{\mathrm{CO}\ \% + \mathrm{CH_4}\% + \mathrm{CO_2}\ \%}{[22.4 \times \mathrm{C}\ \%]} \times 100 \tag{4.1}$$

$$CCE = \frac{12\eta_{Gas}[CO\ \% + CO_2\% + CH_4\%] + 2[C_2H_4\ \% + C_2H_6\ \%]}{[22.4 \times C\ \%]} \times 100 \tag{4.2}$$

where, the gases CO, CO_2, CH_4, C_2H_4, and C_2H_6 are in % Vol., and C is in % of carbon in the dry feedstock from the ultimate analysis, and η_{Gas} is the gas yield, and the factor 12 is the atomic number of carbon.

4.2.3. Gas Yield (η_{Gas})

The amount of gas produced during the gasification or co-gasification process indicates the efficiency of the gasifier. The η_{Gas} is the ratio of the volumetric flow rate of the outlet gas from the gasifier to the mass flow rate of the biomass (or feedstock) to the gasifier, and it is presented in Equation (4.3) [69]:

$$\eta_{Gas} = \frac{Q_{Syngas}}{M_{Biomass}} \tag{4.3}$$

where, Q and M are the volume flow rate and mas flow rate of the gas and biomass, respectively.

4.2.4. Lower heating value of gas (LHV_{Gas})

The amount of heat generated from the combustion of 1 Nm3 of the syngas without water is referred to as the LHV of the gas, and is also expressed mathematically as shown in Equation (4.4) [221, 222]:

$$LHV_{Gas} = 11.76 \times [V_{CO} + 11.882]\left[V_{H_2} + 37.024\right]\left[V_{CH_4}\right] \times \left[\frac{10}{100}\right] \tag{4.4}$$

4.2.5. Product Gas Composition

The composition of gas produced in the gasifier essentially describes well the efficiency of the gasifier. It is influenced by the composition of the feedstock, type of gasifier and the operating conditions used, and the product gas may typically contain CO, CO_2, CH_4, and H_2.

4.3. Uncertainty Analysis

The Mean Square Error (MSE) and coefficient of determination R^2 are commonly used in an ANN model to evaluate the prediction accuracy of the model. On the other hand, to determine the effect of the input variables on the outputs, the PaD shall be employed because of its effectiveness [223], and the expression for the PaD is shown in Equation (4.5) [224,225]:

$$S_I = \frac{1}{N} \sum_{P} \frac{\partial o_k^P}{\partial x_i^P} \tag{4.5}$$

Where N represents the total number of data variables; p is the pattern number; ∂o_k^P is the output value for the pattern p (predicted variable from ANN model); ∂x_i^P is the input value from the pattern p (experimental variable). If a three-layer feedforward neural network is considered, then o_k and o_j follows as shown in Equation (4.6) and Equation (4.7):

$$o_k = f_2\left(\sum_j w_{kj} o_j\right) \tag{4.6}$$

$$o_j = f_1\left(\sum_i w_{ij} x_i\right) \tag{4.7}$$

Where w_{kj} represents the weight between the output neuron k and the hidden neuron j; w_{ij} is the weight between the input neuron i and the hidden neuron j; o_j is the output of the hidden neuron j; f_1 and f_2 represents the activation functions. The chain rule is applied in Equation (4.5), and after which,

the sensitivity of the input variable was obtained by combining Equation (4.6) and Equation (4.7) as expressed in Equation (4.8):

$$S_I = \frac{1}{N}\sum_{P}\frac{\partial o_k}{\partial o_j}\frac{\partial o_j}{\partial x_i} \tag{4.8}$$

Putting the actual values of some of the terms of Equations (4.6 & 4.7) yields the S_I as presented in Equation (4.9):

$$S_i = \frac{1}{N}\sum_{P} f_2'\left(\sum_{j} w_{kj}\, f_1'\right)\sum_{i} w_{ij}x_i\left(\sum_{i} w_{ij}x_i\right)w_{ij} \tag{4.9}$$

Assuming f_1 and f_2 are the Sigmoid function, it means that $f' = 1 - f$, hence; the S_i will be as shown in Equation (4.10):

$$S_i = \frac{1}{N}\sum_{P} o_k\,(1 - o_k)\sum_{i} w_{kj}o_j\,(1 - o_j)w_{ij} \tag{4.10}$$

A crucial point to note about using this method is that the values of the sensitivities are affected by the output values. What it implies is that the patterns with small and large output values has the tendency of being affected because of the terms o_k and $(1 - o_k)$ of Equation (4.11), but if the value of the partial derivative is negative, the output variable result will decrease with an increase in the input variable result and vice-versa. However, the relative contribution of each input variable on a particular output can be measured by estimating the sum of the squares of the partial derivatives as depicted in Equation (4.11):

$$SSD_I = \sum_P \left(\frac{\partial o_k^P}{\partial x_i^P}\right)^2 \quad (4.11)$$

while the contribution or influence of each input variable on the output variables, is presented in Equation (4.12):

$$Contribution\ of\ the\ ith\ Variable = \frac{SSD_i}{\sum_i SSD_i} \quad (4.12)$$

After the computations, the results are screened, and the variable with the highest SSD becomes the most influential variable on the output, hence; the inputs are ranked in the order of their effect on the output. Researchers have used the connection weights method proposed by Garson [226] to determine the relative importance of the input variables on the outputs, but the comparative analysis result of the relative importance of inputs on outputs indicated that the results obtained from the method was not compatible [227,228]. According to Gevrey et al. [225] the Perturbe and step-wise methods are also not stable, and based on these facts, the PaD method is therefore proposed for this paper. where, i and j represents the input variables and hidden layer neurons; β_i is the relative effect of the ith input variable on the output variable; $IW_{j,i}$ and $LW_{j,i}$ are the weight to jth neuron of hidden layer from input variable and weight to output layer from jth neuron of hidden layer, and represents the number of neurons.

4.4. Results and Discussion

4.4.1. Model solutions

In this study, two ANN model approaches were employed to investigate the performance of a gasifier. The models were the Bayesian Regularization (BR) algorithm and Levenberg-Marquardt (L-M)**.** Both methods yield different results that are expected to proffer some reliable information to stake-holders in the sector in solving some energy conversion problems (e.g. efficiency of a gasifier) when different solid fuels are gasified employing different gasifiers and operating conditions.

4.4.2. Bayesian Regularization (BR) algorithm: MIMO layer network

Bayesian regularization (BR) training algorithm was used to predict the performance of the gasifier, and using the MIMO layer networks. The technique consumed a lot of training time, but it is efficient for generalization of difficult and noisy data-sets. In this case, an ANN MIMO layer network was employed, and 11 input variables comprised of C, H, N, S, O, ash, MC, VM, T, ER,

and $LHV_{biomass}$, and 8 output variables comprised of gas composition (CO CO_2, H_2, CH_4), gas yield, LHV of gas, CGE, and CCE were used. The 315 input-output patterns used for the study was divided into three; 70 % (221 datasets) for training; 15 % (47 datasets) for validation; 15 % (47 dataset) for testing of the model. Further, the input datasets were randomised for each of the iterations, while simulations were carried out by varying the number of neurons in the hidden layer using tansigmoid transfer function. The network was evaluated based on the MSE, and the architecture with the lowest MSE is considered the best model. Importantly, high values of the MSE in an indication of poor or non-perfect prediction. It is therefore to train the network such that MSE that tends to zero (0) is obtained.

The convergence characteristics of the MIMO network trained with 23 neurons in the hidden layer is presented in Figure 4.7. It can be observed that the MSE of the training validation and testing decreased until epoch 6 before assuming constant till the epoch 12. The major issue with the result is the MSE value which is high, but it was caused by the nature of the data-sets inputted to the network and not necessary the inability of the network to offer efficient predictions. In this case, the CCE was eliminated from the output variables to be predicted, and to check if the MSE could be reduced and then provide a better result. Figure 4.7 shows the convergence characteristics of the network after the removal of the CCE. 23 neurons in the hidden layer was used to train the network, and the MSE has reduced from 348.6942 to 61.7092 and with best validation performance at iteration 10. This is when the CCE was not included in the prediction. Similarly, Figure 4.8 is the convergence characteristics of the MIMO model, using all the output variables, except CCE (23 neurons) and it yielded the best fitting at epoch 10.

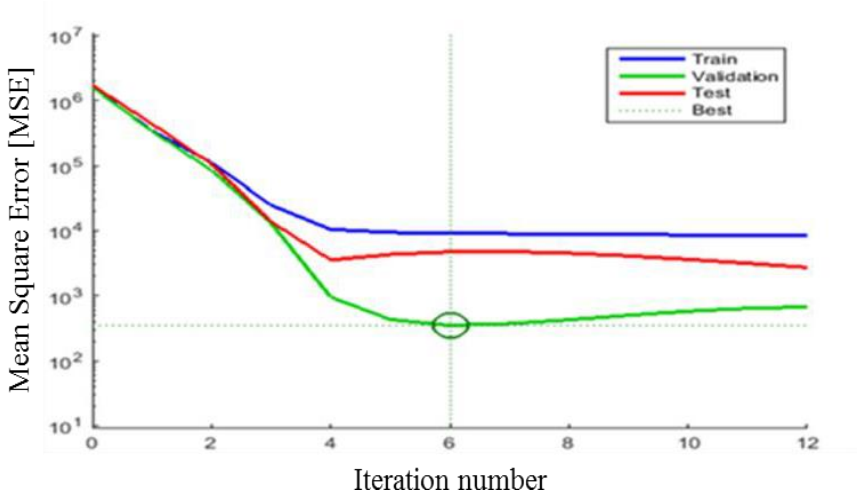


Figure 4. 7: Convergence characteristics of the MIMO model, using all the output variables (23 neurons)

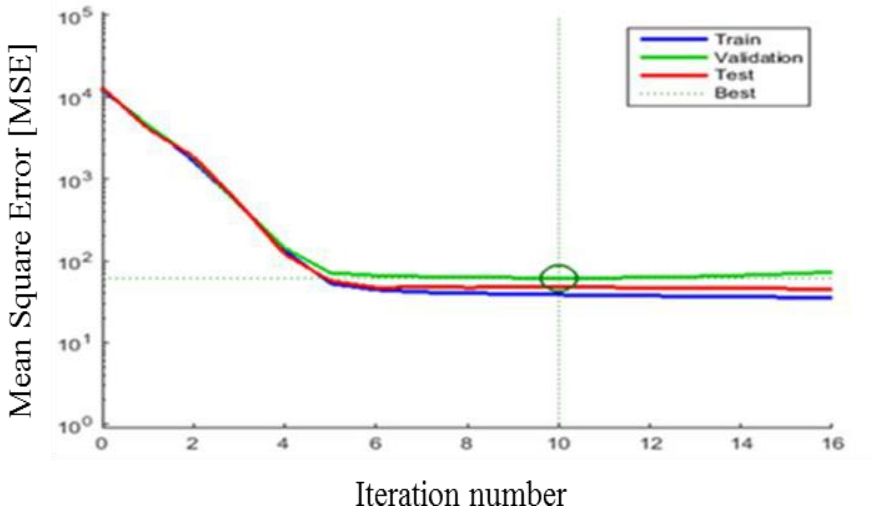


Figure 4. 8: Convergence characteristics of the MIMO model, using all the output variables, except CCE (23 neurons)

4.4.3. Model solutions: Levenberg-Marquardt (L-M) MISO layer network

Results of the ultimate analysis (C, H, and N) were used as input variables to predict the CGE, Gas Yield, and LHV of the gas. These output parameters are considered as one of the major indicators or parameters for evaluating performance of a gasifier.

4.5. Prediction of the CGE [%]

In the prediction of the CGE, 20, 21, and 22 number of neurons in the hidden layer were selected from the several numbers of neurons used for the training of the network as shown in Figure 4.9 to Figure 4.11, and they described how the MSE varies with the number of neuron used in training the networks, and the optimum iteration for each set of the learning program by the model. The best validation performance was obtained at iterations 59, 26, and 166 respectively. The training, validation, and test curves appear close to each other, and with consistent fitting as indicated by the epochs, but the Mean Square Errors (MSE) obtained were on the high side. This could be attributed to the source of the dataset which compelled the network to struggle a lot in memorizing the patterns while correlating the fittings. However, the 21 number of neurons in the hidden layer gave the smallest MSE.

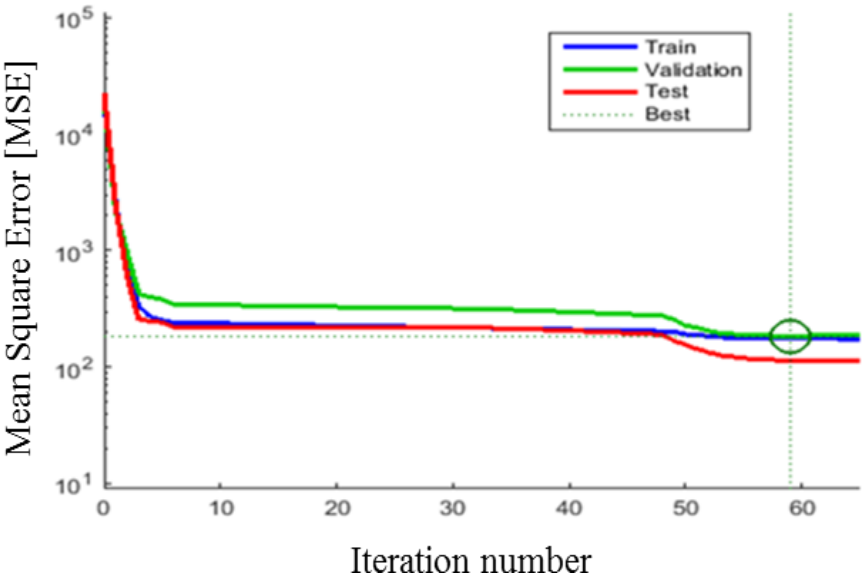


Figure 4. 9: Convergence characteristics of the MISO model, CGE prediction using C, H, & N as the input variables (20 Neurons)

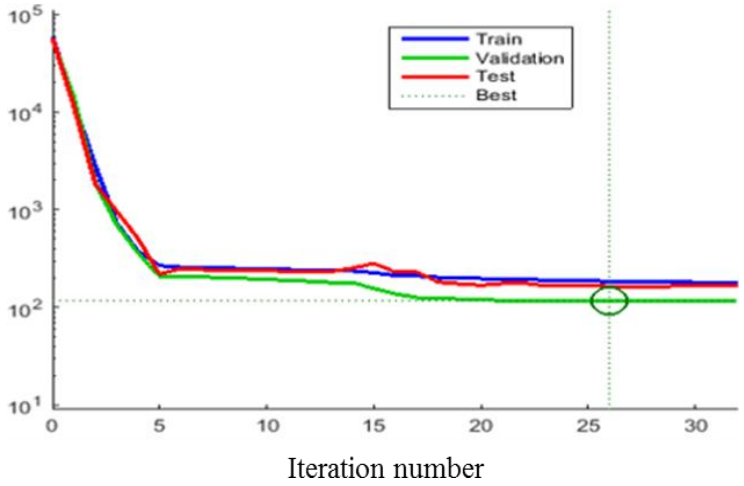


Figure 4. 10: Convergence characteristics of the MISO model: CGE prediction: C, H, & N as the input variables: 21 Neurons

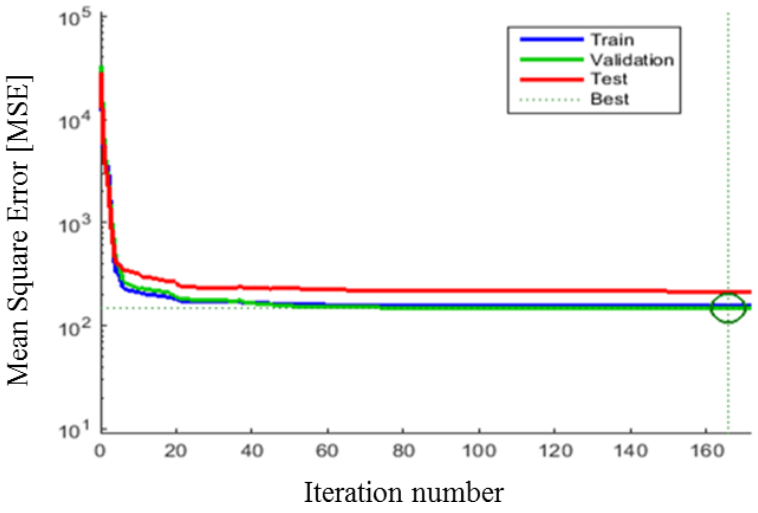


Figure 4. 11: Convergence characteristics of the MISO model: CGE prediction: C, H, & N as the input variables: 22 Neurons

Meanwhile, the coefficient of determination (R^2) obtained for the data fitting using the 20, 21, and 22 number of neurons in the hidden layer is shown in Table 4.2. The highest R^2 (0.84) was obtained from the validation curve from the 22 number of neurons in the hidden layer, but an R^2 of around 0.90 – 0.99 is preferred provided the MSE is small. An R^2 of 0.84 (highest) obtained in this case has not indicated a good correlation and it could be attributed to using a dataset obtained from different gasification system, and under different operating conditions.

Table 4. 2: L-M MISO layer network: R^2 for the CGE using C, H, & N as the inputs

Input variables	Number of neurons	Regression co-efficient (R^2)				Output variables
		Training	Validation	Testing	All*	
C, H, N	20	0.75	0.83	0.80	0.78	CGE
C, H, N	21	0.75	0.81	0.81	0.80	CGE
C, H, N	22	0.78	0.84	0.74	0.82	CGE

C: Carbon; H; Hydrogen; N: Nitrogen; CGE: Cold Gas Efficiency; All*: All data exploited

4.5.1. Prediction of the Gas Yield [kg/Nm^3]: MISO layer network

Figure 4.12 through Figure 4.14 presents the results of the networks trained using 20, 21, and 22 neurons in the hidden layer and with C, H, and N from the ultimate analysis results as the input variables and Gas Yield as the output variable. In this case, the best validation performance was obtained at 36, 25, and 12 iterations respectively, while the highest R^2 of 0.84 was obtained from the network with 21neurons in the hidden layer. It can be observed that the MSE obtained from each of the training were quite high, but the result achieved with the network trained with 21 neurons in the hidden layer produced the smallest MSE of 145.13 at epoch 25. The high values of the MSE is an indication of a wide range of variations in the input and output dataset that were used for the training of the networks, and which resulted from the experimental datasets collected from different gasification systems, that were operated at different process conditions.

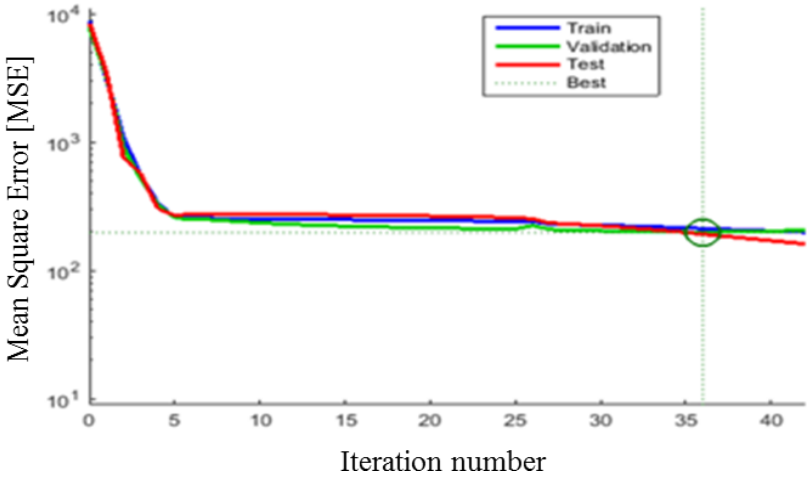


Figure 4. 12: Convergence characteristics of the MISO model: Gas Yield prediction: C, H, & N as the input variables: 20 Neurons

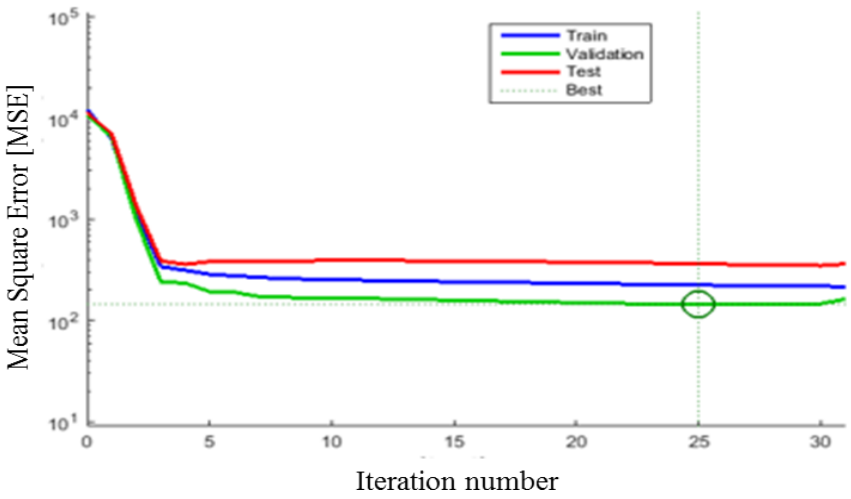


Figure 4. 13: Convergence characteristics of the MISO model: Gas Yield prediction: C, H, & N as the input variables: 21 Neurons

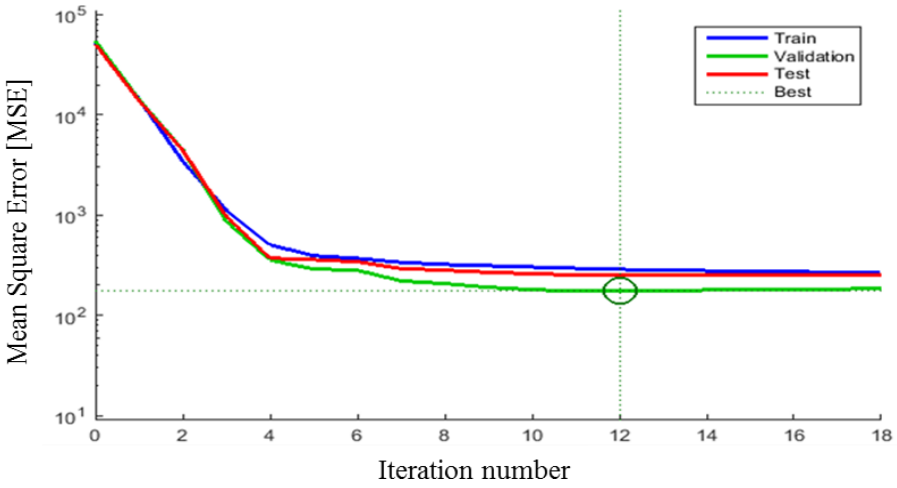


Figure 4. 14: Convergence characteristics of the MISO model: Gas Yield prediction: C, H, & N as the input variables: 22 Neurons

Similarly, the coefficient of determination (R^2) for the training, validation, and testing for the predicted gas yield are shown in Table 4.3. The highest R^2 of 0.84 was obtained from the validation curve of the network with 21 neurons in the hidden layer, the other R^2 are within 70 – 84 % which is not an indication of good result, thus; requires upgrading.

Table 4. 3: L-M MISO layer network: R^2 for the Gas Yield using C, H, & N as the inputs

Input variables	Number of neurons	Regression co-efficient (R^2)				Output variables
		Training	Validation	Testing	All*	
C, H, N	20	0.71	0.71	0.76	0.74	Gas Yield
C, H, N	21	0.80	0.81	0.61	0.85	Gas Yield
C, H, N	22	0.71	0.84	0.67	0.79	Gas Yield

C: Carbon; H; Hydrogen; N: Nitrogen; CGE: Cold Gas Efficiency; All*****: All data exploited

4.5.2. Prediction of the LHV of gas [KJ/Nm^3]: MISO layer network

The same conditions used for the training of the CGE and Gas Yield were equally used to train the networks for the LHV of the gas, and the results are depicted in Table 4.4. It can be observed that the MSE obtained from the each of the training are 0.34, 0.07, and 0.19, respectively, and have decreased very considerably when compared to the MSE obtained from the CGE and Gas Yield as 184.26, 115.28, & 148.47 and 199.61, 145.13, & 173.86. It could be attributed to the individual data in the data-set of the LHV of the gas having values closer to each other than those of CGE and Gas Yield. The training and validation curves for each of the networks fitted perfectly, whereas the testing curves indicated a random relationship. However, the R^2 of the training and validation fittings presented in Table 4.4 for each of the learning sets indicated some improved correlations, and with the validation fittings from the network trained with 21 number of neurons in the hidden layer producing the highest R^2 of 0.96, All the R^2 obtained from each of the training were above 90 % except the validation fitting from the network trained with 20 neurons in the hidden layer and whose R^2 was 89.94 %.

However, the results have revealed that if the individual data in each of the data-set are closer to each other, the MSE will decrease, while the R^2 will increase, thus; yielding a better result. To assure that the individual data are closer to each other for input and output variables, the collection

of the experimental data should generally be based on the type of gasification system (e.g. fixed or fluidised bed gasifiers). The operating conditions should equally be classified (e.g. gasifying agent, gasification temperature, etc. to enhance the overall results of the prediction. The R^2, epochs, and MSE obtained from the prediction of LHV of gas using C, H, and N as inputs and 20, 21, and 22 neurons in the hidden layer respectively are depicted in Table 4.4.

Table 4. 4: Convergence characteristics and R^2 for the LHV of Gas using C, H, & N as the inputs: L-M MISO layer network

Input variables	Number of neurons	Regression co-efficient (R^2)				Epoch	MSE	Output variables
		Training	Validation	Testing	All*			
C, H, N	20	0.95	0.90	0.91	0.90	365.00	0.34	LHV_{Gas}
C, H, N	21	0.93	0.96	0.88	0.94	254.00	0.07	LHV_{Gas}
C, H, N	22	0.90	0.91	0.85	0.85	17.00	0.19	LHV_{Gas}

C: Carbon; H; Hydrogen; N: Nitrogen; CGE: Cold Gas Efficiency; MSE: Mean Square Error; All*****: All data

4.5.3. Prediction using proximate analysis data: MISO layer network

The CGE, Gas Yield, and LHV of the gas were predicted using the results of the proximate analysis and represented in this case by the ash, MC VM as the input variables for the model and employing the MISO layer network. The best validation performance of the network for the each of the predictions are shown in Figures 4.15, 4.16, and 4.17, respectively, and it can be seen from the results that the MSE values remained high irrespective of using the proximate analysis results in predicting the output variables, except the result from the LHV of the gas that has a MSE of 0.30.

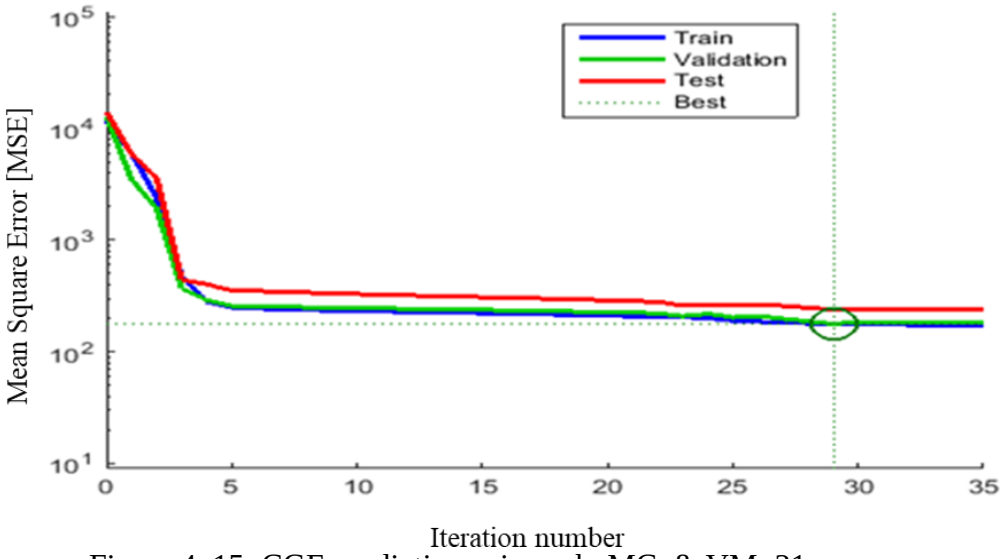


Figure 4. 15: CGE prediction using ash, MC, & VM: 21 neurons

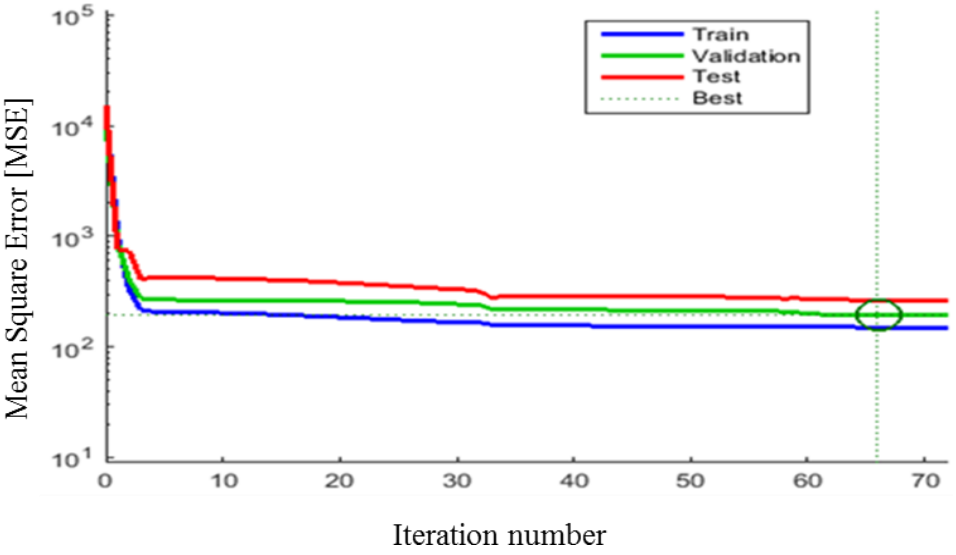


Figure 4. 16: Gas Yield prediction using ash, MC, & VM: 21 Neurons

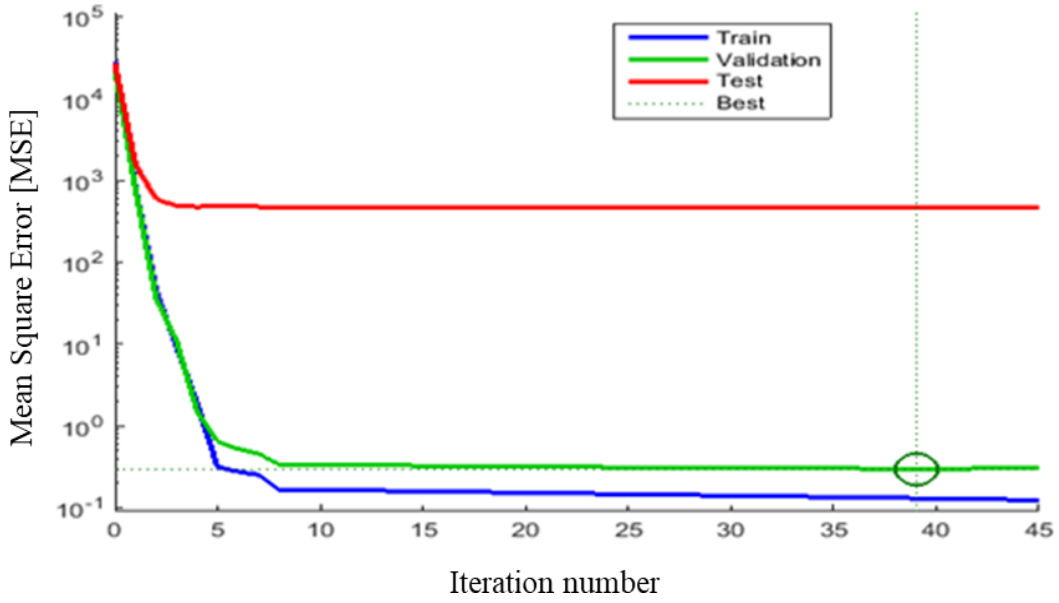


Figure 4. 17: LHV of gas prediction using ash, MC, & VM: 21 Neurons

It can equally be observed in Figure 4.15 and Figure 4.16 that the training, validation and testing curves are very close to each other when compared to Figure 4.17, and have consistent fittings until 29, and 66, epochs, but it is not an indication of a better fitting of the model due to the high values of the MSE and low values of R^2 that are only within the range of 75 – 79 %. On the other hand, a MSE of 0.30 that was produced by the LHV of the gas at iteration 39 is a better result when compared to the results obtained from the CGE and gas yield, and the R^2 obtained from the training and validation were 93 and 81 % respectively, while the testing curve has a lower value. Generally, the results obtained from the ultimate and proximate analysis results as the input variables of the model respectively, indicated a similar trend. Table 4.5 presents the results of the coefficient of determination (R^2), respectively.

Table 4. 5: L-M MISO layer network: R^2 for the CGE, Gas Yield, & LHV of Gas using Ash, MC, & VM as input

Input variables	Number of neurons	Regression Coefficient (R^2)				Output variables
		Training	Validation	Testing	All*	
Ash, MC, VM	21	0.75	0.76	0.71	0.76	CGE
Ash, MC, VM	21	0.76	0.80	0.77	0.79	Gas Yield
Ash, MC, VM	21	0.93	0.81	0.69	0.89	LHV_{Gas}

MC: Moisture content; VM: Volatile Matter; CGE: Cold Gas Efficiency; All*: All data exploited

4.5.4. Prediction using Ultimate, Proximate & Process condition data: Input Variables Representation Technique with Visual Inspection Method (IVRT-VIM): MISO model

The IVRT-VIM was employed to study the improvement of the results of the performance indicators. The method was introduced to minimize the high values of the MSE and enhance the values of the R^2. The technique involves choosing a single input parameter from the 11 input variables to represent the ultimate, proximate, and experimental process condition results respectively, and it was achieved by the screening of the entire data of the input variables using Visual Inspection Method (VIM), and from which the sets having closer values were identified. In this approach, C, VM, & T were chosen as the input variables to represent the ultimate, proximate analysis, and the operating conditions of the gasifier respectively, and were used to predict the CGE, gas yield, and LHV of the gas. Previously, the results obtained from the training involving the ultimate and proximate analysis datasets using the L-M algorithm gave better results, respectively when compared to the model results obtained from the CGE, gas yield and the MIMO layer network involving the entire 11 input variables for the BR algorithm. On this account, only the L-M algorithm is studied in this case.

Figure 4.18 through Figure 4.20 shows the outcome of training the network for the CGE, Gas yield and LHV of the gas, using only 21 neurons in the hidden layer, respectively. It can be observed that the MSE values in each of the case have reduced significantly when compared with the previous results. From Figure 4.18 and Figure 4.19 the best validation performance was at epochs 7 and 3, while the best validation performance for the LHV of the gas was at epoch 16, and with MSE of 0.25. The decrease in the MSE of the three output variables (CGE, Gas yield, and LHV of the gas) is attributed to the refinement of the input datasets by employing the IVRT-VIM. It should be recalled that prior to the application of the IVRT- VIM, the values of the MSE obtained in most cases were high, while the R^2 were as low as around 70 – 80 %. Meanwhile, the R^2 obtained for each of the output variables is presented in Table 4.6, and it can be observed that the R^2 for the

validation of the three performance indicators are between 91.89 – 97.71 %. Similarly, the R^2 obtained for the training and validation of the LHV of gas was 96.83 and 97.71 %, but the R^2 for the testing was small. The ANN model is reliable for predicting the gasification performance indicators studied, but to achieve an enhanced result, the input and output variable datasets may require refinement through IVRT-VIM.

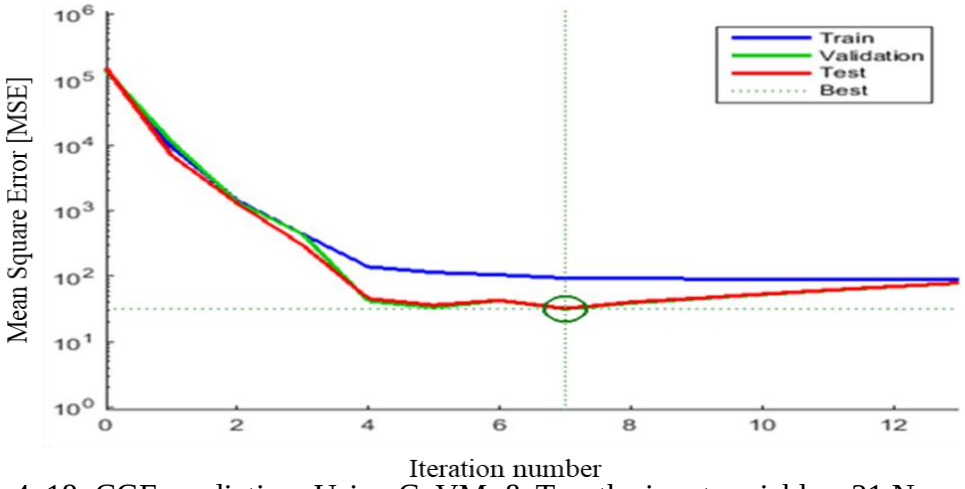


Figure 4. 18: CGE prediction: Using C, VM, & T as the input variables: 21 Neurons

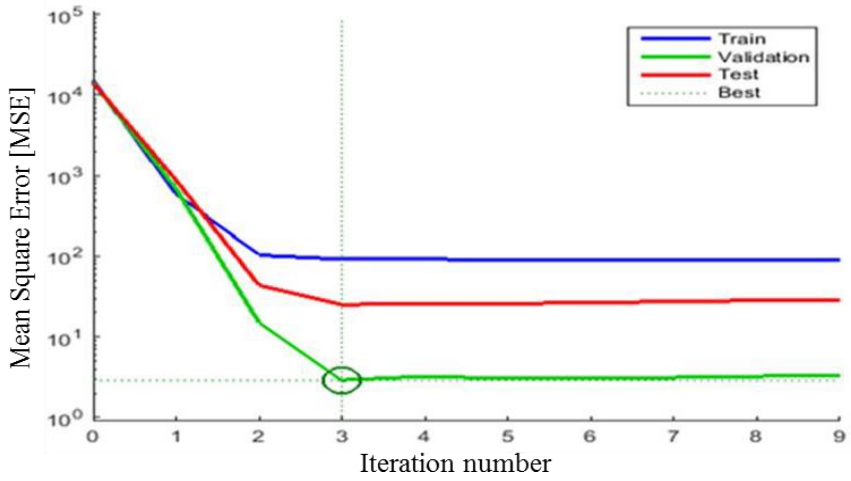


Figure 4. 19: Gas Yield prediction: Using C, VM, & T as the input variables: 21 Neurons.

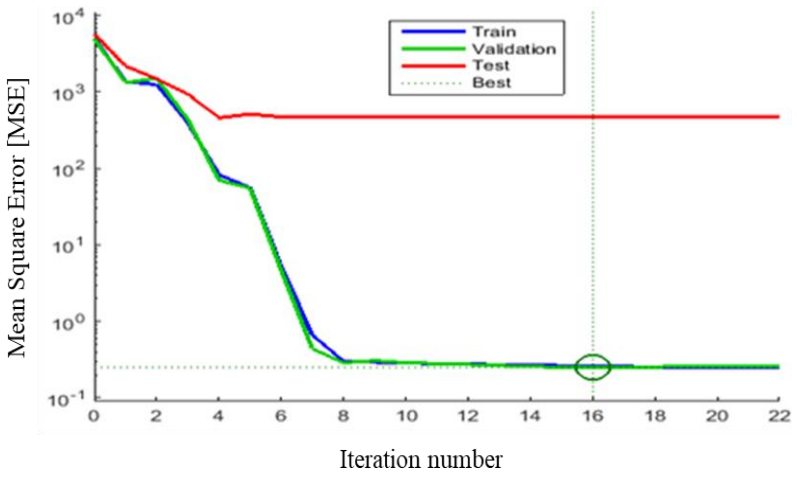


Figure 4. 20: LHV of gas prediction: Using C, VM, & T as the input variables: 21 Neurons

Table 4. 6: R^2 result from ultimate, proximate & operating parameters: Input parameters.

Input variables	Regression Coefficient (R^2)				Output variable
	Training	Validation	Testing	All*	
C, VM, T	0.87	0.92	0.85	0.90	CGE [%]
C, VM, T	0.90	0.95	0.97	0.88	Gas Yield [KJ/Nm^3]
C, VM, T	0.97	0.98	0.33	0.87	LHV_{Gas} [kg/Nm^3]

LHV: Lower Heating Value; R^2: Coefficient of determination; CGE: cold gas efficiency; C: Carbon; VM: Volatile Matter; T: Reaction Temperature; All*: All data exploited

The IVRT-VIM has helped to improve the model results when compared to other results obtained in the study, and it should be applied when several input variables are available for the prediction of the gasification performance indicators, and the results generated by the model are not as good as expected. If after using the IVRT-VIM and the result could not be improved, classifying the datasets into a fixed bed (FB) or fluidised bed gasifier (FBG) during the experimental data collation is another option to be investigated, and which may enhance the model results.

4.5.5. Prediction using L-M algorithm without CCE (WOCCE): Output Variables Representation Technique with Visual Inspection Method (OVRT-VIM): MIMO network layer

The output parameters were screened using the Output Variables Representation Technique - Visual Inspection Method (OVRT-VIM) after which, the model prediction was carried out employing MIMO layer network WOCCE. The remaining variables were used to represent the outputs in the model, and to examine the improvement of the model result. 10 and 23 number of neurons in the

hidden layer was used to study the MIMO layer network and using the L-M algorithm as presented in Figures 4.21 and 4.22, respectively. It can be seen that the best validation performance for Figure 4.21 and Figure 4.22 are at epochs 9 and 5, but the MSE obtained for the networks were 129.31 and 42.15, respectively. The regression results obtained from the network training using the 10 and 23 hidden neuron are also shown in Table 4.7. It can be observed that the R^2 was between 0.84 – 0.94 and 0.91 – 0.95, respectively implying that the model results had been upgraded when compared to the results involving C, H, & N as inputs.

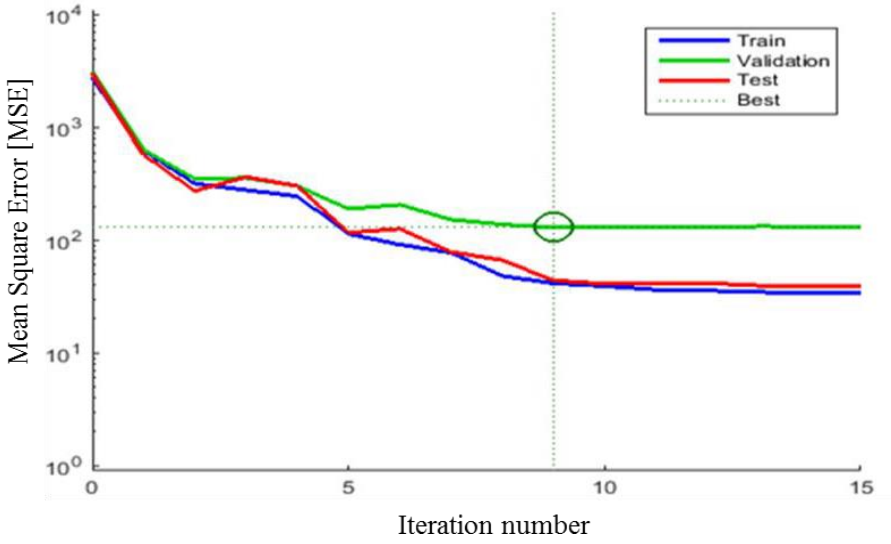


Figure 4. 21: Convergence characteristics of the MIMO L-M model, WOCCE (10 neurons)

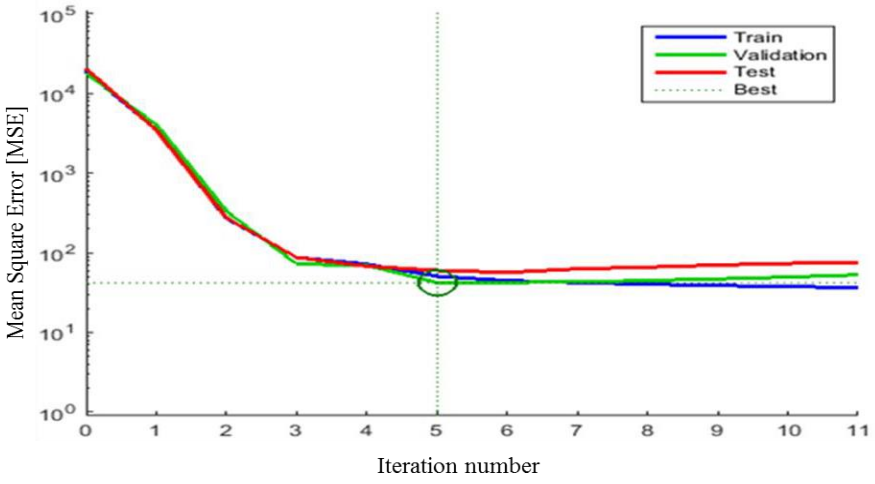


Table 4. 7: Convergence characteristics of the MIMO L-M model, WOCCE (23 neurons)

Inputs	Algo	Coefficient of determination (R^2)					Output
		Neurons	Training	Validation	Testing	All*	CCG, Gas Yield, LHV_{Gas}
C,VM,T	L-M	10	0.94	0.94	0.84	0.92	
		23	0.93	0.91	0.95	0.93	

Algo: Algorithm; L-M: Levenberg-Marquardt, C: Carbon; VM: Volatile Matter; T: Reaction Temperature; CCG: Cold Gas Efficiency; LHV: Lower Heating Value of Gas; All*****: All data exploited.

Similarly, Table 4.8 shows a detailed result of the trained MIMO layer networks that was carried out using different number of neurons in the hidden layer, and BR and L-M algorithms. From Table 4.8, it can be observed that the networks were trained with carbon conversion efficiency (WCCE) and without carbon conversion efficiency (WOCCE), a technique employed to study the upgrade of the model results, and it is referred to as OVRT- VIM. A similar approach (IVRT-VIM) was used for the input variables in section 3.4 to enhance the result of the model. The MSE of 27.23 and R^2 for training and testing of 96 % and 95 % were obtained, respectively from the MIMO layer network that was studied using 23 number of neurons in the hidden layer, WOCCE. Based on the result, the BR algorithm (in this case), is better considered than the L-M algorithm. This implies that the OVRT-VIM is also an effective method of improving the model result. The results of the MISO layer networks (e.g. CO, CO_2, H_2, & CH_4) are provided in one of the published papers from this thesis.

Table 4. 8: BR & L-M algorithm MIMO network results: OVRT-VIM model improvement

Algorithm	Number of Neurons	MSE	Epoch	Training	Validation	Testing	All*
			WCCE				
BR	10	33.35	108.00	0.95	-	0.84	0.90
L-M	10	206.88	8.00	0.86	0.89	0.18	0.65
			WOCCE				
BR	10	6136.99	89.00	0.61	-	0.07	0.80
L-M	10	129.31	9.00	0.95	0.84	0.95	0.92
			WCCE				
BR	23	6174.50	786.00	0.61	-	0.73	0.71
L-M	23	3188.60	5.00	0.45	0.16	0.60	0.61
			WOCCE				
BR	23	27.23	468.00	0.96	-	0.95	0.92
L-M	23	42.15	5.00	0.93	0.95	0.91	0.96

WCCE: With carbon conversion efficiency; WOCCE: Without carbon conversion efficiency; BR: Bayesian Regularisation; L-M: Levenberg Marquardt; MSE: Mean Square Error; OVRT- VIM: Output Variables Representation Technique-Visual Inspection Method; All*****: All data exploited.

4.6. Sensitivity analysis

Although the MSE and R^2 results obtained from this study gave some useful insights about the predictive accuracy of the ANN model, the PaD technique employed in this case had helped to identify the critical parameters and their degree of importance on the model outputs. The sensitivity analysis was carried out using C, VM, & T as the input variables, and Cold gas efficiency (CGE), gas yield, and LHV of gas as the output variables.

The Pareto charts shown in Figure 4.23 to are 4.25 used to describe the relative importance of the input variables (C, VM, and T) on the output variables (CGE, gas yield, and LHV of gas).

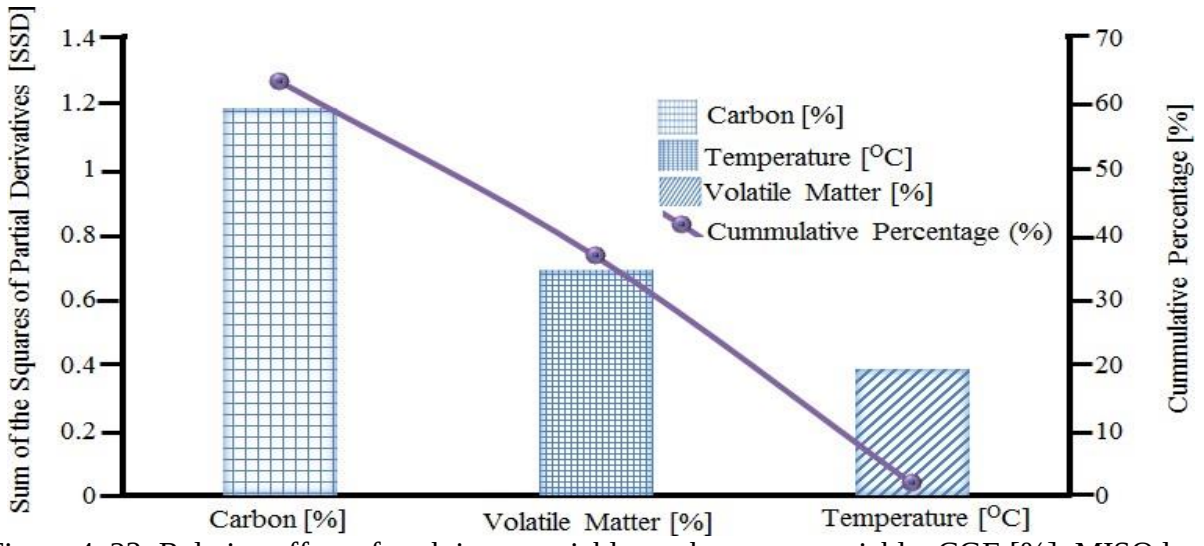


Figure 4. 23: Relative effect of each input variable on the output variable: CGE [%]: MISO layer network: 21 hidden layer neurons

The parameter with the highest sum of squares of the partial derivatives (SSD) has the most effect on the outputs, and from Figure 4.23, carbon is the most influential variable on the CGE. Carbon (C) is one of the major constituents of a fuel alongside H, and O [229]. It makes a significant contribution in the energy value of a fuel which is measured by the higher heating value (HHV) and lower heating value (LHV) of the fuel [37]. The volatile matter (VM) of a fuel describes the presence of organic matter in that fuel, and it accounts for fuel reactivity during thermo-chemical process and in which case, a low or high VM fuel plays a critical role in the overall reaction of the fuel [2230]. The reaction temperature also is another important parameter that plays a key role in energy conversion process, and its effect equally, is dependent on the physio-chemical composition of the fuel such as C, VM, MC, etc. and other operating conditions used in the process (e.g. ER, oxidant, etc,) [231]. High moisture content (MC) fuels may lead to reduction in the gasification temperature which could further lead to tar production and condensation in the gasifier [69].

In this study, there is a decrease and an increase in the MSE of the MISO and MIMO layer networks, respectively, when the MC and VM of fuel as well as C, H, & N and ash, were employed as inputs for the predictions of the CGE, gas yield and LHV of gas. The implication is that different fuels could yield different gasification efficiencies. Similarly, a high gasification temperature may

enhance the cracking of tar (via thermal cracking), thus; resulting to an increase in the amount of product gas formed during gasification [1]. However, beyond certain range of gasification temperature (e.g. 900 -1000^{O}C), the product gas becomes part of the combusting material, and in this case, the product gas yield is decreased [69]. For the CGE prediction, the SSD of carbon was 1.1846, and it is the highest amongst the input parameters studied, hence; ranking it the most important parameter affecting the CGE. Figure 4.23 and Figure 4.25 presents the relative importance of the input parameters on the outputs (gas yield and LHV of gas), respectively.

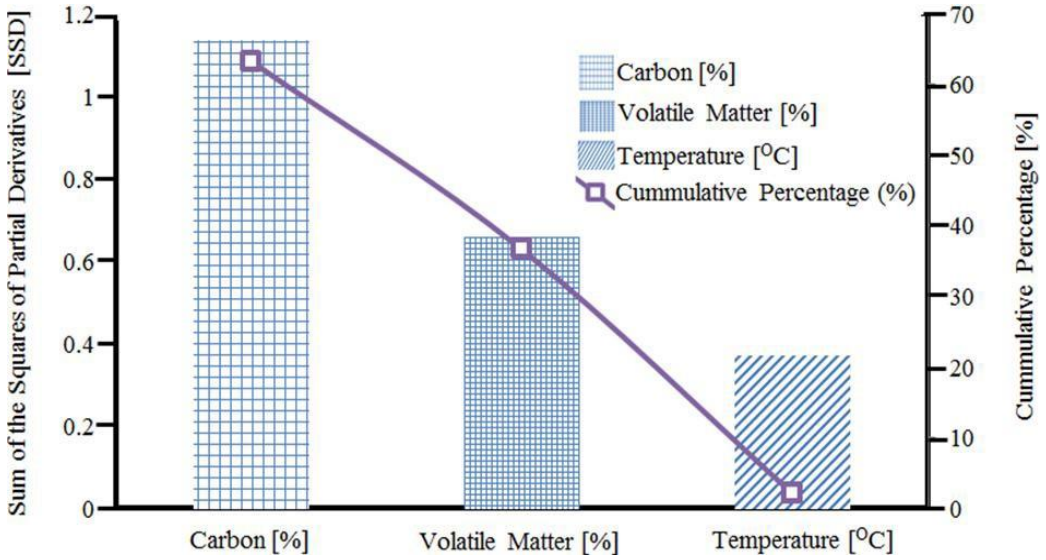


Figure 4. 24: Relative effect of each input variable on the output variable: Gas Yield [kg/Nm^3]: MISO layer network: 21 hidden layer neurons.

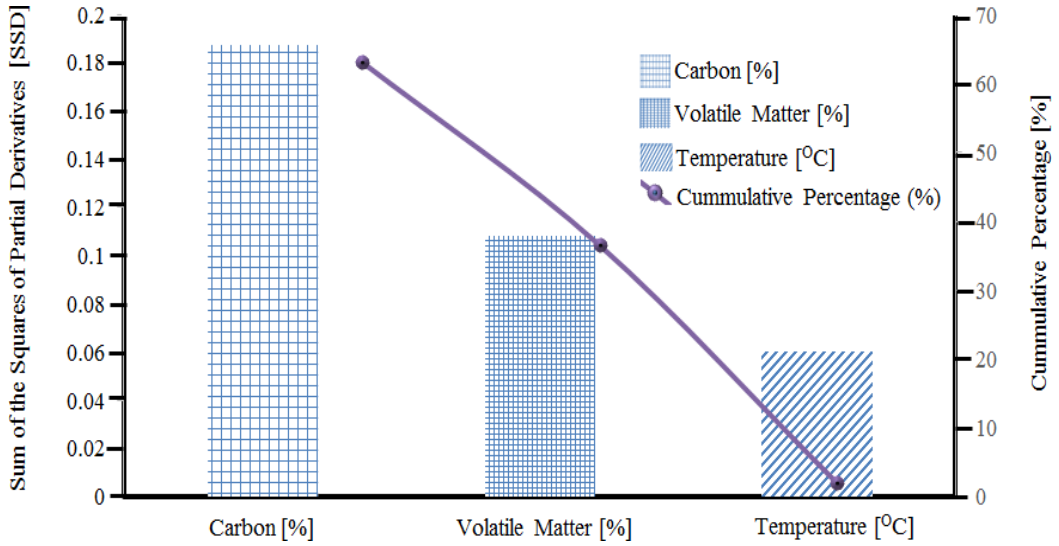


Figure 4. 25: Relative effect of each input variable on the output variable: LHV of Gas [KJ/Nm^3]: MISO layer network: 21 hidden layer neurons

It can be observed that the same trend of result obtained in Figure 4.23 was equally achieved. The SSD value of carbon was 1.1362 and 0.0019 for gas yield and LHV of gas respectively, thus; making it the most effective parameter affecting the outputs. Therefore, from the result of the sensitivity analysis, the use of C, VM, and T as input variables for the model prediction of the gasification performance indicators (CGE, gas yield, and LHV of gas) are in the order of C > VM > T. The order is logical considering the impact of each parameter on the efficiency of biomass and coal gasification processes. The analysis demonstrates that the network output varies relative to the inputs, thus offering essential information about the more sensitive parameters in the investigation, and revealing the reliability of the model parameters. Table 4.9 compares results obtained in this study with literature.

Table 4. 9: Results compared with literature

Reactor	Input variables	Output Variable	Major Findings	Reference
CFBG & BFBG	Ash, MC, C, O, H, ER, T, VM	Gas yield, CO, CO_2, H_2, CH_4	Model predicted efficiently the gasification performance indicators	**[51]**
Remarks: LM-Back-propagation algorithm was used. Model technique: MIMO, Hidden layer Neuron: 2 Sensitivity: Connection weights method [23**]**: All variables have effect on the output, but for CFB: C, H, O has between 31.7 – 54.1 % and for BFB: C, H, O has between 28.9 – 52.3 % effects on the outputs. Generally, ER was the most important factor influencing the gas yield.				
FBG	C, H, O, ash, MC, Reduction zone temperature	Gas composition: CO, CO, CH_4, H_2	Model is reliable in predicting the gas composition, and result in agreement with experimental data.	[213]
Remarks: LM-Back-propagation algorithm was used. Number of neurons: 5 (used to predict CH4, CO), 4 for CO_2 & 3 for H_2 predictions. Training: 70 %, Validation: 15 %, Testing: 15 % dataset. Sensitivity: Connection: Connection weights method. Total number of experimental data: 63 samples.				
FBG	C, H, N, S, O, MC, ash, ER, Tg,	LHV of gas, LHVP (Char, & tar), Gas yield	Model has the ability to predict the gasification performance indicators with low MSE, thus; a viable alternative model for the prediction of the efficiency of a FBG.	[192]
Remarks: L-M MIMO & MISO of single and double layers were used. Number of hidden layer Neuron: 30 for single layer & 15 for the double layer.				
FBG	VM, FC, and Ash	C, H, & O	Predicted the fuel elemental compositions well	[232]

Remarks: ANN (MISI Model), Genetic Algorithm, & Support Vector Regression (SVR) was used. Number of layers: Single layer with 5 hidden neurons & a double layer with 3 hidden number of neurons. Number of data trained: 830 samples.				
FBG		CGE, CCE, total gas yield, LHV of gas	Model offered a reliable prediction	[211]
Remarks: ANN model, Genetic programming (GP) Support vector Regression (SVR) was used. Dataset was obtained from biomass and coal as fuel. Dataset was also obtained from a single gasification system.				
Different Gasifiers	MIMO**:** C, H, N, O, S, VM, Ash, ER, T, $LHV_{biomass}$ MISO: C, VM, T	MIMO: CGE, CCE, gas yield, LHV of gas, Gas composition: CO, CO_2, CH_4, & H_2, MISO: CGE, Gas Yield, LHV of gas.	Model reliably predicted the gasification performance indicators.	This study
Remarks: Dataset: Obtained from different gasifiers, fuels (e.g. biomass, coal, & blends of biomass and coal) & process conditions**.** LM-Back-propagation algorithm & Bayesian Regularisation algorithm were used. Model technique: MIMO & MISO layer networks were studied. Number of hidden neurons: MIMO: 10 & 23. MISO: 20, 21, 22. The MIMO layer network Predictions using 9 & 8 input variables respectively, produced result with high MSE, but has close fittings. The MISO Prediction using C, H, & N and ash, MC, & VM, yielded result with reduced MSE & an R^2 of between 75- 93 "%. MISO model with C, VM, & T as input variables gave better result, after data refinement, with R^2 of between 79 – 98 %, while the MIMO layer network, WOCCE yielded an R^2 of between 95 % - 96 %. A technique called IVRT-VIM and OVRT-VIM were developed, and were used to improve the model result. Sensitivity analysis: The Partial Derivatives (PaD) method was used. The most influential parameter: Carbon (C), with an SSD of 1.1846 for the CGE prediction.				

BFBG: bubbling fluidized bed gasifier; CFBG: circulating fluidized bed gasifier; FBG: Fixed bed gasifier; EFB: Entrained fluidised bed; CGE: cold gas efficiency; CCE: carbon conversion efficiency; ER: equivalence ratio; MC: moisture content; T: reaction temperature, C: carbon; O: oxygen; H: hydrogen; VM: volatile matter; MIMO: Multiple Input-Multiple Output; MISO: Multiple Input-Single Output; L-M: Levenberg- Marquardt; LHV: lower heating value; SSD: sum of squares of partial derivatives; WCCE: without carbon conversion efficiency.

4.7. Concluding remarks

Experimental data obtained from the literature from a few gasifiers (e.g. entrained, fluidised, and fixed bed) operated at varied experimental conditions using blends of feedstocks (e.g. biomass, coal, waste tyre etc.) were employed in a backpropagation L-M and BR algorithms of ANN model with MIMO and MISO layer networks to study the performance efficiency of a gasification unit. The input variables were ash, MC, VM, C, H, N, O, S, T, ER, and $LHV_{biomass}$, while the outputs were CGE, CCE, gas yield, LHV of gas, and gas composition (e.g. CO, CO_2, CH_4, and H_2). The prediction accuracy of the models was assessed using the MSE and R^2, while the Partial Derivatives (PaD) method was employed for the sensitivity analysis. The following conclusions emerged from the study:

- Results of the MIMO and MISO layer networks obtained from the L-M algorithm is better than those of them obtained from the BR algorithm, and it implies that the prediction accuracy of the L-M algorithm is more reliable than the BR algorithm.
- The MISO layer networks trained with 20, 21, and 22 neurons in the hidden layer with C, H, & N and ash, MC, & VM, yielded result with reduced MSE & an R^2 of between 75- 93%, implying that the model is more sensitive to some input variables than others.
- Because of the high values of the MSE and low R^2 obtained from the MIMO layer networks for the BR and L-M algorithm using C, H, & N and ash, MC, & VM in predicting the CGE, gas yield and LHV of gas respectively, the IVRT-VIM and OVRT-VIM were developed to account for the improvement of the model results.
- An application of the IVRT-VIM on the MISO layer networks using C, VM, & T as input variables and the CGE, gas yield and LHV of gas as the outputs gave an R^2 of between 79 % – 98 %, while the OVRT-VIM also gave an R^2 of between 95 % - 96 % for the MIMO layer network, WOCCE indicating that both approaches are effective for the enhancement of the model result.
- Results of the sensitivity analysis reveal that carbon is the most important input parameter affecting the outputs with an SSD of 1.1846 for the CGE prediction, and the relative importance of the inputs to the outputs are of the order of Carbon (1.1846) > volatile matter (0.6863) > temperature (0.0039).
- Performance of a gasifier was assessed via modelling approach and the efficiency of such gasifier can be predicted when different operating conditions and fuels are employed. The information obtained thereof could assist stake-holders in developing gasifiers capable of converting different solid fuel materials into energy. This information could be instrumental to

decision making and serving as a platform for further R & D in this area.

Chapter 5: Comparative study of emission and profit prediction from co-gasification of biomass, tyre, and coal fired CHP plant using Artificial Neural Network in Nigeria and South Africa

5.1. Introduction

In this chapter, artificial neural network model that was developed in chapter 4, and used for the evaluation of the performance efficiency of a gasification system, is also employed here to predict the emissions and profits obtained from solid fuels used in this investigation. The study considered feedstocks from Nigerian and South African origins. The choice for using the two countries as case study was based on the fact that they are the largest producers of the agro-waste materials in the African continent. Secondly, one (South Africa) has regular power supplies, while another (Nigeria) has irregular power supplies to the consumers, therefore, could be used to provide a standard/information for emissions and profits in CHP energy plant. The chapter has provided some results affirming that the emissions and profits from co-gasification CHP energy plants using the same type of fuels from different geographical regions vary. It is noteworthy to mention that a part of this chapter was presented at the International Conference on Engineering for a Sustainable World (Nigeria). It has been published in the Journal of Physic: Conference Series (IOP Indexed). See the list of publications for details. In every nation around the world, constant electric power supply is needed to enhance economic growth. All domestic, industrial, public and private sectors depend on the available power for sustainable economic growth. There are several technologies employed for energy production. Some of which has been described in chapters two and three (e.g. combustion, pyrolysis, and gasification). However, different feedstocks can be used as fuels to operate the systems such as the non-renewables (e.g. coal and petroleum) and renewable fuels (e.g. biomass), solar, wind, hydro, etc. Each of the resources and sources has its own merits and de-merits [1].

South Africa and Nigeria have large deposits of coal available for energy generation. It has been explained in chapter five that around 95 % of electric power production in South Africa is generated from coal. It should also be important to recall that SA has only, an estimated reserve of about 32 million metric tons [8], while the Nigerian estimated coal reserve is around 2.5 Gt [233].

Nigeria with her huge reserve still depends a lot in petroleum as the major source of fuel for energy production. Coal and petroleum have peculiar drawbacks as fuels for power production. They deplete fast and emit gases that are hazardous to the environment. This has been extensively discussed in chapters three and four, respectively. Nigeria and South Africa also have abundant

biomass (e.g. sugarcane bagasse (SCB), corn cob (CC), pine sawdust (PSD). Suberu et al. [234] reported that South Africa, Nigeria, and Egypt are the largest producers of corn (corn cob) in Africa. Gasification of blends of these agro wastes and coal will help to reduce fuel (coal and petroleum) depletion and gas emissions. As reported by the International Energy Agency (IEA), the waste sector was responsible for one-fifth of the global climate change due to about 140 billion metric tons of waste producing GHG which leads to climate change [235]. In this regard, the aforementioned agro-wastes can be well managed by using them as fuel for energy production.

In South Africa, electricity consumers benefit from the constant power supplies and low tariff of about $0.1408 c/kWh [16]. The reason for the low electricity tariff was explained in chapter five. Furthermore, the regular power supply in the country contributes significantly in the nation's economic growth, but most importantly, the emissions from the thermal power plants in the country, constitutes a huge threat to the environment.

In Nigeria, epileptic power supply is very common, irrespective of the exorbitant bills paid by consumers. There is lack of confidence in supplies, and it undermines the overall economy of the country. Different kinds of fuels as mentioned earlier are available in the country to produce electricity. Understanding the feedstocks and emission characteristics of the fuels from both countries therefore, are essential to solving the problems. Meanwhile, the feedstocks can be fed in a gasifier such as Integrated Gasification Combined Cycle (IGCC) or Combined Heat and Power (CHP) plant. Other technologies (though is for clean coal) which may be used are Ultra-Supercritical Combustion (USC), Supercritical- Fluidized Bed Combustion (FBC), and Coal Bed Methane (CBM) [233]. The technologies are efficient in powering communities once the feedstocks are available. A 5 MW capacity CHP plant had been reported by Caputo et al. [236] & Bridgwater et al. [237]. The authors argued that such capacity was feasible for a fluidized bed gasifier. Malek et al. [238] also studied the techno-economic of a 10 MW CHP plant using biomass as fuels. According to the authors, the investment is profitable. Other authors [237,238] have carried out studies using IGCC. They inferred that the technology is viable for power production and can provide around 45 – 50 % energy conversion efficiency. Demirbas [239] also reported that around 20 MWe capacity could be provided by a biomass Integrated Gasification Combined Circle (BIGCC).

Generally, the conversion efficiency of a typical co-gasification plant is about 40 % - 50 %, and the cost of feedstock used for heat and electricity production could equally decrease if a co-gasification technology was employed [238]. In another studies carried out by Ahmadi et al. [240]

it was observed that the overall system efficiency of a typical co-generation system is within the range of 35 % - 40 %. This observation is in affirmation with the findings of Demirbas [239] and Ahmadi et al. [240], thus; implying that co-gasification is an efficient process for energy production. However, emissions and profits are the two crucial factors that must be well understood in an energy generating plant. This is because the amount of gases emitted in the plant determines the environmental impact, and it may affect the overall profit because of the cost of gas cleaning. In this chapter, the emissions and profits from a biomass, tyre, and coal fired co-gasification CHP co-gasification plant are studied using ANN model. The outcome of the study will provide information that will save time and cost of experimentations; affirm that the same type of fuel from different regions can produce different emissions and profits in the same energy plant. The study will assist potential investors and stake-holders in the area in decision making.

5.2. Material & Method

Coal, biomass (e.g. Sugarcane bagasse (SCB), Corn cob (CC), Pine sawdust (PSD)) and Waste-tyre (WT) were the feedstocks used in the study. The collection point for all the South African and Nigerian feedstocks fuel samples has been described in Chapter three. The Nigerian coal was obtained from Onyeama mine, in Enugu state, while the biomass and WT were collected at Enugu-Ogbete Main market and mechanic village 9th mile corner, Ngwo respectively. The feedstock pre-treatment process followed the procedure described in chapter three and Ozonoh et al. [13].

5.2.1. Emission and Profit Estimation

The annual feedstock and feed-rate needed to operate the 10 MW electric power plant were determined from an empirical equation employing the aforementioned feedstocks at coal-to- solid waste ratios of 1:1, 3:2, and 4:1, respectively. Further estimations were carried using different model equations described in chapter 5 to determine the profitability of the feedstocks for power generation in terms of their economic (profits) and environmental (emissions) viabilities.

5.2.2. Artificial Neural Network (ANN)

ANN is a branch of artificial intelligence with information processing structure that allows it to simulate the functions of neurons employing the artificial neurons that behaves like the human brain [192]. A detailed concept of ANN and procedure for training the model can be found in Pandey et al. [192]. In this study, Levenberg-Marquardt (L-M) algorithm with Multiple Input-

Single Output (MISO) layer networks were employed to model the profits and emissions from the Nigerian and South African feedstocks for a period of 20 years, respectively. The range of the input and output variables used for the evaluation (emissions and profits) are presented in Table 5.2 and Table 5.5. The model was developed from the twenty calculated datasets for South African and Nigerian feedstocks in a MATLAB environment using the neural network toolbox (nntool), and 80 %, 10%, and 10 % of the dataset were employed for the training, validation and testing. Meanwhile, Figure 5.1 illustrates the feedforward neural network for the model development. It is crucial to point out that the difference between the model in Figure 5.1 and that of chapter 4 is the number of input and output variables investigated. In this model, MISO layer network was used, while MIMO and MISO layer networks were studied in chapter 4.

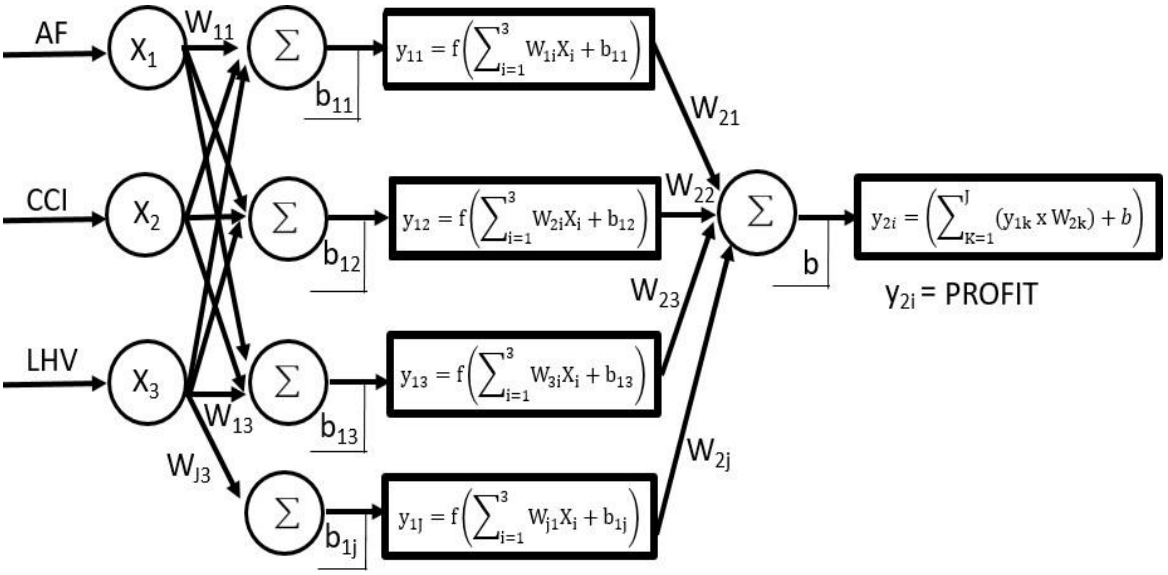


Figure 5. 1: ANN Model Equation development: Feedforward network (MISO layer).

5.2.3. Gaseous Emission estimation

To determine the gaseous emissions from the power plants, three categories of emissions were considered. It includes effective emission reduction, emission reduction by displaced energy, and emissions from transportation of fuels. The equations and their descriptions have been expressed and discussed in chapter 5.

5.2.4. Profit estimation

The annual profit made from the plant is determined based on the Net Present Value (NPV) of the investment. The expression used for the estimations can be found in the techno-economic analysis

reported in Chapter 10. Details of the profits and emission calculation can also be found in Ozonoh et al. [13].

5.3. Results and Discussion

Table 5.1 shows the feedstock characteristics of the Nigerian and South African fuels. A detailed characterization of the South African feedstocks used in this study in terms of the proximate and ultimate analysis can be found in Ozonoh et al. [13]:

Table 5.1: Feedstock characterisation: LHV and MC

South Africa feedstock				
Feedstock Ratio: 1:1				
Parameters	Coal + SCB	Coal + CC	Coal + PSD	Coal + WT
LHV [MJ/kg]	17.58	17.15	19.72	23.57
MC [%]	6.35	5.34	4.65	2.06
Feedstock Ratio: 3:2				
LHV [MJ/kg]	17.65	17.30	18.68	22.87
MC [%]	5.84	5.03	4.48	2.41
Feedstock Ratio: 4:1				
LHV [MJ/kg]	17.77	17.60	18.28	20.16
MC [%]	4.82	4.41	4.14	3.10
Nigerian Feedstock Feedstock Ratio: 1:1				
LHV [MJ/kg]	24.72	24.01	26.16	29.42
MC [%]	5.49	5.52	6.32	1.77
Feedstock Ratio: 3:2				
LHV [MJ/kg]	26.20	25.63	26.48	30.06
MC [%]	4.98	5.02	5.66	2.02
Feedstock Ratio: 4:1				
LHV [MJ/kg]	29.15	28.86	29.29	31.03
MC [%]	4.01	4.03	4.34	2.53

MC: Moisture content; LHV: Lower Heating Value

5.3.1. ANN modelling of South African feedstock: Profit model

Table 5.2 presents the calculated input and output variables used for the prediction of profits in the plant.

Table 5. 2: Input and Output variables employed in the ANN: Profit prediction

Variables	Coal + SCB	Coal + CC	Coal + PSD	Coal + WT
		Nigerian Feedstock		
AF [Ton/Yr.]*	2.91 – 2.47	2.99 – 2.49	2.75 – 2.47	2.45 – 2.30
CCI [$/Yr.]*m	3.52 – 4.01	3.63 – 4.05	3.21–3.93	3.28–3.89
LHV [MJ/kg]*	24.72 – 29.15	24.01 – 28.86	26.15 – 29.29	23.57 – 31.03
PROFIT [$/Yr.]**m	1.57–2.06	1.53 –1.95	1.65 – 2.37	1.69 – 2.30
		South African Feedstock		
AF [Ton/Yr.]*	4.05 – 4.09	4.09 – 4.20	3.65 – 3.95	3.06 – 3.57
CCI [$/Yr.]*m	1.30 – 1.43	1.31 – 1.43	1.26 –1.28	9.47 – 1.09
LHV [MJ/kg]*	17.58 – 17.77	17.15 – 17.60	19.72 – 18.27	23.57 – 20.16
PROFIT [$/Yr.] **m	7.56 – 7.65	7.48 – 7.64	7.45 – 7.67	7.86 – 8.00

*: Input Variable; **: Output Variable; CCI: Capital Cost Investment; LHV: Lower Heating Value; AF: Amount of Feedstock; NGN: Nigerian Naira; ZAR: South African Rand; CC: Corn Cob; PSD: Pine Sawdust; SCB: Sugarcane Bagasse; WT: Waste-Tyre; **m**: Values in the row are in million (i.e. x 10^6)

The results of the MISO layer network employed for the prediction of profits from the South African feedstock are depicted in Table 5.3. To train the networks for Coal + SCB, Coal + CC, Coal + PSD, and Coal + WT, 6, 7, 7, and 6 number of neurons in the hidden layer were used WFC and WOFC, respectively. Two performance evaluation of the efficiency of the model were employed, and it includes the Mean Square Error (MSE) and the coefficient of determination (R^2); for training, validation and testing. The MSE obtained from the South African feedstocks, WFC were between 0.02 – 0.11, while the R^2 were between 90 - 98 %, and the epochs which describe the stability in the convergence characteristics of the model were between 4 -12. An MSE that tends to zero (0) and R^2 tending to 1 indicates better fitting of a model. Similarly, the

MSE obtained for the same feedstocks, WOFC were between 0.10 – 0.41 except Coal + WT whose MSE was 2.06. The R^2 in this case, were between 91 - 97 % excluding Coal + WT with an R^2 of 88 - 89 % for training, validation and testing. The implication of the overall result obtained from the SA feedstock was that the ANN model has the ability of predicting the profit in the plant. Figure 5.2: through Figure 5.5: presents the convergence characteristics performance of the model for Coal + CC, Coal + SCB, Coal + PSD, and Coal + WT, respectively.

Table 5. 3: ANN model result on profits: 10 MW CHP co-gasification power plant

Feedstock	B.R	Algorithm	Neurons**	MSE	Epoch	T*	V*	Ts*
South African Coal [Matla Mine]: WFC								
Coal + SCB	1:1	L-M [MISO]	6	0.02	3	0.98	0.97	0.95
Coal + CC			7	0.03	12	0.96	0.93	0.91
Coal + PSD			7	0.02	4	0.98	0.96	0.98
Coal + WT			6	0.11	4	0.95	0.94	0.90
Nigerian Coal [Onyeama Mine-Enugu]: WFC								
Coal + SCB	1:1	L-M [MISO]	6	0.03	2	0.96	0.95	0.96
Coal + CC			7	0.05	5	0.94	0.97	0.93
Coal + PSD			7	0.03	11	0.97	0.98	0.95
Coal + WT			6	0.01	6	0.90	0.92	0.90
South African Coal [Matla Mine]: WOFC								
Coal + SCB	1:1	L-M [MISO]	6	0.18	6	0.97	0.96	0.94
Coal + CC			7	0.10	8	0.92	0.91	0.90
Coal + PSD			7	0.41	3	0.96	0.95	0.96
Coal + WT			6	2.06	5	0.88	0.89	0.92
Nigerian Coal [Onyeama Mine-Enugu]: WOFC								
Coal + SCB	1:1	L-M [MISO]	6	0.20	3	0.94	0.95	0.97
Coal + CC			7	0.12	5	0.96	0.97	0.95
Coal + PSD			7	0.66	12	0.97	0.95	0.96
Coal + WT			6	2.48	6	0.87	0.88	0.89

L-M: Levenberg Marquardt; MISO: Multiple Input-Single Output; *: Correlation Coefficient

(R^2); MSE: Mean Square Error: **: Number of neurons; WOFC: Without Feedstock Costing WFC: With Feedstock Costing; T: Training; V: Validation; Ts: Testing.

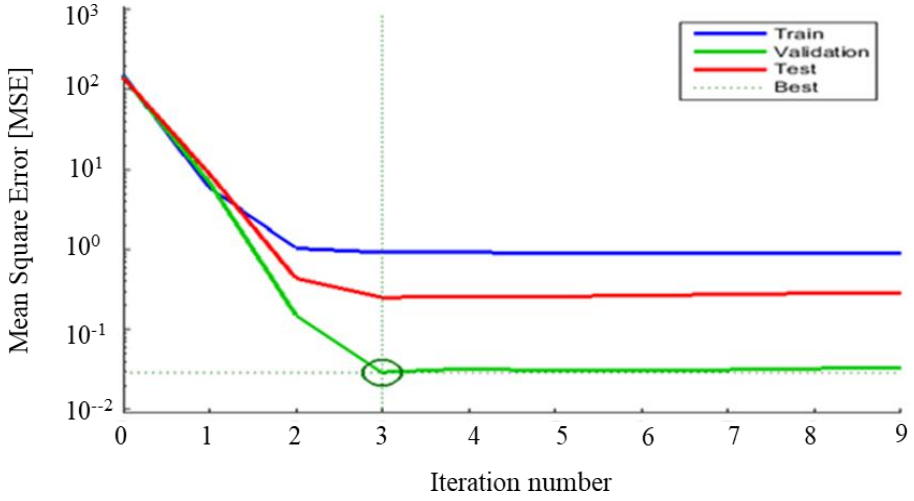


Figure 5. 2: Convergence characteristics for SA Coal + SCB: MISO network: Profit

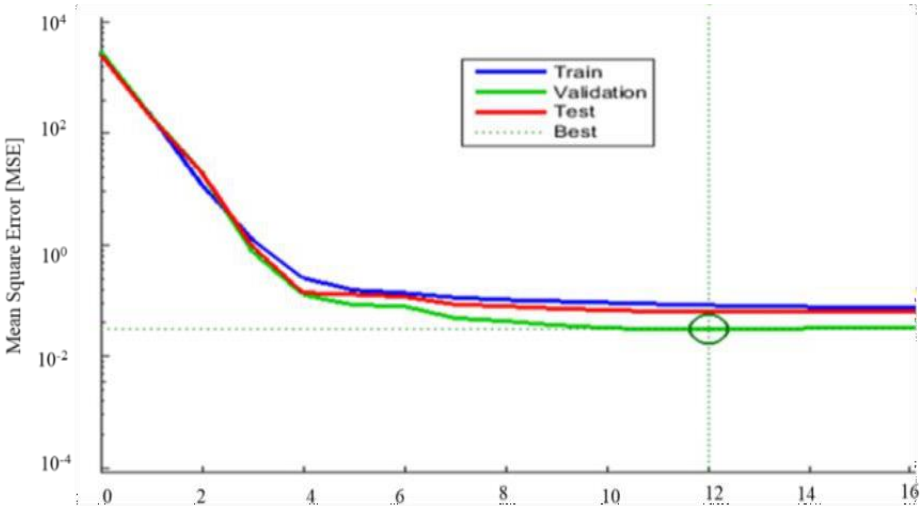


Figure 5. 3: Convergence characteristics for SA Coal + CC: MISO network: Profit

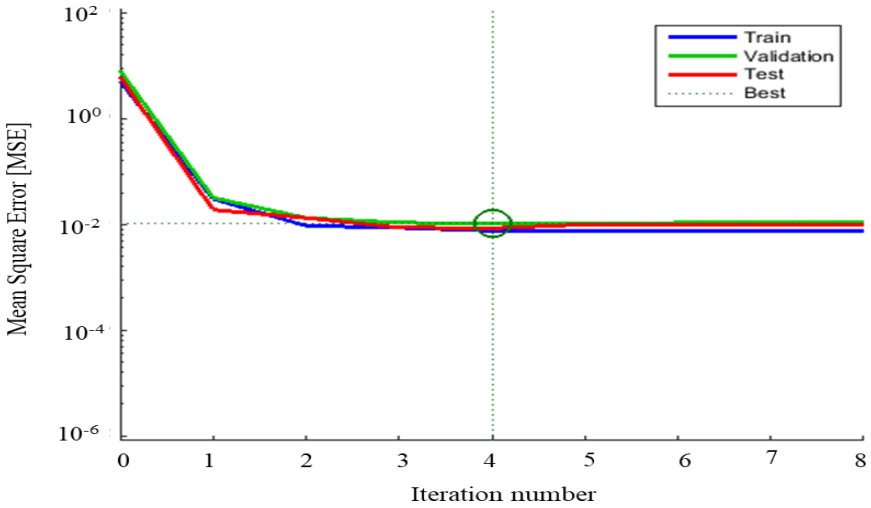


Figure 5. 4: Convergence characteristics for SA Coal + PSD: MISO network: Profit

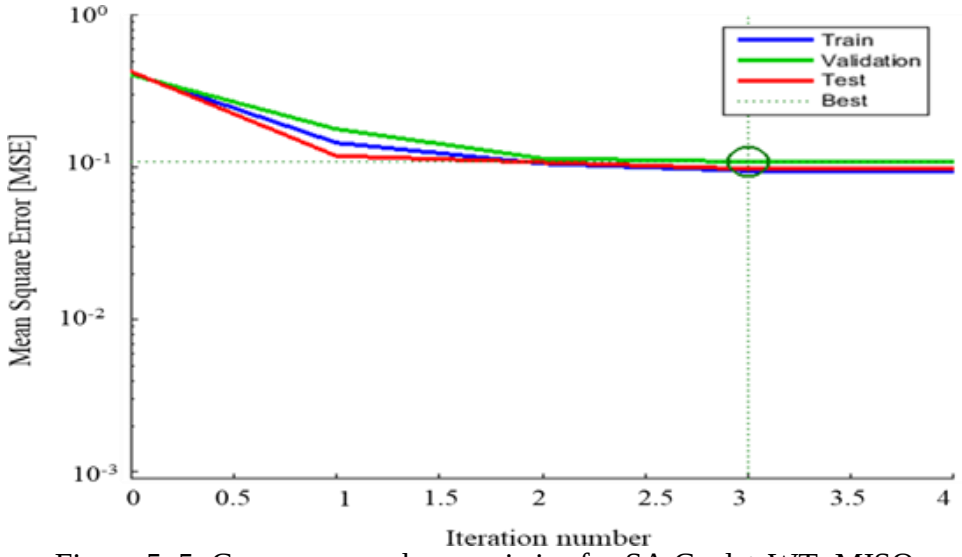


Figure 5. 5: Convergence characteristics for SA Coal + WT: MISO network: Profit

5.3.2. ANN modelling of Nigerian feedstock: Profit Model

The same training conditions employed for the South African feedstocks were used for the Nigerian feedstocks. Figure 5.6 through Figure 5.7 displays the convergence characteristics performance of the fuels; Coal + SCB and Coal + WT, WFC respectively. The model performance in terms of the convergence behaviour is stable, and this was evidenced in the epochs recorded by each of the fuels as contained in Table 5.4. The R^2 and MSE obtained from all the fuels were between 90 - 98 % and 0.01 – 0.05 indicating a better fitted model. From Table 5.5, WOFC, it can be seen that apart from Coal + WT that has an R^2 and MSE of 87 - 89 % and 2.48, the MSE and R^2 of other fuels were between 0.12 – 0.66, and 94 - 97 %, hence; revealing that the model has the capacity of predicting

the profits from Nigerian feedstocks for the 10 MW power production.

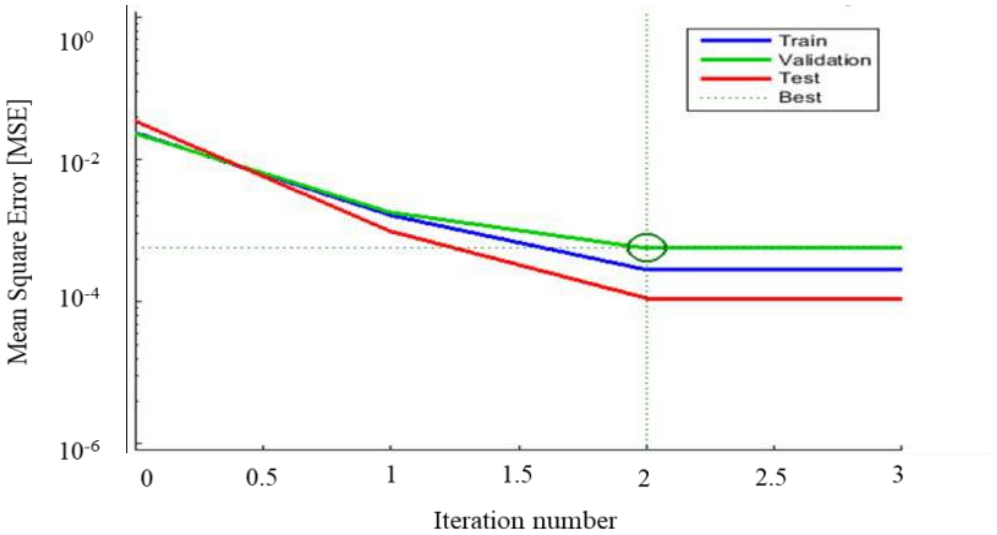


Figure 5. 6: Convergence characteristics for Nigerian Coal + SCB: MISO network: Profit

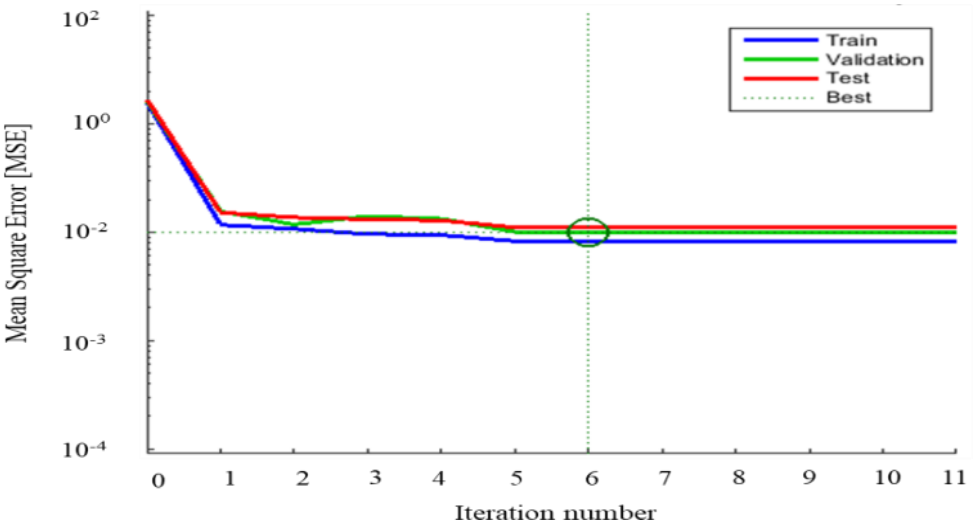


Figure 5. 7: Convergence characteristics for Nigerian Coal + SCB: MISO network: Profit

5.3.3. Comparison of South African and Nigerian feedstock: Profit prediction

The profits accrued from the power plant using South African and Nigerian fuels are compared as shown in Table 5.4. The comparison is carried out based on the highest and lowest profits obtained in the plant from the four feedstocks studied, WFC and WOFC, respectively. The use of South African feedstock to generate 10 MW of electricity produced about 45.18 % and 36.83 % ($3,900,000.07 and $3,179,184.49) profits higher than the Nigerian feedstock, WFC and WOFC, and the feedstocks that yielded the profits were Coal + PSD and Coal + WT, respectively. The SA fuels yielding the higher profit may be attributed to the higher cost of the Nigerian coal. The details

of the evaluation are presented in Table 5.4.

Figure 5.4: Predicted profit from the CHP plant using MISO layer network

Feedstock	South Africa Fuel [WFC]*		Nigerian Fuel [WFC]**	
	Highest Profit (USD million)	Lowest Profit (USD Million)	Highest Profit (USD Million)	Lowest Profit (USD Million)
Coal + SCB Coal + CC		5.68		1.95
Coal + PSD	6.27		2.37	
Coal + WT				
	South African Fuel [WOFC]		Nigerian Fuel [WOFC]	
Coal + SCB Coal + CC		7.48		4.53
Coal + PSD				
Coal + WT	8.00		4.82	

*: Exchange rate of $1.00 = ZAR14.00 **: Exchange rate of $1.00 = NGN350.00;
USD=$=United States Dollars; WOFC: Without Feedstock Costing; WFC: With Feedstock Costing; CC: Corn Cob; SCB: Sugarcane Bagasse; PSD: Pine Sawdust; WT: Waste-Tyre

5.3.4. Modelling of South African fuel: Gaseous Emission model

Table 5.5 presents the calculated input and output variables used for predicting the gaseous e missions in the plant. The negative sign shown on some of the compounds indicates a higher order of gaseous emission reduction as a result of fuel blends.

Table 5. 5: Input and Output variables used in the ANN: Emission Prediction

Parameters	Coal + SCB	Coal + CC	Coal + PSD	Coal + WT
		Nigerian Feedstock		
		Range: Input Variables		
AF [Ton/YR]	2.91 – 2.47	2.99 - 2.49	2.75 - 2.47	2.45 -2.30
LHV [MJ/kg]	24.72 – 29.15	24.01 - 28.89	26.15 - 29.86	29.42 – 31.03
		Range: Output Variables		
CO [kg]	-33.62 – (-40.52)	-33.97 – (-41.75)	-33.45 – (-38.26)	-31.40 – (33.90)
CO_2 [kg]^T	5.84 - 9.39	5.84 – 9.39	5.84 – 9.39	5.85 – 9.39
NO_X [kg]	-111.36 – (-154.36)	-110.61 – (-159.70)	-110.61 – (-144.51)	-101.90–(-125.07)
SO_2 [kg]	69.28 – 111.01	69.28 – 111.01	69.29 – 111.01	69.31 – 111.02
		South African Feedstock		
		Range: Input Variables		
AF [Ton/YR]	4.05 – 2.47	4.09 – 4.20	3.65 – 3.95	3.06 – 3.57
LHV [MJ/kg]	17.58 – 17.77	17.15 – 17.60	19.72 – 18.27	23.42 – 31.03
Range: Output Variables				
CO [kg]	-56.94 – (-57.35)	-56.57 – (-58.81)	-51.03 – (-54.51)	-42.55 – (-49.30)
CO_2 [kg]^T	5.81 – 9.35	5.81– 9.35	5.82 – 9.36	5.83–9.36
NO_X [kg]	-209.29 – (-227.53)	-233.88 – (-211.74)	-200.03 – (-202.19	-162.69–(-179.32)
SO_2 [kg]	69.21 – 110.91	69.21 – 110.91	69.24 – 110.92	69.27 -110.94

AF: Amount of Feedstock; LHV: Lower Heating Value; SCB: Sugarcane Bagasse; CC: Corn Cob; Coal + WT; PSD: Pine Sawdust; ^{T}: The values in the row are in thousand).

Levenberg-Marquardt (L-M) algorithm MISO layer network was used to evaluate the emissions from a 10 MW capacity co-gasification energy plant employing Coal +CC, Coal + PSD, Coal + SCB, and Coal + WT as fuels respectively. CO, CO_2, NO_X, and SO_2 were the major environmental pollutants that were considered. In terms of CO_2 and SO_2 emissions, Coal + WT produced the

highest amounts of around 9363.20 kg and 110.94 kg, respectively. The result was expected (SO_2 emissions) because the fuel has higher Sulphur content when compared to other fuels studied, while the lower amounts of SO_2 were emitted from Coal + SCB, Coal + CC and Coal + PSD because of little or no Sulphur content in the biomass. The amounts of CO and NO_X generated from all the feedstocks were insignificant, with Coal + SCB having the highest of about -57.35 kg and -227.53 kg, respectively.

The result of the MISO layer network assessment is presented in Table 5.6. It can be observed that the MSE obtained from all the fuels, WFC were low except that of the Coal + WT that produced 1.22. The more the value of the MSE tends to zero, the better. The effect has reflected in the correlation coefficient (R^2) of training, validation, and testing for all the fuels investigated where the R^2 were above 90 % excluding the R^2 of Coal + WT. This may be attributed to the dataset used for training the network which has wider data range compared to others. Similarly, Coal + WT has the lowest epoch of 3 while Coal + SCB, Coal + CC, and Coal + PSD have 4, 7, and 9 epochs respectively, implying that the convergence characteristics performance of the fuels is more stable than that of Coal +WT. However, the ANN model is capable of predicting the four major pollutants emitted from the power plant using South African feedstocks.

Table 5. 6: ANN model results on emissions: 10 MW CHP Co-gasification power plant

Feedstock	BR	Algorithm	Neurons**	MSE	Epoch	T*	V*	Ts*
South African Coal [Matla Mine]: WFC								
Coal +SCB			6	0.02	3	0.98	0.97	0.95
Coal + CC		L-M	7	0.03	12	0.96	0.93	0.91
Coal + PSD	1:1	[MISO]	7	0.02	4	0.98	0.96	0.98
Coal + WT			6	0.11	3	0.95	0.94	0.90
Nigerian Coal [Onyeama Mine - Enugu] WFC								
Coal + SCB			6	0.03	2	0.96	0.95	0.96
Coal + CC		L-M	7	0.05	5	0.94	0.97	0.93
Coal + PSD	1:1	[MISO]	7	0.03	11	0.97	0.98	0.95
Coal + WT			6	0.01	6	0.90	0.92	0.90
South African Coal [Matla Mine]: WOFC								
Coal + SCB			6	0.18	6 8	0.97	0.96	0.94
Coal + CC		L-M	7	0.10	3	0.92	0.91	0.90
Coal + PSD	1:1	[MISO]	7	0.41	5	0.96	0.95	0.96
Coal + WT			6	2.06		0.88	0.89	0.92
Nigerian Coal [Onyeama Mine - Enugu] WOFC								
Coal + SCB			6	0.20	3 5	0.94	0.95	0.97
Coal + CC		L-M	7	0.12	12	0.96	0.97	0.95
Coal + PSD	1:1	[MISO]	7	0.66	6	0.97	0.95	0.96
Coal + WT			6	2.48		0.87	0.88	0.89

L-M: Levenberg Marquardt; MISO: Multiple Input-Single Output; *: Correlation Coefficient (R^2); MSE: Mean Square Error: **: Number of neurons in the hidden layer; WFC: With Feedstock Costing, T*: Training; V*: Validation, Ts*: Testing

5.3.5. ANN Modelling of Nigerian Feedstock: Gaseous emission model

The same condition used for training the South African gaseous emission dataset was also employed for the training of Nigerian emission datasets. The MSE from blends of Coal and biomass (i.e. Coal + SCB, Coal + CC, and Coal +PSD) were lower than that of the MSE of Coal + WT. It is shown Table 5.7. Similar result was obtained from the South African feedstock.

Furthermore, the epoch obtained from Coal + WT was the lowest, while Coal + PSD have the highest epoch amongst the fuels investigated. Secondly, all the epochs obtained from other fuels are higher than the epoch obtained from Coal + WT. The implication is that Coal + WT has lower

convergence performance characteristic when compared to the other fuels studied. The reason had been explained in section 3.2. More so, the R^2 obtained from the validation and testing of Coal + WT were 89 % and 88 %, respectively. This is in the same trend with that of South African feedstock, thus indicating that the dataset employed for the training of the networks were similar. Meanwhile, all the R^2 obtained from the fuels except Coal + WT were far above 90 %, and with Coal + PSD having the highest R^2 of 98%, 98 %, and 99 % for training, validation and testing, respectively.

5.3.6. Comparison of South African and Nigerian feedstock: Gaseous emission prediction

The gaseous emission assessment was carried out with the South African and Nigerian feedstocks based on the feedstock that generated the lowest or highest amounts of CO, CO_2, NO_X, and SO_2 in the plant. The model result shown in Table 5.7 effectively describes the emissions from the feedstocks of the two countries. It can be observed that the results of the emission from both countries followed similar trend in terms of the highest and lowest amounts of emissions from each of the fuels, but the exact values the emitted gases vary slightly. For example, the CO_2 emitted by the South African fuel (Coal + WT) was 9363.20 kg, while it was 9390.08 kg for the Nigerian Coal + WT; about 1.36 % higher than the CO_2 emitted from the plant using the South African fuel. The variation of the result is attributed to the difference in the physiochemical properties of the fuels due to different geographical regions. The details of the emissions analysis are displayed in Table 5.7.

Table 5. 7: Predicted emissions from the CHP plant using MIMO layer network

Feedstock	CO [kg]	CO_2 [kg]	NO_X [kg]	SO_2 [kg]	CO [kg]	CO_2 [kg]	NO_X [kg]	SO_2 [kg]
South Africa Fuel								
	Highest Emissions					Lowest Emissions		
Coal + CC	-58.81		-233.88			5809.75		69.21
Coal + WT		9363.20		-110.94	-42.55		-169.69	
Coal+ SCB								
Coal+ PSD								69.21
Nigerian Fuel								
Feedstock	CO [kg]	CO_2 [kg]	NO_X [kg]	SO_2 [kg]	CO [kg]	CO_2 [kg]	NO_X [kg]	SO_2 [kg]
	Highest Emissions					Lowest Emissions		
Coal + CC	-41.75		-159.70			5837.36		69.28
Coal + WT		9390.08		111.02	-31.40		-101.90	
Coal +SCB						5837.36		69.28
Coal +PSD								

PSD: Pine Sawdust; WT: Waste-Tyre; SCB: Sugarcane Bagasse; CC: Corn Cob

5.4. Results of this study compared with literature

In this study, an assessment of gaseous emissions and profit produced from different solid fuels was carried out using a co-gasification CHP plant. A few studies have been reported on emissions and profits using different feedstock and operating conditions [238,10-11,7-14], but most of these works were focused on experimental and empirical model estimations. The capacities of the plant studied by the aforementioned authors were in the range of 5 – 20 MW using biomass and blends of biomass and coal as fuels. The energy conversion efficiency of the plants was between 35 – 50 %. For instance, Malek et al [238] employed the NPV, IRR, and PBP models to determine the emission reduction in a 10 MW biomass-based CHP plant in Malaysia. According to the authors, 50,130.00 t CO_2/y, 750.00 t SO_2/y, 218.65 t NO_X/y, and 22.83 t CO/y emissions were produced from the plant when compare to the existing energy mix, and empty fruit bunch was the optimum feedstock amongst the fuels studied. Ozonoh et al. 2018 [13] used a 5 MW CHP and feedstock of South African origin to study the emissions from the energy plant. About 2910.74 kg CO_2/y, -25.58 kg CO/y, 34.60 kg SO_2/y, and - 100.04 kg NO_X/y were produced using a blend of Coal + PSD as

fuel, and it was the optimum fuel for all the fuels investigated.

Comparing the works of Malek et al. [238] and (Ozonoh et al. [13]. with the current study, an ANN model was employed to predict the emissions and profits from the power plant for the current study, as against an empirical model that was used by the aforementioned authors. Furthermore, biomass and blends of biomass were used by the previous authors respectively, but in the current work, blends of coal and biomass was employed. From the present study, about 5840.78 kg CO_2/y, -33.45 kg CO/y, 69.29 kg SO_2/y, and -110.61 kg NO_X/y emissions were obtained from Nigerian feedstock, while 5821.50 kg CO_2/y, -51.03 kg CO/y, 69.24 kg SO_2/y, and -200.03 kg NO_X/y were produced from South African feedstock. The findings obtained by the previous researchers were quite interesting, but a commercial modelling tool could be better. Consequently, ANN was employed in this article to estimate the emissions and profits in the plant. However, the performance efficiency of the ANN model was attractive when compared to the empirical models and experimental methods used by the previous researchers based on the performance evaluation results.

5.5. Concluding remarks

The prediction of gaseous emissions and profits from biomass, tyre, and coal fired co-gasification CHP Plant using Artificial Neural Network (ANN) was carried out for 20-year-investment period using South Africa and Nigeria as case studies. In this study, twenty datasets with emissions and profits from both countries were employed in the model development using Coal + CC, Coal + SCB, Coal + PSD, and Coal + WT blended at a ratio of 1:1, 3:2, and 4:1, respectively. A MISO layer network was used. The following conclusions were made:

- The profit obtained from the South African feedstock were about 45.18 % and 36.83 % ($3,900,000.07 and $3,179,184.49) higher than that of the Nigerian feedstock, WFC and WOFC.
- The CO_2, NO_X, & SO_2 emissions from Nigerian Coal + PSD and Coal + Torrefied WT were 9327.13 kg, -144.51 kg, & 111.01 kg and 9390.00 kg, -125.07, & 111.02 kg respectively, while the CO_2, NO_X, & SO_2 emissions from same feedstock from South Africa were 9355.53 kg, -202.19 kg, & 110.92 kg and 9363.20 kg, -179.32 kg, 110.94 kg, respectively. The variations in the gaseous emission was an indication of different physio-chemical properties of the feedstock due to different geographical locations.
- The MSE for the profit earned from Nigerian fuels was lower than the MSE obtained from SA fuels, while the R^2 from Nigerian fuel was higher when compared to the SA

fuel. Considering the emissions from the plant, the MSE for the emissions from SA fuels were higher than that of Nigeria, while the same range of result was obtained for the R^2 for both countries, but the emissions generated from Coal + WT was the highest for all the fuels studied.

Chapter 6: Maximization of profit in a co-gasification CHP plant through biomass torrefaction

6.1. Introduction

This chapter focused on how profit in a co-gasification combined heat and power (CHP) was maximized via biomass torrefaction. It should be recalled that chapter 3 of this thesis elaborated amongst other processes the biomass torrefaction as regards to fuel quality enhancement. It is therefore necessary in this chapter, to determine the potentials of torrefied biomass in energy production. This was carried out by estimating the profits maximized in the energy plant due to biomass torrefaction. It is important to state that a section of this chapter has been presented at the European Biomass Conference (EUBC) (Lisbon, Portugal).

It has been proved that one of the promising pathways of producing energy from biomass is its co-gasification with fossil fuels (e.g. coal) [241]. The process could be carried out in plants such as Integrated Gasification Combined Circle (IGCC) or Combined Heat and Power (CHP) plant (either in a newly design or an existing power plant). An existing power plant is considered as a transitional alternative for a total carbon-free power sector that offers advantage in comparison to using biomass in a dedicated power plant with high thermal efficiency, lower capital costs and less operational risk. However, a biomass-fed power plant and coal-fired power plant can be used interchangeably, but slight modification in the design will be required to account for periods when biomass would be un-available [241]. Often, investors may like to invest in plants that require minimal expenditures for effective operations. The use of existing coal-fired power plant for biomass energy generation therefore, could reduce the technical challenges and increase the biomass power capacity [242]. An example of such challenges is the CO_2 abatement cost via Carbon Capture and Storage (CCS) that is on the high side for coal-fired plant compared to biomass-fired plant. Irrespective of using an existing power generating plant, potential investors are equally interested in energy conversion processes that yield more profits.

Biomass as feedstock for energy production is different from coal in terms of handling and combustion characteristics due to the compositional properties. For instance, biomass has higher moisture content, lower energy density, higher chlorine and potassium contents, etc [242], and these could negatively impact on the efficiency of the energy conversion system (e.g. gasifiers and boilers). However, if biomass is co-gasified with traditional fuels such as coal, with reasonable coal-to-biomass ratio, a reasonable efficiency of the energy conversion could be maintained. Irena [241] reported that using blend ratio not above 90:10 could be promising while Bada et al. [243] &

Ozonoh et al. [13] found that 50:50 coal-to-biomass ratio is reasonable for synergetic effect, costs and emission reduction in power plants. Recently, some studies that were carried out using different energy conversion technologies and processes have shown that torrefaction is attractive in terms of increasing the quality of the fuel. The ratio of coal-to-biomass during co-firing or co-gasification is also increased because of fuel pre-treatment. In this case, the hemicellulose matrix and fibres structure of the fuel are decomposed, thus accounting for its de-polymerisation and loss of original nature of the raw fuel [244].

Torrefaction has been studied using different energy conversion technologies and processes and reported to be instrumental to enhancing quality of fuel [245,246]. Generally, the benefits associated with torrefaction include higher energy density (heating value), lower atomic O/C & H/C ratios and moisture content, higher hydrophobicity, enhanced grindabilty, and better uniform properties of biomass fuel [245]. From transportation point of view, the bulk density is reduced and a long-term storage opportunity - without quality degradation is provided. Particularly, an additional profit is gained from the energy plant due to minimal expenditure in the logistics. Further, the use of varieties of feedstock sources in the system (e.g. gasifier) is feasible because of uniformity in the upgraded fuel. It has been reported by Peng et al. [246] that torrefaction of biomass improves the gasification thermal efficiency and reduces tar production due to removal of oxygenated volatile compounds from the biomass during the process. Therefore, investors most times, indicate much interest in investment plans and operating conditions that will enable them to earn more profits at lesser risks. They consider such parameters prior to the venturing into the business.

Several researchers including Park et al. [247], Chen et al. [248], Lu et al. [249], Yan et al [250] Arias et al. [251], and Phanphanich and Mani [252] have studied biomass torrefaction using different kinds of biomass. The reports from these authors have shown an improvement in the quality of the fuel (e.g. energy density) when compared to that of the raw fuel. Secondly, other researchers have reported the positive effect of upgrade of fuel quality on the profitability and environmental impact of power plants [242,253,254].

Many of the studies were carried out using different kinds of biomass without considering blends of these biomass materials with conventional source of fuel like coal. It was expected from the aforementioned works that the authors would consider how the profits earned in the plant reduced over an investment period due to time value of money (TVM), but it was not reported. In this study, the profits earned for a 20-years-investment period in a CHP co- gasification plant were estimated using blends of coal and torrefied biomass as feedstocks. The percentage reduction in the profit over

the time period was equally emphasized. Importantly, the outcome of this investigation will provide statistical evidence that will assist professionals in this sector in critical decision making and as well, open a new window for further R&D in this area.

6.2. Experimental Procedure

In this study, corn cob (CC), sugar cane bagasse (SCB), and pine saw dust (PSD) were torrefied and blended with coal using coal-to-biomass ratios of 50:50, 71:29, & 80:20. The results of the physio-chemical properties and biomass pre-treatment were reported in details in chapter three. The heating value (LHV) and moisture content (MC) of the fuels were used to estimate the feed-rate and annual feedstock requirement of the plant. An estimation of the earned profit from a typical CHP plant for a 20-year-investment period divided into four terms: A, B, C, & D was carried out using the Net Present Value (NPV) and Payback Period (PBP) models as described in section 2.2. The operating cost models considered were with feedstock costing (WFC) and without feedstock costing (WOFC).

6.2.1. Profitability evaluation

To appraise the profits earned in the co-gasification plant, financial intelligence tools used in project management (e.g. Net Present Value (NPV) and Payback Period (PBP) were employed. The model equations for the NPV and PBP were expressed in chapter [238,13], respectively. The profitability evaluation of the plant was carried out for a 20-year period. For emphasis, the 20-year-investment period was divided into four investment terms. It includes term A, B, C, & D, and they are represented by $1^{st} – 5^{th}$, $5^{th} – 10^{th}$, $10^{th} – 15^{th}$, & $15^{th} – 20^{th}$ year. Furthermore, two financial models were considered. They are with Feedstock. Costing (WFC) and Without Feedstock Costing (WOFC) and both financial cases had been defined in the techno-economic analysis presented in Chapter 10. The profit earned at the end of the first year of the investment was used to determine the percentage decrease in the profit as the business progressed. In this case, the Time Value of Money (TVM) on the investment for each of the terms was considered, and its effect on the profit made was determined based on the NPV. Finally, the profit accrued from co-gasification of coal + biomass was compared with that of coal + torrefied biomass to show that biomass torrefaction resulted to an increase in profit of the plant.

6.3. Results and Discussion

6.3.1. Most viable process & profit estimations

The results obtained from the torrefaction experiment and feedstock characterisation are depicted in Table 6.1. The optimum process condition was determined based on the results of the HHV, solid yield, energy yield and the enhancement factor (EF). It is necessary to emphasis that objective function optimization technique was not employed in determining the optimum; referred to as most viable operating conditions in this section and thesis. The optimum process condition was confirmed only by statistically comparing the results/values obtained from the entire process. The order for the optimum process condition are 50:50 (300 ^{O}C at 45 min) > 71:29 (300 ^{O}C at 45 min) > 80:20 (300 ^{O}C at 60 min), while the order for the optimum feedstock are Coal + PSD > Coal + SCB> Coal +CC. Three torrefaction temperature regimes were used for the investigation, but the details of the sever temperature regime employed for the profit evaluation only, was reported in this chapter as shown in Table 6.1. Other temperature regimes investigated can be found in the Appendices.

Table 6. 1: Characterisation and torrefaction experimental results: Sever temperature regime

Feedstock [-]	Temp [^{O}C]	Time [min]	HHV of C+RB	HHV of C+TB	Solid Yield [%]	Energy Yield [%]	EF [-]
	Mixing Ratio: 50:50						
Coal + SCB	300	45	18.72	25.83	54.15	74.73	1.38
Coal + CC	300	45	18.01	24.31	56.68	76.52	1.35
Coal + PSD	300	45	20.05	28.27	52.44	73.94	1.41
	Mixing Ratio: 71:29						
Coal + SCB	300	45	18.65	24.99	62.71	84.03	1.34
Coal + CC	300	45	18.36	24.24	65.28	86.17	1.32
Coal + PSD	300	45	19.18	26.08	59.45	80.85	1.36
	Mixing Ratio: 50:50						
Coal + SCB	300	30	18.65	23.52	76.22	96.04	1.36
Coal + CC	300	30	18.26	22.64	78.55	97.40	1.24
Coal + PSD	300	30	19.44	25.47	74.18	97.18	1.31
	Mixing Ratio: 80:20						
Coal + SCB	300	60	18.67	24.46	69.34	90.84	1.31
Coal + CC	300	60	18.26	23.37	73.15	93.63	1.28
Coal + PSD	300	60	19.44	25.86	66.14	87.97	1.33

E.F: Enhancement Factor; SCB: Sugarcane Bagasse; CC: Corn Cob; PSD: Pine Saw- Dust; C: Coal; RB: Raw Biomass; TB: Torrefied Biomass; Temp: Temperature

The results in Table 6.1 were used to determine the feed-rate and annual feedstock requirements of the power plant, from which the profit earned in the plant, were assessed using the NPV and PBP model calculations adopted from elsewhere [13]. The PBP was employed to estimate the time taken to recover the costs invested on the project, while the NPV was used to evaluate the value of money with respect to the cash flows for the term under consideration. This determines the actual profit. Table 6.2 is the profit made from term A to term D using WFC at coal-to-biomass ratio of 50:50. From Table 6.2, it took around 3 - 4 months for the venture to payback the cost invested in it. Also, the results of the NPV indicated that the four terms (A – D) studied were viable.

Table 6. 2: Profit earning for term A – term D using WFC: 50:50

Feedstock	Investment cost (USD million/yr)	Profit earning (USD million/yr)	PBP [yr]	NPV (USD million/yr)	Investment term
Coal + SCB	2.24	6.71	0.3	4.15	1st
Coal + CC	2.37	6.58	0.4	4.90	
Coal + PSD	1.89	7.05	0.3	4.82	
Coal + SCB	2.24	6.71	0.3	3.01	5th
Coal + CC	2.37	6.58	0.4	2.79	10th
Coal + PSD	1.89	7.05	0.3	3.63	
Coal + SCB	2.24	6.71	0.3	1.88	
Coal + CC	2.37	6.58	0.4	1.67	15th
Coal + PSD	1.89	7.05	0.3	2.44	
Coal + SCB	2.24	6.71	0.3	9.85	
Coal + CC	2.37	6.58	0.4	7.97	
Coal + PSD	1.89	7.05	0.3	1.50	
Coal + SCB	2.24	6.71	0.3	2.87	20th
Coal + CC	2.37	6.58	0.4	1.11	
Coal + PSD	1.89	7.05	0.3	7.64	

USD: United State Dollars; USD1.00 = ZAR14.00; ZAR: South African Rand. PBP: Payback Period; NPV: Net Present Value; WOFC: Without Feedstock Costing; CC: Corn Cob; SCB: Sugarcane Bagasse; PSD: Pine Sawdust.

Table 6.3 represents the profit made in the plant for term A to term D using WOFC at coal- to-biomass ratio of 50:50. From Table 6.3, it can be seen that the capital cost investment for the project was recovered at the first month of each of the evaluation year, as against the WFC that took 3 – 4 months. The results of the NPV equally affirmed the viability of the business for all the terms investigated.

Table 6. 3: Profit earning for term A – term D using WOFC: 50:50

Feedstock	Investment cost (USD million/yr)	Profit earning (USD million/yr)	PBP (yr)	NPV (USD million/yr)	Investment term
Coal + SCB	1.01	7.98	0.1	6.55	1st
Coal + CC	1.06	7.89	0.1	6.45	
Coal + PSD	0.90	7.94	0.1	6.76	
Coal + SCB	1.01	7.98	0.1	5.21	5th
Coal + CC	1.06	7.89	0.1	5.11	10th
Coal + PSD	0.90	7.94	0.1	5.40	
Coal + SCB	1.01	7.98	0.1	3.86	
Coal + CC	1.06	7.89	0.1	3.78	15th
Coal + PSD	0.90	7.94	0.1	4.04	
Coal + SCB	1.01	7.98	0.1	2.81	
Coal + CC	1.06	7.89	0.1	2.73	
Coal + PSD	0.90	7.94	0.1	2.97	
Coal + SCB	1.01	7.98	0.1	1.98	20th
Coal + CC	1.06	7.89	0.1	1.91	
Coal + PSD	0.90	7.94	0.1	2.13	

PBP: Payback Period; NPV: Net Present Value; WOFC: Without Feedstock Costing; CC: Corn Cob; SCB: Sugarcane Bagasse; PSD: Pine Sawdust; USD: United State Dollars; USD1.00 = ZAR14.00; ZAR: South African Rand

As evidenced in Table 6.2, it took a longer time to recover the money invested in the business WFC than WOFC. It was attributed to the logistics cost (e.g. loading & transportation) associated with the WFC estimations. However, the two financial cases (WFC & WOFC) were profitable for the

terms studied.

The profits earned at the end of the 20th year of term D using coal-to-biomass blend ratio of 71:29 and 80:20, WFC and WOFC, respectively are presented in Table 6.4. From Table 6.4, it took between 4 to 6 months to recover all the money invested in the business, WFC, while only 1-month was taken to recover the investment cost, WOFC. It can be seen from Table 6.4 as well, that a profit of between USD5, 902,292.46 – USD6, 489,659.30 was earned. The IRR of 5 ± 1 % and 2 ± 3 % for South Africa electricity price of 0.14 $/c kWh. From the point of view of the investment cost (IC), it was a better project, but from the future value of money point of view, the profits were gradually eroding as shown in the results of the NPV. The implication is that the project is not worth pursuing. In comparison with the result of profits earned WOFC, the venture is more attractive based on the values of the NPV.

Table 6. 4: Profit evaluation at the end of the 20th Year (Term D): WFC & WOFC

Feedstock	B.R	AOF (Kiloton/yr)	IC (USD million/yr)	P.E (USD million/yr)	PBP (yr)	I.T (USD million/yr)
Coal+ SCB		32.8	2.72	6.23	0.4	-37.10
Coal + CC	71:29*	33.9	2.66	6.28	0.4	-0.30
Coal + PSD		30.9	2.46	6.49	0.4	-0.13
Coal +SCB	80:20*	34.8	3.26	5.69	0.6	-0.23
Coal + CC		35.6	3.34	5.61	0.6	-23.00
Coal + PSD		33.4	3.05	5.90	0.5	-0.82
Coal + SCB	71:29**	32.8	1.11	7.83	0.1	-18.40
Coal + CC		33.9	1.15	7.80	0.1	-17.90
Coal + PSD		30.9	1.05	7.90	0.1	-19.30
Coal + SCB		34.8	1.11	7.84	0.1	-18.40
Coal + CC	80:20**	35.6	1.14	7.81	0.1	-18.00
Coal + PSD		33.3	1.06	7.88	0.1	-19.10

AOF: Amount of feedstock; B.R: Blending Ratio; I.T: Investment terms; IC: Investment cost; PE: Profit earning; PBP: Payback Period; WFC: With Feedstock Costing; **: WOFC: Without Feedstock Costing; CC: Corn Cob; SCB: Sugarcane Bagasse; PSD: Pine Sawdust. ZAR: South African Rand; PBP: Payback Period; NPV: Net Present Value; USD: United State Dollars; USD1.00 = ZAR14.00; ZAR: South African Rand.

6.4. Effect of time value of money on profit

The influence of TVM on profit earning for the four investment terms were carried out using Coal + SCB, Coal + CC and Coal + PSD, but only Coal + PSD and Coal + CC results are reported in this paper because they represented the highest and lowest profits earned in the power plant for the considered investment period, respectively. The profits made from Coal + PSD and Coal + CC decreased with an increase in time (investment period) and it is displayed in percentage basis in Figure 6.1 and Figure 6.2, respectively. The results have shown that the reduction in the profit earned in the plant increased from 1^{st} – 5^{th} (term A) through 15^{th} – 20^{th} (term D) year by around 14.09 - 32.48 % and 16.62 - 75.46 %, respectively. The higher the percentage, the lower the profits based on the NPV. This can be well understood by examining the values of the NPV of each of the terms in Table 6.1, and not the actual amounts of profits. It has revealed the effect of TVM on the overall investment and profit. Meanwhile, the result could offer substantive information that will assist investors and stake-holders in the area in decision making.



Figure 6. 1: Profit reduction profile for Coal + PSD: 1^{st} – 5^{th} through 15^{th} – 20^{th} Year

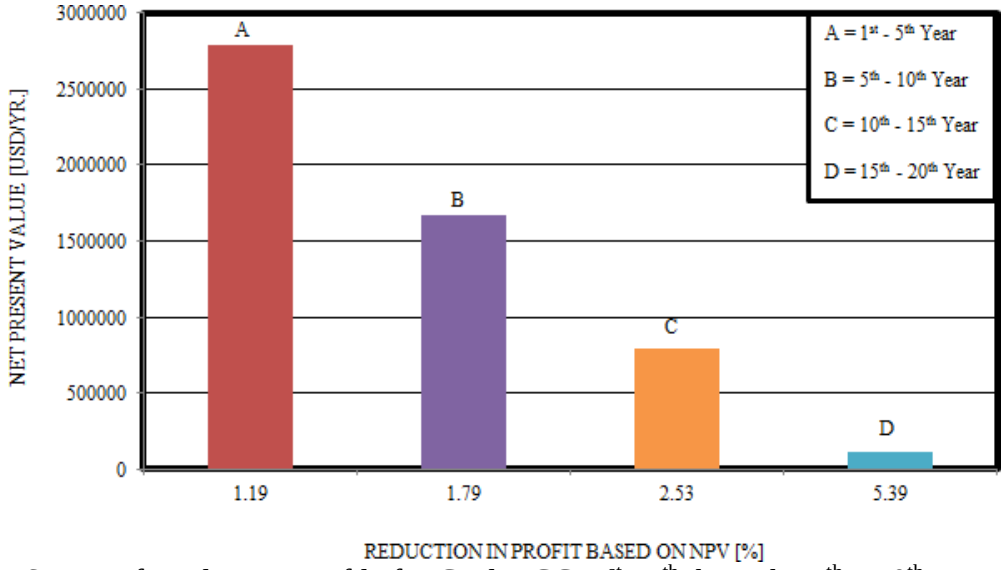


Figure 6. 2: Profit reduction profile for Coal + CC: 1st –5th through 15th – 20th Year

6.5. Effect of blend ratio on profit

Effect of blend ratio on the amount of profit earned was evaluated at the 15th year (in term C) using coal-to-biomass ratios of 71:29 and 80:20 are shown in Figure 6.3 and Figure 6.4, respectively. From Figure 6.3, all the feedstocks used for the power production were very promising based on the values of the NPV, but the highest profit was made from Coal + PSD. The result is expected considering the heating value and other characteristics of the fuel (Table 6.1). From Figure 6.4, it can be observed that the NPV of Coal + CC and Coal + PSD were negative. The implication is that the investment costs were not recovered, hence; investors should not consider the blend ratio as a feasible option. A similar trend of result was observed in our previous work where we carried out the techno-economic analysis of blends of coal and un-treated (raw) biomass, and waste-tyre in a 5-MW CHP plant [13].

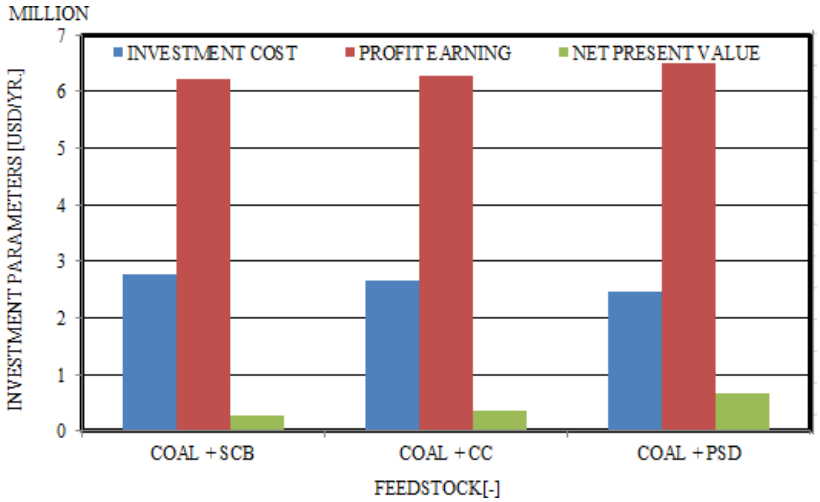


Figure 6. 3: Influence of blend ratio on profit earning: Blend ratio: [71:29]

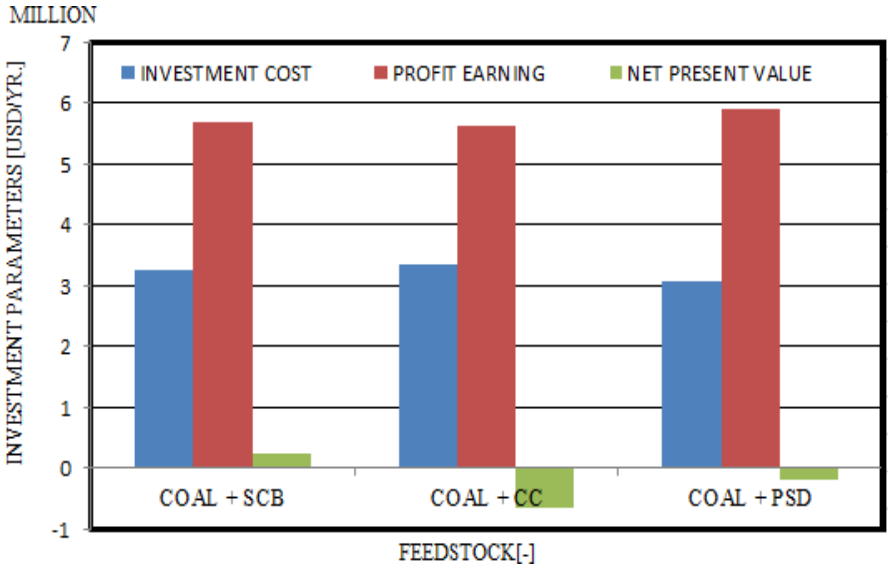


Figure 6. 4: Influence of blend ratio on profit earning: Blend ratio: [80:20]

6.6. Sensitivity analysis

The sensitivity analysis of the profit maximization in the plant was carried out using WFC in the 20th year of term D. Table 6.5 highlights the standard deviation, standard error, and variance of the investment parameters (Annual feedstock Requirement (AFR), Investment Cost (IC), Profit Earning (PE) and Net Present Value (NPV)). Table 6.6 also, describes the mean and Relative Standard Error (RSE) of the investment parameters. It can be seen that the profits decreased as the mean of the investment cost (IC) increased. This increase equally affected the annual feedstock requirement and the NPV, respectively. The increase in the amount of feedstock increased the investment cost, as well. It is evidenced in the negative values of the NPV for 71:29 and 80:20 coal-to-biomass blend

ratios. Similarly, the increase in the blend ratio increased the annual amount of feedstock required and cost of investment in the plant, thus; resulted to reduction in the profits earned. Based on the aforementioned facts, the two most influential parameters affecting the profit are the investment cost (IC) and blend ratio. Following them is the annual feedstock requirement (AFR) that is dependent on the blend ratio, and all these investment parameters determined the NPV.

Table 6. 5: Sensitivity analysis at 20th year, WFC

Annual feedstock requirement (Ton)/yr			Investment cost (USD/yr.)			
X	$\bar{X}$	x - $\bar{x}$	X	$\bar{X}$	x - $\bar{x}$	B.R
[Thousand]	[Thousand]	[Billion]	[Thousand]	[Thousand]	[Billion]	
2.89 *	2.84	28.6	2.24	2.17	7.49	
3.04 **	2.84	413	2.37	2.17	56.1	
2.58***	2.84	6.9	1.89	2.17	105	
Variance		550	Variance		84.1	
Std. Dev		2.3 x 10^{-13}	Std. Dev		2.45 x 10^{-13}	
Std. Error		1.17 x 10^{-14}	Std. Error		1.23 x 10^{-13}	
Profit Earning (USD/yr)			Net Present Value (USD/yr)			1:1
[Million]	[Million]	[Billion]	[Million]	[Million]	[Billion]	
6.07*	6.78	7.49	0.29	0.39	14.2	
6.58 **	6.78	56.1	0.11	0.04	106	
7.05***	6.78	105	0.078	0.04	198	
Variance		84.1	Variance		159	
Std. Dev		0.25	Std. Dev		0.34	
Std. Error		0.12	Std. Error		0.17	

*: Coal + SCB; **: Coal + CC; ***: Coal + PSD; X: Estimated variable (e.g. Annual feed Requirement, Investment Cost, cash flow, Net Present Value); $\bar{X}$: mean of the variable; Std.:

standard; USD: United State Dollars; USD1.00 = ZAR14.00; ZAR: South African Rand; B. Ratio: Blending ratio; Std. Dev: Standard Deviation; Std. Error: Standard Error.

Table 6. 6: Mean NPV and RSE of the investment parameters at 20th Year using WFC

B. Ratio	Annual Feed Requirement		Investment Cost		Profit Earning		Net Present Value	
	Mean AFR [kiloTon/ Yr.]	RSE of AFR [%]	Mean IC [USD/Yr.] [In Million]	RSE of IC [%]	Mean PE [USD/Yr.] [In Million]	RSE of PE [%]	Mean NPV [USD/Yr.] [Thousand]	RSE of NPV [%]
50:50	28.4	0.04	2.17	0.06	6.78	0.02	38.7	0.44
79:21	32.5	0.02	2.61	0.03	6.33	0.01	-22.7	-0.42
80:20	3.46×10^4	0.02	3.26	0.02	5.73	0.01	-6.06×10^4	-0.62

B. Ratio: Blending ratio; RSE: Relative standard error; AFR: Annual Feedstock Requirement; IC: Investment Cost; PE: Profit Earning; NPV: Net Present Value; USD: United State Dollars; USD1.00 = ZAR14.00; ZAR: South African Rand; N. Ratio: Blending Ratio.

The current work is compared with the literature with respect to the feedstock used, torrefaction process experimental conditions, economic assessment and type of energy plant used. Retizelas & Li [225] investigated the environment emissions and economic benefits of using 100 % biomass (palm kernel shell) and 50:50 coal-to-biomass ratio. The authors found that co-gasification of biomass and coal has marginal profit when compared to 100 % biomass gasification having higher profit because of price of coal. Prando et al. [256] used multi-stage modelling technique of a chemical equilibrium model to simulate the energy efficiency due to biomass torrefaction employing a CHP plant, internal combustion engine and gas turbine. The energy efficiency in the plants was enhanced because of torrefaction. Ozonoh et al. [13] studied the profits made from a 5-MW CHP plant using mixture of coal and raw biomass, but torrefied biomass was not used to carry out the evaluation as against the current paper. Caputo et al. [237] and Bridgwater et al. [257] compared the feasibility of power production in power plant with 5-MW capacity using three different energy conversion processes. They assessed the operating efficiency of the plant employing different biomass types, while Malek et al [238] used some selected biomass to investigate the emissions, profits, and the viability of the feedstock for a 10-MW capacity CHP. This paper examined the profits earned from 10-MW CHP plant, percentage reduction in profits earned over investment terms, and effects of blend ratio on the profits for 20-year-investment period. The fuel used in this work was coal mixed with torrefied biomass.

6.7. Comparism of this work and literature

A comparison of this study and literature is presented in Table 6.7. From Table 6.7, Starfelt et al [258] stated that integrating a torrefaction unit into an existing CHP plant was attractive and that using torrefied biomass materials and coal as feedstock was profitable, while the techno-economic model result employed by De & Assadi [259] revealed that the electricity cost per unit emission of CO_2 decreased significantly with increasing plant capacity (15 – 50 MW) and that the reduction in CO_2 emission was due to use of torrefied. Selected biomass materials and torrefied biomass mixed with coal were used by Malek et al. [238] and (Kohl et al. [260] to study the profit and emissions and performance efficiency of a CHP plant respectively. Malek and his co-workers affirmed that palm-kernel empty fruit bunch was the most viable feedstock studied and there was reduction in gas emission and higher profit in the plant when compared to the existing energy mix, but the result of the investigation of Kohl and his research group have shown that the amount of heat generated in the plant for district heat supplies increased from 22 – 38 %. Both Ozonoh et al. [13] & Prando et al. [256] studied the profitability and energy conversion efficiency of a 5-MW and 10-MW CHP employing raw coal and biomass as fuels, respectively. It was observed by Ozonoh et al. [13] that Coal + PSD and coal-to-solid waste ratio of 1:1 were the optimum feedstock and blend ratio respectively, and the amount of gases emitted were very low when compared to solitary gasification of coal. Similarly, there was an enhancement in the energy efficiency of the plant according to Prando et al [256]. Meanwhile, Rentizelas & Li [255] examined the profitability of a CHP using Coal and biomass as fuel and confirmed that co-gasification of biomass and coal produced marginal profit when compared to 100 % use of biomass as fuel in the plant. Particularly, the difference between this study and the literature discussed above are based on the parameters, feedstock, and investment period studied. The profit earned in a 10-MW CHP with respect to 20-year-investment period that was grouped into 4 investment terms was investigated in this article. Secondly, the profitability of using torrefied biomass in the plant and the percentage increase in profit reduction due to TVM were estimated for each of the terms. Furthermore, an un-certainty analysis was carried out and it revealed that the investment cost and blend ratio were the most sensitive parameter that affected the profit. However, blend of coal and torrefied biomass was used as feedstock.

Table 6. 7: Comparison of this work and literature

Feedstock	Plant	Parameters Estimated	Findings	Ref
Coal + Torrefied biomass	CHP	Profitability and performance efficiency of the plant	Very attractive integrating and using torrefied in an existing CHP for power generation	[258]
Coal + Raw biomass	CHP	CO_2 emission and cost of electricity	Techno-economic model indicate that electricity cost per unit cost of CO_2 emission decreased significantly with an increasing plant capacity [15 – 50 MW]. There was increased reduction in CO2 emission due to the use of torrefied biomass.	[196]
Coal + Torrefied biomass	CHP & Pyrolysis power plant	Plant performance efficiency	A considerable increase in the district heat output as well as number of operating hours (22 – 38 %) of the plant was observed.	[260]
Selected biomass materials	CHP [10-MW]	Profitability & Emission	Palm kernel empty fruit bunch was the most viable feedstock studied. Gas emission was reduced when compared to the existing energy mix. Profitability in the plant was also improved.	[238]
Coal + Raw biomass	CHP [5-MW]	Profitability: Energy, Economic, & Environmental	Coal + PSD was the most viable feedstock, while Coal-to-solid waste ratio of 1:1 was the optimum operating condition in terms of profitability in the plant. Emission reduction was also reduced due to the use of blends of coal and biomass as against solitary gasification of coal.	[13]
Coal + Biomass	CHP	Energy efficiency	The energy efficiency of the plant was enhanced due to the use of torrefied biomass	[256]
Coal + Biomass	CHP	Plant profitability	Co-gasification of coal and biomass has marginal profit when compared to 100 % biomass gasification and it has higher profit based on the higher price of coal.	[253]
Coal + Torrefied biomass	CHP [10-MW]	Plant profitability, percentage reduction in profit with time.	Profitability in the plant was enhanced due to the use of torrefied materials. The percentage reduction in profit increased with an increase in the investment time because of TVM. Coal + PSD was the most viable feedstock, while investment cost and fuel blend ratio was the two most influential variables that affected the profit.	This study

TVM: Time Value of Money; CHP: Combined Heat and Power; PSD: Pine Sawdust.

6.8. Concluding remarks

Investigation of profitability of a co-gasification CHP plant through biomass torrefaction for a 20-year-investment period has been carried out and reported in this chapter. Blends of Coal + SCB, Coal + CC, and Coal + PSD with coal-to-biomass ratio of 50:50, 71:29, and 80:20, respectively were used in the study. Four investment terms – A (1^{st} – 5^{th}), B (5^{th} – 10^{th}), C (10^{th} – 15^{th}) & D (15^{th} – 20^{th}) and two operational cost models; with feedstock costing (WFC) and without feedstock costing (WOFC) was employed. The following conclusions were reached:

- Coal + PSD and Coal + CC yielded the highest and lowest profits in the plant, respectively.
- From term A through term D, it took between 3 – 4 months to recover the costs invested in the power plant, WFC while, only 1 month was taken to recover the cost of investment, WOFC.
- At the end of term D (i.e. 20^{th} year), a profit of between USD5,902,292.46 - USD6,489,659.30 and USD7,796,968.80 - USD7,899,284.16 were earned using WFC and WOFC, respectively, but the profits earned from WFC were eroded due TVM, hence; rendered the investment un-attractive.
- The percentage reduction in profits increased from term A through term D by around 1.01 – 2.32 % and 1.19 – 5.39 % using WFC and WOFC. Implying that profitability in the plant is dependent on the future value of money.
- At 15^{th} year (within term C), the NPV of Coal + CC and Coal + PSD were negative for Coal-to-biomass ratio of 80:20, indicating that the business was not lucrative, thus; investors are advised not to consider the blend ratio.
- The investment cost and blend ratio were the two most influential variables that affected the profit

Chapter 7: Investigation of parametric effect of process variables during torrefaction of coal/biomass/waste tyre blends: Comparative study of ANN & RSM

7.1. Introduction

In this chapter, the effect of the process variables of the torrefied fuels using ANN and RSM was carried out. The study was considered necessary to promoting commercial torrefaction plants and profitability in energy production plants. Furthermore, the chapter is an input for the assessment of the gasification of coal and torrefied biomass blends in South Africa. It exposes the potentials of biomass torrefaction with respect to fuel quality enhancement, thus; promoting the performance of gasification systems. A comprehensive study of the effect of process variables during torrefaction of coal/biomass/waste tyre blends is presented in this chapter employing the information obtained from the results of feedstock pre-treatment and characterisation. Currently, a part of this chapter has been accepted for publication in a special edition/issue of the Biomass & Bioenergy journal.

Coal, biomass, tyre, and other solid fuels are the major feedstocks used for gasification. The fuels can be solitary gasified or blended with others to enhance the efficiency of the gasifier. Co-gasification of coal and biomass is considered environmentally friendly due to low emissions when compared to coal gasification process [1]. The process also promotes reduction in the cost of feedstock and tar production during gasification. It is noteworthy to state that raw biomass has enormous potentials as feedstock for gasification, but its applications are limited due to some inherent properties that limit its usage [261]. Some of the fuel properties such as the high moisture content, low bulk density, high oxygen-to-carbon ratio, lower grindabilty, contribute to the handling and gasification difficulties [262] are addressed via torrefaction. Non-torrefied biomass materials when used as fuel for gasification may lead to formation of large amount of tar, and downstream gas cleaning due to the presence of tar is not cost effective.

To solve the aforementioned problems, and equally enhance the quality of the fuel, biomass torrefaction is considered. Torrefaction of biomass is a thermal process that involves heating of fuel in a reactor under an inert atmosphere to enhance its physio-chemical properties. The torrefaction temperature and time are the two major parameters that affect the process, but if different fuel species are blended, the blending ratio plays an important role in the degree of the enhancement of the fuel. Torrefied biomass may be used as a replacement for coal or blended with coal to upgrade the characteristics and the synergetic effects of the fuel in the energy production. Torrefaction of biomass was evaluated by solid yield (SY), enhancement factor (EF), and higher heating value (HHV). The SY is the mass ratio of the torrefied and raw fuel, while the HHV describes the overall energy content of the fuel and the EF is the energy density ratio of raw

and torrefied fuel. The EF is mainly used to evaluate the quality of the fuel after torrefaction. If the quality of the fuel after torrefaction is enhanced, the efficiency of the energy conversion system (e.g. gasifier, combustor, pyrolyser, etc.), will increase, and profitability of the energy plant will equally improve.

Several studies have been carried out on torrefaction process using different biomass and under different operating conditions [263-270]. Results of the studies have revealed that the torrefaction temperature and time have effects on the composition of the fuels. The authors also examined the extent at which the torrefaction variables influenced the properties of the fuels. Other experimental studies were carried out by Park, et al. [271], (Pimchuai et al. [272], Chen et al. [14] & Uemura et al. [273] and they reported that the solid yield (SY) and energy yield (EY) decreased with an increase in temperature, whereas the enhancement factor (EF) increased with an increase in the torrefaction temperature. The authors did not consider the optimisation or construction of a model that described the process [274,275]. Bach et al. [275], Gul et al. [276], & Bach et al. [275], used a linear regression model, Least Square Regression (LSR) model, and Aspen Plus, respectively, while Nhuchhen & Afzal [277] and Ozveren [278] used response surface methodology (RSM) and artificial neural network (ANN) and LSR model to predict the HHV of torrefied biomass, respectively, but their works did not dwell on blends of fuels such as coal and biomass, and WT. Prior to these works, Medic et al [279], have used a numerical approach to determine only, the HHV of a corn Stover. Recently, García et al. [280], used a hybrid particle swarm optimisation (PSO)- support vector machines (SVM) that was fitted in a multilayer performance (MLP) network and random forest (RF) model to predict the HHV of different torrefied biomass fuels, but the study lacks information about blended fuels. The models gave reliable predictions on the parameters studied, although the majority of study focused only on the HHV of the torrefied fuels, and neglecting the enhancement factor (EF) and the solid yield (SY). The EF for example, explains if the quality of a fuel has been improved or not after the torrefaction.

Models describing EF, SY and HHV torrefaction variables, for blends of coal and biomass, and WT employing ANN and RSM are scarce in the literature, but are relevant in torrefaction industries and energy generating plants. Determining the optimum torrefaction process operating conditions and fuel, will save costs and enhance the overall process efficiency in the energy production plants. In this study, Artificial Neural Network (ANN) and Response Surface Methodology (RSM) approach will be used to this effect. The outcome of this work will be beneficial to the agricultural sector that produces the waste from which energy is produced by broadening the market for waste biomass utilizations and promotion of continental or international waste biomass trade. It is achievable because efficient torrefaction technology ensures enhanced biomass material handling and quality

upgrade. This study will also be instrumental to waste management, hence; benefiting the national waste management sector.

Secondly, the findings from this work will enhance the development of commercial torrefaction plant ensuring availability of fuels for sustainable energy production. It will be releasable because biomass fuels outside the ones studied could be pre-treated effectively following the models developed from this study. With enhanced biomass logistics and fuel quality upgrade through torrefaction, the biomass gasification technology is improved and automatically, the energy production sector becomes a potential beneficiary to the current study. Importantly, massive employment is created via the aforementioned sectors, thus; culminating into a stronger national economic development. Above all, information from this work will be employed by stakeholders for decision making and form the basis for further R& D in this area.

7.2. Model formulation

For the Design of Experiment (DoE), an RSM based on Box-Behnken (BBD) technique was employed to model the torrefaction process conditions. It involves a three-level, three-factor BBD with 17 standard experimental runs including 12 factorial points and 5 center points that provided information on the experimental regions for the assessment of the curvature effects. The detailed information of the design (e.g. input variables and responses considered) is shown in Table 7.1.

7. 1: Experimental range and levels of the process variables: Box Behnken Design

		Coded Factor Levels			Model Response (Output Variables)
Independent Process Parameters (Input Variables)	Un-coded Symbols	-1	0	+1	
Torrefaction Temperature (^oC)	X_1	200	250	300	HHV (*****),
Torrefaction Time (Min)	X_2	30	45	60	[MJ/kg], EF [-],
Torrefaction Blending Ratio (-)	X_3	1	2.5	4	and SY[%]

HHV: Higher Heating Value; *: Coal + Torrefied SCB, CC, PSD, WT; SCB: Sugarcane Bagasse; CC: Corn Cob; PSD; Pine Saw-dust; WT; Waste Tyre; EF; Enhancement Factor; SY: Solid Yield.

The generated results were used to carry out the torrefaction experiments following modelling and optimization. In this study, some important torrefaction variables were considered as the outputs in the ANN and RSM models. The variables were used to evaluate the changes in the quality of the fuels. To determine the optimal process variables for the torrefaction process, an ANN and RSM models were employed. The process evaluation will enhance quality upgrade and as well, promote efficiency in the feedstock torrefaction plant. The characteristics of raw and torrefied biomass is presented in Figure 7.1.

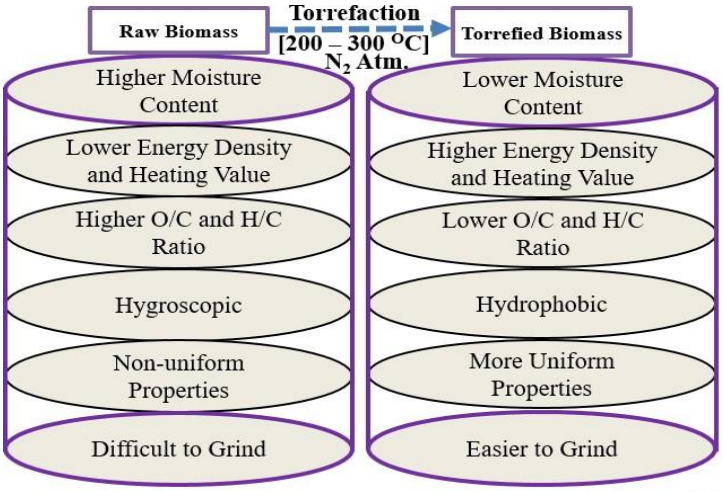


Figure 7. 1: Characteristics of raw and torrefied biomass

7.3. Model formulation: Artificial Neural Network

The ANN process modelling and optimization were carried out in a MATLAB environment. The same input and output variables used for the RSM were also used for the ANN, but a Feed Forward Backpropagation (FFB) network trained with Levenberg-Marquardt algorithm function and Tangent Sigmoid as the activation function was adopted. A Multiple Input- Single Output (MISO) and Multiple Input – Multiple Output (MIMO) layer networks were studied using the 17 standard experimental data-set obtained from the different fuel samples. The architecture of the networks is shown in Figure 7.2 and Figure 7.3, respectively.

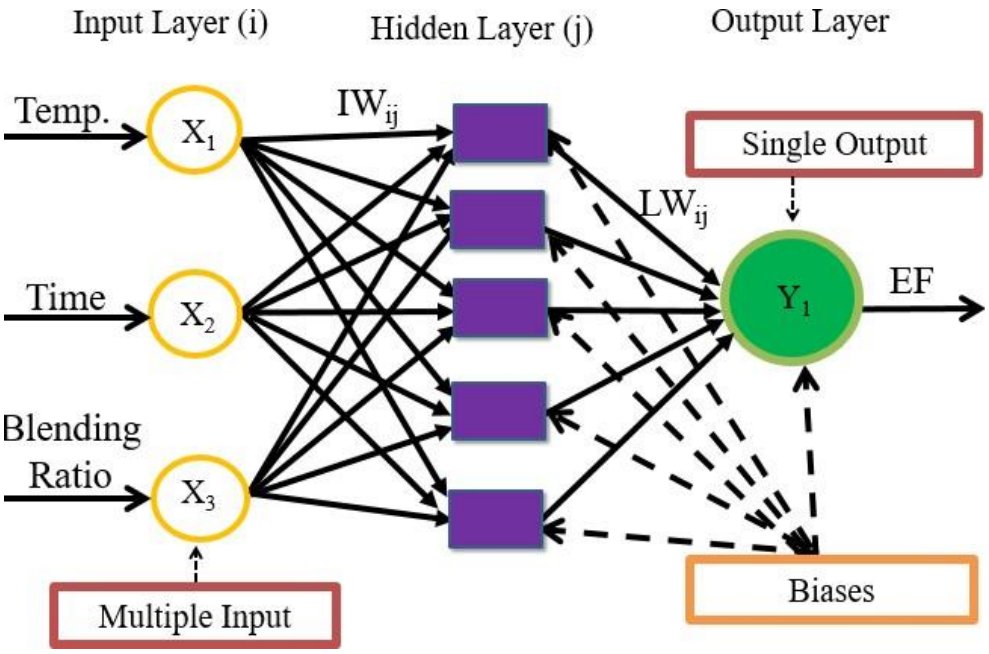


Figure 7. 2: Artificial Neural Networks Architectural Design (3, 5, 1): MISO

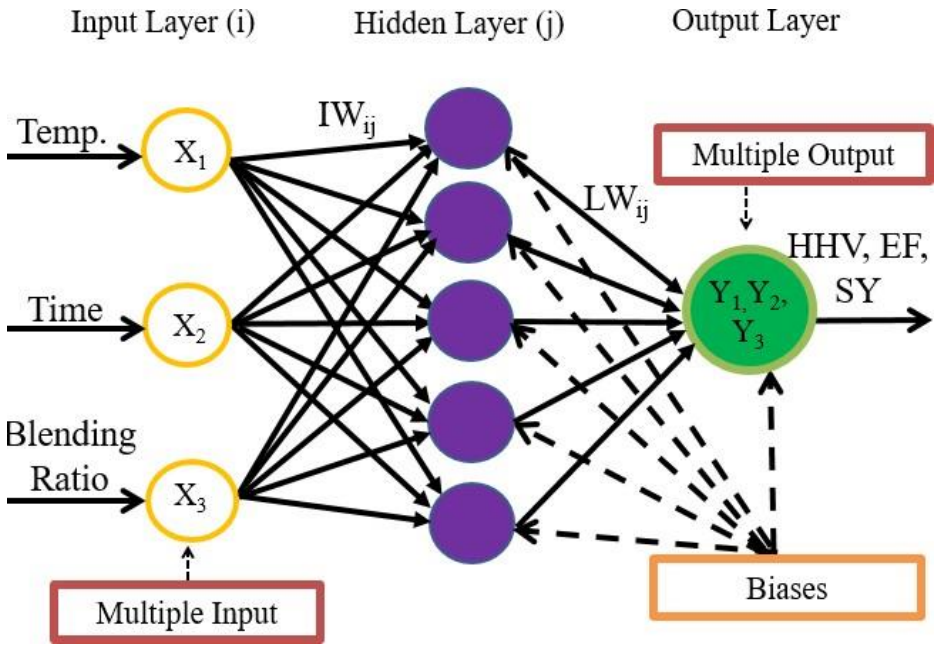


Figure 7. 3: Artificial Neural Networks Architectural Design (3, 5,3): MIMO

In this case, the training, validation and testing of the networks were carried out using 70, 15, and 15% of the experimental dataset, respectively, and the training involves adjusting the connection weights and biases between neurons to reduce the mean square error (MSE) between the predicted and experimental outputs to a threshold acceptable for the network. The training was stopped as soon as the model was able to predict the outputs. This means that once the values yielded by the metrics (MSE & R^2) used for the evaluation of the model are satisfactory, the training is terminated. In this case, the training tends to zero (0), whereas the R^2 should be around 1. A detailed explanation and flow-chart for the ANNs training is available in Azadi & Karimi-Jashni [196]. The validated model was further applied as an evaluation function for the optimization process to predict the optimal values of the torrefaction process variables (X_1, X_2, X_3, and Y_1, Y_2, Y_3) employed in the model development. The performance evaluation of the model was carried out using the Mean-Square-Error (MSE), Absolute Percentage Error (APE), and co- efficient of determination (R^2). The RSM and ANN models are effective for modelling of process variables in gasification, torrefaction, and other related energy conversion processes, respectively, but in this study, both models were employed together to determine the most attractive model amongst the two.

7.4. Torrefaction variables

The torrefaction response variables considered in this study are higher heating value (HHV), Enhancement factor (EF), and solid yield (SY), and energy yield (EY). The EY was not considered as a response variable, but was merely estimated to understand the impact of torrefaction on the feedstocks. They are briefly discussed and expressed as shown in Equations (7.1) – (7.3). The HHV of a torrefied fuel is an essential property of the fuel that determines the overall energy content of the fuel and it is measured with a bomb calorimeter or estimated numerically using different empirical models as shown in Equation (7.1) [39]:

$$\mathrm{HHV} = 0.3491\mathrm{C} + 1.1783\mathrm{H} + 0.1005\mathrm{S} - 0.1034\mathrm{O} - 0.0151\mathrm{N} - 0.0211\mathrm{A} \qquad (7.1)$$

Where C, H, S, O, N are the carbon, hydrogen, Sulphur, oxygen (obtained by difference), and nitrogen contents of the fuel from the ultimate analysis, and A is the ash. Upgrading the HHV of a fuel is one of the major objectives of carrying out torrefaction and it is evaluated by the value of the enhancement factor. The EF of a torrefied fuel is the energy density ratio used to evaluate the quality of a fuel after torrefaction, and it is expressed as shown in Equation (7.2), and its value

is always >1 [281]:

$$EF = \frac{HHV_{TB}}{HHV_{RB}} \tag{7.2}$$

where HHV_{TB} and HHV_{RB} are the higher heating value of torrefied and raw biomass, respectively. In biomass torrefaction, mass loss is inevitable, and it is dependent on the physio-chemical properties of the fuel and operating conditions used. Typically, a larger amount of the mass of the fuel may be consumed due to the thermal degradation of the fuel. The mass ratio of the torrefied and the raw fuel is called the SY, and can be expressed as presented in Equation (7.3) [282]:

$$SY = \frac{[M_{TB}]}{[M_{RB}]} \times 100 \tag{7.3}$$

Where M_{TB} and M_{RB} are the mass of torrefied biomass and raw biomass, respectively. The energy yield is the percentage (%) of the product of ratio of the HHV of torrefied fuel sample to the HHV of the raw fuel sample. This relation was used in the estimation of the energy yield values in Table 7.4 – 7.6.

7.5. Response Surface Methodology (RSM)

The RSM is a combination of mathematical and statistical methods employed in the development, improvement, and optimization of processes involving response variables that are affected by different process input variables. The essence of applying the technique is mainly to evaluate the responses, and also establish the effects of the variables on the responses independently, and the interactive effects of the variables on the responses. It provides useful information from a few numbers of experiments to describe the characteristics of the model and uses this data to generate a second-order polynomial predictive model that relates the independent process input variables to the response variables [283,284]. However, the experiment may be designed using face-centred composite design (FCCD), central composite design (CCD), and Box-Behnken design (BBD). The BBD allows the users to study three input process factors affecting a process and it is consuming lesser amount of time and with fewer numbers of experimental runs when compared to the CCD and FCCD [197].

7.5.1. Artificial Neural Network (ANN)

The ANNs are processing structures with processing units known as neuron that allows it to function like the human brain. They correlate database between themselves without requiring assistance from any external sources. The selecting of the basic structure of the network is the first step in designing of a neural network, and it involves determining the number of neurons and hidden layer in the input and output. Equation (7.4) shows a typical input-output relationship of a neural network.

$$y = b_2 + LW \times \text{tansig}\,(b_1 + IW \times X) \tag{7.4}$$

where y and X represents the input and output vectors respectively; LW represents the connection matrix of weights with respect to all the arcs from the hidden layer; IW represents the connection matrix from the input layer to the hidden layer; b_1 and b_2 are respectively, the hidden and output layers' bias vectors. The functional mechanism of the feedforward ANNs is that the signal is received by the hidden layer and is transferred to the neuron of the output layer, but each unit (yj) of the network in the hidden layer, sums its weighted inputs and uses the activation function to generate the output signal. The principle of the activation function application is expressed in Equation (7.5):

$$y_j = f_{\text{Activation}} \left(\sum_{i=1} W_{ij} X_i + b_j\right) \tag{7.5}$$

where Wij is the weight of the connection between the i^{th} input and the j^{th} neuron of the hidden layer and bj is the bias weight of the unit j. Different activation functions can be applied such as the tansigmoid and Logsigmoid functions which are hyperbolic functions, but an expression for the tansigmoid function which will be used in this work is shown in Equation (7.6):

$$f_{\text{Activation}}(X) = \frac{1}{1 + e^{-x}} \tag{7.6}$$

Normally, the output from neuron yj is transferred to all the units of the output layer, while each

output neuron μk sums the weighted input signals with the application of the activation function according to Equation (7.7):

$$\mu k = f_{Activation}\left(\sum_{j=1} V_{jk} y_f + b_k\right) \quad (7.7)$$

During the network learning, the weights (Wij) of each of the connection between the neurons in the adjacent layers are determined. However, the details of the Levenberg- Marquardt training/learning of the ANN model can be found in [192].

7.6. Model solutions and analysis

7.6.1. Response Surface Methodology

This section presents the model development and optimization study of Coal + Torrefied biomass (PSD, SCB, and CC) and WT using the RSM. The HHV, EF, and SY are independently considered as the response variables in the development of the full quadratic RSM regression models, and using the BBD technique. An illustration of the torrefaction process model is presented in Figure 7.4. The developed concept is expected to enhance the understanding of the torrefaction process model for the fuels studied.

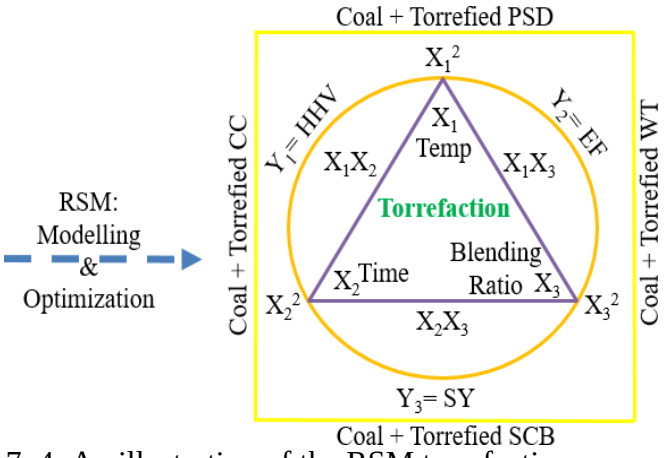


Figure 7. 4: An illustration of the RSM torrefaction process modelling

The optimization analysis was carried out using mathematical models produced by the Design-Expert Software, trial version 8.0.3.1 (Stats-Ease Inc., Minneapolis, MN, USA), and from which

the correlation between PY_1, PY_2, and PY_3 and EY_1, EY_2, and EY_3 for Coal + Torrefied PSD, and other fuels studied were evaluated, where, PY_1, PY_2, and PY_3 and EY_1, EY_2, and EY_3 represents the predicted and experimental response variables of the fuels, respectively.

7.6.2. Artificial Neural Network

The neural networks were studied using MISO and MIMO layer models, but only the MISO layer model results are reported here to allow for a logical comparison between the ANN and RSM model whose response variables were evaluated singly, and with respect to the three input variables (temperature, time and blending ratio). Figure 7.5 and 7.6 shows the computational frame-work in terms of solving for y_{2i} (the output variables from the model equations and the actual architecture of the network), respectively. For the HHV of the Coal+ Torrefied PSD, 5 neurons in the hidden layer was used to train the network, while 6 neurons were used in the training of its EF and SY, and the EF of the other fuels (Coal + SCB, Coal + CC & Coal + WT) investigated.

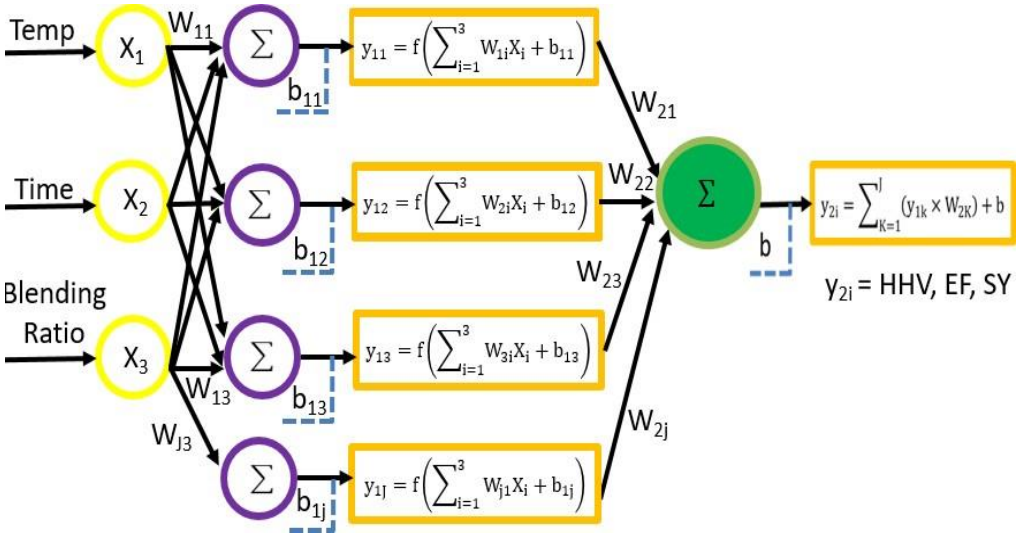


Figure 7. 5: Model equation development for the estimation of y_{2i}: HHV, EF, & SY

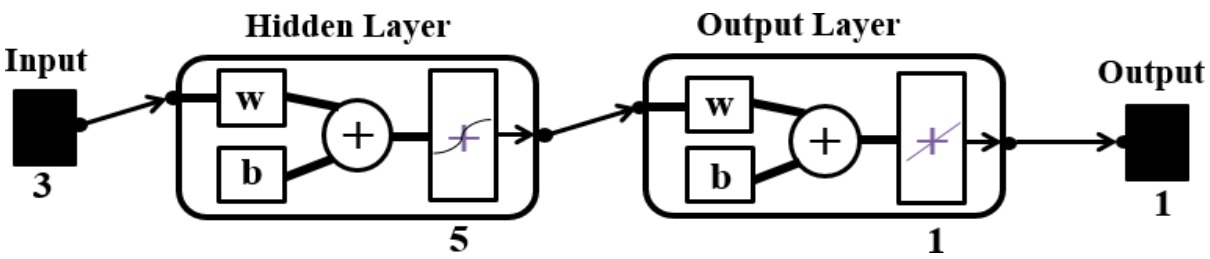


Figure 7. 6: Feedforward neural network (FFNN): 3, 5, 1 architecture

7.6. Results and discussion

The result of the proximate and ultimate analysis of blend of coal and biomass are presented in Table 7.2, while Table 7.3 contained the lower heating value (LHV) and moisture content (MC) of the fuel blends. The results are used for different estimations carried out in this section.

Table 7. 2: Ultimate and Proximate analysis: blend of coal and biomass (Raw fuel)

Feedstock Analysis					
Parameters	Corn Cob	Sugarcane-Bagasse	Pine Saw-dust	Waste-Tyre	Matla Coal
	Proximate analysis determined as air dried basis				
Ash Content (%)	0.29	0.49	0.59	9.92	44.00
Inherent moisture (%)	5.87	8.8	8.55	0.32	3.80
Volatile Matter (%)	72.50	71.50	71.80	63.29	19.90
Fixed Carbon (%)	21.34	19.12	19.06	26.47	32.30
Heating Value					
HHV (MJ/kg)	17.42	18.85	21.50	30.95	18.60
LHV (MJ/kg): Calculated	16.42	17.28	19.86	29.24	17.89
Ultimate analysis determined as air dried basis					
Carbon (%)	24.82	38.67	50.54	87.60	39.09
Hydrogen (%)	3.94	6.40	7.08	8.03	2.90
Nitrogen (%)	0.97	0.23	0.15	0.33	0.92
Sulphur (%)	0.00	0.00	0.57	3.12	0.66
Oxygen (%)	70.27	54.70	41.66	0.92	8.63

Table 7. 3: LHV and MC of feedstocks at different blend ratios (Raw fuel)

Feedstocks: Ratio: 1:1				
Parameters	Coal + SCB	Coal + CC	Coal + PSD	Coal + WT
LHV [MJ/kg]	17.58	17.15	19.72	23.57
MC [%]	6.35	5.34	4.65	2.06
Feedstocks: Ratio: 3:2				
LHV [MJ/kg]	17.65	17.30	18.68	22.87
MC [%]	5.84	5.03	4.48	2.41
Feedstocks: Ratio: 4:1				
LHV [MJ/kg]	17.77	17.60	18.28	20.16
MC [%]	4.82	4.41	4.14	3.10

The results obtained from blends of coal and torrefied biomass at 200, 250, and 300 ^{O}C temperature regimes are displayed in Table 7.4 through Table 7.6

Table 7.4 to Table 7.6 presents the results obtained from the torrefaction experiments at 200, 250, and 300 ^{O}C, respectively. The results obtained at 300 ^{O}C alongside other operating conditions explained in Chapter 3 gave the highest HHV, hence; were used for the evaluation.

Table 7. 4: Light Torrefaction at temperature of 200 ^{O}C

Feedstock	Temp [^{O}C]	Time [Min]	HHV, C + RB [MJ/kg]	HHV, C + TB [MJ/kg]	Solid Yield [%]	Energy Yield [%]	E.F [-]
			Mixing Ratio: 71:29				
Coal + SCB	200	30	18.67	19.79	89.04	94.38	1.06
Coal + CC	200	30	18.26	18.99	89.26	92.83	1.04
Coal + PSD	200	30	19.44	20.99	88.65	95.74	1.08
Coal + SCB	200	60	18.67	19.23	89.95	92.65	1.03
Coal + CC	200	60	18.26	18.44	90.09	90.99	1.01
Coal + PSD	200	60	19.44	20.41	89.24	93.7	1.05
			Mixing Ratio: 50:50				
Coal + SCB	200	45	18.72	20.40	88.13	96.06	1.09
Coal + CC	200	45	18.01	19.27	88.46	94.65	1.07
Coal + PSD	200	45	20.05	22.46	87.93	98.48	1.12
			Mixing Ratio: 80:20				
Coal + SCB	200	45	18.65	19.58	89.77	94.26	1.05
Coal + CC	200	45	18.36	18.91	90.04	92.74	1.03
Coal + PSD	200	45	19.18	20.52	89.53	95.8	1.07

E.F: Enhancement Factor; SCB: Sugarcane Bagasse; CC: Corn Cob; PSD: Pine Saw- Dust; WT: Waste Tyre; C: Coal; RB: Raw Biomass; TB: Torrefied Biomass; Temp: Temperature; *: Raw Tyre; **: Torrefied Tyre.

Table 7. 5: Mild Torrefaction at temperature of 250 ^{O} C

Feedstock	Temp [^{O}C]	Time [Min]	HHV C + RB [MJ/kg]	HHV C + TB [MJ/kg]	Solid Yield [%]	Energy Yield [%]	E.F
			Mixing Ratio: 50:50				
Coal + SCB	250	30	18.72	23.21	80.56	99.89	1.24
Coal + CC	250	30	18.01	21.79	82.44	99.75	1.21
Coal + PSD	250	30	20.05	25.26	79.15	99.73	1.26
			Mixing Ratio: 71:29				
Coal + SCB	250	45	18.67	21.66	85.47	99.15	1.16
Coal + CC	250	45	18.26	20.82	85.66	97.65	1.14
Coal + PSD	250	45	19.44	22.94	84.25	99.42	1.18
			Mixing Ratio: 50:50				
Coal + SCB	250	60	18.72	22.28	83.14	98.94	1.19
Coal + CC	250	60	18.01	21.25	84.07	99.2	1.18
Coal + PSD	250	60	20.05	24.06	82.65	99.18	1.20
			Mixing Ratio: 80:20				
Coal + SCB	250	60	18.65	21.07	86.61	97.87	1.13
Coal + CC	250	60	18.36	20.56	87.19	97.65	1.12
Coal + PSD	250	60	19.18	22.06	86.35	99.3	1.15
Coal + SCB	250	30	18.65	20.89	87.44	97.93	1.12
Coal + CC	250	30	18.36	20.38	87.75	97.4	1.11
Coal + PSD	250	30	19.18	21.87	87.35	99.58	1.14

Table 7. 6: Severe Torrefaction temperature regime (300 ^{O}C)

Feedstock	Temp [^{O}C]	Time [Min]	HHV C+ RB [MJ/kg]	HHV C + TB [MJ/kg]	Solid Yield [%]	Energy Yield [%]	E.F
			Mixing Ratio: 50:50				
Coal + SCB	300	45	18.72	25.83	54.15	74.73	1.38
Coal + CC	300	45	18.01	24.31	56.68	76.52	1.35
Coal + PSD	300	45	20.05	28.27	52.44	73.94	1.41
Coal + WT	300	45	24.78*	24.78**	100.00	100.00	1.00
			Mixing Ratio: 71:29				
Coal + SCB	300	45	18.65	24.991	62.71	84.03	1.34
Coal + CC	300	45	18.36	24.24	65.28	86.17	1.32
Coal + PSD	300	45	19.18	26.08	59.45	80.85	1.36
Coal + WT	300	45	21.07*	21.49**	102.00	104.00	1.02
			Mixing Ratio: 50:50				
Coal + SCB	300	30	18.67	23.52	76.22	96.04	1.26
Coal + CC	300	30	18.26	22.64	78.55	97.4	1.24
Coal + PSD	300	30	19.44	25.47	74.18	97.18	1.31
Coal + WT	300	30	21.18*	21.18**	100.00	100.00	1.00
			Mixing Ratio: 80:20				
Coal + SCB	300	60	18.67	24.46	69.34	90.84	1.31
Coal + CC	300	60	18.26	23.37	73.15	93.63	1.28
Coal + PSD	300	60	19.44	25.86	66.14	87.97	1.33
Coal + WT	300	60	21.18*	21.82**	103.00	106.1	1.03

E.F: Enhancement Factor; SCB: Sugarcane Bagasse; CC: Corn Cob; PSD: Pine Saw- Dust; WT: Waste Tyre; HHV C + RB: higher heating value of coal + raw biomass (SCB, PSD, CC); HHV C + TB: higher heating value of coal + torrefied biomass (SCB, PSD, CC); Temp: Temperature; *: Raw Tyre; **: Torrefied Tyre.

The HHV of a torrefied fuel plays a crucial role in the value of the EF. At some point of the pre-treatment process The HHV stopped to increase even as the torrefaction time was increased from 45 min to 60 min at 300 ^{O}C. The implication was that beyond certain torrefaction time and constant temperature, the HHV of a fuel may not be improved by increasing the time of torrefaction. For example, from Table 7.6, the HHV of Coal + SCB, Coal + CC, and Coal + PSD (25.83 MJ/kg, 24.31 MJ/kg, & 28.27 MJ/kg) at operating conditions of 300 ^{O}C, 45 min, and 50:50 coal-to-biomass ratio were higher than that of Coal + SCB, Coal + CC, and Coal + PSD (24.46 MJ/kg, 23.37 MJ/kg, & 25.86 MJ/kg) at operating conditions of 300 ^{O}C, 60 min, and 80:20 coal-to-biomass ratio, respectively. The emphasis here is on the torrefaction time. It can be seen that the heating values of the fuels did not increase when the torrefaction time was increased from 45 min to 60 min under constant temperature. The result of the SY obtained from Coal + Torrefied PSD is in affirmation with the later argument.

7.7. Regression model result: RSM

A full quadratic RSM regression model was used to develop the mathematical models for the responses, and employing the model formulation described in section and illustrated using Figure 4.3 and 4.4, respectively. The mathematical model equation of the responses (HHV, EF, & SY) for Coal + Torrefied PSD, are written in a coded form and shown in Equations (7.8), (7.9), and (7.10):

$$Y_1\,[\mathrm{MJ/kg}] = 22.94 + 2.66x_1 - 0.15x_2 - 1.19x_3 + 0.24x_1x_2 - 0.060x_1x_3 + 0.35x_2x_3 + 0.63_{X_1^2} - 0.39_{X_2^2} + 0.76_{X_3^2} + E \quad (7.8)$$

$$Y_2\,[-] = 1.18 + 0.14x_1 - 7.500E - 003x_2 - 0.034x_3 + 0.012x_1x_2 + 0.000x_1x_3 + 0.018x_2x_3 + 0.032_{X_1^2} - 0.020_{X_2^2} + 0.028_{X_3^2} + E \quad (7.9)$$

$$Y_3\,[\%] = 85.21 - 12.89x_1 - 0.62x_2 + 2.56x_3 - 2.16x_1x_2 + 1.35x_1x_3 - 1.12x_2x_3 - 8.60_{X_1^2} + 2.94_{X_2^2} - 4.27_{X_3^2} + E \quad (7.10)$$

where X_1, X_2, and X_3 are the input surface factors or variables representing the torrefaction temperature, time and blending ratio, and Y_1, Y_2,, and Y_3, are the output variables or responses representing the HHV, EF, and SY for the Coal + Torrefied PSD, respectively.

The regression models for the enhancement factor (EF) for the other fuels (Torrefied SCB, Coal + Torrefied CC and Coal + Torrefied WT) are shown in Equation (7.11) through Equation (7.13):

$$Y_{11}\,[\%] = 1.16 + 0.13_{X_1} - 2.500E - 003_{X_2} - 0.032_{X_3} + 0.020_{X_1X_2} + 0.000_{X_1X_3} + 0.015_{X_2X_3} + 0.025_{X_1{}^2} - 0.020_{X_2{}^2} + 0.030_{X_3{}^2} + E \quad (7.11)$$

$$Y_{12}\,[\%] = 1.14 + 0.13_{X_1} - 1.250E - 003_{X_2} - 0.029_{X_3} + 0.017_{X_1X_2} + 2.500E - 003_{X_1X_3} + 0.010_{X_2X_3} + 0.020_{X_1{}^2} - 0.018_{X_2{}^2} + 0.033_{X_3{}^2} + E \quad (7.12)$$

$$Y_{13}\,[\%] = 1.00 + 1.000E - 002_{X_1} + 3.750E - 003_{X_2} - 1.250 - E003_{X_3} + 0.000_{X_1X_2} - 5.000E - 003_{X_1X_3} + 2.500E - 003_{X_2X_3} + 6.250E - 003_{X_1{}^2} + 8.750E - 0003_{X_2{}^2} - 1.250E - \ 003_{X_3{}^2} + E \quad (7.13)$$

Where Y_{11}, Y_{12}, and Y_{13} are the responses for the enhancement factors (EF) for Coal + Torrefied SCB, Coal + Torrefied CC and Coal + Torrefied WT, respectively, and X_1, X_2, X_3, are the process factor or independent input variables representing the torrefaction temperature, time and blending ratio, respectively. The model equation for the EF for Coal + Torrefied PSD had been presented in Equation (7.9): Y_2. The developed model equations can be used to describe the torrefaction process of feedstocks similar to the ones used in this study.

7.7.1. Response Surface Methodology: Effect of variables & optimization of the fuels

The coefficient of determination (R^2) obtained from Coal + Torrefied PSD for the HHV, EF, and SY are shown in Figures 7.7, 7.8, and 7.9 and it can be seen that the values of the R^2 for the regression model obtained in each of the case is close to 1, which indicates a good fitting.

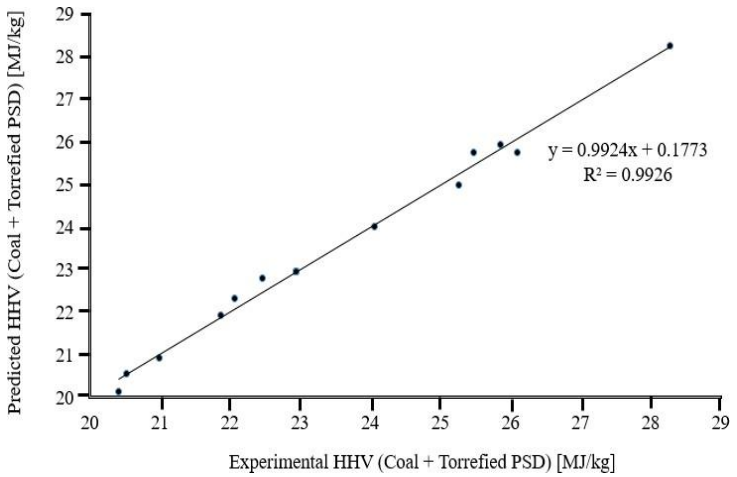


Figure 7. 7: Correlation of Predicted and Experimental HHV: Coal + Torrefied PSD

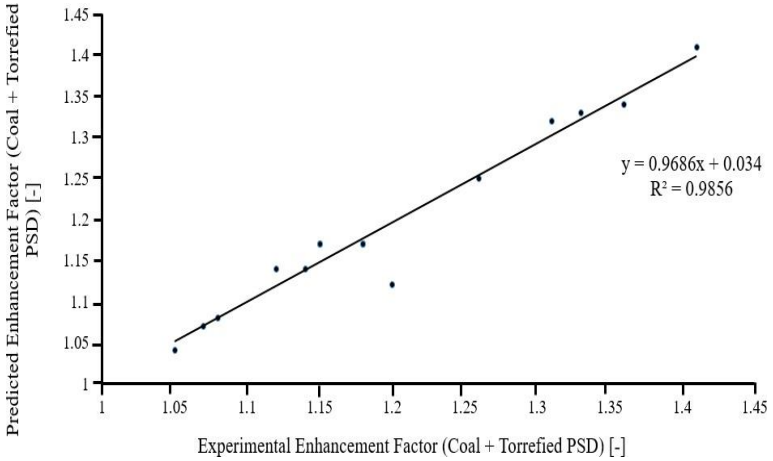


Figure 7. 8: Correlation of Predicted and Experimental EF: Coal + Torrefied PSD

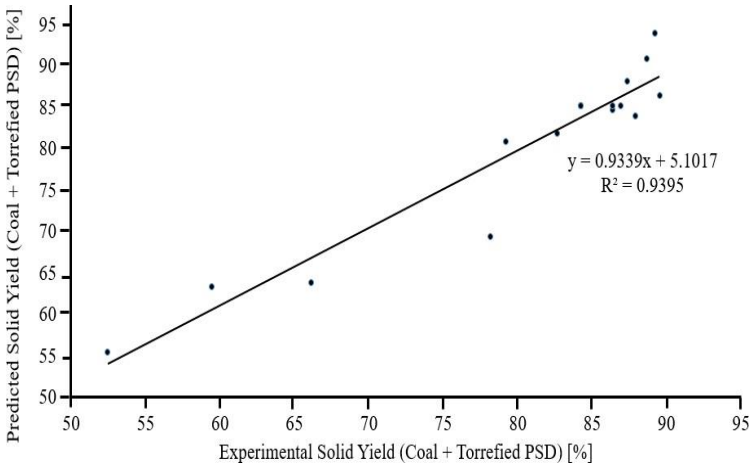


Figure 7. 9: Correlation of Predicted and Experimental SY: Coal + Torrefied PSD

In this study, the statistical significance of the developed quadratic regression models equation for

the different factors that were considered, their interactions, and the goodness of the model's fit are evaluated for all the feedstocks studied, but only the results obtained from Coal + Torrefied PSD; the optimum feedstock is discussed here, and with regard to the ANOVA results of the responses; Y_1, Y_2, and Y_3 = HHV, EF, and SY. In this case, an assessment of the quality of the model fit for each of the response was carried out using the coefficient of determination (R^2), and adjusted R^2, Fisher's test (F-value), probability value (p-value) and lack of fit. A p-value < 0.05 is an indication of the variables having a significant effect on the response. The comprehensive ANOVA and RSM regression analysis results for the other fuels studied are presented in the appendices of this thesis, while the three response variables (HHV, EF, and SY) studied are discussed.

The ANOVA result for the response surface methodology for Coal + Torrefied PSD is shown in Table 7.7.

Table 7. 7: Analysis of Variance (ANOVA) for response surface quadratic model: HHV of Coal + Torrefied PSD: RSM

Source of variance	Sum of squares	DF	Mean square	F-value	P-value
Model	73.75	9	8.19	104.59	<0.0001
T. Temperature, X_1	56.76	1	56.76	724.47	<0.0001
T. Time, X_2	0.18	1	0.18	2.30	0.1734
T. Blending ratio, X_3	11.31	1	11.31	144.28	<0.0001
X_1X_2	0.24	1	0.24	3.00	0.1268
X_1X_3	0.014	1	0.014	0.18	0.6810
X_2X_3	0.48	1	0.48	6.16	0.0420
X_1^2	1.68	1	1.68	21.50	0.0244
X_2^2	0.64	1	0.64	8.17	0.0244
X_3^2	2.45	1	2.45	21.24	0.0008
Residual	0.55	7	0.078	-	-
Lack of fit	0.55	3	0.18	-	-
Pure error	0.000	4	0.000	-	-
Corrected total	74.30	16	-	-	

RSM: R^2 = 0.9926 adj R^2 = 0.9831; Mean-Square-Error (MSE) = 0.381 Mean = 23.41; Standard Error = 0.24; Adequate Precision = 37.828; Coefficient of variation = 1.20 %; Absolute Average Deviation = ±0.038 %; Percentage Relative Error = - 0.6376 %; F: Fisher; P: Probability

From Table 7.7, an F-value of 104.59 and p-value of > 0.0001 was obtained from the quadratic regression model implying that the derived model is statistically significant at the 95 % confidence level. The predicted R^2 is in a reasonable agreement with the adjusted R^2. The adequate precision (signal to noise ratio) was 32.828 which is > 4; the standard adequate precision value recommended for the model. If the physio-chemical properties of a fuel are enhanced, the quality of the syngas will be improved, and most importantly, the profit arising from the sales of heat and electricity from the plant will also increase. The ANOVA result for the enhancement factor of the Coal + Torrefied PSD is shown in Table 7.8. The F-value is 53.38 and the p-value is > 0.0001 indicating that the model is significant, and the significant model terms includes X_1, X_3, X_2X_3, X^2, X^2 and X^2, while one of the main factors; X^2 and the cross product terms such as X_1X_2, and X_1X_3 are not significant.

Table 7.8: Analysis of Variance (ANOVA) for response surface quadratic model: EF of Coal + Torrefied PSD: RSM

Source of variance	Sum of squares	DF	Mean square	F-value	P-value
Model	0.17	9	0.019	53.38	< 0.00
T. Temperature, X_1	0.15	1	0.15	415.00	< 0.00
T. Time, X_2	4.50×10^{-4}	1	4.50×10^{-4}	1.26	0.30
T. Blending ratio, X_3	9.11×10^{-3}	1	9.11×10^{-3}	25.46	0.00
X_1X_2	6.25×10^{-3}	1	6.25×10^{-4}	1.75	0.23
X_1X_3	0.000	1	0.000	0.00	1.00
X_2X_3	1.23×10^{-3}	1	1.23×10^{-3}	3.42	0.11
X_1^2	6.24×10^{-3}	1	6.24×10^{-3}	17.44	0.00
X_2^2	8.25×10^{-3}	1	8.25×10^{-4}	2.31	0.17
X_3^2	4.73×10^{-3}	1	4.73×10^{-3}	13.20	0.00
Residual	2.5×10^{-3}	7	3.58×10^{-4}	-	-
Lack of fit	1.4×10^{-3}	4	4.75×10^{-4}	1.76	0.29
Pure error	1.08×10^{-3}	3	2.70×10^{-4}	-	-
Correlation total	0.17	16	-	-	-

RSM: R^2 = 0.99; adj R^2 = 0.98; Mean-Square-Error (MSE) = 0.00; mean = 1.20; Standard Deviation = 0.02; Adequate Precision = 25.760; Coefficient of variation = 1.58 %; Absolute Average Deviation = ± 0.02 %; Percentage Relative Error = 0.30 %; F: Fisher; P: Probability

From Table 7.7, the predicted R^2 agrees with the adjusted R^2, and the model displayed an adequate precision based on the noise to signal ratio of 34.15 that was obtained from the model. The solid yield during torrefaction process is dependent on the method used [32]. Table 7.9 shows that temperature (X_1, X_1^2) is the only significant factor. Every other model term (X_2, X_3, X_1X_2, X_1X_3, X_2X_3, X_2^2, X_3^2) are not significant, and it may be attributed to torrefaction

method and the experimental design used, and the experimental data generated. Furthermore, there was lack of fit of 21.02 due to noise, which may also be attributed to the nature of experimental data inputted in the system to generate the regression model. However, the model is significant based on the F-value of 12.08 obtained, although the predicted R^2 is not close to the adjusted R^2, but the adequate precision of 12.174 that was obtained was an indication of an adequate signal, and can be used to navigate the design space.

Table 7. 9: Analysis of Variance (ANOVA) for response surface quadratic model: SY of Coal + Torrefied PSD: RSM

Source of variance	Sum of squares	DF	Mean square	F-value	P-value
Model	1842.96	9	204.77	12.08	0.0017
T. Temperature, X_1	1329.73	1	1329.73	78.43	< 0.0001
T. Time, X_2	3.11	1	3.11	0.18	0.6812
T. Blending ratio, X_3	52.38	1	52.38	3.09	0.1222
X_1X_2	18.62	1	18.62	1.10	0.3295
X_1X_3	7.32	1	7.32	0.43	0.5322
X_2X_3	4.97	1	4.97	0.29	0.3295
X_1^2	311.59	1	311.59	18.38	0.05
X_2^2	36.52	1	36.52	2.15	0.01
X_3^2	76.77	1	76.77	4.53	0.07
Residual	118.68	7	16.95	-	-
Lack of fit	111.60	4	37.20	21.02	0.01
Pure error	7.08	3	1.77	-	-
Correlation total	1961.63	16	-	-	-

RSM: R^2 = 0.94; adj R^2 =0.86; Mean-Square-Error (MSE) = 0.96; Mean = 80.54; Standard Deviation = 4.12; Adequate Precision = 12.17; Coefficient of variation = 5.11; Absolute Average Deviation = $\pm$0.02%; Percentage Relative Error = 0.29 %; F: Fisher; P: Probability; T: Torrefaction

The interactive effects of the torrefaction temperature and time (X_1 and X_2) on the HHV of Coal + Torrefied PSD (Y_1) are presented in Figure 7.10 (a), while Figure 7.10 (b) shows the relationship of the X_2 and X_3 on the Y_1. Temperature is the most significant variable influencing the response of the process (Output; HHV) and from Figure 7.10 (a) the blending ratio is the main process factor.

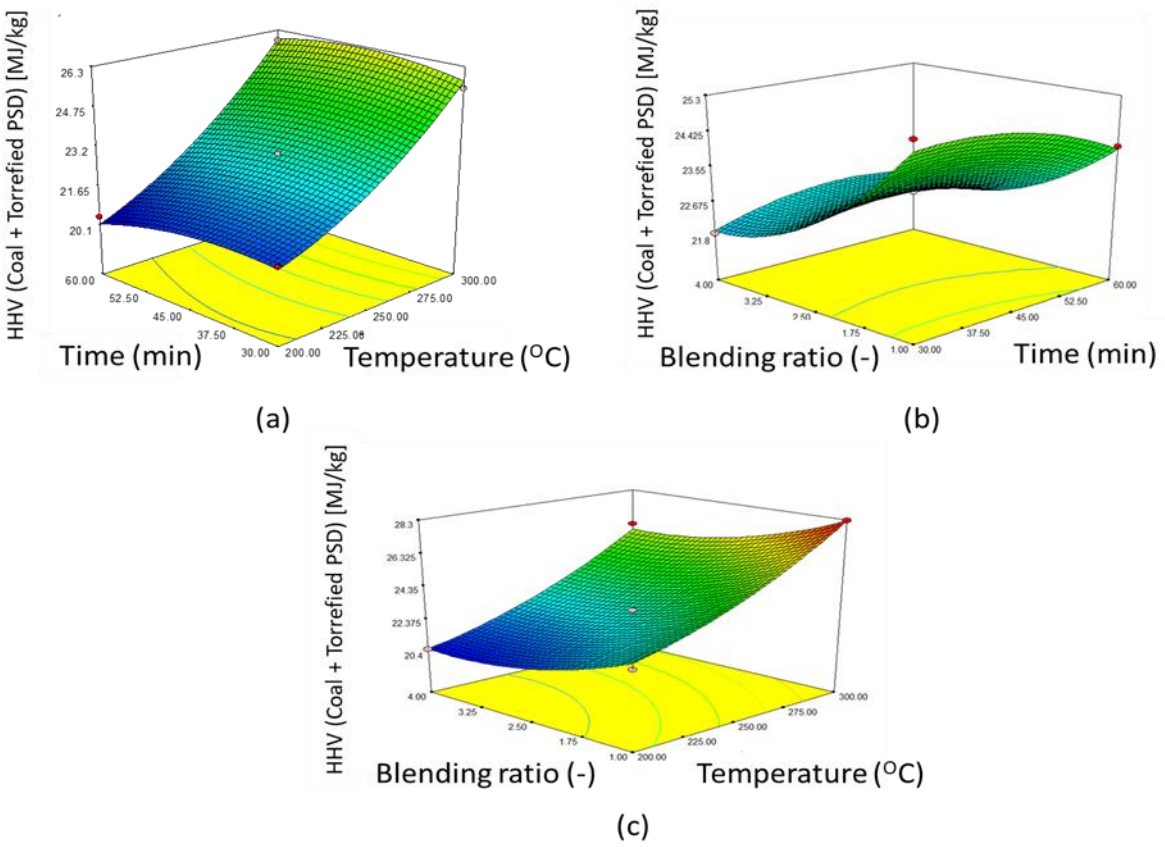


Figure 7. 10: (a) Interactive effects between torrefaction temperature and time on the HHV of Coal + Torrefied PSD for RSM response (3-D) contour plot (b) Interactive effects between torrefaction blending ratio and time on the HHV of the Coal + Torrefied PSD for RSM response (3-D) contour plot (c) Interactive effects between blending ratio and temperature on the HHV of Coal + Torrefied PSD for RSM response (3-D) contour plot.

From Figure 7.10 (c): temperature is the actual process factor and it affected the response (HHV) very considerably. As reported by Dharma et al. [285], improving the performance of a model when there is large number of insignificant model may require model reduction which is achieved by reducing the ranges of the parameters. Further, if lack of fit is displayed by the model, the implication is that several essential terms were not included in the model or that there were large residuals occurring from fitting the model, which amounts to the in- ability of the model to describing the relationship between the input and output variables. Figure 7.11: presents the level of interaction

between the temperature (X_1) and blending ratio (X_3) on the HHV of Coal + Torrefied PSD (Y_1). In this case, the actual process factor is the time, but temperature was the only significant factor that influenced the process.

The torrefaction process for Coal + Torrefied PSD were enhanced by temperature (X_1), and blending ratio (X_3), and time-blending ratio (X_2X_3) for the Y_1 and Y_2, respectively, while the Y_3 was promoted only by the temperature (X_1). The terms; Y_1, Y_2, and Y_3 had been defined earlier in this section.

Figure 7.11 (a) highlights the interactive effects between X_1 and X_2 on the Y_2, while the interaction between X_2 and X_3 on Y_2 is shown in Figure 7.11 (b).

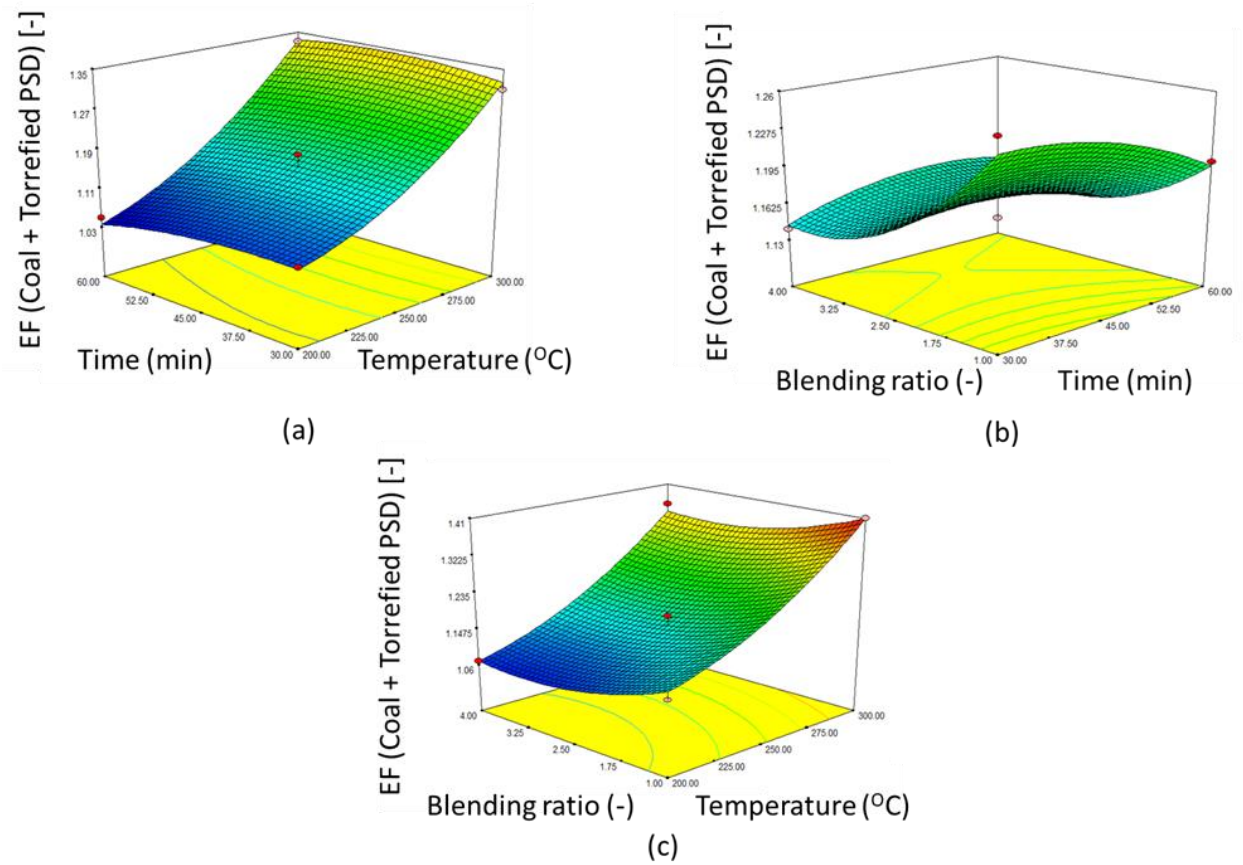


Figure 7. 11: (a) Interactive effects between torrefaction temperature and time on the EF of Coal + Torrefied PSD for RSM response (3-D) contour plot (b) Interactive effects between torrefaction time and blending ratio on the EF of Coal + Torrefied PSD for RSM response (3-D) contour plot (c) Interactive effects between torrefaction temperature and blending ratio on the EF of Coal + Torrefied PSD for RSM response (3-D) contour plot.

Figure 7.11 (c) therefore, presents the level of interaction between the temperature (X_1) and blending ratio (X_3) in terms of the EF (Y_2), and the actual process factor is the time. The interactive effects between the torrefaction time (X_2) and blending ratio (X_3) on the solid yield (Y_3) with the torrefaction temperature as the actual factor, has significant effect on the response variable; EF (Y_2).

Similarly, the interactive effects between the blending ratio and time, torrefaction temperature and time, and blending ratio and temperature on the solid yield (Y_3) are shown in Figure 7.12 (a), Figure 7.12 (b), and Figure 7.12 (c) respectively. From Figures 7.12 (b) and Figure 7.10 (4.12) (c), the temperature affects the solid yield more than the time and blending ratio and is considered as the only significant model term based on the result of the RSM regression analysis contained in the supplementary materials.

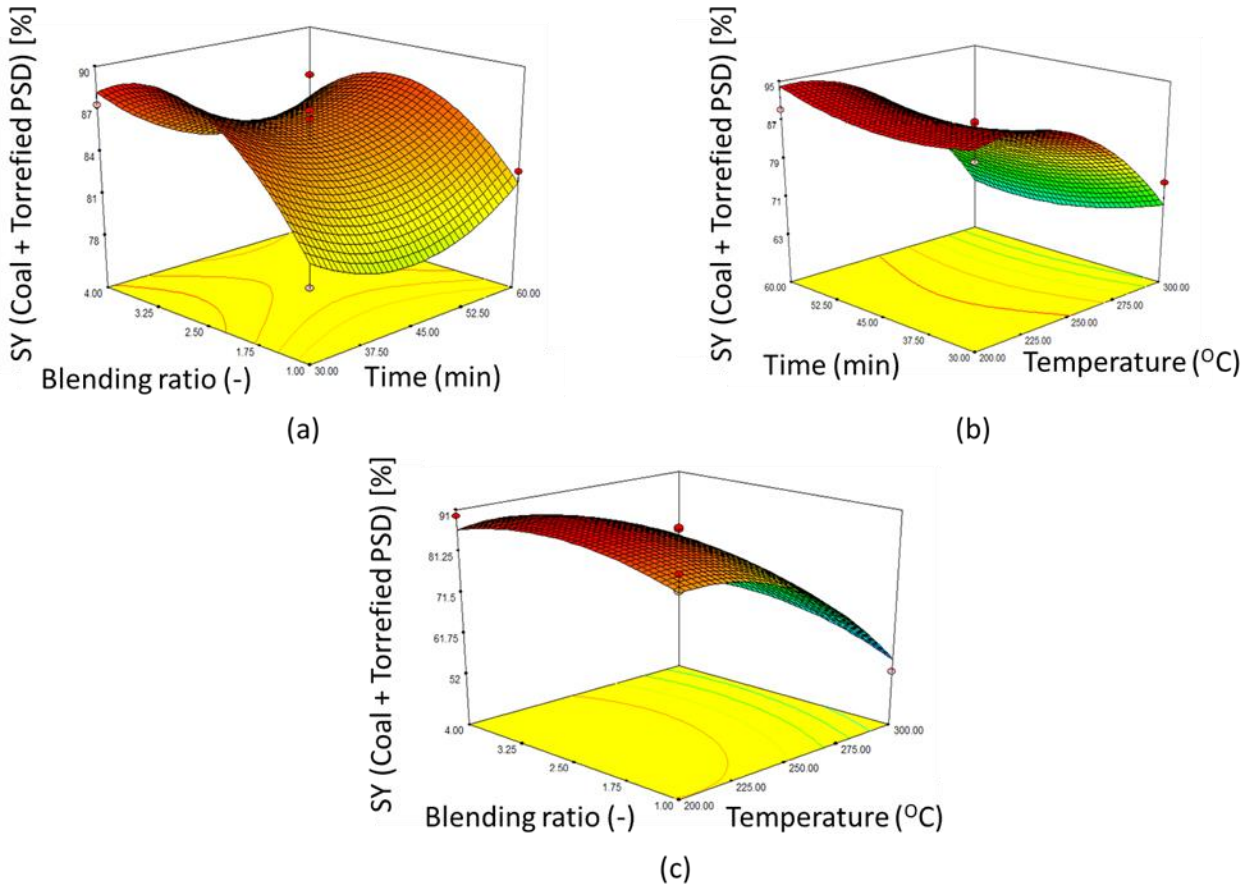


Figure 7. 12: (a) Interactive effects between torrefaction blending ratio and time on the EF of Coal + Torrefied PSD for RSM response (3-D) and contour plot (b) Interactive effects between torrefaction temperature and time on the EF of Coal + Torrefied PSD for RSM response (3-D) contour plot (c) Interactive effects between torrefaction blending ratio and temperature on the EF of Coal + Torrefied PSD for RSM response (3-D) and Contour plot.

7.8. Artificial Neural Network: Effect of variables & optimization of the fuels

Figure 7.13 through Figure 7.15 depicts the convergence characteristics of the ANN model for the, EF, SY, and HHV from Coal + Torrefied PSD using the MISO layer networks. It can be seen from Figure 7.13 (EF) that there was a considerable decrease in the MSE of the training, validation and testing curves till the iteration 5, and it is an indication of better fitting. From Figure 7.14 (SY), all

the MSE curves reduced from the zero (0) epoch to epoch 2 after which, the testing and validation fittings increased slightly till epochs 3 and 4 respectively while the training fitting continued to decrease until the epoch 10 before becoming constant till the last epoch (12). It is a revelation of better fitting, but the best performance in this case was achieved at epoch 7. Figure 7.15 (HHV) shows that the MSE of the training, validation and testing curves continued to decrease until it got to epoch 3 where the testing and training curves became constant, while the validation curve continued to decrease until at epoch 5. It implies that after the epoch 3, the model would not adequately generalize if it was trained beyond this point. Several numbers of neurons were used to identify the best fitting of the network using trial and error technique, but 5 neurons in the hidden layer produced the best fitting unlike in the EF and SY networks where 6 number of neurons in the hidden layer were used. However, the performance evaluation of the network based on the R^2, epoch and MSE is shown in Table 7.9.

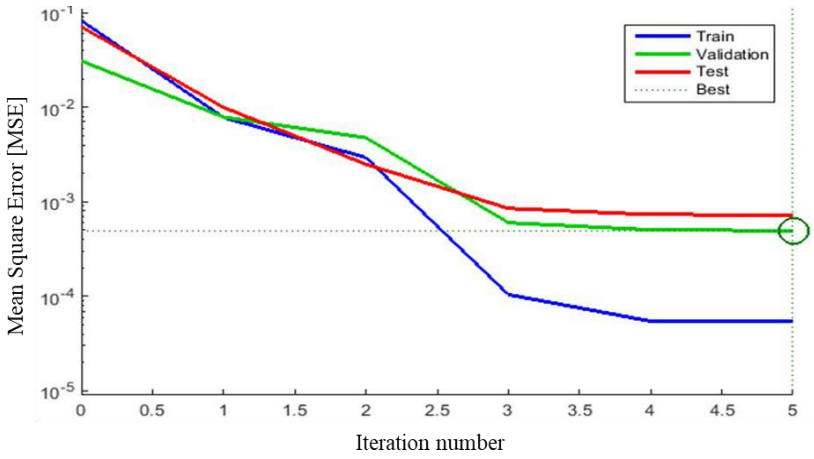


Figure 7. 13: Convergence characteristics of the MISO model for the Coal + Torrefied PSD: EF [with 6 neurons in the hidden layer]

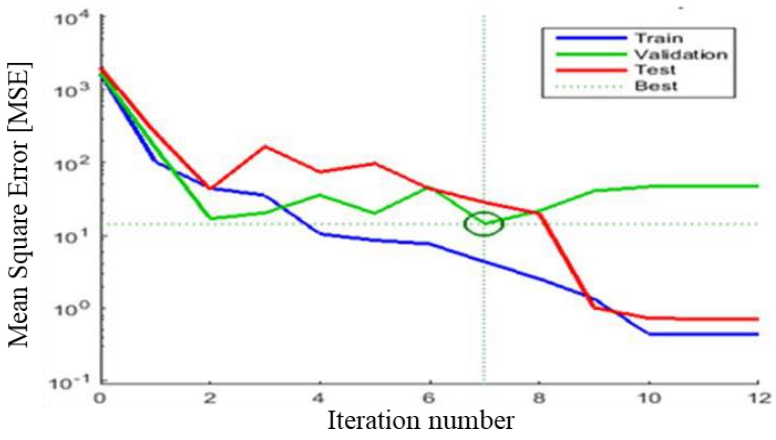


Figure 7. 14: Convergence characteristics of the MISO model for the Coal + Torrefied PSD: SY [with 6 neurons in the hidden layer]

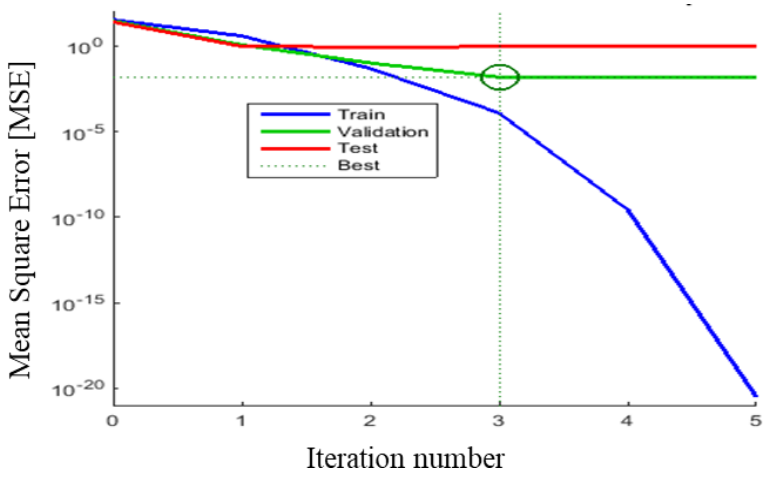


Figure 7. 15: Convergence characteristics of the MISO model for the Coal +Torrefied PSD: HHV: [with 5 neurons in the hidden layer].

The result of the conversion characteristics for the response variables studied are shown in Table 7.10.

Table 7. 10: Correlation coefficient, epoch and MSE of EF, SY & HHV predictions: MISO model

Feedstock	Variable	Training	Validation	Testing	Epoch	MSE
Coal + TPSD	EF	0.99	0.99	0.98	5	0.00
	SY	0.97	0.97	0.99	7	14.45
	HHV	0.99	0.99	0.99	3	0.02

TPSD: Torrefied Pine Sawdust; EF: Enhancement factor; SY: Solid Yield; HHV: Higher Heating Value; MSE: Mean Square Error

The ANN analysis of the other fuels (Coal + Torrefied SCB, Coal + CC, and Coal + Torrefied WT) used in this study were carried out using 3 input and output variables with 6 number of neurons in the hidden layer, but only the EF results obtained from each of the fuels were reported here. Figure 7.16 through Figure 7.18 presents the convergence characteristics of the model for the fuels, respectively. From Figure 7.16 there was a decrease in the MSE of the testing and validation fittings from epoch 0 to 2, after which, a slight increase on both curves were observed till around epoch 6, this may be attributed to the networks struggling to memorize the fittings, but a steady reduction in

the MSE for all the fitting were observed after the epoch 6 till 10 where the best validation performance was achieved. The validation and testing curves remained constant whereas the training fittings continued to decrease till the epoch 13, but the training fitting reduced very considerably from the iteration 0 to 10 hence; revealing a better accuracy for the trained data of the network.

Further, similar patterns were observed in the fittings obtained in Figure 7.17 and Figure 7.18 where the MSE reduced from epoch 0 to 1 for all the curves, but later became horizontally stable for the testing and validation curves till epoch 5 for both fuels. The training fittings for the fuels (Coal + Torrefied CC and Coal + Torrefied WT) continued to reduce from epoch 0 to 5, but the best validation performance for them were found at iterations 4 and 3, respectively. The R^2 values for Coal + Torrefied CC were; training: 0.99, validation: 0.99 and testing: 0.99, while the Coal + Torrefied WT were training: 0.99, validation: 0.99, and testing: 0.71.

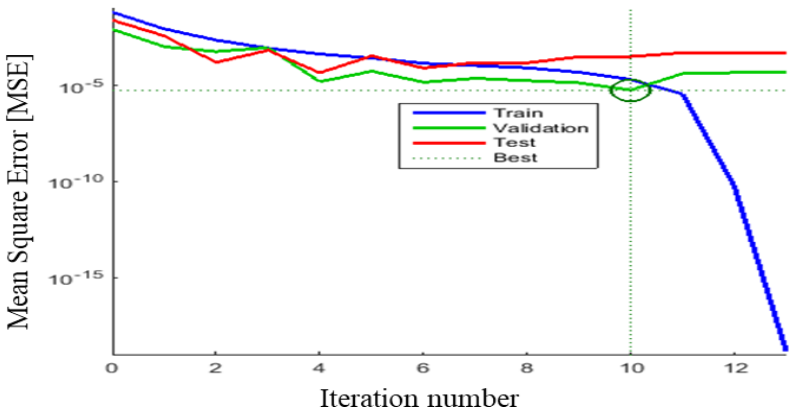


Figure 7. 16: Convergence characteristics of the MISO model for the Coal + Torrefied SCB: EF [with 6 neurons in the hidden layer]

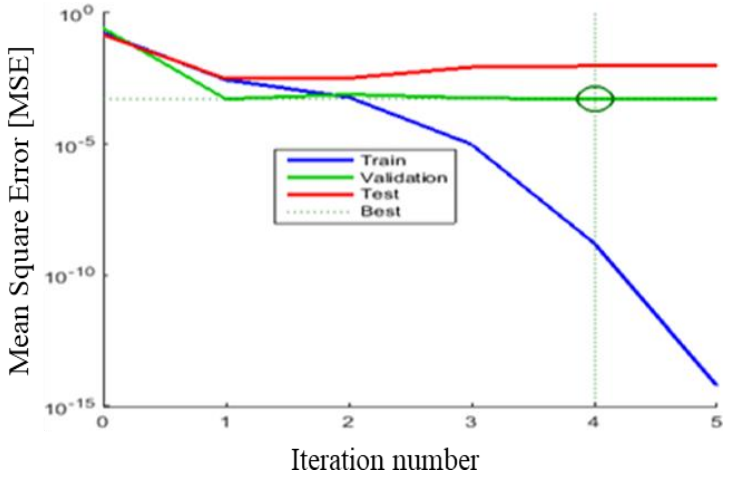


Figure 7. 17: Convergence characteristics of the MISO model for the Coal + Torrefied CC: EF [with 6 neurons in the hidden layer]

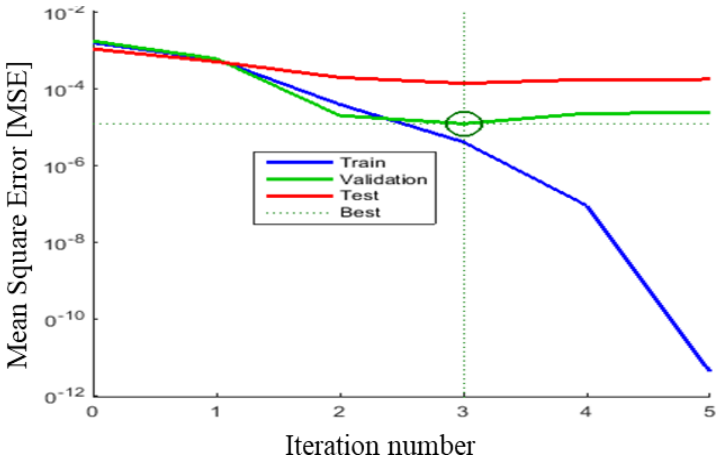


Figure 7. 18: Convergence characteristics of the MISO model for the Coal + Torrefied WT: EF [with 6 neurons in the hidden layer]

It should be noted in Figure 7.16 – Figure 7.18 that the best fitting of the curves was indicated by the number of the iteration referred to in this study as epochs. Typically, the fitting curves (whether perfect or non-perfect) must fall within the iteration number range. The epoch describes the extent of stability of the characteristic curves and are considered a better fitting if an increased number of the epoch are achieved. In this study, the epochs obtained from the different network trainings varied due to the variation in the dataset of the respective parameters or variables employed in the study.

7.9. Sensitivity and Comparative analysis: ANN & RSM models

The experimental and optimization results of the torrefied fuels were compared to determine the optimum process parametric conditions and feedstock. The comparison is based only on the EF and HHV of the fuels.

The RSM regression analyses for the fuels based on the EF (Y_2) for Coal + Torrefied SCB, Coal + Torrefied CC, and Coal + Torrefied WT are shown in Table 7.11 and Table 7.12, respectively.

From the information contained in Table 7.11 and Table 7.12, and based on the model that are significant, it can be found that X_1, X_3, X_1^2, X_3^2 and X_1, X_3, X_3^2 are the significant model terms produced by the model. The F-value of the EF from Coal + Torrefied SCB and Coal + Torrefied CC is 42.04 and 49.39, whereas the F-value from Coal + Torrefied CC is about 8.04 % higher than the Coal + Torrefied SCB. The predicted R^2 and adjusted R^2 for both fuels are not close to each other, but their EF ANOVA results in terms of adequate precision indicated that the signals are adequate, and can be used to navigate the design space. The co- efficient of determination of the

fuels are very close to unity, but the value obtained from the EF of Coal + Torrefied CC is closer by 0.001 % implying that the regression model for the Coal + Torrefied CC is more fitted than Coal + Torrefied SCB, and not that the physio- chemical property (e.g. HHV) of the fuel is more enhanced than Coal + Torrefied SCB (Table 7.6).

Table 7. 11: RSM regression analysis for Coal + Torrefied SCB and Coal + Torrefied CC: Response Y_3: Enhancement Factor

Coal + Torrefied SCB: Enhancement Factor [MJ/kg]						
Factor	Regression Coefficient	DF	Standard Error	95 % Cnf. Level [Low]	95 % Cnf. Level [High]	VIF
Intercept	1.16	1.00	9.18×10^{-3}	1.14	1.18	1.00
X_1	0.13	1.00	9.18×10^{-3}	0.12	0.15	1.00
X_2	-2.50×10^{-3}	1.00	9.18×10^{-3}	-5.00×10^{-2}	0.02	1.00
X_3	-0.03	1.00	1.00×10^{-2}	-2.00×10^{-2}	-0.02	1.00
X_1X_2	0.02	1.00	1.00×10^{-2}	-4.27×10^{-3}	0.04	1.00
X_1X_3	0.00	1.00	1.00×10^{-2}	0.024	0.02	1.00
X_2X_3	0.02	1.00	1.00×10^{-2}	-9.27×10^{-3}	0.04	1.00
X_1^2	0.025	1.00	1.00×10^{-2}	1.34×10^{-3}	0.05	1.01
X_2^2	-0.02	1.00	1.00×10^{-2}	4.40×10^{-2}	3.66×10^{-3}	1.01
X_3^2	0.03	1.00	1.00×10^{-2}	6.34×10^{-3}	0.05	1.01
Coal + Torrefied CC: Enhancement Factor (EF) [-]						
Intercept	1.14	1.00	8.24×10^{-3}	1.12	1.16	
X_1	0.13	1.00	6.51×10^{-3}	0.11	0.15	1.00
X_2	-1.25×10^{-3}	1.00	6.51×10^{-3}	-1.70×10^{-2}	0.014	1.00
X_3	-0.03	1.00	6.51×10^{-3}	-0.044	-0.013	1.00
X_1X_2	0.02	1.00	9.21×10^{-3}	-4.28×10^{-3}	0.039	1.00
X_1X_3	2.50×10^{-3}	1.00	9.21×10^{-3}	-1.90×10^{-2}	0.024	1.00
X_2X_3	0.01	1.00	9.21×10^{-3}	-1.20×10^{-2}	0.032	1.00
X_1^2	-0.02	1.00	8.98×10^{-3}	-1.23×10^{-3}	0.041	1.01
X_2^2	0.02	1.00	8.98×10^{-3}	-3.90×10^{-3}	3.73×10^{-3}	1.01
X_3^2	0.03	1.00	8.98×10^{-3}	1.10×10^{-2}	0.054	1.01

Cfn: Confidence; VIF: Variance Inflation Factor; DF: Degree of Freedom

Similarly, the F-value of 2.86 was obtained from the ANOVA of Coal + Torrefied WT; with X_1 as the only significant model term compared to Coal + Torrefied SCB and Coal + Torrefied CC that has the X_1, X_3, X_1^2, X_3^2 and X_1, X_3, X_3^2 as the significant model terms. Coal + Torrefied WT have a negative predicted R^2 of -2.42 as against other fuels studied that have a positive predicted R^2, respectively. It implies that the overall mean is a better predictor of the response (EF=Y_2) than the current regression model. Again, the F-value obtained from Coal + Torrefied PSD is higher than the value obtained from Coal + Torrefied WT by around 93.99 %. A similar high percentage F-value results were obtained from other fuels, and the adequate precision from Coal + Torrefied WT was only 2.28 above the standard adequate precession value (> 4), whereas the Coal + Torrefied PSD, Coal + Torrefied SCB, and Coal + Torrefied CC have adequate precision values of about 79.03 %, 70.91 %, and 72.54 % higher than the Coal + Torrefied WT, respectively.

Table 7. 12: RSM regression analysis for Coal + Torrefied WT: Response Y_3: Enhancement Factor

Coal + Torrefied WT: Enhancement Factor (EF) [-]						
Factor	Regression Coefficient	DF	Standard Error	95 % Cnf. Level [Low]	95 % Cnf. Level [High]	VIF
Intercept	1.00	1.00	1.46×10^{-3}	1.00	1.00	
X_1	6.25×10^{-3}	1.00	1.16×10^{-3}	3.51×10^{-3}	8.99×10^{-3}	1.00
X_2	8.75×10^{-3}	1.00	1.16×10^{-3}	6.01×10^{-3}	0.01	1.00
X_3	-2.50	1.00	1.16×10^{-3}	-5.24×10^{-3}	2.37×10^{-3}	1.00
X_1X_2	7.50×10^{-2}	1.00	1.64×10^{-3}	3.63×10^{-3}	0.011	1.00
X_1X_3	-5.00×10^{-3}	1.00	1.64×10^{-3}	-8.87×10^{-3}	-1.13×10^{-3}	1.00
X_2X_3	0.00	1.00	1.64×10^{-3}	-3.87×10^{-3}	3.87×10^{-3}	1.00
X_1^2	1.25×10^{-3}	1.00	1.60×10^{-3}	2.52×10^{-3}	5.02×10^{-3}	1.01
X_2^2	6.25×10^{-3}	1.00	1.60×10^{-3}	2.48×10^{-3}	1.00×10^{-2}	1.01
X_3^2	3.75×10^{-3}	1.00	1.60×10^{-3}	-2.20×10^{-3}	7.52×10^{-3}	1.01

Cfn: Confidence; VIF: Variance Inflation Factor; DF: Degrees of Freedom

7.9.1. Comparative analysis: Based on HHV & EF of Coal + PSD & Coal + WT

Coal + PSD and Coal + WT were compared based on their HHV after the torrefaction process. Figure 7.19 and Figure 7.20 describes the relationship between the HHV of raw Coal + WT and Coal + Torrefied WT, and their effects on the enhancement factor as well as the interactive effects between torrefaction temperature and time on the HHV of Coal + Torrefied WT. The assessment was carried

out in order to check the attractiveness of waste tyre (WT) in terms of quality upgrade.

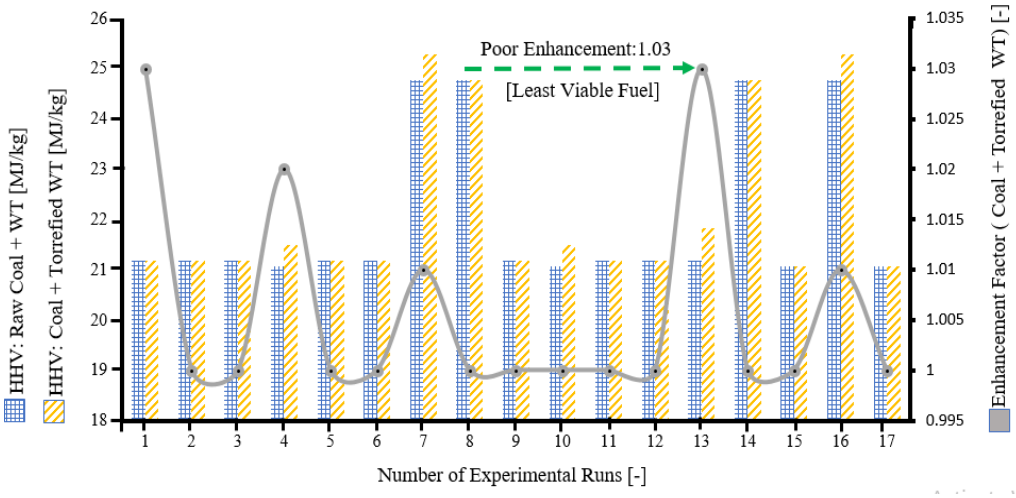


Figure 7. 19: Relationship between enhancement factor, raw Coal + WT and Coal + Torrefied WT

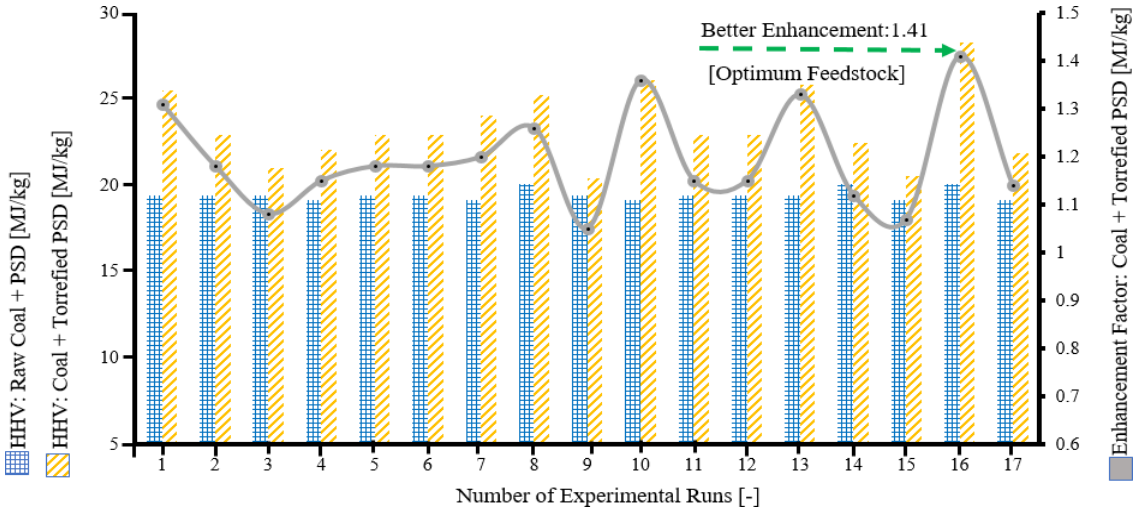


Figure 7. 20: Relationship between enhancement factor, raw Coal + WT and Torrefied Coal + PSD

The EF of Coal + Torrefied WT due to torrefaction was 1.03, and in terms of the physio- chemical properties upgrade, the value is considered very small when compared to other fuels investigated. Figure 7.19 revealed that the difference between the quality of the raw and the torrefied fuel is considerably very small, and based on the processing cost (energy and time), WT torrefaction is not an attractive process of improving the quality of the fuel, hence; is not recommended. Similarly, there was a considerable improvement in the quality of Coal + Torrefied PSD. The relationship between the enhancement factor, raw coal + WT and Coal + Torrefied PSD is depicted in Figure 7.20, and the result shows that the enhancement factor (EF) is 1.41 which is about 10 % higher than the raw fuel, and around 25.23 % higher than the EF of Coal + Torrefied WT; the least viable

feedstock studied.

Generally, the 10 % increase in the HHV of torrefied Coal + PSD when compared to that of the raw fuel (coal + PSD) is clear indication of enhancement of the fuel quality which in overall will lead to reduction in emission due to reduced amount of coal in the mixture, increase in the energy value, and increase in the synergetic effect of the fuel during gasification.

However, the overall results of the ANOVA and RSM regression analysis for the EF from Coal + Torrefied WT shows that Coal + Torrefied WT is not suitable for quality improvement by torrefaction when compared to other fuels studied. From this study, the optimum operating process conditions for different coal-to-torrefied fuel ratio was in this order: 50:50 at 300 ^{O}C and 45 min > 50:50 at 250 ^{O}C and 30 min > 50:50 at 200 ^{O}C and 45 min, while the optimum fuel follows the order of Coal + Torrefied PSD > Coal + Torrefied SCB > Coal + Torrefied CC and > Coal + Torrefied WT.

Similar result has been reported in the literature about the order of feedstock's viability for heat and electricity production in a co-gasification CHP plant [13], except that the rank of Coal + WT viability was higher than that of Coal + biomass fuels investigated. In this work, the highest HHV, EF and SY were 28.27 MJ/kg, 1.41, and 52.44 % respectively, and they were obtained from Coal + Torrefied PSD. Based on the result, Coal + Torrefied PSD is therefore considered the most viable fuel amongst the feedstocks studied, and is recommended for quality enhancement by torrefaction. Secondly, an increase in the calorific value of the fuel due to torrefaction by around 10 % was achieved from the pre- treatment process. It is expected to enhance profitability in the energy generating plant. However, the optimum fuel follows the order of Coal + Torrefied PSD > Coal + Torrefied SCB > Coal + Torrefied CC and > Coal + Torrefied WT.

7 .9.2. Comparative analysis based on model performance: ANN & RSM Models

Table 7.13 through 7.15 shows the results of the sensitivity analysis carried out to determine the most effective model between RSM and ANN with respect to the responses studied and based on the optimum feedstock (Coal + Torrefied PSD).

Table 7. 13: Sensitivity analysis of the RSM Box-Behnken Design and Artificial Neural Network (ANN) models: HHV: (Response Variable Y_1)

Higher Heating Value [MJ/kg]: Response Variable Y_1									
STD Run	X_1	X_2	X_3	Exp. HHV [MJ/kg] RSM	Predicted HHV [MJ/kg] RSM	Residual Value RSM	Exp. HHV [MJ/kg] ANN	Predicted HHV[MJ/kg] ANN	Residual Value ANN
1	-1	-1	0	22.94	25.75	-2.81	22.94	22.96	-0.02
2	1	-1	0	22.94	22.94	0.00	22.94	22.94	0.00
3	0	0	0	20.99	20.91	0.08	20.99	20.99	0.00
4	0	0	0	22.06	22.32	-0.26	22.06	22.05	0.01
5	-1	0	-1	22.94	22.94	0.00	22.94	22.94	0.00
6	1	0	-1	22.94	22.94	0.00	22.94	22.94	0.00
7	-1	0	1	24.06	24.00	0.06	24.06	24.27	-0.21
8	0	0	0	25.26	24.99	0.27	25.26	25.27	-0.01
9	0	-1	-1	20.41	20.13	0.28	20.41	20.41	0.00
10	0	1	-1	26.09	25.75	0.34	26.09	26.08	0.01
11	0	-1	1	22.94	22.94	0.00	22.94	22.94	0.00
12	0	1	1	22.94	22.94	0.00	22.94	22.94	0.00
13	-1	1	0	25.86	25.94	-0.08	25.86	25.86	0.00
14	1	1	0	22.46	22.8	-0.34	22.46	22.46	0.00
15	1	0	1	20.52	20.54	-0.02	20.52	20.52	0.00
16	0	0	0	28.27	28.25	0.02	28.27	28.25	0.02
17	0	0	0	21.87	21.93	-0.06	21.87	21.87	0.00

ANN: Artificial Neural Networks; STD: Standard; X_1: Torrefaction temperature, X_2: Torrefaction time, X_3: Torrefaction blending ratio, RSM: Response Surface Methodology; HHV: Higher Heating Value

Table 7.14: Sensitivity analysis of the RSM-Box-Behnken Design and ANN models: EF: (Response Variable Y_2).

Coal + Torrefied PSD: Enhancement Factor [%]: Response Variable Y_2									
STD Run	X_1	X_2	X_3	Experimental EF [%] RSM	Predicted EF [%] RSM	Residual Value RSM	Experimental EF [%] ANN	Predicted EF [%] ANN	Residual Value ANN
1	-1	-1	0	1.31	1.32	-0.01	1.31	1.31	0.00
2	1	-1	0	1.18	1.17	0.01	1.18	1.17	0.01
3	0	0	0	1.08	1.08	0.00	1.08	1.08	0.00
4	0	0	0	1.15	1.17	-0.02	1.15	1.15	0.00
5	-1	0	-1	1.18	1.17	0.01	1.18	1.17	0.01
6	1	0	-1	1.18	1.17	0.01	1.18	1.17	0.01
7	-1	0	1	1.2	1.12	0.08	1.2	1.20	0.00
8	0	0	0	1.26	1.25	0.01	1.26	1.26	0.00
9	0	-1	-1	1.05	1.04	0.01	1.05	1.08	-0.03
10	0	1	-1	1.36	1.34	0.02	1.36	1.39	-0.03
11	0	-1	1	1.15	1.17	-0.02	1.15	1.17	-0.02
12	0	1	1	1.15	1.17	-0.02	1.15	1.17	-0.02
13	-1	1	0	1.33	1.33	0	1.33	1.36	-0.03
14	1	1	0	1.12	1.14	-0.02	1.12	1.12	0.00
15	1	0	1	1.07	1.07	0.00	1.07	1.07	0.03
16	0	0	0	1.41	1.41	0.00	1.41	1.41	0.03
17	0	0	0	1.14	1.14	0.00	1.14	1.13	0.01

ANN: Artificial Neural Networks; STD: Standard; X_1: Torrefaction temperature, X_2: Torrefaction time, X_3: Torrefaction blending ratio, RSM: Response

Surface Methodology; EF: Enhancement Factor

Table 7.15: Sensitivity analysis of the RSM Box-Behnken Design and ANN Models: SY: (Response Variable Y_3)

Coal + Torrefied PSD: Solid Yield [%]: Response Variable Y_3									
STD Run	X_1	X_2	X_3	Experimental SY [%] RSM	Predicted SY [%] RSM	Residual Value RSM	Experimental SY [%] ANN	Predicted SY [%] ANN	Residual Value ANN
1	-1	-1	0	78.18	69.44	8.74	78.18	71.63	6.55
2	1	-1	0	84.25	85.21	-0.96	84.25	84.94	-0.70
3	0	0	0	88.65	90.91	-2.26	88.65	89.6	-0.90
4	0	0	0	86.35	84.71	1.64	86.35	88.76	-2.40
5	-1	0	-1	84.25	85.21	-0.96	84.25	84.94	-0.70
6	1	0	-1	84.25	85.21	-0.96	84.25	84.94	-0.70
7	-1	0	1	82.65	81.82	0.83	82.65	83.05	-0.40
8	0	0	0	79.19	80.84	-1.65	79.19	79.53	-0.30
9	0	-1	-1	89.24	93.98	-4.74	89.24	87.6	1.64
10	0	1	-1	59.45	63.36	-3.91	59.45	63.55	-4.10
11	0	-1	1	86.36	85.21	1.15	86.36	84.94	1.42
12	0	1	1	86.94	85.21	1.73	86.94	84.94	2.00
13	-1	1	0	66.14	63.88	2.26	66.14	63.93	2.21
14	1	1	0	87.93	84.02	3.91	87.93	87.42	0.51
15	1	0	1	89.53	86.44	3.09	89.53	89.57	-0.00
16	0	0	0	52.44	55.53	-3.09	52.44	61.24	-8.80
17	0	0	0	87.35	88.18	-0.83	87.35	83.22	4.13

ANN: Artificial Neural Networks; STD: Standard; X_1: Torrefaction temperature, X_2: Torrefaction time, X_3: Torrefaction blending ratio, RSM: Response Surface Methodology; SY: Solid Yield.

The ANN and RSM models were evaluated based on the AAD, PRE, and R^2 results obtained from the modelling and optimisation of the torrefaction process. Comparisons of the performance of both models were carried out in two parts. Part one involves an assessment of the three response variables (Y_1, Y_2, and Y_3) of the optimum fuel (Coal + Torrefied PSD), in terms of their AAD, PRE, and R^2 results as shown in Table 7.16, while part two compares only, the enhancement factor of the other fuels investigated using Equation (7.14) through Equation (7.19) and employing also the estimation tools used in part one as presented in Table 7.17.

$$\mathrm{AAD}\ [Y_1] = \left\{\left[\sum_{i=1}^{n}\left(\frac{\mathrm{HHV_{i,Experiment}} - \mathrm{HHV_{i,Predicted}}}{\mathrm{HHV_{i,Experiment}}}\right)\right]\frac{1}{n}\right\} \tag{7.14}$$

$$\mathrm{AAD}\ [Y_2] = \left\{\left[\sum_{i=1}^{n}\left(\frac{\mathrm{EF_{i,Experiment}} - \mathrm{EF_{i,Predicted}}}{\mathrm{EF_{i,Experiment}}}\right)\right]\frac{1}{n}\right\} \tag{7.15}$$

$$\mathrm{AAD}\ [Y_3] = \left\{\left[\sum_{i=1}^{n}\left(\frac{\mathrm{SY_{i,Experiment}} - \mathrm{SY_{i,Predicted}}}{\mathrm{SY_{i,Experiment}}}\right)\right]\frac{1}{n}\right\} \tag{7.16}$$

$$\mathrm{PRE}\ [Y_1] = \frac{[\mathrm{EV_{HHV}} - \mathrm{PV_{HHV}}]}{[\mathrm{EV_{HHV}}]}\ \ \frac{100}{1} \tag{7.17}$$

$$\mathrm{PRE}\ [Y_2] = \frac{[\mathrm{EV_{EF}} - \mathrm{PV_{EF}}]}{[\mathrm{EV_{EF}}]}\ \ \frac{100}{1} \tag{7.18}$$

$$\mathrm{PRE}\ [Y_3] = \frac{[\mathrm{EV_{SY}} - \mathrm{PV_{SY}}]}{[\mathrm{EV_{SY}}]}\ \ \frac{100}{1} \tag{7.19}$$

where AAD and PRE are the Absolute Average Deviation and Percentage Relative Error, $HHV_{i,Experiment}$, $EF_{i,Experiment}$, $SY_{i,Experiment}$ and $HHV_{i,Predicted}$, $EF_{i,Predicted}$, and $SY_{i,Predicted}$ are the experimental and predicted Higher Heating Value, Enhancement Factor, and Solid Yield of the fuels.

Table 7. 16: Summary: Optimization analysis of the optimum fuel: ANN and RSM models

Coal + Torrefied PSD						
Response variable	R^2	RSM AAD	PRE [%]	R^2	ANN AAD	PRE [%]
HHV [Y_1]	0.992	-0.038	0.381	0.999	-0.003	-0.303
EF [Y_2]	0.986	0.018	0.000	0.995	-0.027	-2.657
SY [Y_3]	0.940	0.017	0.955	0.973	-0.003	-0.301

AAD: Absolute Average Deviation; Percentage Relative Error ANN: Artificial Neural Networks; EF: Enhancement Factor; HHV: Higher Heating Value; SY: Solid Yield; PSD: Pine Saw dust; RSM: Response Surface Methodology; R^2: Coefficient of determination

Table 7.17: Summary: Optimization analysis of the other fuels: ANN and RSM model

Response variable	Coal + Torrefied SCB			Coal + Torrefied CC			Coal + Torrefied PSD		
	R^2	AAD	PRE [%]	R^2	AAD	PRE [%]	R^2	AAD	PRE [%]
RSM									
EF [Y1]	0.985	-0.015	-0.250	0.985	0.034	0.559	0.786	-0.025	-0.409
ANN									
EF [Y1]	0.999	-0.004	-0.142	0.999	-0.076	-7.568	0.999	-0.004	-0.351

AAD: Absolute Average Deviation; PRE: Percentage Relative Error; ANN: Artificial Neural Networks; EF: Enhancement Factor; CC: Corn Cob; SCB: Sugarcane Bagasse; WT: Waste-Tyre; RSM: Response Surface Methodology; R^2: Coefficient of determination.

From the results of the R^2 produced by the two models, both of them were found to be effective in predicting and optimizing the torrefaction process variables, but the AAD, PRE, and R^2 results obtained from the ANN shows that the package is more reliable than the RSM.

7.10. Our results compared with the literature

The reports on biomass torrefaction processes are available in the literature, but models describing the HHV, EF, and SY from blends of coal and torrefied biomass, and WT as response or output variables, and using the ANN and RSM models are scarce in the literature. It can be observed from

Table 7.18, that most of the authors studied the predictions of different physio-chemical properties of torrefied fuels, and employing different process conditions, and they are explicitly explained in Table 7.18.

Table 7. 18: Comparison of the present work with previous studies

Model Used	Fuel studied	Major Findings	Reference
ANN & Empirical correlations	250 Biomass samples found in the literature	Developed models were able to predict the HHV of the fuels.	[278]

Remarks: **I**nput variables: Fixed carbon, Volatile matter, and Ash**;** Output Variable: HHV; Hidden layer neurons: 12. A high degree of correlation was achieved by the ANN than the empirical model.

RSM	Timothy hay	The model successfully predicted the HHV of the torrefied fuel.	[277]

Remarks: RSM input variables: Torrefaction temperature; Heating rate; & Residence time. Output variable: Solid & Energy Yield. Optimum Condition: Temperature: 278.7 ºC; Heating rate: 10ºC/min; Time: 15 min. Torrefied fuel Quality improvement compared to raw fuel: by 26 %.

Hybrid PSO-SVM (Fitted in MLP & RF): Machine learning techniques	100 raw and torrefied biomass samples found in the literature	Model capable predicting the HHV of biomass torrefaction process, and with the volatile matter as the most influential parameter. The HHV R^2 obtained was 0.94 %	[280]

Remarks: Parameters used for the predictions were fixed moisture, carbon, and volatile matter contents, reaction temperature, residence time, atomic O/C and H/C ratios. The model was developed also to reduce the costs in the quality assessment of biomass HHV in power plants.

Aspen Plus	Birch branches	Model was reliable in predicting the carbon, oxygen and hydrogen contents of the torrefied biomass. Increase in temperature increased mass and energy yield, but increased the HHV.	[275]

Remarks: Torrefaction temperature and time of 275-278 ^{O}C and 30 min were the optimum process condition for the torrefaction. . Process energy efficiency increases with torrefaction temperature.

Linear Regression Model	Birch branches	Model capable of predicting the residual moisture content & an-hydric weight loss for the improvement of drying and torrefaction. Model also reliable in estimating the mass and energy balance.	[275]

Remarks: The LHV of the gas, solid and gas yield from the torrefied fuel were predicted

-	Corn Stover	Model predicted the improvement of biomass energy density & reduction in the moisture content of the fuel.	[279]

Remarks: Torrefaction conditions: Temp: 200, 250, & 300 ^{O}C; Time: 10, 20, 30 min; Moisture content: 30, 45 and 50 %. Energy density increase: 2 - 19 %; Mass yield decrease: 3 - 45 %; Energy yield decrease: 1 - 35 %.

LSR model	Biomass	Model capable of predicting the kinetic and volatile species released from torrefaction process. Increase in the temperature increases the solid yield. The predicted HHV was dependent on the temperature and not time.	[276]

Remarks: Torrefaction temperature: 510 – 550 & 520 – 550 K. The H/C & O/C ratios decreased with increase in temperature, and with the mild temperature regime as the optimum torrefaction temperature. Enhancement factor (EF) increased rapidly with the mild temperature regime & was the optimum torrefaction temperature. Temperature was the most influential process factor.

ANN & RSM	Coal + TPSD, Coal + TSCB, Coal + TCC, & Coal + TWT	Model capable of predicting the HHV, EF, & SY of the torrefied fuels, but the ANN is more accurate than the RSM for all the fuel blends	Current work

Remarks: Input parameters & Condition**:** Temperature: 200, 250, & 300 ^{O}C; Time: 30, 45, & 60 min; Coal-to- biomass, and WT blending ratio: 50:50, 71:29, & 80:20. Torrefied fuel improvement: by 10 %. The EF increased with an increase in temperature, but with the severe temperature regime as the optimum, and temperature as the most influential process factor investigated.

PSO: Partial swarm optimisation; SVM: Support vector machines; LSR: Least square regression; MLP: Multilayer performance network; RF: Random Forest; ANN: Artificial neural network; RSM: response surface methodology: TPSD: Torrefied pine saw dust; TSCB: Torrefied sugarcane bagasse; TCC: Torrefied corn cob; TWT: Torrefied waste-tyre

7.11. Concluding remarks

The evaluation of process variables for the torrefaction of coal/biomass/waste tyre blends were carried out using ANN and RSM approach. The fuel blends investigated were Coal + Torrefied PSD, Coal + Torrefied SCB, Coal + Torrefied CC, and Coal + Torrefied WT. Three torrefaction temperature regimes (200, 250, & 300), torrefaction times (30, 45, and 60 min), and blend ratios (50:50, 71:29, & 80:20) for Coal-to- solid fuel were studied. The optimum torrefaction process conditions and fuel were determined and the process models were developed for each of the fuel, respectively. The optimum conditions are of the order of 50:50 Coal-to-Torrefied Fuel ratio (300 ^{O}C and 45 min) > 50:50 Coal-to-Torrefied Fuel ratio (250 ^{O}C and 30 min) > 50:50 Coal-to-Torrefied Fuel ratio (200 ^{O}C and 45 min), while the optimum fuel follows the order of Coal + Torrefied PSD > Coal + Torrefied SCB > Coal + Torrefied CC and > Coal + Torrefied WT. The overall process was very critical to promoting sustainable energy development, economic growth and a promising technique for waste to wealth management in developing countries. Based on the aforementioned considerations, the following conclusions were made:

- The most viable torrefaction operating conditions are of the order of 50:50 Coal-to-Torrefied Fuel ratio (300 ^{O}C and 45 min) > 50:50 Coal-to-Torrefied Fuel ratio (250 ^{O}C and 30 min) > 50:50 Coal-to-Torrefied Fuel ratio (200 ^{O}C and 45 min), while the most viable fuel follows the order of Coal + Torrefied PSD > Coal + Torrefied SCB > Coal + Torrefied CC and > Coal + Torrefied WT.

- The Coal + Torrefied PSD have the highest HHV and EF of 28.27 MJ/kg and 1.41, hence; becomes the most viable fuel studied.
- Around 10 % increase in the calorific value of the Coal + Torrefied PSD was obtained when compared to the raw fuel thus; making it the most viable fuel for the fuels studied.
- Torrefaction is not recommended as a method of improving the fuel quality of waste tyre (WT), because it showed a very low enhancement of 1.03 after the pre-treatment. Hence; Potential torrefaction plants should not consider the process.
- A second-order polynomial and ANN models were developed for the response variables for each of the fuels, and they described well the torrefaction process, but the ANN model is more reliable than the RSM on the account of R^2, AAD and PRE results.

Finding a standard method of determining the number of neurons for training the network will save time and improve the model results. However, the developed models are capable of predicting the variables studied and, in the future, can be employed in predicting the profits accrued due to torrefaction of fuels in the energy production plants.

Chapter 8: Development of effective tar treatment technique for production of high-quality syngas from blends of coal and biomass.

8.1. Introduction

In chapter six, profitability of an energy plant was maximized via biomass torrefaction was investigated, but the effect of presence of tar on the operational cost of the plant was not considered. Understanding the tar treatment process prior to co-gasification of biomass and coal is important. The study is required because the presence of tar may affect profitability of energy plant. Based on this argument, four important process schemes were considered for the investigation, and were comprehensively discussed in this chapter. It includes; (1) Biochar production & catalyst synthesis (2) Tar production and treatment (3) tar analysis and (4) model development.

However, it is necessary to state that a part of this chapter was presented at the International Pittsburgh Coal Conference 2019 (Pittsburgh, Pennsylvania) and was included in the conference proceedings. Production of tar is inevitable in gasifiers using biomass or blends of biomass and coal as fuels. Most times, the nature of tar produced is dependent on the physio-chemical compositions of the fuel materials and the operating conditions employed for the gasification process. Tar is a complex mixture of aromatics containing a significant fraction of polycyclic aromatic hydrocarbons (PAH) [286,267] There are different classes of tar namely; primary, secondary and tertiary tars [287]. Irrespective of the type of tar generated, similar gasification or operational difficulties are encountered. The problems may include blockages of coolers, valves, filters, condensers, and feed lines of the gasification unit. Besides that, an entrainment of tarry materials into the produced gas dependent on the amount, affects the quality of the gas, and as well, increases the cost of gas cleaning. Product gas may require cleaning of tar, to meet up with the limit allowed for its use as fuel in different energy conversion systems. For example, the allowable tar limits for gas engines, gas turbines, and fuel cells are 50, 5, and 1 mg/Nm^3, respectively [287]

There are several methods of cracking or treating of tars (e.g. physical, thermal and catalytic cracking processes). The physical treatment may involve separation using suitable separating materials such as filters and precipitators (e.g. electrostatic precipitators) or by absorption, using water and oil. This method is not attractive because the chemical energy contained in the tar is lost, and the discharge of wastewater from the process poses a huge threat to the environment. Thermal cracking is therefore, preferred because the tar is decomposed into permanent gases

with the heating value significantly retained in the gas, but the process is energy intensive (>800 ^{O}C). The implication is that high temperature resistance reactor materials and long residence times are needed to conduct the test, thus increasing the overall experimental cost. For catalytic tar treatment, low temperature process condition (600 – 900 ^{O}C) and fast reaction rate are feasible, which therefore, makes the technique more promising than the physical and thermal methods [288]

Primary and secondary methods can be used to treat tar arising from biomass gasification or co-gasification of biomass and coal using catalysts. The primary treatment is carried out inside the gasifier, while the secondary approach is performed outside the gasifier. Generally, the use of catalyst in biomass or coal and biomass gasification is very essential because it enhances the gas yield [288] Balat [288] argued that hydrogen yield and syngas ratio was increased from 33.3 to 52.5 % and 1.15/2.15 to 1.87/4.45, respectively on application of catalyst during biomass gasification. Additionally, a review on the effect of dolomite, alkaline metal and Nickel catalysts in biomass gasification using different types of gasification agents that were carried out by Devi et al. [290] revealed that the catalysts are effective for elimination of tar.

Fundamentally, there are two types of catalyst used in biomass steam or air-steam gasification. It includes mineral based (e.g. dolomite [291], olivine [292] and alkaline earth metals [293] and synthesised catalyst; transition metal catalyst for gasification [294,295]. In a review carried out by [8] to study the effects of the aforementioned mineral based catalysts on tar elimination, it was observed that all the catalysts were effective for tar treatment, but some merits and demerits exist for each of the catalyst. The use of nickel as a catalyst, could be promoted or supported by biochar material to complement the catalyst production cost, and as well, limit the deposition of carbon on its active sites, thus; resulting to higher activity for tar cracking [296]. Secondly, biochar material which is usually considered as a waste (by-product) from biomass gasification or pyrolysis process has great potentials to be used as a heterogeneous catalyst in co-gasification of biomass and coal [296] hence; affirming a waste to wealth phenomena.

Some researchers have reported that biochar-based catalyst can be used in different capacities. It includes tar removal in gasification [297,298], biomass refining processes (e.g. hydrolysis & dehydration) [299,300], biodiesel [301,302], biomass pyrolysis [303], bio-oil upgrading [302,303], Fischer–Tropsch synthesis of liquid hydrocarbons from syngas [304], and among others. With regard to using biochar and Ni-biochar based catalysts, Hervy et al. [306], argued that the presence of inorganics (e.g. K and Fe) in biochar contributes a lot to catalytic activity for tar cracking, while [307,299,300], reported that biochar surface functional groups could aid the

absorption of metal precursors; a condition required for synthesis of biochar-supported metal catalyst.

According to Simell et al. [291], coal gasification produced tars consisting of aromatic ring compound (e.g. 1-methylnaphthalene, naphthalene, benzene and other poly-cyclic hydrocarbons, while the produced gas from biomass gasification contained tars of mainly poly-aromatic hydrocarbons such as naphthalene and benzene. However, nickel catalyst enhances the enrichment of CO and H_2 formation in the product gas at elevated temperature of around 740 ^{O}C, but with CH_4 formation at a lower temperature. Additionally, it is economical viable to use the in-situ catalytic cracking process to treat biomass and coal tars with Nickel as catalyst [290]. The findings from catalytic cracking of tar obtained from blends of biomass and coal as reported by Brown et al. [308] and Corella et al. [309] proved that an application of catalyst in the gasifier could reduce the production of tar. Several analytic techniques such as Near Infrared (NIR) spectroscopy, thermogravimetric –mass spectroscopy (TG-MS), and TG-MS coupled with Differential Thermogravimetric Analysis (DTG), GC-MS/FID had been used to identify fractions of tar arising from biomass materials [56]. The aforementioned techniques are effective, but an efficient tar treatment method is required to reduce both time and cost of experimentation.

To develop tar treatment model, it is essential to understand the different classifications of tar and how they are formed. This has been presented in chapter two. Meanwhile, the majority of the tar treatment models found in the literature was dependent on naphthalene, toluene, and benzene as tar models. It will be important to study treatment of tar obtained from raw feedstock using catalysts synthesised locally with waste material (biochar) as support, thus; ensuring originality of the investigation. In this study, tars obtained from blends of coal biomass materials were considered, and were treated using biochar and Ni-biochar based catalysts. The catalysts were considered based on availability of the precursors (e.g. biochar), for their synthesis, raw material sustainability (waste biomass), and expected catalyst performance. The outcome of this study will minimise catalyst production cost, provide effective catalysts for tar treatment, and serve as an instrument for harnessing wealth from waste (biochar). Importantly, models for the treatment of tar from similar feedstock are provided.

8.2. Materials & Method

8.2.1. Bio-char production

In this study, three categories of biomass were used to produce biochar used as catalyst, and

catalyst support. The biomasses are woody and herbaceous biomass materials represented by pine sawdust (PSD), sugarcane bagasse (SCB), & corn cob (CC), respectively. Both feedstock was chosen based on their availability. For the biochar production, 100 g of PSD, SCB, and CC were measured using high precision weighing balance, and fed into a quartz tubular reactor using a rectangular ceramic plate, respectively. The process was carried out under nitrogen atmosphere at a flow rate of 350 mL^{-1} and reactor temperature of around 500 ^{O}C at a heating rate of $5^{O}C$/min. After every experimental run with each of the biomass material, the temperature of the reactor was increased to around 700 ^{O}C to burn-out the residual components of the biomass, while nitrogen and air were used to flush the reactor to prevent contamination. The reactor was allowed to cool, after which, the synthesized biochar was packaged in an air-tight plastic container and stored for compositional analysis and other uses (e.g. as catalyst and catalyst support).

8.2.2. Catalyst synthesis

The biochar materials prepared as described in chapter 3 were used as catalysts as well as catalyst support in nickel-biochar catalyst synthesis. The synthesis process involves dissolution of about 15 g of Ni nitrate in a 100 ml of de-ionised water and loading the solution into around 10 g of biochar via incipient wet impregnation method. For the ageing process, the solution was transferred into a 200 ml wide-neck glass reactor containing a magnetic rod and stirrer. The reactor was placed in a hot-plate operated at 250 rpm at 40 ^{O}C for 4hrs. Thereafter, the solution was poured into a glass container with cover and kept till the next day. After the ageing process, it was dried in an oven at 105 ^{O}C for 12 hrs following calcination in an air-flow electric furnace at 900 ^{O}C for 1 hr. The same procedure of synthesis was adopted for the three different biochar materials in synthesising the Nickel-biochar based catalysts. The catalysts were thus; denoted as Ni-PSD-BC, Ni-SCB-BC, and Ni-CC-BC, respectively. Essentially, nickel catalyst may lose its activity because of sintering therefore, it is important to load it with other support material which prevent this occurrence, and as well, ensure product gas enhancement [310].

8.2.3. Tar generation and treatment

The tars used in this study were obtained from blends of coal and biomass materials (Coal + CC, Coal + SCB, & Coal + PSD and raw CC, SCB, & PSD. The last three are biomass tars. All the tars were generated and catalytically treated using the results obtained from the DoE. For experimental control, biomass tars (CC, SCB, & PSD) were equally treated with the optimum catalyst, but only to compare the compounds present on them, with that of coal blends (i.e. Coal

+ CC, Coal + SCB, & Coal + PSD).

8.2.4. Tar treatment experimental setup

The schematic diagram of the apparatus used for the tar treatment is shown in Figure 8.1. The facility is comprised of two inter-connected reactor schemes of A and B, and is referred in this study as, reactor A and reactor B. The decomposition of the feedstock was performed in reactor A, while the actual tar cracking was carried out in reactor B that contained the catalyst bed A detailed description of the procedure used for the tar treatment has been presented in chapter 3.

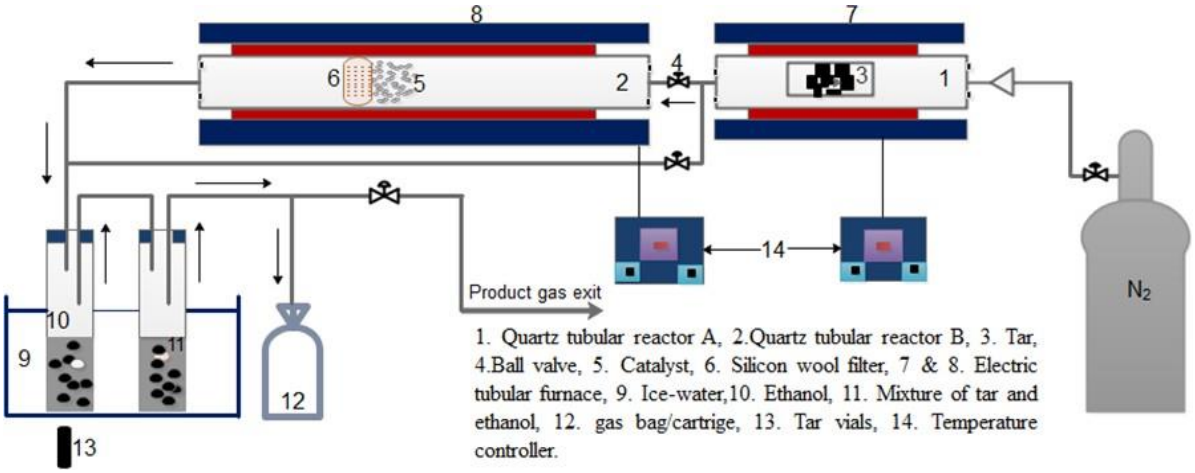


Figure 8. 1: Tar treatment facility

However, the decomposition process is expressed in Equation (8.1) and Equation (8.2), while carbonization reaction is presented in Equation (8.3):

$$C_X H_m O_z \xrightarrow{Pyrolysis} [Tar, H_2O, Char\ (C_n H_m)_s, (C_n H_m)_g, CO_2, CO, N_2] \quad (8.1)$$

$$(C_n H_m)_g \xrightarrow{Secondary\ Pyrolysis} C + H_2 \quad (8.2)$$

$$Char\ (C_n H_m)_s \xrightarrow{Secondary\ Pyrolysis} C + H_2 \quad (8.3)$$

The real gasification process involving the optimum (most viable) feedstock and catalyst was carried out as reported in chapter 9. However, the percentage amount of tar converted during the process was determined using the expression presented in Equation (8.4) [311]:

$$\varphi\ (\%) = \frac{T_{in} - T_{Out}}{T_{in}} X\ 100 \quad (8.4)$$

Where φ, $T_{in,}$ T_{Out} represents the percentage amount of tar converted, amount of inlet tar and outlet tar, respectively. It is important to emphasise that Equation (8.4) was used to estimate the percentage amount of tar converted using the tars and catalysts investigated based on the DoE results. The inlet tar (T_{in}) is the amount of tar used to carry out the tar treatment and analysis, and it was the tar collected and measured after the devolatilization/pyrolysis of the fuels.

8.2.5. Feedstock characterisation

The physio-chemical properties of the blends of coal and biomass used for the tar produced were carried out following the standard procedure of the American Society for Testing and Materials (ASTM E870-82) for the proximate analysis, while the ultimate analysis and the calorific value (CV) of the biochar were measured using the CHNS-O Organic Elemental Analyzers (FLASH 2000) and an oxygen bomb calorimeter (203M 1241), respectively. The results of the CV and CHNS-O analysis for the blends of coal and biomass from which the tars were produced have been presented in Chapter three and elsewhere [13]. The BET analysis, Temperature Programmed Reduction (TPR) analysis, XRD, &n TEM-EDX, of the synthesised catalysts were carried out as explained in chapter 3.

8.2.6. Development of tar treatment model

The effects of tar generation on product gases and gasification efficiency as well as different treatment models have been explained in the earlier sections, respectively. Development of effective models for tar cracking is therefore very crucial because, time and cost of experimentation are saved, and importantly, high quality gasification products (e.g. syngas yield & composition) are assured.

In this study, tar treatment model was developed using Box Behnken Design (BBD) method in Design Expert software. It involves a full quadratic regression model. The Design of Experiment (DoE) from which the model was developed comprised tar conversion temperatures (700, 800 & 900 ^{O}C), conversion time (10, 15, 20 min), and blend ratios (50:50, 71:29, & 80:20) for coal/biomass blends as the input variables. The percentage tar conversion was the output variable, and the tars that were treated (CCC-T, CSCB-T, & CPSD-T) were obtained from blends

of coal and biomass (CC, SCB, & PSD). Two categories of catalysts (biochar: CC-BC, SCB-BC, & PSD-BC and Ni-biochar based: Ni-CC-BC, Ni- SCB-BC, & Ni-PSD-BC) were used to treat the aforementioned tars and employing the results obtained from the DoE. However, the description of the catalysts synthesis and tar production had been presented earlier in sections 2.3 and 2.4, respectively. Table 8.1 shows the experimental range and level, as well as the process variables (inputs & output) used in the study.

Table 8. 1: Experimental range and levels of the process variables: Box Behnken Design

		Coded Factor Levels			
Independent Process Variables (Input)	Un-coded Symbols	-1	0	+1	Model Response (Output Variables)
TCT [^{o}C]	X_1	700	800	900	
TCVT [Min]	X_2	10	15	20	PTC
Coal-Biomass blending Ratio [-]	X_3	1	2.5	4	

TCT: Tar conversion temperature; TCVT: Tar conversion time; PTC: Percentage tar conversion

8.3. Tar treatment and analysis

The pictures of tars produced and method employed for tar analysis were presented and described in chapter 3 respectively, but the operating process conditions used is summarised in Table 8.2:

Table 8. 2: Summary of the GC operating process conditions: Tar analysis

Parameters	Values
Column temperature (^{O}C)	50 ^{O}C for 5 min to 325 ^{O}C at 8 ^{O}C/min
Solvent delay (min)	5
Injection split ratio (-)	1:75
Injection temperature (^{O}C)	275
Detection temperature (^{O}C)	300
Injection volume (µl)	1.0
Carrier gas (cm/s)	Helium
Linear velocity (cm/s)	47.2
Helium pressure (cm/s)	20
Total flow (ml/min)	131.5

GC: Gas chromatography

8.4. Results and Discussion

8.4.1. Characterisation of catalysts

8.4.1.1. Brunauer, Emmett, Teller (BET) characterisation result of catalysts

The BET analyses of the catalysts used for the treatment of the tars were carried out, and the results obtained are presented in Figure 8.2: and Figure 8.3 as well as in Table 8.3, but the pore diameter-pore volume relationships of the two categories of the catalysts is depicted in Figure 8.4. Figure 8.2 and Figure 8.3 describes the adsorption-desorption isotherm plots of the Ni-biochar and biochar based catalysts, while Table 8.3 displayed the structural properties (e.g. surface area, pore volume & pore size) of the catalysts.

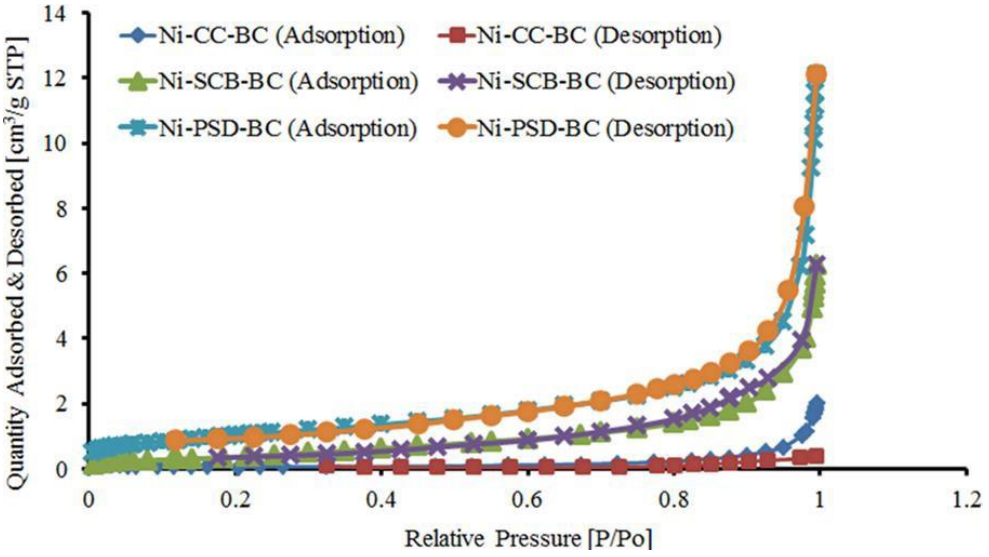


Figure 8. 2: Adsorption-Desorption isotherm plot of the Ni-biochar based catalysts.

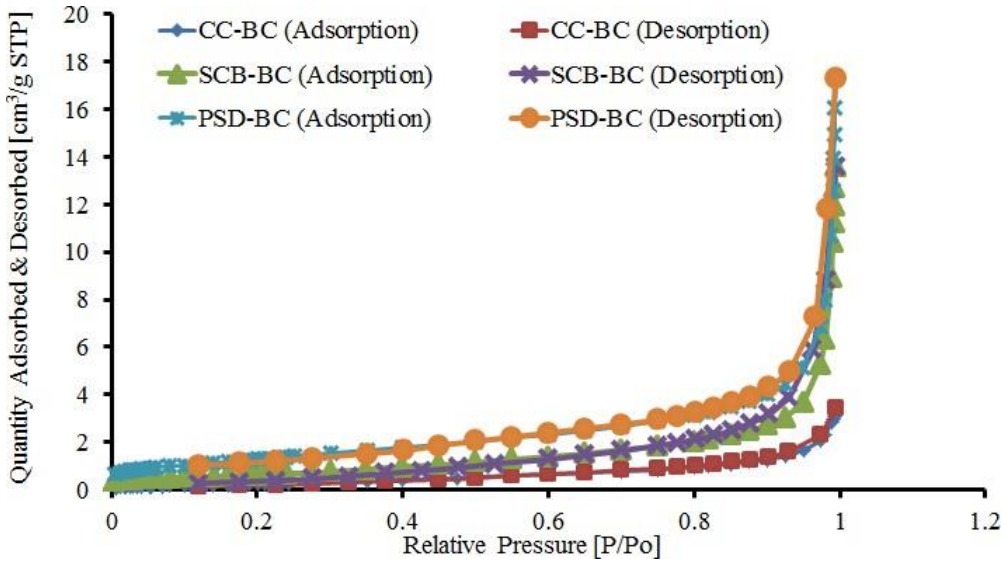


Figure 8. 3: Adsorption-Desorption isotherm plot of the biochar based catalysts

From Figure 8.2, Ni-PSD-BC catalyst has higher surface area and pore volume, and lower pore size when compared to other catalysts. The implication is that higher catalyst activity is expected from the catalyst due to exposition of reacting species to larger surface area and porous medium. Similar result can be seen from Figure 8.3 (the biochar based) and it followed the same trend of interpretation. However, larger catalyst pore size will inhibit reactions of species (tar, gases & catalysts). Therefore, it is also expected that catalysts with higher pore size may not be as effective as that with lower pore size. From Figure 8.4 which describes the pore-volume-pore

diameter relationships of the catalysts, both the Ni-PSD-BC and biochar based catalysts have pore-diameter and sizes higher than other catalysts studied. A higher pore volume and diameter will promote effective mass transfer and sufficient space (pores) for reacting materials, thus; resulting to higher catalysts performance.

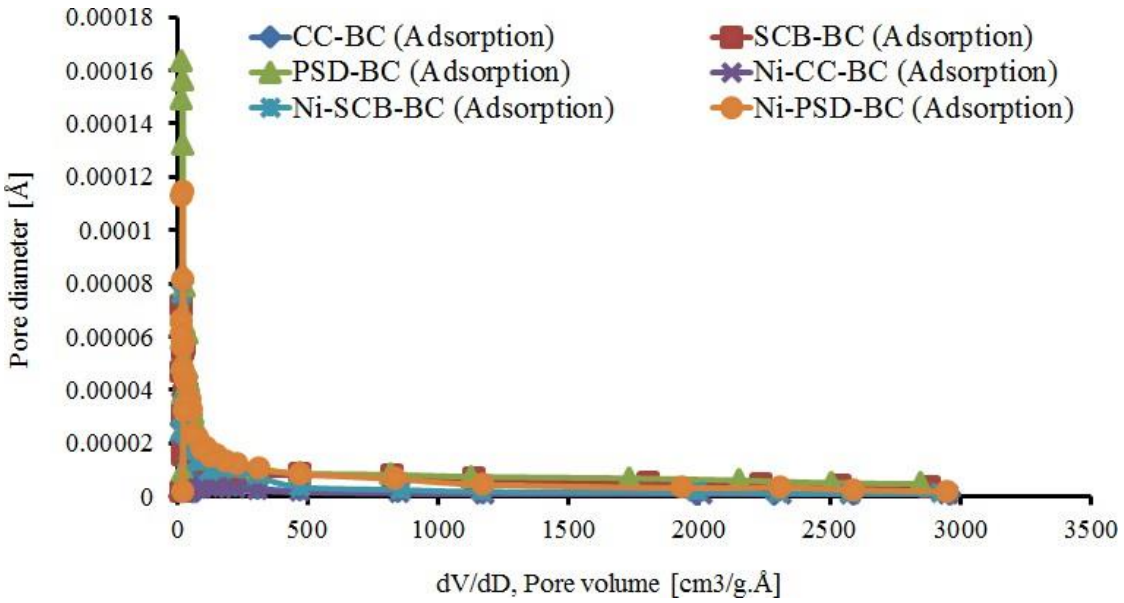


Figure 8. 4: Pore Diameter-Pore volume relationship of the Ni-biochar & biochar based catalysts

Table 8. 3: Summary: Structural properties of the biochar and Ni-biochar based catalysts:

Catalyst	Surface area ($g\ m^2/g$)	Pore Volume (cm^3/g)	BJH adsorption* (cm^3/g)	BJH desorption* (cm^3/g)	Pore size (Å)	BJH adsorption# (Å)	BJH Desorption# (Å)
	Ni-biochar based catalysts						
Ni-PSD-BC	3.752	0.016	0.018	0.019	171.092	184.540	205.853
Ni-SCB-BC	1.399	0.008	0.009	0.009	237.708	161.120	167.394
Ni-CC-BC	0.178	0.003	0.003	0.003	595.416	332.317	273.627
	Biochar based catalysts						
PSD-BC	4.799	0.021	0.0250	0.0269	177.828	188.825	213.019
SCB-BC	2.275	0.017	0.020	0.021	299.569	243.961	228.988
CC-BC	0.9314	0.005	0.005	0.005	201.405	130.133	122.051

BJH: Barrett, Joyner, Halenda; *****: Pore volume BJH; #: Pore size BJH; Ni-PSD-BC: Nickel-pine sawdust-biochar catalyst; Ni-CC-BC: Nickel- corn cob-biochar catalyst; Ni-SCB-BC: Nickel-sugarcane bagasse-biochar catalyst; CC-BC: Corn cob-biochar catalyst; SCB-BC: Sugarcane bagasse-biochar catalyst; PSD-BC: Pine sawdust-biochar catalyst.

The surface area and pore volume of Ni-PSD-BC & PSD-BC catalysts were higher than the other catalysts, while the pore size of Ni-CC-BC & CC-BC catalysts was higher than other catalysts studied, respectively. The pore size of the catalysts is in the order: CC-BC<SCB- BC<PSD-BC (for biochar based) and Ni-CC-BC<Ni-SCB-BC<Ni-PSD-BC (for Ni-biochar based). This is related to the physio-chemical composition of the parent fuel used for the preparation of the biochar. From Table 8.3: it can be seen that the specific surface area, pore volume and pore size of the biochar-based catalysts were higher than that of Ni-biochar based catalysts. It does not necessary mean that the biochar-based catalysts may perform better than the Ni-based catalysts, because stability and crystallinity of the catalysts also has to be considered.

8.4.1.2. Temperature programmed reduction (TPR) of the Ni-based catalysts

The temperature programmed reduction (TPR) test was conducted to investigate the oxidation states of loading of Nickel on the biochar support to understand the oxidation states with the catalyst's activity. The different support used includes PSD, SCB, & CC biochar. The result of the temperature programmed reduction profile for the Ni-biochar based catalysts is presented in Figure 8.5 It can be seen that the oxide reduction signal displayed for all the catalysts followed the same trend, but the signal obtained from Ni-PSD-BC catalysts was the highest for the catalysts studied. This is associated with the oxides composition in the parent fuel; pine sawdust (PSD) when compared to SCB and CC, respectively.

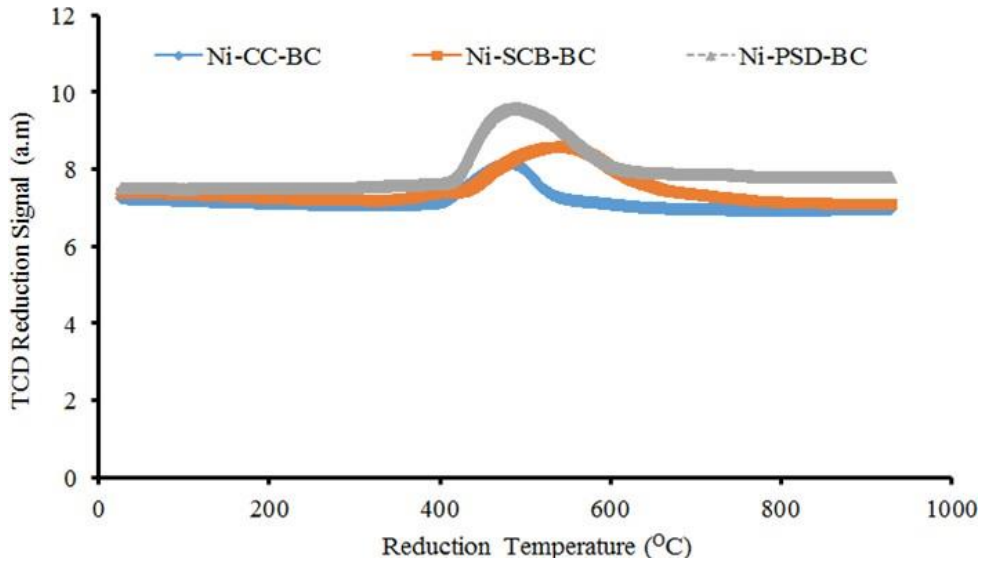


Figure 8. 5: Temperature Programmed Reduction Profile for Nickel biochar based catalysts

The reduction characteristic of Ni-biochar support catalysts mainly dependent on the inherent reducibility of the pure oxide supports. This is based on the fact that the support determines the reactivity of the bridging Ni-O-Support functionalities [312].

From Figure 8.5, the reduction temperatures for Ni-PSD-BC, Ni-SCB-BC, & Ni-CC-BC were in the range of 400 – 600, 400 – 500, & 400 – 500 ^{O}C, respectively. It can also be observed that the oxide reduction process for each of the catalyst commenced almost at the same temperature (400 ^{O}C), but the peaks of the TCD reduction signal of the catalysts varied. It is related to using an equal amount of Ni loading on each of the support and variations in the char characteristics of the bio-char support, respectively. Similar finding was reported by Nguyen et al. [304] when Ni-biochar catalysts were used for hydro-treating bio-oil from micro-algae biomass. Importantly, the peak temperature of reduction of the Ni-biochar catalysts indicated the stability of the Ni^{2+} portions on the catalyst surface as the reduction temperatures were within the aforementioned temperatures for each of the catalyst. This corresponded to the reduction of the bulk NiO portions, the Ni-support (Ni-PSD-BC, Ni- SCB-BC, & Ni-CC-BC) weak interactions or the Ni-support strong interactions respectively [313,314].

Furthermore, the link with medium strength (e.g. 400 – 600 ^{O}C; Ni-PSD-BC catalyst) between NiO and biochar support was considered as the most attractive for the catalyst activity. Finally, on the account that all the NiO portions were assumed to have been reduced from Ni 2+ to NiO, then the produced Ni site density was equal to the moles of the consumed hydrogen during the reduction process. A similar finding was reported by Cheng & Li [314] and Guo et al. [315]. Under this condition, the high percentage of the active NiO portions on the PSD, SCB, & CC biochar surfaces enhanced the catalyst activity in the oxidation- reduction processes, very considerably. It is evidenced in the catalyst activities /results of tar conversion obtained from the Ni-biochar based catalysts.

8.4.1.3. X-ray diffractometer (XRD) analysis

The XRD analyses of the biochar and Ni-biochar based catalysts were also carried out to determine their crystalline structure/phases. The results obtained are displayed in Figure 8.6. The pattern shown by the biochar-based catalysts indicated that they possess strong amorphous structure within the range 6.9161 – 81.4099, 5.1848 – 54.6681, & 5.1084 – 87.2258 (angular locations) for PSD-BC, CC-BC & SCB-BC, and with highest peaks of 243.02, 89.56 & 506.09 (in counts), respectively. This is quite different from the patterns generated from the Ni-based catalysts, and could be attributed to the amorphous nature of the catalyst support (biochar). For the Ni-biochar

based catalysts, it can be seen that very sharp peaks were produced indicating the purity of the catalysts. From Figure 8.6 a, it can be seen that the peaks were not sharp when compared to that of Figure 8.6 b, hence indicating that the catalysts have some impurities. In the case of the Ni-PSD-BC, several distinct peaks in the range of 37.1422 – 79, 2132 theta at 43.0956 angular locations that corresponds to Nickel Copper Oxide phase [$Ni_{.80}$ $Cu_{.2}O$]: JPDS# 01-078-0647. The peaks for the Ni-CC-BC and Ni-CC-BC were in the range of 28.4017 – 79.2818 & 28.1808 – 79.2184 with the highest peaks as 4,314.91 at 44.5098 & 5,097.10 at 43.2066 angular locations, respectively. This corresponds to the Nickel Oxide Silicon Nickel Iron zinc [$NiONi_{17}Si_3Fe_4Zn_9$] & [$Ni_{.9}Zn_{.1}ONiTi_3K_2MgSiO_4SCAlZnO_4$] phases for Ni-CC-BC & Ni- CC-BC, respectively. It can be observed that the angular locations for the highest peak, for each of the Ni-based catalysts were nearly in the same angle (i.e. 43 – 44). It implies that the catalysts have similar crystalline structure which is dependent on the elemental distributions. However, the Ni-PSD-BC displayed the highest purity for the catalysts studied. The purity of the catalysts followed the order: Ni-PSD-BC<Ni-SCB-BC<Ni-CC-BC. The same order was observed for the BET analytical results for the biochar based and Ni-biochar based catalysts, respectively.

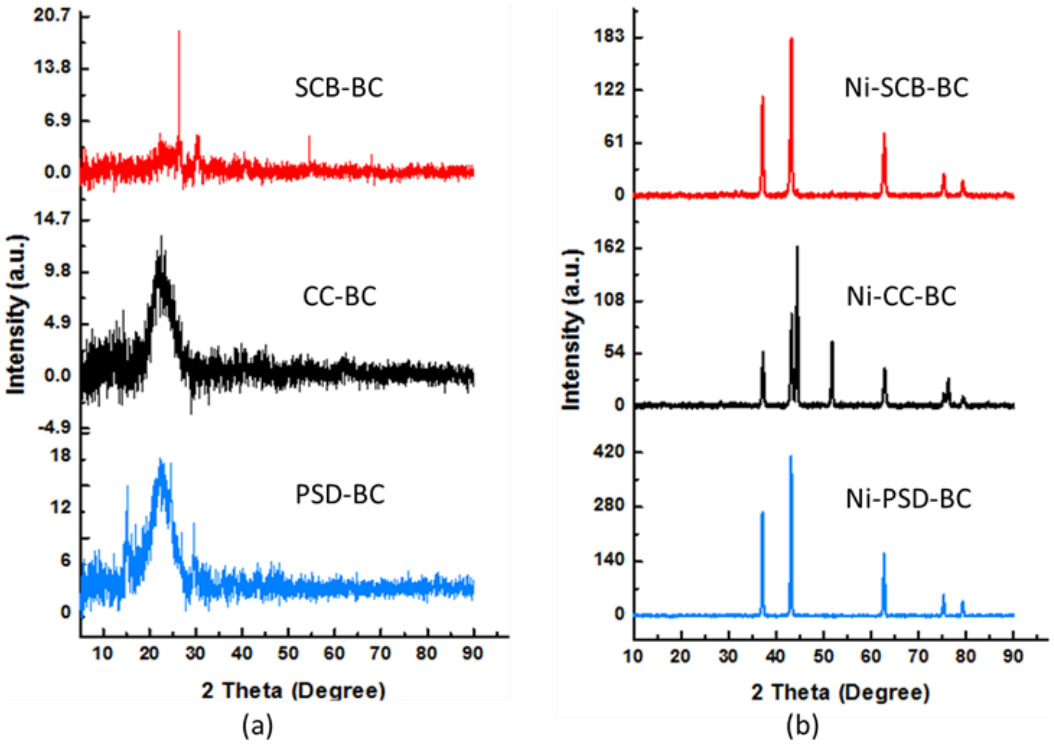


Figure 8. 6: Crystalline phases of the catalysts (a) Biochar based (b) Ni-biochar based:

8.4.1.4. Transmission Electron Microscopy (TEM) analysis

The elemental compositions of the Ni-biochar and biochar based catalysts is shown in Table 8.4, while the morphology of the catalysts are displayed in Figure 8.7. From Table 8.4, it can be observed that there some variations in the elemental compositions of the catalysts due to the difference in physiochemical compositions of the parent fuels.

Table 8.4: Elemental composition of the Ni-biochar & biochar-based catalysts

Element	Mass weight %	Molecular weight %	Atomic weight %	Mass weight %	Molecular Wt. %	Atomic weight %
	Ni-CC-BC				CC-BC	
C	8.37	49.32	0.30	42.31	45.83	60.71
O	20.90	10.09	56.53	19.38	17.54	20.79
Mg	2.63	3.44	6.74	3.18	7.46	2.25
Si	3.71	3.12	5.59	6.31	7.89	3.86
K	5.17	3.28	5.72	23.76	14.25	10.43
Ca	1.00	18.4	1.08	5.06	7.02	2.7
Ni	73.89	28.90	54.58	-	-	-
	Ni-PSD-BC				PSD-BC	
C	-	-	-	85.38	42.29	90.05
O	5.53	25.00	17.53	10.96	33.83	8.69
Mg	40.82	17.86	0.84	-	-	-
Ca	1.09	14.29	1.13	2.41	11.49	0.76
Ni	92.97	42.86	80.26	-	-	-
S	-	-	-	1.26	11.49	0.50
	Ni-CC-BC				CC-BC	
C	-	-	-	92.34	50.00	94.63
O	8.12	80.20	22.49	6.50	37.90	5.00
S	10.99	21.35	15.19	-	-	-
K	3.43	14.06	3.88	1.15	12.10	0.36
Ni	77.46	36.45	58.44	-	-	-

Ni-CC-BC: Nickel-Corncob-Biochar catalyst; Ni-PSD-BC: Nickel-Pine Sawdust-Biochar catalyst; Ni-SCB-BC: Nickel-Sugarcane Bagasse-Biochar catalyst; CC-BC: Corn cob- Biochar catalyst; PSD-BC: Pine sawdust-Biochar catalyst; SCB-BC: Sugarcane bagasse- Biochar catalyst

There is no presence of carbon in the Ni-PSD-BC & Ni-CC-BC catalysts, while its composition in the Ni-CC-BC was low except for the molecular weight. It may be attributed to the total combustion of carbon during calcination. For the biochar-based catalysts, it can be seen that the amount of carbon present is considerably high. This is because the biochar-based catalysts were not calcined, hence; affirming that the carbon (amorphous) were completely burnt leaving only the crystalline phase of the catalyst. However, the elemental composition of the catalysts agrees with those found in the literature [306,308,313,314].

From Figure 8.7, the spectrum of the biochar-based catalysts (d-f), indicates the amorphous nature of the catalyst based on the presence of the area peaks, which could not be found in the Ni-biochar based catalysts. The morphology of the Ni-biochar based catalysts suggests a more solid appearance/block which may be attributed to their crystalline nature when compared to the biochar-based catalysts. This is more prominent in the Ni-PSD-BC catalysts, which therefore affirms the XRD and BET results reported for this catalyst as the optimum catalysts in this study for tar cracking.

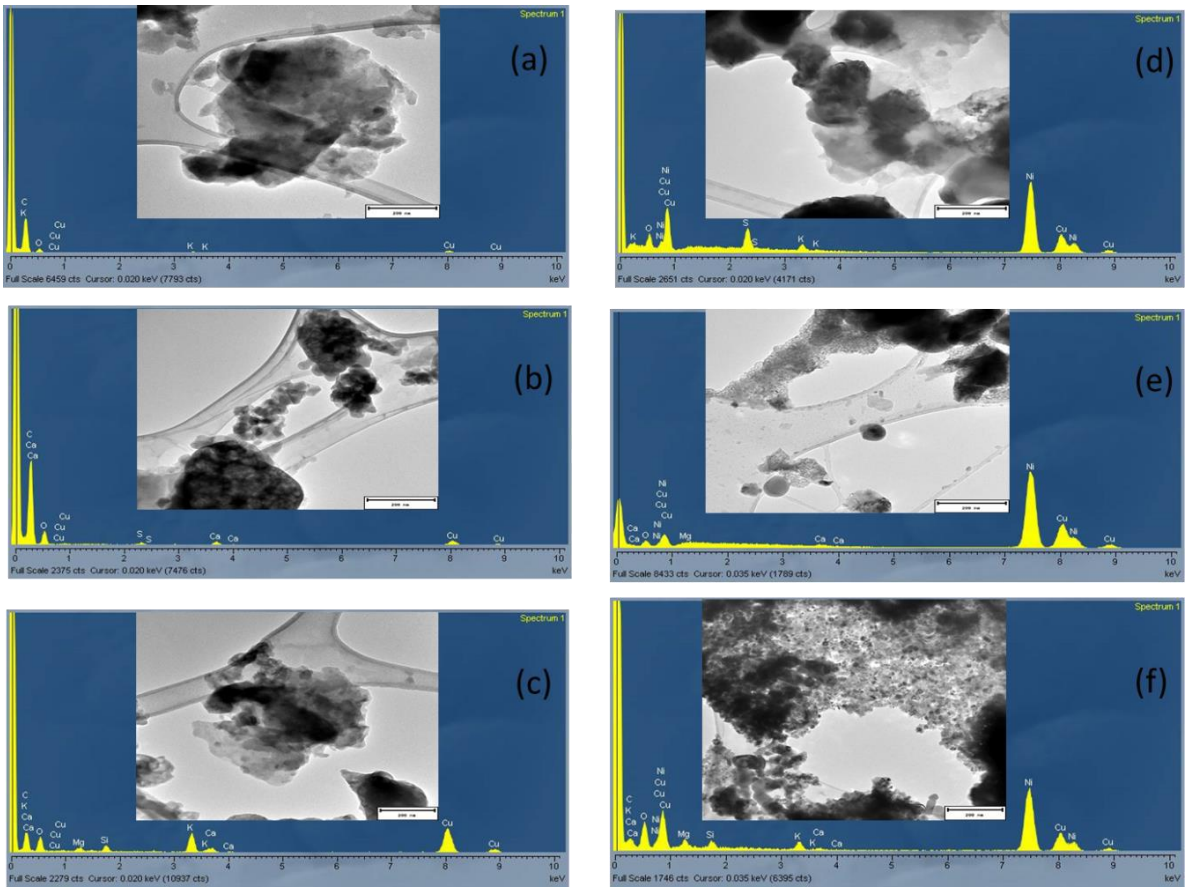


Figure 8. 7: TEM-EDX of the catalysts (a) Nickel-Corn cob-Biochar catalyst (b) Nickel-Pine sawdust-Biochar catalyst (c) Nickel-Sugarcane Bagasse-Biochar catalyst (d) Corn cob- Biochar catalyst (e) Pine sawdust-Biochar catalyst (f) Sugarcane bagasse-Biochar catalyst

8.4.2. Tar treatment: Thermal & catalytic techniques

Three tar conversion temperatures (700, 800, & 900 ^{O}C) were employed to study the treatment of tar samples (CSCB-T, CCC-T, & CPSD-T) obtained from blends of Coal + SCB, Coal + CC, and Coal + PSD respectively.

Biochar (SCB-BC, CC-BC, & PSD-BC) and Ni-biochar based catalysts (Ni-SCB-BC, Ni- CC-BC, & Ni-PSD-BC) were used. From the study, the 900 ^{O}C tar conversion temperature offered the optimum process conditions for the two categories of catalysts as shown in Table 8.5: and Table 8.6:

Table 8.5: Tar cracking temperature of 900 OC: Biochar based catalyst

Feedstock [-]	Tar	Catalyst [-]	TCT [^{O}C]	TCVT [Min]	PTC [%]
Mixing Ratio: 50:50					
Coal + SCB	CSCB-T	SCB-C	900	10	89.51
Coal + CC	CCC-T	CC-C	900	10	89.25
Coal + PSD	CPSD-T	PSD-C	900	10	89.72
Mixing Ratio: 80:20					
Coal + SCB	CSCB-T	SCB-C	900	15	85.55
Coal + CC	CCC-T	CC-C	900	15	86.28
Coal + PSD	CPSD-T	PSD-C	900	15	86.86
Mixing Ratio: 71:29					
Coal + SCB	CSCB-T	SCB-C	900	15	87.53
Coal + CC	CCC-T	CC-C	900	15	87.29
Coal + PSD	CPSD-T	PSD-C	900	15	87.76
Mixing Ratio: 71:29					
Coal + SCB	CSCB-T	SCB-C	900	20	86.46
Coal + CC	CCC-T	CC-C	900	20	86.25
Coal + PSD	CPSD-T	PSD-C	900	20	86.98

CC:

Corn cob; SCB: Sugarcane bagasse; PSD: Pine Sawdust; SCB-C: Sugarcane bagasse biochar-Catalyst; CC-BC: Corncob biochar-Catalyst; PSD-BC: Pine Sawdust biochar-Catalyst; TCT: Tar cracking temperature; TCVT: Tar conversion time; Percentage Tar conversion (PTC); CPSD-T: Coal and pine sawdust blend tar; CSCB-T: Coal and sugarcane blend tar; CCC-T: Coal and corn cob blend tar.

Table 8. 6: Tar cracking temperature of 900 ^{O} C: Ni-based catalyst

Feedstock [-]	**Tar**	**Catalyst [-]**	**TCT [^{O}C]**	**TCVT [Min]**	**TC [%]**
		Mixing Ratio: 50:50			
Coal + SCB	CSCB-T	Ni-SCB-BC	900	10	96.14
Coal + CC	CCC-T	Ni-CC-BC	900	10	94.72
Coal + PSD	CPSD-T	Ni-PSD-BC	900	10	98.25
		Mixing Ratio: 80:20			
Coal + SCB	CSCB-T	Ni-SCB-BC	900	15	95.88
Coal + CC	CCC-T	Ni-CC-BC	900	15	94.71
Coal + PSD	CPSD-T	Ni-PSD-BC	900	15	96.48
		Mixing Ratio: 71:29			
Coal + SCB	CSCB-T	Ni-SCB-BC	900	15	93.75
Coal + CC	CCC-T	Ni-CC-BC	900	15	93.32
Coal + PSD	CPSD-T	Ni-PSD-BC	900	15	94.56
		Mixing Ratio: 71:29			
Coal + SCB	CSCB-T	Ni-SCB-BC	900	20	93.75
Coal + CC	CCC-T	Ni-CC-BC	900	20	93.32
Coal + PSD	CPSD-T	Ni-PSD-BC	900	20	94.56

CC: Corn cob; SCB: Sugarcane bagasse; PSD: Pine Sawdust; Ni-SCB-BC: Nickel- Sugarcane bagasse-Biochar Catalyst; Ni-CC-BC: Nickel- Corn Cob-Biochar Catalyst; Ni-PSD-C: Nickel-Pine

Sawdust-Biochar Catalyst; TCT: Tar cracking temperature; TCVT: Tar conversion time; Percentage Tar conversion (PTC); CPSD-T: Coal and pine sawdust blend tar; CSCB-T: Coal and sugarcane blend tar; CCC-T: Coal and corn cob blend tar.

8.4.3. Effect of time on tar conversion

The effect of time on tar conversion for the biochar and Ni-biochar catalysts at 700, 800, & 900 ^{O}C temperatures was studied using tar conversion times of 10, 15, & 20 minutes. The results are presented in Figure 8.8 through Figure 8.11, respectively. It is important to clarify that the time period < 10 min was considered as the period used for the temperature of the reactor to be stabilised prior to the tar conversion. The percentage amounts of tar converted at 700 – 900 ^{O}C were in the range of 75.81 – 89.72 and 94.81 – 98.25 % for biochar and Ni- biochar based catalysts, respectively. However, it can be seen that the percentage amount of tar converted during the treatment process decreased with an increase in time. From Figures
8.8 and 8.9 and Figures 8.10 and 8.11, it can be observed that tar conversion may reach equilibrium. The implication is that the conversion of tar will continue after 20 minutes and beyond, provided that there are tar and active catalyst available in the reactor for the process.

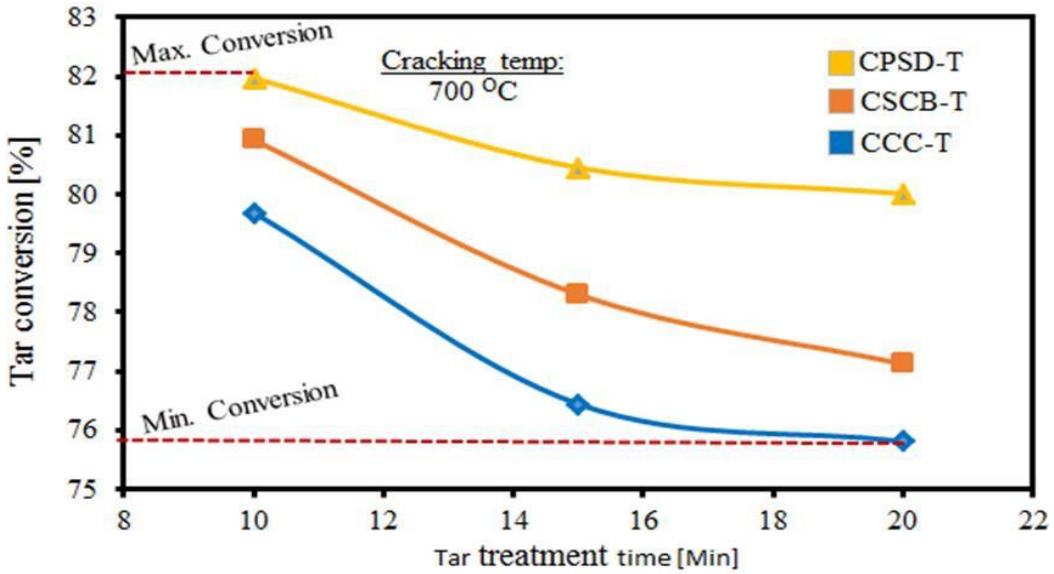


Figure 8. 8: Coal + biomass blend tar: Conversion using biochar-based catalyst at 700 ^{O}C

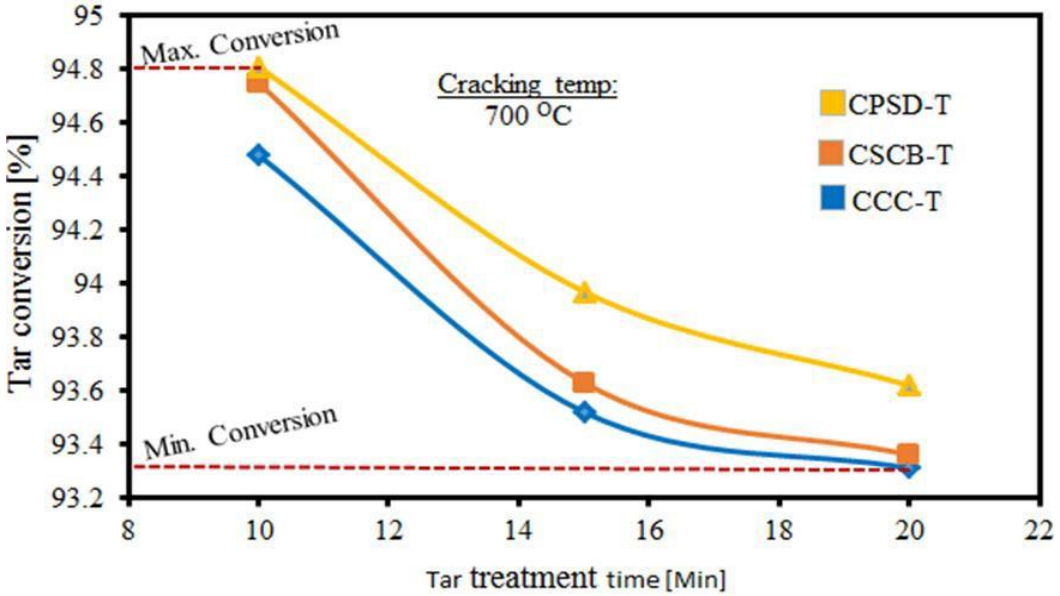


Figure 8. 9: Coal + biomass blend tar: Conversion using Ni-biochar based catalyst at 700 ^{O}C

Similarly, from Figure 8.10 and Figure 8.11, tar conversion decreased with an increase in time, but there is tendency that conversion will terminate after 20 minutes based on two reasons; (1) either that the catalyst has lost its catalytic activity (I.e. de-activation) due to poisoning or (2) that the tar present has been significantly (or completely) cracked in the process. Figures 8.9 & 8.10 and Figures 8.12 & 8.13 which suggested that conversion could reach equilibrium, hence; conversion of tar will continue provided that both tar and catalyst are available in the system for the process.

Generally, the activity of a catalyst during tar conversion can be limited due to catalyst de-activation. This means that the effectiveness of the catalyst in converting the tars to gases over a period of time could be limited by the catalyst poisoning.

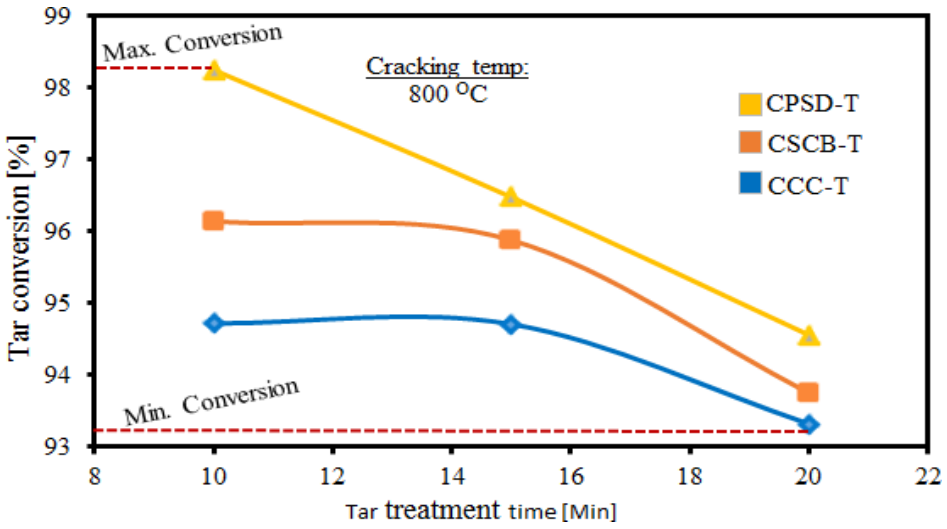


Figure 8. 10: Coal + biomass blend tar: Conversion using biochar based catalyst at 800 ^{O}C

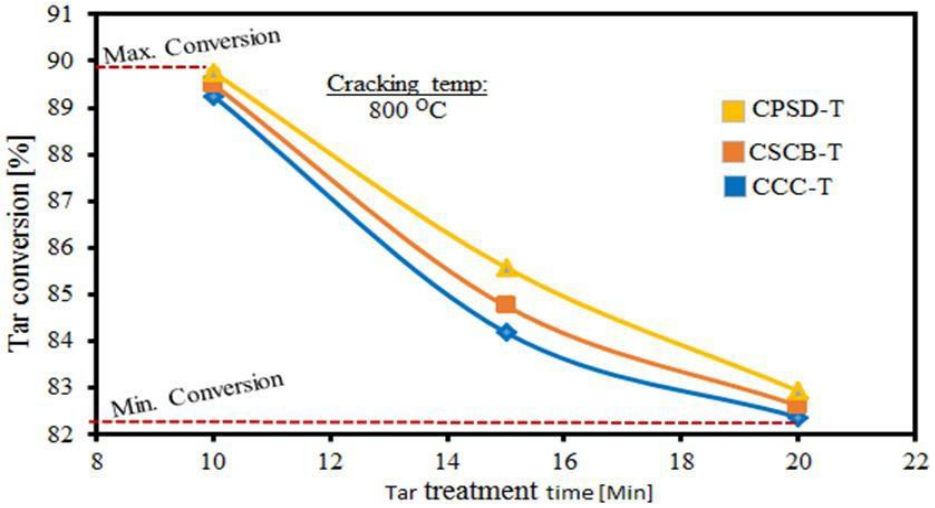


Figure 8. 11: Coal + biomass blend tar: Conversion using biochar-based catalyst at 800 ^{O}C

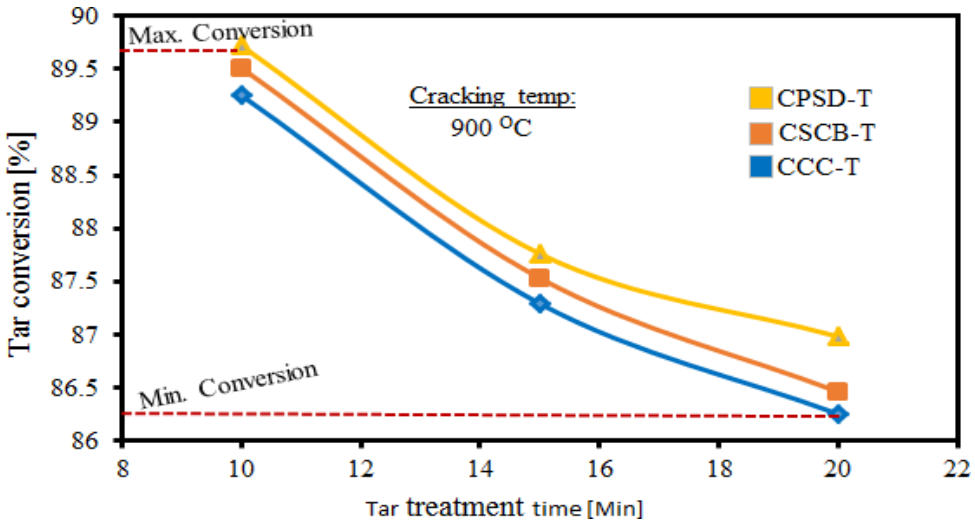


Figure 8. 12: Coal + biomass blend tar: Conversion using biochar-based catalyst at 900 ^{O}C

Generally, it can be observed that the activity of Ni-biochar based catalysts was higher than that of biochar-based catalysts. This was because with biochar as a support to Ni, there was dispersion and stabilisation of the active site of the metal (Ni). The biochar also functioned as an intermediate reductant to convert metal oxides (i.e. the oxides of Ni) to a metallic state, hence; resulting to higher tar conversion [314].

8.4.4. Effect of temperature on tar conversion

The effects of catalyst conversion temperature and catalyst type on tar conversion were considered. To determine that, the average amount of tar converted for 10, 15, and 20 minutes at 700, 800, and 900 ^{O}C using the biochar and Ni-biochar based catalysts, respectively, were evaluated as shown in Figure 8.14 and Figure 8.15. The assessment was carried out to further demonstrate the influence temperature as well as kind of catalyst on tar conversion. The tar conversion increased with an increase in temperature for the two categories of tar studied. The result is expected because more volatile components of the biomass materials linked to the tar were released at higher temperature. Emphatically, the bonds between the aromatic compounds (e.g. polycyclic-aromatic hydrocarbons (PAHs), benzene, etc.) are broken at higher temperature, hence resulting to the transformation of long chain PAHs into short-chain hydrocarbons (tar compounds) Guo et al. [315]. The process cumulatively amounted to an increase in the proportion of single-ring tars, and those present in the product gases were further cracked, thus enabling a higher amount of tar conversion during the treatment. The result is in affirmation with the findings from Li et al. [316]. Li and co-workers reported that the content of tar obtained from the gasification of different proportions of sawdust in the presence of Ni catalysts employing air-steam as the gasifying agent and high temperature (900 ^{O}C), was reduced from 15.1 – 0.4 g/Nm^3. A similar result was also reported by Miccio et al. [317] in which tar content from biomass gasification using $NiAl_2O_3$ as catalyst, was reduced from 110 g/Nm^3 to 10 g/Nm^3 by increasing the reaction temperature from 651 – 826 ^{O}C.

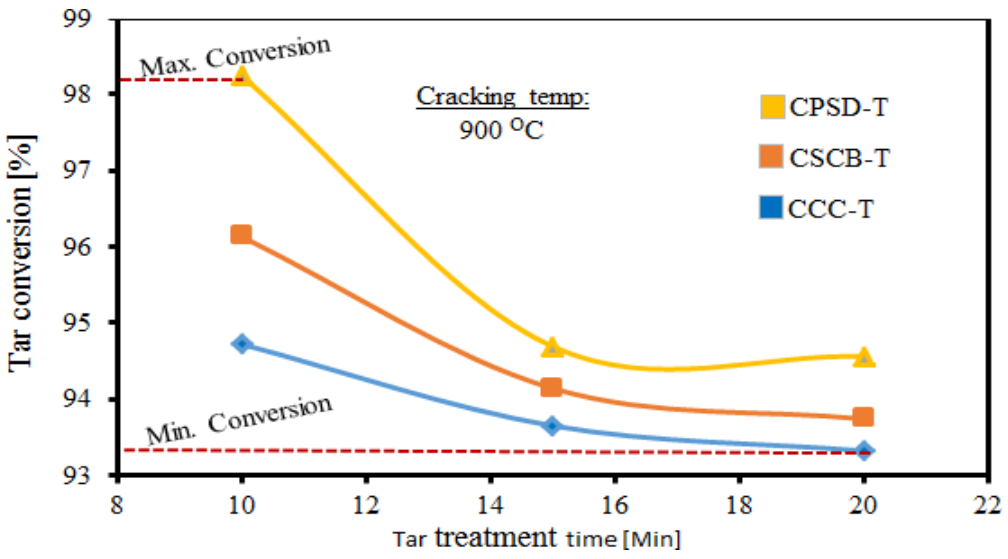


Figure 8. 13: Coal + biomass blend tar: Conversion using Ni-biochar based catalyst at 900 ^{O}C

From Figure 8.14 and Figure 8.15 for example, an average of 96.73, 95.84, & 93.81 % and 89.67, 87.53, & 86.56 % amounts of tar were converted at 900 ^{O}C, for 10, 15, and 20 minutes, respectively. The percentage tar conversion ratios obtained from the tar treatment process were high. The implication was that the synthesised catalysts were effective for tar cracking not only because of the thermal but due to the catalytic treatment of the tars.

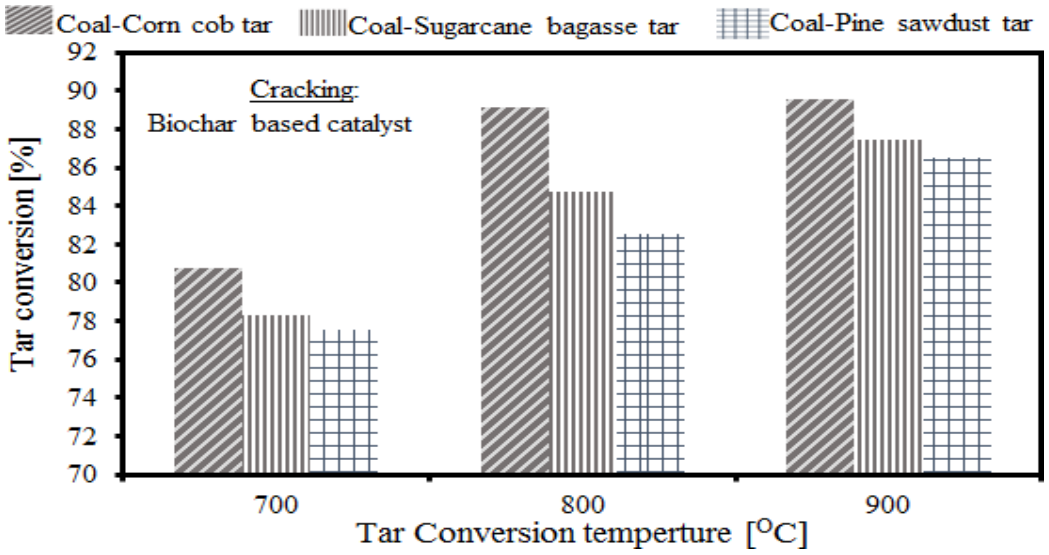


Figure 8. 14: Influence of temperature on tar conversion at 20 minutes: Biochar based catalysts

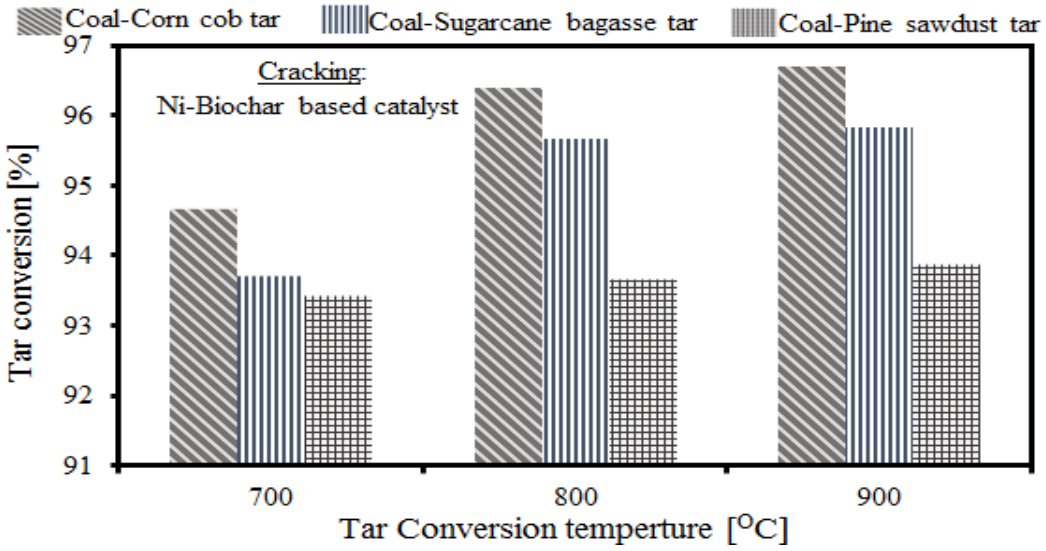


Figure 8. 15: Influence of temperature on tar conversion at 20 minutes: Ni-biochar based catalysts

8.4.5. Catalyst activity: Biochar and Ni-biochar based catalyst

The reforming of polycyclic aromatic hydrocarbons (PAHs) using steam in the gasifier as oxidant at around 1000 ^{O}C is difficult, hence; using catalysts with steam reforming to ensure cracking of the tars (at 700 – 900 ^{O}C) is considered very necessary [318] The catalytic performance of biochar and Ni-biochar based catalysts was carried out based on the conversion temperature and time taken

to crack the different samples of tars used in this study. The percentage difference in the amount of tar converted by each of the catalyst was determined as shown in Table 8.7. Generally, Ni-biochar based catalyst was more efficient than the biochar-based catalyst by 7.87, 3.87, and 3.79 %, respectively. Importantly, the Ni- biochar based catalyst exhibited significantly higher catalyst activity for tar reforming than that of biochar-based catalysts with an average conversion range of 93.43 - 96.73 %, when compared to the biochar with 80.86 – 89.67 %. However, the biochar as a catalyst may be considered more attractive in terms of cost effectiveness. In general, an increase in temperature increased the rate of tar conversion, which decreased with an increase in the tar conversion time.

Table 8. 7: Variation in tar conversion of Ni-biochar and biochar-based catalysts

TCT [^{O}C]	Tar	Catalyst	TCVT [Min]			TCVT [Min]				VTC
			10	15	20	10	15	20		[%]*
		Ni-biochar based catalyst treatment				Biochar based catalyst treatment				
			TC [%]			TC [%]				
700	CCC-T	Ni-CC-BC	94.68	93.71	93.43	CC-BC	80.86	78.4	77.65	7.87
800	CSCB-T	Ni-SCB-BC	96.41	95.69	93.66	SCB-BC	89.23	84.84	82.64	3.87
900	CPSD-T	Ni-PSD-BC	96.73	95.84	93.88	PSD-BC	89.67	87.53	86.56	3.79

TCT: Tar conversion temperature; TCVT; Tar conversion time; VTC: Variation in tar conversion; *: Using Ni-biochar and biochar based catalysts; Ni-CC-BC: Nickel-corn cob-biochar catalyst; Ni-SCB-BC: Nickel-sugarcane bagasse-biochar catalyst; Ni-PSD-BC: Nickel-pine sawdust-biochar catalyst; CC-BC: Corn cob-biochar catalyst; SCB-BC: Sugarcane bagasse-biochar catalyst; PSD-BC: Pine sawdust-biochar-catalyst.

8.4.6. Evaluation of biochar and Ni-biochar based catalysts for tar treatment

An evaluation of the biochar and Ni-biochar based catalysts for tar treatment was carried out to determine the optimum process conditions and catalysts (biochar and Ni-biochar catalysts) for treatment of tar. In this case, 900 ^{O}C and 10 minutes' tar conversion temperature and time, and Coal-to-pine sawdust blend ratio of 50:50 was the optimum process condition. The PSD-BC (biochar based) and Ni-PSD-BC (Ni-biochar based) were the optimal catalysts. The catalysts were used to treat tar including CCC-T, CSCB-T and CPSD-T obtained from blends of Coal + CC, Coal + SCB, and Coal + PSD, respectively. The performance evaluation was based on the activities of the catalysts over the percentage amounts of tar converted. The outcome of the tar treatment is presented in Figure 8.16 and Figure 8.17. However, the result is in affirmation with those obtained from PSD-BC and Ni-PSD-BC.

Importantly, it can be seen from Figure 8.16 and Figure 8.17 that at constant tar conversion temperature (900 ^{O}C), the conversion of tar decreased with an increase in conversion time for both catalysts. The implication is that the cost of energy will be reduced when lesser time (e.g.10 min) is spent for tar treatment when compared to a longer treatment time (e.g. 20 min). However, the activity of the optimum catalysts obtained in this study was tested during the co-gasification of coal and pine sawdust (Coal + PSD) in a fixed bed reactor (Chapter 9). In this case, the effect of catalyst (biochar & Ni-biochar based) on gasification efficiency was evaluated.

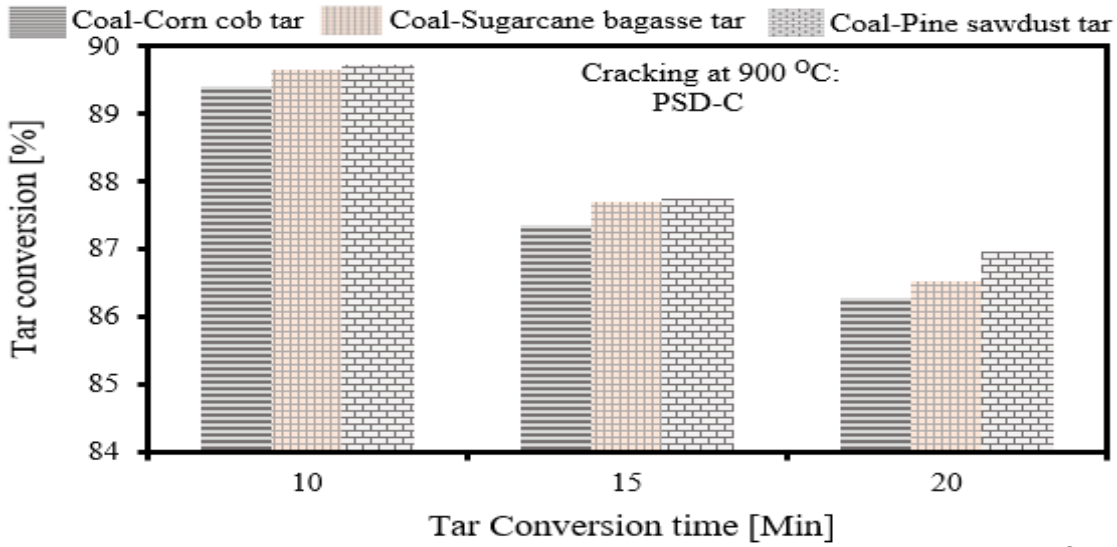


Figure 8. 16: Optimum catalyst evaluation using biochar-based catalyst: 900 ^{O}C

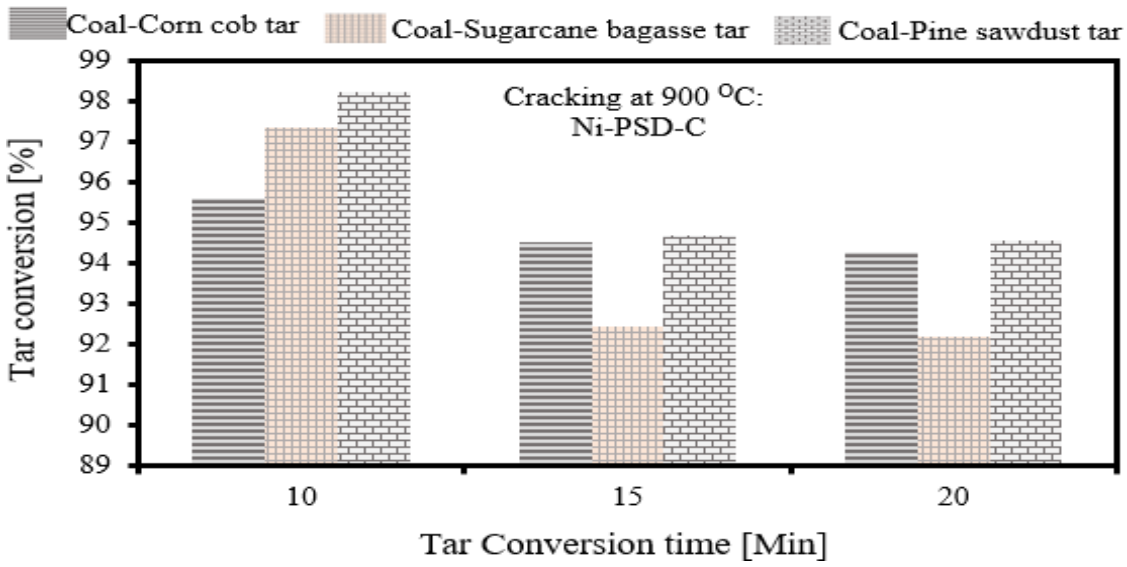


Figure 8. 17: Optimum catalyst evaluation using Ni-biochar based catalyst: 900

8.4.7. Development of tar treatment model

In this study, tar treatment model was developed using Box Behnken Design (BBD) method in Design Expert software. It involves a full quadratic regression model. The Design of Experiment (DoE) from which the model was developed comprised tar conversion temperatures (700, 800 & 900 ^{O}C), conversion time (10, 15, 20 min), and blend ratios (50:50, 71:29, & 80:20) for coal/biomass blends as the input variables. The percentage tar conversion was the output variable, and the tars that were treated (CCC-T, CSCB-T, & CPSD-T) were obtained from blends of coal and biomass (e.g. CC, SCB, & PSD). Two categories of catalysts (biochar: CC-BC, SCB-BC, & PSD-BC and Ni-biochar based: Ni-CC- BC, Ni-SCB-BC, & Ni-PSD-BC) were used to treat the aforementioned tars and employing the results obtained from the DoE. However, the description of the catalysts synthesis and tar production had been presented in the earlier in sections, respectively. Table 8.8: shows the experimental range and level, as well as the process variables (inputs & output) used in the study.

Table 8. 8: Experimental range and levels of the process variables: Box Behnken Design

Independent Process Variables (Input)	Un-coded Symbols	Coded Factor Levels			Model Response (Output Variables)
		-1	0	+1	
TCT [^{o}C]	X_1	700	800	900	
TCVT [Min]	X_2	10	15	20	PTC
Coal-Biomass blending Ratio [-]	X_3	1	2.5	4	

TCT: Tar conversion temperature; TCVT: Tar conversion time; PTC: Percentage tar conversion

The interactions of the process variables obtained from the optimum (most viable) Ni-PSD-BC based catalyst were reported and are depicted in Figure 8.18 through Figure 8.20, while the interactions of other catalysts studied can be found in the appendices. From Figures 8.18 and 8.19 it can be seen that the three process variables studied have significant effects on the amount of tar (%) converted during the treatment. Furthermore, the interactions amongst the variables for example, are well expressed in the results highlighted in all the results displayed in Figure 8.14 through Figure 8.17, hence; affirming the results presented in Figure 8.18 and Figure 8.19.

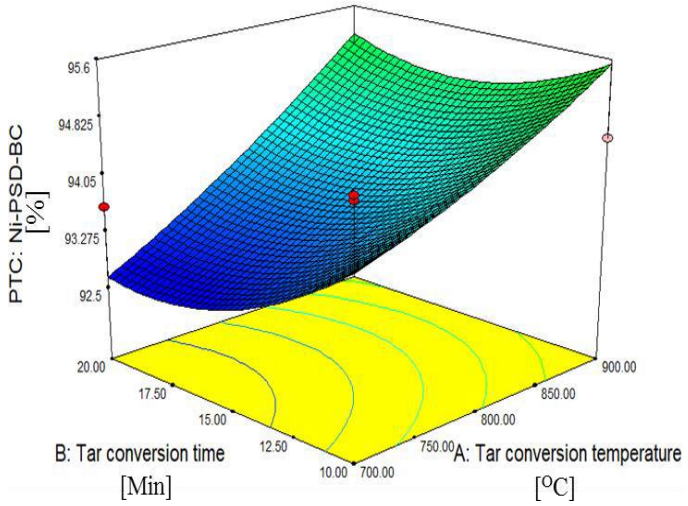


Figure 8. 18: Influence of tar conversion temperature and time on tar conversion (PTC)

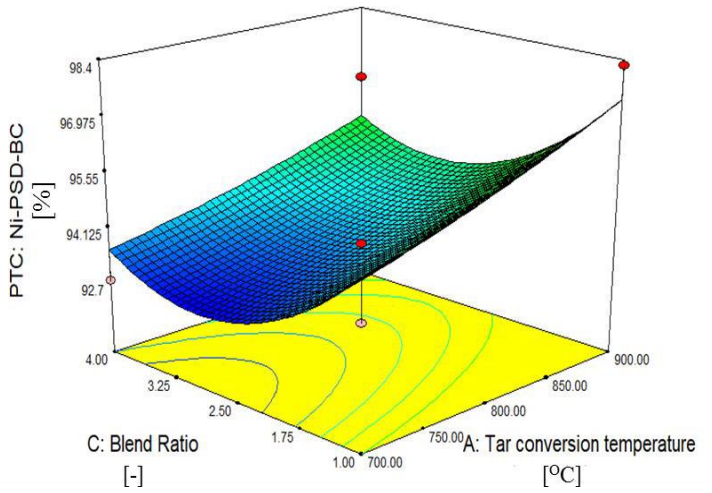


Figure 8. 19: Influence of tar conversion temperature and blend ratio on tar conversion (PTC)

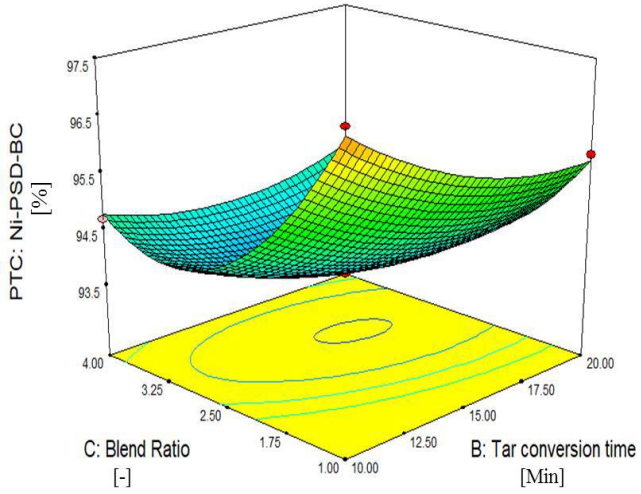


Figure 8. 20: Influence of tar conversion time and blend ratio on tar conversion (PTC)

Based on the aforementioned results, comprehensive tar treatment models were developed as expressed in Equations (8.5) through Equations (8.10):

$$Y_1\,[\%] = 95.88 + 0.50X_1 - 0.48X_2 - 0.64X_3 + 0.29X_1X_2 + 0.68X_1X_3 + 0.11X_2X_3 - 1.17X_1^2 - 1.10X_2^2 - 1.28X_3^2 + E \quad (8.5)$$

$$Z_1\,[\%] = 84.75 + 4.79X_1 - 2.08X_2 - 0.40X_3 - 0.53X_1X_2 - 1.60X_1X_3 + 0.32X_2X_3 - 2.88X_1^2 + 0.13X_2^2 + 0.043X_3^2 + E \quad (8.6)$$

$$Y_2\,[\%] = 94.71 + 0.74x_1 - 0.48x_2 - 0.53x_3 + 0.35x_1x_2 + 0.38x_1x_3 + 0.59x_2x_3 - 0.42x_1^2 - 0.39x_2^2 + 0.081x_3^2 + E \quad (8.7)$$

$$Z_2\,[\%] = 84.76 + 4.09x_1 - 2.43x_2 - 0.45x_3 - 0.19x_1x_2 - 0.93x_1x_3 + 0.29x_2x_3 - 1.82x_1^2 + 0.56x_2^2 - 0.092x_3^2 + E \quad (8.8)$$

$$Y_3\,[\%] = 93.71 + 1.05x_1 - 0.39x_2 - 0.87x_3 + 0.23x_1x_2 - 0.13x_1x_3 + 0.41x_2x_3 + 0.15x_1^2 + 0.46x_2^2 - 1.50x_3^2 + E \quad (8.9)$$

$$Z_3\,[\%] = 85.58 + 3.58x_1 - 2.17x_2 - 0.57x_3 - 0.20x_1x_2 - 0.15x_1x_3 + 0.24x_2x_3 - 1.31x_1^2 + 0.40x_2^2 - 0.46x_3^2 + E \quad (8.10)$$

Where Y_1, Y_2, & Y_3 are the percentage amount of tar conversion for the Ni-biochar based catalysts represented by Ni-CC-BC, Ni-SCB-BC, & Ni-PSD-BC, while Z_1, Z_2, & Z_3 represents the biochar-based catalysts including CC-BC, SCB-BC, & PSD-BC, respectively.

It is noteworthy to state that Equation (8.5) through Equation (8.10) can be very instrumental for the estimation of the percentage tar conversion (PTC) for feedstock (or precursors) similar to the ones investigated, and using the biochar and Ni-biochar based catalysts.

8.4.8. Analysis of coal + biomass & biomass-based tars

Figure 8.21 is the photo images of coal + biomass tars produced, while Figure 8.22 shows the photo images of coal + biomass tars and raw biomass tars dissolved in 2-propanol (Iso- propanol) respectively, and hence; used for the analysis.

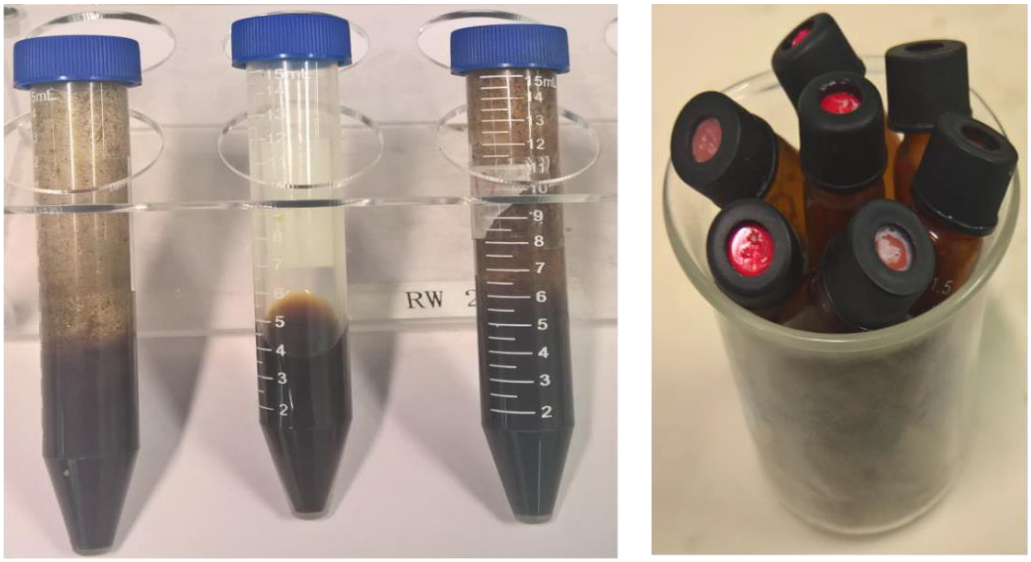


Figure 8. 21: Photo images of blends of coal and biomass tar

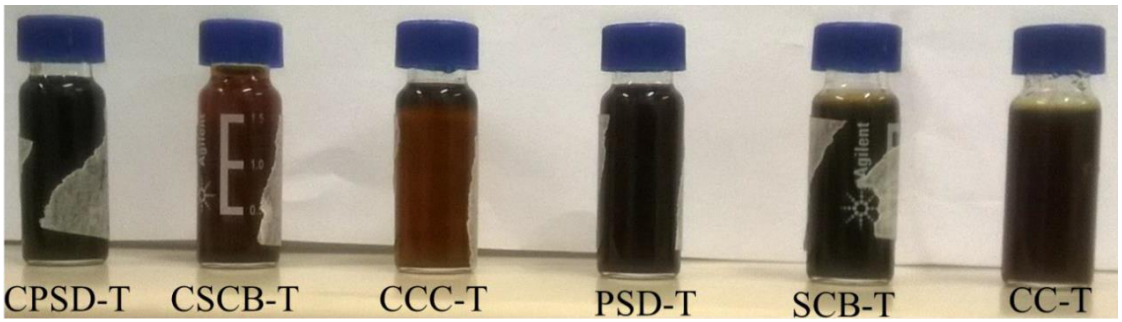


Figure 8. 22: Photo images of analysed tar samples: Blends of coal + biomass & biomass tars

The tars (PSD-T, SCB-T, & CC-T) shown in Figure 8.21 were used as control experiment, in terms of evaluating the compounds present in the tars. The essence of which was to demonstrate the relevance of co-gasification (coal + biomass) in tar reduction as against biomass gasification. An assessment of catalyst activity on the biomass generated tars was not considered, but catalyst performance on coal + biomass generated tars only, were evaluated.

It is important to point out that sample planigraphy pre-treatment was not carried out due to non-availability of the equipment at the time of this test. Planigraphy pre-treatment allows for the separation of the tar samples and other liquids into different categories (e.g. aliphatic, aromatics, esters, and polar). However, the separation was carried out by decantation and the samples of tar collected were analysed. In this case, the aliphatic, aromatics, esters and polar compounds were the same as displayed in Table 8.9 through Table 8.14.

The relative percentage of each compound present in each of the tar species was estimated. It is referred to as the proportion of the relative content of components of each peak (in %) with the total peak, obtained by dividing the individual area peak by the total peaks area. Table 8.9 through Table 8.14 depicts the compositional tar analysis result for blends of coal + biomass and biomass-based tars, respectively.

Table 8. 9: Compositional tar analysis result of Coal + CC tar (CCC-T)

Peak number	Hold time	Compound name	Relative percentage*	% of tar in Coal + CC
1	3.154	Cyclopentanone	0.14	0.71
2	3.458	2-Propanone, 1,1-diethoxy-	0.94	0.99
3	3.510	5-Amino-1-[10-(methylsulpanyl)-7-thia-9,11	0.3	1.03
4	3.618	2-FURANCARBOXALDEHYDE	0.5	1.09
5	3.715	Hydroperoxide, 1-methylbutyl	0.49	0.83
6	3.823	Propane, 2,2'-[ethylidenebis(oxy)]bis-	9.01	0.70
7	3.925	1,6-Hepatadien-4-ol	1.57	0.99
8	4.008	2-FURANCARBOXALDEHYDE	15.20	1.12
9	4.250	1,5-Diazabicyclo[3.1.0]Hexane,6-spiro-cyclic	0.46	1.64
10	4.434	Ethanol, 2-(1-methyl ethoxy)-	8.12	0.86
11	4.505	2-butanone	1.93	0.92
12	4.620	2-Furanmethanol	0.87	1.13
13	4.672	1,3,5-Trioxane	1.33	1.07
14	4.769	2-Propanone, 1-(acetyloxy)-	2.97	1.06
15	5.360	Adenosine, 4'-de(hydroxymethyl)-4'-(N-ethyl)	0.33	0.94
16	5.573	2-Cyclopenten-1-one, 2-methyl-	1.24	0.91
17	5.720	2-ACETYLFURAN	0.34	0.57
18	5.790	Butanoic acid, 4-hydroxy	0.32	0.50
19	5.871	ALPHA., BETA,-CROTONOLACTONE	1.00	1.30

20	6.120	Ethanol 2,2-diethoxy-	4.59	0.92
21	6.556	(2-Methyl-oxiran-2-yl)acetic acid, methyl e	0.84	0.64
22	6.627	Propyl nitrite	1.89	1.17
23	6.742	Beta-D-Glucopyranoside, methyl 3,6 anhydo	1.17	0.95
24	6.917	2-Furancarboxaldehyde, 5- methyl-	1.44	0.90
25	6.980	2-Butanone, 1-(acetyloxy)-	1.39	1.17
26	7.130	Methyl 2-mercaptoacetate	1.18	1.71
27	7.205	2-(2-FURYL)-2-OXAZOLINE	0.85	0.63
28	7.225	Acetic acid, phenoxy-, methyl ester	1.27	0.93
29	7.324	3,5-Octadiene, 2,2,4,7,7-hexamethyl-, (E,	2.27	1.32
30	7.370	6-(Dimethylamino)hex-3-en-5-yn-2-one	0.38	0.34
31	7.447	2,8-NONADIENOIC ACID, ISOPROPYLI	1.66	2.05
32	7.829	Acetic acid, trifluoro-, bicylo[2.2.1]hept-2-	5.85	1.30
33	7.860	Bezenamine, 2-methyl-4-nitro-	8.87	2.12
34	8.064	Furan, 2,5-diethoxytetrahydro-	5.54	0.89
35	8.450	3-Methylcyclopentane-1,2-dione	1.77	0.98
36	8.885	2,5-HEPTADIENE-1-OL	0.47	0.80
37	9.057	n-Octadecyl-N'-6-[N-aziridyl]hexylthiourea	0.31	0.69
38	9.360	Decane-5,6-d2	0.63	0.86
39	9.433	2,4-Dimethyl-1,3-dioxolane (mixed isomers)	2.32	0.85

40	9.491	3,4-Dimethylcyclohexanol	0.57	0.68
41	9.585	2,4-DIHYDOXY-3,3-DIMETHYLBUTAN	0.63	0.88
42	9.665	Thieno[2,3-d]pyrimidin-4(3H)-one,	0.51	0.88
43	9.690	2-Hydroxy-3-hexanone	0.47	1.15
44	9.788	Phenol, 2-methoxy-	4.02	1.03
45	9.958	2,4-Dimethyl-1,3-dioxolane (mixed isomers)	0.99	0.58

RP: Relative Percentage concentration: *: The proportion of the relative content of component of each peak

(in %) with total peak area.

Table 8. 10: Compositional tar analysis result of Coal + SCB tar (CSCB-T)

Peak number	**Hold time**	**Compound name**	**Relative percentage***	**% of tar in Coal + CC**
1	3.144	Cyclopentanone	0.59	0.72
2	3.440	Propanal, 2-oxo-	0.69	2.30
3	3.591	2-FURANCARBOXALDEHYDE	0.64	0.98
4	3.710	3-Pentanone,2,4-dimethyl-	0.15	0.75
5	3.766	2-Ethoxytetrahydrofuran	0.3	0.60
6	3.814	ACETALDEHYDE, DIISOPROPYLACE	0.48	0.68
7	3.924	1,6-Heptadiene-4-ol	1.45	0.70
8	4.006	2-FURANCARBOXALDEHYDE-	28.25	0.90
9	4.500	2-Butanone	2.44	1.33

10	4.614	2-Furamethanol	5.4	1.40
11	4.765	2-Propanone, 1-(acetyloxy)	5.78	0.92
12	5.028	2H-Pyran-3(4H)-one, dihydro-	0.32	1.03
13	5.572	2-Cyclopenten-1-one, 2-methyl-	2.04	1.06
14	5.709	Ethanone, 1-(2-furanyl)-	0.61	0.69
15	5.783	ALPHA., BETA,-CROTONOLACTONE	1.69	0.88
16	5.846	2-BUTENE-1,4-DIOL	2.64	1.21
17	6.025	6-Oxa-bicyclo[3.1.0]hexan -3-one	0.72	1.67
18	6.136	3-Penten-2-one, 3-methyl-	2.45	1.28
19	6.389	Cyclopropene, 1-butyl-2-ethyl-	0.43	0.90
20	6.470	2-Butendioic acid, 2-methyl-	0.06	0.5
21	6.555	2-Furancarboxaldehyde, 5-methyl-	0.24	0.75
22	6.928	Propane, 1-(ethylthio)-	4.22	1.43
23	7.146	2(5H)-Furanone, 3-methyl-	0.16	0.55
24	7.292	2-Cyclopenten-1-one, 3,4-dimethyl-	0.4	1.05
25	7.565	2,3-Dimethyl-2-cyclopenten-1-one	0.16	0.89
26	7.678	Phenol	0.46	1.39
27	7.789	2-Furanmethanol, tetrahydro-	7.87	1.39
28	7.895	Furan,2,5-diethoxytetrahydro-	1.61	1.00
29	8.068	Tripropyl orthoformate	0.53	0.84

30	8.114	3-Methylcyclopentane-1,2-dione	0.46	0.67
31	8.495	5-Hydroxy-2-heptanone	5.78	1.02
32	8.623	PENTANOIC ACID, 2HYDROXY-4-ME	0.77	0.84
33	8.796	6,6-DIDEUTERO-NEONEN-1-OL-3	0.4	1.11
34	8.910	Furan,2,5-diethoxytetrahydro-	0.29	1.38
35	9.045	4-Hexenoic acid, 6-(acetyloxy)-4-methyl	0.21	0.6
36	9.133	FURAN-2-CARBOXAMIDE, N-(5-ME	0.55	1.49
37	9.205	4-Hexenoic acid, 6-(acetyloxy)-4-methyl	0.27	1.08
38	9.297	Phenol, 2-methyl-	2.1	1.02
39	9.370	Decane-5,6-d2	1.09	1.03
40	9.435	2,4-Dimethyl1-,3-dioxolane (mixed isomers)	0.82	0.84
41	9.505	4,4-Dimethyl-1-hexene	0.15	0.54
42	9.570	1-Pentene, 5-bromo-	0.18	0.72
43	9.694	2-Hexanone	0.93	1.27
44	9.799	Phenol, 4-methoxy-	13.01	0.92
45	9.964	UNDECANE, 6,6-DIDEUTERO-	0.21	0.77

RP: Relative Percentage concentration; *: The proportion of the relative content of component of each peak (in %) with total peak area.

Table 8. 11: Compositional tar analysis result of Coal + PSD tar (CPSD-T)

Peak number	Hold time	Compound name	Relative percentage*	% of tar in Coal + CC
1	3.453	Cyclopentanone	0.33	1.14
2	3.812	Propane, 2,2'-[ethylidenebis(oxy)]bis-	1.09	0.52
3	3.923	1,6-Heptadien-4-ol	1.09	0.66
4	4.001	2-FURANCARBOXALDEHYDE	8.89	0.87
5	4.430	PROPANE, 1-(METHYLETHOXY)-	2.08	0.61
6	4.505	2-Butanon	2.09	0.95
7	4.613	2-Furanmethanol	5.26	1.26
8	4.765	2-Propanone, 1-(acetyloxy)-	4.32	0.92
9	5.045	2(3H)-Furanone, dihydro-4,5-dimethyl-	0.52	1.13
10	5.345	Chloroacetic acid 3-methylbutyl ester	0.5	1.11
11	5.520	2-(4-METHYLPHENOXY)N-(1,3-THIA	1.56	1.17
12	5.578	2-Cyclopenten-1-one, 2-methyl-	2.51	1.04
13	5.709	Ethanone,1-(2-furanyl)-	0.94	0.83
14	5.788	2(3H)-Furanone, dihydro-	1.59	0.86

15	5.863	ALPHA., BETA,-CROTONOLACTONE	2.04	1.13
16	5.980	4,5-Trimethylene-2H-1,3-oxazine-3H-2,6-	0.62	0.89
17	6.126	Ethanol, 2,2-diethoxy	6.19	0.83
18	6.397	2(3H)-Furanone, 5-methyl-	0.73	1.12
19	6.553	Butanedioic acid methylene-	0.52	1.00
20	6.626	Propyl nitrite	0.54	0.64
21	6.796	2-Propanamine, N-ethyl-	0.71	1.48
22	6.915	2-Butanone, 1-(acetyloxy)-	1.27	0.68
23	6.967	Octane, 1-axido-	2.46	1.17
24	7.147	Ethanol 2,2-diethoxy-	0.32	0.63
25	7.300	2(5H)-Furanone, 3-methyl-	0.41	0.67
26	7.505	3-Ethyl-5-methyl-4-[3-(thiophen-3-yl)-(1,]-	1.02	1.17
27	7.575	Cyclohex-3-enecarboxaldehyde, 2,4,6-trin	0.66	4.40
28	7.620	4-(METHYLSULPHONYL)TETRAHYDRO	1.27	4.10
29	7.690	2-Decanynoic acid	1.01	2.59
30	7.798	Phenol	5.1	1.28

31	7.886	1,6-Heptadien-4-ol	1.69	0.73
32	8.065	2,3,4,5-TETRAMETHYL-2-CYCLOPEN	22.51	1.50
33	8.310	2-DEOXY-N-(4-METHYL-3-NITROPHENE	0.76	0.75
34	8.355	1,2,4-THIADIAZOL-5-AMINE, 3-ALLYI	0.37	0.64
35	8.472	3-Methylcyclopentane-1,2-dione	3.51	0.96
36	8.545	7H-[1,3]Thiazolo[3,2-a]pyrimidin-7-one	0.59	0.58
37	8.615	5-Hydoxy-2-heptanone	0.46	0.69
38	9.038	Furan, 2,5-diethoxytetrahydro-	0.46	0.58
39	9.104	Ethanone, 1-cyclohexyl-	0.39	0.61
40	9.300	phenol, 2-methyl-	1.37	1.15
41	9.363	Decane-5,6-d2	0.76	0.76
42	9.434	2,4-Dimethyl-1,3-dioxolane (mixed isomers)	0.35	0.45
43	9.583	4-Aminobutyraldehyde diethy acetal	0.47	0.55
44	9.686	N HEPTANAL	1.62	1.45
45	9.794	phenol, 2-methoxy-	5.68	1.03

RP: Relative Percentage concentration; *: The proportion of the relative content of component of each peak (in %) with total peak area.

Table 8. 12: Compositional analysis result of raw CC tar (CC-T)

Peak number	Hold time [s]	Compound name	Relative Percentage*	% of tar in Coal + CC
1	3.031	Butanedial	1.11	0.89
2	3.15	Cyclopentanon	0.38	0.86
3	3.307	1,2,4-BUTANETRIOL	0.09	0.64
4	3.614	3-Furaldehyde	0.31	0.97
5	3.731	Propanedioc acid	0.40	0.98
6	3.815	Propane, 2,2'-[ethylidenebis(oxy)]bis	0.47	0.68
7	3.946	1,6-Heptadien-4-ol	0.40	0.74
8	4.016	2-FURANCARBOXALDEHYDE	13.30	1.08
9	4.444	PROPANE,1-(1-METHYLETHOXY)-	1.16	0.82
10	4.522	1-Methyl-1propenyl acetate	1.57	1.22
11	4.627	2-Furanmethanol	2.47	1.08
12	4.685	Paraformaldehyde	1.42	1.10
13	4.782	2-Propanone, 1-(acetyloxy)-	2.07	0.92
14	5.576	2-Cyclopenten-1-one, 2-methyl-	2.11	1.23
15	5.723	Ethanone, 1-(2-furanyl)-	0.53	0.98
16	5.794	2(3H)-Furanone, dihydro-	0.66	0.94
17	5.862	ALPHA., BETA,-CROTONOLACTONE	2.62	1.53
18	6.031	2-BUTENE-1,4-DIOL	0.84	1.56

19	6.159	6-Oxa-bicyclo[3.1.0]hexane-3-one	4.39	1.42
20	6.315	5-Hydrxy-2-heptanone	0.13	1.18
21	6.402	3-Penten-2-one, 3-methyl-	0.19	0.83
22	6.559	(2-Methyl-oxiran-2-yl)-acetic acid, methyl e	0.70	0.69
23	6.739	6,8-DIOXABICYCLO(3.2.1)OCTAN-3L-C	0.47	0.73
24	6.931	2-Furancarboxaldehyde, 5-methyl-	2.20	0.93
25	6.985	2-Butanone, 1-(acetyloxy)-	1.35	0.94
26	7.09	Ethanone, 1-(3-ethyloxiranyl)-	0.10	0.71
27	7.155	Ethanol, 2,2-diethoxy-	0.13	0.65
28	7.329	2-Propanoic acid, 2-methyl-, 2-hydroxyethy	0.55	0.92
29	7.569	2,4-Hexadiene, 2,3-dimethyl-	0.10	0.59
30	7.665	3-Methylcyclohex-3-en-1-one	0.06	0.75
31	7.807	Phenol	7.86	1.79
32	8.069	Furan, 2,5-diethoxytetrahydro-	2.33	0.64
33	8.121	Tripropyl orthoformate	1.99	0.73
34	8.2	Benzene, 1-methoxy-3-methyl	0.42	1.24
35	8.515	3-Methylcyclopentane-1,2-dione	5.44	1.24
36	8.618	5-Hydroxy-2-heptanone	0.79	0.96
37	8.78	Furan, 2,5-diethoxytetrahydro-	0.85	0.73
38	8.84	2(5H)-FURANONE, 5 METHYL-	0.16	0.80

39	9.038	Furan, 2,5-diethoxytetrahydro-	0.57	0.58
40	9.125	2-(Oxan-3-yl)ethanamine	0.50	1.16
41	9.312	Phenol, 2-methyl-	1.86	1.35
42	9.439	2,4-Dimethyl-1,3-dioxolane (mixed isomers	7.58	0.62
43	9.59	2-PENTENE, 4 BROMO-	0.11	0.69
44	9.717	2,3-Dihydro-5-hydroxy-6-methyl-4H-Pyran-	0.49	0.79
45	9.822	Phenol, 2-methoxy-	26.79	1.00

RP: Relative Percentage concentration; *: The proportion of the relative content of component of each peak (in %) with total peak area.

Table 8. 13: Compositional tar analysis result of raw SCB tar (SCB-T)

Peak number	**Hold time**	**Compound name**	**Relative percentage***	**% of tar in Coal + CC**
1	3.155	Cyclopentanone	0.5	0.93
2	3.480	Propanal, 2-oxo-	0.65	0.89
3	3.536	PENTANOIC ACID	0.94	1.13
4	3.595	3-Furaldehyde	0.39	0.80
5	3.765	Butanoic acid, 2-propenyl ester	0.47	0.78
6	3.818	Propane, 2,2'-[ethylidenebis(oxy)]bis-	0.8	0.69
7	4.017	2-FURANCARBOXALDEHYDE	16.92	1.15

8	4.455	2,2-Diisopropoxy-3-methylbutanal	0.29	0.50
9	4.556	2-Butanone	2.12	1.23
10	4.647	2-Furanmethanol	8.55	1.26
11	4.808	2-Propanone, 1-(acetyloxy)-	5.85	1.00
12	5.588	2-Cyclopenten-1-one, 3-methyl-	2.17	1.02
13	5.720	Ethanone,2,2-diethoxy-	0.78	0.93
14	5.815	2(5H)-Furanone, 3-methyl-	1.68	0.73
15	5.878	ALPHA., BETA,-CROTONOLACTONE	2.37	1.18
16	6.018	2-PIPERIDINONE	0.49	0.83
17	6.040	Petane 1,4-dichloro-	0.3	0.60
18	6.158	Ethanol, 2,2-diethoxy-	8.79	0.82
19	6.325	CIS-DIHYDROCARVONE	0.25	0.86
20	6.416	2(5H)-Furanone, 5-methyl-	0.76	1.25
21	6.565	2,5-Furandione, dihydro-3-methylene	0.50	1.32
22	6.630	Oxiran, (propoxymethyl)-	0.33	0.70
23	6.687	ETHANE, 1,1',1'-[METHYLIDYNETRIS	0.23	0.68
24	6.927	Piperidine-4-carbonitrile	1.20	0.60
25	6.970	Cyclopenten-1-one, 2-methyl	2.20	1.03
26	7.167	Ethanol, 2,2-diethoxy-	0.39	0.64
27	7.316	2(5H)-Furanone, 3-methyl-	0.38	0.81

28	7.415	Butanedioic acid, methyl-	0.29	1.07
29	7.505	1-Deoxy-1-[3-(O-tolyl)-2-thioureido]-b-d-g	0.26	1.13
30	7.586	2,4-Hexadiene, 2,5-dimethyl-	0.25	0.86
31	7.800	Carbamic acid, phenyl ester	10.79	1.63
32	7.900	Butanoic acid, 2-propenyl ester	2.90	1.16
33	8.069	Furan,2,5- diethoxytetrahydro-	4.09	0.66
34	8.476	Furan,2,5- diethoxytetrahydro-	4.33	0.96
35	8.625	3-Methylcyclopentane-1,2-dione	0.57	0.72
36	8.781	5-Hydroxy-2-heptanone	0.75	0.56
37	9.040	Furan,2,5- diethoxytetrahydro	1.52	0.86
38	9.135	6-Hydroxy-7-methyl-5-nitro-bicyclo[4.4.0],	0.23	0.64
39	9.298	Phenol, 2-methyl-	1.25	0.93
40	9.370	UNDECANE, 6,6-DIDEUTER0-3-METHL	0.85	0.92
41	9.432	2,4-Dimethyl-1,3-dioxolane (mixed isomers)	1.22	0.73
42	9.500	Butanoic acid, 2-propenyl ester	0.34	0.57
43	9.675	Butanoic acid, 2-propenyl ester	1.16	1.59
44	9.795	Phenol, 4-methoxy-	7.76	0.99
45	9.959	Butanal, 3-methyl	1.13	0.59

RP: Relative Percentage Concentration; *: The proportion of the relative content of component of each peak (in %) with total peak area.

Table 8. 14: Compositional analysis result of raw PSD tar (PSD-T)

Peak number	Hold time	Compound name	Relative percentage*	Percentage in Coal + CC tar
1	0.22	Cyclopropyl methyl carbinol	0.22	0.65
2	0.67	Cyclopentanone	0.67	0.71
3	0.31	3(2H)-Furanone, dihydro-2-methyl-	0.31	0.94
4	0.34	Propanal, 3-methoxy-	0.34	0.77
5	0.26	Furaldehyde	0.26	0.74
6	1.70	ACETALDEHYDE, DIISOPROPYLACE	1.70	0.70
7	1.26	1,6-Heptadien-4-ol	1.26	0.75
8	23.63	2-FURACARBOXALDEHYDE	23.63	0.83
9	0.40	Pentane, 1-nitro-	0.40	1.48
10	0.99	Ethanol, 2-(1-methylethoxy)-	0.99	0.76
11	1.81	2-Butanone	1.81	1.14
12	4.68	2-Furamethanol	4.68	1.31
13	4.61	2-Propanone, 1-(acetyloxy)-	4.61	0.83
14	0.23	2H-Pyran-3(4H)-one, dihydro-	0.23	0.72
15	1.82	2-Cyclopenten-1-one, 2 methyl-	1.82	1.01
16	0.51	Ethanone, 1-(2-furanyl)-	0.51	0.63
17	1.43	2(3H)-Furanone, dihydro-	1.43	0.82
18	2.23	ALPHA., BETA,-CROTONOLACTONE	2.23	1.20

19	1.05	2-Furanmethanol	1.05	1.48
20	2.38	6-Oxa-bicyclo[3.1.0]hexane-3-one	2.38	1.34
21	0.52	2(5H)-FURANONE, 5 METHYL-	0.52	1.02
22	0.67	2-Butenedioic acid, 2-methyl-, (Z)	0.67	1.46
23	0.43	Propyl nitrate	0.43	0.81
24	0.20	Decane-3,4-d2	0.20	0.95
25	3.66	2-Furancarboxaldehyde, 5-methyl-	3.66	1.47
26	0.22	2(5H)-Furanone, 3-methyl-	0.22	0.69
27	0.17	Pentanoic acid, 4-oxo, methyl ester	0.17	1.00
28	0.33	4-methyl-1,4-heptadiene	0.33	0.69
29	0.47	2-Furamethanol, acetate	0.47	0.80
30	0.70	5-Hydroxy-2-heptanone	0.70	1.00
31	8.13	Phenol	8.13	1.51
32	5.70	Pentane, 1-bromo-	5.70	1.09
33	9.76	Phenol, 4-ethyl-2-methoxy-	9.76	1.86
34	1.47	Tripropyl othoformate	1.47	0.82
35	4.18	3-Methyl-2-dione	4.18	0.98
36	0.4	2-Cyclopenten-1-one, 2,3-dimethyl-	0.40	0.68
37	0.23	1-Octyne	0.23	0.68
38	0.48	3-Hexanone, 2,5-dimethyl-	0.48	1.20

39	0.20	3-Ethyl-2-hydroxy-2-cyclopenten-1-one	0.20	1.25
40	1.10	Phenol, 2-methyl-	1.10	0.95
41	0.40	2,2,9,9-D4-nonadecanone	0.40	0.91
42	0.69	2,4-Dimethyl-1,3dioxolane (mixed isomer)	0.69	0.54
43	0.35	2-Heptanone, 3-methyl-	0.35	0.80
44	8.08	Phenol, 2-methoxy-	8.08	0.93
45	0.88	UNDECANE, 6,6-DIDEUTERO-	0.88	0.54

RP: Relative Percentage concentration; *: The proportion of the relative content of component of each peak (in %) with total peak area.

8.4.9. Quantitative analysis of blends of coal + biomass and biomass-based tars

In this study, the concentration of species presents in the tars produced was emphasised. It is because, according to the research motivational statement, co-gasification was projected as an alternative to minimization of tar during gasification. A comparison of different compounds presents in the analysed tars (Coal + CC, Coal + SCB, & Coal + PSD, and CC, SCB, & PSD) was therefore carried out. To ensure accuracy and standard assessment, five compounds common to each of the tars were employed, and their concentrations were evaluated as shown in Table 8.15. From Table 8.15, the percentage amount of the compounds presents in the raw biomass tars reduced significantly due to catalytic tar cracking. The relative percentages of 2-Furancarboxaldehyde and phenol (also known as hydoxybenzene) in the tar were the highest (23.63 % & 8.15 %), while 2-cyclo Pentene-1-one, 2-methyl- and Cyclopentanone were the lowest (0.38 % & 2.11 %), respectively for the species of tar considered.

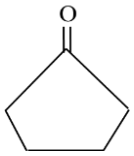
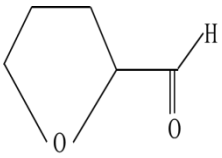
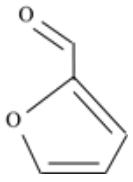
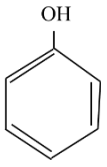
Table 8. 15: Comparison of compounds in tar samples: Coal + biomass & biomass based tars

		Feedstock (tar samples)					
	Tar compounds	CCC-T	CSCB-T	CPSD-T	CC-T	SCB-T	PSD-T
		Percentage amount of compound in the tar sample [%]					
1	Cyclopentanone	0.14	0.50	0.33	0.38	0.59	0.67
2	2-Furacarboxaldehyede	0.50	0.64	8.89	13.30	16.92	23.63
3	Alpha, Beta,-Crotonolactone: 2(5H) -Furanone)	1.00	1.69	2.04	2.62	2.37	2.23
4	Phenol	4.02	0.46	5.10	7.86	1.25	8.13
5	2-cyclo Pentene-1-one, 2-methyl-	1.24	2.04	2.51	2.11	2.17	1.82

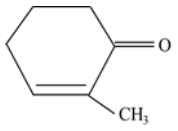
CCC-T: Coal + Corn cob tar; CSCB-T: Coal + Sugarcane bagasse tar; CPSD-T: Coal + Pine sawdust tar; CC-T: Corn cob tar; SCB-T: Sugarcane bagasse tar; PSD-T: Pine sawdust tar

From Table 8.15, the relative amounts of Cyclopentanone formed from PSD-T and reduced in CPSD-T during tar treatment, were the highest (23.63 % & 8.89 %) for all the species of tars studied. It may be attributed to the higher density of woody biomass (e.g. pine sawdust (PSD) when compared to crop residues (sugarcane bagasse (SCB) & corn cob (CC)). The low density crop residues will promote faster decomposition and combustion as against high density biomass at the same temperature condition. It implies that the tar forming compounds present in the crop residues will be more available for cracking than that of woody biomass at the same operating temperature regime. The properties of the tar compounds considered for assessment is depicted in Table 8.16. As explained earlier, five compounds common to each of the tars were used in the estimation.

Table 8. 16: Properties of tar compounds used for assessment

Compound Name	Molecular Formula	MW [g/mol]	MP [^{O}C]	BP [^{O}C]	Structural Formula
Cyclopentanone	C_5H_8O	84.12	-51.3	130	
2- Furancarboxaldehyde	$C_5H_4O_2$	96.08	161.70	-	
Alpha, Beta,- Crotonolactone: 2(5H) -Furanone)	$C_4H_4O_2$	84.08	4.5	86.87	
Phenol	C_6H_5OH	94.11	40.50	181.70	

2-cyclo Pentene-1-one, 2-methyl-	C_6H_8O	96.13	-	157.00



MW: Molecular weight; MP: Melting point; BP: Boiling point

8.4.19. Tar reduction assessment: Coal + biomass & biomass based tar species

To understand the extent of reduction in the content of raw biomass tars (CC-T, SCB-T, & PSD-T) during catalytic treatment, and when compared to blends of coal + biomass tars (CCC-T, CSBC-T & CPSD-T), the percentage reduction or changes in the compounds of tar were estimated. This is displayed in Figure 8.23. From Figure 8.23, for CC-T, SCB, & PSD- T, around 46.15, 8.26, & 34.00 % reduction was obtained from Cyclopentanone, respectively, while 96.21, 92.44, & 45. 35 % reduction was obtained from 2- Furancarboxaldehyde. For the Alpha, Beta, -Crotonolactone (i.e. 2(5H) –Furanone) compound of tar obtained from CC- T, SCB-T, & PSD-T species, about 44.75, 16.75, & 4.45 % reductions in tar were achieved when compared to blends of coal + biomass tars. Around 32.32, 46.20, & 22.90 % and 25.97, 3.09, & 21.01 % reductions were obtained from Phenol and 2-cyclo Pentene-1-one, 2-methyl-, respectively. Secondly, it can be observed that there were variations in the percentage reduction of each of the compounds of tar for each of the species of tar analysed. This could be attributed to the difference in the volatile content and other chemical compositions of the parent fuel from which the tar samples were produced.

Biomass has high volatile matter (VM) content than that of coal. The high volatility contributed to the formation of long chain hydrocarbon (HC) that was cracked during tar treatment. The volatile content of biomass in the mixture (coal + biomass) was decreased, thus; resulting to a decrease in the amount of tar produced. It therefore, affirmed that co-gasification of coal and biomass is instrumental to reducing the formation of tar during gasification process.

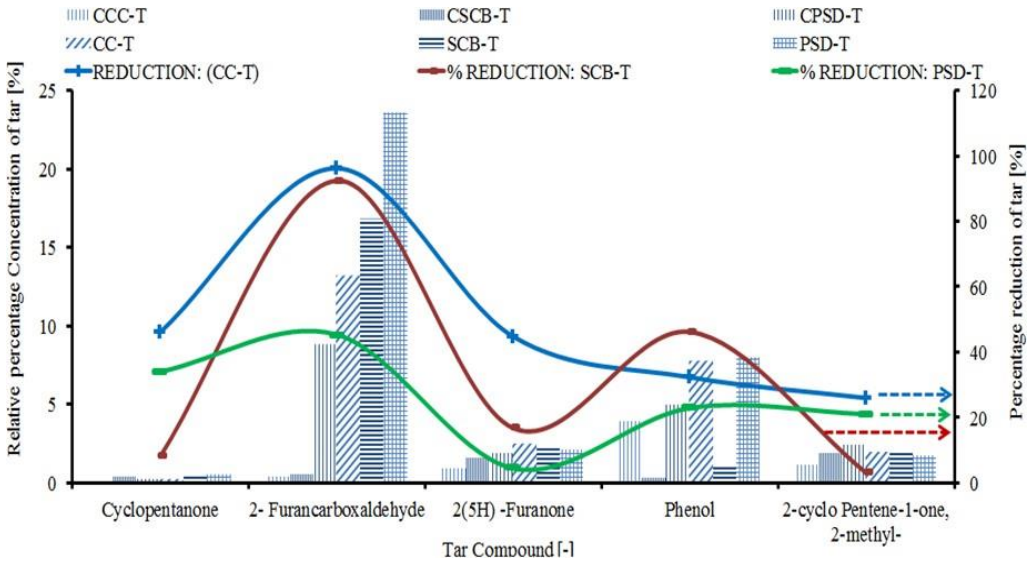


Figure 8. 23: Percentage concentration and tar reduction or changes profile for tar compounds and species

Fundamentally, the problem of tar in end use equipment is not dependent on tar quantity, but is based on the properties and compositional characteristics of the tar [319]. Under this context, the concentration/composition of tars in the syngas produced during co-gasification process and used for fuels in end use facilities will be analysed in the Chapter 9.

8.5. Concluding remarks

A study on treatment of tars produced from blends of coal and biomass using biochar based and Ni-biochar based catalysts was carried out. The tars were produced from Coal + CC, Coal + SCB, & Coal + PSD and CC, SCB, & PSD, and were designated as CCC-T, CSCB-T, & CPSD-T, while the biochar based and Ni-biochar based catalysts used for the treatment were designated as CC-BC, SCB-BC, & PSD-BC and Ni-CC-BC, Ni-SCB-BC, & Ni-PSD- BC, respectively. The results obtained from Box Behnken Design of experiment method that comprised tar conversion temperature (700 – 900 ^{O}C), tar conversion time (10 – 20 min), & Coal-to-biomass blend ratio (1 – 4) as the input variables, and Percentage tar conversion as the output variable were employed. A comprehensive tar treatment model was developed based on the catalysts, tars and process variables investigated, and the following conclusions were made:

- The optimum catalysts were PSD-BC and Ni-PSD-BC and the average percentage amount of tar conversion by the catalysts were 89.76 and 96.73 %, respectively.
- Ni-PSD-BC was more efficient for tar cracking than PSD-BC based on tar conversion

time of 10, 15, & 20 min at 900 ^{O}C by around 7.87, 3.87, & 3.79 %, respectively, but PSD-BC may be more attractive if sustainability and cost effectiveness of precursors are considered.

- Increase in temperature increased the rate of tar conversion, but the conversion decreased with an increase in time. The implication was that higher volatile components in the tar were released and the bonds linking the hydrocarbons were broken, hence; resulting to cracking of higher amount of tar. Also, majority of the tars may have undergone cracking, thus; leading to a lower conversion as the treatment process progressed.

Chapter 9: Co-gasification of coal and biomass to hydrogen enriched syngas in a fixed bed gasifier with catalyst (WCAT) and without catalysts (WOCAT)

9.1. Introduction

In the previous chapter, the treatment of tars obtained from feedstocks used in this study employing biochar and Ni-biochar based catalysts was studied. It was therefore considered very crucial investigating the influence of the synthesised catalysts on the co-gasification products of blend of coal and biomass. The process was carried out in a fixed bed gasifier using the optimum (most viable) feedstock (Coal + PSD) and catalysts (PSD-BC & Ni-PSD-BC), obtained from techno-economic analysis (chapter 5) and tar treatment (chapter 8), respectively. The details of the study are therefore, elaborated in this chapter.

Gasification is one of the thermo-chemical energy conversion technologies used for the conversion of solid fuels into product gases (e.g. CO, CO_2, CH_4, H_2). The gases are used for different domestic and industrial applications. The process has existed for many decades [1], but the technology and operating process conditions are constantly modified (improved), while the feedstock employed are variably pre-treated to ensure quality upgrade and effective performance of the gasifier. Coal and biomass materials can be gasified independently or co-gasified to generate producer gas, but the experimental process conditions, type of fuel, and gasifier determines the efficiency of the gasifier and gas quality [13]. The quality of the gas produced influences the type of energy devise it could be fed as fuel to produce electricity. Some of the examples of energy conversion system where the fuel can be used are fuel cells, gas turbines, internal combustion engines, etc. Each of the facility has an allowable limit of impurities (e.g. tar) in the gas to achieve efficient performance. Therefore, efforts should be made to ensure that the tar limit in the produced gas is not exceeded.

It is necessary to emphasise that co-gasification of coal and biomass has several benefits such as: (1) reduction in tar production and cost of feedstock for energy generation (2) reduction in the fast depletion of coal due to its solitary gasification (3) provision of an effective means of waste management (4) provision of sustainability in the energy production sector, hence; resulting to enhanced economic growth and development [320]. To achieve the aforementioned benefits, some critical factors and aspects of gasification must be well understood. It includes the techno-economic analysis of the feedstock that will be used, performance of the gasification systems efficiency, and cracking of tars produced from the feedstock using suitable catalysts. The three important areas had been well investigated and were presented as chapters, in this study. Importantly, from the result of the techno- economic analysis, blend of coal and biomass was the

most viable feedstock in terms of profitability in the power plant. Secondly, an evaluation of the performance efficiency of the gasification system carried out via an ANN model revealed the most important input variables on the outputs. The ANN model result was considered during feedstock pre- treatment to upgrade the quality of the fuel, and to achieve better gasification efficiency. Additionally, biochar and Ni-biochar based catalysts were produced from the feedstock investigated in this study and the optimum catalysts (PSD-BC & Ni-PSD-BC) were employed for tar cracking to ensure effective gasification efficiency and production of high quality syngas. The findings obtained from the key areas associated with the co-gasification process as elaborated in the earlier chapters were therefore, employed to carry out the co-gasification test presented in this chapter.

To carry out the co-gasification test in this study, Coal + PSD and PSD-BC & Ni-PSD-BC were used as fuel and catalysts, respectively. The effects of the catalyst on tar production and gasification efficiency (e.g. product gas yield and composition (quality), etc) were determined. The outcome of this study affirmed the state-of-the-art of catalyst effectiveness in co-gasification process. Above all, it will encourage production of catalyst from local source (e.g biochar waste) to minimize catalyst production cost, and improve energy sustainability.

9.2. Materials & methods

9.2.1. Materials

Coal and Pine sawdust (Coal + PSD) were the feedstock used for the gasification test. Details of their origin, pre-treatment, and characterisations were reported in chapter 3. From the techno-economic analysis of the feedstock reported in chapter 10, coal-to-biomass ratio of 1:1 was established as the most viable blend ratio, hence; is used in this chapter for the gasification experiment.

9.2.2. Method

A schematic of the experimental setup used in this study for the co-gasification test is presented in Figure 10.1.

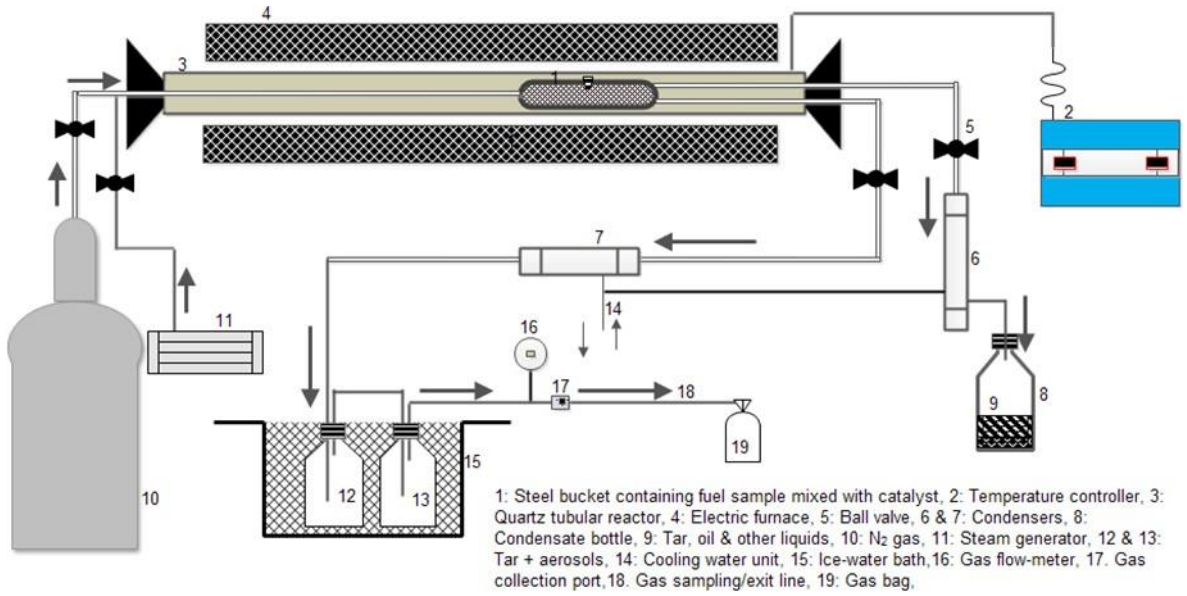


Figure 9. 1: Bench-scale fixed bed gasifier (Located at the FT-Lab, School of Chemical & Metallurgical Engineering, University of the Witwatersrand, Johannesburg).

The gasifier has an internal diameter and length of 45 mm and 550 mm respectively, and is made of stainless steel (Cr25Ni20) with high temperature resistance. Also fitted with the gasifier is an electric furnace and temperature regulator used for the heating and controlling of temperature of the reactor, steel-sheet bucket bed for feeding of feedstock, steam generator for steam supplies, flexible gasification fluid-line, condenser fitted to a water cooling line, ice-water bath housing two condensate bottles for the collection of the gasification liquid product (tar & liquid aerosols), and product gas collection port (where gas is collected for GC analysis). The method used for the co-gasification test was described in chapter 3, the features and operating process conditions for the gasification system is shown in Table 9.1.

Table 9.1: Features and experimental conditions of the gasifier

S/N	Items /parameters	Values
1	Type/configuration of gasifier	Bench scale FBG
2	Geometric parameter	ID: 45 mm and length: 550 mm
3	Heating system/medium	External electric heating
4	Cooling system/medium	Water & ice

5	Gasifying agent	Air & Steam
6	Operating temperature	700 - 900 ^{O}C
7	Type of catalyst	Ni-Biochar & Biochar based
8	Gas collection	Gas syringe
9	Feedstock used	Blend of coal and biomass
10	Fuel blend ratio	1:1
11	Air & steam flow rates	200 ml/min & 0.2 g/min

FBG: Fixed Bed Gasifier; ID: Internal diameter

9.2.3. Feedstock characterisation

The results of feedstock characterisation used for the co-gasification test includes; proximate and ultimate analysis results as well as the calorific values. The lower heating value (LHV) was calculated from the higher heating value (HHV) that was determined experimentally using an oxygen bomb calorimeter. All the model equations and analytic results obtained were presented in chapter 3.

9.3. Results and Discussion

The characterisation results of blend of Coal + PSD used for the investigation is presented in Table 9.2. It is within the range of results reported in the literature.

Table 9. 2: Results of feedstock characterisation: Coal + PSD

Proximate Analysis				Ultimate Analysis				
Feedstock: Coal + PSD								
Ash	MC	VM	FC	C	H	N	S	O
22.30	6.18	45.85	25.68	48.82	9.03	0.54	0.62	25.25
HHV of fuel [MJ/kg]				20.05				
LHV of fuel [MJ/kg]				18.88				

HHV: Higher heating value; LHV: Lower Heating Value; PSD: Pine Sawdust

The Matla coal used in this study is known to have a very high ash content of around 44.00 %, while the ash content of pine sawdust was as low as 0.59 % [13] which is nearly of zero ash content.

Gasification of high ash content coal poses a big threat to gasification efficiency because of possibility of melting of ash during the gasification process. When ash is melted inside the gasifier, it could result to slag plugging the reactor tapping system [321]. From Table 9.2, it can be seen that the ash content of blend of Coal + PSD has reduced when compared to the ash content of coal. Around 97.35 % reduction in the amount of ash was achieved by gasifying a blend of Matla coal and pine sawdust against solitary gasification of Matla coal. Majority of the South African coal samples are known for their high ash contents. This study therefore has offered an opportunity for utilising them via co-gasification with low ash content fuels such as PSD. On the other hand, biomass has high volatility when compared to coal, and it contributes to high tar formation in biomass gasification [320]. Co-gasification of Coal + PSD is instrumental to tar reduction based on the value of the volatile matter (VM) content of the blend as displayed in Table 9.2. Generally, the physio-chemical composition of blend of Coal + PSD was improved in terms of fuel quality for better operating and gasification efficiency.

9.3.1. Estimation of gasification systems efficiency

Table 9.3 depicts the results of the gasification system efficiency. For the evaluation, five efficiency indicators including gas composition, carbon conversion efficiency, cold gas efficiency, gas yield, and LHV of gas were employed. The expressions defining each of the indicator has been presented in chapter 4. From Table 9.3, the cold gas efficiency increased with an increase in temperature from 50.35 – 55.95 % at 700 – 800 ^{O}C, but decreased to 46.66 % at 900 ^{O}C, while the carbon conversion efficiency (CCE) also increased with an increase in the temperature. From a test carried out by Baskara et al. [322], the CCE increased from 60.25 – 67.88 % at 650 - 900 ^{O}C. The result obtained in this study was similar to that obtained by Baskara and his co-workers, except that in this study, there was slight decrease in the CCE from 800 - 900 ^{O}C. This may be attributed to variation in the experimental process conditions used in each of the studies. For the CCE, the result was expected because higher amount of carbon was decomposed at higher temperatures, but a time may reach when temperature increase may not lead or have significant effect on the conversion of carbon. The implication could be that most of the carbon present in the fuels may have been converted to gasification products (e.g. char & gases). For the LHV of the gas and in terms of catalyst performance, there was an increase in the heating value

of the gas when Ni-PSD-BC catalyst was used when compared to that of the PSD-BC catalyst. Baskara et al. [322] reported similar result, and in this case, the LHV of gas increased from 5.90 – 6.01 MJ/m^3 and decreased from 5.55 – 5.75 MJ/m^3 using variable catalysts and 800 – 900 ^{O}C temperature, respectively. It was a confirmation of the fact that for the catalyst utilisation, the Ni-PSD-BC has higher catalytic activity than the biochar based (PSD-BC) catalyst.

Table 9. 3: Results of performance of gasification system efficiency & amount of tar in the product gas: Bench scale FBG

Gasification efficiency parameters	Temperature condition [^{O}C]			Catalysts Temperature: 900^{O}C	
	700	800	900	Ni-PSD-BC	PSD-BC
Carbon conversion efficiency [%]	57.90	68.59	70.78	53.93	50.11
Cold gas efficiency [%]	50.35	55.95	46.66	88.49	64.65
Gas Yield [kg/Nm^3]	1.71	1.95	2.27	2.85	2.51
LHV of gas [MJ/Nm^3]	5.50	5.36	3.80	5.80	4.81
Tar content (g/Nm^3)	12.96	8.25	8.01	4.55	4.96

Ni-PSD-BC: Nickel-Pine sawdust-biochar catalysts; PSD-BC: Pine sawdust-biochar catalysts; LHV: Lower Heating Value; FBG: Fixed Bed Gasifier.

9.4. Effect of catalyst on gas composition

The influence of catalyst on the product gas composition was evaluated using Ni-PSD-BC and PSD-BC based catalysts respectively. The composition of gas formed with catalyst (WCAT) was compared with that of without catalyst (WOCAT), and is represented in Figure 9.2. It can be seen that the gas composition increased significantly on application of catalysts than WOCAT for each of the product gas specie studied. This is because; the release of more volatile components of the fuel was enhanced by the catalyst (even at lower temperature) hence; resulting to conversion of the volatile materials into product gases.

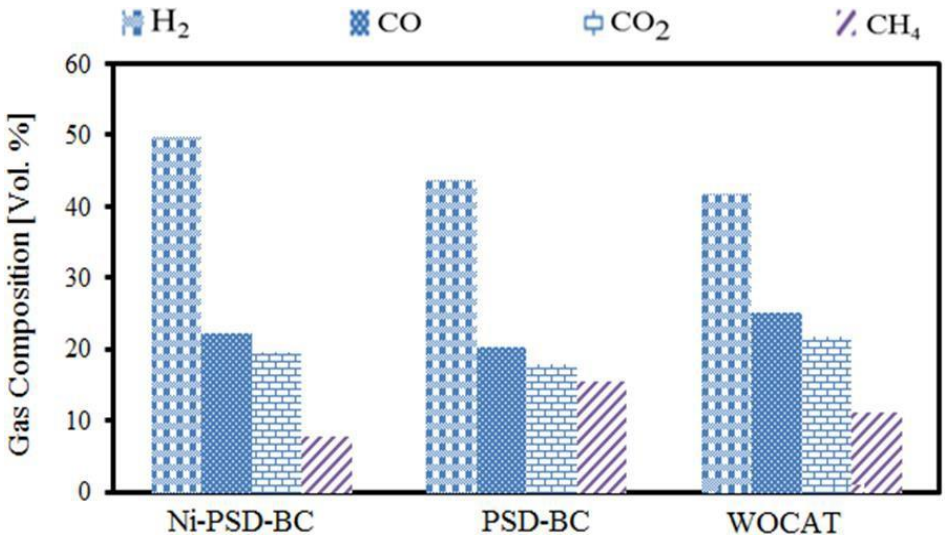


Figure 9. 2: Influence of catalyst on product gas composition: At 900 ^{O}C & steam as oxidant

9.3.1.1. Effect of temperature on gas composition

The influence of temperature on the product gas composition during co-gasification of Coal + PSD is presented in Figure 9.3. The composition of producer gas varied at different operating temperature conditions studied. From Figure 9.3, syngas (H_2 & CO) composition increased with an increase in the gasification temperature, while the CO_2 and CH_4 contents were decreased. The increase in the H_2 content could be attributed to decomposition of the volatiles or cracking of the hydrocarbons (HCs) at increased temperature [323].

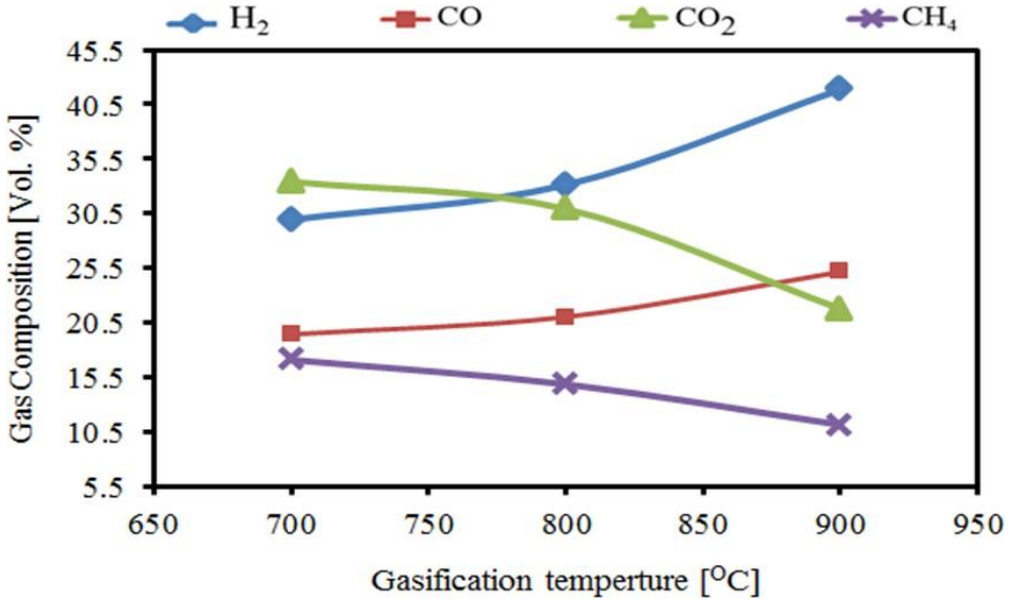


Figure 9. 3: Influence of gasification temperature on product gas composition: At temperature range of 700 – 900 ^{O}C, & steam as oxidant (WOCAT)

For example, the H_2 and CO contents (syngas) increased from 29.95 – 41.87 % and 19.45 –

25.18 % when the temperature was increased from 700 – 900 ^{O}C, respectively. This is in affirmation with the result obtained by Baskara et al. [322] during the gasification of groundnut shells to product gases. According to Baskara and co-workers, there was an increase in the H_2 content from 10 – 20 % when the reaction temperature was increased from 730 – 830 ^{O}C, while a decrease in the long chain HCs from 3 – 5 % was also observed for the aforementioned temperature condition. The reduction in the HCs enhanced the production of H_2 and CO during the process [322]. A similar finding was also reported by Yu et al. [324] during pine sawdust and rice husk gasification using CO_2/air as gasifying agent. There was an increase in the syngas yield, but the content of CO_2 was higher than that of H_2, which could be related to the use of CO_2/air as against air/steam employed in this study which yielded hydrogen-enriched syngas. Generally, the syngas produced at 900 ^{O}C was higher than that of 700 ^{O}C by 16.65 % and lower than that produced WCAT (at 900 ^{O}C) by about 8.61 %. The composition of syngas in the produced gas WCAT was equally higher than that WOCAT (at 900 ^{O}C) by 5.82 %. This is related to the increase in conversion of volatiles and tarry compounds at increased temperature and catalyst activity on the reacting species.

9.3.1.2. Effect of temperature on gas yield

Figure 9.4 and Figure 9.5 shows how gas yield is affected by temperature during co- gasification of coal and biomass (i.e. the overall gas yield). Figure 9.4 explains only the temperature effect on the gas yield, while Figure 9.5 described both the effect of temperature and catalysts on gas yield. From Figure 9.5, the gas yield increased from 1.71 – 2.27 kg/Nm^3 when the temperature was increased from 700 – 900 ^{O}C. There was a significant increase in the gas yield from the minimum (700 ^{O}C) to maximum (900 ^{O}C) gasification temperature by around 14.07 %; thus indicating that increase in temperature favoured the product gas yield.

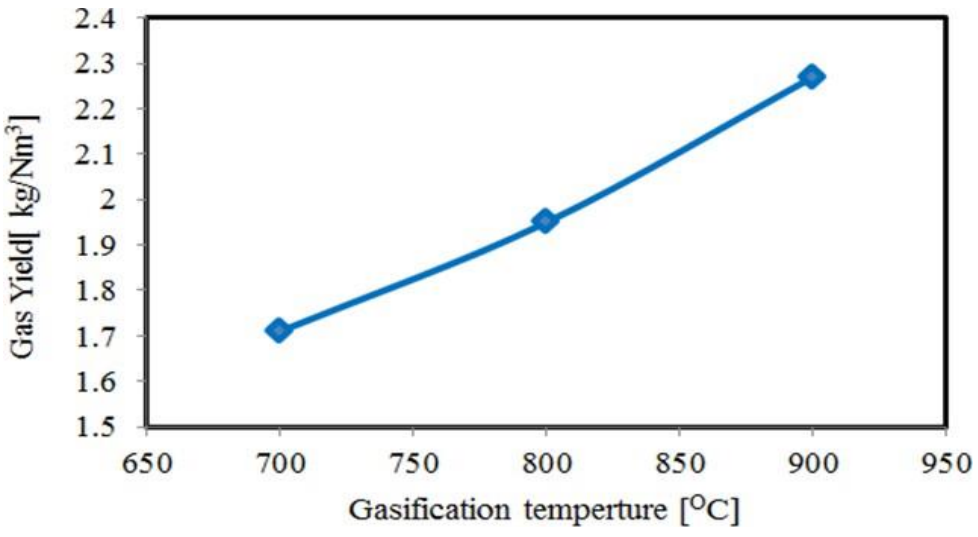


Figure 9. 4: Influence of gasification temperature on product gas yield

The relationship between gasification temperature and gas yield with catalyst (WCAT) and without catalyst (WOCAT) for the co-gasification reaction is displayed in Figure 9.5.

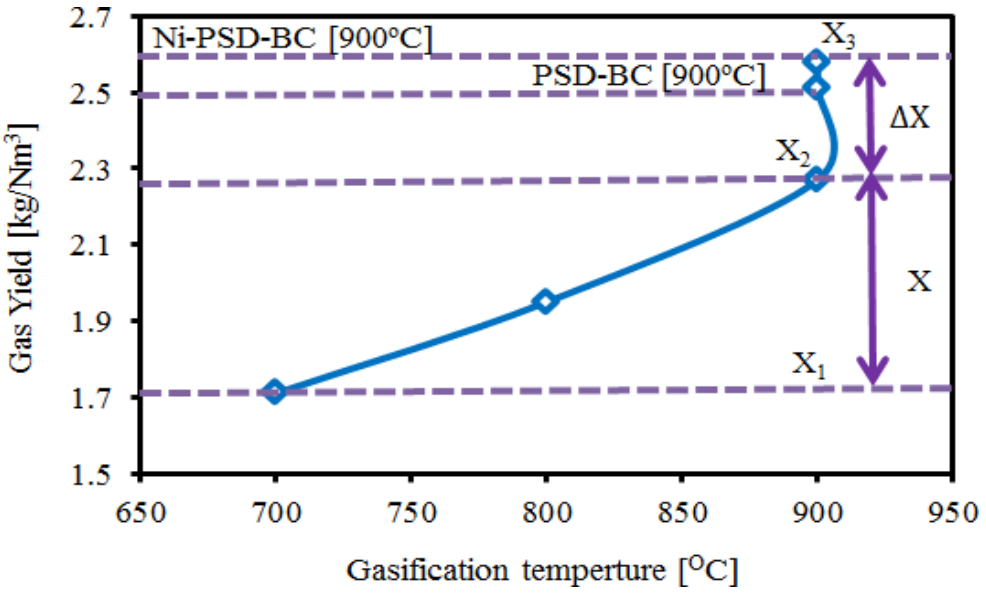


Figure 9. 5: Influence of gasification temperature on product gas yield

From Figure 9.5, Δ*X* is the change in gas yield due to utilisation of catalysts during co- gasification test. It was calculated from the difference in gas yield between co-gasification test without catalyst (WOCAT); X_2 and co-gasification test with catalyst (WCAT); X_3 at 900 ^{O}C, respectively. The value of Δ*X* obtained when Ni-PSD-BC and PSD-BC catalysts were used for the co-gasification reaction were 11.33 % and 5.02 % higher than that of co- gasification process without catalyst (WOCAT). Secondly, the gas yield, WOCAT (i.e. by thermal cracking) which is represented in Figure 9.5 with X, is the difference between the gas yield at 700 ^{O}C (X_1) and gas yield at 900 ^{O}C (X_2). In this case, the product gas yield for X_1, is higher than that of X_2 by around 14.07 %, but X, is lower than that of Δ*X* (WCAT) by 11.33 % at gasification temperature of 900 ^{O}C. Similar result (in terms of use of catalyst) had been reported by Shen et al. [325] and Zhang et al. [326], respectively. The implication as can equally be seen in Table 10.3 is that, gas yield increased with an increase in temperature, but increased further, when the Ni-PSD-BC and PSD-BC based catalysts were employed in the co-gasification process. It could also be attributed to the conversion of more chars, volatile materials, and cracking of tars by the gasifying medium and catalysts [327,322].

As explained earlier, the increase in the gasification temperature increased the gas yield on the basis that more tars were converted into small molecular HCs and gases, while higher gas yields were observed when catalysts were employed. Evidently, the increase in the product gas yield could be attributed to the thermo-chemical reactions amongst the reacting species (e.g. gas, char and catalyst). The reaction condition can be well understood as described in Equation (9.1) through Equation (9.9):

$$Tar_{Coal+PSD} \rightarrow \mathrm{C} + C_nH_m + Product\ gases \tag{9.1}$$

$$C_nH_m + \mathrm{n}CO_2 \rightarrow 2\mathrm{nCO} + \left(\frac{m}{2}\right)H_2 \tag{9.2}$$

$$C_nH_m + \mathrm{n}H_2\mathrm{O} \rightarrow \mathrm{nCO} + \left(\frac{n+m}{2}\right)H_2 \tag{9.3}$$

$$C_nH_m + 2\mathrm{n}H_2\mathrm{O} \rightarrow \mathrm{n}CO_2 + \left(\frac{2n+m}{2}\right)H_2 \tag{9.4}$$

$$CH_4 + H_2\mathrm{O} \leftrightarrow \mathrm{CO} + 3H_2 \tag{9.5}$$

$$\mathrm{C} + H_2\mathrm{O} \leftrightarrow \mathrm{CO} + H_2 \tag{9.6}$$

$$\mathrm{C} + CO_2 \leftrightarrow 2\mathrm{CO} \tag{9.7}$$

$$2\mathrm{CO} \rightarrow \mathrm{C} + CO_2 \tag{9.8}$$

$$CO + H_2O \leftrightarrow CO_2 + H_2 \quad (9.9)$$

The presence of water (H_2O) and carbon monoxide (CO) in the volatiles allowed for the regenerations of syngas (H_2 and CO) via Equation (9.2) through Equation (9.4) at high temperature. In this case, the component of tar (from Coal+PSD) was cracked into gaseous compounds via dry reforming over PSD-BC and Ni-PSD-BC based catalysts, respectively. It is important to state that char reacted with the gases (e.g. H_2O or CO_2) during the process expressed in Equation (9.6) through Equation (9.7), hence; producing more syngas [328] which in this study, is the product of interest.

9.4. Tar in the product gases

The amount of tar present in the product gases obtained from co-gasification of Coal + PSD at 700, 800, & 900 ^{O}C, WCAT and WOCAT were studied as displayed in Table 10.3. Temperature was found to have a very significant influence in the cracking of tar. It was demonstrated on the concentration or amount of tar contained in the product gas. The amount of tar present in the gas decreased with an increase in temperature studied. A more significant decrease in the content of tar was observed when the co-gasification was carried out using catalysts. From Table 10.3, it can be seen that the amount of tar when Ni-PSD-BC catalyst was used at 900 ^{O}C was lower than that of the WOCAT under the same temperature condition, thus; implying that catalyst has strong effect on tar reduction. Emphatically, the amount of tar in the product gas when Ni-PSD-BC was employed in the co-gasification experiment was lower than that of PSD-BC catalyst by around 4.31 %. Furthermore, the tar content in the product gas WOCAT at 900 ^{O}C was higher than that of WCAT at same temperature (900 ^{O}C) by around 27.55 %. The use of catalysts has significantly enhanced reduction of tar in the produced gases. Meanwhile, a comprehensive study on catalytic cracking of tars produced from the feedstocks used in this study and synthesised catalysts had been reported in chapter 8.

Importantly, from the aforementioned results, the quality of gases generated at 700, 800 & 900 ^{O}C WOCAT respectively, do not meet with the standard recommended for applications in fuel cells and gas turbines (in terms of tar contents) for electricity production. The allowable tar limit for different energy conversion devices can be found in the literature review section of this thesis. Similarly, the gases produced WCAT at 900 ^{O}C can be used in internal combustion engines and gas turbines, but unfortunately, have a low quality to be used in fuel cells for electric power

generation. For the produced gas to be considered of high quality for use in fuel cells it must undergo cleaning in a secondary reactor, however, gas cleaning is not a cost effective process. In this case, modification of the current gasifier or use of fluidised bed gasifier (BFB & CFB) or other conversion technologies, as well as improvement of experimental process conditions is required to upgrade the quality of the gas.

9.6. Concluding remarks

The co-gasification of coal and biomass to hydrogen enriched syngas in a fixed bed gasifier was carried out with catalyst (WCAT) at 900 ^{O}C and without catalyst (WOCAT), at 700, 800, and 900 ^{O}C temperatures, respectively. Coal and pine sawdust (Coal + PSD) of 1:1 blend ratio was used as the feedstock, while Nickel-pine sawdust- biochar (Ni-PSD-BC) and pine sawdust-biochar (PSD-BC) were employed as catalysts. The gases and tars produced from the aforementioned process conditions were analysed in a GC and the results obtained were used to estimate the performance of the gasification system efficiency. The following conclusions were therefore, drawn from the investigation:

- Co-gasification of Coal + PSD is instrumental to using high ash content South African coal such as Matla coal for the production of syngas for electricity generation.
- The co-gasification performance efficiency of the gasifier was significantly improved when the co-gasification process was carried out WCAT as against WOCAT.
- In terms of gas yield, co-gasification process WCAT (Ni-PSD-BC and PSD-BC based catalysts) were higher than that of WOCAT by 11.33 % and 5.02 %, respectively, but the product gas yield at 900 ^{O}C was higher than that of 700 ^{O}C (i.e. thermal cracking) by 14.07 %. The implication is that increase in temperature and use of catalyst favoured gas production.
- H_2 and CO (syngas) contents increased from 29.95 – 41.87 % and 19.45 – 25.18 % at 700 – 900 ^{O}C, respectively. The syngas composition was significantly enhanced during co-gasification WCAT. The implication is that production of hydrogen- enriched syngas was promoted by using catalyst due to tar cracking and reactivity amongst species (e.g. char, gases, and catalyst).
- The content of tar in the product gas is in the range of 8.01 – 12.96 g/Nm^3 for 700 – 900 ^{O}C temperature condition and 4.55 – 4.96 g/Nm^3 when PSD-BC and Ni-PSD-BC catalysts were used, respectively. It implies that catalytic cracking is more effective than thermal cracking in terms of tar reduction.

- The quality of gases produced at 700, 800 & 900 ^{O}C WOCAT were not suitable for use in fuel cells and gas turbines, while others produced at 900 ^{O}C WCAT, can be used in internal combustion engines and gas turbines, but unfortunately, have lower quality to be employed in fuel cells for electricity production.

Chapter 10: Environmental, economic and energy assessment in the co-gasification plant via proximate and ultimate analysis

10.1. Introduction

In this chapter, the techno-economic analysis of the feedstocks used for the energy production in a CHP co-gasification plant were studied using biomass, coal, and tyre. It dwelled on the economic, energy and environmental parameters of the plant. In this chapter, CO_2, SO_2, and equipment costing were not considered. Energy value of the feedstock, logistics, and gaseous emissions from the fuels were considered. The outcome of this work will open window for future works such as the aforementioned factors that were not studied in this research. Meanwhile, the information obtained from the proximate and ultimate analysis of the aforementioned fuels, empirical model equations, and some project evaluation tools were employed for the investigation.

Importantly, a part of the information contained in this chapter has been published in the Journal of Cleaner Production [13] and the abstract can be found in the appendices. Secondly, another important scientific data considered very useful to stake-holders in the energy sector and potential investors was published from this chapter in Data-In-Brief Journal article [13]. An abstract of the peer-reviewed article is attached in the appendices. Presently, the quest for energy utilizations around the globe has continued to increase and resulting to the rapid depletion of the available source of fuel. The world equally has continued to make use of fossil fuels (e.g. coal and petroleum) as the major fuels for power generation. Unfortunately, both coal and crude oil constitute a big threat to the environment because of the amount of emissions generated from them. Obviously, there are some variations in the amount of coal and petroleum deposited in different countries across the world. On the other hand, some countries do not have these fuels, hence resulting to such countries using other types/sources of fuel as a replacement. In South Africa (SA), coal is the major source of fuel for power production. It provides around 95 % of the electric power generation in the country. Currently, the estimated coal reserve in the SA is about 32 million tons. The reserve has been projected to last not more than a century [8].

Secondly, the present electricity tariff in the country is about ZAR1.74 /kWh [16], and it is considered as one of the lowest around the globe. This could be attributed to local availability and lower price of coal in the country. In contrary, coal is available and the cost of electricity supplies to consumers is equally low when compared to other countries, but the emissions

generated from it are tending to override the benefits. Similarly, Biomass materials and other solid waste are in abundant in South Africa, but their gasification is quite expensive, because of the high cost of the feedstock. They also have peculiar issues such as large amounts of tar generation when used in energy generation, and the presence of tar in product gas downgrades its quality, hence; limiting its applications. Co-gasification has higher efficiency than the solitary coal gasification. It is because the cellulose, hemicellulose and lignin content of biomass help to ignite and enhance the rate of reaction [329]. The process (co-gasification) has the capacity of reducing the aforementioned drawbacks, and equally be instrumental to waste management in South Africa.

Based on this background, there is need to understand the physio-chemical and gasification characteristics of the feedstocks used for energy production. The use of coal, biomass, solid wastes or mixture of them in electric and thermal power production have been reported by some researchers. For example, the structure and gasification characteristics of selected South African bituminous coals using a bubbling fluidized bed reactor was reported by Oboirien et al. [330], while Bridgwater [331] and Caputo et al. [332] investigated the pyrolysis, combustion and gasification processes for energy generation using a 5MW power plant. The findings from the authors were very attractive, and they were able to determine the most viable technology amongst the conversion technologies investigated. Unfortunately, the reports from the studies were devoid of the optimum feedstock for the power production with reference to both profit and emission reduction. To identify the order of viability of some selected feedstocks for power production, a techno-economic analysis of electricity production was conducted by Malek et al. [333] using a 10 MW biomass-based steam power plant. Malek and co-workers did not consider blends of the feedstocks in their investigation, but the report contained vital information.

The results contained in the investigation reported by Bridgwater [331], Mitchell et al. [334], Searcy & Flynn [335] revealed that biomass integrated gasification and combined gas- steam power cycle (IGCC) is a promising technology providing not less than 40 % - 50 % total conversion efficiency. Furthermore, Demirbas [336] argued that around 40 % could be achieved from a biomass integrated gasification combined cycle (BIGCC) plant of around 20MWe capacity. The IGCC technology as reported by the above authors is quite attractive, but the studies lacked the information on the viability of the feedstocks for a definite period of investment; an aspect that potential investors usually show a very kin interest about.

Generally, the Co-gasification process in a fluidized bed system may support an overall conversion efficiency of about 40 % - 50 % and minimize the cost of fuel for energy production. The works of Ahmadi et al. [337] have shown that the overall system efficiency of a typical co-

generation system is in the range of 35 % - 40 %.

Energy production via combustion, pyrolysis and gasification of biomass using 5 MW, 10 MW, and 20 MW CHP plants have been reported by several authors in the literature, but the studies did not consider blends of biomass and other solid fuels (e.g. coal and waste-tyre). In this study, a 5 MW CHP plant was employed to investigate blends of South African feedstocks. The order of feedstock viability and their energy contents, annual feedstock requirement and feed-rate, and the optimum assessment year were considered. It is expected from this study that the rapid depletion of South African coal reserve and huge CO_2 emissions in the country (1^{st} in Africa) will be reduced. Additionally, the outcome of the investigation could be instrumental to decision-making by the government and the key players in energy sector in South Africa and Africa at large.

10.2. Materials

Coal, sugarcane bagasse, corn cob, pine saw-dust and waste tyre were the feedstocks used for the investigation. The biomass materials were pre-treated, characterized and packaged as described in chapter 3 (methodology).

10.3. Method

10.3.1. Blending of feedstock and cost estimation

The method used in this study involved three steps namely; blending of coal and biomass and waste tyre (using the blend ratio shown in Table 10.1), estimation of the LHV, and the annual federate of the feedstocks, and Estimation of fuel requirement for the CHP plant. To determine the potentials of the fuels for electric and thermal power production with reference to energy, emissions and profit in the plant, the coal and biomass & waste tyre were blended in the ratio of 1:1, 3:2, and 4:1, respectively. The feedstocks and their blends are shown in Table 10.1, but the estimated results from the blends are presented in Table 10.4.

Table 10. 1: Feedstock blends and their ratio

Blended Feedstocks	Coal + SCB	Coal + CC	Coal + PSD	Coal + WT
Blend Ratio	1:1, 3:2, 4:1			

SCB: sugarcane bagasse; CC: corn cob; PSD: pine sawdust; WT: waste tyre

Cost analysis was carried out in the plant, and it is comprised of two financial cases namely; "blending with feedstocks costing (WFC)" and "blending without feedstock costing (WOFC)" were considered and studied. The WFC considered the actual costs of the feedstock together with cost of packaging and transportation of the feedstocks, and WOFC considers only the cost of packaging and transportation of feedstocks to the plant room. The relative advantage of WFC over WOFC is to specify the cost implications of the venture to potential investors. The information will serve as a guide to those investors in this business area. In addition, the techno-economic analysis considered the energy, economic, and environmental parameters of a typical co-gasification plant. To achieve this, an empirical model equation presented in Equation (10.1) was used to estimate the lower heating value of the fuel, and was used to determine both the annual feedstocks requirement and the feed rate for the plant. For profitability, the NPV, IRR, and PBP were used to assess the viability of the power generation at the 10^{th}, 11^{th}, 17^{th} and 18^{th} year business periods.

10.3.2. Estimation of the LHV and annual feed rate of the feedstocks

There are many important properties used to evaluate the qualities of fuels used for energy production, but the heating value of the fuel (LHV) is one of the most important [338,339]. The parameter is very useful in design, planning, operations, and development of a power generating plant. For efficient operations, Huang et al. [340] argued that the ultimate and proximate analysis data and the calorific value of the fuel play essential roles. The heating value of a fuel determines the amount of feedstock required for energy production in a power plant, and it has a strong influence of the feed rate. It has been reported by Ahmaruzzuman [341], Parikh et al. [342], Sheng & Azevedo [343], Thipkhunthod et al. [344] & Yin [345] that proximate and ultimate analysis data were efficient in estimating the HHV and LHV of fuels. In this study, Equation (10.1) [346] and Equation (10.2) [333] were used to estimate the LHV and annual feed rate of the feedstock for the co-gasification power plant.

$$LHV = HHV - (0.212 \times M_H) - (0.0245 \times MC) \tag{10.1}$$

$$F_{R\ ANNUAL} = \frac{\gamma}{\frac{LHV_{FEEDSTOCK}}{NOH}} \tag{10.2}$$

where HHV is the higher heating value of the fuel, MH is the mass fraction of the hydrogen, and MC is the moisture content of the fuel, NOH is the number of the operating hours, and $LHV_{Feedstock}$,

10.3.3. Estimation of fuel requirement for the CHP plant

Understanding the amount of fuel required to operate an energy production plant is very crucial. To achieve this, the LHV of the solid fuels was used to estimate the amount of feedstock required annually for the power production. The estimation was based on the moisture content (MC) and the efficiency of the system. According to Verma et al. [347], the annual feedstock requirement can be determined using Equation (10.3):

$$A_{FR} = \frac{\varpi \times 3.6}{LHV \times \eta_0} \tag{10.3}$$

Where A_{FR} annual feedstock requirement (t/y), ϖ is the energy demand (MWh/y) and η_0 is the operating efficiency of the plant (%). It is worthy to state that the LHV and MC of fuels are two vital parameters in thermochemical energy conversion process. The implication is that feedstock with low or high MC offers different operational efficiencies. A low MC fuel saves the cost of feedstocks pre-treatment (e.g. drying), improves the heating value of fuel, and consequently, enhances the overall efficiency of the energy production plant. High MC fuel reduces the heat transfer coefficient of the system, hence; resulting to several operational difficulties [333].

10.3.4. Economic Analysis of a co-gasification Power Plant

10.3.4.1. Net Present Value (NPV)

In project management, some evaluations tools such as the NPV are used to evaluate profitability of an investment. The NPV of an investment is referred to as the sum of the present values for an expected returns overtime offset by its up-front costs. It is used to determine projects that will yield the highest return over a specific period of time, and demonstrate the viability of the business. To estimate the NPV, the total earnings of the consecutive number of years for the business are discounted from the Marginal Rate of Return [333].

Estimation of the NPV in this study employed the Equation (10.5), the modified form of model presented by (Malek et al. [338]):

$$NPV = -\beta + \frac{\phi_1}{(1+R)^1} + \frac{\phi_2}{(1+R)^2} + \frac{\phi_3}{(1+R)^3} + \ldots\ldots\ldots\ldots \frac{\phi}{(1+R)^T} \quad (10.4a)$$

Where β the capital cost of investment also known as initial investment is, ϕ is the cash flow. According to Seifert & Litster [348], the NPV can be represented as shown in Equation (10.4b) [348]:

$$NPV = 0 + \sum_{t=1}^{N} \frac{I_t}{(1+i)^j} \quad (10.4b)$$

Where I_t, represents the net income in year t assuming there is no inflation in price/cost, N represents the power plant total lifetime, while I is the inflation-adjusted rate of return.

The β is a sensitive parameter in the NPV relation that depends on the feedstock cost. Feedstock cost is one of the factors that impacts on the investment cost (a significant variable) in the present evaluation. Therefore, profit or loss from a business is proportional to the increase or decrease in the β, and this equally affects the IRR of the business.

10.3.4.2. Internal Rate of Return (IRR)

The IRR is a parameter used in capital budgeting to measure the profitability of potential investments. It discounts all the cash back, hence; causing the NPV to become zero for the stipulated life of the business venture [333].

A project is more desirable to be undertaken than the other if it generates higher IRR. At times, different types of business investments may yield uniform IRR, but the tool can be applied to rank multiple potential ventures a firm may consider as the most viable option(s). Estimation of IRR in this study was according to Equation (10.5):

$$NPV = -\beta + \sum_{j=1}^{T} \frac{\phi_j}{(1+IRR)^j} = 0 \quad (10.5)$$

10.3.4.3. Payback Period (PBP)

Information describing the time it will take to recover the capital expenditure of a business venture is necessary in every investment. The time required for the amount of money invested in an asset to be repaid by the net cash flow generated by the asset is referred to as the PBP [333].

An investment with shorter PBP is better because it gives the investor a quick picture of the amount of time the initial investment will be on risk. Alternatively, PBP can be referred to as the number of years it takes a project to recover its total investment (δ) by earning after interest and tax (μ). However, the δ is a sensitive parameter in the PBP expression, because if the cash flows or profit made from the business is poor; then, the business status can be adjusted on the side of profit scale by changing the δ in order to shorten the PBP. Further re- adjustment can be made if economic condition appears better. Kong et al. [349] and Hasanuzzaman et al. [350] have developed an expression for the estimation of the PBP as shown in Equation (10.6). Equation (10.6) was used for the estimation of PBP in this study.

$$PBP = \frac{\delta}{\mu} \tag{10.6}$$

Emissions from a 5 MW co-gasification energy production plant

Emissions arising from energy plants pose a huge threat to the environment; therefore, emission reduction must be vigorously pursued. To generate energy from fuels, especially the fossils, various forms of emissions are produced, but co-gasification has the capacity of reducing the amount. Notable amongst these emissions and which will be studied in this research are CO, CO_2, SO_2, and NO_X.

10.4. Emissions reduction by displaced energy

Environmental Management and Control (EMC) is one of the top issues in the agenda of the United Nations. It is because of the impact emissions has on the environment, hence; resulting to a global issue. It is useful to know the amount of emissions that can be reduced if fossil fuel such as coal is replaced with renewable raw material such as biomass, or other solid waste. The emission of power generation can be estimated using the Equation (10.7) [351]. If the power plant is scaled up by increasing the ϖ to either10 MW, 15 MW or 20 MW, then the ξ will be increased, resulting in the increase in amount of emissions from the system, thus; increasing the amount emissions in the system.

$$\xi = \varpi \times [(\alpha^1 \times \tau^1) + (\alpha^2 \times \tau^2)] + \cdots\cdots\cdots\cdots \alpha^n \times \tau^m \quad (10.7)$$

In energy production or fuel processing, different fuels have different emission factors. The energy mix in the current study involves coal, biomass, and tyre. Table 10.2 presents the emission factors of different fossil fuels.

Table 10. 2: Emission factors of fossil fuels [350]

Fuel Sources Emission factor (kg/kWh)

	CO_2	SO_2	NO_X	CO
Coal	1.1800	0.0139	0.0052	0.0002
Petroleum oil	0.8500	0.0164	0.0025	0.0002
Natural gas	0.5300	0.0005	0.0009	0.0005

Furthermore, to determine the emission reduction from the co-gasification process, the emission factors of coal and biomass (or solid waste) are considered very essential. Table 10.3 presents the life cycle emission factors for renewable energy sources.

Table 10. 3: Life cycle emission: renewable energy sources [351]

Green-House-Gas Emissions			
Energy Sources	CO_2 (kg/kWh)	SO_2 (kg/kWh)	NO_X (kg/kWh)
Small hydro	0.009	0.00003	0.00007
Large hydro	0.0036 - 0.0116	0.000009 – 0.000024	0.000003- 0.000006
Wind	0.007 – 0.009	0.00002 – 0.00009	0.00002 – 0.00006
Solar photovoltaic	0.098 – 0.167	0.0002 – 0.00034	0.00018 – 0.0003
Solar Thermal Photovoltaic	0.0026 – 0.0038	0.00013 – 0.00027	0.00006 – 0.00013
Energy crops (Biomass)	0.017 – 0.027	0.00007 – 0.00016	0.0011 – 0.0025
Biomass: Current practice Improved	0.015 – 0.018	0.00006 – 0.00008	0.00035 – 0.00051
Geo-thermal	0.007 – 0.009	0.00002 – 0.00009	0.00028

10.4.1. Emissions from the transportation of biomass, tyres and coals

Often, the site for a power generating plant may differ from the feedstock production site. The implication is that the fuels should be transported to the plant room, and using different sizes of trucks. In the process, different amounts of emissions are generated. The emission arising from the fuel transportation was estimated in this study from Equation (10.8) [252]:

$$\lambda = \left[\frac{A_{FR} \times \gamma \times \omega}{T_{LPT}}\right] \quad (10.8)$$

where λ is the emission from transportation of biomass (eCO_2/y), T_{LPT}, γ is the hauling distance (km)

Similarly, and according to the US EAP [352] report, the emissions arising from different sizes of trucks in gross vehicles weight (GLT) rating for biomass transportation is presented in Table 10.4.

Table 10. 4: Heavy-duty diesel classification [352]

Type of Vehicles	Class	Mass Unit
Full size pickup truck	2b	3.86 – 4.54
Enclosed delivery truck	3	> 4.54 – 6.36
City delivery truck	4	> 6.36 – 7.27
Large work-in delivery truck	5	> 7.27 – 8.86
Rack trucks	6	> 8.86 – 11.82
Garbage collection truck	7	> 11.82 –15.00
Long-haul semi-tractor trailer rigs	8a	> 15.00 –27.27
Double long-haul semi-tractor trailer rigs	8b	> 27.27

10.4.2. Effective Emissions Reduction: Biomass Power Plant

The possibility of emission reduction in a power production plant is feasible when some factors (e.g. type of fuel, mode of transportation, etc.) are considered. Based on the life cycle of GHG emission intensity from biomass (ε) as 0.045 $kgCO_2$ e/kWh, the effective emission reduction arising from a biomass energy plant is expressed as in Equation (10.9) [353]. The distance covered and type of truck used in transporting fuels has direct impact on the φ model. For example, if the distance is reduced, and an electric-powered truck is used instead of a diesel truck, then the amount of emission, λ, will decrease enormously.

$$\varphi = \xi - \varepsilon - \lambda \tag{10.9}$$

where φ is the effective emission reduction, ξ is the emission reduction by displaced energy ε life cycle GHG emission intensity from biomass, and λ is the emission from transportation of biomass (eCO_2/y)

10.5. Results and Discussion

10.5.1. Physio-chemical characterization of the feedstocks

The physio-chemical properties of the feedstocks were determined and the result is presented in Table 10.5. It is evident from Table 10.5 that the Matla coal has high ash content, whereas; the biomass samples have very low ash content as well as little or no Sulphur content. Therefore, mixture of the two feedstocks as fuel in gasification, will limit the problems that are usually caused by ash and Sulphur from coal such as agglomeration and emissions, respectively, [86]. Furthermore, the volatile matter for all the biomass feedstocks and waste tyre were above 71 % and 60 %, respectively. High volatility in fuel samples (e.g. inorganic matter) is an indication of high reactivity, impacted on the coal sample (with low volatile content) by the other solid samples to enhance the overall gasification reactivity of the char [355]. According to Kumabe et al. [86] & (Alzate et al. [95], the co-gasification of high ash coal and biomass has the synergy for enhancing the H_2/CO in the gaseous product that is required for liquid fuel synthesis. The product gas composition and quality, is dependent on several factors including, but not limited to, the MC of the feedstock [356]. In addition, the heating value of the biomass and coal does not indicate a very wide range of value compare to the waste tyre that has the highest calorific value. These results eventually may influence the energy and economic analysis of the individual feedstocks.

However, each fuel possesses characteristics for efficient co-gasification process for energy production.

Table 10. 5: Characterization of feedstocks

Feedstock Analysis					
Parameters	Corn Cob	Sugarcane-Bagasse	Pine Saw-dust	Waste-Tyre	Matla Coal
	Proximate analysis determined as air dried basis				
Ash Content (%)	0.29	0.49	0.59	9.92	44.00
Inherent moisture (%)	5.87	8.8	8.55	0.32 63.29	3.80
Volatile Matter (%)	72.50	71.50	71.80	26.47	19.90
Fixed Carbon (%)	21.34	19.12	19.06		32.30
Heating Value					
HHV (MJ/kg)	17.42	18.85	21.50	30.95	18.60
LHV (MJ/kg): Calculated	16.42	17.28	19.86	29.24	17.89
Ultimate analysis determined as air dried basis					
Carbon (%)	24.82	38.67	50.54	87.60	39.09
Hydrogen (%)	3.94	6.40	7.08	8.03	2.90
Nitrogen (%)	0.97	0.23	0.15	0.33	0.92
Sulphur (%)	0.00	0.00	0.57	3.12	0.66
Oxygen (%)	70.27	54.70	41.66	0.92	8.63

10.5.2. Energy analysis of Feedstocks and their blends

The moisture content of a fuel affects the performance of the energy conversion system which in-turn determines the electric and heat production of the plant. Table 10.6 presents the MC and LHV of the various feedstock mixtures used in the co-gasification power generation plant. The table describes the relationship between the MC and LHV of the fuels. It can be observed that the MC

of the entire feedstocks except the Coal + PSD (with the highest LHV), decreased with an increase in the LHV of the fuels, both MC and LHV increased with the blending ratio. In most cases, higher energy content fuels are more efficient in electric and thermal power production than the lower energy content fuels. In addition, Table 10.6 (a) shows the results of the feedstocks at different blend ratio.

Table 10. 6: LHV and MC of feedstocks at different blend ratios

Parameters	Coal + SCB	Coal + CC	Coal + PSD	Coal + WT
Feedstocks: Ratio: 1:1				
LHV [MJ/kg]	17.58	17.15	19.72	23.57
MC [%]	6.35	5.34	4.65	2.06
Feedstocks: Ratio: 3:2				
LHV [MJ/kg]	17.65	17.30	18.68	22.87
MC [%]	5.84	5.03	4.48	2.41
Feedstocks: Ratio: 4:1				
LHV [MJ/kg]	17.77	17.60	18.28	20.16
MC [%]	4.82	4.41	4.14	3.10

MC: Moisture content; LHV: Lower Heating Value; SCB: Sugarcane bagasse; PSD: Pine sawdust; WT: Waste Tyre.

Table 10.6 (b) presents the economic assumptions used for the techno-economic estimations. It is important to mention that the economic analysis basically was focused only in the feedstock used in the power plant. Material/equipment costing was no considered.

Table 10.6 (b): Data and economic assumption used for the techno-economic analysis

S/N	Item	Price**	Unit
1	Cost of electricity in South Africa	0.14	$/c kWh
2	South Africa coal spot price	74.46	$/Ton Coal
3	Cost of bagging and transportation of biomass to plant room (PSD, SCB, & CC)*: Assume 10 kilometers distance	40	$/Ton biomass
4	Cost of bagging and transportation of coal to plant room*	30	$/Ton Coal
5	Cost of bagging and transportation of waste tyre to plant room*	32	$/Ton WT
6	Revenue generated from the sale of steel-wire obtained from WT crumbling*	20	$/Ton WT
7	PSD Price (SA)	2.5	$/Ton PSD
8	SCB price (SA)	10.7	$/Ton SCB
9	CC Price (SA)	11.43	$/Ton CC
10	Cost of WT (and Crumbling) in south Africa)	42.86	$/Ton WT

SCB: Sugarcane bagasse; PSD: Pine sawdust; WT: Waste Tyre. *: assumptions; **: Exchange rate of United States Dollar (USD) to South African Rand (ZAR): 1USD = 1ZAR.

10.5.3. Feedstocks requirements for the different blends

Researchers have developed different empirical models for the estimation of the heating value of fuels. The model shown in Equation (10.1) was applied to calculate the lower heating value (LHV) of the feedstocks, employing the data from the proximate and ultimate analysis depicted in Table 10.5. The HHV was experimentally determined using a bomb calorimeter. The results obtained from the model were in the same trend with those found in the literature (16.80 MJ/kg – 19.50 MJ/kg) [38]. Figure 10.1 and Figure 10.2 depict the co-gasification CHP process plant and flowchart/schematic diagram of the proposed technical approach. The flowchart shows a hypothetical case for design to generate about 5 MW (130 TJ/Yr) of electricity if operated for about 300 days per annum (7200 h./Yr). Caputo et al. [332] has reported that the total electrical efficiency of a gasification plant with about 5 MW electric power production capacity is 36 %. Based upon this assumption, the utilization of Matla coal and ‘Coal + PSD” as feedstocks as shown in Figure 10.2, generated 5 MW of electricity using 20 million kg/Yr and 18 million kg/Yr

of Matla coal and Matla coal + PSD respectively. Furthermore, on the basis that the number of operating hours was 7,200 h/Yr, about 2,795 kg/h of Matla coal and 2,535 kg/h of Matla Coal + PSD were converted into power by the co-gasification plant, respectively, to produce about 5 MW (130 TJ/Yr) of electricity.

Similarly, to recover some costs associated with the electricity production and also maximize the heat arising from the gasification or co-gasification process, condensers or heat exchangers were installed in the form of combined heat and power (CHP) plant. Bridgwater [357] reported that the overall thermal efficiency of a gasification plant could be assumed as about 40 %. Under this scenario, about 5.56 MW (144 TJ/Yr) of heat power was produced from the steam-gas unit using Matla coal and Matla Coal + PSD, respectively. However, the details of gasification of the Matla coal and blends of Matla coal and solid wastes in terms of heat and power production are shown in Figure 10.1. In this case, evaluation involving only coal was used as control for blends of coal + solid waste tests.

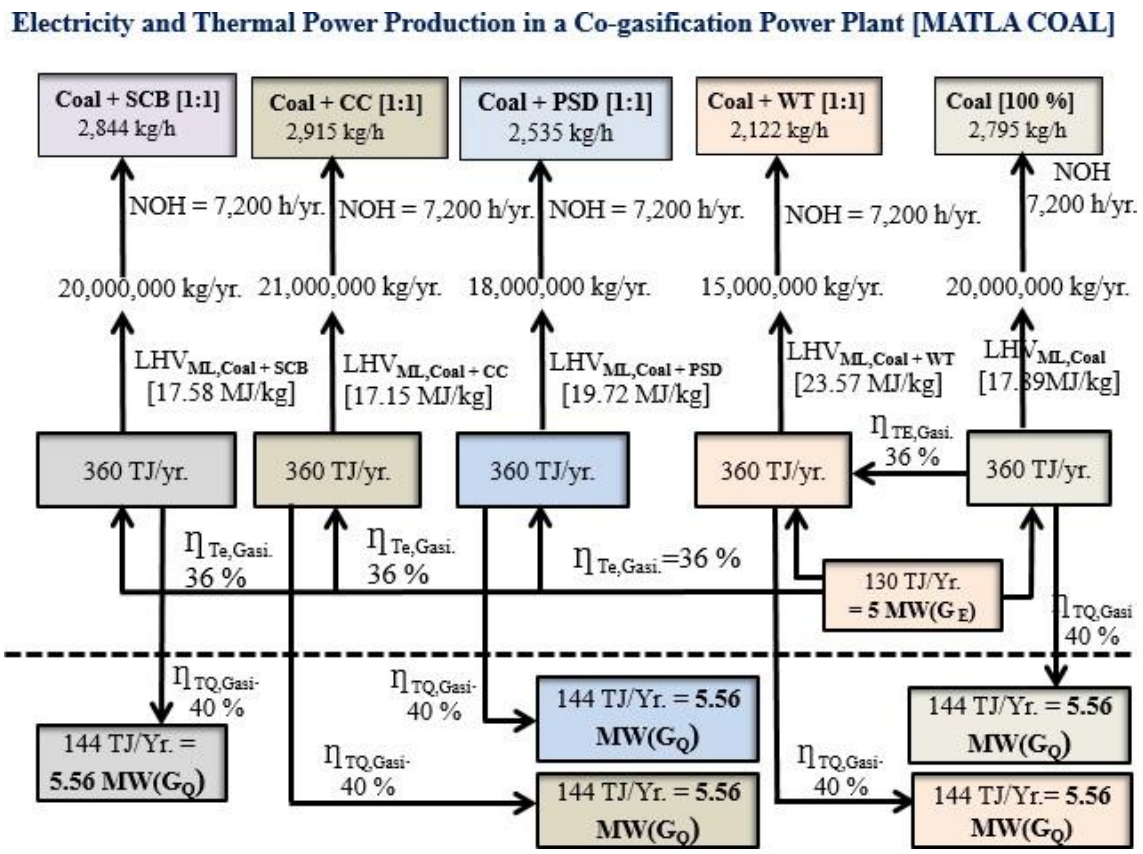


Figure 10. 1: Schematic illustration of a co-gasification process plant: Electric and Thermal Power Generation

Figure 10.2 therefore presents the proposed co-gasification CHP plant (5 MW Capacity) used in this study.

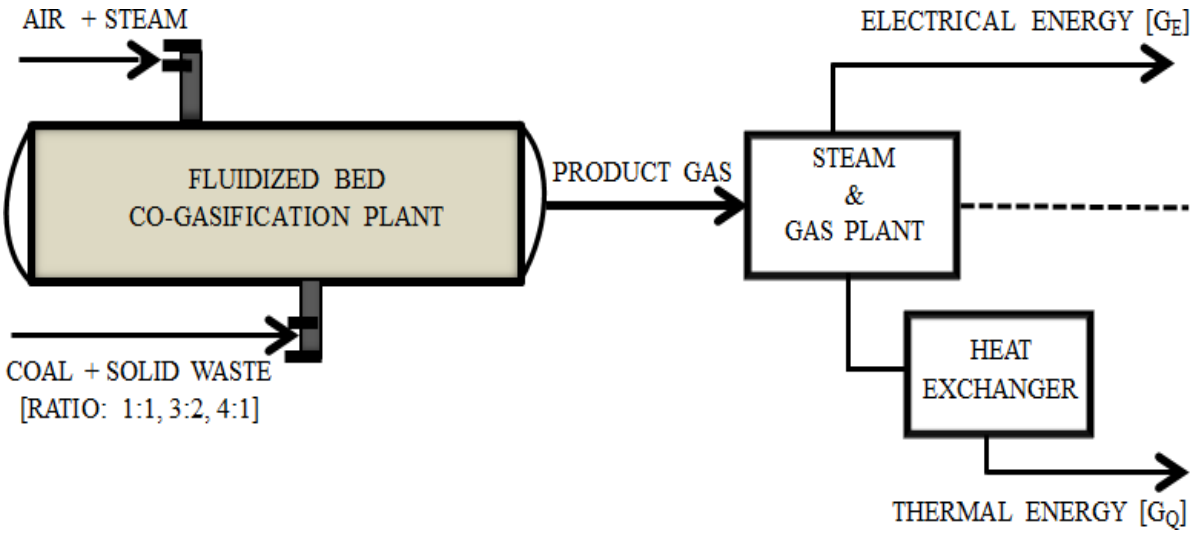


Figure 10. 2: Schematic diagram of the proposed co-gasification plant [13].

10.6. Relationship between the amount of feedstocks, expenditure and profit for an electric power generating co-gasification plant with 5 MW production capacity

The Matla Coal + PSD indicated the highest yield of profit and lowest expenditure compared to other feedstocks investigated, because PSD was the cheapest feedstock amongst the fuels studied. Normally, fuel with higher calorific value produces higher amount of energy. In this study, the power generating capacity of the plant is known, so the interest is on the feedstock blend that offers the highest profit and of lower emissions with 130 TJ/Yr standard targets. The energy content of Coal + WT was higher than the energy value of Coal + PSD. Thus, higher electric and thermal powers are expected from the blend, but the expectation was not the case under WFC condition. Expectedly, Coal + WT should have yielded more profit WFC, but more profit was obtained from Coal + WT under WOFC. It has been shown that the calorific value of a fuel and the expenses incurred on the feedstocks determine the amount of loss or profit that could be expected during power production. However, it can be observed from Figure 10.4 that more profit was accrued under WOFC than in Figure 10.3 under WFC.

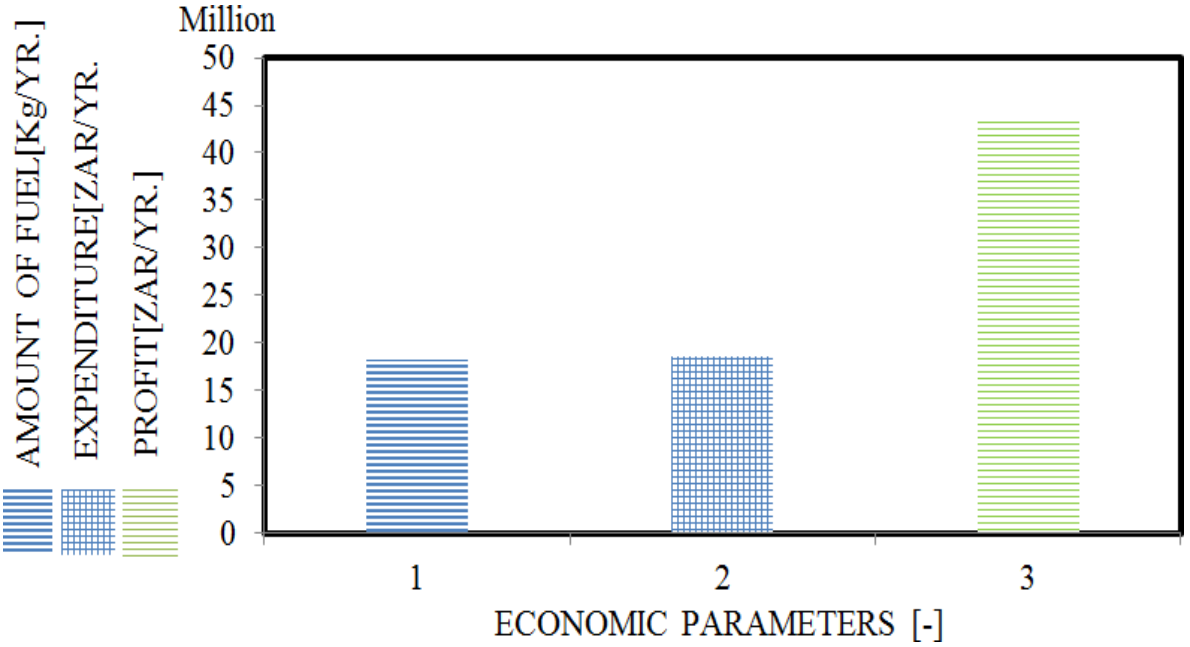


Figure 10. 3: Relationship between the amount of fuel and expenditure & profit (Matla coal + PSD: 1:1) using WFC

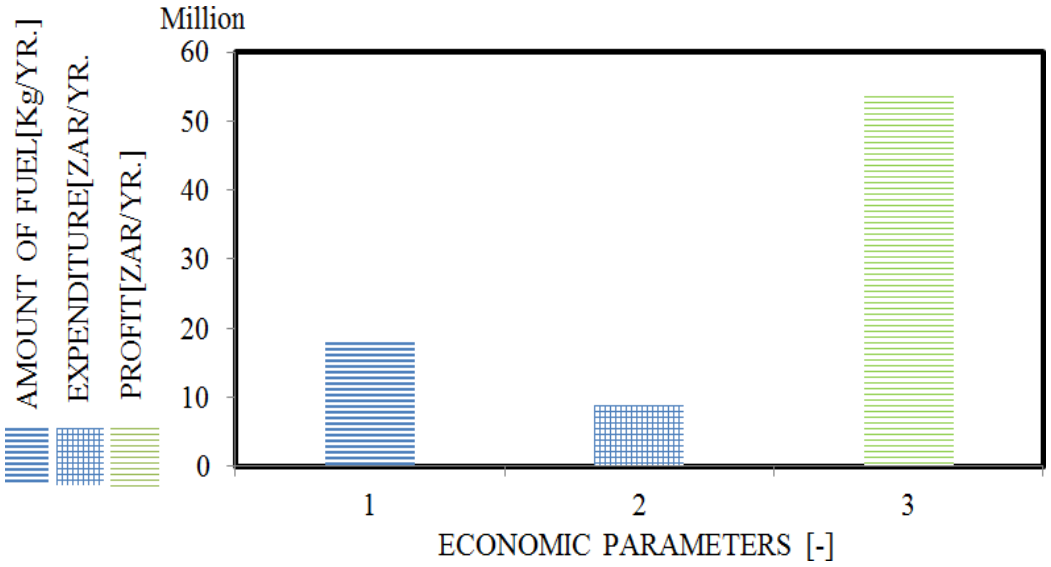


Figure 10. 4: Relationship between the amount of fuel and expenditure & profit (Matla coal + PSD: 1:1) using WOFC

10.6.1. Economic evaluation of coal gasification

In this study, control gasification analysis was firstly, developed by solitary gasification of coal. This was followed by the analysis of co-gasification of coal and other solid wastes as presented in Figure 10.5. The result obtained revealed that the amount of feedstocks used for the power production as depicted in Figures 10.5 and 10.6 was different from the amount of Matla coal used for the same purpose (see Figure 10.5). Higher amount of fuel was consumed in the plant that used Matla coal than that of Matla Coal + PSD co-gasification plant. It was observed that about 1,868,806.40 kg of fuel could be saved annually by using a blend of Matla Coal + PSD for power production as against using 100 % Matla coal. The implication is that the operating cost of the plant was reduced due to annual feedstock savings.

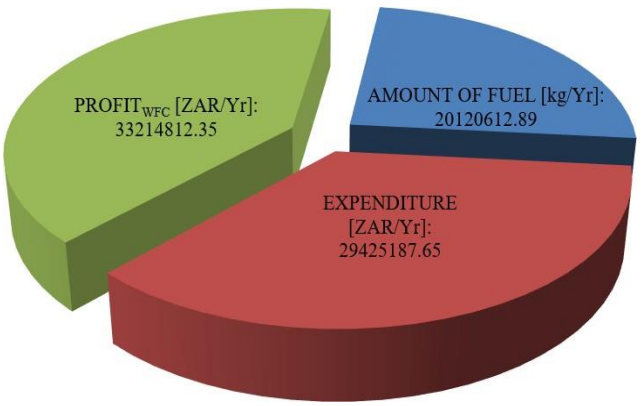


Figure 10. 5: 100 % Matla coal economic analysis: 5 MW & 5.56 MW electric & thermal power generations

10.6.2. Co-gasification of the feedstocks

In this study, synergetic effects are achieved via co-gasification of the feedstocks, and the results obtained are reported based on the two financial cases investigated. Figure 10.6 and Figure 10.7 highlight the influence of the various feedstocks investigated and their economic parameters for WFC and WOFC, respectively. The reported blend ratio of 1:1 Coal + solid waste blend ratio in this study is the optimum blending ratio. Figure 10.6 shows that Coal + CC blend yielded the lowest profit, because corn cob is costlier than SCB and PSD

.

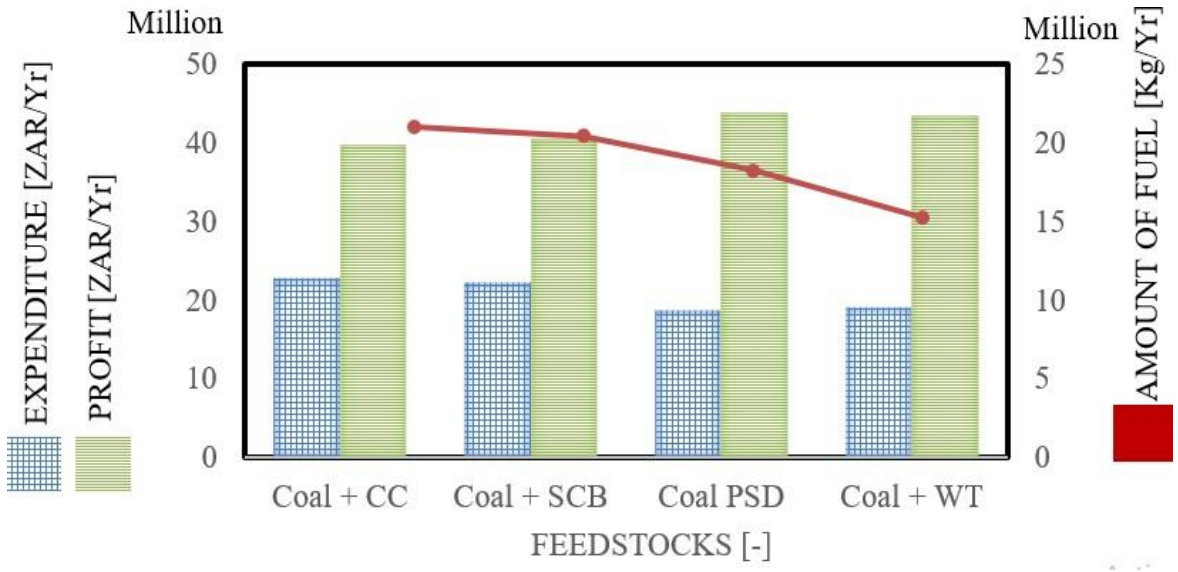


Figure 10. 6: Influence of feedstocks on the economic parameters using WFC

The heating values of the fuels are in the increasing order of Coal + CC < Coal + SCB < Coal+ PSD, < Coal + WT, and the profit increased with an increase in the heating value of the feedstock (Figure 10.7). However, the ultimate analysis result (Table 10.6) from WT has the highest amounts of carbon and hydrogen amongst the feedstocks studied. Carbon and hydrogen are the major combustible part of a fuel and determines the energy content of the fuel. The energy content of WT is higher than the energy content of all other fuels studied. Thus; the use of Coal + PSD as shown in Figure 10.7 displayed the optimum during WOFC.

10.6.3. Effect of Feedstocks blend ratio

Figures 10.8 and 10.9 present the economic evaluation of Matla Coal + PSD of WFC and WOFC, respectively, at a blend ratio of 4:1. Figures 10.8 and Figure 10.9 were compared to Figures 10.3

and Figure 10.4 (1:1).

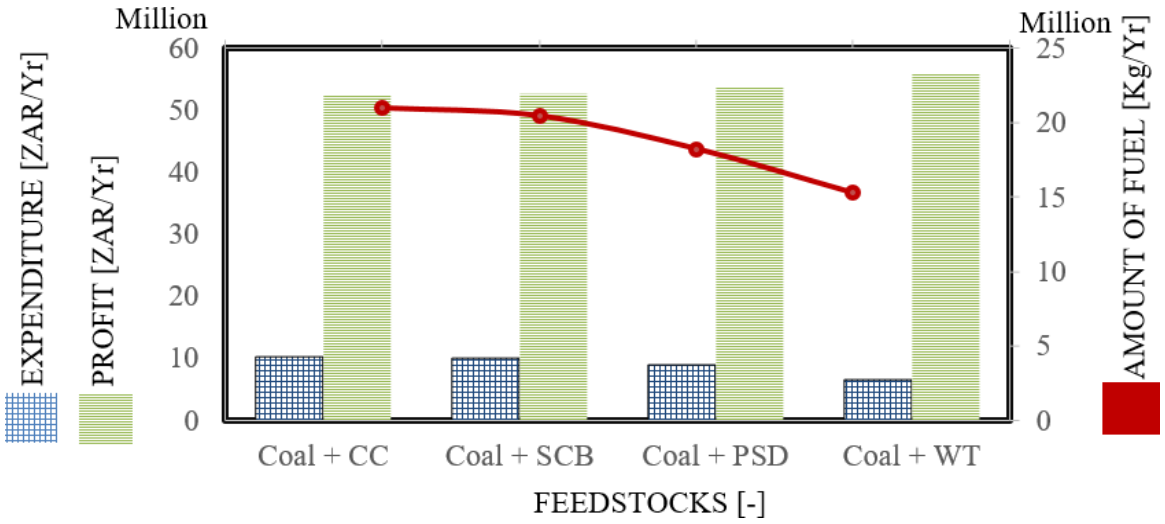


Figure 10. 7: Influence of feedstocks on the economic parameters using WOFC

The results obtained from Coal + PSD mixture at a ratio of 4:1 depicted in Figure 10.8, and compared to results from Coal + PSD mixture at a ratio of 1:1 depicted in Figure 10.3, reveal that increasing the content of Matla coal in the blend increased the expenses in the power generation by about 14.68 %. This in turn decreased the profit accrued by about 7.95 %. In this scenario also, the amount of feedstock used in the 4:1 blend ratio was increased by 3.78 % compared to that of 1:1 mixture, thus amounted to a loss of ZAR6, 461,301.771 for WFC. This was considered as a loss based on the fact that the same quantity of heat and electricity were produced using different amounts of feedstock at different fuel blend ratios. The 4:1 blend ratio increased the amount of feedstock, thereby leading to the huge loss of money. In a study carried out by Bada et al. [358], it was reported that co-firing coal and biomass at the ratio of 1:1resulted to a 50 % reduction in CO_2 emissions. The current report has also demonstrated that around ZAR6, 461,301.771 could be saved by using 1:1 coal to solid waste mixture as against 4:1 mixture, for a co-gasification plant of 5 MW power generation capacity. Similarly, at WOFC and with the same increase in the amount of fuel of 3.78 %, an increase in the expenditure by 0.70 % was observed. This therefore led to a decrease in the profit by 0.12 %

(ZAR 123,782.50). Table 10.7 highlights the prices of the feedstocks as obtained in South Africa and some parts of the globe. The prices are landing cost.

Table 10. 7: Cost of feedstocks in South Africa and some parts of the globe.

S/N	Type of Feedstock	Price of Feedstock (ZAR/Ton)
1	Pine Saw-dust*	35.00 – 55.00
2	Sugarcane Bagasse*	150.00 – 200.00
3	Corn-Cob*	160.00
4	Waste-tyre*	550.00 – 600.00
5	Corn-Cob**	1946.00 – 2646.00
6	Sugarcane Bagasse***	2380.00
7	Corn Cob***	2380.00
8	Sugarcane Bagasse**	1680.00 – 2800.00
9	Coal, SA*	1042.44

*: Local Price (South Africa); **: International Price (Vietnam); ***: USA; S/N: Serial number.

The increase or decrease in the amount of feedstock and expenditure or profit have been typically attributed to the price of South African Coal which at present is $74.46/ton Coal (ZAR1, 042.44/ton Coal) compared to the solid wastes (sugarcane bagasse, corn cob, pine saw-dust, and waste-tyre) which is within the range of $10.71/ton – $42.86/ton (ZAR149.94/ton – ZAR600.04/ton). Under this context, if biomass fuels (not waste biomass - e.g. miscanthus, switch-grass, beech- wood, etc.) are purchased either within or outside South Africa at the rate of around $120.00/ton – $170.00/ton of biomass, then it will be cheaper to generate electricity and heat from South African Matla coal than from the biomass. The analysis presented in section 3.2.1– 3.2.4 indicates that the energy content of the feedstock (LHV), cost of fuel, and the blend ratio are the most significant factors influencing the estimation, although the future value of money determined in each investment year through the NPV, and reported in section 3.3, is equally a crucial influencing factor in the assessment.

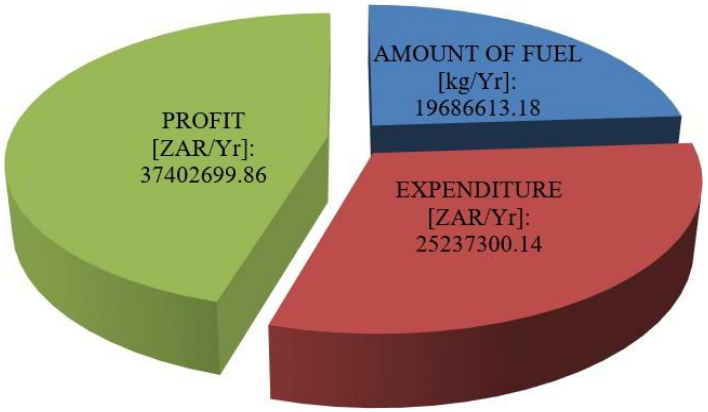


Figure 10. 8: Effect of the amount of feedstocks blending ratio on expenditure and profit (Matla Coal + PSD: 4:1) using WFC

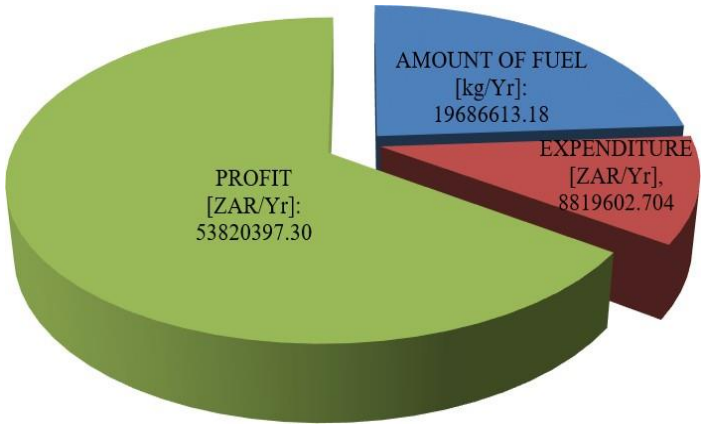


Figure 10.9: Effect of the amount of feedstocks blending ratio on expenditure and profit (Matla Coal + PSD: 4:1) using WOFC

10.6.4. Effect of Feedstocks on the Economic Parameters: Percentage basis

The percentage changes in the economic and energy production of a power production plant were studied here. Understanding the changes in the economic parameters of feedstocks used for electric and thermal power production with regard to their percentage changes is a very important aspect of energy and economic analysis. Table 10.8 presents the variation in feedstocks economic parameters, for the WFC and for the WOFC, and Table 10.9 describes (in percentage basis) the potentials of the other solid wastes studied over coal, for power generation. At this point, the analysis describes the benefits in terms of profit making, of using mixtures of coal and other solid wastes over the use of coal.

Table 10. 8: Variation in feedstocks economic parameters [Coal + Solid Wastes] at WOFC

Parameters	Amount of Fuel [Kg/Yr] [In Million]	Expenditure [ZAR/Yr] [In Million]	Profit [ZAR/Yr] [In Million]
WFC			
Coal	20.1	29.43	33.21
Coal + CC	20.99	22.90	39.74
VEP*	8.65×10^{-3}	6.52×10^{-3}	65.26
Coal + SCB	20.47	22.24	40.402
VEP**	3.53×10^{-3}	7.19×10^{-3}	7.19×10^{-3}
Coal + PSD	18.25	18.78	43.86
VEP***	18.69	10.65	10.65
Coal + WT	15.28	19.18	43.46
VEP****	4.84×10^{-3}	10.25	10.25
WOFC [Except Coal]			
Coal	20.12	29.43	22.80
Coal + CC	20.99	10.28	52.37
VEP*	8.65×10^{-3}	19.14	19.14
Coal + SCB	20.47	10.03	10.0
VEP**	3.53×10^{-3}	19.40	19.40
Coal + PSD	3.53×10^{-3}	8.94×10^{-3}	19.40
VEP***	18.25	20.48	20.48
Coal + WT	15.28	6.63×10^{-3}	56.01
VEP****	4.844×10^{-3}	22.80	22.78

*: Coal & Coal + CC; **: Coal & Coal + SCB; ***: Coal & Coal + PSD; ****: Coal & Coal + WT; “: Blend Ratio: 1:1; WFC: With Feedstock Costing; WOFC: Without Feedstock Costing; VEP: Variation in the Economic Parameters;

Table 10.8 in real terms, describes the annual fuel savings and cost savings from the individual feedstocks, and as well, highlights how each feedstock differs from one another in terms of

power production economy.

Table 10.9: Variation in feedstocks economic parameters: Percentage basis

Feedstock	Parameters: Amount of Fuel	Expenditure	Profit
	WFC [%]		
Coal & Coal + CC*	0.02	12.47	8.94
Coal & Coal + PSD**	4.87	22.09	32.87
	WOFC [%]		
Coal & Coal + CC*	2.11	48.21	22.37
Coal & Coal + WT**	13.69	63.72	25.55

*: Lowest economy; **: Highest economy; SCB: sugarcane bagasse; CC: corn cob; PSD: pine sawdust; WT: waste tyre

Meanwhile, with reference to profit making, Coal + PSD & Coal + CC; Coal + SCB & Coal + CC; Coal + WT & Coal + CC; Coal + SCB & Coal + PSD; Coal + WT & Coal + PSD; and Coal + WT & Coal + SCB were evaluated at WFC and 1:1 ratio. Low or high profit had been described to be related to the CV of the fuel, and the investment cost. It was observed that higher profits were made from Coal + PSD, Coal + SCB, and Coal + WT blend than the blends they were compared with. And more profits were equally made from Coal + PSD and Coal + WT blends than the blends they were compared with. Details of the analysis at 10^{th} year at WFC & WOFC are presented in the appendices.

10.7. Profitability analysis using NPV, IRR and PBP

In this study, the capital cost investment is referred to as the total expenditure incurred on the feedstocks to generate 5 MW of electricity, and the cash flow is regarded as the annual profit obtained by subtracting the total expenditure from the revenue generated from the sales of electricity at the rate of ZAR1.74/kWh [16] of electric power. The venture embarked on from the 1^{st} year to the 10^{th} year is attractive, except for the coal-to- solid waste blend of 4:1 at WFC. The status of the venture is illustrated in Figures 10.10 –10.12. The capital cost investment from Coal + CC is higher than the rest of the feedstocks studied. Figure 10.11 thereby resulting in the

lowest NPV. On the other hand, the NPV from the Coal + PSD is the highest out of the fuels investigated due to its lowest capital cost investment.

Figure 10. 9: Economic assessment at the 10th year using WFC at coal to biomass/waste ratio of 1:1

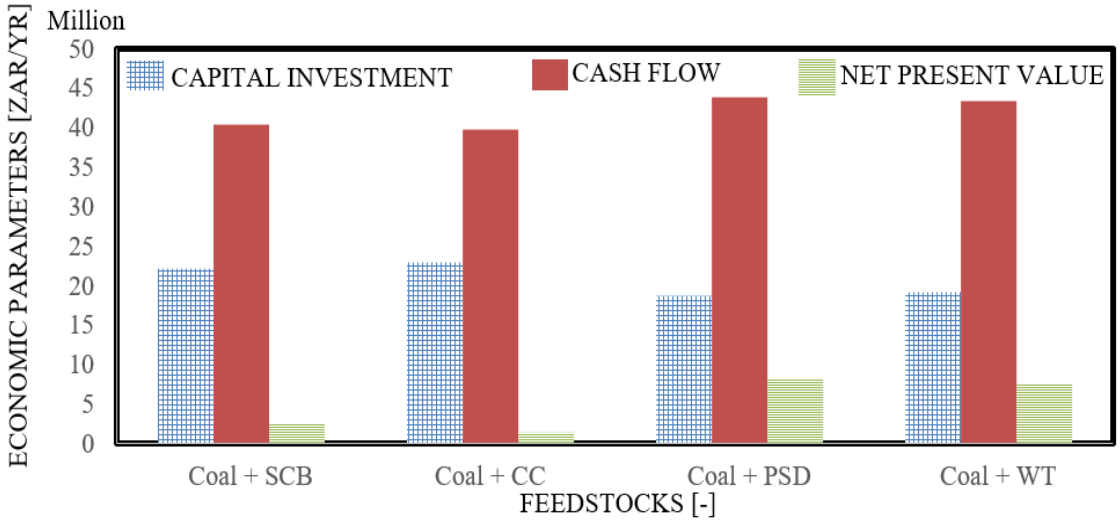


Figure 10.11 shows a significant increase in the NPV of all the feedstocks, because of the lower capital investments incurred from the individual feedstocks when compared to Figure 10.10. The price of WT (Table 10.8) is highest of all the prices of all the agro-wastes studied. In spite of the highest fuel price, the blend still displays the highest NPV at WOFC due to its highest heating value.

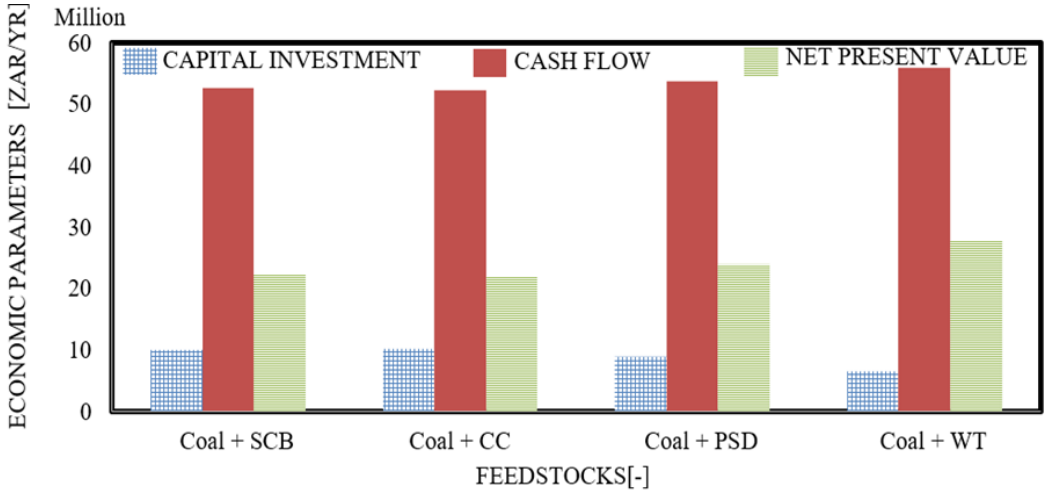


Figure 10. 10: Economic assessment at the 10th year using WOFC at coal to biomass/waste ratio of 1:1. Figure 10.12 presents similar assessment using Coal-Solid waste blend ratio of 4:1 at WFC.

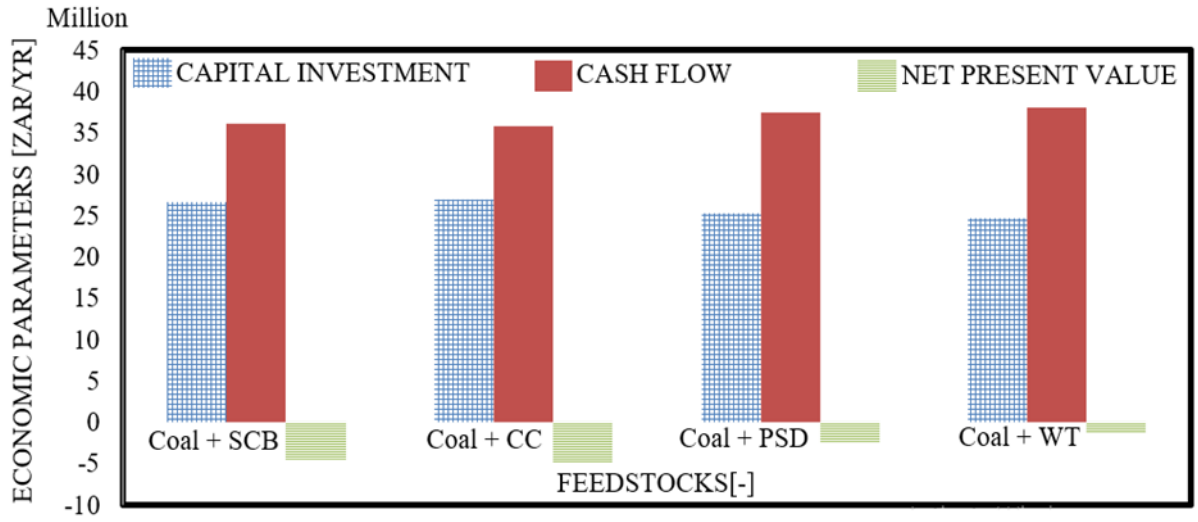


Figure 10. 11: Economic assessment at the 10th year using WFC at coal to biomass/waste ratio of 4:1

From Figure 10.12, a poor investment was recorded because, the NPV at the end of the 10-year period is negative, and the cash returns are insufficient to encourage further investment, under the conditions and feedstocks investigated.

10.7.1. Effect of elongation of business period on the business viability

Time has a very big influence on business ventures. In this study, the business life was increased from 10 to 11 years to investigate the effect of the business period elongation on viability. All the fuel mixtures from the 1:1 and 3:2 ratios except the Coal + SCB from 3:2 fuel blend, remained viable. However, all the investment made with the 4:1 fuel ratio is not viable because of the effect of the capital cost investment and time value of money on the NPV. Similarly, the use of all the feedstocks remained viable for the power production at WOFC, and the use of Coal-to-Solid waste ratio of 1:1 displays the most attractive venture. The details of the analysis of the cost and profitability at WFC and WOFC at the 11th year can be found in the appendices.

10.7.2. Effect of business period elongation on the venture from 11 – 17 years

As stated earlier, a business may suffer profitability risks at the course time, but that is dependent on the type of business. The essence of this analysis is to determine when exactly the investment would turn into a fruitless venture. The information will be a guide both to the Energy Analysts and potential investors prior to investing in the area. The result obtained under this context

indicated that only Coal-to-PSD of blend ratio 1:1 was viable, and the IRR from the use of all the feedstocks for the venture was lower than 5 % (the initial annual interest rate). A comprehensive result of the assessment at WFC is shown in Table 10.10.

Table 10. 10: Investment evaluation at 17th Year using WFC

Feedstocks [-]	Capital Cost Investment [δ] [ZAR/Yr] [In Million]	Cash Flow [μ] [ZAR/Yr] [In Million]	Net Present Value [NPV] [ZAR/Yr] [In Million]	Internal Rate of Return [IRR] [%]	Payback Period [PBP] [Year]
Ratio: [1:1], Interest Rate: [5 %] - WFC					
Coal + SCB	22.24	40.40	-4.61	3.57	0.6
Coal + CC	22.90	39.74	-5.56	3.29	0.6
Coal + PSD	18.78	43.86	361,720.25^{T}	5.12	0.5
Coal + WT	19.18	43.46	-211,931.82^{T}	4.93	0.5
Ratio: [3:2], Interest rate: [5 %] - WFC					
Coal + SCB	23.70	38.94	-6.70	2.97	0.6
Coal + CC	22.922	39.72	-5.59	3.30	0.6
Coal + PSD	21.50	41.14	-3.55	3.90	0.4
Coal + WT	20.41	42.23	-1.99	4.37	0.4
Ratio: [4:1], Interest Rate: [5 %] - WFC					
Coal + SCB	26.58	36.06	-4.44	1.79	0.7
Coal + CC	26.88	35.76	-11.28	1.69	0.8
Coal + PSD	25.24	37.40	-8.92	2.31	0.7
Coal + WT	24.63	38.01	-8.05	2.58	0.7

WFC: With Feedstock Costing; SCB: sugarcane bagasse; CC: corn cob; PSD: pine sawdust; WT: waste tyre; ^{T}: In thousand

10.7.3. Effect of power production period on the investment viability from 2017 – 2035

A specific investment period (2017 – 2035) was projected and studied to further understand the influence of time on the profitability of the energy plant. From 2017 - 2035 was 18th year of the investment. At this time, none of the ventures is viable. Figure 10.13 highlights the viability status of the business for coal-to-solid waste ratio of 1:1 and indicates a negative NPV for all the feedstocks investigated at WFC. Similar observations were made in other blends, as well. Therefore, investing in the business till 2035 using any of the feedstocks will be a waste of resources, but the analysis at WOFC proofed otherwise.

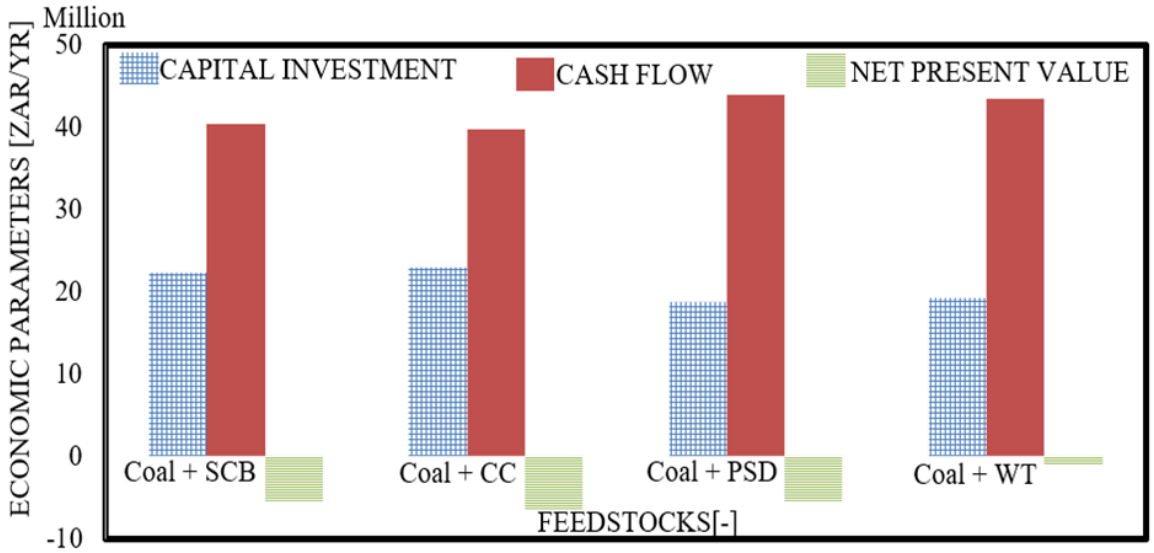


Figure 10. 12: Economic assessment from 2017 – 2035 (I.e. the 18th year) using WFC at coal to biomass/waste ratio of 1:1

10.8. Environmental Impact Assessment of the 5 MW co-gasification power plant

A co-gasification power generation plant operating at 5MW capacity can use Coal + SCB, Coal + CC, Coal + PSD, and Coal + WT of about 20,473,451.41 kg, 20,986,049.96 kg, 18,251,806.49 kg, and 15,276,277.85 kg, respectively, to produce the 5 MW of electricity annually. Coal is commonly used for power production in South Africa and if these feedstocks replace coal for energy production it is expected that the amount of GHG emitted from power plant will reduce. Most importantly, the amount of CO_2 that will be available for sequestration will also reduce. Arias et al. [359] investigated the optimal design and sensitivity analysis of post-combustion CO_2 capture process by chemical absorption with amines. The authors were able to identify the operating conditions that minimize the specific total cost of the CO_2 capture. Also, in a review carried out by Chen et al. [360] on emerging N-nitrosamines and N-nitramines from amine-based post-combustion CO_2 capture, it was revealed that the process is a promising option.

However, a change in the capacity of the existing plant to about 1.5 or 2 times the current capacity will definitely increase the feed rate and annual feedstock requirements, investment cost and profit, and as well, the emissions in the plant. Table 5.11 presents the effective emission reduction expected from different feedstocks studied. The values contained in Table 10.11 were calculated from Equation (10.9).

Table 10. 11: Estimated emission reduction from the plant at different blend ratio

Feedstock	CO [kg]	CO_2 [kg]	SO_2 [kg]	NO_X [kg]
Blending Ratio: [1:1]				
Coal + SCB	-28.70	2905.96	34.58	-113.79
Coal + CC	-29.43	2904.89	34.58	-116.96
Coal + PSD	-25.54	2910.74	34.60	-100.04
Coal + WT	-21.30	2918.87	34.63	-81.61
Blending Ratio: [3:2]				
Coal + SCB	-28.50	3496.52	41.53	-110.75
Coal + CC	-29.07	3495.65	41.53	-113.25
Coal + PSD	-26.89	3498.95	41.54	-103.74
Coal + WT	-21.86	3510.02	41.57	-81.91
Blending Ratio: [4:1]				
Coal + SCB	-28.10	4676.41	55.43	-104.67
Coal + CC	-28.38	4675.99	55.43	-105.89
Coal + PSD	-27.28	4677.65	55.44	-101.12
Coal + WT	-24.67	4682.28	55.45	-89.78

SCB: sugarcane bagasse; CC: corn cob; PSD: pine sawdust; WT: waste tyre

The coal-to-solid waste ratio of 1:1 (Table 5.11) produced the lowest amounts of CO_2 and SO_2

emissions, and the emissions increased as the amount of coal in the various mixtures increased for all the feedstocks investigated. Similarly, Coal + PSD produced the lowest amounts of CO_2 and SO_2 emission reductions, whereas; Coal + WT gave the lowest CO and NO_X emission for all the feedstocks investigated. In overall, it is possible to reduce the CO, CO_2, SO_2, and NO_X emissions by approximately 3.4 %, 23.28 %, 22.97 %, and 0.55 %, respectively, using the Coal-to-PSD of blend ratio 1:1 as against the blend ratio of 4:1. The CO_2 emission from the Matla coal is estimated using Equation (10.9) as 5900 kg CO_2/kWh, whereas the CO_2 emission from Coal + PSD or other biomass and waste investigated at a blend ratio of 1:1 is estimated as 2950 kg CO_2/kWh (a 50 % reduction). Meanwhile, Bada et al. [358] have also reported a similar trend using coal-to-biomass blend ratio of 1:1 thereby corroborating the findings of this study.

A co-gasification power generation plant operating at 5MW capacity can use Coal + SCB, Coal + CC, Coal + PSD, and Coal + WT of about 20,473,451.41 kg, 20,986,049.96 kg, 18,251,806.49 kg, and 15,276,277.85 kg, respectively, to produce the 5 MW of electricity annually. Coal is commonly used for power production in South Africa and if these feedstocks replace coal for energy production it is expected that the amount of GHG emitted from power plant will reduce. Most importantly, the amount of CO_2 that will be available for sequestration will also reduce. Arias et al. [359] investigated the optimal design and sensitivity analysis of post-combustion CO_2 capture process by chemical absorption with amines. The authors were able to identify the operating conditions that minimize the specific total cost of the CO_2 capture. Also, in a review carried out by Chen et al. [360] on emerging N-nitrosamines and N-nitramines from amine-based post-combustion CO_2 capture, it was revealed that the process is a promising option. However, a change in the capacity of the existing plant to about 1.5 or 2 times the current capacity will definitely increase the feed rate and annual feedstock requirements, investment cost and profit, and as well, the emissions in the plant. Table 10.11 presents the effective emission reduction expected from different feedstocks studied.

Table 10. 11: Estimated emission reduction from the plant at different blend ratio

Feedstock	CO [kg]	CO_2 [kg]	SO_2 [kg]	NO_X [kg]
Blending Ratio: [1:1]				
Coal + SCB	-28.70	2905.96	34.58	-113.79
Coal + CC	-29.43	2904.89	34.58	-116.96
Coal + PSD	-25.54	2910.74	34.60	-100.04
Coal + WT	-21.30	2918.87	34.63	-81.61
Blending Ratio: [3:2]				
Coal + SCB	-28.50	3496.52	41.53	-110.75
Coal + CC	-29.07	3495.65	41.53	-113.25
Coal + PSD	-26.89	3498.95	41.54	-103.74
Coal + WT	-21.86	3510.02	41.57	-81.91
Blending Ratio: [4:1]				
Coal + SCB	-28.10	4676.41	55.43	-104.67
Coal + CC	-28.38	4675.99	55.43	-105.89
Coal + PSD	-27.28	4677.65	55.44	-101.12
Coal + WT	-24.67	4682.28	55.45	-89.78

SCB: sugarcane bagasse; CC: corn cob; PSD: pine sawdust; WT: waste tyre

The coal-to-solid waste ratio of 1:1 (Table 10.11) produced the lowest amounts of CO_2 and SO_2 emissions, and the emissions increased as the amount of coal in the various mixtures increased for all the feedstocks investigated. Similarly, Coal + PSD produced the lowest amounts of CO_2 and SO_2 emission reductions, whereas; Coal + WT gave the lowest CO and NO_X emission for all the feedstocks investigated. In overall, it is possible to reduce the CO, CO_2, SO_2, and NO_X emissions by approximately 3.4 %, 23.28 %, 22.97 %, and 0.55 %, respectively, using the Coal-

to-PSD of blend ratio 1:1 as against the blend ratio of 4:1. The CO_2 emission from the Matla coal is estimated as 5900 kg CO_2/kWh, whereas the CO_2 emission from Coal + PSD or other biomass and waste investigated at a blend ratio of 1:1 is estimated as 2950 kg CO_2/kWh (a 50 % reduction). Meanwhile, Bada et al. [358] have also reported a similar trend using coal-to-biomass blend ratio of 1:1 thereby corroborating the findings of this study.

10.9. Results compared with literature

Table 10.12 presents the comparison of the present work with other previous works. The information contained in this section is basically the analysis of different previous studies on electricity and thermal power generations including the technology, system capacity, and feedstock. (Malek et al. [333] used a biomass-based steam generating plant to study the energy efficiencies, cost implications, environmental effect, and the potentials of a 10 MW biomass power plant in Malaysia. Two financial cases namely: assessment with loan and assessment without loan were investigated. MC, heating value, and investment cost were considered as the major variables in the study and NPV, IRR, and PBP were the appraisal tools. In addition, the authors considered plant efficiencies of 20 %, 30 % and 40 % with corresponding investment years of 2015, 2020, 2030, and 2050. Consequently, the authors reported savings of about MYR 0.88 – 2.43 million from the plant with raw Empty Fruit Bunch (EFB) as the feedstock. In the current study, a 5 MW CHP plant was assessed using feedstocks originated from South Africa, and about 1,868,805.41 Kg of fuel was saved by using Coal-to-PSD ratio of 1:1 at WFC, hence; making the fuel mixture the most viable feedstock amongst the feedstocks studied. Malek and co-workers also reported that system efficiency of 25 % - 40 % could be achieved from various biomass-based steam plant, and that significant amounts of CO_2, SO_2, NO_X, and CO emissions (Table 10.12) were reduced in the plant when compared to the existing Malaysian energy mix (see Table 10.12) The effective emission reduction of 3.4 %, 23.28 %, 22.9 %, and 0.55 %, is CO, CO_2, SO_2 & NO_X, respectively, were obtained from the 5 MW CHP assessed in the present work. The energetic efficiencies and cost of investment were the most uncertain variables reported by Voets et al. [361] during their estimations using biomass of Belgium origin, and the variables rendered the analysis of the 20 MW technology option unclear. However, the current study, 10^{th} year, and Coal-to- Solid waste ratio of 1:1 are the optimum investment year and blending ratio, respectively.

Table 10. 12: Comparison of the present work with previous studies

Technology Used	Plant Capacity	Fuel Used	Major Findings	References
Flash Pyrolysis & Gasification plants: Electricity & CHP generation Units	5 MW, 10 MW, & 20 MW	Short rotation Coppices (Belgium)	For the 5 MW & 10 MW electric power productions, flash pyrolysis was more viable in terms of plants profitability. But higher profit was produced from the 5 MW CHP productions. The 20MW technology option was unclear because of the energetic efficiencies and investment cost; the most uncertain variables.	[361]
Remarks: Feedstock origin: Flanders, Belgium Evaluation Target: Plant with the highest profit Investment evaluation year: 10 yrs. Appraisal tool used: NPV				
Biomass-based Rankine-Cycle Steam power Plant	10 MW	EFB, MCF, PKS, OPF, OPT, & WB	Feedstock cost of around MYR 0.88 –2.43 million, was	[333]

Remarks: Feedstocks Origin: Malaysia. Two Hypothetical Financial Cases: Investment with Loan & Investment without Loan. Major Variables Considered: Moisture content, Heating value & Investment Cost. Project Appraisal tools: NPV, IRR, & PBP. Specific Compares: Biomass-based Plant & existing energy mix in Malaysia, system efficiencies: 20 %, 30 % and 40 %, investment years studied: 2015, 2020, 2030 & 2050.			saved by using raw EFB in the power plant, and an application of various biomass- based gasification technologies could enhance system efficiency by around 25 % to 40 %. Emission analysis indicated that lower emission reductions of about 50,130 t of CO_2, 750 t of SO_2, 218.65 t of NO_X, & 22.83 t of CO were produced from the plant as compared to the existing energy mix in Malaysia.	
Co-gasification CHP Plant	5 MW	Biomass & Solid Waste	About 1,868,805.41kg of feedstock was	Current Work.

Remarks: Feedstock Origin: South Africa. Feedstocks: Coal, SCB, CC, PSD, & WT. Two hypothetical cases: WFC & WOFC. Major Variables: Energy (Heating value), Moisture content,		saved in the plant annually, by using Coal-to-PSD ratio of 1:1. A higher profit of around 13.82 %,	

Economic (investment cost & profit), and Environmental (emissions). Project appraisal tools: NPV, IRR, & PBP Compares: Coal & other solid wastes, various blends of Coal & other solid wastes, investment years: 10^{th}, 11^{th}, 17^{th} & 18^{th} year. Evaluation target: The most viable feedstock for power production with regard to: Profitability: Energy content, annual feedstock savings, cost savings, and emissions reduction.	& 23.56 % were made from Coal + PSD compared to 100 % Matla coal WFC & WOFC. %, 22.9 %, and 0.55 %, of CO, CO_2, SO_2 & NO_X emissions were reduced in the plant by using Coal-to-PSD ratio of 1:1, respectively. The 10^{th} year & Coal + PSD were the optimum investment year and feedstock studied.	

EFB: empty fruit bunch; MCF: Mesocarp fiber; PKS: palm kernel shell; OPF: Oil palm frond; OPT: oil palm trunk; WB: wood biomass; WFC: with feedstock costing; WOFC: without feedstock costing; NPV: net present value; IRR: internal rate of return; PBP: payback period; PSD: pine saw-dust

Secondly, if environment regulations and/or policy are to be promulgated, and restricting the transportation of biomass only with specific type of trucks such as electric powered trucks (batteries) and solar vehicles, emissions will be further reduced. In this case, the overall result of the present analysis will be changed.

10.9.1. Sulphur and CO_2 capture

In this study, the capture of Sulphur and CO_2 were not considered, but the amounts of the gases and other gases such as CO and NO_X generated from each of the feedstock studied in the co-

gasification process were determined. The estimations of the gaseous emissions from the gasification operations were carried out to understand the influence of gasification of biomass and coal blends as against solitary coal gasification over the emitted gases. The information provided in this section will assist stakeholders in the design, building, and modification of similar power generation plants.

Meanwhile, different works has been reported in the literature on Sulphur and CO_2 capture, but an extensive work was carried out in CO_2 capture by Seifert and Litster [348]. Integrated Gasification Combined Cycle (IGCC) coupled with Integrated Gasification Fuel Cell power plants was investigated. In this study, a stand-alone Combined Heat and Power (CHP) plant of 5 MW capacity was investigated, while the total power output (plus the Rankine Cycle steam turbine) reported by Seifert and Litster was 808 MW capacity. The data obtained in this study will enhance the modification of Figure 10.2 of this chapter to address the CO_2/and or Sulphur capture based on the coal and waste biomass available in Africa.

10.10. Sensitivity of the NPV and impact of uncertainty

To evaluate the sensitivity of the NPV and impact of uncertainty on the viability of the feedstocks for energy production in the 5 MW power plant, the standard deviation (SD), the variance, and the standard error of the major Equations (10.10), (10.11), and (10.12), respectively [361].

$$SD = \sqrt{\frac{\Sigma(X-\overline{X})^2}{N-1}} \tag{10.10}$$

$$Variance = \frac{\Sigma(X-\overline{X})^2}{N-1} \tag{10.11}$$

$$Standard\ Error = \frac{SD}{(N)^{1/2}} \tag{10.12}$$

X represents the variables including amount of feedstock, capital cost investment, cash flow and

net present value, while $\bar{x}$ is the mean of the variables.

Results of the analysis are presented in Table 10.13

Table 10. 13: Sensitivity Analysis of 10th Year using WFC

Amount of Feedstock [Kg]			Capital Cost Investment [ZAR/Yr]			B.R
X	$\bar{X}$ [Million]	$(X - \bar{X})^2$ [Billion]	X [Million]	$\bar{X}$ [Million]	$(X - \bar{X})^2$ [Billion]	
2.05	18.70	29.80	22.20	16.50	32.40	
2.10	18.70	50.10	22.90	16.50	40.40	
1.83	18.70	24.50	18.80	16.50	21.50	
1.53	18.70	12.00	19.20	16.50	69.00	
Variance	676*		Variance	98.30		
Std. Deviation	2.6		Std. Dev.	99.10		
Standard Error	13.0		Std. Error	49.60		
Cash Flow [ZAR/Yr.]			Net Present Value [ZAR/Yr.]			
[Million]	[Million]	[Million]	[Million]	[Million]	[Billion]	
40.4	41.9	25.0	13.8	3.71	53.90	
39.7	41.9	45.3	3.34	3.71	11.40	**1:1**
43.7	41.9	39.9	6.87	37.1	10.00	
43.5	41.9	255*	6.24	3.71	64.1	
Variance		440*	Variance		1.10×10^{-4}	
Std. Deviation		210*	Std. Deviation		3.27×10^{-3}	
Standard Error		1.05×10^{-3}	Standard Error		1.05×10^{-3}	
Amount of Feedstock [Kg]			Capital Cost Investment [ZAR/Yr]			
[Million]	[Billion]		[Billion]	[Million]	[Billion]	
20.4	19.1	18.1	2.37×10^{-4}	22.1	245	

20.8	19.1	37.0	2.29×10^{-4}	22.1	62.0
19.3	19.1	46.2	21.5	22.1	40.3
15.7	19.1	11.0	20.4	22..1	295
Variance		530	Variance		214
Std. Deviation		2.30×10^{-3}	Std. Deviation		1.46×10^{-3}
Standard Error		1.15×10^{-3}	Standard Error		7.31×10^{-2}

Cash Flow [ZAR/Yr.] [Million]		[Billion]	Net Present Value [ZAR/Yr.] [Million]	[Million]	[Billion]	B.R
X	$\bar{X}$	$(X - \bar{X})^2$	X	$\bar{X}$	$(X - \bar{X})^2$	
38.9	40.5	245	2.13	2.74	638	
39.7	40.5	620	1.47	2.74	16	
41.1	40.5	403	3.76	2.74	105	
42.2	40.5	250	5.51	2.74	767	
Variance		214	Variance		557	
Std. Deviation		1.43×10^{-2}	Std. Dev.		236	
Standard Error		7.31×10^{-2}	Std. Error		1.18×10^{-3}	**3:2**
Amount of Feedstock [Kg] [Million]		[Billion]	Capital Cost Investment [ZAR/Yr] [Million]	[Million]	[Billion]	
20.3	19.6	483	26.6	258	559	
20.5	19.6	79	26.9	25.8	110	
19.7	16 .0	147	25.2	25.8	355	
17.9	19.6	292	24.0	25..8	1440	
Variance		141	Variance		115	**4:1**
Std. Deviation		11.9×10^{-3}	Std. Deviation		1.07×10^{-2}	
Standard Error		59.3×10^{-3}	Standard Error		5.36×10^{-2}	
Cash Flow [ZAR/Yr.] [Million]		[Billion]	Net Present Value [ZAR/Yr.] [Million]	[Million]	[Billion]	

36.1	36.8	559	-4.44	-3.24	145
35.8	36.8	110	-4.93	-3.24	28
37.4	36.8	355	-2.26	-3.4	924
38.00	36.8	144	-1.30	-3.24	375
Variance		115	Variance		300
Std. Deviation		1.07×10^{-3}	Std. Deviation		1.70×10^{-3}
Standard Error		5.36×10^{-3}	Standard Error		8.66×10^{-3}

B.R: Blending Ratio; X: Estimated variable (e.g. amount of feedstock, capital cost investment, cash flow, net present value); $\bar{X}$: mean of the variable; Std.: standard; *: In billion.

The standard error of the mean (SEOM) is referred to as a measure for the variance of NPV distributions [362], which is dependent on the blend ratio of the variables mentioned earlier, and their SEOM were equally estimated. To enhance the comparability of this measure for different blend ratio of the fuel, the SEOM was divided by the mean value of the NPV of the feedstocks from the various blends. The mean and relative standard (percentage) error (RSE) of all the feedstocks, the amount of feedstock, capital cost investment, cash flow, NPV obtained were from the three different fuel blends studied in the plant (10^{th} year) at WFC are shown in Table 10.14.

Table 10.14: Mean NPV and RSE of Variables (10^{th} Year) using WFC

BR	AOF [kg/yr]		CCI [kg/yr]		Cash Flow [kg/yr]		NPV [kg/yr]	
	Mean AOF*	RSE of AOF [%]	Mean CCI [kg/yr*	RSE of CCI [kg/yr]	Mean CF [kg/yr*	RSE of CF [kg/yr]	Mean NPV [kg/yr*	RSE of NPV [%]
1:1	18.75	0.07	18.55	0.30	41.86	0.03	37.07	0.45
3:2	19.06	0.06	21.13	0.03	40.50	0.02	27.38	0.43
4:1	19.57	0.03	25.83	0.02	36.81	0.01	-32.37	-0.27

B.R: Blending Ratio; RSE: Relative standard error; AOF: amount of feedstock; CCI: Capital cost investment; CF: cash flow; NPV: net present value; B. Ratio: feedstock blend ratio; *: In Million

According to Table 10.14, the feedstock blend ratio and investment cost were considered as the most significant variables. Both the amount of fuel and energy content of the fuel (not shown in

Table 10.14 have direct impact on the investment cost, as can be observed in the mean value of the RSE in Table 10.14. According to the report of Australian Bureau of Statistics [363] on Labour Force Standard Error, a RSE $\geq$ 25 % is prone to high sampling error and should be used with caution. Most of the RSE presented in Table 10.14 are less than 25 % indicating less sampling error. Meanwhile, coal-to-solid waste ratio of 1:1 is the optimum blend in terms of fuel and investment cost savings and emission reduction. This blend has the highest mean NPV as shown in Table 10.14, and it provides information that will assist investors to make their decisions about the investment.

However, the sensitivity analysis was carried out using Figure 10.7 and Figure 10.8 as well as Table 10.12 as the base model; the most viable investment conditions in the plant. From Table 10.14, the coal-to-solid waste ratio of 1:1 has the highest mean NPV, whereas; in the absent of 4:1 mixture, the lowest RSE was produced by the 3:2 feedstock blend. The 4:1 blend clearly indicated an un-attractive investment, as can be observed from the negative value of the mean NPV, thus; should not be ventured by investors. Figure 10.7 (base model) have demonstrated that Coal-to-PSD ratio of 1:1 at WFC was the optimum feedstock and blend ratio for the energy production following the variables earlier mentioned. With reference to the value of NPV of the base model, for the most profitable condition, there was no deviation with the option of the most viable condition for the highest mean NPV.

On the basis of emission reduction in the plant, the optimal condition (1:1 blend ratio) can as well, be observed in Table 10.11. The Coal + PSD produced higher CO and NO_X emissions, as well as lower amounts of CO_2 and SO_2 when compared to Coal + WT that yielded lower CO and NO_X, plus higher CO_2 and SO_2 emission. However, the results of the mean of AOF, CCI, and CF variables of the 1:1 fuel mixture in Table 10.14 confirmed the most viable option based on the results presented in Figure 10.7.

Similarly, the sensitivity analysis for the variables at WOFC is presented in Table 10.15. It can be seen from the table that the mean value of the NPV of 4:1 fuel blend is higher than the mean value of NPV of the 1:1 blend. However, the RSE value of the 4:1 fuel blend is lower than the RSE value of 1:1 fuel blend. This implies that based on analysis at WOFC, where the actual cost of the feedstock is discounted; investors may consider the investment to be viable. However, it is noteworthy to mention that the cost of transfer of the feedstock is very crucial in the overall decision-making if the plant is not located very close to the source of raw material. Furthermore, the variance in the NPV is an indication of the degree of the influence of the investment cost on the economic analysis. Nevertheless, investment cost and blend ratio are the most sensitive

variables in the analysis.

Table 10.15: Mean NPV and RSE of Variables (10th Year) using WOFC

BR	AOF [kg/yr.]		CCI [kg/yr.]		Cash Flow [kg/yr.]		NPV [kg/yr.]	
	Mean AO*	RSE of AOF [%]	Mean CCI (kiloton/yr)	RSE of CCI (kg/yr)	Mean CF (kiloton/yr)	RSE of CF (kg/yr)	Mean NPV (kiloton/yr)	RSE of NPV [%]
1:1	18.75	0.07	8.97	0.09	53.67	0.02	23.98	0.06
3:2	19.06	0.06	8.89	0.08	53.75	0.01	24.10	0.05
4:1	19.57	0.09	8.67	0.04	53.97	0.01	24.47	0.02

B.R: Blending Ratio; RSE: Relative standard error; AOF: amount of feedstock; CCI: Capital cost investment; CF: cash flow; NPV: net present value; B. Ratio: feedstock blend ratio.

Comparison of the NPV in Figure 10.7 and that of Table 10.15 indicates that the investment cost has a significant impact on the NPV and should be considered in the decision-making by prospective investors. Considering investment cost for the two cost analysis scenarios presented in this study (i.e. WFC & WOFC), the use of Matla Coal + PSD at blend ratio 1:1 is the most attractive for WFC while the use of Matla Coal + WT at blend ratio of 1:1 is the most viable option for WOFC.

10.11. Concluding remarks

An evaluation of the economic, energy and environmental viability of a 5 MW co- gasification power plant has been carried out, using coal blended with SCB, CC, PSD, and WT. The evaluation considered two scenarios namely: WFC and WOFC. The blend ratios investigated were 1:1, 3:2, and 4:1. The heating value, investment cost and emission were estimated for the blends of coal and solid waste, but investment cost and feedstock blend ratio were the most significant factors considered. The NPV, IRR, and PBP tools were used to evaluate the power generation project at different business periods namely: 10th, 11th, 17th and 18th year. Coal + PSD blend at a ratio of 1:1 evaluated at WFC is the most attractive feedstock for the energy generation in the investigated power plant. The business viability order is Coal + PSD > Coal + WT > Coal + SCB, > Coal + CC at WFC. At WOFC, the order is Coal + WT > Coal + PSD > Coal + SCB, > Coal + CC. The use of 100 % Matla coal is not cost effective, and it produces higher emissions when compared to other feedstocks investigated. A higher profit of 13.82 % and 23.56 % are predicted for the use of Coal + PSD at WFC and WOFC, respectively, when compared to 100

% Matla coal, thereby enabling a savings of about 1,868,805.41 kg of feedstock, annually. In addition, the following conclusions emanated from the study:

- The use of Coal-to-PSD ratio of blend 4:1 for the power generation as against 1:1 Coal-to-PSD of blend ratio 1:1 resulted to an annual loss of about ZAR6, 461,301.77 ($90,458,224.70) and ZAR123,782.47 ($1,732,954.58) WFC and WOFC, respectively. The IRR were 5 ±1 %/yr. and 2 ± 3/yr. for 1:1 & 4:1 Coal-to-PSD blend ratio based on South Africa electricity price of $0.14 c/kWh, respectively.

- The use of Coal-to-PSD ratio of blend 4:1 for the power generation as against 1:1 Coal-to-PSD of blend ratio 1:1 resulted to an annual loss of about ZAR6, 461,301.77 ($90,458,224.70) and ZAR123,782.47 ($1,732,954.58) WFC and WOFC, respectively.
- At the 10^{th} year, coal-to-solid waste blend of ratio 4:1 is not viable at WFC but Coal + PSD is viable at the 17^{th} year, but at the 18^{th} year the use of none of the feedstocks is attractive for the business venture, at WFC.
- The power plant will use 20,473,451.41 kg, 20,986,049.96 kg, 18,251,806.49 kg, and 15,276,277.85 kg of Coal + SCB, Coal + CC, Coal + PSD, and Coal + WT to produce the 5 MW and 5.56 MW electric and thermal power, annually.
- Coal-to-solid waste ratio of 1:1 produced the lowest amounts of CO_2 and SO_2 emission, and emissions increases as the amount of coal in the blend increases for all the feedstocks studied. But the emission is reduced significantly when Coal + PSD blend with ratio 1:1 is used.
- Change of energy, economic and environmental policies in the future will affect the estimated results. The speculated future policies may include: basing the price of fuel on its heating value, restricting fuel transportations only with electric-powered trucks, and allowing electricity consumers to use non-central grid units without payment of utility bills to the government.

Chapter 11: General conclusion and recommendation

11.1. Conclusions

In this study, co-gasification of coal and solid waste to hydrogen-enriched syngas in a fixed bed gasified (FBG) was carried out. It involved 11 different activities including: (1) review of literature and sample collection, (2) feedstock pre-treatment, (3) feedstock characterisation, (4) optimisation of process variables of biomass torrefaction using response surface methodology (RSM) and artificial neural network (ANN) technique, (5) assessment of the environmental, economic and energy parameters in the co-gasification plant using the results of the ultimate analysis of some selected feedstocks such as sugar bagasse, corn cob, waste tyre, and coal in South Africa (i.e. techno-economic analysis of the feedstock), (6) evaluation of performance of gasification systems efficiency using ANN model, (7) maximization of profit in a co-gasification CHP plant via biomass torrefaction, (8) Prediction of emissions and profits from a biomass, tyre, and coal fired co-gasification CHP plant using Artificial Neural Network: Nigerian and South African perspectives, (9) development of effective tar treatment technique for production of high quality syngas from blends of coal and biomass**,** (10) co-gasification of coal and biomass to hydrogen enriched syngas in a fixed bed gasifier, and (11) writing of the Ph.D. thesis. Activities 5, 6, & 9 are the specific research objectives, while activity 10 represents the main aim of the study. From activity 1 through activity 10, the 11^{th} activity was achieved and the following conclusions were made:

- Important gaps were identified in the reviewed literature and were addressed through the specific research objectives of this thesis.
- Different methods were employed to carry out the tasks/activities in this study, and majority of them were effective for accomplishment of the tasks.
- Performance efficiency of gasification systems was evaluated using Experimental data obtained from a few gasifiers (e.g. entrained, fluidised, and fixed bed) operated at varied experimental conditions using blends of feedstocks (e.g. biomass, coal, waste tyre etc.). A backpropagation L-M and BR algorithms of ANN model with MIMO and MISO layer networks were considered. Results of the MIMO and MISO layer networks obtained from the L-M algorithm are better than that of BR algorithm. To improve the model result, the Input Variables Representation Technique-by- Visual Inspection Method (IVRT-VIM) and Output Variables Representation Technique-by-Visual Inspection Method (OVRT-VIM) were employed. The sensitivity analysis revealed that carbon (%) was the most important input variable affecting the outputs. In overall,

information obtained thereof could assist stake- holders in developing gasifiers capable of converting different solid fuel materials into energy. This information could be instrumental to decision making and serving as a platform for further R & D in this area.

- The prediction of emissions and profits from biomass, tyre, and coal fired co-gasification CHP Plant using Artificial Neural Network (ANN) was carried out for 20-year-investment period using South Africa and Nigeria as case studies. Coal + CC, Coal + SCB, Coal + PSD, and Coal + WT blended at a ratio of 1:1, 3:2, and 4:1, were considered, respectively. A MISO layer network model was developed using twenty datasets with emissions and profits obtained from both countries. Profitability was higher using South African feedstock as against Nigerian feedstock, WFC and WOFC. The CO, NO_X, & SO_2 emissions from Nigerian feedstock were lower than that of South Africa, but the emissions obtained from Coal + WT for both countries, were the highest.

- Profitability of a co-gasification CHP plant through biomass torrefaction for a 20- year-investment period has been carried out using blends of Coal + SCB, Coal + CC, and Coal + PSD with coal-to-biomass ratio of 50:50, 71:29, and 80:20, respectively. Four investment terms – A (1^{st} – 5^{th}), B (5^{th} – 10^{th}), C (10^{th} – 15^{th}) & D (15^{th} – 20^{th})

  and two operational cost models; with feedstock costing (WFC) and without feedstock costing (WOFC) was employed. At the end of term D (i.e. 20^{th} year), a profit of between USD5,902,292.46 - USD6,489,659.30 and USD7,796,968.80 - USD7,899,284.16 were earned using WFC and WOFC, respectively. The Internal Rate of Return (IRR) was 5 ± 1 %/yr. and 7 ± 4 %/yr. based on South African electricity price of 0.14 $/ kWh, respectively. The profits earned from WFC were eroded due Time Value of Money (TVM), hence; resulted to un-attractive venture. The percentage reduction in profits increased from term A through term D, thus; implying that profitability in the plant is dependent on the future value of money. In terms of input-output variable relationship, the investment cost and blend ratio were the two most influential variables that affected the profit (output).

- From the investigation of the parametric effect of process variables during torrefaction via ANN and RSM models, the most viable torrefaction process conditions and fuel were determined. Process models were developed for each of the fuel, respectively. The operating process conditions are of the order: 50:50 Coal-to-Torrefied Fuel ratio (300 ^{O}C and 45 min) > 50:50

  Coal-to-Torrefied Fuel ratio (250 ^{O}C and 30 min) > 50:50 Coal-to-Torrefied Fuel ratio

(200 ^{O}C and 45 min), while the optimum fuel follows the order of Coal + Torrefied PSD > Coal + Torrefied SCB > Coal + Torrefied CC and > Coal + Torrefied WT. Torrefaction of WT is not a suitable option for fuel quality upgrade.

- Effective tar treatment was studied using tars produced from biomass and blends of coal and biomass using biochar based and Ni-biochar based catalysts, respectively. Box Behnken Design of Experiment (DoE) method; (RSM model) that comprised tar conversion temperature (700 – 900 ^{O}C), tar conversion time (10 – 20 min), & Coal-to-biomass blend ratio (1 – 4) as the input variables, and Percentage tar conversion as the output variable were employed. Tar treatment model was developed for each fuel based on the catalysts, tars and process variables investigated. An increase in temperature increased the rate of tar conversion, but the conversion decreased with an increase in time. The most effective catalysts for the tar conversion were PSD-BC and Ni- PSD-BC but on the account of the cost of production, the PSD-BC may be considered more attractive.
- Co-gasification of coal and pine sawdust (PSD) to hydrogen enriched syngas in a fixed bed gasifier was carried out with catalyst (WCAT) at 900 ^{O}C and without catalyst (WOCAT), at 700, 800, and 900 ^{O}C temperatures, respectively. Coal-to-PSD ratio of 1:1 was used, while Nickel-pine sawdust-biochar (Ni-PSD-BC) and pine sawdust-biochar (PSD-BC) were employed as catalysts. The process is instrumental to using high ash content South African coal such as Matla coal for the production of syngas for electricity generation. Blending this type of coal and biomass for example, promotes the H_2/CO content in the product gas which is needed for liquid fuel synthesis [86,95]. The efficiency of the gasifier was considerably improved via WCAT as against WOCAT. The gases produced at 700, 800 & 900 ^{O}C, WOCAT cannot be used in fuel cells and gas turbines due to poor quality, while others produced at 900 ^{O}C WCAT, can be used in internal combustion engines and gas turbines, but unfortunately, have lower quality to be employed in fuel cells for electricity production.
- An assessment of the economic, energy and environmental viability of a 5 MW co-gasification power plant was carried out, using blends of coal and biomass (SCB, CC, & PSD) and WT at ratios of 1:1, 3:2, and 4:1, respectively. The evaluation considered two financial scenarios namely: with feedstock costing (WFC) and without feedstock costing (WOFC) and using the NPV, IRR, & PBP models. Coal-to- PSD ratio of 1:1 (WFC) is the most attractive feedstock in the plant. The business viability order (for WFC) is Coal + PSD > Coal + WT > Coal + SCB, > Coal + CC at WFC. At WOFC, the order is Coal + WT > Coal + PSD > Coal + SCB, > Coal + CC. Huge amount of

money was saved in the energy plant annually by using coal-to- solid waste ratio of 1:1 as against other blend ratios studied. 100 % coal generated higher emissions when compared to blends of coal and biomass/WT

11.2. Recommendations

Based on the findings made and the experiences encountered from this study, the following points are recommended:

- To save time and ensure accuracy of result in artificial neural network (ANN) learning, a standard method of determining the number of neurons in the hidden layer should be studied.
- It is recommended that large number of datasets should be provided in the neural network training to achieve a better result.
- For the evaluation of gasification systems efficiency, the classification of the experimental dataset into fixed and fluidised bed gasifiers, and experimental process conditions is expected to improve the model results, and therefore is recommended.
- With reference to the Input Variables Representation Technique-by-Visual Inspection Method (IVRT-VIM) and Output Variables Representation Technique-by-Visual Inspection Method (OVRT-VIM), it is recommended that different sets of output variables should be studied using different sets of inputs and Vis versa, to verify/improve the ANN model results.
- From the result of the techno-economic analysis, coal-to-biomass ratio of 4:1 should be avoided because it increased the cost of investment, hence; resulting to huge profit loss in the plant, annually. However, coal-to-biomass ratio of 1:1 is recommended.
- In some cases, where only one coal sample (e.g. Matla coal (South Africa) & Onye-ama coal (Nigeria) was used for assessment, it is very useful to consider variety of coal samples for their profitabilities because of the expected difference in compositional characteristics and calorific values.
- For fuel quality improvement, torrefaction of waste tyre (WT) is not recommended, but other pre-treatment methods such as chemical pre-treatment may be investigated. Additionally, the biomass materials (PSD, SCB, & CC) should be pre-treated by biological and chemical methods to improve their qualities hence; resulting to increase in profits of the fuel materials.
- For profit and emission predictions in a co-gasification CHP plant, other commercial packages such as Aspen Plus, General Algebraic Modelling Systems (GAMS), and

others should be considered.

- It is important to carry out the kinetic studies of the biochar and Ni-biochar based catalysts used in this study. The durability test of the catalysts in terms of commercial scale development is also recommended. Furthermore, it will be necessary to estimate the percentage amount of tar conversion using commercial predictive modelling tool (e.g. Artificial Neural Network or General Algebraic Modelling System (GAMS).
- Modification of the fixed bed reactor used in this study and improvement of the experimental process conditions are recommended. It will enhance the production of syngas that will be of high quality for use in gas turbines and fuel cells for electric power generation. The modification will include but not limited to connecting of a secondary unit of reactor for gas cleaning process. The aforementioned modifications will also reduce operating costs.

References

[1] J. Udomsirichakorn, P.A. Salam, P.A. (2014). Review of hydrogen-enriched gas production from steam gasification of biomass: the prospect of CaO-based chemical looping gasification. Renew. Sust. Energy Rev. 30, 565-579

[2] M.L. Long, R.Y. Zhi, R.Y. Biomass gasification Principles and Application. Liaoning Institute of Energy Resources (2009).

[3] S. Farzad, M.A. Mandegari. A critical review of biomass gasification, co-gasification, and their environmental assessment. Biofuel Research Journal 12, (2016), 483 – 495.

[4] D. Mallick, P. Mahanta, V. S. Moholkar. Co-gasification of coal and biomass blends: Chemistry and engineering. Fuel 204, (2017), 106–128.

[5] J.G.J. Olivier, G. J. Maenhout, M. Muntean, J. A. H. W. Peters. Trends in global CO_2 emissions: 2015 Report. PBL Netherlands Environmental Assessment Agency, The Hague; European Commission, Joint Research Centre (JRC), Institute for Environment and Sustainability (IES). JRC98184, PBL1803.

[6] IEA. Energy and Air Pollution: World Energy Outlook Special Report (2016)

[7] SA Yearbook. Published by government Communication and Information Systems (GCIS) (2014).

[8] Stats SA. Electricity generated and available distribution (P4141) (2015). Retrieved from STATS SA (Statistics South Africa) website on 20-02-17: Available online at: http://.www.statssa.gov.za.

[9] SA Stats. Gross Domestic Products (P0441), 3rd Quarter (2014).

[10] Bryson. Greenhouse Gas Protest S.Africa Coal Plant: 9 arrested. Published by the

Associate Press, Donna Bryson (2011).

[11] J. Subramoney, J. Van Wyk, M. Dithupe, A. Molapo, N. Mahlangu, R. Morumudi. Digest of South African Energy Statistics Department of Energy, Republic of South Africa, Pretoria, (2009), 73.

[12] Greenpeace Africa. Greenpeace Confronts ESKOM – End Coal Addiction and Embrace Renewable Energy (2011). Retrieved from Greenpeace Africa website on 25-4-17. Available online at: http://www.greenpeace.org/africa/en/News/news/Greenpeace-Confronts-Eskom/

[13] [M. Ozonoh, T.C. Aniokete, B.O. Oboirien, M.O. Daramola. Techno-economic analysis

of electricity and heat production by co-gasification of coal, biomass and waste tyre in South Africa. Journal of Cleaner Production 201 (2018) 192-206.

[14] K. Premlall, M. Mabuza, N. Wagner. Evaluating CO_2 sorption capacity of a number of South African (SA) coal types: comparative study of the different coal properties at incremental pressures up to supercritical pressures Energy Procedia 5, (2014), 299-30

[15] J. Viljoen, F. Stapelberg, M. Cloete. Technical Report on the Geological Storage of Carbon Dioxide in South Africa. Council for Geoscience, Pretoria (2010), 1-237

[16] SA Power Network (2017). Retrieved from SA Power Network website on 22-03-19. Available online at: https://www.sapowernetworks.com.au/centric/industry/our_network/network_tariffs.jsp

[17] NERSA: National Energy Regulator of South Africa. NERSA approves electricity tariff, (2019). www.iafrica.com/nersa-approves-electricity...

[18] US NUS Consulting Group. South Africa Electricity Prices vs The World. US NUS Consulting Electricity & Natural Gas Group, (2014).

[19] Sheppard. Jump up Sheppard; Your Tax Dollars at Work: A Giant Coal Plant in South Africa 'Mother Jones' (2011).

[20] M.D. Aminu, S.A. Nabavi, C.A. Rochelle, V. Manovic. A review of developments in carbon dioxide storage. Appl. Energy 208, (2017), 1389-1419.

[21] C.M. White, D.H. Smith, K.L. Jones, A.L. Goodman, S.A. Jikich, R.B. LaCount, S.B. Du Bose, E. Ozdemir, B.I. Morsi, K.T. SchroederSequestration of carbon dioxide in coal with enhanced coalbed methane recovery – a review. Energy Fuel, 19 (2005), pp. 659-724.

[22] K. Kumabe T. Hanaoka S. Fujimoto T. Minowa K. Sakanishi. Co-gasification of woody biomass and coal with air and steam. Fuel 86 , (2007) 684-689.

[23] Z. Chen, M. Wang, E. Jiang, D. Wang, K. Zhang, Y. Ren, Y. Jiang. Pyrolysis of Torrefied Biomass 36, (2018), 1287-1298.

[24] M. Akia, F. Yazdani, E. Motaee, D. Han, H. Arandiyan. A review on conversion of biomass to biofuel by nanocatalysts. Biofuel Res. J. 1, (2014), 16-25.

[25] A. Bauen, G. Berndes, M. Junginger, M. Londo, F. Vuille, R. Ball, T. Bole, C. Chudziak, A. Faaij, H. Mozaffarian, H. (2009). Bioenergy-a sustainable and reliable energy source: A review of status and prospects. IEA Bioenergy, (2009). 108

[26] R. Saidur, E.A. Abdelaziz, A. Demirbas, M.S. Hossain, S. Mekhilef. A review on biomass as a fuel for boilers. Renewable and Sustainable Energy Reviews. Volume 15, Issue 5, June 2011, Pages 2262-2289.

[27] USADA: United States Department of Agriculture, Crop Estimates Committee, (2017).

Retrieved from UASDA website on 01-09-19. Available online at: https://www.pecad.fas.usda.gov/cropexplorer/pecad_stories.aspx?regionid=safrica&ftype=prodbriefs.

[28] SA CEC Committee (South African Crop Estimate Committee 2013. Available online at: ipad.fas.usda.gov/highlights/2013/04/SouthAfrica.

[29] USADA. (2016). Retrieved from GAIN (Global Agriculture Information Network) Report website on 01-09-17. Available online at:https://gain.fas.usda.gov/Recent%20GAIN%20Publications/Sugar%20Annual_Pretoria_South%20Africa%20-%20Republic%

[30] Mbohwa. Energy Management in the South African Sugar Industry. Proceedings of the World Congress on Engineering, (2013), WCE 1, ISSN: 2078-0966.

[31] REDISA. Waste Tyre Bioremediation Plan (2015). Retrieved from urban EARTH website on 12-11-16. Available online at: http://www.urbanearth.co.za/articles/waste-tyre-management-plan-and-fee-now-operational- south-africa.

[32]SA FMVC. South African forest market value chain (2016). www.nda.agric.za/doaDev/sideMenu/Marketing/Annual..

[33] MCSA - Mineral Council of South Africa (2019): https://www.mineralscouncil.org.za/sa-mining/coal

[34]. Mintek Annual Report, (2007): www.mintek.co.za/wp-content/uploads/2007/11/AR...

[35] CGS. Council for Geoscience South Africa; Applied Geoscience Solutions (2016). Available online at: www.researchgate.net/profile/GerritS_Kock/.

[36] H. Shi, N. Mahinpey, A. Aqsha, R. Silbermann. Characterization, thermochemical conversion studies, and heating value modelling of municipal solid waste. Waste Manag 48, (2016), 34-47.

[37] J. Posom, P. Sirisomboon. Evaluation of lower heating value and elemental composition of bamboo using near infrared spectroscopy. Energy 12, (2017), 147-158.

[38] D.R. Nhuchhen, P.A. Salam, P.A. Estimation of higher heating value of biomass from proximate analysis: A new approach 99, (2012), 55-63.

[39] S.A. Channiwala, P.P. Parikh. A unified correlation for estimating higher heating value of solids, liquids and gaseous fuels. Fuel 81, (2002), 1051-1063.

[40] C. Sheng, J.L.T. Azevedo. Estimating the higher heating value of biomass fuels from basic analysis data. Biomass and Bioenergy 28 (2005) 499–507.

[41] J. Posom, P. Sirisomboon. Evaluation of the moisture content of Jatropha curcas kernels and the heating value of the oil extracted residue using near-infrared spectroscopy. Biosyst Eng 130, (2015), 52-59.
[42] Fagan, C.C., Everard, C.D., & McDonnell, K. (2011). Prediction of moisture, calorific value, ash and carbon content of two dedicated bioenergy crops using near-infrared spectroscopy. Bioresour Technol 102, 5200-5206.
[43] J.M. Andres, M.T. Bona, M.T. ASTM clustering for improving coal analysis by near infrared spectroscopy. Talanta 70, (2006), 711-719.

[44] A. McPhail, R. Griffin, M. El-Halwagi, K. Medlock, P. J. J. Alvarez. Environmental,

Economic, and Energy Assessment of the Ultimate Analysis and Moisture Content of Municipal Solid Waste in a Parallel Co-Combustion Process. Energy Fuels 2014, 28, 2, 1453- 1462.

[45] Y. Huang D.R. McIlveen-Wright S. Rezvani M.J. Huang, Y.D. Wang, A.P. Roskilly,

N.J. Hewitt. Comparative techno-economic analysis of biomass fuelled combined heat and power for commercial buildings. Applied energy 112, (2013), 518-525.

[46] Luis E. Rincon, Luis A. Becerra, Jonathan Moncada, Carlos A. Cardona (2014). Techno-Economic Analysis of the Use of Fired Cogeneration Systems Based on Sugar Cane Bagasse in South Eastern and Mid-Western Regions of Mexico. Waste Biomass Valor 5, (2014), 189– 198

[47] S.R. Wood, P.N. Rowley. A techno-economic analysis of small-scale, biomass-fuelled combined heat and power for community housing. Biomass bioenergy 35, (2011), 3849- 3858.

[48] S. Sokhansanj, S. Mani, S. Tagore. A.F. Turhollow. Techno-economic analysis of using corn stover to supply heat and power to a corn ethanol plant – Part 1: Cost of feedstock supply logistics. Biomass and bioenergy 34, (2010), 75-81.

[49] J. Moncada, M.M. El-Halwagi, C. A. Cardona. Techno-economic analysis for a sugarcane biorefinery: Colombian case. Bioresource technology 135, (2013), 533-543

[50] J. Turner , G. Sverdrup, M.K. Mann, P.C. Maness, B. Kroposki, M. Ghirardi, R. J. Evans, D. Blake. Renewable hydrogen production. Int. J. Energy Res. 32, (2008), 379–407.
[51] M. Puig-Arnavat, J.A. Hernandez, J.C. Bruno, A. Coronas, (2013). Artificial neural network models for biomass gasification in fluidized bed gasifiers. Biomass Bioenergy 49, 279–289.
[52] A.M. Shakorfow. Biomass, Incineration, Pyrolysis, Combustion and Gasification. International

Journal of Science and Research (IJSR) 5, (2016), 2319-7064.
[53] S.K. Sansaniwala, K. Pal, M.A. Rosen, S.A. Tyagi. Recent advances in the development of biomass gasification technology: A comprehensive review. Renewable and Sustainable Energy Reviews. 72, (2017), 363-384
[54] A.K. Rajvanshi, A.K. Biomass gasification. Boca Raton, Florida, United States: CRC Press (1986), 83-102.
[55]. A. Mustafa, R.K. Calay, M.Y. Mustafa. Techno-economic of Biomass Gasification

Plant for the Production of Transport Biofuel for Small Communities. Energy Procedia 112, (2017), 521-536.
[56] V.S. Sikarwar, M. Zhao, P. Clough, J. Yao, X. Zhong, M.Z. Memon, N. Shah, E. Anthony, P. Fennell. An overview of advances in biomass gasification. Energy Environ. Sci. 9, (2016), 2939-2977.
[57] R.F Probstien, R.E. Hicks. Synthetic Fuels (2006), 189. 3rd edition. McGraw- Hill Books Company New York. Dover Publication Inc. 31 East 2nd street, Mineola NY 11501.
[58] S. Farzad, M.A. Mandegari. A critical review of biomass gasification, co-gasification, and their environmental assessment. Biofuel Research Journal 12, (2016), 483 – 495.
[59] A.A. Erakhrumen. Biomass gasification: Documented information for adoption/adaptation as further improvements towards suitable utilisation of renewable natural resources. Renew Energy, (2012), 1 – 8.
[60] Y.H. Kiang. Fuel property estimation and combustion process characterization: conventional fuels, biomass, biocarbon, waste fuels, refuse derived fuel, and other alternative fuels. Academic Press, 2018.
[61] P. Basu. Biomass Gasification and Pyrolysis. Academic Press Boston, (2010), 117-156.

[62] J.P. Ciferno, J.J. Marano, J.J. Benchmarking biomass gasification technologies for fuels, chemicals, and hydrogen production. US department of Energy, National Energy Technology Laboratory (Washington DC) (2002).
[63] C. Pfeifer, S. Koppatz, H. Hofbauer, H. Steam gasification of various feedstocks at a dual fluidised bed gasifier: Impact of operating condition and bed material. Biomass Convers Biorefine 1, (2011), 39 – 53.

[64] US Department of Energy National Energy Technology Laboratory,). Worldwide synthetic gas production (2016). Retrieved from: http://www.netl.doe.gas/research/coal/energysystems/gasification/gasification-plant-

databases/current-brand.

[65] H. Karatas, H. Olgum, F. Akgum. Experimental results of gasification of waste tire with air & CO2, air & steam and steam in a bubbling fluidised bed gasifier. Fuel processing Technology 102, (2012), 166 – 174.

[66] Z.A.B.Z. Alauddin, P. Lahijani, M. Mohammadi, A.F. Mohamed, Gasification of lignocellulosic biomass in fluidised bed for renewable energy development: A review. Renew Sustain Energy Rev 14, (2010), 2852 -2862.

[67] E. Natarajan, M. Ohman. Experimental determination of bed agglomeration tendencies of some common agricultural residues in fluidised bed combustion and gasification. Biomass Bioenergy 15, (1998), 163 -169.

[68] L. Shen, Y. Gao, J. Xiao. Simulation of hydrogen production from biomass gasification in interconnected fluidized beds. Biomass and Bioenergy 32, (2008), 120-127.

[69] T.K Patra, P. N. Sheth. Biomass gasification models for downdraft gasifier: A state –of-the-art review. Renewable and Sustainable Energy 50, (2015), 583 – 593.

[70] C. Wang, B. Dou, H. Chen Y. Chen, S. Y. Xu, X. Du, T. Luo, C. Tan. Hydrogen production from steam reforming of glycerol by Ni–Mg–Al based catalysts in a fixed-bed reactor. Chemical Engineering Journal 220, (2013) 133-142

[71] L. Wei, S. Xu L, Zhang, C. Liu, H. Zhu, S. Liu. Steam gasification of biomass for hydrogen-rich gas in a free-fall reactor. Int J Hydrogen Energy 32, (2007), 24–31.

[72] S. Sharma, P.N. Sheth. Air-steam biomass gasification: experiments, modelling and simulation. Energy Convers. Manage 110, (2016), 307-318

[73] M. Campoy, A. Gomez-Barea, A.L. Villanueva, P. Olvera. Air−Steam Gasification of Biomass in a Fluidized Bed under Simulated Autothermal and Adiabatic Conditions. Ind. Eng. Chem. Res.47, (2008), 5957–5965.

[74] Cheng, J., Zhang, X., Luo, Z., Liu, F., Ye, Y., Yin, W., Liu, W., & Han, Y. Carbon nanotubes synthesis andparametricstudyusingCaCO3 nanocrystals as catalyst support by CVD. Mater.Chem.Phys 95, (2006), 5–11.

[75] J. Corella, J.M. Toledo, G. Molina. Biomass gasification with pure steam in fluidised bed: 12 variables that affect the effectiveness of the biomass gasifier. Int. J. Oil Gas Coal Technol 1, (2008), 194-207.

[76]. J. Udomsirichakorn, P. Basu, P.A. Salam, B. Acharya. Effect of CaO on tar reforming to hydrogen-enriched gas with in-process CO2 capture in a bubbling fluidized bed biomass steam

gasifier. Int. J. Hydrogen Energy 38, (2013), 14495-14504.

[77] Cheng, J., Zhang, X., Luo, Z., Liu, F., Ye, Y., Yin, W., Liu, W., & Han, Y. Carbon nanotubes synthesis andparametricstudyusingCaCO3 nanocrystals as catalyst support by CVD. Mater.Chem.Phys 95, (2006), 5–11.

[78] L.Q. Wang, Z.S. Chen. Experimental Studies on H_2-Rich Gas Production by Co- Gasification of Coal and Biomass in an Intermittent Fluidized Bed Reactor. Advanced Materials Research 201, (2013), 1127-1131, 2013.

[79] L. Narvaez, A. Orio, M.P. Aznar, J. Corella. Biomass Gasification with Air in an Atmospheric Bubbling Fluidised Bed. Effect of Six Operating Variables on the Quality of the Produced Raw Gas. Ind. Eng. Chem. Res 35, (1996), 2110-2120

[80] M. A. Hamad, A.M. Radwan, D. A. Heggo, T. Moustafa. Hydrogen rich gas production from catalytic gasification of biomass. Renewable Energy 85, (2016), 1290-1300.

[81] A. Inayat, M.M. Ahmad, M.I.A. Mutalib, S. Yusup. Process modelling for parametric study on oil palm empty fruit bunch steam gasification for hydrogen production. Fuel Process Technol 93, (2012), 26–34.

[82] S. Luo, B. Xiao, X. Guo, Z. Hu, S. Liu, S. M. He. Hydrogen-rich gas from catalytic steam gasification of biomass in a fixed bed reactor: influence of particle size on gasification performance. Hydrogen Energy 34, (2009), 1260-1264

[83] L. Wei, S. Xu, L. Zhang, C. Liu, H. Zhu, S. Liu Steam gasification of biomass for hydrogen-rich gas in a free-fall reactor. Energy Convers Manage 43, (2007), 897-909

[84] L. Wei, S. Xu, L. Zhang, C. Liu, H. Zhu, S. Liu. Steam gasification of biomass for

hydrogen-rich gas in a free-fall reactor. Int J Hydrogen Energy 32, (2007), 24–31.

[85] Demirbas, A. (2002). Gaseous products from biomass by pyrolysis and gasification: effects of catalyst on hydrogen yield. Energy Convers Manage 43, 897–909.

[86] K. Kumabe, T. Hanaoka, S. Fujimo S, T. Minowa, S. kinya. Co-gasification of woody biomass and coal with air and steam. Fuel 86, (2007), 684-689.

[87] P. Straka, Z. Bucko, Z. Co-gasification of Lignite/waste-tyre mixture in a moving bed. Fuel Processing Technology 90, (2009), 1202-1206.

[88] D.A. Ali, M.A. Gadalla, O.Y. Adelazzi, C.P. Hulleberg. Co-gasification of coal and biomass in an entrained flow gasifier: Modelling, Simulation and Integration Opportunities. Journal of Natural Gas Science and Engineering 37, (2017), 126-137.

[89] I. Aigner, C. Pfeifer, H. Hofbauer. Co-gasification of coal and wood in a dual fluidized bed gasifier. Fuel 90, (2011), 2404-2412.

[90] D.R. Mcllveen-Wright, F. Pinto, L. Armestro, M.A. Caballero, M.P. Aznar, A. Cabanilla A comparism of CFB Combustion and Gasification Power Plant technologies for processing mixtures of coal, biomass and plastic waste. Fuel process Technol 87, (2006), 793-801.

[91] R.N. Andre, F. Pinto, C. Franco, M. Dias, I. Gulyurtlu, M.A.A. Matos, Fluidised bed Co-gasification of Coal and Olive oil industry waste and wood in a bubbling fluidized bed reactor. Fuel 89, (2010), 2991-3000.

[92] F. Pinto, H. Lopes, R.N. Andre, M. Mirinda, I. Gulyurtlu, I. Cabrita. Effect of catalyst in the quality of coal and wastes 1: Tars and Nitrogen Compounds Abatment. Fuel 86, (2007), 2051-2063.

[93] F. Pinto, C. Franco, R.N. Andre, M. Mirinda, I. Gulyurtlu, I. Cabrita,. Co-gasification study of biomass mixed with plastic waste. Fuel 81, (2002), 291-297.

[94] Alzate, C.A., Chejne, F., Valdes, C.F., Berrio, A., Cruz, J.D.L., & Londono, C.A. (2009). Co-gasification of pelletized wood residues. Fuel 88, (2002), 437-445.

[95] J. Fermoso, B. Arias, M.G. Plaza, C. Pevida, F. Rubiera, J.J. Pis. High pressure co- gasification of coal with biomass and petroleum coke. Fuel process Technol 90, (2009), 926- 932.

[96] W. De Joug, J. Andries, K.R.G. Hein, Coal/biomass co-gasification in a pressurized bed reactor. Renew Energy 16, (1999), 1110-1113.

[97] X.M. Zhang, L.J. Guo, Y.J. Lu, C.M. Ji, Y. Guan, A.X. Pei. Hydrogen production by biomass gasification in supercritical water: A systematic experimental and analytical study. Catalysis Today 129, (2007), 275-286.

[98] K.J. Andersson, M. Skov-Skjøth Rasmussen, P.E. Hojlund NielsenIndustrial-scale gas conditioning including Topsoe tar reforming and purification downstream biomass gasifiers: an overview and recent examples. Fuel, 203 (2017), pp. 1026-1030

[99] S. Anis, Z.A. Zainal. Tar reduction in biomass producer gas via mechanical, catalytic and thermal methods: a review. Renew Sustain Energy Rev, 15 (2011), pp. 2355-2377

[100] H.L. Iversen, B. Gobel. Update on gas cleaning technologies for biomass gasification for different application, Biomass Gasification Group, Denmark, (2006)

[101] V. Rios, M. Lucia V. Rios, A. M. González, E.E.S. Lora, O.A.A. Del Olmo. Reduction of tar generated during biomass gasification: A review. Biomass and Bioenergy108, (2018), 345-370

[101] J. Gil, J. Corella, M. Aznar, M.A. Caballero, Biomass gasification in atmospheric and bubbling fluidized bed: effect of the type of gasifying agent on the product distribution, Biomass Bioenergy 17, (1999), 389–403

[103] C.A.V.B. de Sales, D.M.Y. Maya, E.E.S. Lora, R.L. Jaén, A.M.M. Reyes,A.M. González, R.V. Andrade, J.D. Martínez, Experimental study on biomass (eucalyptus spp.) gasification in a two-stage

downdraft reactor by using mixtures of air, saturated steam and oxygen as gasifying agents, Energy Convers. Manag. 145, (2017), 314–323

[104] H. de Lasa, E. Salaices, J. Mazumder, R. Lucky, Catalytic steam gasification of biomass: catalysts, thermodynamics and kinetics, Chem. Rev. 111, (2011), 5404–5433

[105] F.L. Chan, A. Tanksale, Review of recent developments in Ni-based catalysts for biomass gasification, Renew. Sustain. Energy Rev. 38, (2014), 428–438

[106] D. Wang, W. Yuan, W. Ji, Char and char-supported nickel catalysts for secondary syngas cleanup and conditioning, Appl. Energy 88, (2011), 1656–1663

[107] F.P. Nagel, S. Ghosh, C. Pitta, T.J. Schildhauer, S. Biollaz, Biomass integrated gasification fuel cell Systems-Concept development and experimental results, Biomass Bioenergy 35, (2011) ,354–362

[108] Y. Ueki, T. Torigoe, H. Ono, R. Yoshiie, J.H. Kihedu, I. Naruse, Gasification characteristics of woody biomass in the packed bed reactor, Proc. Combust. Inst. 33, (2011), 1795–1800,

[109] M. Dogru, C.R. Howarth, G. Akay, B. Keskinler, A.A. Malik, Gasification of hazelnut shells in a downdraft gasifier, Energy 27, (2002), 415–427

[110] P. Lv, Z. Yuan, L. Ma, C. Wu, Y. Chen, J. Zhu, Hydrogen-rich gas production from biomass air and oxygen/steam gasification in a downdraft gasifier, Renew. Energy 32, (2007), 2173–2185.

[111] A.L. Galindo, E. Silva, R. Viera, S.Y. Giraldo, R.L. Jae, V. Melian. Biomass gasification in a downdraft gasifier with a two-stage air supply: effect of operating conditions on gas quality, Biomass Bioenergy 61, (2014), 236–244

[112] C.A.V.B. de Sales, D.M.Y. Maya, E.E.S. Lora, R.L. Jaén, A.M.M. Reyes, A.M. González, R.V. Andrade, J.D. Martínez, Experimental study on biomass (eucalyptus spp.) gasification in a two-stage downdraft reactor by using mixtures of air, saturated steam and oxygen as gasifying agents, Energy Convers. Manag. 145 (2017) 314–323,

[113] J. Gil, J. Corella, M. Aznar, M.A. Caballero, Biomass gasification in atmospheric

and bubbling fluidized bed: effect of the type of gasifying agent on the product distribution, Biomass Bioenergy 17, (1999), 389–403

[114] P. Mckendry, Energy production from biomass (part 3): gasification technologies,

Bioresour. Technol. 83, (2002), 55–63
[115] J. Gil, M. a. Caballero, J. a. Martín, M.-P. Aznar, J. Corella, Biomass gasification with air in a fluidized bed: effect of the in-bed use of dolomite under different operation conditions, Ind. Eng. Chem. Res. 38 (1999) 4226–4235

[116] F. Miccio, B. Piriou, G. Ruoppolo, R. Chirone, Biomass gasification in a catalytic fluidized reactor with beds of different materials, Chem. Eng. J. 154, (2009), 369–374

[117] K. Tasaka, T. Furusawa, A. Tsutsumi, Biomass gasification in fluidized bed reactor with Co catalyst, Chem. Eng. Sci. 62, (2007), 5558–5563

[118] A. Olivares, M.P. Aznar, M. a. Caballero, J. Gil, E. Francés, J. Corella, Biomass gasification: produced gas upgrading by in-bed use of dolomite, Ind. Eng. Chem. Res. 36, (1997), 5220–5226

[119] P. Lv, Z. Yuan, C. Wu, L. Ma, Y. Chen, N. Tsubaki, Bio-syngas production from biomass catalytic gasification, Energy Convers. Manag. 48, (2007), 1132–1139,
[120] S. Turn, C. Kinoshita, D. Ishimura, J. Zhou, The fate of inorganic constituents of biomass in fluidized bed gasification, Fuel 77, (1998), 135–146

[121] S. Rapagnà, N. Jand, A. Kiennemann, P.U. Foscolo, Steam-gasification of biomass in a fluidised-bed of olivine particles, Biomass Bioenergy 19, (2000),187–197

[122] A. Narváez, M.P. Orío, J. Aznar, J. Corella, Biomass gasification with air in an atmospheric bubbling fluidized bed. Effect of six operational variables on the quality of the produced raw gas, Ind. Eng. Chem. Res. 35, (1996) 2110–2120

[123] J. Delgado, M.P. Aznar, J. Corella, Biomass gasification with steam in fluidized bed: effectiveness of CaO, MgO, and CaO-MgO for hot raw gas cleaning, Ind. Eng. Chem. Res. 36, (1997), 1535–1543.
[124] C. Pfeifer, B. Puchner, H. Hofbauer, Comparison of dual fluidized bed steam gasification of biomass with and without selective transport of CO2, Chem. Eng. Sci.

64 (2009) 5073–5083

[125] A. Van Der Drift, J. Van Doorn, J.W. Vermeulen, Ten residual biomass fuels for circulating gasification, Biomass Bioenergy 20, (2001), 45–56.

[126] X.T. Li, J.R. Grace, C.J. Lim, A.P. Watkinson, H.P. Chen, J.R. Kim, Biomass gasi- fication in a circulating fluidized bed, Biomass Bioenergy 26 (2004) 171–193, http://dx.doi.org/10.1016/S0961-

9534(03)00084-9.

[127] J.J. Hernández, G. Aranda-Almansa, A. Bula, Gasification of biomass wastes in an entrained flow gasifier: effect of the particle size and the residence time, Fuel Process.
Technol. 91, (2010), 681–692
128] Luan, J. Qian, Experimental study on sawdust air gasification in an entrained-flow reactor, Fuel Process. Technol. 91,
(2010), 910–914
[129] P.K. Senapati, S. Behera, Experimental investigation on an entrained flow type biomass gasification system using coconut coir dust as powdery biomass feedstock, Bioresour. Technol. 117, (2012), 99–106.

[130] R.H. Hurt, J.R. Gibbens. Residual carbon from pulverized coal fired boilers: 1. Size distribution and combustion reactivity Fuel 74, (1995), 471-480
[131] S. Kajitani, N. Suzuki, M. Ashizawa, S. HaraCO_2 gasification rate analysis of coal char in entrained flow coal gasifier. Fuel 85, (2006), 163-169
[132] H. Slaghuis, T.J. Van der Walt, D. Glasser, D. Hildebrand. Anomalies in gasification kinetic behaviour of some South African coal chars. Proceedings of 1993 international Pittsburgh coal conference on coal-energy and environment, Pittsburgh, USA (1993)
[133] A. Molina, A. Montoya, F. Mondragon. CO_2 strong chemisorption as an estimate of coal char gasification reactivity. Fuel 78, (1999), 971-977
[134] F. Pinto, R.N. Andre, C. Carolino, M. Miranda. Hot treatment and upgrading of syngas obtained by co-gasification of coal and wastes. Fuel Processing Technology126, (2014), 19- 29.
[135] M. L. Mastellone, L. Zaccariello, U. Arena. Co-gasification of coal, plastic waste and wood in a bubbling fluidized bed reactor. Fuel 89, (2010), 2991-3000
[136] S. Gaqa, S. Mamphweli, D. Katwire, E. Meyer. The Properties and Suitability of
Various Biomass/Coal Blends for Co-Gasification Purposes. Journal of Sustainable Bioenergy Systems4, (2015), 175-182
[137] G. Zhang M. Reinmoller, M. Klinger, B. Meyer Ash melting behavior and slag infiltration into alumina refractory simulating co-gasification of coal and biomass. Fuel 139, (2015), 457-465

[138] H. Balat, E. Kırtay. Hydrogen from biomass – present scenario and future prospects. Int J Hydrogen Energy 35, (2010), 7416-7426.

[139] J.H. Chang, K.S. Lee, P.J. Lin. Bio-hydrogen production with fixed-bed bioreactors Int J Hydrogen Energy 27, (2002), 1167-1174.

[140] P. Parthasarathy, K.S. Narayanan. Hydrogen production from steam gasification of biomass: Influence of process parameters on hydrogen yield – A review. Renewable Energy 66, (2014), 570-579.

[141] A. Arregi, M. Amutio, G. Lopez, J. Bilbao M. Olazar. Evaluation of thermochemical routes for hydrogen production from biomass: A review. Energy Conversion and Management 165, (2018), 696-719. Y.

[142] Y. Xiao, S. Xu, Y. Liu, C. Qiao. Catalytic steam co-gasification of biomass and coal in a dual loop gasification system using olivine catalysts. Journal of Energy Institute 3, (2020), 1074 – 1082.

[143] Y.K. Choi, M.H. Cho, J.S. Kim. Steam/oxygen gasification of dried sewage sludge in a two-stage gasifier: effects of the steam to fuel ratio and ash of the activated carbon on the production of hydrogen and tar removal. Energy 91, (2015), 160-167.

[144] Amal S. Al-Rahbi Paul T. Williams. Hydrogen-rich syngas production and tar removal from biomass gasification using sacrificial tyre pyrolysis char. Applied Energy, (2017), 501- 509

[145] R.C. Saxena, D. Seal, S. Kumar, H.B. Golay. Thermochemical routes for hydrogen rich gas from biomass: a review. Renew Sustain Energy Rev 12, (2008), 1909-1927.

[146] M. Asadullah, M. Tomohisa, I. Shin-ichgi, K. Kimio, T. KeiichiDemonstration of real biomass gasification drastically promoted by effective catalyst Appl Cataly A General, 8514 (2003), 1 – 14

[147] R. Rozas, N. Escalona, C. Sepulveda, K.Leiva, R.J. Chimentao, R. Garcia, J.L.G. Fierro. Catalytic gasification of pine-sawdust: Effect of primary and secondary catalysts. Journal of the Energy Institute 92, (2019), 1727-1735.

[148] W. Duan, Q. Yu, T. Wu, F. Yang, Q. Qin. Experimental study on steam gasification of coal using molten blast furnace slag as heat carrier for producing hydrogen-enriched syngas. Energy Conversion and Management 117, (2016), 513-519.

[149] M. Zribi, M. Lajili, F.J. Escudero-Sanz. Hydrogen enriched syngas production via gasification of biofuels pellets/powders blended from olive mill solid wastes and pine sawdust under different water steam/nitrogen atmospheres. International Journal of Hydrogen Energy 44, (2019), 11280-11288

[150] S. Kordoghli, B. Khiari, M. Paraschiv, F. Zagrouba, M. Tazerout. Production of hydrogen and hydrogen-rich syngas during thermal catalytic supported cracking of waste tyres in a bench-scale fixed bed reactor. International Journal of Hydrogen Energy 44, (2019), 11289-11302.

[151] Y. Xiao S. Xu, Y. Song, Y. Shan, C. Wang, G. Wan. Biomass steam gasification for hydrogen-rich gas production in a decoupled dual loop gasification system. Fuel Processing Technology 165,

(2017), 54-61.
[152] A. D. Orazio S. Rapagna P.U. Foscolo K. Gallucci, M. Nacken, S. Heidenreich, A. Di Carlo, A. Dell Era. Gas conditioning in H_2 rich syngas production by biomass steam gasification: Experimental comparison between three innovative ceramic filter candles. International Journal of Hydrogen Energy 40, (2015), 7282-7290.
[153] J. Fermoso, B.Arias, M.V.Gil, M.G.Plaza, C. Pevida, J.J.Pis, F. Rubiera. Co- gasification of different rank coals with biomass and petroleum coke in a high-pressure reactor for H_2-rich gas production. Bioresource Technology 101, (2010), 3230-3235
[154] N. Howaniec, A.S. Ski. Effect of fuel blend composition on the efficiency of hydrogen-rich gas production in co-gasification of coal and biomass. Fuel 128 (2014) 442– 450.

[155] R.C. Brown, Q. Liu, G. Norton 2000. Catalytic effects observed during the co- gasification of coal and switch grass. Biomass Bioenergy 18, 499–506.

[156] T. Chmielniak M. Sciazko. Co-gasification of biomass and coal for methanol synthesis. Applied Energy 74, (2003) 393–403.

[157] T.R. McLendona, A.P. Luib, R.L. Pineaulta, S.K. Beera, S.W. Richardson. High- pressure co-gasification of coal and biomass in a fluidized bed. Biomass and Bioenergy 26 (2004) 377–388.

[158] W. de Jong, J. Andries, k. R. G. Hem. Coal/Biomass co-gasification in a pressurized fluidised bed reactor. Renewable Energy 16 (1999), 1110-1113.

[159] K. Li, R. Zhang, J. Bi. Experimental study on syngas production by co-gasification of coal and biomass in a fluidized bed.
[160] Basu, P. (2010). Biomass Gasification and Pyrolysis. Academic Press Boston, Academic Press, 117-156.
[161] Sharma, A.K. (2008). Modelling of biomass gasification applied to a combined gasifier-combustor unit: equilibrium and kinetic approaches. Energy Convers. Manage 49, 832–84
[162]. H.L. Friedman. Kinetics of thermal degradation of char-forming plastics from

thermogravimetry – application to a phenolic plastic. J Polym Sci C, 6 (1963), pp. 183-195

[163] C.E. Greenhalf, D.J. Nowakowski, A.V. Bridgwater, J. Titiloye, N.Yates, A.Riche, I.Shield. Thermochemical characterisation of straws and high yielding perennial grasses. Industrial Crops and Products36, (2012), 449-459.
[164] K. Jayaraman, I. Gokalp. Thermogravimetric and evolved gas analyses of high ash Indian and Turkish coal pyrolysis and gasification. Journal of Thermal Analysis and Calorimetry 121, (2015),

919–927,
[165] T. Damartzis, D.Vamvuka, S.S. fakiotakis, A. Zabaniotou. Modeling of cardoon
(Cynara cardunculus) pyrolysis using thermogravimetric analysis (TGA). Bioresource Technology102, (2011), 6230-6238.
[166] L. Shao, Z. X. Xu, W. Jin, H. L. Yin. Rice Husk as Carbon Source and Biofilm Carrier for Water Denitrification. Pol. J. Environ. Stud18, (2009), 693–699.
[167] A. Inayat, M.M. Ahmad, M.I.A. Mutalib, S.Yusup. Process modelling for parametric study on oil palm empty fruit bunch steam gasification for hydrogen production Fuel Process Technol 93, (2012), 26–34.
[168] E.D. Gordillo, A. Belghit. A downdraft high temperature steam-only solar gasifier
of biomass char: a modelling study. Biomass Bioenergy 35, (2011), 2034–2043.
[169] C.C. Sreejith, C. Muraleedharan, P. Arun. Air–steam gasification of biomass in fluidized bed with CO 2 absorption: A kinetic model for performance prediction. Fuel Process Technol 130, (2015), 197–207.
[170] R. Khonde, A. Chaurasia. Rice husk gasification in a two-stage fixed-bed gasifier: Production of hydrogen rich syngas and kinetics. Int. J. Hydrogen Energy 41, (2016), 8793– 8802.
[171] G. Mirmoshtaghi, J. Skvaril, P.E.Campana, H. Li, E.Thorin, E. Dahlquist. The influence of different parameters on biomass gasification in circulating fluidized bed gasifiers. Energy Conversion and Management 126, (2016), 110-123.
[172] A. Gagliano, F. Nocera, M. Bruno, G.Cardillo. Development of an Equilibrium-based Model of Gasification of Biomass by Aspen Plus. Energy Procedia
111, (2017), 1010-1019
[173] K.G. Mansaray A.M. Al-Taweel, A.E. Ghaly, F. Hamdullahpur V.I. Ugursal. Mathematical modeling of a fluidized bed rice husk gasifier. Energy Sources 22 (2000) 83- 98.
[174] M.B. Nikoo, N. Mahinpey. Simulation of biomass gasification in fluidized bed reactor using ASPEN PLUS. Biomass Bioenergy, 32 (2008), 1245-1254.
[175] Z.Y. Liu, Y.T. Fang, S.P. Deng, J.J. Huang, J.T. Zhao, Z.H. Cheng. Simulation of pressurized ash agglomerating fluidized bed gasifier using ASPEN PLUS Energ. Fuel 26, (2012), 1237-1245.
[176] G. Li, Z. Liu, J. Li, Y. Fang, J. Shan, S. Guo, Z. Wang. Modeling of ash agglomerating fluidized bed gasifier using back propagation neural network based on particle swarm optimization. Applied Thermal Engineering 129, (2018), 1518-1526.

[177] M. Costa, M. La Villetta, N. Massarotti. Optimal tuning of a thermo-chemical equilibrium model for downdraft biomass gasifiers. Chem Eng Trans 43, (2015), 439-444.

[178] I.I. Ahmed, A.K. Gupta. Sugarcane bagasse gasification: Global reaction mechanism of syngas evolution. Applied Energy 91 (2012) 75–81.

[179] M.Anil, S.Rupesh, C.Muraleedharan, P.Arun. Performance Evaluation of Fluidised Bed Biomass Gasifier using CFD. Energy Procedia 90, (2016), 154-162.

[180] R. Jayathilake, S Rudra. Numerical and experimental investigation of Equivalence Ratio (ER) and feedstock particle size on birchwood gasification. Energies 10, (2018), 1232.

[181] X. Gao, Y. Zhang, F. Bao, B. Li, Y. Zhao, C. Ke, B. Jiang. CFD modeling of sawdust gasification in a lab-scale entrained flow reactor based on char intrinsic kinetics. Part 1: Model development. Chemical Engineering and Processing - Process Intensification 125, (2018), 280-289.

[182] E. Monteiro, T. M. Ismai, A. Ramos, M. A. El-Salam, P.S.D. Brito, A. Rouboa. Assessment of the miscanthus gasification in a semi-industrial gasifier using a CFD model.
Applied Thermal Engineering123, (2017) 448-457

[183] H. Liu, R. J.Cattolica, R. Seiser. Operating parameter effects on the solids circulation rate in the CFD simulation of a dual fluidized-bed gasification system. Chemical Engineering Science 169, (2017), 235-245.

[184] D. A. Ali, Mamdouh, A. Gadalla, O. Y. Abdelaziz, C. P. Hulteberg, F. H. Ashou. Co-gasification of coal and biomass wastes in an entrained flow gasifier: Modelling, simulation and integration opportunities. Journal of Natural Gas Science and Engineering 37 (2017) 126- 137.

[185] A. Slezak, J. M. Kuhlman, L. J.Shadle, S. Shi. CFD simulation of entrained-flow coal gasification: Coal particle density/size fraction effects. Powder Technology 203, Issue1, (2010), 98-108.

[186] L.Q. Wang, Z.S. Chen. Experimental Studies on H_2-Rich Gas Production by Co- Gasification of Coal and Biomass in an Intermittent Fluidized Bed Reactor. Advanced Materials Research 201, (2013), 1127-1131.

[187] N. Couto, V. Silva, E. Monteiro, P. Brito, A. Rouboa. Using an Eulerian-granular 2-D multiphase CFD model to simulate oxygen air enriched gasification of agro-industrial residues. Renewable Energy 77, (2015), 174-181.

Savuto, A., Di-Carol, A., Bocci, E., Dorazio, A., Villarini, M., Carlini, M., & Foscolo,

[188] P.U. (2015). Development of a CFD model for the simulation of tar and methane steam reforming through a ceramic catalytic filter. International J. Hydrogen Energy 40, 7991-8004

[189] C.D. Blasi. Modeling chemical and physical processes of wood and biomass pyrolysis.

Progress in Energy and Combustion Science 34, (2008), 47-90.

[190] M. J. Diamantopoulou E. Milios. Modelling total volume of dominant pine trees in reforestations via multivariate analysis and artificial neural network models. Biosystems Engineering105, (2010), 306-315.

[191] D. Strusnik, J. Avsec. Artificial neural networking and fuzzy logic exergy controlling model of combined heat and power system in thermal power plant. Energy 80, (2015), 318- 330.

[192] D.S. Pandey, S. Das, I. Pan, J.J. Leahy, W. Kwapinski. Artificial neural network based modelling approach for municipal solid waste gasification in a fluidized bed reactor. Waste Management 58, (2016), 202-213.

[193] R. Mikulandric, D. Loncar, D. Bohning, R. Bohme, M. Beckman. Process performance improvement in a co-current, fixed bed biomass gasification facility by control system modifications. Energy Conversion and Management 104, (2015), 135-146.

[194] C. C. Sreejith, C. Muraleedharan, P. Arun. Performance prediction of fluidised bed gasification of biomass using experimental data-based simulation models. Biomass Conversion and Biorefiney 3, (2013), 283–304.

[195] Z.Q. Bian, B. Han, Z.M. Du, J.N. Jaubert, M.J. Li. Integrating support vector regression

with genetic algorithm for CO_2-oil minimum miscibility pressure (MMP) in pure and impure CO_2 streams. Fuel 182, (2016), 550-557.

[196] S. Azadi, A. Karimi-Jashni. Verifying the performance of artificial neural network and multiple linear regression in predicting the mean seasonal municipal solid waste generation rate: a case study of Fars province, Iran Waste Manage 48, (2016), 14-23.

[197] I. Estiati, F. B. Freire, J. T. Freire, R. Aguado, M. Olazar. Fitting performance of artificial neural networks and empirical correlations to estimate higher heating values of biomass. Fuel 180, (2016), 377-383.

[198] S. E. Onoji, S. E. Iyuke, A. I. Igbafe, D. B. Nkazi. Rubber seed oil: A potential renewable source of biodiesel for sustainable development in sub-Saharan Africa. Energy Conversion and Management 15, (2016), 125-134.

[199] D. Baruah, D.C. Baruah, M.K. Hazarika. Artificial neural network based modeling of biomass gasification in fixed bed downdraft gasifiers. Biomass and Bioenergy 98, (2017), 264-271.

[200] S. Azadi A.R. Sepaskhah. Annual precipitation forecast for west, southwest, and south provinces of Iran using artificial neural networks. Theoretical and Applied Climatology 109,

(2012), 175–189.

[201] A.E. Bakyani, H. Sahebi, M. M.Ghiasi, N. Mirjordavi, F. Esmaeilzadeh, M. Lee, A. Bahador. Prediction of CO_2–oil molecular diffusion using adaptive neuro-fuzzy inference system and particle swarm optimization technique. Fuel 181, (2016), 178-187.

[202] R.L. Grob, E.F. Barry. Modern practice of gas chromatography. John Wiley & Sons; N. Rakesh, S. Dasappa Energy Conversion and Management 167, (2018) 134–146

[203] E. De Hoffmann, V. Stroobant. Mass spectrometry: principles and applications. John Wiley & Sons; 2007.

[204] F.W. McLafferty, F. Turecek. Interpretation of mass spectra. University Science Books (1993).

[205] O.D. Sparkman Z. Penton, F.G. Kitson. Chromatography Gas. Gas chromatography and mass spectrometry: a practical guide. Academic Press, 138 (2011), 471, ISBN 13: 978-0- 12-373628-

[206] H. Nair H, W. Clark. Mass Spectrometry for the Clinical Laboratory. Academic Press; 2016

[207] S.E. Stein. Estimating probabilities of correct identification from results of mass spectral library searches. J Am Soc Mass Spectrom 5, (1999), 316–23.

[208] P. Ausloos, C.L. Clifton, S.G. Lias, A. L. Mikaya, S.E. Stein, D.V. Tchekhovskoi, The critical evaluation of a comprehensive mass spectral library. J Am Soc Mass
Spectrom10, (1999), 287–99.

[209] Q.V. Batch, O. Skreiberg, C.J. Lee. Process modeling and optimization for torrefaction of forest residues. Energy 138, (2017), 348 - 354.

[210] P.J.G. Nieto, E. Garcia-Gaonzalo, J.P. Paredes-Sanches, A.S.M. Bernardo, M.M. Fernandez. Prediction modelling of higher heating value in biomass for energy treatment process using machine learning techniques. Fuel, (2018), 1 – 14.

[211] S. Tiwary, S.B. Ghugare, P.D. Chavan, S. Saha, S. Datta, J. Sahu, S.S. Tambe. Co- gasification of High Ash Coal–Biomass Blends in a Fluidized Bed Gasifier. Experimental Study and Computational Intelligence-Based Modeling Waste and Biomass Valorization (2018), https://doi.org/10.1007/s12649-018-0378-7

[212] J. George, P. Arun, C. Muraleedharan. Assessment of producer gas composition in air gasification of biomass using artificial neural network model. International Journal of Hydrogen Energy 43, (2018), 9558 – 9568.

[213] D. Baruah, D.C. Baruah, M.K. Hazarika. Artificial neural network based modeling of biomass

gasification in fixed bed downdraft gasifiers. Biomass and Bioenergy 98, (2017), 264 -271

[214] J.J. Montano, A. Palmer. Numeric sensitivity analysis applied to feedforward neural networks. Neural Computing and Applications 12, (2003), 119 – 125

[215] W. Wang, P. Jones, D. Partridge. Assessing the impact of input features in a feedforward neural network. Neural Computing and Applications 9, (2000), 101–112.

[216] M. Gevrey, I. Dimopoulos, S. Lek. Review and comparison of methods to study the contribution of variables in artificial neural network models. Ecological Modelling160, (2003), 249–264.

[217] P. Lahijani, Z.A. Zainal. Gasification of palm empty fruit bunches in a fluidised bed; a performance study. Bioresource Technol 102, (2011), 2068 – 2076.

[218] J. Dascomb, A. Krothapall. Hydrogen-Enriched Syngas from Biomass Steam Gasification for Use in Land-Based Gas Turbine Engines. Novel combustion Concept for sustainable for sustainable energy development (conference paper), (2014), 89 - 110.

[219] P.M. Lv, Z.H. Xiong, C.Z. Jang, Y. Wu, J.X. Chen, Z.X. Zhu. An experimental study of biomass air-steam gasification in a fluidized bed. Bioresource Technology 95, (2004), 95 – 101.

[220] F. Guo, Y. Dong, L. Dong, C. Guo, C. Effect of Design and Operating Parameters on the Gasification Process of Biomass in a Downdraft Fixed Bed: An Experimental Study.

International Journal of Hydrogen Energy 39, (2014), 5625–5633

[221] F. Guo, Y. Dong, L. Dong, C. Guo, C. Effect of Design and Operating Parameters on the Gasification Process of Biomass in a Downdraft Fixed Bed: An Experimental Study.

International Journal of Hydrogen Energy 39, (2014), 5625–5633

[222] L.Q. Wang, Y. Chen. Experimental Studies on H2-Rich Gas Production by Co- Gasification of Coal and Biomass in an Intermittent Fluidized Bed Reactor. Advanced Materials Research 201, (2013), 1127-1131.

[223] M.H. Shojaeefard, M. Akbari, M. Tahani, F. Farhani. Sensitivity Analysis of the Artificial Neural Network Outputs in Friction Stir Lap Joining of Aluminum to Brass. Advances in Materials Science and Engineering. (2013), 1-7

[224] T. Tchaban, M.J. Taylor, J.P. Grifn. Establishing impacts of the inputs in a feedforward neural network," Neural Computing and Applications, (1998), 7309 – 7317.

[225] M. Gevrey, I. Dimopoulos, S. Lek, Review and comparison of methods to study the contribution of variables in artificial neural network models, Ecol. Model.

(2003) 249-264

[226] G.D. Garson, G.D. Interpreting neural-network connection weights. AI Expert, 6, (1991), 46 – 51.

[227] J. Montano, A. Palmer, Numeric sensitivity analysis applied to feedforward neural networks, Neural Comput. Appl. 12 (2003) 119-125

[228] W. Wang, P. Jones, D. Partridge, Assessing the impact of input features in a feedforward neural network, Neural Comput. Appl. 9 (2000) 101-112.

[229] C.C. Fagan, C.D. Everard, K. McDonnell. Prediction of moisture, calorific value, ash, and carbon content of two dedicated bioenergy crops using near-infrared spectroscopy. Bioresour Technol 102, (2011), 5200-5206

[230] R. Khonde, A. Chaurasia. Rice husk gasification in a two-stage fixed-bed gasifier: Production of hydrogen rich syngas and kinetics. Int. J. Hydrogen Energy 41, (2016), 8793– 8802.

[231] S. Sharma, P.N. Sheth, Air-steam biomass gasification: experiments, modelling and simulation, Energy Convers. Manag. 110 (2016) 307-318.

[232] S.B. Ghugare, S. Tiwary, S.S. Tambe. Computational intelligence based models for prediction of elemental composition of solid biomass fuels from proximate analysis. Int J Syst Assur Eng Manag 8, (2014), doi 10.1007/s13198-014-0324-4.

[233] Oboirien, B. O., North, B. C., Obayopo, S. O., Odusote, J. K., & Sadiku, E. R. (2018). Analysis of clean coal technology in Nigeria for energy generation, Energy Strategy Reviews 20, 64-70.

[234] Suberu, M.Y., Mokhtar, A. S., Bahir, N. (2012). Potential capability of corn cob residue for small power generation in rural Nigeria. ARPN Journal of Engineering and Applied Sciences, 7(8), 1037 - 1046

[235] UNDP. (2009) Converting waste Agricultural Biomass into Resources. Compedium of Technology United Nations Environmental Programme, Japan, 2009.

[236] A. C. Caputo, M. Palumbo, P.M. Pelaggage, F. Scacchia. Economics of biomass energy utilization in combustion and gasification plants: effects on logistic variables. Biomass Bioenerg 28,

(2005), 35-51.

[237] A.V. Bridgwater, A.J. Toft, J.G. Brammer. A techno-economic comparison of power production by biomass fast pyrolysis with gasification and combustion. Renew Sust Energ Rev 6, (2002), 181-248.

[238] A. A.M.M. Malek, M. Hasanuzzaman, N.S. Rahim, Y.A.A. Turki. Techno-economic analysis and environmental impact assessment of a 10 MW biomass-based power plant in Malaysia. Journal of Cleaner Production 141, (2017), 502-513.

[239] A. Demirbas. Biomass resource facilities and biomass conversion processing for fuels and chemicals. Energy Conv. Manag. 42, (2001), 1357-1378.

Bioenerg 34, (2010), 798 – 804.

[240] F. Ahmadi, A.Q. Al Amin, M. Hasanuzzaman, R. Saidur. Alternative energy resources in Bangladesh and future prospect. Renew. Sust. Energ. Rev. 25 (2013), 698-707.

[241] I.E.A, IRENA. Biomass Co-firing: Technology Brief. IEA-ETSAP (International Energy Agency – Energy Technology Systems Analysis Program) and IRENA (International Renewable Energy Agency) Technology Brief E21, (2013).

[242] L.J.R., Nunes, J.C.O. Mtias, J.P.S. Catalao. A review on torrefied biomass pellets as a sustainable alternative to coal in power generation, (2014), Pag.153 – 160

[243] A.M. Arias, P.L. Mores, N.J. Scenna, S.F. Mussati. Optimal design and sensitivity analysis of post-combustion CO2 capture process by chemical absorption with amines. Journal of Cleaner Production 115, (2016), 315-331.

[244] N. Kongkeaw, S. Patumsawad. Thermal upgrading of biomass as a fuel by torrefaction, (2011), Pag.38-42.

[245] W.H. Chen, J. Peng, X.Y. Bi. A state-of-the-art review of biomass torrefaction, densification and applications, (2015), Pag.847 - 866

[246] J.H. Peng, X.T. Bi, S. Sokhansanj, C.J. Lim. Torrefaction and densification of different species of softwood residues, (2013), Pag.411 – 421.

[247] S.W. Park, C.H. Jang, K.R. Baek, J.K. Yang. Torrefaction and low-temperature carbonization of woody biomass: evaluation of fuel characteristics of the products, (2012),
Pag.676 – 685.

[248] W.H. Chen, W.Y. Cheng, K.M. Lu, Huang, Y.P. Huang. An evaluation on improvement of pulverized biomass property for solid fuel through torrefaction, (2012),
Pag.3636 –3644

[249] K.M. Lu, W.J. Lee, Chen, W.H, S.H. Liu, T.C. Lin. Torrefaction and low temperature carbonization of oil palm fiber and eucalyptus in nitrogen and air atmospheres, (2012), Pag.98 – 100

[250] W. Yan, T.C. Acharjee, C.J. Coronella, V.R. Vasquez. Thermal pretreatment of lignocellulosic biomass, (2009), Pag.35 – 40

[251] B. Arias, C. Pevida, J. Fermoso, M.G. Plaza, F. Rubiera, J.J. Pis. Influence of torrefaction on the grindabilty and reactivity of woody biomass, (2008), Pag.169 – 175.

[252] M. Phanphanich, S. Mani. Impact of torrefaction on the grindabilty and fuel characteristics of forest biomass, (2007), Pag.1246 – 1253

[253] W.J. Hall. Assessment of carbon dioxide emissions reductions achievable by using torrefaction, (2012), Pag.103 - 113

[254] B. Batidzirai, A.P. Mignot, W.B. Schakel, H.M. Junginger, A.P. Faaij. Biomass torre- faction technology: techno-economic status and future prospects. Energy, (2013), Pag.196 – 214

[255] A.A. Rentizelas, J. Li. Techno-economic and carbon emissions analysis of biomass torrefaction downstream in international bioenergy supply chains for co-firing, (2016), Pag.129 – 142.

[256] D. Prando, F. Patuzzi, P. Baggio, M. Baratieri. CHP Gasification Systems Fed by Torrefied Biomass: Assessment of the Energy Performance, (2014), Pag.147 – 155

[257] F. Starfelt, E. T. Aparicio, H. Li, E. Dotzauer. Integration of torrefaction in CHP plant – A case study, (2015), Pag.427-435.

[258] A.V. Bridgwater, A.J. Toft, J.G. Brammer. A techno-economic comparison of power production by biomass fast pyrolysis with gasification and combustion. Renew Sust Energ Rev 6, (2002), 181-248.

[259] S. De, M. Assadi. Impact of co-firing biomass with coal in power plants: techno- economic assessment, (2009), Pag.283 – 293.

[260] T. Kohl, T. Laukkanen, M. Jarvinen, C.J. Fogelholm. Energetic and Environmental Performance of three biomass upgrading processes integrated with a CHP plant, (2013) Pag.124 – 134

[261] H.W. Chen, J. Peng, X.T. Bi. A state-of-the-art review of biomass torrefaction, densification and applications. Renewable and Sustainable Energy Reviews 44 (2015), 847– 866.

[262] M.K. Raut, P. Basu, B. Acharya. The Effect of Torrefaction Pre-Treatment on the Gasification of Biomass. International Journal of Renewable Energy & Biofuels 2016 (2016), 1-13.

[263] W.H. Chen, S.C. Ye, H.K. Sheen. Hydrothermal carbonization of sugarcane bagasse via wet torrefaction in association with micro wave heating. Bio-resour Technol118 (2012), 195 –203.

[264] A. Ohliger, M. Forster, R. Kneer. Torrefaction of beech wood: a parametric study including

heat of reaction and grindabilty. Fuel 104 (2013), 607–613.
[265] J. Wannapeera, K. Worasuwannara, B. Fungtammasan. Effect of temperature and holding time during torrefaction on the pyrolysis behaviours of woody biomass. J Anal Appl Pyrolysis 92, (2009), 99 – 105.
[266] K.T. Wu, C.J. Tsai, C.S. Chen, H.W. Chen. The characteristics of torrefied micro- algae. Appl Energy100, (2012), 52–57.
[267] K.M. Lu, W.J. Lee, W.H. Chen, S.H. Liu. T.C. Lin. Torrefaction and low temperature carbonisation of oil palm fibre and eucalyptus in nitrogen and atmospheres. Bioresource Technol 123, (2012), 98 – 105.
[268] T.G, Bridgeman J.M, Jones, A. Williams, D. Waldron. An investigation of grindability of two torrefied energy residues. Energy 138, (2010), 348 – 354
[269] J.H. Peng, X.T. Bi, J. Lim, S. Sakhansanj. Development of torrefaction kinetics for British Columbia softwoods. Int J Chem React Eng10 (1) (2012), 1542 – 6580
[270] M. Phanphanich, S. Mani. Impact of torrefaction on the grindability and fuel characteristics of forest biomass. Bioresour Technol 102 (2011), 1246 – 1253.
[271] S.W. Park, C.H. Jang, K.R. Baek, J.K. Yang. Torrefaction and low-temperature carbonization of woody biomass: evaluation of fuel characteristics of the products. Energy 45 (2012), 676–685.
[272] A. Pimchuai, A. Dutta, P. Basu. Torrefaction of agriculture residue to enhance combustible properties. Energy Fuels 24, (2010), 4638–4645.
[273] W.H. Chen, H.C. Hsu, K.M. Lu, W.C. Lee, D.C. Lin. Thermal pretreatment of wood (Lauan) block by torrefaction and its influence on the properties of the biomass. Energy 36 (2011), 3012–3021.
[274] Y. Uemura, W. Omar, N.A. Othman, S. Yusup, T. Tsutsui. Torrefaction of oil palm wastes. Fuel 90, (2011), 2585 – 2591.
[275] Q.V. Batch, O. Skreiberg, C.J. Lee. Process modeling and optimization for torrefaction of forest residues. Energy 138, (2017), 348 - 354.
[276] S. Gul, N. Ramzan M. Abrar, H.S. Bano. Kinetic, volatile release modeling and optimization of torrefaction. Journal of Analytical and Applied Pyrolysis 128, (2017), 44-53.
[277] D. R. Nhuchhen, M.T. Afzal. HHV Predicting Correlations for Torrefied Biomass Using Proximate and Ultimate Analyses. Bioengineering 4(1), (2017), 7
[278] U. Ozveren. An artificial intelligence approach to predict gross heating value of lignocellusic fuels. J. Energy Inst 90(3), (2017), 397 – 407.
[279] D. Medic, M. Darr, A. Shah, B. Potter, J. Zimmerman. Effects of torrefaction process parameters on biomass feedstock upgrading. Fuel 91 (2012), 147–154

[280] P.J.G. Nieto, E. Garcia-Gaonzalo, J.P. Paredes-Sanches, A.S.M. Bernardo, M.M. Fernandez. Prediction modelling of higher heating value in biomass for energy treatment process using machine learning techniques. Fuel, (2018), 1 – 14.

[281] Y. Wei, T.C. Acharjee, C.J. Coronella, V.R. Vasquez. 2009. Thermal pretreatment of lignocellulosic biomass. Environmental progress and sustainable energy 28, (2009), 435 – 440

[282] B. Batidzirai, A.P.R. Mignot W.B. Schakel H.M. Junginger A.P.C. Faaij. Biomass torrefaction technology: Techno-economic status and future prospects. Energy 62, (2013), 196 – 214

[283] M.D. Kostic, N.M, Jokovic, O.S. Stamenkovic. Optimization of hamp seed oil extraction by n-hexane. Ind Crops Prod. 48 (2013), 133–143.

[284] D. Bas, I.H. Boyaci. Modeling and optimization I: usability of response surface methodology. J Food Eng.78 (3), (2007a) 836–845.

[285] S. Dharma, H.H. Masjuki, H.C. Ong, A.H. Sebayang, A.S. Silitonga, F. Kusumo. Optimization of biodiesel production process for mixed Jatropha curcas-Ceiba pentandra biodiesel using response surface methodology. Energy Conv Manage, 115 (2016), 178 -190

[286] L.J. Guo, X.M. Zhang, Y.J. Lu, C.M. Ji, Y. Guan, A.X. Pei. Hydrogen production by biomass gasification in supercritical water: A systematic experimental and analytical study. Catalysis Today 129, (2007), 275-286.

[287]. S. Thapa, P. R. Bhoi, A. Kumar, R. L. Huhnke. Effects of Syngas Cooling and Biomass Filter Medium on Tar Removal. Energies 10 (2017) 349-361.

[288]. S. Rapagna, A. Latif. Steam gasification of almond shells in a fluidised bed reactor: the influence of temperature and particle size on product yield and distribution. Biomass- Bioenergy 12 (1997) 281-288.

[289]. M. Balat. Potential importance of hydrogen as a future solution to environmental and transportation problems. International Journal of Hydrogen Energy 33 (2008) 4013-4029.

[290]. L. Devi, K.J. Ptasinski, F.J. Janssen. A review of the primary measures for tar elimination in biomass gasification processes. Biomass- Bioenergy 24 (2003) 125–40.

[291]. P.A. Simell, J.K. Leppalahti, E.A. Kurkela, Tar-decomposing activity of carbonate rocks under high CO2 partial pressure, Fuel 74 (6) (1995) 938–945.

[292]. D. Swierczynski, S. Libs, C. Courson, A. Kiennemann. Applied Catalysis B: Environmental 74 (2007) 211-222.

[293]. L. Devi, K.J. Ptasinski F.J. Janssen S.V. van Paasen P.C. Bergman, J.H. Kiel. Catalytic decomposition of biomass tars: use of dolomite and untreated olivine. Renew Energy 30 (2005) 565–587.

[294]. D. Sutton, B. Kelleher, J.R. Ross. Review of literature on catalysts for biomass gasification.

Fuel Process Technol 73 (2001) 155–73.
[295]. A. Bridgwater. Catalysis in thermal biomass conversion. Appl Catal A: Gen 116 (1994) 5–47
[296]. L.D. Felice, C. Courson, P.U. Foscolo, A. Kiennemann. Iron and nickel doped alkaline-earth catalysts for biomass gasification with simultaneous tar reformation and CO2 capture. Int J Hydrog Energy 36 (2011) 5296–5310.
[297]. Y. Shen. Chars as carbonaceous adsorbents/catalysts for tar elimination during biomass pyrolysis or gasification. Renew. Sustain. Energy Rev. 43 (2015) 281–295.
[298]. H. Luo, L. Bao, H. Wang, L. Kong, L. Y. Sun. Microwave-assisted in-situ elimination of primary tars over biochar: Low temperature behaviours and mechanistic insights. Bioresour. Technol. 267 (2018) 333–340.
[299]. Cao, S. Sun, R. Sun. Application of biochar-based catalysts in biomass upgrading: A review. RSC Adv. 7 (2017) 48793–48805.
[300]. X. Xiong, I.K.M. Yu L. Cao, D.C.W. Tsang, S. Zhang, Y.S.A. Ok. A review of biochar-based catalysts for chemical synthesis, biofuel production, and pollution control. Bioresour. Technol. 246 (2017) 254–270.
[301]. A.M. Dehkhoda, A.H. West, N. Ellis. Biochar based solid acid catalyst for biodiesel production. Appl.Catal. A 382 (2010) 197–204.
[302]. T. Dong, D. Gao, C. Miao, X. Yu, C. Degan, M. Garcia-Perez B. Rasco, S.S. Sablani, S. Chen. Two-step microalgal biodiesel production using acidic catalyst generated from pyrolysis-derived bio-char. Energy Convers. Manag. 105 (2015) 1389–1396.
[303]. S. Ren, H. Lei, L. Wang, Q. Bu, S. Chen, J. Wu. Hydrocarbon and hydrogen-rich syngas production by biomass catalytic pyrolysis and bio-oil upgrading over biochar catalysts. RSC Adv. 4 (2014) 10731–10737.
[304]. H.K.D. Nguyen, V.V. Pham, H.T. Do. Preparation of Ni/biochar catalyst for hydro treating of bio-oil from microalgae biomass. Catal. Lett. 2016, 146, 2381–2391
[305]. Q.Yan, C. Wan, J. Liu, J. GAO, F. Yu, J. Zhang, Z. Cai. Iron nanoparticles in situ encapsulated in biochar-based carbon as an effective catalyst for the conversion of biomass- derived syngas to liquid hydrocarbons. Green Chem. 15 (2013) 1631–1640.
[306]. M. Hervy, S. Berhanu, E. Weiss-Hortala, A. Chesnaud, C. Gerente, A. Villot, D.P. Minh, A. Thorel, L. Le Coq, A. Nzihou. Multi-scale characterisation of char's mineral species for tar cracking. Fuel 189 (2017) 88–97.
[307]. M.M. Titirici, R.J. White, C. Falco, M. Sevilla. Black perspectives for a green future: Hydrothermal carbons for environment protection and energy storage. Energy Environ. Sci. 5 (2012) 6796–6822.

[308]. R.C. Brown, Q. Liu, G. Norton. Catalytic effects observed during the co-gasification of coal and switchgrass. Biomass- Bioenergy 18 (2000) 499–506.
[309]. J. Corella, M.P. Aznar, J. Gil, M.A. Caballero. Biomass gasification in fluidized bed: where to locate the dolomite to improve gasification? Energy Fuels 13 (1999) 1122–1127.
[310]. J. Srinakruang, K. Sato, T. Vitidsant, K. Fujimoto. A highly efficient catalyst for tar gasification with steam. Catal Commun 6 (2005) 437–440.
[311]. Q. Huang, P. Lu, B. Hu, Y. Chi, J. Yan. Cracking of Model Tar Species from the Gasification of Municipal Solid Waste Using Commercial and Waste-Derived Catalysts. Energy & Fuels 30 (2016) 5740-5748.
[312] E.R. Stobbe, B.A. de Boer, J.W. Geus, Catal. Tar cracking. Today 47 (1999) 167
[313] L. Yingxin, C. Jixiang, Z. Jiyan. Effects of the supports on activity of supported nickel catalysts for hydrogenation of m-dinitrobenzene to m-phenylenediamine. Chin J Chem Eng 15, (2007), 63–67
[314] F. Cheng, X. Li. Preparation and Application of Biochar-Based Catalysts for Biofuel Production. Catalysts 8, 346, (2018), doi:10.3390/catal8090346
[315] F. Guo, X. Li, Y. Liu, K. Peng, C. Guo, Z. Rao. Catalytic cracking of biomass pyrolysis tar over char-supported catalyst. Energy conversion management, 167 (2018), 81-90.
[316] X.T. Li, J.R. Gracea, C.J. Lima, A.P. Watkinsona, H.P. Chenb, J.R. Kim. Biomass gasification in a circulating fluidised bed X.T. Biomass and Bioenergy 26 (2004) 171–193.
[317] F. Miccio, A. Picarelli, G. Ruoppolo. Increasing tar and hydrocarbons conversion by catalysis in bubbling fluidized bed gasifier. Fuel Processing Technology 141 (2016) 31–37.
[318] Amal S. Al-Rahbi Paul T. Williams. Hydrogen-rich syngas production and tar removal from biomass gasification using sacrificial tyre pyrolysis char. Applied Energy, (2017), 501- 509.
[319] C. Li, K. Suzuki. Tar property, analysis, reforming mechanism and model for biomass gasification—An overview. Renewable and Sustainable Energy Reviews 13 (2009) 594–604
[320] M. Ozonoh, B.O. Oboirien, A. Higginson, M.O. Daramola. Performance evaluation of gasification system efficiency using artificial neural network. Renewable Energy 145, (2020), 2253-2270). ‘
[321] M. Ramarao, S. Vivekanandan (2016). Evaluation of carbon conversion efficiency of mixed biomass gasification. International Journal of Mechanical Engineering and Technology (IJMET) 7, (2016), 555–564.
[322] S.S. Baskara, K.M. Deepak, B.D. Dinesh, M.I. Dhamodharan. Gasification of Biomass Using Fluidized Bed. International Journal of Innovative Research in Science, Engineering and Technology 3, (2014), 8995 - 9002
[323] D. Wang, W. Yuan W. Ji. Char and char-supported nickel catalysts for secondary syngas

cleanup and conditioning. Appl Energy 88, (2011), 1656–63
[324] H. Yu, G. Chen, Y. Xu, D. Chen. Experimental study on the gasification characteristics of biomass with CO2/air in an entrained-flow gasifier, BioRes. 11, (2016), 6085-6096.
[325] Y.F. Shen, M.D. Chen, T.H. Sun, J.P. Jia. Catalytic reforming of pyrolysis tar over metallic nickel nanoparticles embedded in pyrochar. Fuel 159, (2015), 570–9.
[326] S.P. Zhang, Q. Dong, L. Zhang Y.Q. Xiong. High quality syngas production from microwave pyrolysis of rice husk with char-supported metallic catalysts. Bioresour Technol 191, (2015)17–23.
[327] F. Guo, X. Li, Y. Liu, K. Peng, C. Guo, Z. Rao. Catalytic cracking of biomass pyrolysis tar over char-supported catalyst. Energy conversion management, 167 (2018), 81-90.
[328] L.E. Taba, M.F. Irfan, A.M.W.D. Wan, M.H. Chakrabarti. The effect of temperature on various parameters in coal, biomass and CO-gasification: a review. Renew Sust
Energy Rev 16 (2012), 5584–96.
[329] A.D. Kamble, V.K. Saxena, P.D. Chavan, V.D. Mend. Co-gasification of coal and biomass an emerging clean energy technology: Status and prospects of development in Indian context. International Journal of Mining Science and Technology 29, (2018), 171–186.y A.

[330] B.O. Oboirien, A.D. Engelbrecht, B.C. North, V.M. Du Cann, S. Veryn, R. Falcon. Study on structure and gasification characteristics of selected South African bituminous coal in fluidized bed gasification. Fuel Processing Technology 92, (2011), 735-742.

[331] A.V. Bridgwater. Biomass fast pyrolysis. Therm Sci 8, (2004), 21-49.

(332) A.C. Caputo, M. Palumbo, P.M. Pelaggage, F. Scacchia. Economics of biomass energy utilization in combustion and gasification plants: effects on logistic variables. Biomass Bioenerg 28, (2005), 35-51.

[333] A. A.M.M. Malek, M. Hasanuzzaman, N.S. Rahim, Y.A.A. Turki. Techno-economic analysis and environmental impact assessment of a 10 MW biomass-based power plant in Malaysia. Journal of Cleaner Production 141, (2017), 502-513.

[334] C.P. Mitchell, A.V. Bridgwater, D.J. Stevens, A.J. Toft, M.P. Watters. Techno- economic assessment of biomass to energy. Biomass Bioenerg 9, (1995), 205-26.
[335] E. Searcy, P.C. Flynn. A criterion for selecting renewable energy processes. Biomass

[336] A. Demirbas. Biomass resource facilities and biomass conversion processing for fuels and chemicals. Energy Conv. Manag. 42, (2001), 1357-1378.
Bioenerg 34, (2010), 798 – 804.

[337] F. Ahmadi, A.Q. Al Amin, M. Hasanuzzaman, R. Saidur. Alternative energy resources in Bangladesh and future prospect. Renew. Sust. Energ. Rev. 25 (2013), 698-707.
[338] D.R. Nhuchhen, P.A. Salam. Estimation of higher heating value of biomass from proximate analysis: A new approach. Fuel 99, (2012), 55-63.

[339] P. Pepiot, C.J. Dibble, T.D. Foust). Computational fluid dynamics modelling of biomass gasification and pyrolysis, in Computational Modelling in Lignocellulosic Biofuel Production, ACS Symposium Series, National Renewable Energy Laboratory, USA 1052, (2010), 273–298.

[340] C.J. Huang, L.J. Han, L. Liu, Z. Yang. Proximate analysis and calorific value estimation of rice straw by near infrared reflectance spectroscopy. Journal Energy Institute 81, (2008), 153-157.

[341] M. Ahmaruzzuman. Proximate analysis and predicting higher heating value of chars obtained from co-cracking of petroleum vacuum residue with coal, plastic and biomass.
Bioresource Technol 99 (2008), 5043-5080

[342] J. Parik, S.A. Channiwala, G.K. Ghosal. A correlation for calculating HHV from proximate analysis of solid fuels. Fuels 84, (2005), 487-494.

[343] C. Sheng, J.L.T. Azevedo. Estimating the higher heating value of biomass fuels from basic analysis data. Biomass Bioenergy 28, (2005), 499-507.

[344] P. Thipkhumthod, V. Meeyoo, P. Rangsunvigit, B. Kitiyanan, K. Siemanond, T. Rirksomboon. Fuel 84, (2005), 849-857.

[345] C.Y. Yin. Prediction of higher heating value of biomass from proximate and ultimate analysis. Fuel 90, (2011), 1128–1132.

[346] C.D. Cooper, B. Kim, J. MacDonald. Estimating the Lower Heating Values of Hazardous and Solid Wastes. Journal of the Air & Waste Management Association 49, (1999), 471-476.

[347] V.K. Verma, S. Bram, F. Delattin, P. Laha, I. Vandendael, A. Hubin, J. De Ruyck. Agro-pellets for domestic heating boilers: standard laboratory and real life performance. Appl. Energ 90, (2012), 17-23.
[348] N.S. Siefert, S. Litster. Energy and Economic analysis of advanced IGCC-CCS and IGFC-CCS power plants. Applied Energy 107 (2013) 315 – 328.
[349] X.Q. Kong, R.R. Wang, X.H. Huang. Energy efficiency and economic feasibility of CCHP driven by Stirling engine. Energ. Convers. Manage 45, (2004), 1433-1442

[350] M. Hasanuzzaman, N.A. Rahim, R. Saidur, R. S.N. Kazi. Energy savings and emissions reductions for rewinding and replacement of industrial motor. Energy 36, (2011), 233-240.

[351] T.M.I. Mahlia. Emissions from electricity generation in Malaysia. Renew. Energy 27, (2002), 293-300.

[352] B. Varun, I.K., R. Prakash. LCA of renewable energy for electricity generation systems

- a review. Renew. Sustain. Energy Rev. 13, (2009) 1067-1073.

[353] PDD. Project Design Document (A report). Bell eco power sdn bhd _Biomass based power generation project. In: CDM-UNFCCC. CDM-SSC-PDD (2006), Clean Development

[354] US EPA. Average In-use Emissions from Heavy-duty Trucks Emission Facts. A report from MI, USA: Office of Transportation and Air Quality (2008).

[355] WNA. Comparison of Lifecycle GHG Emissions for Various Electricity Generation Sources. World Nuclear Association Report, London, UK (2011). Retrieved on 15-08-17. Available online at: www.worldnuclear.org/World Nuclear- Association/Publications/Reports/Lifecycle GHG Emissions- of-Electricity-Generation

[356] Y. Zhang, Y. Zheng, M. Yang, Y. Song. Effect of fuel origin on synergy during co- gasification of biomass and coal in CO_2. Bioresource Technology 200, (2016), 789–794.

[357] A.V. Bridgwater, A.J. Toft, J.G. Brammer. A techno-economic comparison of power production by biomass fast pyrolysis with gasification and combustion. Renew Sust Energ Rev 6, (2002), 181-248.

[358] S.O. Bada, E.M.S. Falcon, L.M. Falcon, C.P. Bergmann. Co-firing potential of raw and thermally treated Phyllostachys aurea bamboo with coal. Energy Sources, Part A: Recovery, Utilization, and Environmental Effect 38, (2016), 1345-1354.

[359] A.M. Arias, P.L. Mores, N.J. Scenna, S.F. Mussati. Optimal design and sensitivity analysis of post-combustion CO_2 capture process by chemical absorption with amines. Journal of Cleaner Production 115, (2016), 315-331.

[360] X. Chen, G. Huang, G. C. An, Y. Yao, S. Zhao. Emerging N-nitrosamines and N- nitramines from Amine-based Post-combustion CO_2 Capture- A Review. Chemical Engineering Journal 335, (2017), 921-935.

[361] T. Voets, T. Kuppens, T. Cornelissen, T. Thewys. Economics of electricity and heat production by gasification or flash pyrolysis of short rotation coppices in Flanders (Belgium). Biomass Bioenergy 35, (2011), 1912-1924.

[362] M.F Zady, 2009. Z-5: Sum of squares, Variance, and the Standard Error of the Mean Basic Statistics. Clinical Laboratory Science Program. University of Louisville, Louisville Kentucky. Accessed on: 03/08/2018. Available online at: www. wstgard.com/lessen35.htm.

[363] ABS. Australian Bureau of Statistics, Labour Force Survey Standard Error, Datacube (2009) (Cat.no.6298.0.55.001). Available online at: http://.www.abs.gov.au

Appendix A: Dataset for ANN Predictive modelling in Chapter 6 of this thesis

Table 1: Input variables

C	H	N	S	O	MC	Ash	Tg	VM	LHV	ER	Reference
46.8	5.74	0.66	0.11	41.40	15.00	5.10	750	72.15	15.00	0.25	Yang et al.,
46.8	5.74	0.66	0.11	41.40	15.00	5.10	750	72.15	15.00	0.25	2018
35.42	4.62	0.47	0.18	31.28	12.2	15.83	800	60.01	16.38	0.32	
35.42	4.62	0.47	0.18	31.28	12.2	15.83	800	60.01	16.38	0.26	Pei et al., 2018
35.42	4.62	0.47	0.18	31.28	12.2	15.83	800	60.01	16.38	0.25	
35.42	4.62	0.47	0.18	31.28	12.2	15.83	800	60.01	16.38	0.26	
35.42	4.62	0.47	0.18	31.28	12.2	15.83	850	60.01	16.38	0.32	
35.42	4.62	0.47	0.18	31.28	12.2	15.83	850	60.01	16.38	0.26	
35.42	4.62	0.47	0.18	31.28	12.2	15.83	850	60.01	16.38	0.25	
35.42	4.62	0.47	0.18	31.28	12.2	15.83	850	60.01	16.38	0.26	
46.6	5.08	0.04	0.02	47.76	13.74	0.51	900	78.69	18.73	0.30	
46.6	5.08	0.04	0.02	47.76	13.74	0.51	900	78.69	18.73	0.30	Villetta et al.,
46.6	5.08	0.04	0.02	47.76	13.74	0.51	900	78.69	18.73	0.30	2018
46.6	5.08	0.04	0.02	47.76	13.74	0.51	900	78.69	18.73	0.30	
36.1	3.86	0.56	0.12	20.46	11.17	36.53	900	30.21	14.42	0.75	
36.1	3.86	0.56	0.12	20.46	11.17	36.53	1000	30.21	14.42	0.75	
36.1	3.86	0.56	0.12	20.46	11.17	36.53	1100	30.21	14.42	0.75	Rodrigues et al.,
36.1	3.86	0.56	0.12	20.46	11.17	36.53	1200	30.21	14.42	0.75	2018
36.1	3.86	0.56	0.12	20.46	11.17	36.53	900	30.21	14.42	0.75	
36.1	3.86	0.56	0.12	20.46	11.17	36.53	1000	30.21	14.42	0.75	
36.1	3.86	0.56	0.12	20.46	11.17	36.53	1100	30.21	14.42	0.75	
36.1	3.86	0.56	0.12	20.46	11.17	36.53	1200	30.21	14.42	0.75	
33.39	3.47	0.61	2.15	16.68	11.06	42.91	1100	20.291	12.85	0.10	
33.39	3.47	0.61	2.15	16.68	11.06	42.91	1100	20.291	12.85	0.2	
33.39	3.47	0.61	2.15	16.68	11.06	42.91	1100	20.291	12.85	0.60	
33.39	3.47	0.61	2.15	16.68	11.06	42.91	1100	20.291	12.85	0.20	Rodrigues et al.,
33.39	3.47	0.61	2.15	16.68	11.06	42.91	1100	20.291	12.85	0.40	2018
33.39	3.47	0.61	2.15	16.68	11.06	42.91	1100	20.291	12.85	0.60	
33.39	3.47	0.61	2.15	16.68	11.06	42.91	1100	20.291	12.85	0.20	
33.39	3.47	0.61	2.15	16.68	11.06	42.91	1100	20.291	12.85	0.40	
33.39	3.47	0.61	2.15	16.68	11.06	42.91	1100	20.291	12.85	0.60	
33.39	3.47	0.61	2.15	16.68	11.06	42.91	1100	20.291	12.85	0.20	
33.39	3.47	0.61	2.15	16.68	11.06	42.91	1100	20.291	12.85	0.40	
33.39	3.47	0.61	2.15	16.68	11.06	42.91	1100	20.291	12.85	0.60	
51.46	6.10	0.26	0.01	41.85	11.78	0.35	900	86.44	19.31	0.10	
51.46	6.10	0.26	0.01	41.85	11.78	0.35	900	86.44	19.31	0.20	
51.46	6.10	0.26	0.01	41.85	11.78	0.35	900	86.44	19.31	0.60	
51.46	6.10	0.26	0.01	41.85	11.78	0.35	900	86.44	19.31	0.20	
51.46	6.10	0.26	0.01	41.85	11.78	0.35	900	86.44	19.31	0.40	Rodrigues et al.,
51.46	6.10	0.26	0.01	41.85	11.78	0.35	900	86.44	19.31	0.60	2018
51.46	6.10	0.26	0.01	41.85	11.78	0.35	900	86.44	19.31	0.20	
51.46	6.10	0.26	0.01	41.85	11.78	0.35	900	86.44	19.31	0.40	
51.46	6.10	0.26	0.01	41.85	11.78	0.35	900	86.44	19.31	0.60	
51.46	6.10	0.26	0.01	41.85	11.78	0.35	900	86.44	19.31	0.20	
51.46	6.10	0.26	0.01	41.85	11.78	0.35	900	86.44	19.31	0.40	
51.46	6.10	0.26	0.01	41.85	11.78	0.35	900	86.44	19.31	0.60	
49.00	6.30	0.20	0.10	44.4	8.15	0.79	850	77.86	18.39	0.40	
49.00	6.30	0.20	0.10	44.4	8.15	0.79	850	77.86	18.39	0.40	
49.00	6.30	0.20	0.10	44.4	8.15	0.79	850	77.86	18.39	0.40	
49.00	6.30	0.20	0.10	44.4	8.15	0.79	850	77.86	18.39	0.40	

49.00	6.30	0.20	0.10	44.4	8.15	0.79	850	77.86	18.39	0.40	
49.00	6.30	0.20	0.10	44.4	8.15	0.79	850	77.86	18.39	0.40	De sales et al.
49.00	6.30	0.20	0.10	44.4	8.15	0.79	850	77.86	18.39	0.40	2017
49.00	6.30	0.20	0.10	44.4	8.15	0.79	850	77.86	18.39	0.40	
49.00	6.30	0.20	0.10	44.4	8.15	0.79	850	77.86	18.39	0.40	
49.00	6.30	0.20	0.10	44.4	8.15	0.79	850	77.86	18.39	0.40	
49.00	6.30	0.20	0.10	44.4	8.15	0.79	850	77.86	18.39	0.40	
49.00	6.30	0.20	0.10	44.4	8.15	0.79	850	77.86	18.39	0.40	
49.00	6.30	0.20	0.10	44.4	8.15	0.79	850	77.86	18.39	0.40	
49.00	6.30	0.20	0.10	44.4	8.15	0.79	850	77.86	18.39	0.40	
99.00	0.00	0.00	0.90	42.51	0.10	10.1	600	5.40	31.5	0.45	
99.00	0.00	0.00	0.90	42.51	0.10	10.1	750	5.40	31.5	0.45	
99.00	0.00	0.00	0.90	42.51	0.10	10.1	800	5.40	31.5	0.45	
99.00	0.00	0.00	0.90	42.51	0.10	10.1	850	5.40	31.5	0.45	
99.00	0.00	0.00	0.90	42.51	0.10	10.1	900	5.40	31.5	0.45	
85.81	13.86	0.12	0.06	0.00	0.02	0.15	700	99.81	38.04	0.30	
85.81	13.86	0.12	0.06	0.00	0.02	0.15	900	99.81	38.04	0.30	Konstantinou &
85.81	13.86	0.12	0.06	0.00	0.02	0.15	900	99.81	38.04	0.30	Marsh, 2015
85.81	13.86	0.12	0.06	0.00	0.02	0.15	900	99.81	38.04	0.30	
85.81	13.86	0.12	0.06	0.00	0.02	0.15	900	99.81	38.04	0.30	
51.81	5.76	0.26	0.36	30.32	0.00	5.98	700	82.28	21.31	0.60	
51.81	5.76	0.26	0.36	30.32	0.00	5.98	950	82.28	21.31	0.60	
51.81	5.76	0.26	0.36	30.32	0.00	5.98	950	82.28	21.31	0.60	He et al., 2009
51.81	5.76	0.26	0.36	30.32	0.00	5.98	950	82.28	21.31	0.60	
51.81	5.76	0.26	0.36	30.32	0.00	5.98	950	82.28	21.31	0.60	
51.81	5.76	0.26	0.36	30.32	0.00	5.98	950	82.28	21.31	0.60	
50.54	7.08	0.15	0.57	41.11	8.00	0.55	900	82.29	19.15	0.22	
50.54	7.08	0.15	0.57	41.11	8.00	0.55	900	82.29	19.15	0.25	He et al., 2009
50.54	7.08	0.15	0.57	41.11	8.00	0.55	900	82.29	19.15	0.24	
50.54	7.08	0.15	0.57	41.11	8.00	0.55	900	82.29	19.15	0.26	
50.54	7.08	0.15	0.57	41.11	8.00	0.55	900	82.29	19.15	0.25	
50.54	7.08	0.15	0.57	41.11	8.00	0.55	900	82.29	19.15	0.25	
50.54	7.08	0.15	0.57	41.11	8.00	0.55	900	82.29	19.15	0.25	
50.54	7.08	0.15	0.57	41.11	8.00	0.55	900	82.29	19.15	0.28	
50.54	7.08	0.15	0.57	41.11	8.00	0.55	900	82.29	19.15	0.27	LV et al., 2006
50.54	7.08	0.15	0.57	41.11	8.00	0.55	900	82.29	19.15	0.24	
50.54	7.08	0.15	0.57	41.11	8.00	0.55	900	82.29	19.15	0.27	
50.54	7.08	0.15	0.57	41.11	8.00	0.55	900	82.29	19.15	0.27	
50.54	7.08	0.15	0.57	41.11	8.00	0.55	900	82.29	19.15	0.27	
50.54	7.08	0.15	0.57	41.11	8.00	0.55	900	82.29	19.15	0.27	
50.54	7.08	0.15	0.57	41.11	8.00	0.55	900	82.29	19.15	0.27	
51.30	6.10	0.00	0.01	42.6	7.90	1.16	770	79.67	18.35	0.25	
51.30	6.10	0.00	0.01	42.6	7.90	1.16	770	79.67	18.35	0.25	
51.3	6.10	0.00	0.01	42.6	7.90	1.16	770	79.67	18.35	0.25	
43.43	5.95	0.97	0.13	45.01	6.17	5.93	700	75.95	17.75	0.18	
43.43	5.95	0.97	0.13	45.01	6.17	5.93	800	75.95	17.75	0.21	
43.43	5.95	0.97	0.13	45.01	6.17	5.93	800	75.95	17.75	0.24	
43.43	5.95	0.97	0.13	45.01	6.17	5.93	800	75.95	17.75	0.28	
43.43	5.95	0.97	0.13	45.01	6.17	5.93	800	75.95	17.75	0.32	
43.43	5.95	0.97	0.13	45.01	6.17	5.93	800	75.95	17.75	0.36	Rapagna et al.,
43.43	5.95	0.97	0.13	45.01	6.17	5.93	800	75.95	17.75	0.41	2000
52.84	5.37	0.59	0.49	41.01	10.12	5.40	690	84.48	16.88	0.40	
52.84	5.37	0.59	0.49	41.01	10.12	5.40	730	84.48	16.88	0.40	
52.84	5.37	0.59	0.49	41.01	10.12	5.40	750	84.48	16.88	0.40	Gai & Dong,
52.84	5.37	0.59	0.49	41.01	10.12	5.40	750	84.48	16.88	0.40	2012

52.84	5.37	0.59	0.49	41.01	10.12	5.40	750	84.48	16.88	0.40	
52.84	5.37	0.59	0.49	41.01	10.12	5.40	770	84.48	16.88	0.40	
52.84	5.37	0.59	0.49	41.01	10.12	5.40	690	84.48	16.88	0.35	
52.84	5.37	0.59	0.49	41.01	10.12	5.40	730	84.48	16.88	0.35	
52.84	5.37	0.59	0.49	41.01	10.12	5.40	750	84.48	16.88	0.35	
52.84	5.37	0.59	0.49	41.01	10.12	5.40	750	84.48	16.88	0.35	
52.84	5.37	0.59	0.49	41.01	10.12	5.40	750	84.48	16.88	0.35	Loha et al.,
52.84	5.37	0.59	0.49	41.01	10.12	5.40	770	84.48	16.88	0.35	2011
52.84	5.37	0.59	0.49	41.01	10.12	5.40	770	84.48	16.88	0.35	
52.84	5.37	0.59	0.49	41.01	10.12	5.40	770	84.48	16.88	0.35	
52.84	5.37	0.59	0.49	41.01	10.12	5.40	770	84.48	16.88	0.35	
52.84	5.37	0.59	0.49	41.01	10.12	5.40	770	84.48	16.88	0.35	
52.84	5.37	0.59	0.49	41.01	10.12	5.40	770	84.48	16.88	0.35	
36.42	5.40	5.50	1.90	31.5	9.50	29.70	800	51.8	14.86	0.25	
36.42	5.40	5.50	1.90	31.5	9.50	29.70	800	51.8	14.86	0.25	
44.20	6.10	2.10	1.00	42.5	8.50	6.30	950	42.5	17.63	0.25	
44.20	6.10	2.10	1.00	42.5	8.50	6.30	950	42.5	17.63	0.25	
48.90	5.90	0.57	0.57	33.2	8.69	10.37	700	69.83	16.14	0.20	
48.90	5.90	0.57	0.57	33.2	8.69	10.37	750	69.83	16.14	0.20	
48.90	5.90	0.57	0.57	33.2	8.69	10.37	800	69.83	16.14	0.20	
48.90	5.90	0.57	0.57	33.20	8.69	10.37	800	69.83	16.14	0.20	
48.90	5.90	0.57	0.57	33.20	8.69	10.37	800	69.83	16.14	0.20	
44.30	5.90	0.10	0.00	44.40	8.40	0.30	780	74.20	18.30	0.30	
44.30	5.90	0.10	0.00	44.40	8.40	0.30	780	74.20	18.30	0.30	
44.30	5.90	0.10	0.00	44.40	8.40	0.30	780	74.20	18.30	0.30	Ong et al., 2015
44.30	5.90	0.10	0.00	44.40	8.40	0.30	780	74.20	18.30	0.30	
44.30	5.90	0.10	0.00	44.40	8.40	0.30	780	74.20	18.30	0.3	
44.30	5.90	0.10	0.00	44.40	8.40	0.30	780	74.20	18.30	0.30	
35.70	1.90	4.60	0.00	38.20	4.80	19.52	650	69.83	13.20	0.30	Serrano et al.,
12.10	0.62	2.60	0.00	54.00	1.50	79.86	650	15.64	5.50	0.33	2016
38.45	2.97	0.49	0.07	36.36	9.95	19.52	650	14.99	14.70	0.25	
38.45	2.97	0.49	0.07	36.36	9.95	19.52	675	14.99	14.70	0.25	
38.45	2.97	0.49	0.07	36.36	9.95	19.52	700	14.99	14.70	0.25	
38.45	2.97	0.49	0.07	36.36	9.95	19.52	725	14.99	14.70	0.25	
38.45	2.97	0.49	0.07	36.36	9.95	19.52	600	14.99	14.70	0.35	Miccioa et al.,
38.45	2.97	0.49	0.07	36.36	9.95	19.52	650	14.99	14.70	0.35	2009
38.45	2.97	0.49	0.07	36.36	9.95	19.52	700	14.99	14.70	0.35	
38.45	2.97	0.49	0.07	36.36	9.95	19.52	725	14.99	14.70	0.35	
38.45	2.97	0.49	0.07	36.36	9.95	19.52	750	14.99	14.70	0.35	
38.45	2.97	0.49	0.07	36.36	9.95	19.52	600	14.99	14.70	0.45	
38.45	2.97	0.49	0.07	36.36	9.95	19.52	650	14.99	14.70	0.45	
38.45	2.97	0.49	0.07	36.36	9.95	19.52	700	14.99	14.70	0.45	Thakkar et al.,
38.45	2.97	0.49	0.07	36.36	9.95	19.52	725	14.99	14.70	0.45	2016
38.45	2.97	0.49	0.07	36.36	9.95	19.52	800	14.99	14.70	0.45	
38.45	2.97	0.49	0.07	36.36	9.95	19.52	650	14.99	14.70	0.25	Karmakar et al.,
38.45	2.97	0.49	0.07	36.36	9.95	19.52	675	14.99	14.70	0.25	2013
38.45	2.97	0.49	0.07	36.36	9.95	19.52	700	14.99	14.7	0.25	
38.45	2.97	0.49	0.07	36.36	9.95	19.52	725	14.99	14.70	0.25	
38.45	2.97	0.49	0.07	36.36	9.95	19.52	600	14.99	14.70	0.35	
38.45	2.97	0.49	0.07	36.36	9.95	19.52	650	14.99	14.70	0.35	
38.45	2.97	0.49	0.07	36.36	9.95	19.52	700	14.99	14.70	0.35	
38.45	2.97	0.49	0.07	36.36	9.95	19.52	725	14.99	14.70	0.35	
38.45	2.97	0.49	0.07	36.36	9.95	19.52	750	14.99	14.70	0.35	
38.45	2.97	0.49	0.07	36.36	9.95	19.52	600	14.99	14.70	0.45	
38.45	2.97	0.49	0.07	36.36	9.95	19.52	650	14.99	14.70	0.45	

38.45	2.97	0.49	0.07	36.36	9.95	19.52	700	14.99	14.70	0.45	
38.45	2.97	0.49	0.07	36.36	9.95	19.52	725	14.99	14.70	0.45	
38.45	2.97	0.49	0.07	36.36	9.95	19.52	800	14.99	14.70	0.45	
38.45	2.97	0.49	0.07	36.36	9.95	19.52	650	55.54	14.70	0.45	
38.45	2.97	0.49	0.07	36.36	9.95	19.52	690	55.54	14.70	0.45	
38.45	2.97	0.49	0.07	36.36	9.95	19.52	730	55.54	14.70	0.45	
38.45	2.97	0.49	0.07	36.36	9.95	19.52	770	55.54	14.70	0.45	
38.45	2.97	0.49	0.07	36.36	9.95	19.52	750	55.54	14.70	0.45	
38.45	2.97	0.49	0.07	36.36	9.95	19.52	750	55.54	14.70	0.45	
38.45	2.97	0.49	0.07	36.36	9.95	19.52	750	55.54	14.70	0.45	
38.45	2.97	0.49	0.07	36.36	9.95	19.52	750	55.54	14.70	0.45	
47.18	3.60	1.01	0.01	48.20	13.63	6.00	880	73.40	16.15	0.30	
47.18	3.60	1.01	0.01	48.20	13.63	6.00	880	73.40	16.15	0.30	
47.18	3.60	1.01	0.01	48.20	13.63	6.00	880	73.40	16.15	0.30	
47.18	3.60	1.01	0.01	48.20	13.63	6.00	880	73.40	16.15	0.30	
47.18	3.60	1.01	0.01	48.20	13.63	6.00	880	73.40	16.15	0.30	
47.18	3.60	1.01	0.01	48.20	13.63	6.00	880	73.40	16.15	0.30	
47.18	3.60	1.01	0.01	48.2	13.63	6.00	880	73.4	16.15	0.30	
47.18	3.60	1.01	0.01	48.2	13.63	6.00	880	73.4	16.15	0.30	
47.18	3.60	1.01	0.01	48.2	13.63	6.00	880	73.4	16.15	0.30	
47.18	3.60	1.01	0.01	48.2	13.63	6.00	880	73.4	16.15	0.30	
47.18	3.60	1.01	0.01	48.2	13.63	6.00	880	73.4	16.15	0.30	
47.18	3.60	1.01	0.01	48.2	13.63	6.00	880	73.4	16.15	0.30	
47.18	3.60	1.01	0.01	48.2	13.63	6.00	880	73.4	16.15	0.30	
47.18	3.60	1.01	0.01	48.2	13.63	6.00	880	73.4	16.15	0.30	
47.18	3.60	1.01	0.01	48.2	13.63	6.00	880	73.4	16.15	0.30	
47.18	3.60	1.01	0.01	48.2	13.63	6.00	880	73.4	16.15	0.30	Subramanian, et al., 2011
47.18	3.60	1.01	0.01	48.2	13.63	6.00	880	73.4	16.15	0.30	
47.18	3.60	1.01	0.01	48.2	13.63	6.00	880	73.4	16.15	0.30	
38.92	5.10	2.17	0.12	53.69	8.10	19.33	880	63.8	15.81	0.40	
38.92	5.10	2.17	0.12	53.69	8.10	19.33	880	63.8	15.81	0.40	
38.92	5.10	2.17	0.12	53.69	8.10	19.33	880	63.8	15.81	0.40	
38.92	5.10	2.17	0.12	53.69	8.10	19.33	880	63.8	15.81	0.40	
38.92	5.10	2.17	0.12	53.69	8.10	19.33	880	63.8	15.81	0.40	
38.92	5.10	2.17	0.12	53.69	8.10	19.33	880	63.8	15.81	0.40	
38.92	5.10	2.17	0.12	53.69	8.10	19.33	880	63.8	15.81	0.40	
38.92	5.10	2.17	0.12	53.69	8.10	19.33	880	63.8	15.81	0.40	
38.92	5.10	2.17	0.12	53.69	8.10	19.33	880	63.8	15.81	0.40	
38.92	5.10	2.17	0.12	53.69	8.10	19.33	880	63.8	15.81	0.40	
38.92	5.10	2.17	0.12	53.69	8.10	19.33	880	63.8	15.81	0.40	
38.92	5.10	2.17	0.12	53.69	8.10	19.33	880	63.8	15.81	0.40	
38.92	5.10	2.17	0.12	53.69	8.10	19.33	880	63.8	15.81	0.40	
38.92	5.10	2.17	0.12	53.69	8.10	19.33	880	63.8	15.81	0.40	
38.92	5.10	2.17	0.12	53.69	8.10	19.33	880	63.8	15.81	0.40	
38.92	5.10	2.17	0.12	53.69	8.10	19.33	880	63.8	15.81	0.40	Subramanian, et al., 2011
38.92	5.10	2.17	0.12	53.69	8.10	19.33	880	63.8	15.81	0.40	
51.33	6.13	0.12	0.02	41.97	9.30	1.80	880	77.76	15.81	0.50	
51.33	6.13	0.12	0.02	41.97	9.30	1.80	880	77.76	17.62	0.50	
51.33	6.13	0.12	0.02	41.97	9.30	1.80	880	77.76	17.62	0.50	
51.33	6.13	0.12	0.02	41.97	9.30	1.80	880	77.76	17.62	0.50	
51.33	6.13	0.12	0.02	41.97	9.30	1.80	880	77.76	17.62	0.50	
51.33	6.13	0.12	0.02	41.97	9.30	1.80	880	77.76	17.62	0.50	
51.33	6.13	0.12	0.02	41.97	9.30	1.80	880	77.76	17.62	0.50	
51.33	6.13	0.12	0.02	41.97	9.30	1.80	880	77.76	17.62	0.50	
51.33	6.13	0.12	0.02	41.97	9.30	1.80	880	77.76	17.62	0.50	

51.33	6.13	0.12	0.02	41.97	9.30	1.80	880	77.76	17.62	0.50	
51.33	6.13	0.12	0.02	41.97	9.30	1.80	880	77.76	17.62	0.50	
51.33	6.13	0.12	0.02	41.97	9.30	1.80	880	77.76	17.62	0.50	
51.33	6.13	0.12	0.02	41.97	9.30	1.80	880	77.76	17.62	0.50	
51.33	6.13	0.12	0.02	41.97	9.30	1.80	880	77.76	17.62	0.50	
51.33	6.13	0.12	0.02	41.97	9.30	1.80	880	77.76	17.62	0.50	
51.33	6.13	0.12	0.02	41.97	9.30	1.80	880	77.76	17.62	0.50	
51.33	6.13	0.12	0.02	41.97	9.30	1.80	880	77.76	17.62	0.50	
51.33	6.13	0.12	0.02	41.97	9.30	1.80	880	77.76	17.62	0.50	Subramanian, et
37.6	5.42	0.38	0.03	36.56	0.00	20.00	665	13.6	14.22	0.25	al., 2011
37.6	5.42	0.38	0.03	36.56	0.00	20.00	744	13.6	14.22	0.30	
37.6	5.42	0.38	0.03	36.56	0.00	20.00	811	13.6	14.22	0.35	
37.6	5.42	0.38	0.03	36.56	0.00	20.00	670	13.6	14.22	0.25	
37.6	5.42	0.38	0.03	36.56	0.00	20.00	750	13.60	14.22	0.30	
37.6	5.42	0.38	0.03	36.56	0.00	20.00	822	13.60	14.22	0.35	
37.6	5.42	0.38	0.03	36.56	0.00	20.00	700	13.60	14.22	0.25	
37.6	5.42	0.38	0.03	36.56	0.00	20.00	766	13.60	14.22	0.30	
37.6	5.42	0.38	0.03	36.56	0.00	20.00	828	13.60	14.22	0.35	
77.58	4.30	0.22	0.05	17.88	6.20	2.70	975	91.10	15.38	0.25	
77.58	4.30	0.22	0.05	17.88	6.20	2.70	975	91.10	15.38	0.25	
77.58	4.30	0.22	0.05	17.88	6.20	2.70	975	91.10	15.38	0.25	
77.58	4.30	0.22	0.05	17.88	6.20	2.70	975	91.10	15.38	0.25	
77.58	4.30	0.22	0.05	17.88	6.20	2.70	975	91.10	15.38	0.25	
77.58	4.30	0.22	0.05	17.88	6.20	2.70	975	91.10	15.38	0.25	
77.58	4.30	0.22	0.05	17.88	6.20	2.70	975	91.10	15.38	0.25	
77.58	4.30	0.22	0.05	17.88	6.20	2.70	975	91.10	15.38	0.25	
77.58	4.30	0.22	0.05	17.88	6.20	2.70	975	91.10	15.38	0.25	Mansaray et al.,
77.58	4.30	0.22	0.05	17.88	6.20	2.70	975	91.10	15.38	0.25	1999
77.58	4.30	0.22	0.05	17.88	6.20	2.70	975	91.10	15.38	0.25	
77.58	4.30	0.22	0.05	17.88	6.20	2.70	975	91.10	15.38	0.25	
77.58	4.30	0.22	0.05	17.88	6.20	2.70	975	91.10	15.38	0.25	
77.58	4.30	0.22	0.05	17.88	6.20	2.70	975	91.10	15.38	0.25	
77.58	4.30	0.22	0.05	17.88	6.20	2.70	975	91.10	15.38	0.25	
77.58	4.30	0.22	0.05	17.88	6.20	2.70	975	91.10	15.38	0.25	
77.58	4.30	0.22	0.05	17.88	6.20	2.70	975	91.10	15.38	0.25	
45.40	6.50	0.70	0.30	24.20	9.10	20.40	849	0.00	18.60	0.26	
45.40	6.50	0.70	0.30	24.20	9.10	20.40	852	0.00	18.60	0.26	Salam &
45.40	6.50	0.70	0.30	24.20	9.10	20.40	869	0.00	18.60	0.27	Bhattacharya,
45.40	6.50	0.70	0.30	24.2	9.10	20.40	879	0.00	18.00	0.30	2006
45.40	6.50	0.70	0.30	24.2	9.10	20.40	898	0.00	18.60	0.32	
45.40	6.50	0.70	0.30	24.2	9.10	20.40	932	0.00	18.60	0.33	
79.34	5.72	1.20	0.66	48.9	9.80	4.50	849	15	14.00	0.20	
37.60	5.42	0.38	0.03	36.56	0.00	20.00	665	66.40	13.55	0.25	
37.60	5.42	0.38	0.03	36.56	0.00	20.00	744	66.40	13.55	0.30	
37.60	5.42	0.38	0.03	36.56	0.00	20.00	811	66.40	13.55	0.35	
37.60	5.42	0.38	0.03	36.56	0.00	20.00	670	66.40	13.55	0.25	
37.60	5.42	0.38	0.03	36.56	0.00	20.00	750	66.40	13.55	0.30	
37.60	5.42	0.38	0.03	36.56	0.00	20.00	822	66.40	13.55	0.35	
37.60	5.42	0.38	0.03	36.56	0.00	20.00	700	66.40	13.55	0.25	
37.60	5.42	0.38	0.03	36.56	0.00	20.00	766	66.40	13.55	0.30	
37.60	5.42	0.38	0.03	36.56	0.00	20.00	828	66.40	13.55	0.35	
44.48	6.49	0.73	0.07	48.23	8.48	1.23	702	75.23	17.88	0.28	
44.48	6.49	0.73	0.07	48.23	8.48	1.23	760	75.23	17.88	0.28	
44.48	6.49	0.73	0.07	48.23	8.48	1.23	846	75.23	17.88	0.28	
49.42	7.82	0.12	0.06	42.49	8.61	1.02	702	76.50	18.21	0.28	

49.42	7.82	0.12	0.06	42.49	8.61	1.02	760	76.50	18.21	0.28	
49.42	7.82	0.12	0.06	42.49	8.61	1.02	846	76.50	18.21	0.28	Arena &
49.42	7.82	0.12	0.06	42.49	8.61	1.02	846	76.50	18.21	0.28	Gregorio, 2014.
49.42	7.82	0.12	0.06	42.49	8.61	1.02	846	76.50	18.21	0.28	
49.42	7.82	0.12	0.06	42.49	8.61	1.02	846	76.50	18.21	0.28	
50.54	6.14	0.96	0.03	42.59	6.30	0.50	755	93.20	17.10	0.20	
50.54	6.14	0.96	0.03	42.59	6.30	0.50	840	93.20	17.10	0.22	
50.54	6.14	0.96	0.03	42.59	6.30	0.50	755	93.20	17.10	0.45	
50.54	6.14	0.96	0.03	42.59	6.30	0.50	840	93.20	17.10	0.23	Lahijani et al.,
50.54	6.14	0.96	0.03	42.59	6.30	0.50	755	93.20	17.10	0.42	2011
50.54	6.14	0.96	0.03	42.59	6.30	0.50	840	93.20	17.10	0.32	Mansaray et al.,
50.54	6.14	0.96	0.03	42.59	6.30	0.50	755	93.20	17.10	0.60	1999
50.54	6.14	0.96	0.03	42.59	6.30	0.50	840	93.20	17.10	0.31	
50.54	6.14	0.96	0.03	42.59	6.30	0.50	755	93.20	17.10	0.58	
50.54	6.14	0.96	0.03	42.59	6.30	0.50	840	93.20	17.10	0.33	
50.54	6.14	0.96	0.03	42.59	6.30	0.50	755	93.20	17.10	0.56	
50.54	6.14	0.96	0.03	42.59	6.30	0.50	840	93.20	17.10	0.31	
50.54	6.14	0.96	0.03	42.59	6.30	0.50	755	93.20	17.10	0.61	
50.54	6.14	0.96	0.03	42.59	6.30	0.50	840	93.20	17.10	0.10	
50.54	6.14	0.96	0.03	42.59	6.30	0.50	755	93.20	17.10	0.29	
50.54	6.14	0.96	0.03	42.59	6.30	0.50	840	93.20	17.10	0.36	Hu et al., 2016
50.54	6.14	0.96	0.03	42.59	6.30	0.50	755	93.20	17.10	0.54	
50.54	6.14	0.96	0.03	42.59	6.30	0.50	840	93.20	17.10	0.57	
50.54	6.14	0.96	0.03	42.59	6.30	0.50	755	93.20	17.10	0.30	
50.54	6.14	0.96	0.03	42.59	6.30	0.50	840	93.20	17.10	0.56	
41.82	6.07	0.77	0.14	50.3	10.4	7.90	740	64.40	16.36	0.36	
41.82	6.07	0.77	0.14	50.3	10.4	7.90	700	64.40	16.36	0.36	
41.82	6.07	0.77	0.14	50.3	10.4	7.90	740	64.40	16.36	0.36	
41.82	6.07	0.77	0.14	50.30	10.40	7.90	700	64.40	16.36	0.36	
41.82	6.07	0.77	0.14	50.30	10.40	7.90	740	64.40	16.36	0.36	Campoy et al.,
41.82	6.07	0.77	0.14	50.30	10.40	7.90	700	64.40	16.36	0.36	2009
35.42	4.62	0.47	0.18	31.38	12.20	15.83	620	60.01	16.38	0.18	
35.42	4.62	0.47	0.18	31.38	12.20	15.83	720	60.01	16.38	0.20	
35.42	4.62	0.47	0.18	31.38	12.20	15.83	620	60.01	16.38	0.21	
35.42	4.62	0.47	0.18	31.38	12.20	15.83	720	60.01	16.38	0.20	
35.42	4.62	0.47	0.18	31.38	12.20	15.83	850	60.01	16.38	0.32	
35.42	4.62	0.47	0.18	31.38	12.20	15.83	850	60.01	16.38	0.26	
35.42	4.62	0.47	0.18	31.38	12.20	15.83	850	60.01	16.38	0.25	
35.42	4.62	0.47	0.18	31.38	12.20	15.83	850	60.01	16.38	0.26	
44.42	3.80	0.89	0.50	13.9	7.80	33.50	800	24.50	17.40	0.00	
42.18	5.70	1.59	0.50	27.54	7.80	33.50	800	24.50	15.70	1.00	
											George et al., 2018

	Pei et al., 2018 Thengane et al., 2019

Table 2: Output dataset (Output variables)

CO	H_2	CH_4	CO_2	LHV	Gas yield	CGE	CCE	Reference
38.30	36	0.40	23.50	4.00	1.50	81.40	52.11	Yang et al., 2018
38.30	35.8	0.60	23.50	4.00	1.30	83.10	31.71	
18.50	6.10	5.80	13.7	5.10	1.17	34.99	67.24	Pei et al., 2018
18.90	5.70	6.80	13.4	5.40	1.29	40.86	76.29	
21.70	6.90	5.40	11.9	5.40	1.44	45.61	84.94	
16.10	6.00	6.30	14.4	4.90	1.24	35.64	69.02	
12.90	11.00	0.60	9.10	3.00	2.75	48.39	94.00	
13.90	12.30	1.20	8.90	3.50	2.62	53.78	95.10	
15.50	13.70	13.70	8.20	3.70	2.7	58.59	152.73	
35.80	19.10	19.10	5.80	6.70	1.90	74.66	174.43	
12.50	11.80	1.00	8.50	3.27	2.22	36.55	56.11	Villetta et al., 2018
14.10	13.40	1.20	9.50	3.72	2.16	40.56	61.70	
14.200	14.00	1.50	10.40	3.91	2.29	45.12	68.73	
15.10	14.10	1.50	10.20	4.03	2.10	42.67	64.75	
21.50	10.60	0.00	5.51	4.31	0.66	44.00	28.60	Rodrigues et al., 2018
23.10	12.20	0.00	8.64	6.26	0.96	53.40	42.62	
24.10	13.80	0.00	6.03	9.12	1.34	55.90	44.85	
23.60	14.60	0.00	6.77	9.37	1.44	66.10	45.53	
28.10	13.30	0.00	3.29	13.70	1.76	75.90	45.40	
22.00	14.50	0.00	8.15	7.79	1.27	60.70	46.00	
21.80	14.90	0.00	7.54	8.03	1.32	66.80	44.91	
21.50	13.70	0.00	8.35	6.84	1.12	56.50	38.50	
28.10	22.40	0.03	0.17	3.76	0.59	50.20	26.79	Rodrigues et al., 2018
31.10	19.00	0.01	0.39	4.85	0.68	58.40	34.37	
11.60	4.920	0.00	10.5	2.85	0.59	24.90	20.92	
27.7	22.8	0.00	3.39	4.33	0.79	75.30	39.41	
16.9	12.3	0.00	7.83	3.34	0.70	48.40	27.77	
9.16	5.89	0.00	11.30	2.19	0.62	26.50	20.35	
21.10	23.40	0.00	6.47	3.32	0.82	82.90	36.27	
12.80	12.80	0.00	9.42	2.51	0.71	51.50	25.31	
6.81	6.13	0.00	11.9	1.59	0.61	36.70	18.31	
10.8	20.50	0.00	9.41	1.74	0.78	95.40	25.29	
6.26	10.90	0.00	10.60	1.21	0.65	52.70	17.58	
2.74	4.42	0.00	11.70	0.62	0.53	20.80	12.28	
38.7	33.20	0.00	0.12	9.82	1.46	90.50	59.00	Rodrigues et al., 2018
39.40	27.60	0.00	0.58	11.90	1.63	100.00	67.84	
13.30	7.23	0.00	11.20	6.54	1.27	38.00	32.39	
34.80	28.30	0.00	2.88	10.00	1.67	104.10	65.51	
21.00	15.20	0.00	7.97	7.87	147	68.20	44.33	
11.80	7.59	0.00	11.7	5.45	1.28	39.40	31.31	
29.90	28.1	0.00	5.09	8.24	1.67	105.40	60.83	

18.00	15.20	0.00	9.18	6.39	1.45	67.50	41.03	
9.93	7.01	0.00	12.30	4.31	1.26	37.60	29.15	
19.70	25.70	0.00	8.77	5.01	1.54	97.50	45.64	
11.30	13.40	0.00	11.20	3.63	1.30	56.50	30.45	
15.36	5.73	0.00	13.20	2.09	1.08	25.60	32.11	
17.80	17.00	1.40	4.00	4.61	0.811	18.93	17.01	De sales et al. 2017
15.40	16.2	1.60	4.00	4.27	0.95	20.49	17.61	
21.00	16.00	1.70	4.00	5.02	1.08	27.44	26.78	
12.20	19.00	1.60	4.00	4.22	0.81	17.33	12.23	
8.70	21.00	1.40	4.00	3.89	0.95	18.67	10.46	
8.30	18.00	1.60	4.00	3.59	1.08	19.62	11.68	
7.20	19.00	1.60	4.00	3.52	0.81	14.45	7.80	
12.80	18.00	1.70	4.00	4.20	0.95	20.15	15.02	
11.10	20.00	1.70	4.00	4.20	1.08	22.96	15.10	
23.20	34.10	3.50	4.00	7.90	0.17	6.81	4.97	
20.80	34.70	3.20	4.00	7.66	0.20	7.71	5.21	
24.30	27.40	5.40	4.00	7.96	0.23	9.15	7.37	
17.80	32.60	3.60	4.00	7.07	0.17	6.10	3.98	
24.80	33.00	4.50	4.00	8.35	0.20	8.40	6.36	
18.00	33.3	3.40	4.00	7.13	0.23	8.20	5.31	
11.80	30.2	0.50	4.00	4.90	3.90	16.00	29.10	Konstantinou & Marsh,
12.30	49.1	1.90	4.00	7.50	7.20	25.10	62.02	2015
17.40	42.1	2.90	4.00	7.80	7.50	25.20	92.37	
12.90	38.9	2.80	4.00	6.80	6.10	24.40	58.10	
11.90	34.7	3.10	4.00	6.40	5.70	20.60	53.38	
20.33	16.92	21.44	35.28	12.44	1.22	39.9	67.87	
21.53	21.31	18.91	32.46	12.15	1.31	41.83	69.00	He et al., 2009
22.83	28.94	14.87	27.91	11.67	1.47	45.09	70.22	
25.87	34.96	34.96	21.84	11.36	1.81	54.07	80.68	
27.37	36.98	36.98	20.78	11.31	2.04	60.67	86.54	
9.34	27.01	20.30	35.25	14.44	0.74	49.58	62.05	
11.16	34.70	17.89	30.86	13.47	0.85	52.58	62.13	He et al., 2009
12.65	40.64	15.57	26.61	12.62	0.98	55.49	64.74	
13.46	45.60	12.24	24.23	11.74	1.12	57.74	68.18	
14.85	48.63	9.62	23.59	10.74	1.28	63.52	72.37	
16.92	53.29	5.76	22.05	9.36	1.48	68.36	74.51	
29.56	31.40	6.23	30.02	5.44	0.91	24.10	63.48	
24.59	28.44	6.50	36.41	5.04	0.88	21.59	62.96	LV et al., 2006
25.53	28.93	6.82	34.88	4.76	0.82	19.00	58.44	
25.2	29.16	8.21	34.36	5.05	0.85	20.90	61.06	
27.92	35.39	4.36	30.11	5.17	0.94	23.66	62.16	
28.77	31.88	5.54	31.76	4.78	0.91	21.18	63.73	
27.52	31.47	5.70	33.39	4.60	0.88	19.71	62.13	
25.81	31.17	6.01	33.32	4.82	0.86	20.18	59.38	
25.2	29.16	8.21	34.36	5.05	0.85	20.90	61.06	
25.07	27.12	9.02	35.62	5.26	0.78	19.97	57.64	
36.85	26.42	3.52	31.96	9.04	1.50	66.02	115.00	
39.21	30.51	3.29	25.75	9.88	1.62	77.92	117.20	
38.66	28.58	6.01	24.45	11.11	1.42	76.81	104.04	
42.65	29.91	3.58	22.29	10.37	1.24	62.60	90.06	
37.65	27.17	4.78	28.89	9.75	1.32	62.66	99.79	
33.20	43.60	11.5	11.7	13.01	1.10	77.99	64.79	
24.00	55.50	6.40	14.1	10.94	1.90	113.28	88.29	Rapagna et al., 2000
23.00	52.20	7.90	19.9	11.37	1.70	105.34	90.18	
11.35	6.11	1.27	23.93	2.69	1.35	21.17	60.30	
13.55	8.23	1.84	20.37	3.32	1.47	28.46	64.24	Gai & Dong, 2012

16.72	10.92	2.98	16.48	4.43	1.62	41.85	71.62	
18.99	12.78	3.96	13.11	5.30	1.81	55.94	79.76	
14.81	13.51	3.72	11.58	5.39	2.14	67.26	78.74	
17.97	12.26	3.65	13.82	4.99	2.53	73.61	109.57	
15.16	10.58	1.57	18.41	3.69	2.86	61.54	122.81	
14.30	50.50	8.60	26.60	6.80	1.68	90.79	62.60	
16.30	52.20	7.90	23.50	6.60	1.85	96.34	66.90	Loha et al., 2011
23.70	49.50	5.60	21.20	5.60	1.43	78.84	43.88	
17.75	52.90	7.40	22.25	6.90	2.43	85.65	91.87	
16.40	52.90	7.80	22.9	5.20	2.75	79.44	78.36	
18.00	54.40	7.70	19.40	6.20	2.82	138.85	95.80	
12.99	48.76	7.03	31.21	6.60	1.94	86.42	70.16	
15.45	50.71	5.06	28.74	6.90	1.88	57.53	71.08	
20.59	50.37	4.02	25.01	6.40	1.96	80.59	68.73	
16.64	51.43	4.28	27.65	6.10	1.84	84.66	61.50	
13.50	52.26	4.50	29.74	5.00	2.78	78.72	76.16	
17.72	52.00	3.62	26.66	6.80	2.15	80.56	80.11	
16.26	48.40	6.46	28.88	6.50	2.88	67.21	102.58	
18.94	50.14	4.60	26.33	6.20	2.15	90.15	73.04	
24.22	49.64	3.62	22.52	6.50	1.90	93.66	67.67	
20.15	50.76	3.82	25.22	5.50	1.87	99.87	56.36	
16.78	51.67	4.08	27.47	5.60	1.85	97.61	56.77	
21.28	51.24	3.25	24.25	6.90	2.55	93.55	96.41	
17.10	17.30	11.90	1.70	4.70	2.73	66.9	71.28	
15.90	17.10	12.20	2.00	4.60	2.52	66.2	64.40	Ong et al., 2015
15.60	16.80	12.70	2.10	4.50	1.83	45.75	45.75	
12.00	13.40	12.50	1.80	3.60	1.96	39.2	39.20	
10.01	13.38	5.33	17.37	5.80	2.54	83.09	83.09	
15.05	16.51	4.89	16.77	5.97	2.15	72.39	72.39	Serrano et al., 2016
10.68	12.62	4.88	16.98	6.24	2.19	77.08	77.08	
13.89	13.64	5.29	16.83	6.66	2.51	94.28	94.28	
16.71	16.26	4.87	16.56	6.81	2.66	102.17	102.17	
15.2	20.2	4.70	16.4	6.89	1.12	41.71	44.18	
16.4	19.8	4.9	15.9	5.69	1.14	35.06	46.08	Miccioa et al., 2009
13.8	20.3	4.40	16.9	5.22	1.02	28.78	38.90	
11.7	22.8	4.10	17.7	6.54	1.01	35.70	36.77	
16.7	28.7	2.02	14.5	6.86	1.14	42.27	41.15	
17.60	30.3	1.49	14.3	6.44	1.21	42.12	43.90	
15.20	2.70	3.10	9.30	5.16	1.89	59.0	85.00	
14.20	2.50	2.70	10.90	5.22	1.98	57.0	88.00	Thakkar et al., 2016
26.02	18.71	1.96	13.91	6.38	1.09	49.28	71.51	
27.03	19.18	1.53	13.14	6.44	1.12	51.07	72.44	Karmakar et al., 2013
27.84	19.49	1.19	12.47	6.46	1.16	53.09	74.07	
28.56	19.69	0.92	11.91	6.50	1.19	54.82	75.82	
16.15	13.82	2.32	18.74	5.13	1.18	42.84	73.43	
18.46	14.78	1.39	16.94	5.19	1.25	46.94	77.77	
20.18	15.18	0.82	15.62	5.24	1.32	48.94	82.68	
20.86	15.24	0.63	15.10	5.26	1.43	53.24	83.91	
21.48	15.22	0.63	14.64	5.28	1.46	54.62	85.43	
10.93	9.89	0.48	21.56	3.53	1.32	33.00	75.46	
12.88	10.47	1.62	20.06	3.61	1.39	35.58	80.20	
14.35	11.10	0.94	18.46	3.69	1.44	37.65	84.17	
14.95	11.54	0.53	17.51	3.77	1.48	39.48	88.57	
16.39	11.14	0.40	16.44	3.86	1.52	41.55	92.83	
24.84	17.22	0.17	40.4	6.38	1.09	49.28	71.51	
25.04	17.93	2.46	40.29	6.44	1.12	51.07	72.44	

25.31	18.12	2.38	40.63	6.46	1.16	53.09	74.07	
26.59	18.49	1.96	40.35	6.50	1.19	54.82	75.82	
17.48	14.13	2.79	45.67	5.13	1.18	42.84	73.43	
20.63	14.22	1.92	45.59	5.19	1.25	46.94	77.77	
20.47	14.63	1.32	44.91	5.24	1.32	48.94	82.68	
22.89	15.88	1.43	46.18	5.26	1.43	53.24	83.91	
22.24	16.08	1.46	46.12	5.28	1.46	54.62	85.43	
11.72	8.92	1.32	54.15	3.53	1.32	33.00	75.46	
13.47	9.32	1.39	53.41	3.61	1.39	35.58	80.20	
15.13	10.15	1.44	52.09	3.69	1.44	37.65	84.17	
16.61	10.27	1.48	51.16	3.77	1.48	39.48	88.57	
17.78	10.22	1.52	50.53	3.86	1.52	41.55	92.83	
11.25	42.25	9.60	31.9	11.28	1.03	62.99	84.10	
12.83	50.50	8.16	28.51	11.23	1.12	68.78	85.82	
15.90	52.20	6.25	25.65	11.16	1.16	65.58	85.83	
17.85	53.08	5.17	23.90	11.09	1.21	66.06	87.88	
27.48	47.81	6.62	19.09	12.21	1.05	65.75	86.33	
22.7	48.88	6.22	22.20	11.59	1.09	65.96	86.25	
19.65	51.17	6.03	23.19	11.42	1.16	66.1	87.68	
17.38	51.89	5.92	14.81	11.18	1.21	66.15	90.11	
8.71	8.49	1.52	14.62	2.65	1.98	30.47	55.87	
9.26	7.89	1.36	14.88	2.58	2.02	30.26	58.49	Subramanian, et al., 2011
10.12	9.54	1.89	12.12	3.08	2.26	40.42	61.92	
10.28	10.17	1.53	11.63	3.04	2.18	38.49	58.02	
11.53	10.55	2.67	11.58	3.67	2.21	47.10	64.69	
12.57	10.61	3.82	11.05	4.23	2.32	56.99	72.28	
8.24	7.54	1.08	15.61	2.31	2.24	30.05	63.41	
9.21	8.62	1.59	15.22	2.75	2.12	33.86	62.64	
10.52	8.79	1.32	14.17	2.82	2.24	36.68	66.16	
11.12	9.53	2.54	12.83	3.44	2.68	53.54	80.61	
10.91	10.46	2.50	11.69	3.52	2.52	51.51	71.82	
12.68	10.57	3.60	11.83	4.16	2.69	64.98	85.86	
6.54	5.62	1.91	16.24	2.18	2.73	34.56	76.53	
8.94	6.87	1.21	15.48	2.36	3.14	43.03	91.38	
8.31	7.23	1.86	14.32	2.57	2.83	42.23	78.70	
10.52	9.61	1.33	13.67	2.93	3.24	55.13	93.89	
11.61	9.78	2.42	13.14	3.49	2.9	58.77	89.47	
12.47	9.64	2.91	12.68	4.14	2.84	68.29	90.49	
10.54	6.18	1.04	15.24	2.40	1.86	27.83	68.67	
11.26	7.54	1.25	14.31	2.73	2.14	36.42	79.00	Subramanian, et al., 2011
10.12	6.09	1.49	12.87	2.51	1.79	28.01	60.31	
14.67	7.46	2.88	12.19	3.75	2.18	50.97	89.24	
15.42	8.59	3.21	11.68	4.10	2.25	57.51	93.87	
19.55	8.62	3.24	10.21	4.61	2.31	66.39	104.93	
10.11	5.54	1.08	16.28	2.29	2.23	31.84	84.32	
9.87	6.65	1.27	15.44	2.47	2.37	36.50	86.71	
10.53	6.78	1.66	13.89	2.71	2.31	39.03	82.92	
12.64	6.59	2.26	12.17	3.16	2.49	49.05	92.78	
14.78	7.42	2.01	10.66	3.43	2.56	54.74	96.73	
16.13	7.77	2.78	10.68	3.92	2.57	62.81	104.67	
9.32	5.34	1.03	17.14	2.15	2.18	29.22	82.45	
10.24	5.88	1.19	16.82	2.39	2.35	35.02	91.38	
10.11	6.65	1.57	15.96	2.61	2.42	39.38	92.07	
12.57	7.49	1.62	14.56	3.02	2.57	48.39	101.70	
15.48	7.12	1.71	12.92	3.36	2.68	56.14	111.07	
15.29	7.42	2.06	11.76	3.51	2.81	61.49	112.59	

14.23	6.54	1.02	14.51	2.88	2.42	39.94	75.16	
15.19	7.54	1.81	12.62	3.42	2.51	49.19	77.59	Subramanian, et al., 2011
16.28	7.98	2.04	13.89	3.69	2.43	51.39	81.69	
15.61	8.23	1.60	12.18	3.47	2.52	50.11	77.30	
17.38	9.98	2.45	11.96	4.21	2.71	65.38	89.91	
17.54	10.14	3.21	10.78	4.54	2.64	68.69	86.87	
13.55	5.59	1.06	15.31	2.70	2.84	43.94	88.68	
14.41	6.78	1.17	14.87	2.99	2.92	50.03	92.80	
15.82	7.69	1.24	13.25	3.29	2.89	54.49	91.42	
15.67	7.82	1.8	12.55	3.50	3.01	60.37	94.31	
16.32	8.12	2.14	11.16	3.75	3.15	67.69	97.38	
17.73	9.35	2.62	11.87	4.24	3.21	77.99	107.94	
12.62	5.24	0.98	16.84	2.52	3.01	43.47	95.63	
12.39	5.63	1.25	15.56	2.64	3.41	51.59	103.92	
13.42	6.87	1.62	14.24	3.05	3.61	63.10	110.31	
14.56	7.29	1.24	12.63	3.09	3.57	63.22	105.93	
15.85	7.38	1.82	12.81	3.48	3.64	72.59	115.79	
16.48	8.42	2.18	12.33	3.82	3.70	80.99	119.67	
19.20	4.00	2.90	14.45	5.03	1.50	53.06	76.00	
14.95	3.78	2.27	16.25	3.83	1.73	46.60	78.30	Mansaray et al., 1999
12.75	3.39	1.98	17.14	3.28	1.98	45.67	81.00	
18.29	3.77	2.36	14.5	4.38	1.49	45.89	70.40	
14.23	3.4	2.00	16.46	3.54	1.71	42.57	72.60	
12.50	3.26	1.85	17.23	3.15	1.97	43.64	78.60	
15.13	3.41	2.00	14.82	3.75	1.30	34.28	55.00	
13.00	3.32	1.91	16.62	3.36	1.50	35.44	66.00	
12.29	3.25	1.84	17.42	3.09	1.70	36.94	67.00	
13.96	12.39	0.56	14.08	3.69	2.59	44.23	56.12	
14.44	13.01	0.69	13.66	3.89	2.57	46.34	56.17	Salam & Bhattacharya,
12.31	11.36	0.57	15.42	3.35	2.59	40.07	55.54	2006
12.79	12.74	0.94	13.9	3.74	2.69	46.6	56.36	
16.02	11.89	0.77	13.62	3.99	2.82	52.04	65.10	
13.79	12.43	0.68	13.9	3.73	2.74	47.22	58.92	
14.77	13.48	0.93	13.86	4.10	2.63	49.78	58.83	
15.64	12.6	0.61	14.75	3.96	2.73	50.11	64.25	
14.49	11.61	0.55	15.08	3.66	2.64	44.63	60.25	
17.65	11.44	0.68	13.58	4.10	2.58	48.98	62.46	
16.58	11.55	0.51	14.22	3.91	2.65	47.95	62.99	
17.19	11.64	0.62	13.41	4.04	2.60	48.53	61.42	
19.76	11.62	0.93	12.39	4.51	2.59	54.05	65.05	
16.00	11.90	0.84	14.41	4.01	2.61	48.36	61.74	
17.68	12.27	0.75	13.14	4.24	2.60	51.11	62.31	
18.42	11.29	0.85	12.87	4.25	2.68	52.72	65.30	
15.5	10.75	0.90	14.19	3.82	2.52	44.6	58.54	
15.32	10.9	0.88	14.05	3.81	2.48	43.58	56.75	
9.74	8.48	4.18	13.36	2.42	1.62	53.00	70.00	
8.98	7.11	4.20	15.68	2.71	1.73	56.00	80.00	
10.47	8.44	4.51	12.28	2.66	1.72	58.00	75.00	Arena & Gregorio, 2014.
10.4	8.24	4.51	12.83	2.78	1.91	61.00	81.00	
12.73	7.08	4.35	14.04	2.79	2.04	61.00	92.00	
11.66	7.68	3.33	11.66	2.61	2.00	57.00	79.00	
10.00	6.00	4.00	10.00	4.53	1.76	40.00	71.00	
19.2	4.00	2.9	14.45	5.03	1.50	55.68	76.00	
14.45	3.78	2.37	16.25	3.83	1.73	48.90	78.30	Lahijani et al., 2011
12.75	3.39	1.98	17.14	3.28	1.98	47.93	81.00	Mansaray et al., 1999
18.29	3.77	2.36	14.5	4.38	1.49	48.16	70.40	

14.43	3.40	2.00	16.46	3.54	1.71	44.67	72.60	
12.5	3.26	1.85	17.23	3.15	1.97	45.80	78.60	
15.13	3.41	2.00	14.82	3.75	1.30	35.98	55.00	
13.00	3.32	1.91	16.62	3.36	1.50	37.20	60.00	
12.00	3.25	1.84	17.42	3.09	1.70	38.78	67.00	
25.75	33.91	8.14	21.83	14.28	0.93	62.41	78.11	
18.42	40.23	8.11	25.36	12.81	1.12	70.09	83.73	
26.90	46.31	6.41	16.99	11.61	1.36	72.92	87.14	Hu et al., 2016
13.74	21.31	12.25	33.18	15.31	0.53	33.43	51.61	
17.57	24.73	11.13	29.14	14.94	0.70	43.16	64.82	
22.32	27.14	10.35	25.43	14.51	0.78	48.30	71.30	
17.31	24.42	11.37	31.60	14.8	0.71	45.62	64.47	
22.80	28.92	9.33	25.91	14.57	0.83	51.35	74.47	
25.73	33.91	9.14	21.83	14.28	0.93	56.21	78.11	
15.80	8.70	5.10	1.03	4.76	1.03	59.000	93.00	
15.40	11.90	4.80	1.11	4.95	1.11	62.00	90.00	
13.80	13.30	4.60	1.14	4.83	1.14	61.00	92.00	Campoy et al., 2009
15.00	140	4.70	0.97	5.09	0.97	54.00	90.00	
11.90	16.20	5.30	1.06	5.15	1.06	57.00	91.00	
18.90	16.40	5.55	1.13	6.12	1.13	64.00	94.00	
15.70	18.30	5.70	1.08	6.00	1.08	60.00	95.00	
20.80	20.00	6.70	0.98	7.18	0.98	61.00	96.00	
15.30	17.50	70.10	20.3	6.88	1.04	60.00	96.00	
20.00	16.60	5.60	16.8	6.14	1.14	66.00	95.00	
17.50	21.80	6.10	18.00	6.00	1.00	60.00	90.00	
23.90	22.40	7.30	12.60	8.06	0.97	64.00	96.00	
19.30	25.10	7.40	16.20	7.81	1.04	65.00	96.00	
27.40	18.30	7.30	16.20	8.06	1.05	67.00	97.00	
25.10	23.10	6.50	13.70	8.00	1.09	69.00	96.00	
23.90	22.30	6.70	14.60	7.83	1.09	69.00	96.00	
20.20	24.50	6.80	16.70	7.67	1.05	64.00	97.00	
19.30	25.7	6.70	17.00	7.62	1.10	66.00	96.00	
28.50	25.7	8.10	9.20	9.28	0.96	68.00	97.00	
23.50	27.5	7.70	14.60	8.70	0.98	63.00	97.00	
9.84	8.74	3.97	7.10	3.61	1.46	35.23	39.00	
9.49	7.68	3.89	7.20	3.42	1.43	32.71	37.70	
9.10	6.90	8.10	7.80	4.80	1.69	59.20	54.80	George et al., 2018
7.60	5.90	5.40	8.90	3.53	1.55	39.90	40.70	
10.70	7.46	5.60	9.20	4.16	1.60	47.57	50.60	
9.84	6.60	4.60	9.05	3.63	1.54	39.75	44.90	
9.10	11.00	0.60	12.92	3.00	2.75	46.98	67.90	
8.90	12.30	1.20	12.30	3.50	2.65	52.82	68.60	
8.20	13.70	0.90	13.70	3.70	2.70	56.89	72.20	Pei et al., 2018
5.80	19.10	0.40	19.10	6.70	1.90	72.49	87.00	
13.70	6.10	5.80	18.50	5.10	1.17	33.98	48.50	
13.40	5.70	6.80	18.90	5.40	1.29	39.67	54.90	
11.90	6.90	5.40	21.70	5.40	1.44	44.28	61.00	
14.40	6.00	6.30	16.10	4.90	1.24	34.60	49.90	
6.70	7.20	1.20	11.70	2.07	1.94	22.87	45.86	
11.20	8.20	1.40	15.40	2.74	1.98	30.90	70.41	Thengane et al., 2019

References

S. Yang, B. Li, J. Zheng, R.K. Kankala. Biomass-to-Methanol by dual-stage entrained flow gasification: Design and techno-economic analysis based on system modeling. Journal of Cleaner Production 205, (2018), 364-374

H. Pei, X. Wang, X. Dai, B. Jin, Y. Huang. A novel two-stage biomass gasification concept: Design and operation of a 1.5 MWth demonstration plant. Bioresource Technology 267, (2018), 102-109.

M. La Villetta , M. Costa, D. Cirillo , N. Massarotti, L.Vanoli. Performance analysis of a biomass powered micro-cogeneration system based on gasification and syngas conversion in a reciprocating engine. Energy Conversion and Management175, (2018), 33-48.

R. Rodriguez, G. Mazza, A. Fernandez, A. Saffe, M. EchegarayPrediction of the lignocellulosic winery wastes behavior during gasification process in fluidized bed: experimental and theoretical study. J. Environ. Chem. Eng. 6, (2018), 5570-5579.

C.A.V.B. de Sales, D.M.Y. Maya, E.E.S. Lora, R.L. Jaen, A.M.M. Reyes, A.M.M. Gonzalez, R.V. Andrade, J.D. Martínez. Experimental study on biomass (*eucalyptus* spp.) gasification in a two-stage downdraft reactor by using mixtures of air, saturated steam and oxygen as gasifying agents. Energy Conversion and Management 145, (2017), 314-323.

E. Konstantinou, R. Marsh. Coal char to combustible gas products in the context of Underground Coal Gasification. Fuel 159, (2015), 508-518.

W. He, C.S Park, J.M. Norbeck. Rheological study of comingled biomass and coal slurries with hydrothermal pretreatment. Energy & Fuels, 23, 10, (2009), 4763-4767.

P. Lv, Z. Yuan, C. Wu, L. Ma, Y. Chen, N. Tsubaki. Bio-syngas production from biomass catalytic gasification. Energy Conversion and Management 48, (2007), 1132-1139.

S. Rapagna, N. Jand, A. Kiennemann, P.U. Foscolo. Steam-gasification of biomass in a fluidised-bed of olivine particles. Biomass and Bioenergy19, (2000), 187-197.

C. Gai, Y. Dong. Experimental study on non-woody biomass gasification in a downdraft gasifier. International Journal of Hydrogen Energy 37, (2012), 4935-4944.

C. Loha, P. K. Chatterjee, H. Chattopadhyay. Performance of fluidized bed steam gasification of biomass – Modeling and experiment. Energy Conversion and Management 52, (2011), 1583-1588.

Z. Ong, Y. Cheng, T. Maneerung, Z. Yao, Y.W. Tong, C.H. Wang, Y. Dai. Co-gasification of woody biomass and sewage sludge in a fixed-bed downdraft gasifier. AIChE Journal 61, (2015), 2508-2521.

D. Serrano, M. Kwapinska, A. Horvat, S. S.Delgado, J. J.Leahy. *Cynara cardunculus* L. gasification in a bubbling fluidized bed: The effect of magnesite and olivine on product gas, tar and gasification performance. Fuel 173, (2016), 247-259.

F.Miccio, B.Piriou, G.Ruoppolo, R.Chirone. Biomass gasification in a catalytic fluidized reactor with beds of different materials. Chemical Engineering Journal 154, (2009), 369-374.

M.Thakkar, J.P.Makwana, P. Mohanty, M. Shah, V. Singh. In bed catalytic tar reduction in the autothermal fluidized bed gasification of rice husk: Extraction of silica, energy and cost analysis. Industrial Crops and Products 87, (2016), 324-332.

M.K.Karmakar, J.Mandal, S.Haldar, P.K.Chatterjee. Investigation of fuel gas generation in a pilot scale fluidized bed autothermal gasifier using rice husk. Fuel

111, (2013), 584-591.

P.Subramanian A.Sampathrajan, P.Venkatachalam. Fluidized bed gasification of select granular biomaterials. Bioresource Technology 102, (2011), 1914-1920.

K.G. Mansaray, A.E. Ghaly, A.M. Al-Taweel, F. Hamdullahpur, V.I. Ugursa. Air gasification of rice husk in a dual distributor type fluidized bed gasifier. Biomass and Bioenergy 17, (1999) 315-332.

P. Abdul Salam, S.C. Bhattacharya. A comparative study of charcoal gasification in two types of spouted bed reactors. Energy 31, (2006), 228-243.

U. Arena, F. Di Gregorio. Energy generation by air gasification of two industrial plastic wastes in a pilot scale fluidized bed reactor. Energy 68, (2014), 735-743.

[31]. P. Lahijani, Z.A. Zainal. Gasification of palm empty fruit bunch in a bubbling fluidized bed: A performance and agglomeration study. Bioresource Technology 102, (2011), 2068-2076.

J. Hu J. Shao, H. Yang, G. Lin Y. Chen, X. Wang, W. Zhang, H. Chen. Co-gasification of coal and biomass: Synergy, characterization and reactivity of the residual char. Bioresource Technology 244, (2017), 1-7.

M. Campoy, A. Gomez-Barea, F. B. Vidal P. Ollero. Air–steam gasification of biomass in a fluidised bed: Process optimisation by enriched air. Fuel Processing Technology 90, (2009), 677- 685.

J. George, P. Arun, C Muraleedharan. Assessment of producer gas composition in air gasification of biomass using artificial neural network model. International Journal of Hydrogen 43, (2018), 9558-9568.

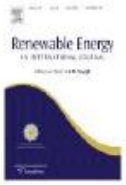
H. Pei, X. Wang, X. Dai, B. Jin, Y. Huang. A novel two-stage biomass gasification concept: Design and operation of a 1.5 MWth demonstration plant. Bioresource Technology 267, (2018), 102-109.

S. K. Thengane, A. Gupta, S. M. Mahajani. Co-gasification of high ash biomass and high ash coal in downdraft gasifier. Bioresource Technology 273, (2019), 159-168.

AppendiX B: Copyright permission for making use of the contents of the journals stated in the copyrights in my thesis.

Copyright Clearance Center | RightsLink®

Home | Help | Email Support | Sign in | Create Account



Performance evaluation of gasification system efficiency using artificial neural network

Author: M. Ozonoh,B.O. Oboirien,A. Higginson,M.O. Daramola

Publication: Renewable Energy

Publisher: Elsevier

Date: January 2020

© 2019 Elsevier Ltd. All rights reserved.

Please note that, as the author of this Elsevier article, you retain the right to include it in a thesis or dissertation, provided it is not published commercially. Permission is not required, but please ensure that you reference the journal as the original source. For more information on this and on your other retained rights, please visit: https://www.elsevier.com/about/our-business/policies/copyright#Author-rights

BACK | CLOSE WINDOW

© 2019 Copyright - All Rights Reserved | Copyright Clearance Center, Inc. | Privacy statement | Terms and Conditions

Comments? We would like to hear from you. E-mail us at customercare@copyright.com

Copyright Clearance Center | RightsLink®

Home | Help | Email Support | Sign in | Create Account



Techno-economic analysis of electricity and heat production by co-gasification of coal, biomass and waste tyre in South Africa

Author: M. Ozonoh,T.C. Aniokete,B.O. Oboirien,M.O. Daramola

Publication: Journal of Cleaner Production

Publisher: Elsevier

Date: 10 November 2018

© 2018 Elsevier Ltd. All rights reserved.

Please note that, as the author of this Elsevier article, you retain the right to include it in a thesis or dissertation, provided it is not published commercially. Permission is not required, but please ensure that you reference the journal as the original source. For more information on this and on your other retained rights, please visit: https://www.elsevier.com/about/our-business/policies/copyright#Author-rights

BACK | CLOSE WINDOW

© 2019 Copyright - All Rights Reserved | Copyright Clearance Center, Inc. | Privacy statement | Terms and Conditions

Copyright Clearance Center | RightsLink®

Home | Help | Email Support | Sign In | Create Account

Dataset on the assessment of the environmental, economic and energy parameters of 5 MW CHP co-gasification plant using South African coal, biomass and waste-tyre

Author: M. Ozonoh,T.C. Aniokete,B.O. Oboirien,M.O. Daramola

Publication: Data in Brief

Publisher: Elsevier

Date: December 2018

Copyright © 2018, Elsevier

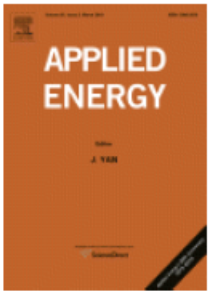
Creative Commons

This is an open access article distributed under the terms of the Creative Commons CC-BY license, which permits unrestricted use, distribution, and reproduction in any medium, provided the original work is properly cited.

You are not required to obtain permission to reuse this article.

To request permission for a type of use not listed, please contact Elsevier Global Rights Department.

Are you the author of this Elsevier journal article?



Thank you for your order!

Dear Maxwell Ozonoh,

Order Summary

Licensee: 1 JAN SMUTHS AVE, JOHANNESBURG

Order Date: Dec 6, 2019

Order Number: 4722910205667

Publication: Applied Energy

Title: Comparative techno-economic analysis of biomass fuelled

Order Total: 0.00 USD

View or print complete details of your order and the publisher's terms and conditions.

Sincerely,

Tel: +1-855-239-3415 / +1-978-646-2777

customercare@copyright.com

Copyright Clearance Center

RightsLink®

Appendix C: Copies of publication

Journal of Cleaner Production 201 (2018) 192e206

Contents lists available at ScienceDirect

Journal of Cleaner Production

Techno-economic analysis of electricity and heat production by co-gasification of coal, biomass and waste tyre in South Africa

M. Ozonoh [a], T.C. Aniokete [a], B.O. Oboirien [b], M.O. Daramola [a, *]

[a] School of Chemical and Metallurgical Engineering, Faculty of Engineering and the Built Environment, University of the Witwatersrand, Wits 2050, Johannesburg, South Africa

[b] Department of Chemical Engineering, University of Johannesburg, Doornfontein, Johannesburg 2028, South Africa

articleinfo

Article history:
Received 16 March 2018
Received in revised form
18 July 2018
Accepted 21 July 2018
Available online 2 August 2018

Keywords:
Co-gasification
Biomass
Solid waste Coal
Energy generation
Techno-economic assessment

0959-6526/© 2018 Elsevier Ltd. All rights reserved.

abstract

South Africa has large deposit of coal that supports about 95% of electric power generation in the country. The fuel is fast depleting, though the current reserve may serve for the next century. However, the emissions from the coal projects huge threat to the environment. Similarly, the country has abundant solid wastes that can be co-gasified with coal to H_2 enriched syngas for clean energy production. A 5 MW combined heat and power plant was studied using different coal-to-solid waste ratios of 1:1, 3:2, and 4:1 and economy of the plant was evaluated with feedstock costing (WFC) and without feedstock costing (WOFC). The lower heating value of the fuels, determined from a model equation was applied to estimate the annual feedstock requirement and the feed rate. Net Present Value (NPV), Internal Rate of Return (IRR), and Payback Period (PBP) were used to evaluate the viability of the power generation at the 10th, 11th, 17th and 18th year business periods. The predicted optimum period of the plant is the 10th year. The use of Coal þ Pine saw-dust (PSD) blend of blend ratio 1:1, is the most attractive feedstock for the energy generation. A higher profit of about 13.82%, and 23.56% were estimated for the use of Coal þ PSD as compared to the use of 100% Matla coal at WFC and WOFC, thus; enabling a savings of about 1,868.81 t

feedstock per annum. The use of Coal þ PSD blend of blend ratio 1:1 reduces the CO, CO_2, SO_2, and NO_x emissions by 3.4%, 23.28%, 22.9%, and 0.55%, respectively.

© 2018 Elsevier Ltd. All rights reserved.

1. Introduction

Currently, global energy consumption is rising very rapidly, and amounting to the fast depletion of the available source of fuel. Fossil fuels such as coal and crude oil are the two major fuels used for energy generation in the world. The emissions arising from both fuels raise huge concern to the society at large, because of their contributions in global warming that result in climate change. In South Africa, coal is the major source of fuel for power production, and around 95% of the electric power generation in the country comes from coal. At the moment, the estimated coal reserve in the country is about 32 million tons, and it may last for about a century (Stats SA, 2015).

The local availability of coal in South Africa has also contributed so immensely in the low electricity tariff in the country of about $0.1408 c/kWh (SA Power Networks, 2017), and the tariff is one of the lowest around the world. It is true that the cost of electricity supply to consumers in South Africa is low, but at the same time, the emissions associated with the production is equally very high. Similarly, power production from biomass is not cost effective; if waste biomass is not used, and besides, biomass feedstock produces high amounts of tar that causes operational difficulties in the gasifiers and end use facilities. Biomass fuels (e.g. agro-waste) and other solid waste are in abundant in South Africa, and can be co-gasified with coal to produce electricity. Co-gasification has higher efficiency than the solitary coal gasification because the cellulose, hemicellulose and lignin content of biomass help to ignite and enhance the rate of gasification (Kamble et al., 2018). The process will also reduce emissions, cost of feedstock, tar produc- tion, and as well be instrumental to waste management in South Africa.

Some researchers have investigated the use of coal, biomass, solid wastes or mixture of them in electric and thermal power production. Understanding the physio-chemical and gasification characteristics of coal that can be blended with any of these solid fuels to produce energy is very essential. Oboirien et al. (2011) have

* Corresponding author.
E-mail address: Michael.Daramola@wits.ac.za (M.O. Daramola).

https://doi.org/10.1016/j.jclepro.2018.07.209

0959-6526/© 2018 Elsevier Ltd. All rights reserved.

Nomenclature

	annual feedstock requirement (t/y)
	bubbling fluidized bed
A_{FR}	
BFR	bubbling fluidized bed gasifier
BFBG	corn cob
CC	
CHP	combined heat and power plant
	annual feed rate (t/y)
FR_{ANNUAL}	
G_E	electric power efficiency (%)
	greenhouse gas
GHG	
$LHV_{FEEDSTOCK}$	lower heating value of feedstock (MJ/kg)
MC	moisture content (%) MW mega-watts
M	million
NPV	
NOH	net present value (million ZAR/y)
PSD	number of hours
R	
SCB	pine saw-dust
SA	
	annual rate of return (%)
t	ton
T_{LPT}	
WT	truck load per trip (t)
ZAR	waste tyre
Y	
	South African rand
	year
6	
	CO_2 emission factor of diesel based transportation (t CO_2/Km)
f	
$h_{TeGasi:}$	
$h_{TQGasi:}$	energy demand (MWh/y)
h_o	cash flow (million ZAR)
b	overall electrical efficiency of a gasification plant (%)
	overall thermal efficiency of a gasification plant (%)
Y	operating efficiency of the plant (%)
IRR	
PBP	capital investment (ZAR/y)
	hauling distance (Km)
x	internal rate of return (%)
	payback period (y)
m	

studied the structure and gasification characteristics of selected South African bituminous coals using a bubbling fluidized bed reactor. Bridgwater et al. (2002) and Caputo et al. (2005) have equally carried out some work on pyrolysis, combustion and gasification processes, and reported that about 5 MW of electrical power capacity are feasible for most fluidized bed systems. The authors were also able to determine the most viable technology amongst the conversion technologies investigated, but could not report on the optimum feedstock for the power production with reference to both profit and emission reduction. Malek et al. (2017), carried out the techno-economic analysis of electricity production in 10 MW biomass-based steam power plant to identify the order of viability of the various feedstocks for power production, but blends of the feedstocks were not used to evaluate the same goal aimed in the study.

Other researchers including; Bridgwater et al., 2002; Mitchell et al. (1995); Searcy and Flynn (2010) have also indicated that biomass integrated gasification and combined gas-steam power cycle (IGCC) is an attractive technology providing about 40%e50% total conversion efficiency, whereas; Demirbas (2001) argued that a biomass integrated gasification combined cycle (BIGCC) plant of around 20 MWe capacity may be as high as about 40%. The IGCC technology as reported by the above authors is quite promising, although the feedstock that could remain viable for a known period of investment was not determined, and the information is consid- ered very useful for investors. However, the Co-gasification process in a fluidized bed system is expected to support an overall con- version efficiency of about 40%e50%, reduce the cost of feedstocks used for electric and thermal power generation as well. The overall system efficiency of a typical co-generation system is within the range of 35%e40% as reported by Ahmad et al. (2013).

Gasification of blends of coal and biomass, and other solid wastes can minimize some of the problems earlier mentioned. Although some researchers have reported on the energy produc- tion via combustion, pyrolysis and gasification of biomass with reference to 5 MW, 10 MW, and 20 MW CHP plants, but their studies did not consider blends of biomass and other solid fuels such as coal and waste-tyre, available in south Africa. Consequently, there is no available data in the literature describing the energy production in a 5 MW CHP plant using blends of South African feedstocks, and with emphasis on the blending ratios, energy content of the feedstock, feed-rate and annual feedstock require- ment, optimum assessment year, and the most viable feedstock for energy generation in the plant. The findings of this study could pave way to elongate the consumption period of coal reserve that is fast depleting in the South African and the CO_2 emissions for which South Africa is the number one emitter in Africa. In addition, the availability of data on techno-economic analysis of electricity and heat production from co-gasification of coal, biomass and solid waste (e.g. waste-tyre) could be instrumental to decision-making by the government and the key players in energy sector in South Africa and Africa at large.

2. Materials and method

2.1. Materials

Feedstocks used for the investigation in this study were coal, sugarcane bagasse, corn cob, pine saw-dust and waste tyre, ob- tained in South Africa The biomass materials were reduced from their original size of 6.0e10.0 mm to 0.5e2.0 mm with Retsch biomass cutter (SM 200 Rostire), and the coal (Matla coal) was milled to 0.2e2.0 mm using the milling machine located at the Coal Lab of the University of the Witwatersrand, Johannesburg. The waste tyre was shredded to 0.5e3.0 mm and the re-enforced ma- terials removed. Physio-chemical properties of the feedstocks were checked through ultimate and proximate analysis prior to deter- mining their heating values.

2.2. Blending of feedstocks and cost estimation

The coal and other solid wastes of South African origin were blended in the ratio of 1:1, 3:2, and 4:1, respectively to examine their potentials for electric and thermal power production. The feedstocks and their blends are shown in Table 1, but the estimated results from the blends is presented in Table 5.

Table 1
Feedstock blends and their ratio.

Blended Feedstocks	Coal þ SCB	Coal þ CC	Coal þ PSD	Coal þ WT
Blend Ratio	1:1, 3:2, 4:1			

SCB: sugarcane bagasse; CC: corn cob; PSD: pine sawdust; WT: waste tyre.

For the cost estimation, two hypothetical cases namely; "blending with feedstocks costing (WFC)" and "blending without feedstock costing (WOFC)" were considered and studied. The WFC considered the actual costs of the feedstock together with cost of packaging and transportation of the feedstocks, and WOFC considers only the cost of packaging and transportation of feedstocks to the plant room. The relative advantage of WFC over WOFC is to provide elaborate cost information and guidance to investors who are interested in the business area. In addition, the techno-economic analysis considered the energy, economic, and environmental parameters of a typical co-gasification plant. The lower heating value (LHV) of the fuels was estimated using an empirical model (shown in equation (1)), and was used to determine both the annual feedstocks requirement and the feed rate for the plant. For profitability, the NPV, IRR, and PBP were used to assess the viability of the power generation at the 10th, 11th, 17th and 18th year business periods.

2.3. Estimation of the LHV and annual feed rate of the feedstocks

One of the most important characteristics of biomass or other fuels used for energy conversion processes and systems is the heating value (Nhuchhen and Salam, 2012). The parameter is very useful in design, planning, operations, and development of a power generating plant. The ultimate and proximate analysis data, as well as the calorific value of the fuel play essential roles in efficient operations (Huang et al., 2008). The heating value of a fuel can also be influencial to the amount of feedstock that is required for energy production in a power plant, which in-turn affects the feed rate of the fuel. Several researchers including Ahmaruzzuman (2008); Parik et al. (2005); Sheng and Azevedo, 2005; Thipkunthod et al. (2005) and Yin, 2011 have studied the use of proximate and ultimate analysis data in estimating the HHV and LHV of fuels. In this study, Equation (1) (Cooper et al., 1999) and Equation (2) (Malek et al., 2017) were used to estimate the LHV and annual feed rate of the feedstock for the co-gasification power plant.

$$LHV = HHV - (0.212 \times M_H) - (0.0245 \times MC) \quad (1)$$

$$F = \frac{g}{LHV_{FEEDSTOCK} \cdot NOH} \quad (2)$$

2.4. Estimation of fuel requirement for the CHP plant

The LHV of the solid fuels was used to estimate the amount of feedstock required annually for the power production, and was based on the MC and the efficiency of the system. According to Verma et al. (2012), the annual feedstock requirement can be determined using Equation (3):

$$A = \frac{6 \times 3.6}{LHV \times h_0} \quad (3)$$

It is interesting the mention that the LHV and MC of fuels are two important parameters in thermochemical energy conversion process. Feedstocks with low or high MC can be used in an energy conversion system, but this results in different operational efficiencies. A low water content fuel saves the cost of feedstocks drying, improves the heating value of fuel and consequently enhances the overall efficiency of the energy production plant. However, the use of a high MC fuel is associated with several operational difficulties such as lowering the heat transfer of the system and many others.

2.5. Economic analysis: Co-gasification power plant

2.5.1. Net present value (NPV)

The NPV of an investment is referred to as the sum of the pre- sent values for an expected returns overtime offset by its up-front costs. It is used to identify projects that will yield the most return over a specific period of time, and demonstrate the viability of the business. To estimate the NPV, the total earnings of the consecutive number of years for the business are discounted from the Marginal Rate of Return. Estimation of the NPV in this study employed the Equation (5), the modified form of model presented by Malek et al. (2017):

$$NPV = -b + \frac{f_1}{(1+R)^1} + \frac{f_2}{(1+R)^2} + \frac{f_3}{(1+R)^3} + \cdots + \frac{f}{(1+R)^T} \quad (4)$$

The b is a sensitive parameter in the NPV relation that depends on the feedstock cost. Feedstock cost is one of the factors that im- pacts on the investment cost (a significant variable) in the present evaluation. Profit or loss from a business is proportional to the increase or decrease in the b, and this equally affects the IRR of the business.

2.5.2. Internal rate of return (IRR)

The IRR is a parameter used in capital budgeting to measure the profitability of potential investments. It discounts all the cash back, hence; causing the NPV to become zero for the stipulated life of the business venture.

A project is more desirable to be undertaken than the other if it generates higher IRR. At times, different types of business investments may yield uniform IRR, but the tool can be applied to rank multiple potential ventures a firm may consider as the most viable option(s). Estimation of IRR in this study was according to Equation (5).

$$\sum_{j=1}^{T} \frac{f}{(1+IRR)^j} - b + \frac{i}{j} = 0 \quad (5)$$

2.5.3. Payback period (PBP)

The time required for the amount of money invested in an asset to be repaid by the net cash flow generated by the asset is referred to as the PBP. An investment with shorter PBP is better because it gives the investor a quick picture of the amount of time the initial investment will be on risk. Alternatively, PBP can be referred to as the number of years it takes a project to recover its total investment (d) by earning after interest and tax (m). However, the d is a sensitive parameter in the PBP expression, because if the cash flows or profit made from the business is poor; then, the business status can be adjusted on the side of profit scale by changing the d in order to shorten the PBP. Further re-adjustment can be made if economic condition appears better. Kong et al. (2004) and Hasanuzzaman et al. (2011) have developed an expression for the estimation of the PBP as shown in Equation (6). Equation (6) was used for the estimation of PBP in this study.

$$PBP = \frac{d}{m} \quad (6)$$

2.6. Emissions from a 5 MW co-gasification energy production plant

In order to generate energy from fuels, various forms of emis- sions accompany the process. Notable amongst these emissions are CO, CO_2, SO_2, and NO_X in this article.

2.6.1. Emissions reduction by displaced energy

Environmental management is a worldwide issue especially as it concerns global warming caused by emissions from fossil fuels utilization. It is useful to know the amount of emissions that can be reduced if fossil fuel such as coal is replaced with renewable raw material such as biomass, or other solid waste. The emission of power generation can be estimated using the Equation (7) (Mahlia, 2002). If the power plant is scaled up by increasing the 6 to either 10 MW, 15 MW or 20 MW, then the x will be increased, resulting in the increase in amount of emissions from the system. Hence; increasing the amount emissions in the system.

$$x = 6 \times \left(a^1 \times t^1 + a^2 \times t^2 + \cdots + a^n \times t^m \right) \quad (7)$$

In energy production or fuel processing, various emission fac- tors are produced from the fuels. The energy mix in the current study involves coal, biomass, and tyre. Table 2a presents the emission factors of different fossil fuels.

To calculate the emission reduction from the co-gasification process, the emission factors of coal and biomass (or solid waste) are very crucial. Table 2b presents the life cycle emission factors for renewable energy sources.

2.6.2. Emissions from the transportation of biomass, tyres and coals

At times, power plants are not sited near the source of raw materials. Produced fuel-carrying raw materials such as biomass is transported to the plant room with different sizes of trucks, hence; generating different amounts of emissions during the process. The emission arising from the fuel transportation was estimated in this study from Equation (8) (PDD, 2006):

$$\frac{1}{T_{LPT}} \quad \frac{\delta A_{FR} \times g \times \mu}{} \quad (8)$$

Similarly, and according to the US EAP (2008) report, the emissions arising from different sizes of trucks in gross vehicles weight (GLT) rating for biomass transportation is presented in Table 3.

2.6.3. Effective emissions reduction: biomass power plant

With regards to the life cycle of GHG emission intensity from biomass (ε) as 0.045 kg CO_2 e/kWh, the effective emission reduction arising from a biomass energy plant is expressed as in Equation (9)

Table 2a
Emission factors of fossil fuels (Mahlia and Yanti, 2010). Fuel

Sources	Emission factor (kg/kWh)			
	CO_2	SO_2	NO_X	CO
Coal	1.1800	0.0139	0.0052	0.0002
Petroleum oil	0.8500	0.0164	0.0025	0.0002
Natural gas	0.5300	0.0005	0.0009	0.0005

(WNA, 2011). The distance covered and type of truck used in transporting fuels have direct impact on the 4 model. For example, if the distance is reduced, and an electric-powered truck is used instead of a diesel truck, then the amount of emission, 1 , will decrease enormously.

$$4 = x - \varepsilon - 1 \quad (9)$$

3. Results and discussion

3.1. Physio-chemical characterization of the feedstocks

The physio-chemical properties of the feedstocks were deter- mined and the result shown in Table 4. From Table 4, it is evident that the Matla coal has high ash content, whereas; the biomass samples have very low ash content as well as little or no Sulphur content. Mixture of the two feedstocks as fuel in gasification, will limit the problems that are usually caused by ash and Sulphur from coal such as agglomeration and emissions, respectively, (Kumabe et al., 2007). Furthermore, the volatile matter for all the biomass feedstocks and waste tyre were above 71% and 60%, respectively. High volatility in fuel samples (e.g. inorganic matter) is an indica- tion of high reactivity, impacted on the coal sample (with low volatile content) by the other solid samples to enhance the overall gasification reactivity of the char (Zhang et al., 2016). According to Kumabe et al. (2007) & Alzate et al. (2009), the co-gasification of high ash coal and biomass has the synergy for enhancing the H_2/CO in the gaseous product that is required for liquid fuel synthesis. The product gas composition and quality, is dependent on several fac- tors including, but not limited to, the MC of the feedstock (Kamble et al., 2018). In addition, the heating value of the biomass and coal does not indicate a very wide range of value compare to the waste tyre that has the highest calorific value. These results eventually may influence the energy and economic analysis of the individual feedstocks, and each fuel possesses characteristics for efficient co-gasification process for energy production.

3.2. Energy analysis of the various feedstocks and their blends

Generally, the MC of a fuel plays a major role in the electric and thermal power production. Table 5 presents the MC and LHV of the various feedstock mixtures used in the co-gasification power gen- eration plant. The table describes the relationship between the MC and LHV of the fuels. It can be observed that the MC of the entire feedstocks except the Coal PBD (with the highest LHV), decreased with an increase in the LHV of the fuels, but MC and LHV increased with the blending ratio. In most cases, higher energy content fuels are more efficient in electric and thermal power production than the lower energy content fuels. In addition, Table 5 shows there- sults of the feedstocks at different blend ratio.

3.2.1. Feedstocks requirements for the different blends

Different empirical models had been developed by researcher for the estimation of the calorific values of fuels. The model pre- sented in Equation (1) was applied to determine the lower heating value (LHV) of the feedstocks, using the data from the proximate and ultimate analysis presented in Table 4. The HHV was experi- mentally determined using a bomb calorimeter. The results ob- tained from the model were in agreement with some results obtained from the literature (16.80 MJ/kge19.50 MJ/kg) (Nhuchhen and Salam, 2012).

Fig. (1a) and (1b) depict the flowchart of the proposed technical approach for the system and the schematic representation for a co-

Table 2b
Life cycle emission: renewable energy sources (Varun, et al., 2009).

Green-House-Gas Emissions			
Energy Sources	CO_2 (t/kWh)	SO_2 (t/kWh)	NO_x (t/kWh)
Small hydro	9.0E-6	3.0E-8	7.0E-11
Large hydro	3.6E-6 - 1.16E-5	9.0E-9e2.4E-8	3.0E-9- 6.0E-9
Wind	7.0E-6e9.0E-6	2.0E-8e9.0E-8	2.0E-8e6.0E-8
Solar photovoltaic	9.8E-5e1.67E-4	2.0E-7e3.4E-7	1.8E-7e3.0E-7
Solar Thermal Photovoltaic	2.6E-6e3.8E	1.3E-7e2.7E-7	6.0E-8e1.3E-7
Energy crops (Biomass)	1.7E-5e2.7E-5	7.0E-8e1.6E-7	1.1E-7e2.5E-6
Biomass: Current practice Improved	1.5E-5e1.8E-5	6.0E-8e8.0E-8	3.5E-7e5.1E-7
Geo-thermal	7.0E-6e9.0E-6	2.0E-8e9.0E-8	2.8E-7

Table 3
Heavy-duty diesel classification (US EPA, 2008).

Type of Vehicles	Class	Mass Unit
Full size pickup truck	2b	3.86e4.54
Enclosed delivery truck	3	>4.54e6.36
City delivery truck	4	>6.36e7.27
Large work-in delivery truck	5	>7.27e8.86
Rack trucks	6	>8.86e11.82
Garbage collection truck	7	>11.82e15.00
Long-haul semi-tractor trailer rigs	8a	>15.00e27.27
Double long-haul semi-tractor trailer rigs	8b	>27.27

Table 5
LHV and MC of feedstocks at different blend ratios.

Parameters	Coal þ SCB	Coal þ CC	Coal þ PSD	Coal þ WT
Feedstocks: Ratio: 1:1				
LHV [MJ/kg]	17.58	17.15	19.72	23.57
MC [%]	6.35	5.34	4.65	2.06
Feedstocks: Ratio: 3:2				
LHV [MJ/kg]	17.65	17.30	18.68	22.87
MC [%]	5.84	5.03	4.48	2.41
Feedstocks: Ratio: 4:1				
LHV [MJ/kg]	17.77	17.60	18.28	20.16
MC [%]	4.82	4.41	4.14	3.10

gasification electric and thermal power plant. The flowchart shows a hypothetical case for design to generate about 5 MW (130 TJ/y) of electricity if operated for about 300 days per annum (7200 h./y). Caputo et al. (2005) has reported that the total electrical efficiency of a gasification plant with about 5 MW electric power production capacity is 36%. Based upon this assumption, the utilization of Matla coal and 'Coal PSD" as feedstocks as shown in Fig. (1b), generated 5 MW of electricity using 20,000 t/y and 18,000 t/y of Matla coal and Matla coal PSD respectively. Furthermore, on the basis that the number of operating hours was 7200 h/y, about
2.80 t/h of Matla coal and 2.54 t/h of Matla Coal þ PSD were converted into power by the co-gasification plant, respectively, to produce about 5 MW (130 TJ/y) of electricity.
Similarly, to recover some costs associated with the electricity production and also maximize the heat arising from the gasification or co-gasification process, condensers or heat exchangers were installed in the form of combined heat and power (CHP) plant. Bridgwater (2004) reported that the overall thermal efficiency of a gasification plant could be assumed as about 40%. Under this scenario, about 5.56 MW (144 TJ/y) of heat power was produced from the steam-gas unit using Matla coal and Matla Coal þ PSD.

However, the details of gasification of the Matla coal (as a control process) and Matla coal plus other solid wastes as indicated in the Fig. (1b) were evaluated for power production. It can be observed from Fig. (1b) that the lower heating value (LHV), a sensitive parameter considered in the estimation, affects both the feed rate and the annual feedstock requirements of the system.

3.2.2. *Relationship between the amount of feedstocks, expenditure and profit for an electric power generating co-gasification plant with 5 MW production capacity*

The Matla Coal PSD indicated the highest yield of profit and lowest expenditure compared to other feedstocks investigated, because PSD was the cheapest feedstock amongst the fuels studied. Normally, fuel with higher calorific value produces higher amount of energy. In this study, the power generating capacity of the plant is known, so the interest is on the feedstock blend that offers the highest profit and of lower emissions with 130 TJ/y standard tar- gets. The energy content of Coal WT was higher than the energy value of Coal PSD. Higher electric and thermal power are ex- pected from the blend, but the expectation was not the case under

Table 4
Characterization of feedstocks.

Parameters	Corn Cob	Sugarcane-Bagasse	Pine Saw-dust	Waste-Tyre	Matla Coal
Proximate analysis determined as air dried basis					
	Feedstock Analysis				
Ash Content (%)	0.29	0.49	0.59	9.92	44.00
Inherent moisture (%)	5.87	8.8	8.55	0.32	3.80
Volatile Matter (%)	72.50	71.50	71.80	63.29	19.90
Fixed Carbon (%)	21.34	19.12	19.06	26.47	32.30
	Heating Value 18.85				
HHV (MJ/kg)	17.42		21.50	30.95	18.60
LHV (MJ/kg): Calculated	16.42	17.28	19.86	29.24	17.89
	Ultimate analysis determined as air dried basis				
Carbon (%)	24.82	38.67	50.54	87.60	39.09
Hydrogen (%)	3.94	6.40	7.08	8.03	2.90
Nitrogen (%)	0.97	0.23	0.15	0.33	0.92
Sulphur (%)	0.00	0.00	0.57	3.12	0.66
Oxygen (%)	70.27	54.70	41.66	0.92	8.63

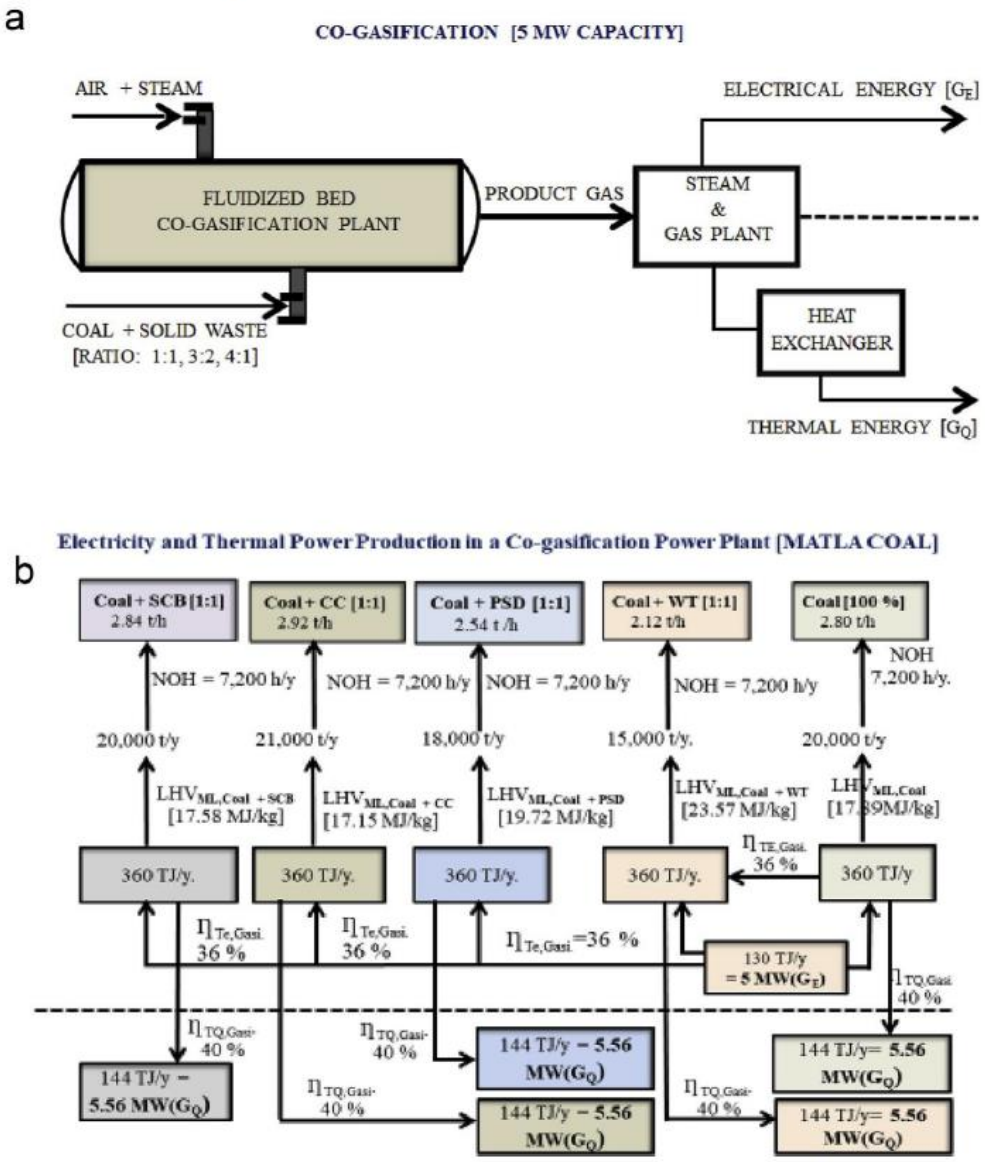


Fig. 1. a: Flow-chart of a 5 MW power plant: Proposed technical approach, b): Schematic illustration of a co-gasification process plant: Electric and Thermal Power Generation.

WFC condition. Expectedly, Coal WT should have yielded more profit under WOFC. It has been shown that the calorific value of a fuel and the expenses incurred on the feedstocks determine the amount of loss or profit that could be expected during power production. How- ever, it can be observed from Fig. (2b) that more profit was accrued under WOFC than in Fig. (2a) under WFC.

3.2.3. Economic evaluation of coal gasification

The use of Matla coal in the gasification process serves as a control for the co-gasification of the Matla coal with other solid wastes as shown in Fig. 3. It can be observed that the amount of feedstocks used for the power production as depicted in Fig. (2a) and (2b) was different from the amount of Matla coal used for the same purpose (see Fig. 3). More fuel was consumed in the Matla coal plant than in Matla Coal PSD co-gasification power plant. About 18,251.81 t of fuel could be saved annually by using a mixture of Matla Coal PSD for power production as against using 100% Matla coal. This implies a reduction in operating cost per annum as a result of savings in the yearly cost of the feedstock.

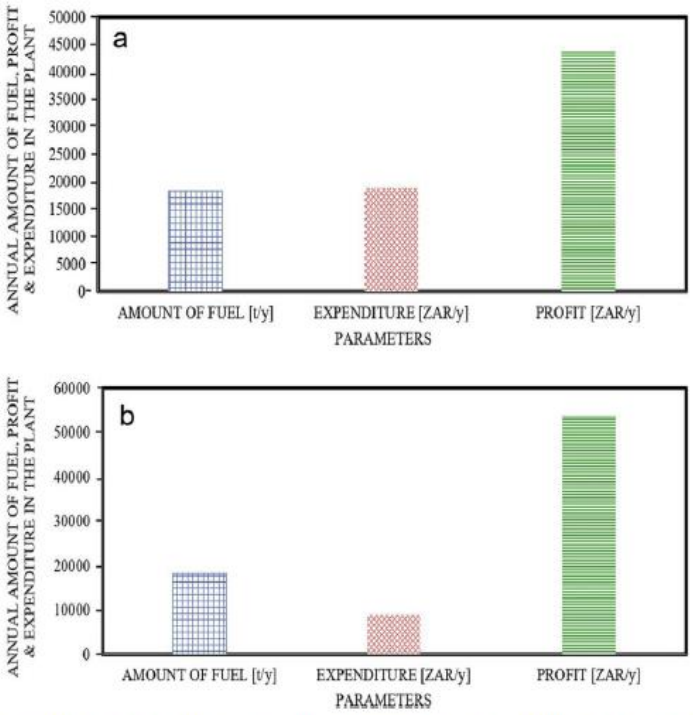


Fig. 2. a: Relationship between the amount of fuel and expenditure & profit (Matla coal þ PSD: 1:1) using WFC. b): Relationship between the amount of fuel and expenditure & profit (Matla coal þ PSD: 1:1) using WOFC.

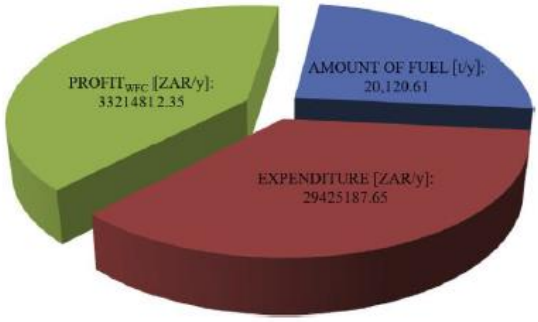


Fig. 3. 100% Matla coal economic analysis: 5 MW & 5.56 MW electric & thermal power generation.

3.2.4. Co-gasification of the various feedstocks

Figs. 4 and 5 highlight the influence of the various feedstocks investigated and their economic parameters for WFC and WOFC. The reported blend ratio of 1:1 Coal þ solid waste blend ratio in this study is the optimum blending ratio. Fig. 4 shows that Coal þ CC blend yielded the lowest profit, because corn cob is costlier than SCB and PSD.

The heating values of the fuels are in the increasing order of Coal CC > Coal þ SCB > Coal þ PSD, > Coal þ WT, and the profit increased with an increase in the heating value of the feedstock (Fig. 5). However, the ultimate analysis result (Table 4) from WT has the highest amounts of carbon and hydrogen amongst the feedstocks studied. Carbon and hydrogen are the major combustible part of a fuel and determines the energy content of the fuel. The energy content of WT is higher than the energy content of all other fuels studied, and the use of Coal PSD þ as shown in Fig. 5 displayed the optimum during WOFC.

3.2.5. Effect of feedstocks blend ratio

Fig. 6a and b present the economic evaluation of Matla Coal PSD of þ WFC and WOFC, respectively, at a blend ratio of 4:1. Fig. 6a and b were compared to Fig. 2a and b (1:1). The results obtained from Coal PSD mixture at a ratio of 4:1 depicted in Fig. (6a), and compared to results from Coal PSD mixture at a ratio of 1:1 depicted in Fig. (2a), reveal that increasing the content of Matla coal in the blend increased the expenses in the power gen- eration by about 14.68%. This in turn decreased the profit accrued by about 7.95%. In this scenario also, the amount of feedstock used in the 4:1 blend ratio was increased by 3.78% compared to that of 1:1 mixture, thus amounted to a loss of ZAR6, 461,301.77 for WFC. It was considered as a loss because, the same amount of fuel from 1:1 Coal PSD fuel mixture were used to produce the same quantity of electricity and thermal power of 5 MW and 5.56 MW, which on the utilization of the 4:1 blend ratio, increased the amount of feedstock, and leading to the huge loss of money.

Bada et al. (2016) have reported that co-firing coal and biomass at the ratio of 1:1 will cause the reduction in the CO_2 emissions by 50%. The current report has also demonstrated that around ZAR6, 461,301.77 could be saved by using 1:1 coal to solid waste mixture

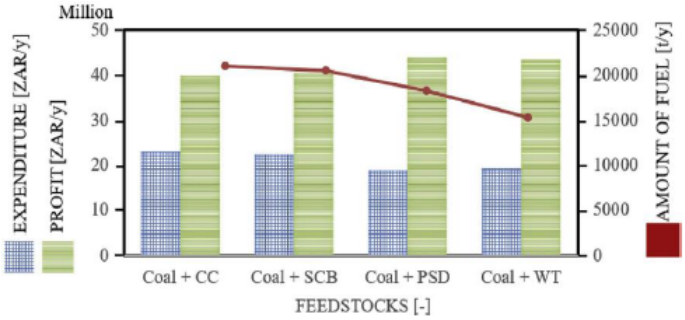


Fig. 4. Influence of feedstocks on the economic parameters using WFC.

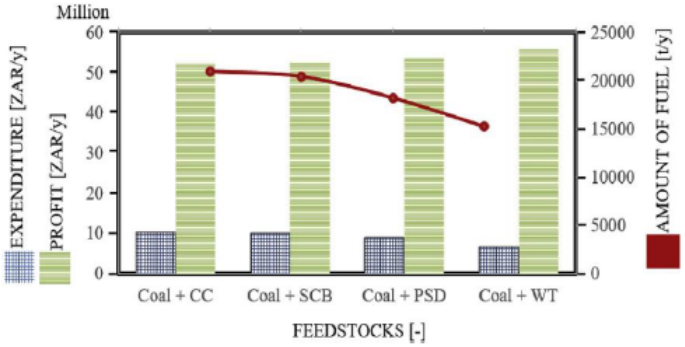


Fig. 5. Influence of feedstocks on the economic parameters using WOFC.

as against 4:1 mixture, for a co-gasification plant of 5 MW power generation capacity. On the other hand, at WOFC and with the same increase in the amount of fuel of 3.78%, an increase in the expenditure by 0.70% was observed. This also led to a decrease in the profit by 0.12% (ZAR 123,782.50).

The increase or decrease in the amount of feedstock and expenditure or profit have been basically attributed to the price of South African Coal which currently stand at $74.46/kg Coal (ZAR1, 042.44/kg Coal) compared to the solid wastes (sugarcane bagasse, corn cob, pine sawdust, and waste-tyre) which is within the range of $10.71/te$42.86/t (ZAR149.94/kgeZAR600.04/kg). Table 6 highlights the prices of the feedstocks as obtained in South Africa and some parts of the globe.

Under this context, if biomass fuels (not waste biomass - e.g. miscanthus, switch grass, beech-wood, etc.) are purchased either within or outside South Africa at the rate of around $120.00/kge $170.00/kg of biomass, then it will be cheaper to generate electricity and heat from South African Matla coal than from the biomass. The analysis presented in Section 3.2.1e3.2.4 indicates that the energy content of the feedstock (LHV), cost of fuel, and the blend ratio are the most significant factors influencing the esti- mation, although the future value of money determined in each investment year through the NPV, and reported in Section 3.3, is equally a crucial influencing factor in the assessment.

3.2.6. Effect of feedstocks on the economic parameters: percentage basis

Understanding the changes in the economic parameters of feedstocks used for electric and thermal power production with regard to their percentage changes is a very important aspect of energy and economic analysis. Table 7a presents the variation in feedstocks economic parameters, for the WFC and for the WOFC, and Table 7b describes (in percentage basis) the potentials of the other solid wastes studied over coal, for power generation. At this point, the analysis describes the benefits in terms of profit making, of using mixtures of coal and other solid wastes over the use of coal. Table 7a in real terms, describes the annual fuel savings and cost savings from the individual feedstocks, and as well, highlights how each feedstock differs from one another in terms of power production economy.

With reference to profit making, Coal PSD & Coal CC; Coal SCB & Coal CC; Coal WT & Coal CC; Coal SCB & Coal PSD; Coal WT & Coal PSD; and Coal WT & Coal SCB were evaluated at WFC and 1:1 ratio. Low or high profit had been described to be related to the CV of the fuel, and the investment cost. It was observed that higher profits were made from Coal PSD, Coal SCB, and Coal WT blend than the blends they were compared with. And more profits were equally made from Coal PSD and Coal WT blends than the blends they were compared with. Details of the analysis at 10th year at WFC & WOFC are presented in the supplementary material that accompanies this article.

3.3. Profitability analysis using NPV, IRR and PBP

In this study, the capital cost investment is referred to as the

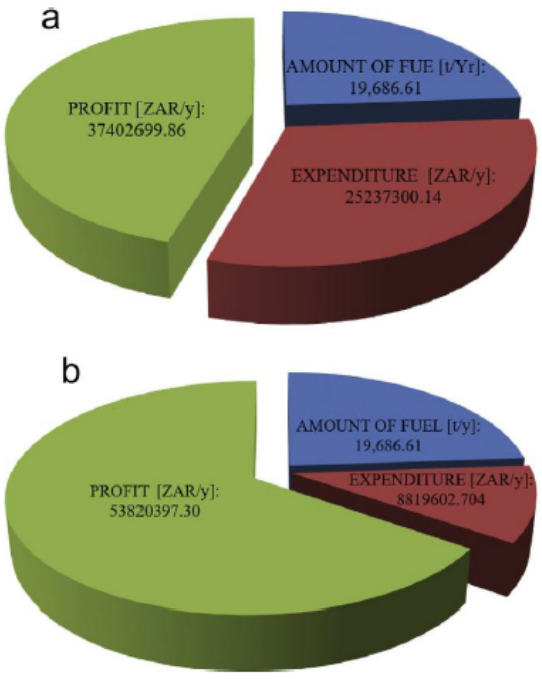


Fig. 6. aEffect of the amount of feedstocks blending ratio on expenditure and profit (Matla Coal þ PSD: 4:1) using WFC. b): Effect of the amount of feedstocks blending ratio on expenditure and profit (Matla Coal þ PSD: 4:1) using WOFC.

Table 6
Cost of feedstocks in South Africa and some parts of the globe.

Serial Number	Type of Feedstock	Price of Feedstock (ZAR/t)
1	Pine Saw-dust[i]	35.00e55.00
2	Sugarcane Bagasse[i]	150.00e200.00
3	Corn-Cob[i]	160.00
4	Waste-tyre[i]	550.00e600.00
5	Corn-Cob**	1946.00e2646.00
6	Sugarcane Bagasse[iii]	2380.00
7	Corn Cob[iii]	2380.00
8	Sugarcane Bagasse[ii]	1680.00e2800.00
9	Coal, SA[i]	1042.44

*: Local Price (South Africa); **: International Price (Vietnam); ***: USA.

total expenditure incurred on the feedstocks to generate 5 MW of electricity, and the cash flow is regarded as the annual profit obtained by subtracting the total expenditure from the revenue generated from the sales of electricity at the rate of ZAR1.74/kWh (SA Power Network, 2017) of electric power.

The venture embarked on from the 1st year to the 10th year is attractive, except for the coal-to-solid waste blend of 4:1 at WFC. The status of the venture is illustrated in Figs. 7e9. The capital cost investment from Coal þSCB is higher than the rest of the feedstocks studied. Fig. 8 thereby resulting in the lowest NPV. On the other hand, the NPV from the Coal þPSD is the highest out of the fuels investigated due to its lowest capital cost investment.

Fig. 8 shows a significant increase in the NPV of all the feedstocks, because of the lower capital investments incurred from the individual feedstocks when compared to Fig. 7. The price of WT (Table 6) is highest of all the prices of all the agro-wastes studied. In

Table 7a
Variation in feedstocks economic parameters [Coal þ Solid Wastes] at WOFC.

Parameters	Amount of Fuel [t/y]	Expenditure [ZAR/y]	Profit [ZAR/y]
WFC			
Coal	20,120.61	29425188.20	33214812.41
Coal þ CC	20,986.05	22900607.35	39739393.33
VEP*	8654.38	6524580.10	6524580.24
Coal þ SCB	20,473.45	22238058.20	40401942.13
VEP**	3528.40	7187129.10	7187129.04
Coal þ PSD	18,251.81	18775998.40	43864002.15
VEP***	18,688.05	10649189.11	10649189.22
Coal þ WT	15,2762.78	19175395.02	43464605.31
VEP****	4844.33	10249793.30	10249793.14
WOFC [Except Coal]			
Coal	20,120.61	29425188.17	22795283.00
Coal þ CC	20,986.05	10283164.03	52356836.25
VEP*	8654.38	19142023.25	19142023.11
Coal þ SCB	20,473.45	10031991.22	10031991.42
VEP**	35,283.40	19393197.06	19393197.05
Coal PSD	35,283.40	8943385.12	19393197.01
VEP[iii]	18,251.81	20481802.00	20481802.41
Coal WT	15,276.28	6629905.32	56010095.33
VEP****	4844.33	22795283.14	22795283.15

*: Coal & Coal þ CC; [ii]: Coal & Coal þ SCB; ***: Coal & Coal þ PSD; ****: Coal & Coal þ WT; [v]: Blend Ratio: 1:1; WFC: With Feedstock Costing; WOFC: Without Feedstock Costing; VEP: Variation in the Economic Parameters.

spite of the highest fuel price, the blend still displays the highest NPV at WOFC due to its highest heating value.

Fig. 9 presents similar assessment using Coal-Solid waste blend ratio of 4:1 at WFC.

A poor investment is indicated in Fig. 9 because the NPV at the end of the 10-year period is negative, and the cash returns are insufficient to encourage further investment, under the conditions and feedstocks investigated.

3.3.1. *Effect of business period elongation on the business viability*

In this study, the business life was increased from 10 to 11 years to investigate the effect of the business period elongation of its viability. All the fuel mixtures from the 1:1 and 3:2 ratios except the Coal þSCB from 3:2 fuel blend, remained viable. However, all the investment made with the 4:1 fuel ratio is not viable because of the effect of the capital cost investment and time value of money on the NPV. Similarly, the use of all the feedstocks remained viable for the power production at WOFC, and the use of Coal-to-Solid waste ratio of 1:1 displays the most attractive venture. The details of the analysis of the cost and profitability at WFC and WOFC at the 11th year can be found in the supplementary data.

3.3.2. *Effect of business period elongation on the venture from 11 to 17 years*

The essence of this analysis is to identify when exactly the investment would become a wasteful venture. The information will be a guide both to the Energy Analysts and potential investors prior to investing in the area. Only Coal-to-PSD of blend ratio 1:1 is viable, and the IRR from the use of all the feedstocks for the venture is lower than 5% (the initial annual interest rate). A comprehensive result of the assessment at WFC is shown in Table 8 but the detailed analysis at WOFC is presented in the supplementary data.

3.3.3. *Effect of power production period on the investment viability from 2017 to 2035*

The business period starting from 2017 and ending at the 18th year has its period as 2017e2035, but none of the ventures is viable at this period Fig. 10 highlights the viability status of the business for coal-to-solid waste ratio of 1:1 and indicates a negative NPV for all the feedstocks investigated at WFC. Similar observations were

Table 7b
Variation in feedstocks economic parameter: Percentage basis.

Parameters			
Feedstock	Amount of Fuel	Expenditure	Profit
WFC [%]			
Coal & Coal þ CC*	0.02	12.47	8.94
Coal & Coal þ PSD**	4.87	22.09	32.87
WOFC [%]			
Coal & Coal þ CC*	2.11	48.21	22.37
Coal & Coal þ WT**	13.69	63.72	25.55

*: Lowest economy; **: Highest economy; SCB: sugarcane bagasse; CC: corn cob; PSD: pine sawdust; WT: waste tyre.

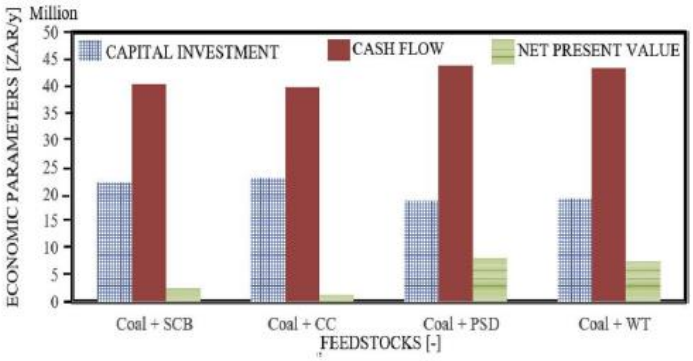


Fig. 7. Economic assessment at the 10th year using WFC at coal to biomass/waste ratio of 1:1.

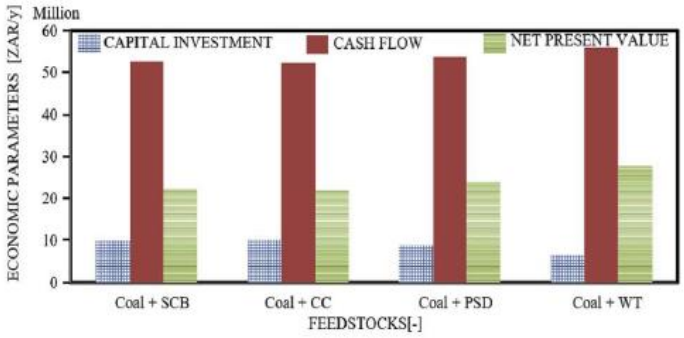


Fig. 8. Economic assessment at the 10th year using WOFC at coal to biomass/waste ratio of 1:1.

made in other blends, as well. Therefore, investing in the business till 2035 using any of the feedstocks will be a waste of resources, but the analysis at WOFC proofed otherwise.

3.4. Environmental impact assessment of the 5 MW co-gasification power plant

A co-gasification power generation plant operating at 5 MW capacity can use Coal SCB, Coal þ CC, Coal þ PSD, and Coal WT of about 20,473.45 t, 20,986.05 t, 18,251.81 t, and 15,276.28 t, to produce the 5 MW of electricity annually. Coal is commonly used for power production in South Africa and if these feedstocks replace coal for energy production it is expected that the amount of GHG emitted from power plant will reduce. Most importantly, the amount of CO_2 that will be available for sequestration will also reduce. Arias et al. (2016) investigated the optimal design and sensitivity analysis of post-combustion CO_2 capture process by chemical absorption with amines. The authors were able to identify the operating conditions that minimize the specific total cost of the CO_2 capture. Also, in a review carried out by Chen et al. (2017) on emerging N-nitrosamines and N-nitramines from amine-based post-combustion CO_2 capture, it was revealed that the process is a promising option. However, a change in the capacity of the existing plant to about 1.5 or 2 times the current capacity will definitely increase the feed rate and annual feedstock re- quirements, investment cost and profit, and as well, the emissions in the plant. Table 9 presents the effective emission reduction ex- pected from different feedstocks studied.

The coal-to-solid waste ratio of 1:1 (Table 9) produces the lowest amounts of CO_2 and SO_2 emissions, and the emissions

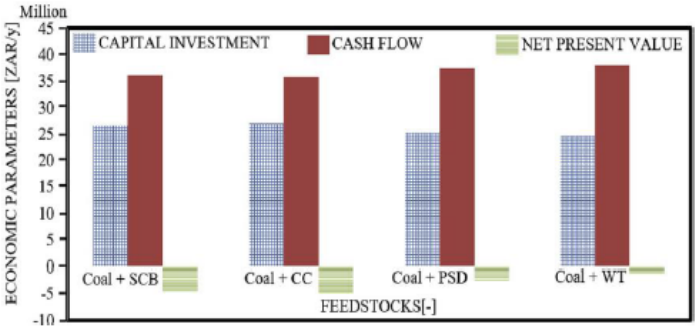


Fig. 9. Economic assessment at the 10th year using WFC at coal to biomass/waste ratio of 4:1.

Table 8
Investment evaluation at 17th Year using WFC.

Feedstocks [-]	Capital Cost Investment [d] [ZAR/y]	Cash Flow [m] [ZAR/y]	Net Present Value [NPV] [ZAR/y]	Internal Rate of Return [IRR] [%]	Payback Period [PBP] [Year]
Ratio: [1:1], Interest Rate: [5%] - WFC					
Coal þ SCB	22238058.18	40401941.82	−4610824.80	3.57	0.6
Coal þ CC	22900607.30	39739392.70	−5562441.90	3.29	0.6
Coal þ PSD	18775998.37	43864001.63	361720.25	5.12	0.5
Coal þ WT	19175395.01	43464604.99	−211931.82	4.93	0.5
Ratio: [3:2], Interest rate: [5%] - WFC					
Coal þ SCB	23695579.21	38944420.79	−6704257.43	2.97	0.6
Coal þ CC	22918288.46	39721711.54	−5587837.29	3.30	0.6
Coal þ PSD	21496041.75	41143958.25	−3545069.05	3.90	0.4
Coal þ WT	20414617.14	42225382.86	−1991822.46	4.37	0.4
Ratio: [4:1], Interest Rate: [5%] - WFC					
Coal þ SCB	26580269.34	36059730.66	−4442722.76	1.79	0.7
Coal þ CC	26881014.28	35758985.72	−11279487.30	1.69	0.8
Coal þ PSD	25237300.14	37402699.86	−8918626.08	2.31	0.7
Coal þ WT	24632996.13	38007003.87	−8050666.23	2.58	0.7

WFC: With Feedstock Costing; SCB: sugarcane bagasse; CC: corn cob; PSD: pine sawdust; WT: waste tyre.

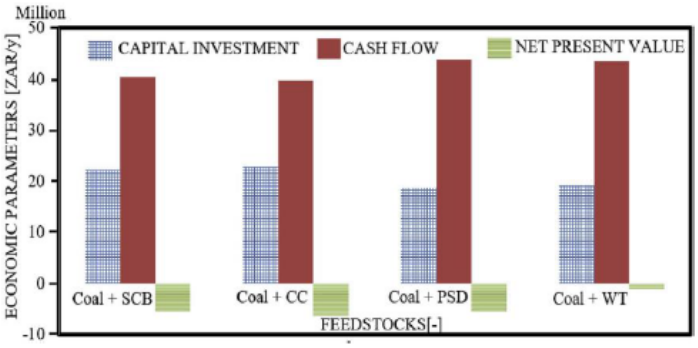


Fig. 10. Economic assessment at the 18th year using WFC at coal to biomass/waste ratio of 1:1.

increased as the amount of coal in the various mixtures increased for all the feedstocks investigated. Similarly, Coal þ PSD produced the lowest amounts of CO_2 and SO_2 emission reductions, whereas; Coal þ WT gave the lowest CO and NO_X emission for all the feed- stocks investigated. In overall, it is possible to reduce the CO, CO_2, SO_2, and NO_X emissions by approximately 3.4%, 23.28%, 22.97%, and 0.55%, respectively, using the Coal-to-PSD of blend ratio 1:1 as against the blend ratio of 4:1. The CO_2 emission from the Matla coal is estimated as 5,9000 kg CO_2/kWh, whereas the CO_2 emission from Coal þ PSD or other biomass and waste investigated at a blend ratio of 1:1 is estimated as 2950 kg CO_2/kWh (a 50% reduction). Bada et al. (2016) have also reported a similar trend using coal-to-biomass blend ratio of 1:1. The result corroborates the findings of this study.

3.5. *Our results compared with literature*

Table 10 presents the comparison of the present work with

Table 9
Estimated emission reduction from the plant at different blend ratio.

Feedstock	CO [kg]	CO_2 [kg]	SO_2 [kg]	NO_x [kg]
Blending Ratio: [1:1]				
Coal þ SCB	−28.70	2905.96	34.58	−113.79
Coal þ CC	−29.43	2904.89	34.58	−116.96
Coal þ PSD	−25.54	2910.74	34.60	−100.04
Coal þ WT	−21.30	2918.87	34.63	−81.61
Blending Ratio: [3:2]				
Coal þ SCB	−28.50	3496.52	41.53	−110.75
Coal þ CC	−29.07	3495.65	41.53	−113.25
Coal þ PSD	−26.89	3498.95	41.54	−103.74
Coal þ WT	−21.86	3510.02	41.57	−81.91
Blending Ratio: [4:1]				
Coal þ SCB	−28.10	4676.41	55.43	−104.67
Coal þ CC	−28.38	4675.99	55.43	−105.89
Coal þ PSD	−27.28	4677.65	55.44	−101.12
Coal þ WT	−24.67	4682.28	55.45	−89.78

SCB: sugarcane bagasse; CC: corn cob; PSD: pine sawdust; WT: waste tyre.

other previous works. The information contained in this section is basically the analysis of different previous studies on electricity and thermal power generations including the technology, system ca- pacity, feedstock. Malek al. (2017) used a biomass-based steam generating plant to study the energy efficiencies, cost implications, environmental effect, and the potentials of a 10 MW biomass power plant in Malaysia. Two financial cases namely: assessment with loan and assessment without loan were investigated. MC, heating value, and investment cost were considered as the major variables in the study and NPV, IRR, and PBP were the appraisal tools. In addition, the authors considered plant efficiencies of 20%, 30% and 40% with corresponding investment years of 2015, 2020, 2030, and 2050. Consequently, the authors reported savings of about MYR 0.88e2.43 M from the plant with raw Empty Fruit Bunch (EFB) as the feedstock. In the current study, a 5 MW CHP plant was assessed using feedstocks originated from South Africa, and about 1868.81 t of fuel was saved by using Coal-to-PSD ratio of 1:1 at WFC. This makes the fuel mixture the optimum amongst the feedstocks studied. Malek and co-workers also reported that system efficiency of 25%e40% could be achieved from various biomass-based steam plant, and that significant amounts of CO_2, SO_2, NO_x, and CO emissions (Table 10) were reduced in the plant when compared to the existing Malaysian energy mix (see Table 10) The effective emission reduction of 3.4%, 23.28%, 22.9%, and 0.55%, is CO, CO_2, SO_2 & NO_x, respectively. Were obtained from the 5 MW CHP assessed in the present work. The energetic efficiencies and cost of investment were the most uncertain variables reported by Voets et al. (2011) during their estimations using biomass of Belgium origin, and the variables rendered the analysis of the 20 MW technology option unclear. However, the current study, 10th year, and Coal-to-Solid waste ratio of 1:1 are the optimum investment year and blending ratio, respectively.

Secondly, if environment regulations and/or policy are to be promulgated, and restricting the transportation of biomass only with specific type of trucks such as electric powered trucks (bat- teries) and solar vehicles, emissions will be further reduced. In this case, the overall result of the present analysis will be changed.

3.6. Sensitivity of the NPV and impact of uncertainty

To evaluate the sensitivity of the NPV and impact of uncertainty on the viability of the feedstocks for energy production in the 5 MW power plant, the standard deviation (SD), the variance, and the standard error of the major Equations (10)e(12) (Zady, 2009), respectively. Results of the analysis are presented in Table 11a

Table 10
Comparison of the present work with previous studies.

Technology Used	Plant Capacity	Fuel Used	Major Findings	Reference
Flash Pyrolysis & Gasification plants: 5 MW, Electricity & CHP generation Units 10 MW, & 20 MW Remarks: Feedstock origin: Flanders, Belgium Evaluation Target: Plant with the highest profit Investment evaluation year: 10 yrs. Appraisal tool used: NPV		Short rotation Coppices (Belgium)	For the 5 MW & 10 MW electric power productions, flash pyrolysis was more viable in terms of plants profitability. But higher profit was produced from the 5 MW CHP productions. The 20 MW technology option was unclear because of the energetic efficiencies and investment cost; the most uncertain variables.	Voets et al., 2011
Biomass-based Rankine-Cycle Steam power Plant Remarks: Feedstocks Origin: Malaysia. Two Hypothetical Financial Cases: Investment with Loan & Investment without Loan. Major Variables Considered: Moisture content, Heating value & Investment Cost. Project Appraisal tools: NPV, IRR, & PBP. Specific Compares: Biomass-based Plant & existing energy mix in Malaysia, system efficiencies: 20%, 30% and 40%, investment years studied: 2015, 2020, 2030 & 2050.	10 MW	EFB, MCF, PKS, OPF, OPT, & WB	Feedstock cost of around MYR 0.88e2.43 million, was saved by using raw EFB in the power plant, and an application of various biomass-based gasification technologies could enhance system efficiency by around 25%e40%. Emission analysis indicated that lower emission reductions of about 50,130 t of CO_2, 750 t of SO_2, 218.65 t of NO_x, & 22.83 t of CO were produced from the plant as compared to the existing energy mix in Malaysia.	Malek et al., 2017
Co-gasification CHP Plant Remarks: Feedstock Origin: South Africa. Feedstocks: Coal, SCB, CC, PSD, & WT. Two hypothetical cases: WFC & WOFC. Major Variables: Energy (Heating value), Moisture content, Economic (investment cost & profit), and Environmental (emissions). Project feedstock studied. appraisal tools: NPV, IRR, & PBP Compares: Coal & other solid wastes, various blends of Coal & other solid wastes, investment years: 10th, 11th, 17th & 18th year. Evaluation target: The most viable feedstock for power production with regard to: Profitability: Energy content, annual feedstock savings, cost savings, and emissions reduction.	5 MW	Biomass & Solid Waste	About 1,868,805.41 Kg of feedstock was saved in the plant annually, by using Coal-to-PSD ratio of 1:1. A higher profit of around 13.82%, & 23.56% were made from Coal þ PSD compared to 100% Matla coal WFC & WOFC. Around 3.4%, 23.28%, 22.9%, and 0.55%, of CO, CO_2, SO_2 & NO_x emissions were reduced in the plant by using Coal-to-PSD ratio of 1:1, respectively. The 10th year & Coal þ PSD were the optimum investment year and	Current Work.

EFB: empty fruit bunch; MCF: Mesocarp fiber; PKS: palm kernel shell; OPF: Oil palm frond; OPT: oil palm trunk; WB: wood biomass; WFC: with feedstock costing; WOFC: without feedstock costing; NPV: net present value; IRR: internal rate of return; PBP: payback period; PSD: pine saw-dust.

Table 11a
Sensitivity Analysis of 10th Year using WFC.

Amount of Feedstock [t]			Capital Cost Investment [ZAR/y]			Ratio
×	$\bar{X}$	$\delta X - \bar{X}$ þ²	×	$\bar{X}$	$\delta X - \bar{X}$ þ²	1:1
20,473.45	18,746.90	2.98099Eþ9	22238058.18	16547914.72	3.23777Eþ13	
20,986.045	18,746.90	5.01381Eþ9	22900607.3	16547914.72	4.03567Eþ13	
18,251.81	18,7468.96	2.45114Eþ8	1877598.37	16547914.72	2.15218Eþ14	
15,276.28	18,746.90	1.20452Eþ10	19175395.01	16547914.72	6.90365Eþ12	
Variance	6.7617Eþ9		Variance	9.82854Eþ13		
Std. Deviation	2600.33		Std. Deviation	9913900.512		
Standard Error	1300.16		Standard Error	4956950.256		
Cash Flow [ZAR/y]			Net Present Value [ZAR/y]			
40401941.82	41867485.29	2.14782Eþ12	1384120.434	3706536.818	5.39362Eþ12	
39739392.7	41867485.29	4.52878Eþ12	334192.5751	3706536.818	1.13727Eþ13	
43864001.63	41867485.29	3.98608Eþ12	6870374.924	3706536.818	1.00099Eþ13	
43464604.99	41867485.29	2.55079Eþ12	6237459.338	3706536.818	6.40557Eþ12	
Variance	4.4045Eþ12		Variance	1.10606Eþ13		
Std. Deviation	2098687.25		Std. Deviation	3325746.228		
Standard Error	1049343.63		Standard Error	1662873.114		
Amount of Feedstock [t]			Capital Cost Investment [ZAR/y]			3:2
20,401.90	19,055.91	1.81167Eþ9	23695579.21	22131131.64	2.4475Eþ12	
20,807.06	19,055.91	3.0665Eþ9	22918288.46	22131131.64	6.19616Eþ11	
19,270.94	19,055.91	4.623706Eþ7	21496041.75	22131131.64	4.03339Eþ11	
15,743.76	19,055.91	1.09704Eþ10	20414617.14	22131131.64	2.94642Eþ12	
Variance	5.29826Eþ9		Variance	2.13896Eþ12		
Std. Deviation	2301.80		Std. Deviation	1462517.607		
Standard Error	1150.90		Standard Error	731258.8037		
Cash Flow [ZAR/y]			Net Present Value [ZAR/y]			Ratio
×	$\bar{X}$	$\delta X - \bar{X}$ þ²	×	$\bar{X}$	$\delta X - \bar{X}$ þ²	3:2
38944420.79	40508868.36	2.4475Eþ12	212916.8565	2737799.533	6.37503Eþ12	
39721711.54	40508868.36	6.19616Eþ11	1467396.71	2737799.533	1.61392Eþ12	
41143958.25	40508868.36	4.03339Eþ11	3762779.525	2737799.533	1.05058Eþ12	
42225382.86	40508868.36	2.94642Eþ12	5508105.041	2737799.533	7.67459Eþ12	
Variance	2.13896Eþ12		Variance	5.57138Eþ12		
Std. Deviation	1462517.607		Std. Deviation	2360376.556		
Standard Error	731258.8037		Standard Error	1180188.278		
Amount of Feedstock [t]			Capital Cost Investment [ZAR/y]			
20,260.28	19,565.16	4.83182Eþ8	26580269.34	25832894.97	5.58568Eþ11	4:1
20,458.08	19,565.16	7.97294Eþ8	26881014.28	25832894.97	1.09855Eþ12	
19,686.61	19,565.16	1.4749684Eþ7	25237300.14	25832894.97	3.54733Eþ11	
17,855.69	19,565.16	2.9223Eþ9	24632996.13	25832894.97	1.43976Eþ12	
Variance	1.40584Eþ9		Variance	1.15054Eþ12		
Std. Deviation	1185.68		Std. Deviation	1072631.183		
Standard Error	592,841.27		Standard Error	536315.5915		
Cash Flow [ZAR/y]			Net Present Value [ZAR/y]			
36059730.66	36807105.03	5.58568Eþ11	−4442722.763	−3236525.37	1.45491Eþ12	
35758985.72	36807105.03	1.09855Eþ12	−4928099.02	−3236525.37	2.86142Eþ12	
37402699.86	36807105.03	3.54733Eþ11	−2275286.976	−3236525.37	9.23979Eþ11	
38007003.87	36807105.03	1.43976Eþ12	−1299992.719	−3236525.37	3.75016Eþ12	
Variance	1.15054Eþ12		Variance	2.99682Eþ12		
Std. Deviation	1072631.183		Std. Deviation	1731133.687		
Standard Error	536315.5915		Standard Error	865566.8433		

X: Estimated variable (e.g. amount of feedstock, capital cost investment, cash flow, net present value); $\bar{X}$: mean of the variable; Std.: standard.

$$SD = \sqrt{\frac{\sum (X - \bar{X})^2}{N-1}} \quad (10)$$

$$Variance = \frac{\sum (X - \bar{X})^2}{N-1} \quad (11)$$

$$Standard\ Error = \frac{SD}{\delta N þ^{1=2}} \quad (12)$$

X represents the variables including amount of feedstock, capital cost investment, cash flow and net present value, while $\bar{X}$ is the mean of the variables.

The standard error of the mean (SEOM) is referred to as a measure for the variance of NPV distributions (Voets et al., 2011), which is dependent on the blend ratio of the variables mentioned earlier, and their SEOM were equally estimated. To enhance the comparability of this measure for different blend ratio of the fuel, the SEOM was divided by the mean value of the NPV of the feedstocks from the various blends. The mean and relative standard (percentage) error (RSE) of all the feedstocks, the amount of feedstock, capital cost investment, cash flow, NPV obtained were from

Table 11b
Mean NPV and RSE of Variables (10th Year) using WFC.

B. RATIO	Amount of Feedstock		Capital Cost Investment		Cash Flow		Net Present Value	
	Mean AOF [t/y]	RSE of AOF [%]	Mean CCI [t/y]	RSE of CCI [%]	Mean CF [t/y]	RSE of CF [%]	Mean NPV [t/y]	RSE of NPV [%]
1:1	18,746.90	0.07	16,547.91	0.30	41,861.49	0.03	3706.54	0.45
3:2	19,055.91	0.06	22,131.13	0.03	40,508.87	0.02	2737.80	0.43
4:1	19,565.16	0.03	25,832.89	0.02	36,807.11	0.01	−3236.53	−0.27

RSE: Relative standard error; AOF: amount of feedstock; CCI: Capital cost investment; CF: cash flow; NPV: net present value; B. Ratio: feedstock blend ratio.

Table 11c
Mean NPV and RSE of Variables (10th Year) using WOFC.

B. RATIO	Amount of Feedstock		Capital Cost Investment		Cash Flow		Net Present Value	
	Mean AOF [t/y]	RSE of AOF [%]	Mean CCI [t/y]	RSE of CCI [%]	Mean CF [t/y]	RSE of CF [%]	Mean NPV [t/y]	RSE of NPV [%]
1:1	18,746.90	0.07	8972.10	0.09	53,667.80	0.02	23,975.32	0.06
3:2	19,055.91	0.06	8894.28	0.08	53,745.17	0.01	24,100.92	0.05
4:1	19,565.16	0.03	8665.20	0.04	53,974.78	0.01	24,470.64	0.02

RSE: Relative standard error; AOF: amount of feedstock; CCI: Capital cost investment; CF: cash flow; NPV: net present value; B. Ratio: feedstock blend ratio.

the three different fuel blends studied in the plant (10th year) at WFC are shown in Table 11b.

According to Table 11b, the feedstock blend ratio and investment cost were considered as the most significant variables. Both the amount of the fuel and energy content of the fuel (not shown in Table 11b) have direct impact on the investment cost, as can be observed in the mean value of the RSE in Table 11b. According to the report of Australian Bureau of Statistics (ABS, 2009) on Labour Force Standard Error, a RSE 25% is prone to high sampling error and should be used with caution. Most of the RSE presented in Table 11b are less than 25% indicating less sampling error. Coal-to-solid waste ratio of 1:1 is the optimum blend in terms of fuel and investment cost savings and emission reduction. This blend has the highest mean NPV as shown in Table 11b, and Table 11b provides information that will assist investors to make their decisions about the investment.

However, the sensitivity analysis was carried out using Figs. 7 and 8 as well as Table 9 as the base model; the optimum investment conditions in the plant. From Table 11b, the coal-to-solid waste ratio of 1:1 has the highest mean NPV, whereas; in the absent of 4:1 mixture, the lowest RSE was produced by the 3:2 feedstock blend. The 4:1 blend clearly indicated an unattractive investment, as can be observed from the negative value of the mean NPV, and as such, should not be ventured by investors. Fig. 7 (base model) have demonstrated that Coal-to-PSD ratio of 1:1 at WFC was the optimum feedstock and blend ratio for the energy production following the variables earlier mentioned. With reference to the value of NPV of the base model, for the most profitable condition, there was no deviation with the option of the most viable condition for the highest mean NPV.

On the basis of emission reduction in the plant, the optimal condition (1:1 blend ratio) can as well, be observed in Table 9. The Coal þ PSD produced higher CO and NO_x emissions, as well as lower amounts of CO_2 and SO_2 when compared to Coal þ WT that yielded lower CO and NO_x, plus higher CO_2 and SO_2 emission. However, the results of the mean of AOF, CCI, and CF variables of the 1:1 fuel mixture in Table 11b confirmed the most viable option based on the results presented in Fig. 7.

Similarly, the sensitivity analysis for the variables at WOFC is presented in Table 11c. It can be seen from the table that the mean value of the NPV of 4:1 fuel blend is higher than the mean value of NPV of the 1:1 blend. The RSE value of the 4:1 fuel blend is lower than the RSE value of 1:1 fuel blend. This implies that based on analysis at WOFC, where the actual cost of the feedstock is discounted, investors may consider the investment to be viable. However, it is noteworthy to mention that the cost of transfer of the feedstock is very crucial in the overall decision-making if the plant is not located very close to the source of raw material. Furthermore, the variance in the NPV is an indication of the degree of the influence of the investment cost on the economic analysis. The investment cost and blend ratio are the most sensitive variables in the analysis.

Comparison of the NPV in Fig. 7 and that of Table 11c indicates that the investment cost has a significant impact on the NPV and should be considered in the decision-making by prospective investors. Considering investment cost for the two cost analysis scenarios presented in this studies (i.e. WFC & WOFC), the use of Matla Coal PSD at blend ratio 1:1 is the most attractive for WFC while the use of Matla Coal WT at blend ratio of 1:1 is the most viable option for WOFC.

4. Conclusions

An evaluation of the economic, energy and environmental viability of a 5 MW co-gasification power plant has been carried out, using coal blended with SCB, CC, PSD, and WT. The evaluation considered two scenarios namely: WFC and WOFC. The blend ratios investigated were 1:1, 3:2, and 4:1. The heating value, investment cost and emission were estimated for coal-blended fuel at coal:- solid waste but investment cost and feedstock blend ratio were the most significant factors considered. The NPV, IRR, and PBP tools were used to evaluate the power generation project at different business periods namely: 10th, 11th, 17th and 18th year. Coal PSD blend at a ratio of 1:1 evaluated at WFC is the most attractive feedstock for the energy generation in the investigated power plant. The business viability order is Coal PSD > Coal WT > Coal SCB, > Coal CC at WFC. At WOFC, the order is Coal WT > Coal PSD > Coal SCB, > Coal CC. The use of 100% Matla coal is not cost effective, and it produces higher emissions when compared to other feedstocks investigated. A higher profit of 13.82% and 23.56% are predicted for the use of Coal PSD at WFC and WOFC respectively, when compared to 100% Matla coal, thereby enabling a savings of about 1868.81 t of feedstock, annually. In addition, the following conclusions emanated from the study:

The use of Coal-to-PSD ratio of blend 4:1 for the power generation as against 1:1 Coal-to-PSD of blend ratio 1:1 resulted to an

annual loss of about ZAR6, 461,301.77 ($90,458,224.70) and ZAR123,782.47 ($1,732954.58) WFC and WOFC.

At the 10th year, coal-to-solid waste blend of ratio 4:1 is not viable at WFC but Coal PSD is viable at the 17th year, but at the 18th year the use of none of the feedstocks is attractive for the business venture, at WFC.

The power plant will use 20,473.45 t, 20,986.05 t, 18,251.81 t, 15,276.28 t of Coal SCB, Coal CCB, Coal PSD and Coal PWT to produce the 5 MW and 5.56 MW electric and thermal power, annually.

- Coal-to-solid waste ratio of 1:1 produced the lowest amounts of CO_2 and SO_2 emission, and emissions increases as the amount of coal in the blend increases for all the feedstocks studied. But the emission is reduced significantly when Coal PSD blend with ratio 1:1 is used.

Change of energy, economic and environmental policies in the future will affect the estimated results. The speculated future policies may include: basing the price of fuel on its heating value, restricting fuel transportations only with electric- powered trucks, and allowing electricity consumers to use non-central grid units without payment of utility bills to the government.

This study considered only one coal sample from Matla mine. It is very useful to consider variety of coal samples because of ex- pected difference in compositional characteristics and calorific contents. Future R&D should consider using variety of coal samples especially from different geographical locations in South Africa. Computational analysis of this study could be carried out using computational tools such as artificial neural networks, Aspen plus or in General Algebraic Modelling System (GAMS) environment for improved results. Regardless of the aforementioned areas not considered in the present study, the outcome of this study could serve as a platform upon which further R&D in this area could be built.

Acknowledgment

The authors acknowledge the support of Dr. S. O. Bada for his help in biomass processing, Mr. Jubril Abdulsalam and Mrs. Angela Ozonoh for proof reading the work.

References

ABS, 2009. Australian Bureau of Statistics, Labour Force Survey Standard Error. Datacube (Cat.no.6298.0.55.001). Available online at: http://.www.abs.gov.au.

Ahmaruzzuman, M., 2008. Proximate analysis and predicting higher heating value of chars obtained from co-cracking of petroleum vacuum residue with coal, plastic and biomass. Bioresour. Technol. 99, 5043e5080.

Ahmed, F., Al Amin, A.Q., Hasanuzzaman, M., Saidur, R., 2013. Alternative energy resources in Bangladesh and future prospect. Renew. Sustain. Energy Rev. 25, 698e707.

Alzate, C.A., Chejne, F., Valdés, C.F., Berrio, A., Cruz, J.D.L., Londoño, C.A., 2009. CO-gasification of pelletized wood residues. Fuel 88, 437e445.

Arias, A.M., Mores, P.L., Scenna, N.J., Mussati, S.F., 2016. Optimal design and sensi-tivity analysis of post-combustion CO_2 capture process by chemical absorption with amines. J. Clean. Prod. 115, 315e331.

Bada, S.O., Falcon, E.M.S., Falcon, L.M., Bergmann, C.P., 2016. Co-firing potential of raw and thermally treated Phyllostachys aurea bamboo with coal. Energy Sources, Part A Recovery, Util. Environ. Eff. 38, 1345e1354.

Bridgwater, A.V., 2004. Biomass fast pyrolysis. Therm. Sci. 8, 21e49.

Bridgwater, A.V., Toft, A.J., Brammer, J.G., 2002. A techno-economic comparison of power production by biomass fast pyrolysis with gasification and combustion. Renew. Sustain. Energy Rev. 6, 181e248.

Caputo, A.C., Palumbo, M., Pelagagge, P.M., Scacchia, F., 2005. Economics of biomass energy utilization in combustion and gasification plants: effects on logistic variables. Biomass Bioenergy 28, 35e51.

Chen, X., Huang, G., An, C., Yao, Y., Zhao, S., 2017. Emerging N-nitrosamines and N-nitramines from amine-based post-combustion CO ₂ capture- a review. Chem. Eng. J. 335, 921e935.

Demirbas, A., 2001. Biomass resource facilities and biomass conversion processing for fuels and chemicals. Energy Convers. Manag. 42, 1357e1378.

Hasanuzzaman, M., Rahim, N.N., Saidur, R., Kazi, S.N., 2011. Energy savings and emission reductions for rewinding and replacement of industrial motor. Energy 36, 233e240.

Huang, C.J., Han, L.J., Liu, L., Yang, Z., 2008. Proximate analysis and calorific value estimation of rice straw by near infrared reflectance spectroscopy. J. Energy Inst. 81, 153e157.

Kamble, A.D., Saxena, V.K., Chavan, P.D., Mend, V.A., 2018. Co-gasification of coal and biomass an emerging clean energy technology: status and prospects of development in Indian context. Int. J. Min. Sci. Technol. https://doi.org/10.1016/ j.ijmst.2018.03.011. (Accessed 7 July 2018).

Kong, X.Q., Wang, R.Z., Huang, X.H., 2004. Energy efficiency and economic feasibility of CCHP driven by Stirling engine. Energy Convers. Manag. 45, 1433e1442.

Kumabe, K., Hanaoka, T., Fujimoto, S., Minowa, T., Sakanish, K., 2007. Co-gasification of woody biomass and coal with air and steam. Fuel 86, 684e689.

Mahlia, T.M.I., 2002. Emissions from electricity generation in Malaysia. Renew. Energy 27, 293e300.

Mahlia, T.M.I., Yanti, P.A.A., 2010. Cost efficiency analysis and emission reduction by implementation of energy efficiency standards for electric motors. J. Clean. Prod. 18, 365e374.

Malek, A.A.B.M., Hasanuzzaman, M., Rahim, N.S., Turki, Y.A.A., 2017. Techno-eco-nomic analysis and environmental impact assessment of a 10 MW biomass- based power plant in Malaysia. J. Clean. Prod. 141, 502e513.

Mitchell, C.P., Bridgwater, A.V., Stevens, D.J., Toft, A.J., Watters, M.P., 1995. Techno-economic assessment of biomass to energy. Biomass Bioenergy 9, 205e226.

Nhuchhen, D.R., Salam, P.A., 2012. Estimation of higher heating value of biomass from proximate analysis: a new approach. Fuel 99, 55e63.

Oboirien, B.O., Engelbrecht, A.D., North, B.C., Du Cann, V.M., Veryn, S., Falcon, R., 2011. Study on structure and gasification characteristics of selected South Af- rican bituminous coal in fluidized bed gasification. Fuel Process. Technol. 92, 735e742.

Parik, J., Channiwala, S.A., Ghosal, G.K., 2005. A correlation for calculating HHV from proximate analysis of solid fuels. Fuels 84, 487e494.

PDD, Project Design Document, 2006. Bell eco power sdn bhd _Biomass based power generation project. In: CDM-UNFCCC. CDM-SSC-PDD: Clean Develop- ment Mechanism (CDM) Executive Board Report - Version 03, 1-85 Accessed on: 06/07/2018. Available online at: mer.markit.com/br-reg/services/processDocument/downloadDocumentById/103000000014897.

SA Power Network, 2017. South Africa Power Network. Retrieved from SA Power Network website on 22-03-17. Available online at: https://www.sapowernetworks.com.au/centric/industry/our_network/network_tariffs.jsp.

Searcy, E., Flynn, P.C., 2010. A criterion for selecting renewable energy processes. Biomass Bioenergy 34, 798e804.

Sheng, C., Azevedo, J.L.T., 2005. Estimating the higher heating value of biomass fuels from basic analysis data. Biomass Bioenergy 28, 499e507.

Stats SA, 2015. Stats SA: Electricity Generated and Available Distribution (P4141). Retrieved from STATS SA (Statistics South Africa) website on 20-02-17: Avail- able online at: http://.www.stats.

Thipkhunthod, P., Meeyoo, V., Rangsunvigit, P., Kitiyanan, B., Siemanond, K., Rirksomboon, T., 2005. Fuel 84, 849e857.

US EPA, 2008. Average In-use Emissions from Heavy-duty Trucks Emission Facts. A Report from MI. Office of Transportation and Air Quality, USA.

Varun, Bhat, I.K., Prakash, R., 2009. LCA of renewable energy for electricity gener- ation systemsda review. Renew. Sustain. Energy Rev. 13, 1067e1073.

Verma, V.K., Bram, S., Delattin, F., Laha, P., Vandendael, I., Hubin, A., De Ruyck, J., 2012. Agro-pellets for domestic heating boilers: standard laboratory and real life performance. Appl. Energy 90, 17e23.

Voets, T., Kuppens, T., Cornelissen, T., Thewys, T., 2011. Economics of electricity and heat production by gasification or flash pyrolysis of short rotation coppices in Flanders (Belgium). Biomass Bioenergy 35, 1912e1924.

WNA, 2011. Comparison of Lifecycle GHG Emissions for Various Electricity Gener-ation Sources. World Nuclear Association Report, London, UK. Retrieved on 15- 08-17. Available online at: www.worldnuclear.org/World Nuclear-Association/Publications/Reports/Lifecycle GHG Emissions- of-Electricity-Generation.

Yin, C.Y., 2011. Prediction of higher heating value of biomass from proximate and ultimate analysis. Fuel 90, 1128e1132.

Zady, M.F., 2009. Z-5: Sum of squares, Variance, and the Standard Error of the Mean Basic Statistics. Clinical Laboratory Science Program. University of Louisville, Louisville Kentucky. Accessed on: 03/08/2018. Available online at: www.wstgard.com/lessen35.htm.

Zhang, Y., Zheng, Y., Yang, M., Song, Y., 2016. Effect of fuel origin on synergy during co-gasification of biomass and coal in CO_2. Bioresour. Technol. 200, 789e794.

Data in Brief 21 (2018) 2598–2608

Contents lists available at ScienceDirect

Data in Brief

Data Article

Dataset on the assessment of the environmental, economic and energy parameters of 5 MW CHP co-gasification plant using South African coal, biomass and waste-tyre

M. Ozonoh [a], T.C. Aniokete [a], B.O. Oboirien [b], M.O. Daramola [a,n]

[a] School of Chemical and Metallurgical Engineering, Faculty of Engineering and the Built Environment, University of the Witwatersrand, Wits 2050, Johannesburg, South Africa
[b] Department of Chemical Engineering, University of Johannesburg, Doornfontein, Johannesburg 2028, South Africa

articleinfo

Article history:
Received 24 July 2018
Received in revised form 14 October 2018
Accepted 23 October 2018
Available online 27 October 2018

Keywords:
Co-gasification
Biomass waste
Coal
Electricity and heat production
Techno-economic
South Africa

abstract

The data provided in this article supplements the data information provided in "Techno-economic analysis of electricity and heat production by co-gasification of coal, biomass and waste tyre in South Africa" [1]. The generation of the data considered co-generation of a coal sample (Matla coal) with pine sawdust, sugarcane bagasse, corn cob, and waste tyre at a blend ratio of 1:1, 3:2, and 4:1. The cost evaluation of the use of the feedstocks was considered with feedstock costing (WFC) and without feedstock costing (WOFC). Profitability assessment tools for the case study included NPV, IRR and PBP. The data as contained in this article could be useful for a quick decision making on a similar project by the government and stakeholders in the sector.

& 2018 The Authors. Published by Elsevier Inc. This is an open access article under the CC BY license (http://creativecommons.org/licenses/by/4.0/).

DOI of original article: https://doi.org/10.1016/j.jclepro.2018.07.209
[n] Corresponding author.
E-mail address: michael.daramola@wits.ac.za (M.O. Daramola).

https://doi.org/10.1016/j.dib.2018.10.117
2352-3409/& 2018 The Authors. Published by Elsevier Inc. This is an open access article under the CC BY license (http://creativecommons.org/licenses/by/4.0/).

Specifications table

Subject area	Electricity and Thermal Power Production
More specific subject area	Chemical Engineering
Type of data	Table, graph, figure
How data was acquired	CHNS-O Organic Elemental Analyzer (FLASH 2000), TGA-SDT (600), Oxygen-bomb calorimeter (203 M 1241).
Data format	Raw and analyzed.
Experimental factors	Feedstocks of South African origin were milled (size reduction) and sieved for analysis.
Experimental features	Results from the proximate and ultimate analysis was fitted into an empirical model to estimate the LHV of the fuels, and was then used in the model equations shown in the experimental design, material and method section, to determine the annual feed rate and feedstock requirements for the 5 MW electric and thermal power plant.
Data source location	Johannesburg, South Africa
Data accessibility	Data are with this article
Related research article	Techno-economic analysis of electricity and heat production by co-gasification of coal, biomass and waste tyre in South Africa [1]

Value of the data

- South African coal reserve depletes very fast, and the CO_2 emission in the country is the highest in the whole of Africa. In this regard, the use of this data article could be instrumental to the reduction in the rapid depletion of the coal reserve, and emissions.
- As far as could be ascertained, data describing the electrical and thermal power production in a 5 MW CHP plant using South African feedstock is not available in the open literature; thus, a set of data provided in this article, could be used as a platform for decision making and further R&D in this area.
- With the provided dataset, investors can have a good understanding of the techno-economic analysis of the power generation in the plant before embarking on the investment, meaning that the dataset provides a working guide for interested investors.
- Policy-making in energy, economic and environmental sectors could consider the dataset, for the modification of existing policies.

1. Data

The dataset provided in this article supplements the data information provided in [1], recently published in the Journal of Cleaner Production, and it contains 11 tables and 6 figures. Figs. 1 and 2 present the flowchart of the proposed technical approach and the scheme of the 5 MW co-gasification process plant. Tables 1 and 2 are the variation in feedstocks economic parameters at the 10th year estimated with feedstock costing (WFC) and without feedstock costing (WOFC), respectively, and both data were estimated using the lower heating value (LHV) data, moisture content (MC) data and the South Africa and other parts of the globe feedstock prices [1]. Tables 3 and 4 emphasize the results of the appraisal tools at the 10th year assessment at WFC and WOFC. Tables 5 and 6 indicate the business viability estimation at the 11th year, at WFC and WOFC. The economic evaluation at the 17th year at WOFC is shown in Table 7. Figs. 3–6 depict the comparism of the feedstocks economic parameters obtained at WFC and WOFC, as well as the economic assessment at the 18th year with blend ratio 3:1 and 4:1. Table 8 describes the emissions reduction assessment of the plant via co-gasification, while Table 9 presents the statistical sensitivity analysis of the statistical estimation showing the mean of the variables amount of feedstock, capital cost investment, cash flows and net

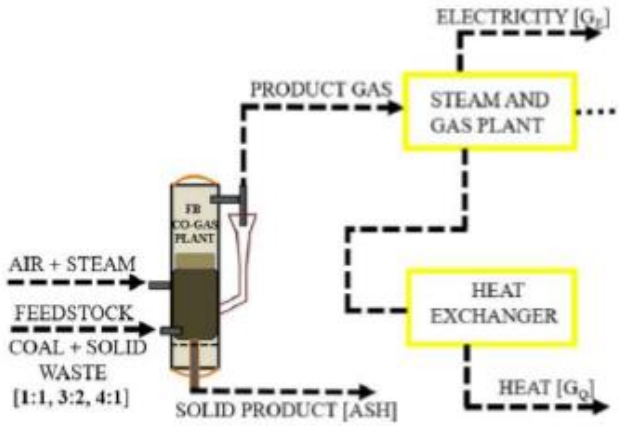


Fig. 1. Fluidised bed co-gasification CHP plant [5 MW]: proposed technical approach.

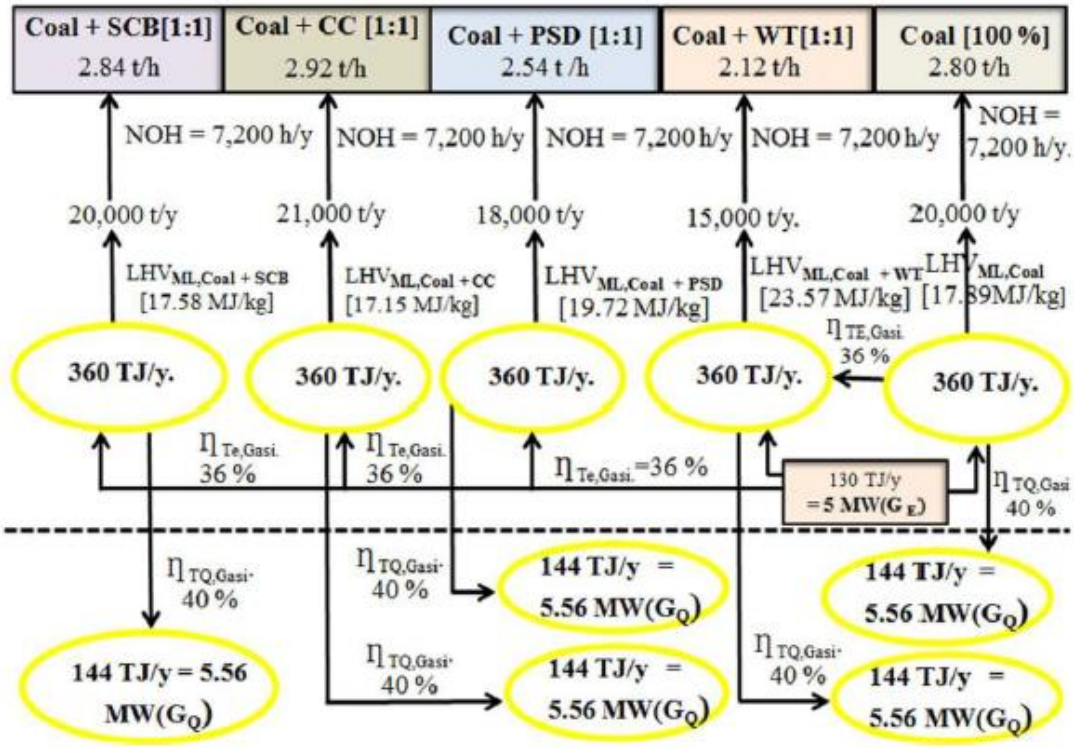


Fig. 2. Proposed process flow diagram for the fluidized bed co-gasification CHP plant (5 MW).

present value (NPV), as well as the variance, standard deviation and standard error of the overall evaluations at 10th year, using WOFC.

2. Experimental design, materials and methods

South African feedstocks comprising coal and solid waste (sugarcane bagasse, corn cob, pine saw- dust, and waste-tyre) were pre-treated by milling and sieving and kept in air-tight bags for analysis.

Table 1
Variation in feedstocks economic parameters *[10th year]: WFC.

Feedstocks	Amount of Fuel [t/y]	Expenditure [ZAR/y]	Profit [ZAR/y]	Feedstock with Highest Profit	Percentage Profit [%]
WFC					
CoalþCC &	20,986.05	22,900,607.05	39,739,393.16	CoalþSCB	4.93
CoalþSCB	20,473.45	22,238,058.01	4,0401,942.41		
VEP*	5125.49	662,549.42	662,549.22		
CoalþCC &	20,986.05	22,900,607.19	39,739,393.16	CoalþPSD	0.83
CoalþPSD	18,251.81	18,775,998.00	43,864,002.00		
VEP**	2734.24	4,124,609.47	4,124,609.03		
CoalþCC &	20,986.05	22,900,607.11	39,739,393.15	CoalþWT	4.48
Coal WTþ	15,276.28	19,175,395.25	43,464,605.06		
VEP***	5709.77	3,725,212.03	3,725,212.00		
CoalþPSD &	18,251.81	18,775,998.04	43,864,002.42	CoalþPSD	4.11
CoalþSCB	20,473.45	22,238,058.15	40,401,942.15		
VEP#	2221.65	3,462,060.11	3,462,060.42		
CoalþPSD &	18,251.81	18,775,998.42	43,864,002.11	CoalþPSD	0.46
CoalþWT	15,276.28	19,175,395.02	43,464,605.02		
VEP##	2975.53	399,397.00	399,397.15		
CoalþSCB &	20,473.45	22,238,058.31	40,401,942.33	CoalþWT	3.65
CoalþWT	15,276.28	19,175,395.08	43,464,605.12		
VEP###	5197.17	3,062,663.04	3,062,663.04		

*CoalþCC & CoalþSCB; **: CoalþCC & CoalþPSD; ***: CoalþCC & CoalþWT; #: CoalþPSD & CoalþSCB; ##: CoalþPSD & CoalþWT; ###: CoalþSCB & CoalþWT; þ: Kg/Yr; þþ: ZAR/Yr; VEP: variation in the economic parameters; ": blending ratio of 1: 1; WFC: with feedstock costing.

Table 2
Variation in feedstocks economic parameters *[10th year]: WOFC.

Parameters	Amount of fuel [t/y]	Expenditure [ZAR/y]	Profit [ZAR/y]	Feedstock with highest profit	Percentage profit [%]
WOFC [except coal]					
CoalþCC &	20,986.05	10,283,164.00	5,356,836.06	Coalþ SCB	1.26
CoalþSCB	20,473.45	10,031,991.21	52,608,009.35		
VEP*	5125.99	251,173.35	251,173.03		
CoalþCC &	20,986.05	10,283,165.00	52,356,836.12	Coalþ PSD	0.24
CoalþPSD	18,251.81	8,943,385.03	53,696,615.00		
VEP**	2734.24	1,339,779.11	1,339,779.07		
CoalþCC &	20,986.05	10,283,164.42	52,356,836.44	Coalþ WT	3.37
CoalþWT	15,276.26	6,629,905.06	56,010,095.21		
VEP***	5709.77	3,402,087.14	3,653,260.07		
CoalþPSD &	18,251.81	8,943,385.11	53,696,615.14	Coalþ PSD	1.02
CoalþSCB	20,473.45	10,031,991.00	52,608,009.25		
VEP#	2221.65	1,088,606.02	1,088,606.36		
CoalþPSD &	18,251.81	894,338.14	53,696,615.11	Coalþ WT	2.11
CoalþWT	15,276.28	6,629,905.25	56,010,095.07		
VEP##	2975.53	2,313,481.11	2,313,481.04		
CoalþSCB &	20,473.45	10,031,991.04	52,608,009.16	Coalþ WT	3.13
CoalþWT	15,276.28	6,629,905.06	56,010,095.22		
VEP###	5197.17	3,402,087.17	3,402,087.00		

*: Coalþ CC & Coalþ SCB; **: CoalþCC & Coalþ PSD; ***: Coalþ CC & CoalþWT; #: CoalþPSD & Coalþ SCB; ##: Coalþ PSD & Coalþ WT; ###: Coalþ SCB & Coalþ WT; ": with a blending ratio of: 1:1; WOFC: without feedstock costing; VEP: variation in the economic parameter.

Table 3
Plant assessment at 10th year, WFC: emphasis on appraisal tools.

Feedstocks [-]	Amount of fuel [t]	Capital cost investment [δ] [ZAR/y]	Cash flow [μ] [ZAR/y]	Net present value [NPV] [ZAR/y]	Internal rate of return [IRR] (%)	Payback period [PBP] (Year)
Ratio: [1:1], Interest rate: [5%] - WFC						
CoalþSCB	20,473.45	22,238,058.18	40,401,941.82	25,652,29.37	6.15	0.55
CoalþCC	20,986.05	22,900,607.30	39,739,392.70	1,495,932.57	5.66	0.58
CoalþPSD	18,251.81	18,775,980.37	43,864,001.63	8,152,693.59	8.85	0.43
CoalþWT	15,276.28	19,175,395.01	43,464,604.99	7,508,102.06	8.52	0.44
Ratio: [3:2],	Interest rate: [5%] - WFC					
CoalþSCB	20,401.90	23,695,579.21	38,944,420.79	212,916.87	5.09	0.61
CoalþCC	20,807.06	22,918,288.46	39,721,711.54	1,467,396.71	5.65	0.58
CoalþPSD	19,270.94	21,496,041.75	41,143,958.25	3,762,779.53	6.70	0.52
CoalþWT	15,743.76	20,414,617.14	42,225,382.86	5,508,105.04	7.73	0.48
Ratio: [4:1],	Interest rate: [5%] - WFC					
CoalþSCB	20,260.28	26,580,269.34	36,059,730.66	-4,442,722.76	3.09	0.74
CoalþCC	20,458.08	26,881,014.28	35,758,985.72	-4,928,099.02	2.89	0.75
CoalþPSD	19,686.61	25,237,300.14	37,402,699.86	-2,275,286.98	4.01	0.67
CoalþWT	17,855.69	24,632,996.13	38,007,003.87	-1,299,992.72	4.43	0.65

Table 4
Plant assessment at 10th year, WOFC: emphasis on appraisal tools.

Feedstocks [-]	Amount of fuel [t]	Capital cost investment [δ] [ZAR/y]	Cash flow [μ] [ZAR/y]	Net present value [NPV] [ZAR/y]	Internal rate of return [IRR] (%)	Payback period [PBP] (Year)
Ratio: [1:1], Interest rate: [5%] - WFC						
CoalþSCB	20,473.45	10,031,991.19	52,608,008.81	22,264,762.66	18.02	0.17
CoalþCC	20,986.05	10,283,164.48	52,356,835.52	21,859,390.76	17.67	0.17
CoalþPSD	18,251.81	8,943,385.18	53,696,614.82	24,021,678.33	19.63	0.16
CoalþWT	15,276.28	6,629,904.59	56,010,095.41	27,755,435.32	23.78	0.14
Ratio: [3:2],	Interest rate: [5%] - WFC					
CoalþSCB	20,401.90	9,711,302.96	52,928,697.04	22,782,325.65	18.47	0.18
CoalþCC	20,807.06	9,904,159.23	52,735,840.77	22,471,072.36	18.20	0.19
CoalþPSD	19,270.94	9,172,968.27	53,467,031.74	23,651,151.15	19.27	0.17
CoalþWT	15,743.76	6,788,708.79	55,851,291.21	27,499,139.12	23.46	0.12
Ratio: [4:1], Interest rate: [5%] - WFC						
CoalþSCB	20,260.28	9,076,604.62	53,563,395.38	23,806,673.71	19.43	0.10
CoalþCC	20,458.08	9,165,218.93	53,474,781.07	23,663,657.91	19.29	0.20
CoalþPSD	19,686.61	8,819,602.70	53,820,397.30	24,221,452.51	19.83	0.17
CoalþWT	17,855.69	7,599,381.80	55,040,618.20	26,190,783.20	21.90	0.12

WOFC: without feedstock costing.

Characterization of the feedstocks was carried out using CHNS-O Organic Elemental Analyzer (FLASH 2000), TGA-SDT (600), Oxygen-bomb calorimeter (203 M 1241) for the ultimate, and proximate analysis and heating value determinations, respectively, and using coal-to-solid waste ratios of 1:1, 3:2, and 4:1. The result from characterization analysis was used in the empirical model (Eq. (1)) to obtain the lower heating value (LHV) of the fuels, and the value was then applied in Eqs. (2) and (3) to estimate the annual feed rate and feedstock requirements shown in the model for the co-gasification power plant presented in Fig. 2

$$LHV = HHV - (0.212 \times M_H) - (0.0245 \times MC) \quad (1)$$

Table 5
Estimation of the business viability at the 11th year: WFC.

Feedstocks [-] Capital cost investment [δ] [ZAR/y]		Cash flow [μ] [ZAR/y]	Net present value [NPV] [ZAR/y]	Internal rate of return [IRR] (%)	Payback period [PBP] (Year)
Ratio: [1:1], Interest rate: [5%] - WFC					
CoalþSCB	22,238,058.18	40,401,941.82	1,384,120.43	5.58	0.6
CoalþCC	22,900,607.30	39,739,392.70	334,192.58	5.13	0.6
CoalþPSD	18,775,98O.37	43,864,001.63	6,870,374.92	8.01	0.5
CoalþWT	19,175,395.01	43,464,604.99	6,237,459.34	7.71	0.5
Ratio: [3:2], Interest rate: [5%] - WFC					
CoalþSCB	23,695,579.21	38,944,420.79	−925,582.96	4.62	0.6
CoalþCC	22,918,288.46	39,721,711.54	306,173.61	5.2	0.6
CoalþPSD	214,96,041.75	41,143,958.25	2,559,978.51	6.08	0.4
CoalþWT	20,414,617.14	42,225,382.86	4,273,689.70	6.83	0.4
Ratio: [4:1], Interest rate: [5%] - WFC					
CoalþSCB	26,580,269.34	36,059,730.66	−4,442,722.76	2.81	0.7
CoalþCC	26,881,014.28	35,758,985.72	−5,973,475.94	2.63	0.8
CoalþPSD	25,237,300.14	37,402,699.86	−3,368,716.17	3.64	0.7
CoalþWT	24,632,996.13	38,007,003.87	−2,411,088.12	4.02	0.7

WFC: with feedstock costing.

Table 6
Estimation of the business viability at the 11th year: WOFC.

Feedstocks [-] Capital cost investment [δ] [ZAR/y]		Cash flow [μ] [ZAR/y] Net present value [NPV] [ZAR/y]		Internal rate of return [IRR] [%]	Payback period [PBP] [Year]
Ratio: [1:1], Interest rate: [5%] - WOFC					
CoalþSCB	10,031,991.19	52,608,008.81	20,726,822.00	16.23	0.2
CoalþCC	10,283,164.48	52,356,835.52	20,328,792.89	15.95	0.2
CoalþPSD	8,943,385.18	53,696,614.82	22,451,913.40	17.69	0.2
CoalþWT	6,629,904.59	56,010,095.41	26,118,038.18	21.41	0.1
Ratio: [3:2], Interest rate: [5%] - WOFC					
CoalþSCB	9,711,302.96	52,928,697.04	21,235,010.00	18.47	0.2
CoalþCC	9,904,159.23	52,735,840.77	20,929,394.67	16.42	0.2
CoalþPSD	9,172,968.27	53,467,031.74	22,088,097.84	17.38	0.2
CoalþWT	6,788,708.79	55,851,291.21	25,866,384.46	21.12	0.1
Ratio: [4:1], Interest rate: [5%] - WOFC					
CoalþSCB	9,076,604.62	53,563,395.38	22,240,803.31	17.51	0.2
CoalþCC	9,165,218.93	53,474,781.07	22,100,378.06	17.39	0.2
CoalþPSD	8,819,602.70	53,820,397.30	22,648,068.92	17.87	0.2
CoalþWT	7,599,381.80	55,040,618.20	24,581,727.73	19.73	0.1

WOFC: without feedstock costing.

$$\frac{F_{FEEDSTOCK}}{NOH} \quad \frac{1}{RANNUAL} \quad \frac{\gamma}{} \qquad \delta 2\flat$$

$$\frac{\varpi \times 3{:}6\ LHV \times \eta_0}{A_{FR}} \qquad \delta 3\flat$$

where LHV and HHV are the lower heating value and higher heating value of the feedstocks in MJ/kg, respectively; $F_{RANNUAL}$ is the annual feed-rate of the plant in t/y; A_{FR} is the annual feedstock requirement of the plant in t/y; η_0 is the operating efficiency of the plant in %, respectively, M_H and MC are the mass fractions of hydrogen and moisture content of the feedstocks in %, NOH is the

Table 7
Economic evaluation at the 17th Year: WOFC.

Feedstocks [-]	Capital cost investment [δ] [ZAR/y]	Cash flow [μ] [ZAR/t]	Net present value [NPV] [ZAR/y]	Internal rate of return [IRR] [%]	Payback period [PBP] [Year]
Ratio: [1:1], Interest rate: [5%] - WOFC					
CoalþSCB	22,238,058.18	40,401,941.82	12,920,708.80	26.22	0.2
CoalþCC	22,900,607.30	39,739,392.70	12,559,949.43	26.00	0.2
CoalþPSD	18,775,998.37	43,864,001.63	14,484,270.01	27.24	0.2
CoalþWT	19,175,395.01	43,464,604.99	17,807,114.51	29.82	0.1
Ratio: [3:2], Interest rate: [5%] - WOFC					
CoalþSCB	23,695,579.21	38,944,420.79	13,381,312.24	18.47	0.2
CoalþCC	22,918,288.46	397,21,711.54	13,104,313.42	11.01	0.2
CoalþPSD	21,496,041.75	41,143,958.25	1,4154,520.58	10.34	0.2
CoalþWT	20,414,617.14	42,225,382.86	17,579,024.57	10.92	0.1
Ratio: [4:1], Interest rate: [5%] - WOFC					
CoalþSCB	26,580,269.34	36,059,730.66	14,292,927.36	11.01	0.2
CoalþCC	26,881,014.28	35,758,985.72	14,165,650.93	10.93	0.2
CoalþPSD	252,37,300.14	37,402,699.86	14,662,058.36	11.22	0.2
CoalþWT	24,632,996.13	38,007,003.87	16,414,657.61	12.36	0.1

WOFC: without feedstock costing.

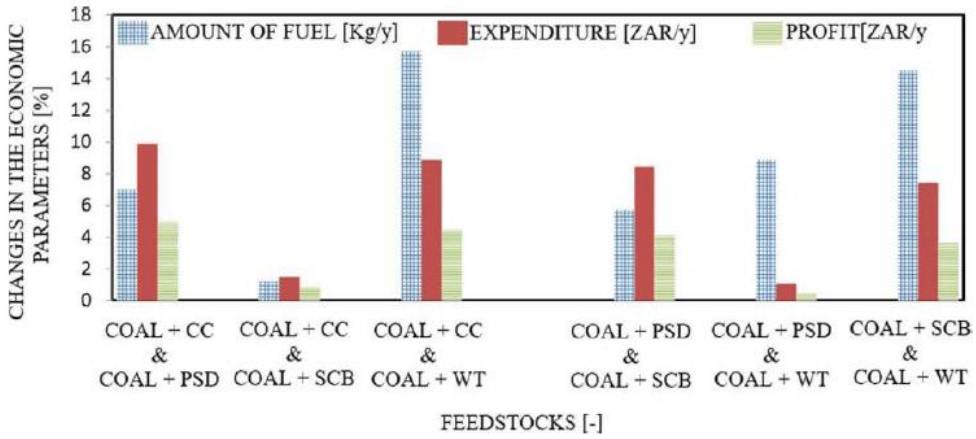


Fig. 3. Comparism of economic parameters of the feedstocks at WFC.

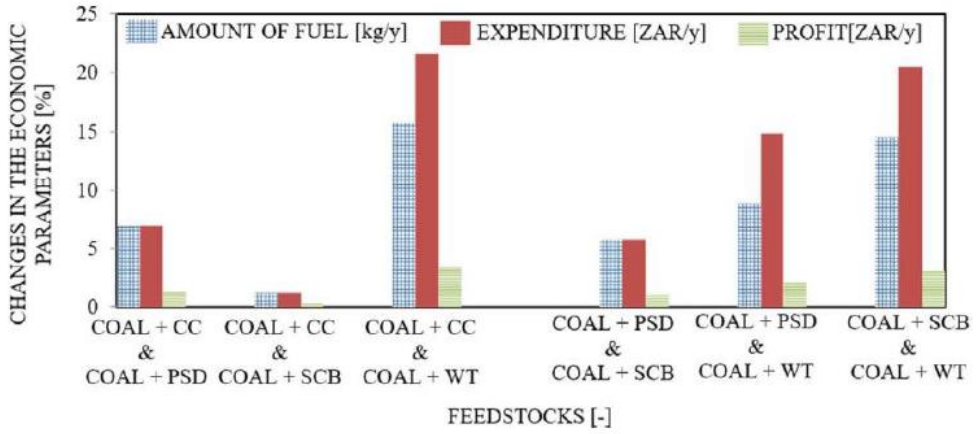


Fig. 4. Comparism of economic parameters of the feedstocks at WOFC.

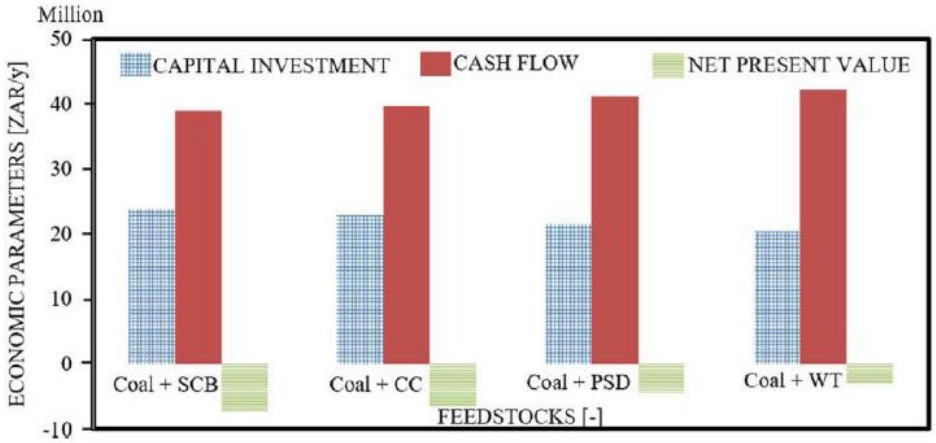


Fig. 5. Economic assessment at 18th year at WFC with blend ratio of 3:2.

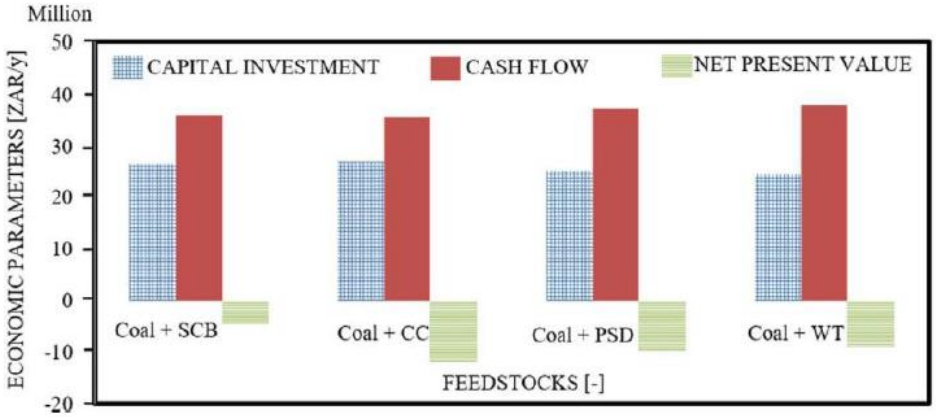


Fig. 6. Economic assessment at 18th year at WFC with blend ratio of 4:1.

Table 8
Emission reduction assessment from the plant (Coal & Coalþ Solid Waste).

Feedstock	CO [kg]	CO_2 [kg]	SO_2 [kg]	NO_x [kg]
Coal (Matla)	1.00	5900.00	69.50	26.00
Blending ratio: [1:1]				
CoalþSCB	0.50	2950.01	34.75	13.00
CoalþCC	0.50	2950.01	34.75	13.00
CoalþPSD	0.50	2950.01	34.75	13.00
CoalþWT	0.50	2950.01	34.75	13.00
Blending ratio: [3:2]				
CoalþSCB	0.60	3540.42	41.70	15.60
CoalþCC	0.60	3540.42	41.70	15.60
CoalþPSD	0.60	3540.42	41.70	15.60
CoalþWT	0.60	3540.42	41.70	15.60
Blending ratio: [4:1]				
CoalþSCB	0.80	4720.00	55.60	20.80
CoalþCC	0.80	4720.00	55.60	20.80
CoalþPSD	0.80	4720.00	55.60	20.80
CoalþWT	0.80	4720.00	55.60	20.80

SCB: sugarcane bagasse; CC: corn cob; PSD: pine saw-dust; WT: waste tyre.

Table 9
Sensitivity analysis WOFC: At 10th year (1:1, 3:2, 4:1 Coalþ Solid Waste).

Amount of feedstock [t]			Capital costinvestment [ZAR/y]			Ratio
X	$\bar{X}$	$\sum(X-\bar{X})^2$	X	$\bar{X}$	$\sum(X-\bar{X})^2$	
20,473.45*	18,746.90	2.98099Eþ 9	10,031,991.19	16,547,914.72	4.24573Eþ13	1:1
20,986.05**	18,746.90	5.01381Eþ9	10,283,164.48	16,547,914.72	3.92471Eþ13	
18,251.81***	18,746.90	2.45114Eþ8	8,943,385.18	16,547,914.72	5.78289Eþ 13	
15,276.28****	18,746.90	1.20452Eþ10	6,629,904.59	16,547,914.72	9.83669Eþ 13	
Variance	6.7617Eþ9		Variance	2.77632Eþ12		
Std. deviation	2600.33		Std. deviation	1,666,229.60		
Standard Error	1300.16		Standard Error	833,114.80		
Cash flow [ZAR/y]			Net present value [ZAR/y]			
52,608,008.81	41,867,485.29	1.15359Eþ14	22,264,762.66	3,706,536.82	3.44408Eþ 14	
52,356,835.52	41,867,485.29	1.10026Eþ14	21,859,390.76	3,706,536.82	3.29526Eþ 14	
53,696,614.82	41,867,485.29	1.39928Eþ14	24,021,678.33	3,706536.82	4.12705Eþ14	
56,010,095.41	41,867,485.29	2.00013Eþ14	27,755,435.32	3,706,536.82	5.7835Eþ14	
Variance	2.77632Eþ12		Variance	7.23153Eþ12		
Std. deviation	1,666,229.60		Std. deviation	2,689,150.05		
Standard Error	833,114.80		Standard Error	1,344,575.02		
Amount of feedstock [t]			Capital cost investment [ZAR/y]			
20,401.90*	19,055.91	1.81167Eþ9	9,711,302.96	22,131,131.64	1.54252Eþ14	3:2
20,807.06**	19,055.91	3.0665Eþ9	9,904,159.23	22,131,131.64	1.49499Eþ14	
19,270.94***	19,055.91	4.623706Eþ7	9,172,968.27	22,131,131.64	1.67914Eþ14	
15,743.76****	19,055.91	1.09704Eþ10	6,788,708.79	22,131,131.64	2.3539Eþ14	
Variance	5.29826Eþ9		Variance	2.06616Eþ 12		
Std. Deviation	2301.80		Std. deviation	1,437,414.328		
Standard Error	1150.90		Standard Error	718,707.1639		
Cash flow [ZAR/y]			Net present value [ZAR/y]			
52,928,697.04	40,508,868.36	1.54252Eþ14	22,782,325.65	2,737,799.53	4.01783Eþ14	
52,735,840.77	40,508,868.36	1.49499Eþ14	22,471,072.36	2,737,799.53	3.89402Eþ 14	
53,467,031.74	40,508,868.36	1.67914Eþ14	23,651,151.15	2,737,799.53	4.37368Eþ 14	
55,851,291.21	40,508,868.36	2.3539Eþ14	27,499,139.12	2,737,799.533	6.13124Eþ14	
Variance	2.06616Eþ12		Variance	5.38176Eþ12		
Std. deviation	1,437,414.33		Std. deviation	2,319,862.04		
Standard Error	718,707.16		Standard Error	1,159,931.02		
Amount of feedstock [t]			Capital cost investment [ZAR/y			
20,260.28*	19,565.16	4.83182Eþ11	9,076,604.62	25,832,894.97	2.80773Eþ 14	
20,458.08**	19,565.16	7.97294Eþ11	9,165,218.93	25,832,894.97	2.77811Eþ14	
19,686.61***	19,565.16	1.474969Eþ10	8,819,602.70	25,832,894.97	2.89452Eþ 14	
17,855.69****	19,565.16	2.9223Eþ12	7,599,381.80	25,832,894.97	3.32461Eþ 14	
Variance	1.40584Eþ12		Variance	5.2636Eþ11		
Std. deviation	1,185,682.54		Std. deviation	725,507.02		
Standard Error	592,841.27		Standard Error	362,753.51		
Cash flow [ZAR/y]			Net present value [ZAR/y]			
53,563,395.38	36,807,105.03	2.80773Eþ14	23,806,673.71	−3,236,525.37	7.31335Eþ14	4:1
53,474,781.07	36,807,105.03	2.77811Eþ14	23,663,657.91	−3,236,525.37	7.2362Eþ 14	
53,820,397.30	36,807,105.03	2.89452Eþ14	24,221,452.51	−3,236,525.37	7.53941Eþ14	
55,040,618.20	36,807,105.03	3.32461Eþ14	26,190,783.26	−3,236,525.37	8.65966Eþ 14	
Variance	5.2636Eþ11		Variance	1.37102Eþ12		
Std. deviation	725,507.02		Std. deviation	1,170,905.43		
Standard Error	362,753.51		Standard Error	585,452.71		

*: Coal þ SCB, **: Coal þ CC, ***: Coal þ PSD, ****: Coal þWT, X: Estimated variable. X: estimated variable (e.g. amount of feedstock, capital cost investment, cash flow, net present value) $\bar{X}$: mean of the variable; Std.: standard.

number of operating hours in the plant in h; ϖ is the energy demand in MWh/y; and γ is the gasification conversion efficiency in %.

The economic evaluation of electricity and thermal power generation from the plant was then carried out using the net present value (NPV), internal rate of return (IRR), and payback period (PBP) as the project tools at 10th, 11th, 17th and 18th investment years based on two financial situations namely: with feedstock costing (WFC) and without feedstock costing (WOFC). The appraisal tools and emission models

used are provided in Eqs. (4)–(10). The NPV was estimated with Eq. (4) [2]. Eqs. (5) and (6) [2] were applied to estimate the IRR and PBP, respectively. Eq. (7) [3] and Eq. (8) [4] were used to estimate the emissions from the plant. Sensitivity analysis that considers the standard deviation, variance, and stan- dard error was carried out on the variables using Eqs. (9), (10), and (11), respectively [5]

$$NPV = -\beta + \frac{\phi_1}{(1+R)^1} + \frac{\phi_2}{(1+R)^2} + \frac{\phi_3}{(1+R)^3} + \cdots + \frac{\phi_T}{(1+R)^T} \quad (4)$$

$$NPV = -\beta + \sum_{j=1}^{T} \frac{\phi_j}{(1+IRR)^j} = 0 \quad (5)$$

$$PBP = \frac{\beta}{\mu} \quad (6)$$

where NPV, IRR, and PBP are the net present value, internal rate of return, and payback period, respectively; β is the capital investment in ZAR/y; ϕ is the cash flow in million (M) ZAR; R is the annual rate of return in %; T is the economic life of the plant or business period

$$\xi = \varpi \times (\alpha^1 \times \tau^1 + \alpha^2 \times \tau^2 + \cdots \alpha^n \times \tau^m) \quad (7)$$

$$\varphi = \xi - \varepsilon - \lambda \quad (8)$$

where ξ is the emission reduction by displaced energy from the grid; φ is the effective emission reduction; ε is the life cycle GHG emission intensity of biomass; λ is the emission from transportation of biomass; α is the percentage of feedstock used for the blend; τ is the emission factor of the fuel used

$$SD = \sqrt{\frac{\Sigma(X - \bar{X})^2}{N-1}} \quad (9)$$

$$Variance = \frac{\Sigma (X - \bar{X})^2}{N-1} \quad (10)$$

$$Standard\ Error = \frac{SD}{(N)^{1/2}} \quad (11)$$

SD is the standard deviation of the sensitivity analysis variables; X is the variables including the amount of feedstock, capital cost investment, cash flow, and NPV; *N* is the number of sample population.

Acknowledgments

The authors thank Dr. S. O. Bada for his help in the pretreatment of the feedstocks, Mr. Nonye Ozonoh, and Mrs. Angela Ozonoh for their moral and financial support.

Transparency document. Supporting information

Transparency data associated with this article can be found in the online version at https://doi.org/10.1016/j.dib.2018.10.117.

References

[1] M. Ozonoh, T.C. Aniokete, B.O. Oboirien, M.O. Daramola, Techno-economic analysis of electricity and heat production by co-gasification of coal, biomass and waste tyre in South Africa, J. Clean. Prod. 201 (2018) 192–206.

[2] A.A.B.M. Malek, M. Hasanuzzaman, N.S. Rahim, Y.A.A. Turk, Techno-economic analysis and environmental impact assessment of a 10 MW biomass-based power plant in Malaysia, J. Clean. Prod. 141 (2017) 502–513.
[3] WNA, Comparison of Lifecycle GHG Emissions for Various Electricity Generation Sources, World Nuclear Association Report, London, UK. Retrieved on 15 August 2017. Available online at: (www.worldnuclear.org/WorldNuclear-Association/Publications/Reports/LifecycleGHGEmissions-of-Electricity-Generation), 2011.
[4] T.M.I. Mahlia, Emissions from electricity generation in Malaysia, Renew. Energy 27 (2002) 293–300.
[5] M.F. Zady, Z-5: Sum of Squares Variance, and the Standard Error of the Mean Basic Statistics, Clinical Laboratory Science Programme, University of Louisville, Louisville, Kentucky, 2009, Accessed on: 06 May 2018(www.wstgard.com/lessen35.htm).

Renewable Energy 145 (2020) 2253e2270

Contents lists available at ScienceDirect

Renewable Energy

Performance evaluation of gasification system efficiency using artificial neural network

M. Ozonoh [a], B.O. Oboirien [b], A. Higginson [a], M.O. Daramola [a, *]

[a] School of Chemical and Metallurgical Engineering, Faculty of Engineering and the Built Environment, University of the Witwatersrand, Wits 2050, Johannesburg, South Africa
[b] Department of Chemical Engineering, University of Johannesburg, Doornfontein, Johannesburg 2028, South Africa

articleinfo

Article history:
Received 5 March 2019
Received in revised form 23 July 2019
Accepted 29 July 2019
Available online 30 July 2019

Keywords:
Artificial neural network Coal and biomass Energy conversion Gasification efficiency Performance evaluation

abstract

Gasification is one of the thermo-chemical energy conversion processes with energy self-sufficiency, recoverability and controllable efficiency when compared to combustion and pyrolysis. Gasification process is carried out using different systems (gasifiers), different types of fuels and process conditions, and these factors determine the efficiency of the overall process. The performance of a gasifier is eval- uated by some parameters such as Cold Gas Efficiency (CGE), Carbon Conversion Efficiency (CCE), gas yield, gas composition, and lower heating value (LHV) of gas. To understand how efficient a gasifier is, several experiments are needed, but conducting these experiments is time consuming and capital intensive, and the information is vital in energy production plants. Meanwhile, a model that could accurately predict the aforementioned parameters irrespective of the type of gasifier, fuel, and operating conditions is imperative for some time conditions. In this study, Levenberg-Marquardt (LM) back- propagation and Bayesian Regularisation (BR) training algorithms for an Artificial Neural Networks (ANN) were used to study a dataset containing 315 experimental data of biomass, coal, and blends of biomass and coal from various gasifiers and process conditions. Eleven input variables were used in the study, and the result shows that the Mean Square Error (MSE) of the BR algorithm was higher than that of the L-M algorithm. To reduce the MSE, techniques called Input Variables Representation Technique with Visual Inspection method (IVRT-VIM) and Output Variables Representation Technique with Visual In-
spection Method (OVRT-VIM) were developed, and their applications produced smaller MSE and an R^2 of between 79 e 98% and 95e96%, respectively. Further, the results of the sensitivity analysis revealed that carbon (% amount) is the most important input parameter affecting the outputs, and with sum of the Squares of the Partial Derivatives (SSD) value of 1.18 for the CGE prediction.
© 2019 Elsevier Ltd. All rights reserved.

1. Introduction

Different kinds of fuels are available for energy generation around the world, but some fuels are more abundant in some countries than the another. Solid fuels such as biomass and coal seem to be more abundant than every other solid fuels used for energy production. Coal may be used as a major source of fuel in an area based on its low price and availability, while biomass may also be considered in another area due to its environmental friendliness compared to coal that poses environmental threats. Presently, concerns about energy security and environmental apprehensions have compelled stakeholders and policymakers in the energy sector to consider renewable and sustainable energy options to meet the increasing energy demands of the world. On the envi- ronmental regulations point of view and fuel cost savings, biomass and coal can be co-gasified, and the efficiency of the gasifier also maintained, but it requires several experiments to establish the process conditions for better efficiency. A lot of time and money are needed to achieve this, and a model that has the capacity of pre- dicting the efficiency parameters irrespective of the type of gasifier, solid fuel, and process condition could be instrumental to reducing costs and saving time. Presence of a dependable model could also pave the way to control and optimisation of process.

The assessment of gasification performance is an important aspect of the gasification process, and some parameters including the Cold gas efficiency (CGE), carbon conversion efficiency (CCE),

* Corresponding author.
E-mail address: michael.daramola@wits.ac.za (M.O. Daramola).

https://doi.org/10.1016/j.renene.2019.07.136
0960-1481/© 2019 Elsevier Ltd. All rights reserved.

lower heating value (LHV) of gas, and product gas composition (e.g. CO, CO_2, CH_4, & H_2) are used in the evaluation [1]. These performance indicators may be studied using different predictive commercial soft-wares such as an artificial neural network (ANN), Genetic programming, Aspen-plus, etc. In a study carried out by Pandey et al. [2], it was reported that the ANN model offered high prediction accuracy. An ANN model is used to study some of the processes occurring in the gasification system, as well as prediction of the lower heating value (LHV) of fuels used in the gasifier [3,4]. With regard to the relevance of evaluating the performance of a gasifier, several researchers have carried out some investigations to understand the process.

Tiwary et al. [5] studied the performance efficiency of a co-gasification fluidised bed gasifier (FBG) using blends of biomass and coal as fuel, employing ANN, genetic programming, and sup- port vector regression models. The authors used eleven (11) input variables including the gasification temperature, air/fuel ratio, steam/fuel ratio, C, H, O, reaction rate constant, biomass feed rate, coal feed rate, FC, VM, ash, and total gas yield, CCE, CGE, and LHV of gas as the output variables. Their results were comparable with other results reported in the literature in terms of the effectiveness of the models in predicting the gasification performance parame- ters, but the experimental dataset used by the authors was ob- tained from only one type of gasifier operated at the same process conditions (e.g. gasifying agent).

In the same vein, Pandey et al. [2] employed ANN Multiple Input-Multiple Output (MIMO) and Multiple Input-Single Output layer networks to predict the syngas yield, LHV of gas, and LHV of the gasification products (char and tar) from municipal solid waste in a fluidised bed gasifier (FBG) In addition, George et al. [6] employed MIMO layer network to assess product gas composition (CO, CO_2, CH_4, & H_2) in a bubbling fluidised bed (BFB) gasifier. The studies of George et al. [6] and Pandey et al. [2] are very promising with respect to the reliability of the models to evaluate perfor- mance of the gasifier. However, these studies considered a type of gasifier and few experimental conditions. Baruah et al. [7] pre- dicted the concentrations of the four major producer gas compo- sitions. Proximate analysis results and experimental process conditions data were the input parameters used in the ANN model. Although, the model result was in agreement with the experi- mental data, unfortunately, Baruah and co-workers could not use other fuels such as coal and blends of coal and biomass, instead their report used only biomass and a type of gasifier as inputs.

Earlier, Puig-Arnavat et al. [8] investigated the performance efficiency of a bubbling fluidised bed (BFB) and circulating fluidised bed (CFB) gasifiers using the proximate analysis and operating condition data from biomass gasification and employing an ANN model. The producer gas composition and gas yield were the predicted outputs, and the results obtained have high agreement with published experimental data, but the study was dwelled on only the MIMO layer networks using Levenberg-Marquardt algorithm, and did not consider the MISO layer networks and Bayesian Regularization algorithm, and besides that, the dataset used was obtained only from biomass gasification experiment, and without using data from fixed bed systems. Further, the sensitivity analysis that was carried out by these authors to understand the relative importance of the input variables on the outputs overlooked the partial derivatives (PaD) method which some authors including Montano et al. [9], Wang et al. [10] & Gevrey et al. [11] affirmed that it is more reliable than the connection weights, step-wise, Perturbe methods that are commonly used by other authors such as those mentioned earlier.

An ANN model study that covers the performance evaluation of gasifiers using dataset obtained from different gasification systems, fuels such as biomass and coal, and blends of biomass and coal, and different operating process conditions is not available in the literature. Carrying out gasification experiments to understand the performance of a gasifier using different solid fuels and gasification systems is very challenging in terms of time and cost of experimentation. Using a predictive model such as an ANN model, an interesting predictive model, could be instrumental to saving cost and reducing time. ANN is self-manipulated and can solve problems that are difficult to be resolved by human brain; provide nonlinear relations without seeking for external assistance. It does not need the formulation of complex numerical equations to provide solutions; and very reliable in terms of accuracy of results [12,13]. Therefore, experimental data obtained from a few gasifiers (e.g. entrained, fluidised, and fixed bed) operated at varied experimental conditions using fuels and blends of feedstock (e.g. biomass, coal, waste tyre etc.) were employed in a backpropagation L-M and BR algorithms of ANN model with MIMO and MISO layer networks to study the performance of a gasification unit. It is ex- pected that this study will: (i) enhance understanding of perfor- mance of a gasifier via modelling approach without conducting actual gasification tests; thereby saving time and reducing cost of experimentation; (ii) allow for the prediction of the efficiency of gasifiers operated at different process conditions and using different fuels (e.g. biomass, coal, and their blends); (iii) provide information that could assist stake-holders to develop gasifiers capable of converting different solid fuel materials into energy. Importantly, this information could be instrumental to decision making as well and could serve as a platform for further R & D in this field.

2. Materials and methods

2.1. Experimental data

315 fuel samples used in this study included biomass, coal, and blends of biomass and coal. Information about their proximate, ultimate, process condition data, and performance indicators were obtained from the literature. The proximate analysis data used were ash, moisture content (MC), and volatile matter (VM), while the ultimate analysis data includes Carbon (C), hydrogen (H), ni- trogen (N), oxygen (O), and sulphur (S), and LHV_{Fuel}. The experi- mental data considered in this study were equivalence ratio (ER) and reaction temperature (T), and the gasification performance efficiency parameters were cold gas efficiency (CGE), carbon con- version efficiency (CCE), gas yiled, lower heating value (LHV) of gas, and gas composition (e.g. CO, CO_2, CH_4, H_2). The dataset was grouped into input and output variables as shown in Table 1. It was then saved in an excel document for use in the training of the models.

These gasification experiments were performed using different types of gasifiers namely; updraft, downdraft, fluidised bed and entrained bed, and they are illustrated in Fig. 1. The system effi- ciencies varied based on the mechanisms and the capacity of the gasifiers. For instance, a circulating fluidised bed (CFB) gasifier is known for excellent heat and mass transfer efficiencies and ac- commodating of a wide range of feedstocks. However, amongst the key factors that affect the efficiency of the gasifiers is the quality of the feedstock and process conditions. In this study, the fuel prop- erties evaluated includes C, H, N, S, O, ash, MC, VM, and LHV, while the process parameter were ER and T. These parameters were used to develop the ANN Model. Hence our model is capable of pre- dicting the gasification efficiency of any of the four gasifiers based on 8 output variables comprised of gas composition (CO CO_2, H_2, CH_4), gas yield, LHV of gas, CGE, and CCE.

For the Bayesian regularization (BR) training algorithm, a MIMO layer networks were employed. The use of the techniques needs a

Table 1
Input and output variables employed in ANN.

Input variables	Data range	Output variables	Data range
C (wt.% dry basis)	12.10e99.00	CGE (%)	3.98e174.43
H (wt. % dry basis)	0.62e13.86	CCE (%)	6.10e138.85
N (wt. % dry basis)	0.04e5.50	Gas Yield (kg/Nm³)	0.17e7.50
S (wt. % dry basis)	0.00e2.15	LHV of gas (MJ/Nm³)	0.62e15.31
O (wt.% dry basis)	13.90e54.00	Gas composition (Vol. %):	2.74e42.68
MC (wt.% dry basis)	0.02e15.00	CO	0.12e54.15
Ash (wt. % dry basis)	0.15e79.16	CO_2	0.00e70.10
T (°C)	600.00e1200.00	CH_4 H_2	2.50e55.55
VM (%)	5.40e99.81		
ER (–)	0.10e1.00		
Fuel LHV*	5.5e38.04		

h_{Gas}: Gas yield; CGE: Cold Gas Efficiency; CCE: Carbon Conversion Efficiency; T: Gasification Temperature; ER: Equivalence Ratio; VM: Volatile Matter; LHV: Lower Heating Value.*: Biomass, coal, & coal þ biomass.

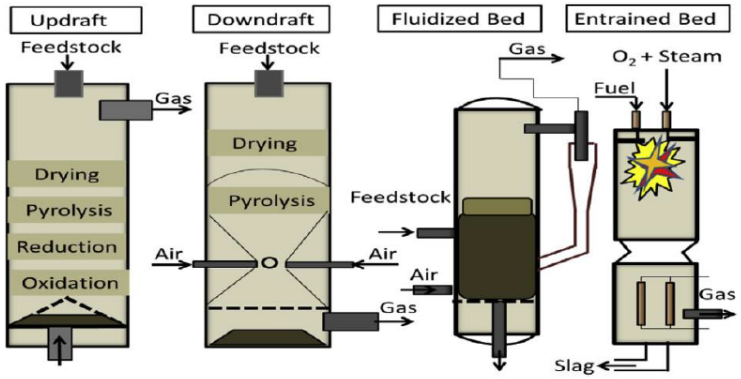


Fig. 1. Schematic diagram of some gasification systems (Adapted from Sikarwar et al. [14]).

lot of training time, but it is efficient for generalization of difficult and noisy data-sets. In this case, 11 input variables comprising C, H, N, S, O, ash, MC, VM, T, ER, and $LHV_{biomass}$; and 8 output variables comprising gas composition (CO CO_2, H_2, CH_4), gas yield, LHV of gas, CGE, and CCE were used. The 315 input-output patterns used for the study were divided into three namely: 70% (221 datasets) for training; 15% (47 datasets) for validation; 15% (47 dataset) for testing the model. Further, the input datasets were randomised for each of the iterations, while simulations were carried out by varying the number of neurons in the hidden layer using tansig- moid transfer function. Similar approach was used for the Levenberg-Marquardt (LM) back-propagation algorithm. The net- works were evaluated based on the Mean Square Error (MSE) and coefficient of determination (R^2) obtained, and the architecture with the lowest MSE and highest R^2 were considered as the best candidate model.

2.2. Artificial neural network (ANN) working principles

The neurons in the hidden layer receives signal from the input layer and transfers it to the neurons in the output layer, but the units (yi) of the network in the hidden layer must have summed its weighted inputs and used the activation function to produce the output signal. The mode of operations of the activation function is expressed in Equation (1):

$$y_j = f_{Activation}\left(\sum_{i=1} W_{ij}X_i + b_j\right) \quad (1)$$

where Wij represents the weight of the connection between the ith input and the jth neuron of the hidden layer and bj is the bias weight of the unit j. A hyperbolic function is commonly employed to provide effective learning of the network, and the tansigmoid and Logsigmoid functions are the two main functions that are used to achieve this purpose. A tansigmoid function has been proposed for this work and it is presented in Equation (2) [12]:

$$f_{Activation}(X) = \frac{1}{1 + e^{-x}} \quad (2)$$

In this case, the output from neuron yj is transferred to all the units of the output layer, while each output neuron mk sums the weighted input signals with the application of the activation function as shown in Equation (3):

$$m_k = f_{Activation}\left(\sum_{j=1} V_{jk}y_f + b_k\right) \quad (3)$$

The weights (Wij) of each of the connection between the adja- cent layers and the neurons are calculated, and may also be used in the sensitivity analysis for the estimation of the effect of the input parameters on the outputs, if the connection weight method is to be used.

2.2.1. Levenberg-Marquardt (LM) & Bayesian Regularization (BR) algorithms

The L-M algorithm is the most stable and fastest training algo- rithm that uses two combination minimization techniques such as the Gradient-descent and the Gauss Newton methods [13]. It is expressed in Equation (4):

$$J^t J + mI = J^t \times E \quad (4)$$

where J represents the Jacobian matrix for the network; I is the identity matrix; m is the L-M training algorithm; E is the error vector (e.g. Mean Square Error (MSE)). The $J^t J$ can also be referred to as the approximated Hessian. The BR algorithm is equally used to train the network. It consumes a lot of training time, but it offers a good generalisation for difficult or noisy datasets.

2.2.2. Multiple Input-Multiple Output (MIMO) and Multiple Input- Single Output (MISO) layer

The MIMO and MISO layer networks will be studied using the input and output data characteristics shown earlier in Table 1, and the architectures are presented in Fig. 1a and Fig. 1b. The number of neurons in the hidden layer varies, and it is usually determined by trial and error [2].

Meanwhile, the neural network is trained using the methodol- ogy in Fig. 2.

The details of the Levenberg-Marquardt (L-M) training/learning of the ANN model can be found in Ref. [2].

2.3. ANN model development and applications

The ANN model was developed from the 315 dataset using the neural network toolbox (nntool) under MATLAB environment. A backpropagation L-M and BR algorithms using a Multiple Input-Multiple Output (MIMO) and Multiple Input-Single Output (MISO) layer networks were employed to study the performance indicators. For the MIMO layer network, C, H, N, S, O, MC, Ash, VM, T, ER, and $LHV_{biomass}$ were used as the input variables, while CGE, CCE, gas yield, LHV of gas, and product gas composition (CO, CO_2, CH4, and H_2) were used as the output variables. The ER and T represents the operating conditions of the gasifier, while C, H, N, S, O, MC, Ash, VM, and $LHV_{biomass}$ represents the fuel characteristics in the input layer. The output layer is represented by the gasifier performance indicators which considerably are influenced by the properties of the fuels and operating condition. In the MISO layer

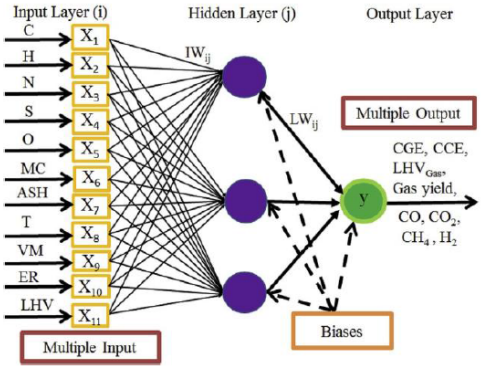


Fig. 1a. Architectural design of Multiple Input-Multiple Output (MIMO) layer of the neural network.

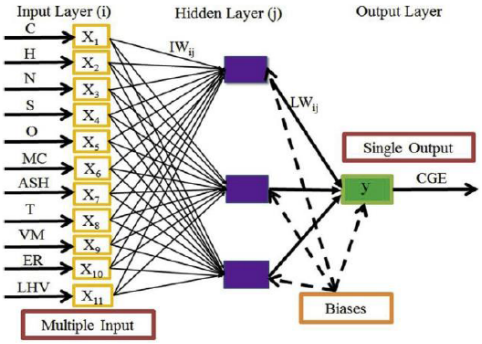


Fig. 1b. Architectural design of the Multiple Input-Single Output (MISO) layer of the neural network.

networks, the performance indicators (output parameters) are considered independently, unlike the Multiple Output (MO) of the MIMO layer that jointly examines the output variables. In this case, a single architecture of the neural network was designed for the MIMO network, while one architecture was developed for the each of the performance indicators, and thus; referred to as a MISO layer network. The MIMO and MISO layer architectures for the networks have been shown in Fig. 1a and b, respectively, but Fig. 3a describes the computational frame-work and equations that were used for the estimation of the value of y_{2i}; the output variables, while 3b shows the actual topography used to train the network. In this case, C, VM, and T are the inputs, whereas CGE, gas yield, and LHV of gas are the outputs. It is important to point out that the three output variables which are shown in Fig. 3a, are trained separately in the network, hence; making it a MISO layer network, but a similar network accounting for the 11 inputs and 8 outputs (MIMO layer network) is presented in the supplementary material accompa- nying this paper.

2.4. Gasification performance evaluation

The efficiency of a gasifier for biomass and coal gasification or co-gasification of biomass and coal can be evaluated using the gasification performance indicators such as Cold Gas Efficiency (CGE), Carbon Conversion Efficiency (CCE), product gas yield, LHV of gas, and gas composition (e.g. CO, CO_2, CH_4, & H_2).

2.4.1. Cold gas efficiency (CGE)

The CGE is a measure of the gasification performance. It is the ratio of the product of the gas yield and lower heating value (LHV) of the product gas to the LHV of the feedstock (biomass or coal). Mathematically, the CGE is expressed in Equation (5) [15,16]:

$$CGE = \frac{[Gas\ Yield]_{Gas} \times LHV_{Syngas}}{LHV_{Biomass}} \times 100 \quad (5)$$

2.4.2. Carbon conversion efficiency (CCE)

The CCE describes the percentage of the total carbon in the gasifier feed-stocks, and converted to product gases that contain carbon such as CO, CO_2, and CH_4. The CCE is presented in Equation (6) [17,18]. If the gas analysis also contains C_2H_4, and C_2H_6 alongside the CO, CO_2, and CH_4, it can be expressed as shown in Equation (7) [19]:

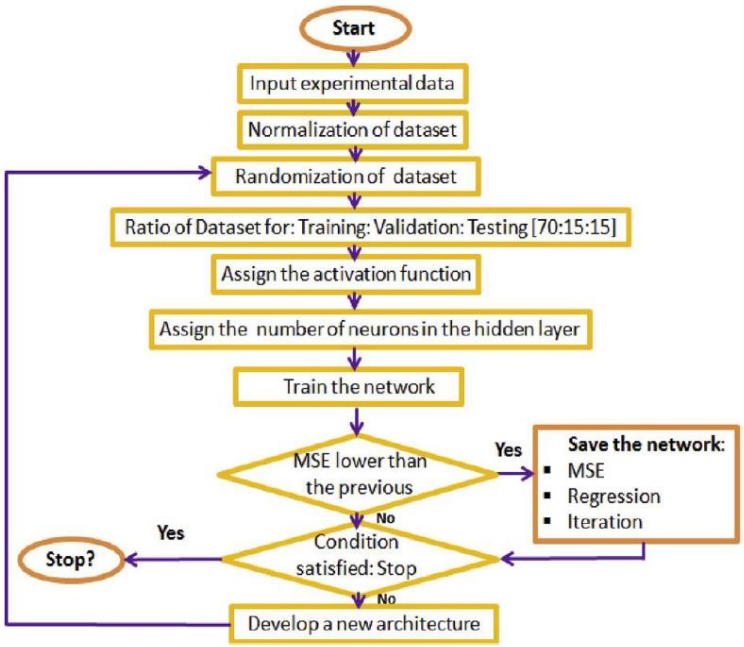


Fig. 2. ANN network training flow-sheet.

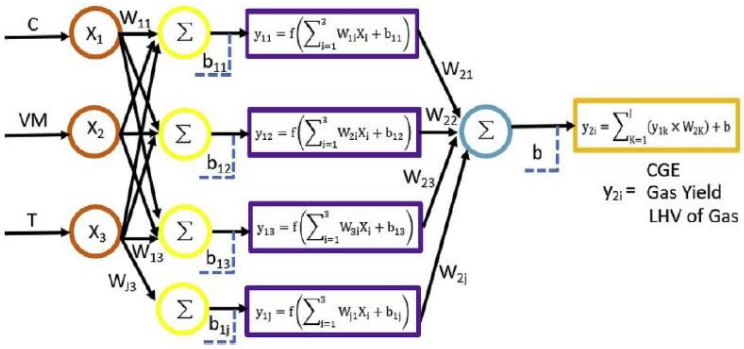


Fig. 3a. Model equation development for the estimation of y2i (output variables).

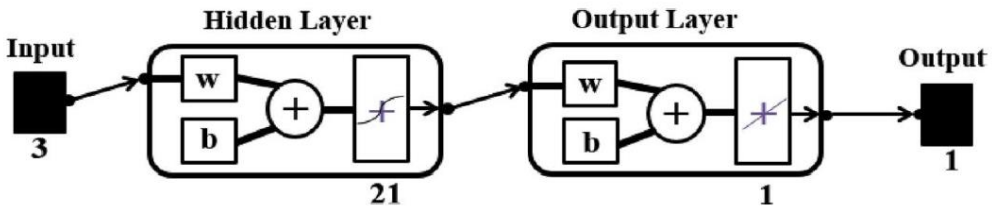


Fig. 3b. Feedforward neural network (FFNN): 3, 21, 1 architecture.

$$CCE = \frac{[CO\% + CH_4 + CO_2\%]}{[22.4\ X\ C\%]} X\ 100 \quad (6)$$

$$CCE = \frac{12\,\eta_{Gas}[CO\% + CO_2\% + CH_4\%] + 2[C_2H_4\% + C_2H_6\%]}{[22.4\ X\ C\%]} X\ 100 \quad (7)$$

where, the gases CO, CO_2, CH_4, C_2H_4, and C_2H_6 are in % Vol., and C is in % of carbon in the dry feedstock from the ultimate analysis, and η_{Gas} is the gas yield.

2.4.3. Gas yield (η_{Gas})

The amount of gas produced during the gasification or co-gasification process indicates the efficiency of the gasifier. The η_{Gas} is the ratio of the volumetric flow rate of the outlet gas from the gasifier to the mass flow rate of the biomass (or feedstock) to the gasifier, and it is presented in Equation (8) [16]:

$$\eta_{Gas} = \frac{Q_{Syngas}}{M_{Biomass}} \quad (8)$$

where, Q and M are the volume flow rate and mas flow rate of the gas and biomass, respectively.

2.4.4. Lower heating value of gas (LHV$_{Gas}$)

The amount of heat generated from the combustion of 1 Nm^3 of the syngas without water is referred to as the LHV of the gas, and is also expressed mathematically as shown in Equation (9) [19,20]:

$$LHV_{Gas} = 11.76\ X\ [V_{CO} + 11.882]X\ V_{H_2} + [37.024]X\ V_{CH_4} \quad (9)$$

2.4.5. Product gas composition

The composition of gas produced in the gasifier essentially de- scribes well the efficiency of the gasifier. It is influenced by the composition of the feedstock, type of gasifier and the operating conditions used, and the product gas may typically contain CO, CO_2, CH_4, and H_2.

2.5. Uncertainty analysis

The Mean Square Error (MSE) and coefficient of determination R^2 are commonly used in an ANN model to evaluate the prediction accuracy of the model. On the other hand, to determine the effect of the input variables on the outputs, the PaD shall be employed because of its effectiveness [21], and the expression for the PaD is shown in Equation (10) [11,22]:

$$S_I = \frac{1}{N}\sum_p \frac{o^P}{x_i^P} \quad (10)$$

where N represents the total number of data variables; p is the pattern number; o^P is the output value for the pattern p (predicted variable from ANN model); x_i is the input value from the pattern p (experimental variable).

If a three-layer feedforward neural network is considered, then o_k and o_j follows as shown in Equation (11) and Equation (12):

$$o_k = f_2\left(\sum_j w_{kj} o_j\right) \quad (11)$$

$$o = f\left(\sum_i w_{ij} x_i\right) \quad (12)$$

where w_{kj} represents the weight between the output neuron k and the hidden neuron j; w_{ij} is the weight between the input neuron i and the hidden neuron j; o_j is the output of the hidden neuron j; f_1 and f_2 represents the activation functions. The chain rule is applied in Equation (10), and after which, the sensitivity of the input variable was obtained by combining Equation (11) and Equation (12) as expressed in Equation (13):

$$S_I = \frac{1}{N}\sum_p \frac{\partial o_k}{\partial o_j}\frac{\partial o_j}{\partial x_i} \quad (13)$$

Putting the actual values of some of the terms of Equations (11) and (12) yields the S_I as presented in Equation (14):

$$S_i = \frac{1}{N}\sum_p f_2'\left(\sum_j w_{kj} f_1'\left(\sum_i w_{ij}x_i\right) w_{ij}\right) \quad (14)$$

Assuming f_1 and f_2 are the Sigmoid function, it means that $f' = 1 - f$, hence; the S_i will be as shown in Equation (15):

$$S_i = \frac{1}{N}\sum_p o_k(1 - o_k)\left(\sum_i w_{kj} o_j (1 - o_j) w_{ij}\right) \quad (15)$$

A crucial point to note about using this method is that the values of the sensitivities are affected by the output values. What it implies is that the patterns with small and large output values has the tendency of being affected because of the terms o_k and $1 - o_k$ of Equation (16), but if the value of the partial derivative is negative, the output variable result will decrease with an increase in the input variable result and vice-versa. However, the relative contri- bution of each input variable on a particular output can be measured by estimating the sum of the squares of the partial de- rivatives as depicted in Equation (16):

$$SSD_I = \sum_p \left(\frac{\partial o^P}{\partial x_i^P}\right)^2 \quad (16)$$

while the contribution or influence of each input variable on the output variables, is presented in Equation (17):

$$\text{Contribution of the ith Variable} = \frac{SSD_i}{\sum_i SSD_i} \quad (17)$$

After the computations, the results are screened, and the vari- able with the highest SSD becomes the most influential variable on the output, hence; the inputs are ranked in the order of their effect on the output.

Researchers have used the connection weights method pro- posed by Garson [23] to determine the relative importance of the input variables on the outputs, but the comparative analysis result of the relative importance of inputs on outputs indicated that the results obtained from the method is not compatible [9,24]. Ac- cording to Gevrey et al. [11], the Perturbe and step-wise methods are also not stable, and based on these facts, the PaD method is therefore proposed for this paper.where, i and j represents the input variables and hidden layer neurons; b_i is the relative effect of the ith input variable on the output variable; IW_{ji} and LW_{ji} are the weight to jth neuron of hidden layer from input variable and weight

to output layer from jth neuron of hidden layer, and represents the number of neurons.

3. Results and discussion

3.1. Model solutions

In this study, two ANN model approaches were employed to investigate the performance of a gasifier without actually per- forming the gasification experiments. The models were the Bayesian Regularization (BR) algorithm and Levenberg-Marquardt (L-M). Both methods yield different results that are expected to proffer some reliable information to stake-holders in the sector in solving some energy conversion problems (e.g. efficiency of a gasifier) when different solid fuels are gasified employing different gasifiers and operating conditions.

3.1.1. Bayesian Regularization (BR) algorithm: MIMO layer network

Bayesian regularization (BR) training algorithm was used to predict the performance of the gasifier, and using the MIMO layer networks. The technique consumed a lot of training time, but it is efficient for generalization of difficult and noisy data-sets. In this case, an ANN MIMO layer network was employed, and 11 input variables comprised of C, H, N, S, O, ash, MC, VM, T, ER, and $LHV_{biomass}$, and 8 output variables comprised of gas composition (CO CO_2, H_2, CH_4), gas yield, LHV of gas, CGE, and CCE were used. The 315 input-output patterns used for the study was divided into three; 70% (221 datasets) for training; 15% (47 datasets) for vali- dation; 15% (47 dataset) for testing of the model. Further, the input datasets were randomised for each of the iterations, while simu- lations were carried out by varying the number of neurons in the hidden layer using tansigmoid transfer function. The network was evaluated based on the MSE, and the architecture with the lowest MSE is considered the best model.

The convergence characteristics of the MIMO network trained with 23 neurons in the hidden layer is presented in Fig. 4a. It can be observed that the MSE of the training validation and testing decreased until epoch 6 before assuming constant till the epoch 12. The major issue with the result is the MSE value which is high, but it was caused by the nature of the data-sets inputted to the network and not necessary the inability of the network to offer efficient predictions.

In this case, the CCE was eliminated from the output variables to be predicted, and to check if the MSE could be reduced and then provide a better result. Fig. 4b shows the convergence character- istics of the network after the removal of the CCE. 23 neurons in the hidden layer was used to train the network, and the MSE has reduced from 348.6942 to 61.7092 and with best validation per- formance at iteration 10. This is when the CCE was not included in the prediction.

3.2. Model solutions: Levenberg-Marquardt (L-M) MISO layer network

Results of the ultimate analysis (C, H, and N) shown in section 3.2.1 were used as input variables to predict the CGE, Gas Yield, and LHV of the gas. These output parameters are considered as one of the major indicators or parameters for evaluating performance of a gasifier.

3.2.1. Prediction of the CGE [%]

In the prediction of the CGE, 20, 21, and 22 number of neurons in the hidden layer were selected from the several number of neurons used for the training of the network as shown in Fig. 5a through 5c, and they described how the MSE varies with the number of neuron used in training the networks, and the optimum iteration for each set of the learning program by the model. The best validation performance was obtained at iterations 59, 26, and 166 respec- tively. The training, validation, and test curves appear close to each other, and with consistent fitting as indicated by the epochs, but the Mean Square Errors (MSE) obtained were on the high side. This could be attributed to the source of the dataset which compelled the network to struggle a lot in memorizing the patterns while correlating the fittings. However, the 21 number of neurons in the hidden layer gave the smallest MSE.

Meanwhile, the coefficient of determination (R^2) obtained for the data fitting using the 20, 21, and 22 number of neurons in the hidden layer is shown in Table 2. The highest R^2 (0.84) was obtained from the validation curve from the 22 number of neurons in the hidden layer, but an R^2 of around 0.90e0.99 is preferred provided the MSE is small. An R^2 of 0.84 (highest) obtained in this case has not indicated a good correlation and it could be attributed to using a dataset obtained from different gasification system, and under different operating conditions.

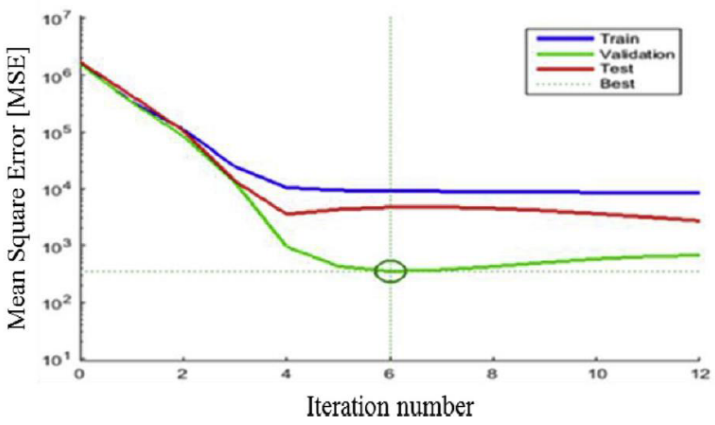


Fig. 4a. Convergence characteristics of the MIMO model, using all the output variables (23 neurons).

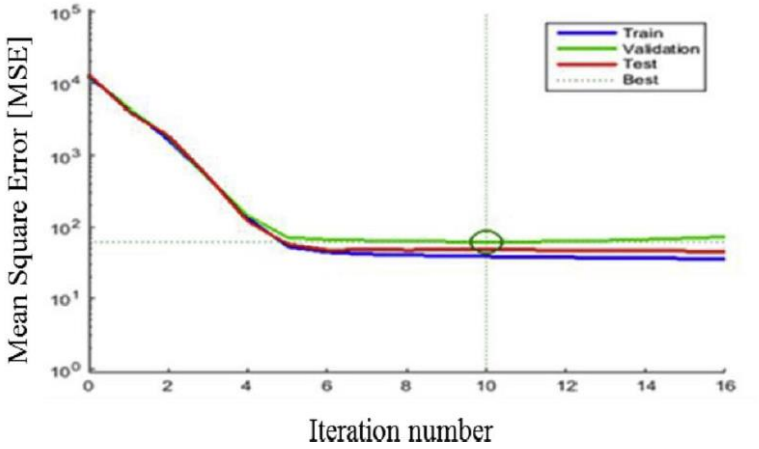


Fig. 4b. Convergence characteristics of the MIMO model, using all the output variables, except CCE (23 neurons).

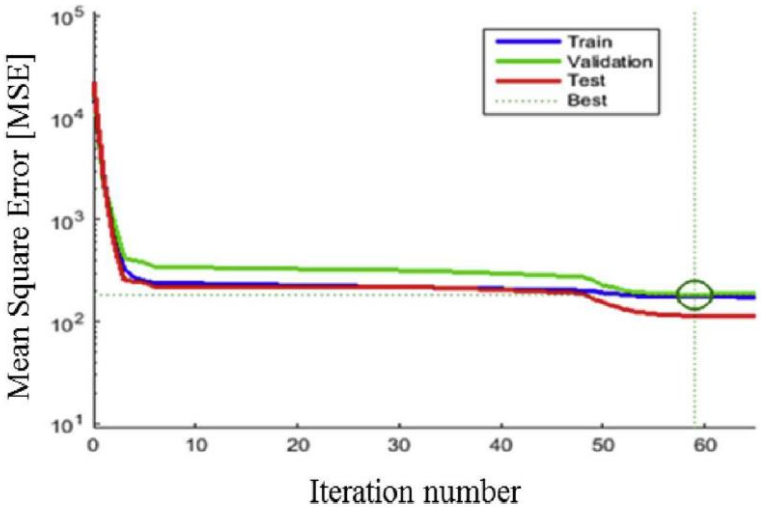


Fig. 5a. Convergence characteristics of the MISO model, CGE prediction using C, H, & N as the input variables (20 Neurons).

3.2.2. Prediction of the gas yield [kg/Nm³]: MISO layer network

Fig. 6a through Fig. 6c presents the results of the networks trained using 20, 21, and 22 neurons in the hidden layer and with C, H, and N from the ultimate analysis results as the input variables and Gas Yield as the output variable. In this case, the best validation performance was obtained at 36, 25, and 12 iterations respectively, while the highest R^2 of 0.84 was obtained from the network with 21neurons in the hidden layer. It can be observed that the MSE obtained from each of the training were quite high, but the result achieved with the network trained with 21 neurons in the hidden layer produced the smallest MSE of 145.13 at epoch 25. The high values of the MSE is an indication of a wide range of variations in the input and output dataset that were used for the training of the networks, and which resulted from the experimental datasets collected from different gasification systems, that were operated at different process conditions.

Similarly, the coefficient of determination (R^2) for the training, validation, and testing for the predicted gas yield are shown in Table 3. The highest R^2 of 0.84 was obtained from the validation curve of the network with 21 neurons in the hidden layer, the other R^2 are within 70e84% which is not an indication of good result, thus; requires upgrading.

3.2.3. Prediction of the LHV of gas [KJ/Nm³]: MISO layer network

The same conditions used for the training of the CGE and Gas Yield were equally used to train the networks for the LHV of the gas, and the results are depicted in Table 4. It can be observed that the MSE obtained from the each of the training are 0.34, 0.07, and 0.19, respectively, and have decreased very considerably when compared to the MSE obtained from the CGE and Gas Yield as 184.26, 115.28, & 148.47 and 199.61, 145.13, & 173.86. It could be attributed to the individual data in the data-set of the LHV of the

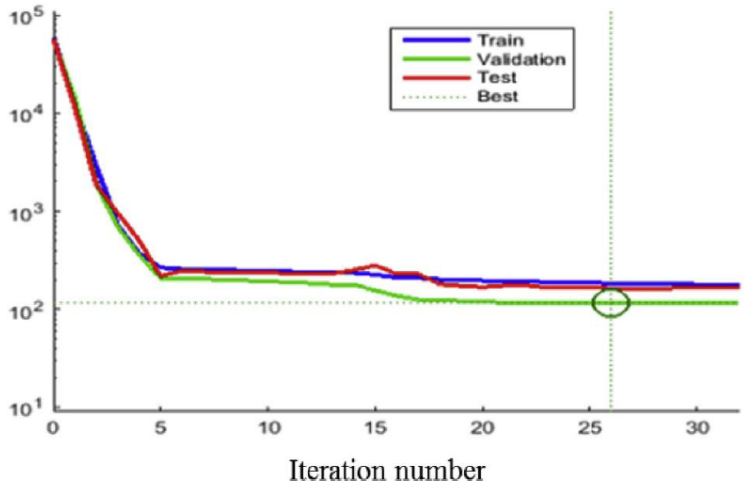


Fig. 5b. Convergence characteristics of the MISO model: CGE prediction: C, H, & N as the input variables: 21 Neurons.

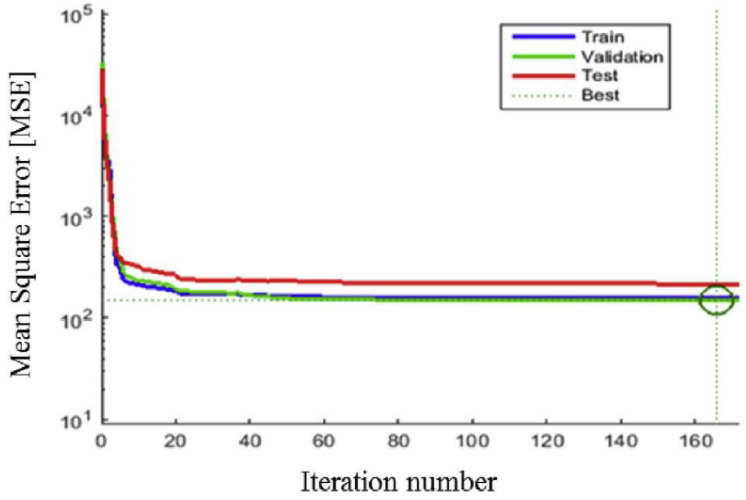


Fig. 5c. Convergence characteristics of the MISO model: CGE prediction: C, H, & N as the input variables: 22 Neurons.

Table 2
L-M MISO layer network: R^2 for the CGE using C, H, & N as the inputs.

Input variables	Number of neurons	Regression co-efficient (R^2)			Output variables
		Training	Validation	Testing All'	
C, H, N	20	0.75	0.83	0.80 0.78	CGE
C, H, N	21	0.75	0.81	0.81 0.80	CGE
C, H, N	22	0.78	0.84	0.74 0.82	CGE

C: Carbon; H; Hydrogen; N: Nitrogen; CGE: Cold Gas Efficiency; All': All data exploited.

gas having values closer to each other than those of CGE and Gas Yield. The training and validation curves for each of the networks fitted perfectly, whereas the testing curves indicated a random relationship. However, the R^2 of the training and validation fittings presented in Table 4 for each of the learning sets indicated some improved correlations, and with the validation fittings from the network trained with 21 number of neurons in the hidden layer producing the highest R^2 of 0.96, All the R^2 obtained from each of

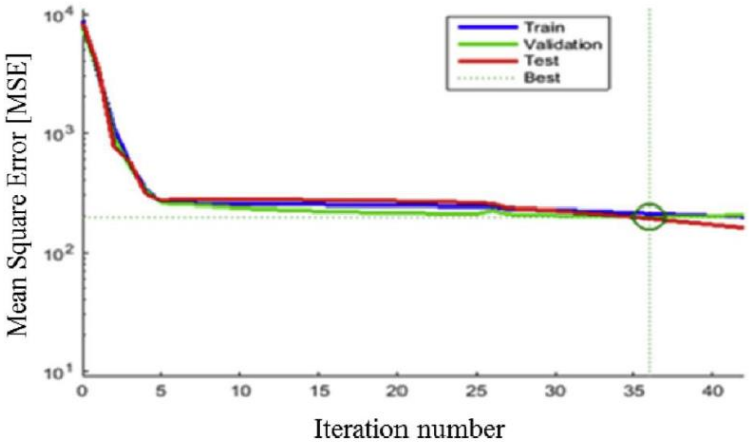


Fig. 6a. Convergence characteristics of the MISO model: Gas Yield prediction: C, H, & N as the input variables: 20 Neurons.

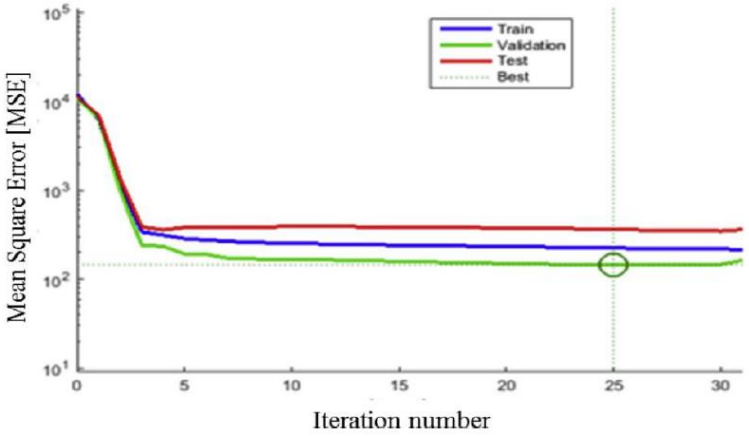


Fig. 6b. Convergence characteristics of the MISO model: Gas Yield prediction: C, H, & N as the input variables: 21 Neurons.

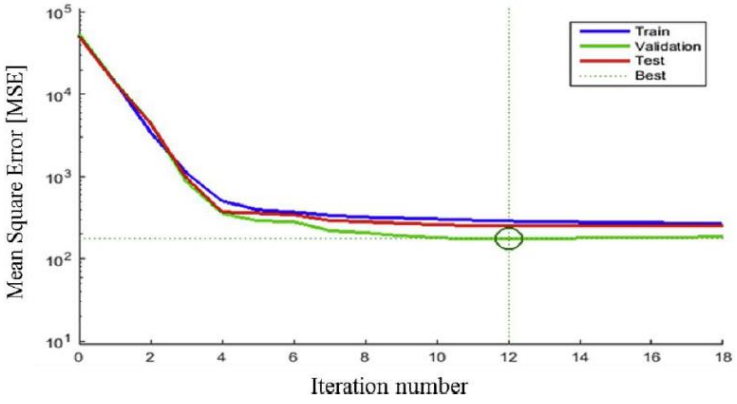


Fig. 6c. Convergence characteristics of the MISO model: Gas Yield prediction: C, H, & N as the input variables: 22 Neurons.

Table 3
L-M MISO layer network: R^2 for the Gas Yield using C, H, & N as the inputs.

Input variables	Number of neurons	Regression co-efficient (R^2)				Output variables
		Training	Validation	Testing	All*	
C, H, N	20	0.71	0.71	0.76	0.74	Gas Yield
C, H, N	21	0.80	0.81	0.61	0.85	Gas Yield
C, H, N	22	0.71	0.84	0.67	0.79	Gas Yield

C: Carbon; H; Hydrogen; N: Nitrogen; CGE: Cold Gas Efficiency; All*: All data exploited.

Table 4
Convergence characteristics and R^2 for the LHV of Gas using C, H, & N as the inputs: L-M MISO layer network.

Input variables	Number of neurons	Regression co-efficient (R^2)			Epoch		MSEOutput variables
		Training	Validation	Testing	All*		
C, H, N	20	0.95	0.90	0.91	0.90	365.00	0.34LHV of Gas
C, H, N	21	0.93	0.96	0.88 0.85	0.94	254.00	0.07LHV of Gas
C, H, N	22	0.90	0.91		0.85	17.00	0.19LHV of Gas

C: Carbon; H; Hydrogen; N: Nitrogen; CGE: Cold Gas Efficiency; MSE: Mean Square Error; All*: All data.

the training were above 90% except the validation fitting from the network trained with 20 neurons in the hidden layer and whose R^2 was 89.94%.

However, the results have revealed that if the individual data in each of the data-set are closer to each other, the MSE will decrease, while the R^2 will increase, thus; yielding a better result. To assure that the individual data are closer to each other for input and output variables, the collection of the experimental data should generally be based on the type of gasification system (e.g. fixed or fluidised bed gasifiers). The operating conditions should equally be classified (e.g. gasifying agent, gasification temperature, etc. to enhance the overall results of the prediction.

The R^2, epochs, and MSE obtained from the prediction of LHV of gas using C, H, and N as inputs and 20, 21, and 22 neurons in the hidden layer respectively are depicted in Table 4.

3.3. Prediction using proximate analysis data: MISO layer network

The CGE, Gas Yield, and LHV of the gas were predicted using the results of the proximate analysis and represented in this case by the ash, MC VM as the input variables for the model and employing the MISO layer network. The best validation performance of the network for the each of the predictions are shown in Fig. 7a, b, and 7c, respectively, and it can be seen from the results that the MSE values remained high irrespective of using the proximate analysis results in predicting the output variables, except the result from the LHV of the gas that has a MSE of 0.30.

It can equally be observed in Fig. 7a and b that the training, validation and testing curves are very close to each other when compared to Fig. 7c, and have consistent fittings until 29, and 66, epochs, but it is not an indication of a better fitting of the model due to the high values of the MSE and low values of R^2 that are only within the range of 75e79%. On the other hand, a MSE of 0.30 that was produced by the LHV of the gas at iteration 39 is a better result when compared to the results obtained from the CGE and gas yield, and the R^2 obtained from the training and validation were 93 and 81% respectively, while the testing curve has a lower value.

Generally, the results obtained from the ultimate and proximate analysis results as the input variables of the model respectively, indicated a similar trend. Table 5 presents the results of the coefficient of determination (R^2), respectively.

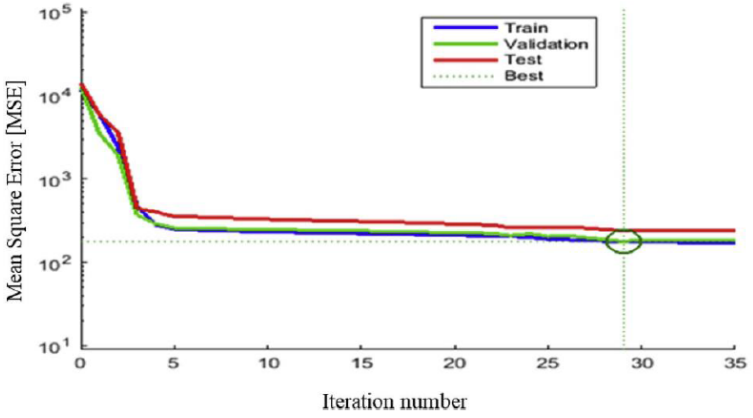


Fig. 7a. CGE prediction using ash, MC, & VM: 21 Neurons.

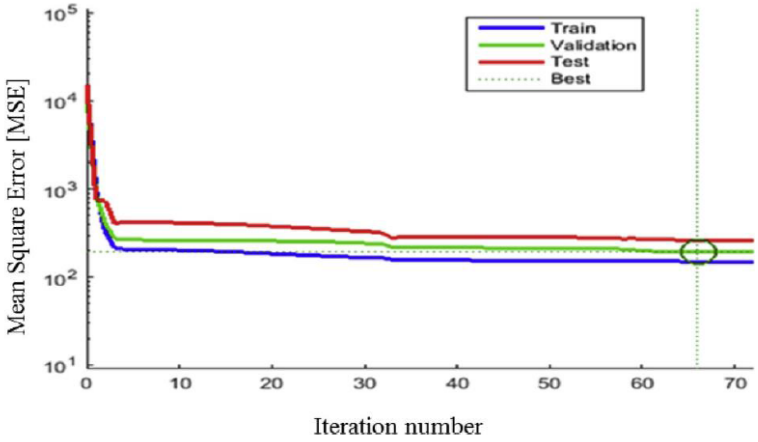


Fig. 7b. Gas Yield prediction using ash, MC, & VM: 21 Neurons.

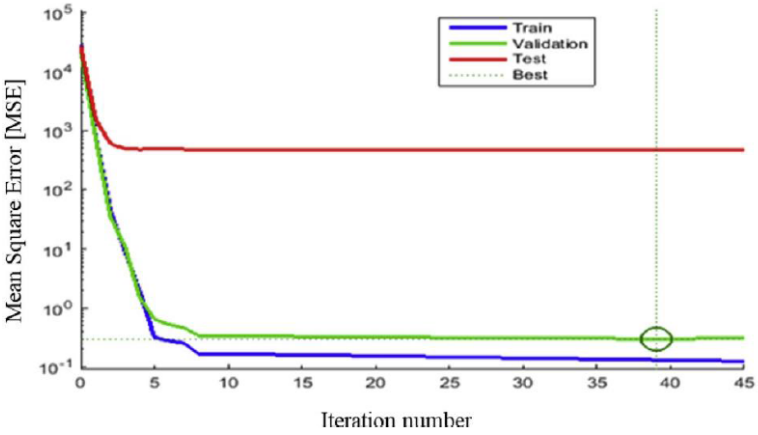


Fig. 7c. LHV of gas prediction using ash, MC, & VM: 21 Neurons.

Table 5
L-M MISO layer network: R^2 for the CGE, Gas Yield, & LHV of Gas using Ash, MC, & VM as inputs.

Input variables	Number of neurons	Regression co-efficient (R^2)			Output variables	
		Training	Validation	Testing	All*	
Ash, MC, VM	21	0.75	0.76	0.71	0.76	CGE
Ash, MC, VM	21	0.76	0.80	0.77	0.79	Gas Yield
Ash, MC, VM	21	0.93	0.81	0.69	0.89	LHV of Gas

MC: Moisture content; VM: Volatile Matter; CGE: Cold Gas Efficiency; All*: All data exploited.

3.4. Prediction using ultimate, proximate & process condition data: Input Variables Representation Technique with Visual Inspection Method (IVRT-VIM): MISO model

The IVRT-VIM was employed to study the improvement of the results of the performance indicators. The method was introduced to minimize the high values of the MSE and enhance the values of the R^2. The technique involves choosing a single input parameter from the 11 input variables to represent the ultimate, proximate, and experimental process condition results respectively, and it was achieved by the screening of the entire data of the input variables using Visual Inspection Method (VIM), and from which the sets having closer values were identified. In this approach, C, VM, & T were chosen as the input variables to represent the ultimate, proximate analysis, and the operating conditions of the gasifier respectively, and were used to predict the CGE, gas yield, and LHV of the gas. Previously, the results obtained from the training involving the ultimate and proximate analysis datasets using the L-M algorithm gave better results, respectively when compared to the model results obtained from the CGE, gas yield and the MIMO layer

network involving the entire 11 input variables for the BR algo- rithm. On this account, only the L-M algorithm is studied in this case.

Fig. 8a through Fig. 8c shows the outcome of training the network for the CGE, Gas yield and LHV of the gas, using only 21 neurons in the hidden layer, respectively. It can be observed that the MSE values in each of the case have reduced significantly when compared with the previous results. From Fig. 8a and b, the best validation performance was at epochs 7 and 3, while the best validation performance for the LHV of the gas was at epoch 16, and with MSE of 0.25. The decrease in the MSE of the three output variables (CGE, Gas yield, and LHV of the gas) is attributed to the refinement of the input datasets by employing the IVRT-VIM. It should be recalled that prior to the application of the IVRT-VIM, the

values of the MSE obtained in most cases were high, while the R^2 were as low as around 70**e**80%.

Meanwhile, the R^2 obtained for each of the output variables is presented in Table 6, and it can be observed that the R^2 for the validation of the three performance indicators are between 91.89 and 97.71%. Similarly, the R^2 obtained for the training and valida- tion of the LHV of gas was 96.83 and 97.71%, but the R^2 for the testing was small. The ANN model is reliable for predicting the gasification performance indicators studied, but to achieve an enhanced result, the input and output variable datasets may require refinement through IVRT-VIM.

The IVRT-VIM has helped to improve the model results when compared to other results obtained in the study, and it should be applied when several input variables are available for the predic- tion of the gasification performance indicators, and the results generated by the model are not as good as expected. If after using the IVRT-VIM and the result could not be improved, classifying the datasets into a fixed bed (FB) or fluidised bed gasifier (FBG) during the experimental data collation is another option to be investi- gated, and which may enhance the model results.

3.5. Prediction using L-M algorithm without CCE (WOCCE): Output Variables Representation Technique with Visual Inspection Method (OVRT-VIM): MIMO network layer

The output parameters were screened using the Output Vari- ables Representation Technique -Visual Inspection Method (OVRT- VIM) after which, the model prediction was carried out employing MIMO layer network WOCCE. The remaining variables were used to represent the outputs in the model, and to examine the improve- ment of the model result. 10 and 23 number of neurons in the hidden layer was used to study the MIMO layer network and using the L-M algorithm as presented in Fig. 9a and b, respectively. It can be seen that the best validation performance for Fig. 9a and b are at epochs 9 and 5, but the MSE obtained for the networks were 129.31 and 42.15, respectively. The regression results obtained from the network training using the 10 and 23 hidden neuron are also shown in Table 7. It can be observed that the R^2 was between 0.84 **e** 0.94 and 0.91**e**0.95, respectively implying that the model results had been upgraded when compared to the results involving C, H, & N as inputs.

Similarly, Table 8 shows a detailed result of the trained MIMO layer networks that was carried out using different number of neurons in the hidden layer, and BR and L-M algorithms. From Table 8, it can be observed that the networks were trained with carbon conversion efficiency (WCCE) and without carbon conver- sion efficiency (WOCCE), a technique employed to study the up- grade of the model results, and it is referred to as OVRT-VIM. A similar approach (IVRT-VIM) was used for the input variables in section 3.4 to enhance the result of the model. The MSE of 27.23 and R^2 for training and testing of 96% and 95% were obtained, respec- tively from the MIMO layer network that was studied using 23 number of neurons in the hidden layer, WOCCE. Based on the result, the BR algorithm (in this case), is better considered than the L-M algorithm. This implies that the OVRT-VIM is also an effective method of improving the model result. The results of the MISO layer networks (e.g. CO, CO_2, H_2, & CH_4) are contained in the sup- plementary material accompanying this paper.

4. Sensitivity analysis

Although the MSE and R^2 results obtained from this study gave some useful insights about the predictive accuracy of the ANN model, the PaD technique employed in this case had helped to identify the critical parameters and their degree of importance on the model outputs. The sensitivity analysis was carried out using C, VM, & T as the input variables, and Cold gas efficiency (CGE), gas yield, and LHV of gas as the output variables. The details of the other sensitivity analysis performed with other input and output variables are contained in the supplementary material accompa- nying this paper.

The Pareto charts shown in Fig. 10a through 10c are used to describe the relative importance of the input variables (C, VM, and T) on the output variables (CGE, gas yield, and LHV of gas).

The parameter with the highest sum of squares of the partial derivatives (SSD) has the most effect on the outputs, and from

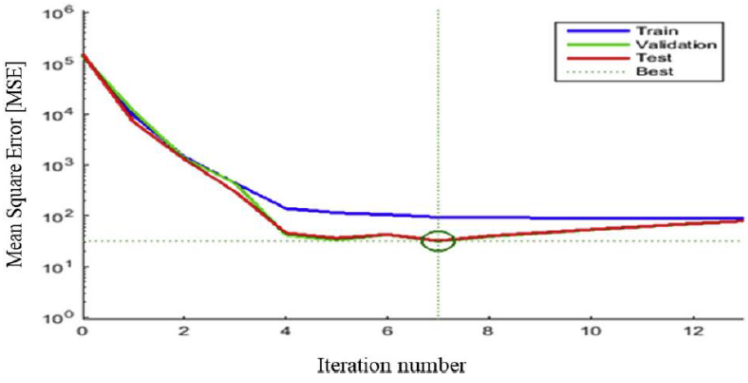


Fig. 8a. CGE prediction: Using C, VM, & T as the input variables: 21 Neurons.

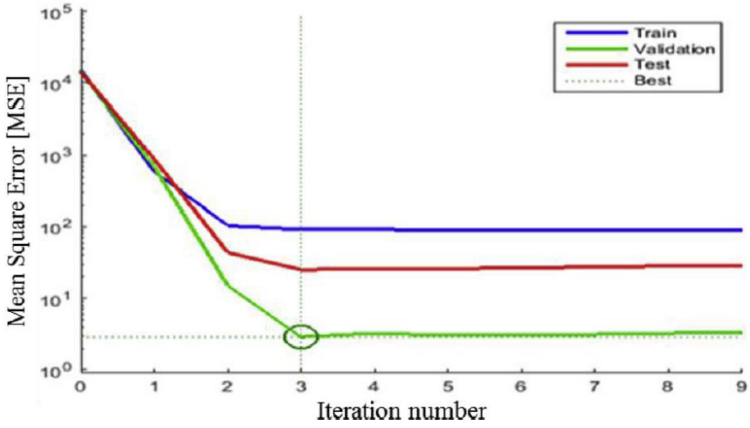


Fig. 8b. Gas Yield prediction: Using C, VM, & T as the input variables: 21 Neurons.

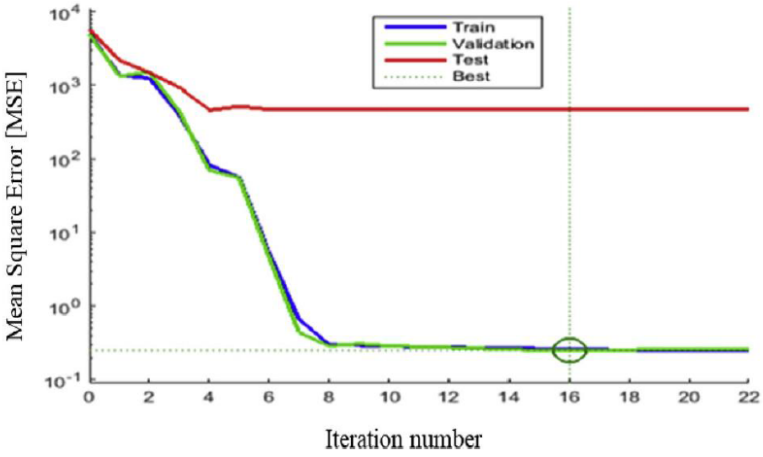


Fig. 8c. LHV of gas prediction: Using C, VM, & T as the input variables: 21 Neurons.

Table 6
R^2 result from ultimate, proximate & operating parameters: Input parameters.

Input Variables	Regression co-efficient (R^2)			Output Variables
	Training	Validation	Testing	All*
C, VM, T	0.87	0.92	0.85	0.90 CGE [%]
C, VM, T	0.90	0.95	0.79	0.88 Gas Yield [KJ/Nm³]
C, VM, T	0.97	0.98	0.33	0.87 LHV of Gas [kg/Nm³]

LHV: Lower Heating Value; R^2: Coefficient of determination; CGE: cold gas efficiency; C: Carbon; VM: Volatile Matter; T: Reaction Temperature; All*: All data exploited.

Fig. 10a, carbon is the most influential variable on the CGE. Carbon (C) is one of the major constituents of a fuel alongside H, and O [25]. It makes a significant contribution in the energy value of a fuel which is measured by the higher heating value (HHV) and lower heating value (LHV) of the fuel [26]. The volatile matter (VM) of a fuel describes the presence of organic matter in that fuel, and it accounts for fuel reactivity during thermo-chemical process and in which case, a low or high VM fuel plays a critical role in the overall reaction of the fuel [27]. The reaction temperature also is another important parameter that plays a key role in energy conversion process, and its effect equally, is dependent on the physio-chemical composition of the fuel such as C, VM, MC, etc. and other operating conditions used in the process (e.g. ER, oxidant, etc) [28]. High moisture content (MC) fuels may lead to reduction in the gasification temperature which could further lead to tar production and condensation in the gasifier [16]. In this study, there is a decrease and an increase in the MSE of the MISO and MIMO layer networks, respectively, when the MC and VM of fuel as well as C, H, & N and ash, were employed as inputs for the predictions of the CGE, gas yield and LHV of gas. The implication is that different fuels could yield different gasification efficiencies. Similarly, a high gasification temperature may enhance the cracking of tar (via thermal cracking), thus; resulting to an increase in the amount of product gas formed during gasification [29]. However, beyond certain range of gasification temperature (e.g. 900 -1000°C), the product gas becomes part of the combusting material, and in this case, the product gas yield is decreased [16].

For the CGE prediction, the SSD of carbon was 1.1846, and it is

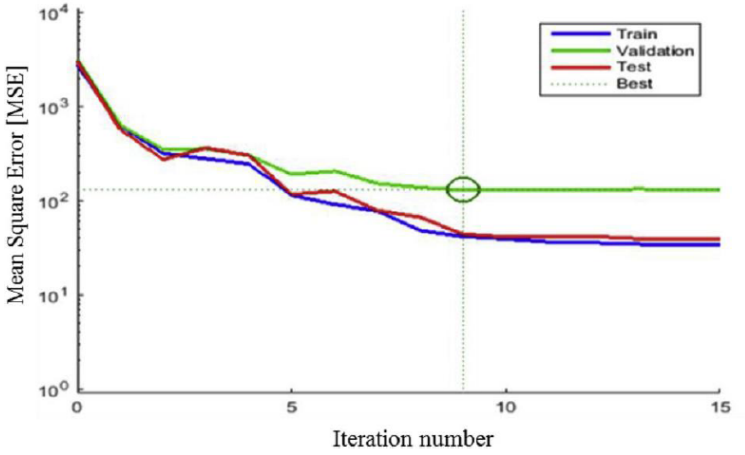


Fig. 9a. Convergence characteristics of the MIMO L-M model, WOCCE (10neurons).

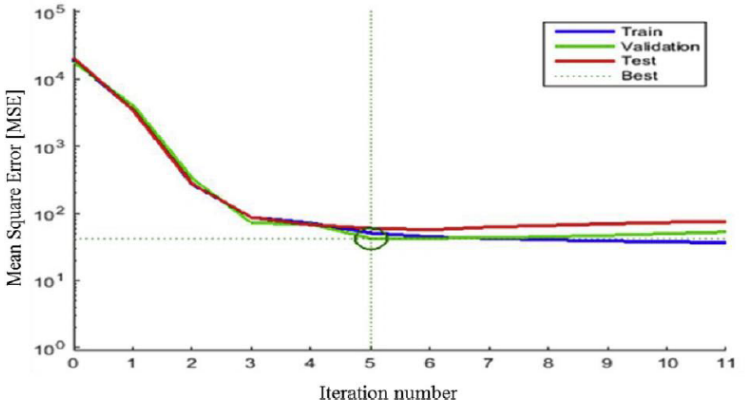


Fig. 9b. Convergence characteristics of the MIMO L-M model, WOCCE (23neurons).

Table 7
Model improvement using OVRT-VIM: MIMO L-M algorithm, WOCCE.

Inputs	Algorithm	Coefficient of determination (R^2)					
C, VM, T	L-M	Neurons	Training	Validation	Testing	All*	Outputs
		10	0.94	0.94	0.84	0.92	CCG, gas yield, LHV of gas
		23	0.93	0.91	0.95	0.93	

L-M: Levenberg-Marquardt, C: Carbon; VM: Volatile Matter; T: Reaction Temperature; CCG: Cold Gas Efficiency; LHV: Lower Heating Value of Gas; All*: All data exploited.

the highest amongst the input parameters studied, hence; ranking it the most important parameter affecting the CGE. Fig. 10b and c presents the relative importance of the input parameters on the outputs (gas yield and LHV of gas), respectively.

It can be observed that the same trend of result obtained in Fig. 10a was equally achieved. The SSD value of carbon was 1.1362 and 0.0019 for gas yield and LHV of gas respectively, thus; making it the most effective parameter affecting the outputs.

Therefore, from the result of the sensitivity analysis, the use of C, VM, and T as input variables for the model prediction of the gasi- fication performance indicators (CGE, gas yield, and LHV of gas) are in the order of C > VM > T. The order is logical considering the impact of each parameter on the efficiency of biomass and coal gasification processes. The analysis demonstrates that the network output varies relative to the inputs, thus offering essential infor- mation about the more sensitive parameters in the investigation, and revealing the reliability of the model parameters.

5. Results compared with literature

Table 9 compares results obtained in this study with literature. BFBG: bubbling fluidized bed gasifier; CFBG: circulating

Table 8
BR & L-M algorithm MIMO network results: OVRT-VIM model improvement.

Algorithm	Number of Neurons	MSE	Epoch	Training	Validation	Testing All*
WCCE						
BR	10	33.35	108.00	0.95	e	0.84 0.90
L-M	10	206.88	8.00	0.86	0.89	0.18 0.65
WOCCE						
BR	10	6136.99	89.00	0.61	e	0.07 0.80
L-M	10	129.31	9.00	0.95	0.84	0.95 0.92
WCCE						
BR	23	6174.50	786.00	0.61	e	0.73 0.71
L-M	23	3188.60	5.00	0.45	0.16	0.60 0.61
WOCCE						
BR	23	27.23	468.00	0.96	e	0.95 0.92
L-M	23	42.15	5.00	0.93	0.95	0.91 0.96

WCCE: With carbon conversion efficiency; WOCCE: Without carbon conversion efficiency; BR: Bayesian regularisation; L-M: Levenberg Marquardt; MSE: Mean Square Error; OVRT-VIM: Output Variables Representation Technique-Visual Inspection Method; All*: All data exploited.

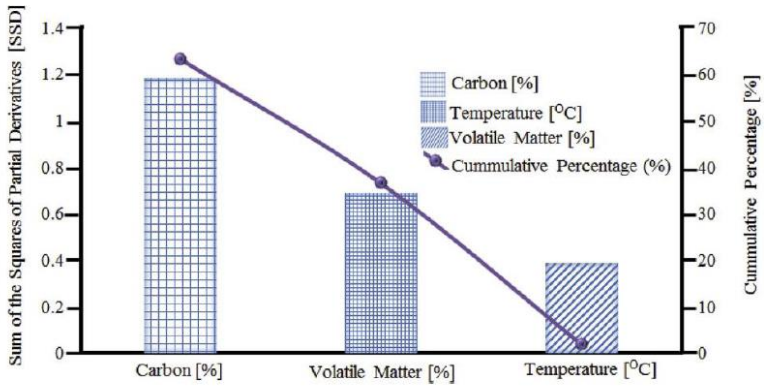


Fig. 10a. Relative effect of each input variable on the output variable: CGE [%]: MISO layer network: 21 hidden layer neurons.

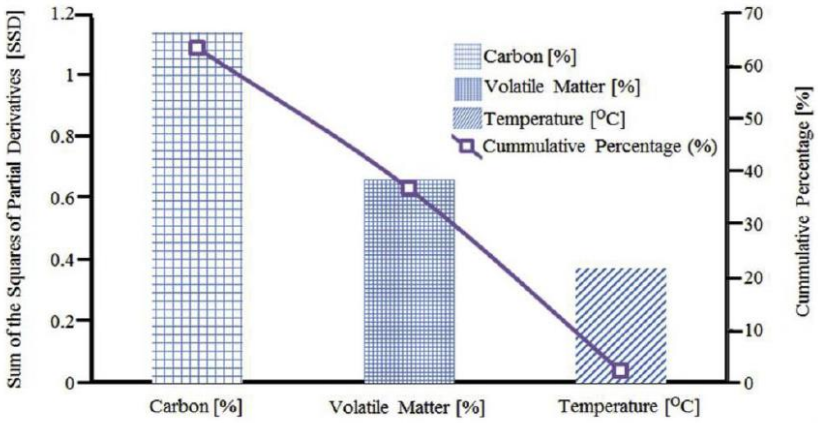


Fig. 10b. Relative effect of each input variable on the output variable: Gas Yield [kg/Nm³]: MISO layer network: 21 hidden layer neurons.

fluidized bed gasifier; FBG: Fixed bed gasifier; EFB: Entrained fluidised bed; CGE: cold gas efficiency; CCE: carbon conversion efficiency; ER: equivalence ratio; MC: moisture content; T: reaction temperature, C: carbon; O: oxygen; H: hydrogen; VM: volatile matter; MIMO: Multiple Input-Multiple Output; MISO: Multiple Input-Single Output; L-M: Levenberg- Marquardt; LHV: lower heating value; SSD: sum of squares of partial derivatives; WCCE: without carbon conversion efficiency.

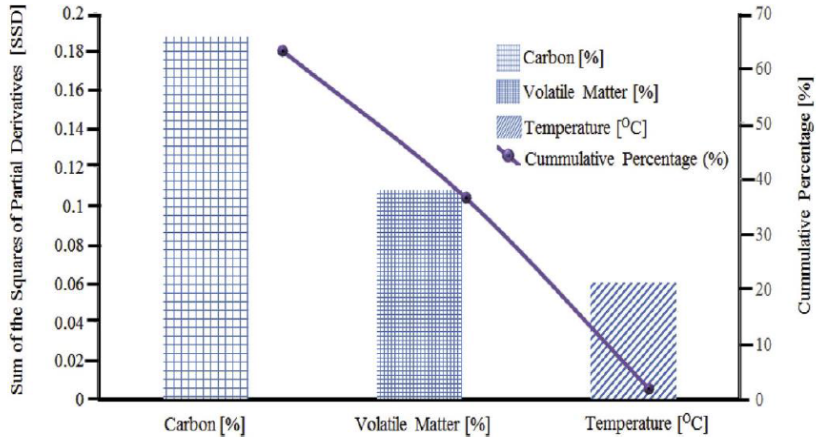


Fig. 10c. Relative effect of each input variable on the output variable: LHV of Gas [KJ/Nm³]: MISO layer network: 21 hidden layer neurons.

Table 9
Results compared with literature.

Reactor	Input variables	Output Variable	Major Findings	Reference
CFBG & BFBG	Ash, MC, C, O, H, ER, T, VM	Gas yield, CO, CO_2, H_2, CH_4	Model predicted efficiently the gasification performance indicators	[8]
Remarks: LM-Back-propagation algorithm was used. Model technique: MIMO, Hidden layer Neuron: 2 Sensitivity: Connection weights method [23]: All variables have effect on the output, but for CFB: C, H, O has between 31.7 and 54.1% and for BFB: C, H, O has between 28.9 and 52.3% effects on the outputs. Generally, ER was the most important factor influencing the gas yield.				
FBG	C, H, O, ash, MC, Reduction zone temperature	Gas composition: CO, CO, CH_4, H_2 composition, and result in agreement with experimental data.	Model is reliable in predicting the gas	[7]
Remarks: LM-Back-propagation algorithm was used. Number of neurons: 5 (used to predict CH4, CO), 4 for CO_2 & 3 for H_2 predictions. Training: 70%, Validation: 15%, Testing: 15% dataset. Sensitivity: Connection: Connection weights method. Total number of experimental data: 63 samples.				
FBG	C, H, N, S, O, MC, ash, ER, Tg,	LHV of gas, LHVP (Char, & tar), Gas yield	Model has the ability to predict the	[2]
gasification performance indicators with low MSE, thus; a viable alternative model for the prediction of the efficiency of a FBG.				
Remarks: L-M MIMO & MISO of single and double layers were used. Number of hidden layer Neuron: 30 for single layer & 15 for the double layer.				
FBG	VM, FC, and Ash	C, H, & O	Predicted the fuel elemental	
compositions well				
				[30]
Remarks: ANN (MISI Model), Genetic Algorithm, & Support Vector Regression (SVR) was used. Number of layers: Single layer with 5 hidden neurons & a double layer with 3 hidden number of neurons. Number of data trained: 830 samples.				
FBG		CGE, CCE, total gas yield, LHV of gas	Model offered a reliable prediction	[5]
Remarks: ANN model, Genetic programming (GP) Support vector Regression (SVR) was used. Dataset was obtained from biomass and coal as fuel. Dataset was also obtained from a single gasification system.				
Different Gasifiers	MIMO: C, H, N, O, S, VM, Ash, ER, T, $LHV_{biomass}$, MISO: C, VM, T			
MIMO: CGE, CCE, gas yield, LHV of gas, Gas composition: CO, CO_2, CH_4, & H_2, MISO: CGE, Gas Yield, LHV of gas.			Model reliably predicted the gasification performance indicators.	This study
Remarks: Dataset: Obtained from different gasifiers, fuels (e.g. biomass, coal, & blends of biomass and coal) & process conditions. LM-Back-propagation algorithm & Bayesian Regularisation algorithm were used. Model technique: MIMO & MISO layer networks were studied. Number of hidden neurons: MIMO: 10 & 23. MISO: 20, 21, 22. The MIMO layer network Predictions using 9 & 8 input variables respectively, produced result with high MSE, but has close fittings. The MISO Prediction using C, H, & N and ash, MC, & VM, yielded result with reduced MSE & an R^2 of between 75 and 93%. MISO model with C, VM, & T as input variables gave better result, after data refinement, with R^2 of between 79 and 98%, while the MIMO layer network, WOCCE yielded an R^2 of between 95% and 96%. A technique called IVRT-VIM and OVRT-VIM were developed, and were used to improve the model result. Sensitivity analysis: The Partial Derivatives (PaD) method was used. The most influential parameter: Carbon (C), with an SSD of 1.1846 for the CGE prediction.				

6. Conclusions

Experimental data obtained from a few gasifiers (e.g. entrained, fluidised, and fixed bed) operated at varied experimental condi- tions were using blends of feedstocks (e.g. biomass, coal, waste tyre etc.) were employed in a backpropagation L-M and BR algorithms of ANN model with MIMO and MISO layer networks to study the performance efficiency of a gasification unit. The input variables were ash, MC, VM, C, H, N, O, S, T, ER, and $LHV_{biomass}$, while the outputs were CGE, CCE, gas yield, LHV of gas, and gas composition (e.g. CO, CO_2, CH_4, and H_2). The prediction accuracy of the models was assessed using the MSE and R^2, while the Partial Derivatives (PaD) method was employed for the sensitivity analysis. The following conclusions emerged from the study:

Results of the MIMO and MISO layer networks obtained from the L-M algorithm is better than those of them obtained from the BR algorithm, and it implies that the prediction accuracy of the L-M algorithm is more reliable than the BR algorithm.

The MISO layer networks trained with 20, 21, and 22 neurons in the hidden layer with C, H, & N and ash, MC, & VM, yielded result with reduced MSE & an R^2 of between 75 and 93%, implying that the model is more sensitive to some input vari- ables than others.

Because of the high values of the MSE and low R obtained from the MIMO layer networks for the BR and L-M algorithm using C, H, & N and ash, MC, & VM in predicting the CGE, gas yield and LHV of gas respectively, the IVRT-VIM and OVRT-VIM were developed to account for the improvement of the model results. An application of the IVRT-VIM on the MISO layer networks using C, VM, & T as input variables and the CGE, gas yield and LHV of gas as the outputs gave an R^2 of between 79%e98%, while the OVRT-VIM also gave an R^2 of between 95% and 96% for the MIMO layer network, WOCCE indicating that both approaches

are effective for the enhancement of the model result.

Results of the sensitivity analysis reveal that carbon is the most important input parameter affecting the outputs with an SSD of 1.1846 for the CGE prediction, and the relative importance of the inputs to the outputs are of the order of Carbon (1.1846) > volatile matter (0.6863) > temperature (0.0039).

Performance of a gasifier was assessed via modelling approach (without carrying out the actual gasification tests) and the efficiency of such gasifier can be predicted when different operating conditions and fuels are employed. The information obtained thereof could assist stake-holders in developing gasifiers capable of converting different solid fuel materials into energy. This information could be instrumental to decision making and serving as a platform for further R & D in this area.

Though, different number of neurons in the hidden layer was extensively used to train the MIMO and MISO neural networks to achieve better results, it is noteworthy to mention that vast time was consumed to upgrade the models. This could be attributed to the nature of the dataset used. The classification of the experi- mental dataset into fixed and fluidised bed gasifiers, and the pro- cess conditions is expected to improve the overall model results, and this could be investigated. Furthermore, it will be crucial in the future, to eliminate other outputs (e.g. CGE & LHV of gas) to verify the extent of the model improvement. However, the ANN model has demonstrated its robustness in the estimation of the gasifica- tion efficiency parameters.

Acknowledgment

Ozonoh acknowledges Mrs. Angela Ozonoh for her financial support.

Appendix A. Supplementary data

Supplementary data to this article can be found online at https://doi.org/10.1016/j.renene.2019.07.136.

References

[1] A.S. Englebrecht, B.C. North, B.O. Oboirien, R.C. Everson, H. Neomagus, Fluidized bed gasification of high-ash South Africa coals: an experimental and modelling study. IFSA 2011 Industrial Fluidization South Africa 145-160, in: A Lukos & P Den Hoed Johannesburg Southern African Institute of Mining and Metallurgy, 2011.

[2] D.S. Pandey, S. Das, I. Pan, J.J. Leahy, W. Kwapinski, Artificial neural network based modelling approach for municipal solid waste gasification in a fluidized bed reactor, Waste Manag. 58 (2016) 202e213.

[3] Q.V. Bach, O. Skreiberg, C.J. Lee, Process modeling and optimization for torrefaction of forest residues, Energy 138 (2017) 348e354.

[4] P.J.G. Nieto, E. Garcia-Gonzalo, J.P. Paredes-Sanchez, A. Bernardo Sanchez, M. Menendez Fernandez, Predictive Modelling of the Higher Heating Value in Biomass Torrefaction for the Energy Treatment Process Using Machine- Learning Techniques. Fuel, 2018, pp. 1e14.

[5] S. Tiwary, S.B. Ghugare, P.D. Chavan, S. Saha, S. Datta, J. Sahu, S.S. Tambe, Co-gasification of high ash coalebiomass blends in a fluidized bed gasifier. Experimental study and computational intelligence-based modeling waste and biomass valorization. https://doi.org/10.1007/s12649-018-0378-7, 2018.

[6] J. George, P. Arun, C. Muraleedharan, Assessment of producer gas composition in air gasification of biomass using artificial neural network model, Int. J. Hydrogen Energy 43 (2018) 9558e9568. https://doi.org/10.1016/j.ijhydene.2018.04.007.

[7] D. Baruah, D.C. Baruah, M.K. Hazarika, Artificial neural network based modeling of biomass gasification in fixed bed downdraft gasifiers, Biomass Bioenergy 98 (2017) 264e271.

[8] M. Puig-Arnavat, J.A. Hernandez, J.C. Bruno, A. Coronas, Artificial neural network models for biomass gasification in fluidized bed gasifiers, Biomass Bioenergy 49 (2013), 2 7 9-2 8 9.

[9] J.J. Montano, A. Palmer, Numeric sensitivity analysis applied to feedforward neural networks, Neural Comput. Appl. 12 (2003) 119e125.

[10] W. Wang, P. Jones, D. Partridge, Assessing the impact of input features in a feedforward neural network, Neural Comput. Appl. 9 (2000) 101e112.

[11] M. Gevrey, I. Dimopoulos, S. Lek, Review and comparison of methods to study the contribution of variables in artificial neural network models, Ecol. Model. (2003) 249e264.

[12] E. Idoia, B.F. Fabio, T.F. Jose, A. Roberto, O. Martin, Fitting performance of artificial neural networks and empirical correlations to estimate higher heating values of biomass, Fuel 180 (2016) 377e383.

[13] D.R. Nhuchhen, P.A. Salam, Estimation of higher heating value of biomass from proximate analysis: a new approach, Fuel 99 (2012) 55e63.

[14] V.S. Sikarwar, M. Zhao, P. Clough, J. Yao, X. Zhong, M.Z. Memon, N. Shah, E. Anthony, P. Fennell, An overview of advances in biomass gasification, En- ergy Environ. Sci. 9 (2016) 2939e2977.

[15] P. Lahijani, Z.A. Zainal, Gasification of palm empty fruit bunches in a fluidised bed; a performance study, Bioresour. Technol. 102 (2011) 2068e2076.

[16] N. Nipattummakul, I.I. Ahmed, S. Kerdsuwan, A.K. Gupta, Hydrogen and syngas production from sewage sludge via steam gasification, Int. J. Hydrogen Energy 35 (2010) 11738e11745.

[17] J. Dascomb, A. Krothapall, Hydrogen-Enriched syngas from biomass steam gasification for use in land-based gas turbine engines, in: Novel combustion concept for sustainable for sustainable energy development (conference paper), 2014, pp. 89e110.https://doi.org/10.1007/978-81-322-2211-8_6.

[18] P.M. Lv, Z.H. Xiong, C.Z. Jang, Y. Wu, J.X. Chen, Z.X. Zhu, An experimental study of biomass air-steam gasification in a fluidized bed, Bioresour. Technol. 95 (2004) 95e101.

[19] F. Guo, Y. Dong, L. Dong, C. Guo, Effect of design and operating parameters on the gasification process of biomass in a downdraft fixed bed: an experimental study, Int. J. Hydrogen Energy 39 (2014) 5625e5633.

[20] L.Q. Wang, Y. Chen, Experimental studies on H_2-rich gas production by Co-gasification of coal and biomass in an intermittent fluidized bed reactor, Adv. Mater. Res. 201 (2013) 1127e1131.

[21] M.H. Shojaeefard, M. Akbari, M. Tahani, F. Farhani, Sensitivity analysis of the artificial neural network outputs in friction stir lap joining of aluminum to brass, Adv. Mater. Sci. Eng. (2013) 1e7. https://doi.org/10.1155/2013/574914.

[22] T. Tchaban, M.J. Taylor, J.P. Grifn, Establishing impacts of the inputs in a feedforward neural network, Neural Comput. Appl. (1998) 7309e7317.

[23] G.D. Garson, Interpreting neural-network connection weights, AI Expet. 6 (1991) 46e51.

[24] W. Wang, P. Jones, D. Partridge, Assessing the impact of input features in a feedforward neural network, Neural Comput. Appl. 9 (2000) 101e112.

[25] C.C. Fagan, C.D. Everard, K. McDonnell, Prediction of moisture, calorific value, ash, and carbon content of two dedicated bioenergy crops using near-infrared spectroscopy, Bioresour. Technol. 102 (2011) 5200e5206.

[26] J. Posom, P. Sirisomboon, Evaluation of lower heating value and elemental composition of bamboo using near infrared spectroscopy, Energy 12 (2017) 147e158.

[27] R. Khonde, A. Chaurasia, Rice husk gasification in a two-stage fixed-bed gasifier: production of hydrogen rich syngas and kinetics, Int. J. Hydrogen Energy 41 (2016) 8793e8802.

[28] S. Sharma, P.N. Sheth, Air-steam biomass gasification: experiments, modelling and simulation, Energy Convers. Manag. 110 (2016) 307e318.

[29] J. Udomsirichakorn, P.A. Salam, Review of hydrogen-enriched gas production from steam gasification of biomass: the prospect of CaO-based chemical looping gasification, Renew. Sustain. Energy Rev. 30 (2014) 565e579.

[30] S.B. Ghugare, S. Tiwary, S.S. Tambe, Computational intelligence based models for prediction of elemental composition of solid biomass fuels from proximate analysis, Int. J. Syst. Assur. Eng. Manag. 8 (2014), https://doi.org/10.1007/s13198-014-0324-4.

MAXIMIZATION OF PROFIT IN A CO-GASIFICATION CHP PLANT THROUGH BIOMASS TORREFACTION

M. Ozonoh[a], B. O. Oboirien[b], M.O. Daramola[a*]
[a]School of Chemical and Metallurgical Engineering, Faculty of Engineering and the Built Environment, University of the Witwatersrand, Wits 2050, Johannesburg, South Africa
[b]Department of Chemical Engineering, University of Johannesburg, Doomfontein Johannesburg, 2028, South Africa
[*]Corresponding author: michael.daramola@wits.ac.za

ABSTRACT: Co-gasification of coal and biomass is a well-known energy conversion technology that reduces the cost of feedstock required for power production. The amount of heat and electricity generated, as well as the profit made from the power plant is dependent on the quality of the feedstock used in generating the energy. Torrefaction improves the quality of feedstock used for syngas generation and earning of profit in a power plant such as Combined Heat and Power (CHP) plant is improved if the fuel quality is enhanced. In this study, waste biomass such as corn cob, sugar cane bagasse, and pine saw dust were torrefied and blended with coal using coal-to-biomass ratios of 50:50, 71:29, & 80:20. The feedstocks was characterized and then the heating value and moisture content of the fuels were measured and used to estimate the feed-rate and annual feedstock requirement of the plant. An estimation of the earned profit from a typical CHP plant for a 20-year-investment period divided into four terms: A, B, C, & D was carried out using the Net Present Value and Payback Period models. The operating cost models considered were with feedstock costing (WFC) and without feedstock costing (WOFC). A profit of between USD5,902,292.46 - USD 6,489,659.30, and USD7,654,111.66 – USD7,899,284.01 were earned with percentage reduction in profit increased from A - D by about 1.01 – 2.32 % and 1.19 – 5.39 % using WFC and WOFC, respectively.
Keyword: Biomass, Coal, Co-gasification, Energy Production, Profit Maximization, Torrefaction.

1 INTRODUCTION

One of the potential pathways of producing energy from biomass is its co-gasification with fossil fuels (e.g. coal) which could be carried out in plants such as Integrated Gasification Combined Circle (IGCC) or Combined Heat and Power (CHP) plant (either in a newly design or an existing power plant). An existing power plant is considered as a transitional alternative for a total carbon-free power sector that offers advantage in comparison to using biomass in a dedicated power plant with high thermal efficiency, lower capital costs and less operational risk. However, a biomass-fed power plant and coal-fired power plant can be used interchangeably, but slight modification in the design will be required to account for periods when biomass would be un-available [1]. Often, investors may like to invest in plants that require minimal expenditures for effective operations. The use of existing coal-fired power plant for biomass energy generation therefore, could reduce the technical challenges and increase the biomass power capacity [2]. An example of such challenges is the CO_2 abatement cost via Carbon Capture and Storage (CCS) that is on the high side for coal-fired plant compared to biomass-fired plant. Irrespective of using an existing power generating plant, potential investors are equally interested in energy conversion processes that yield more profits.

Biomass as feedstock for energy production is different from coal in terms of handling and combustion characteristics due to the compositional properties. For instance, biomass has higher moisture content, lower energy density, higher chlorine and potassium contents, etc [2], and these could negatively impact on the efficiency of the energy conversion system (e.g. gasifiers and boilers). However, if biomass is co-gasified with traditional fuels such as coal, with reasonable coal-to- biomass ratio, a reasonable efficiency of the energy conversion could be maintained. Irena [1] reported that using blend ratio not above 90:10 could be promising while Bada et al [3] and Ozonoh et al [4] found that 50:50 coal-to-biomass ratio is reasonable for synergetic effect, costs and emission reduction in power plants.

Recently, some studies that were carried out using different energy conversion technologies and processes have shown that torrefaction is attractive in terms of increasing the quality of the fuel. The ratio of coal-to- biomass during co-firing or co-gasification is also increased because of fuel pre-treatment. In this case, the hemicellulose matrix and fibres structure of the fuel are decomposed, thus accounting for its de-polymerisation and loss of original nature of the raw fuel [5].

Torrefaction has been studied using different energy conversion technologies and processes and reported to be instrumental to enhancing quality of fuel [7]. Generally, the benefits associated with torrefaction include higher energy density (heating value), lower atomic O/C & H/C ratios and moisture content, higher hydrophobicity, enhanced grindabilty, and better uniform properties of biomass [6]. From transportation point of view, the bulk density is reduced and a long-term storage opportunity - without quality degradation is provided. Particularly, an additional profit is gained from the energy plant due to minimal expenditure in the logistics. Further, the use of varieties of feedstock sources in the system (e.g. gasifier) is feasible because of uniformity in the upgraded fuel. It has been reported by Peng et al [7] that torrefaction of biomass improves the gasification thermal efficiency and reduces tar production due to removal of oxygenated volatile compounds from the biomass during the process. Therefore, investors most times, indicate much interest in investment plans and operating conditions that will enable them to earn more profits at lesser risks. They consider such parameters prior to the venturing into the business.

Several researchers including Park et al [8]; Chen et al [9]; Lu et al [10]; Yan et al [11]; Arias et al [12] Phanphanich & Mani [13] have studied biomass torrefaction using different kinds of biomass. The reports from these authors have shown an improvement in the quality of the fuel (e.g. energy density) when compared to that of the raw fuel. Secondly, other researchers have reported the positive effect of upgrade of fuel quality on the profitability and environmental impact of power plants [2,14,15]. Many of the studies were carried out

using different kinds of biomass without considering blends of these biomass materials with conventional source of fuel like coal. It was expected from the aforementioned works that the authors would consider how the profits earned in the plant reduced over an investment period due to time value of money (TVM), but it was not reported. In this study, the profits earned for a 20-years-investment period in a CHP co-gasification plant were estimated using blends of coal and torrefied biomass as feedstocks. The percentage reduction in the profit over the time period was equally emphasised. Importantly, the outcome of this investigation will provide statistical evidence that will assist professionals in this sector in critical decision making and as well, open a new window for further R&D in this area.

2 EXPERIMENTAL

2.1 Materials and Methods

The biomass and coal used in this study were of South African origin. The biomass materials were corn cob (CC), pine sawdust (PSD) and sugarcane bagasse (SCB), Corn cob (CC). Specifically, the coal and biomass were obtained from the Matla mine and Hill-brow market, respectively. They were pre-treated by milling and sieving and the method used can be found elsewhere Ozonoh et al [4].

Blends of coal and torrefied biomass were used as feedstocks to investigate the profitability of a co-gasification CHP plant. The torrefaction was carried out using the experimental design (Box Behnken Design (BBD)) obtained from Design Expert Software (version 8.0 using 3 input variables (torrefaction temperature, torrefaction time and blend ratio) and output variable (Higher Heating Value). The torrefaction temperature and torrefaction time considered in this study were in the range of 200 - 300 ^{O}C and 30 - 60 minutes respectively, and the blend ratio (coal-to-biomass) were 50:50, 71:29, & 80:20. The torrefaction experiments were conducted in a tubular furnace reactor under inert (nitrogen) atmosphere using the statistically designed experiment discussed above. Thereafter, the torrefied biomass was blended with coal and characterized for the heating value, proximate and ultimate analysis using the procedures described in Ozonoh et al [4].

2.2 Profitability evaluation

The results from characterization and torrefaction experiments were used to estimate the annual feed-rate and feedstock requirements in the plant. Financial intelligence tools used in project management such as Net Present Value (NPV) and Payback Period (PBP) were employed to appraise the profits earned. The NPV and PBP are expressed in Equation (1) and Equation (2) [16; 4], respectively:

$$NPV = -\beta + \sum_{j=1}^{T} \frac{\Phi_j}{(1+IRR)^j} = 0 \quad (1)$$

$$PBP = \frac{\delta}{\mu} \quad (2)$$

Where β is the capital cost investment; T is economic life of the plant (investment period); Φ is the cash flow (profit); IRR is the Internal Rate of Return; δ is the number of years taking to recover the total investment cost; and is the earnings after interest and tax. In this study, the 20-year-investment period was divided into four investment terms. It includes term A, B, C, & D, and they are represented by 1st – 5th, 5th – 10th, 10th – 15th, & 15th – 20th year. Furthermore, two financial cases were considered. They are with Feedstock Costing (WFC) and Without Feedstock Costing (WOFC) and both financial cases had been defined in our previous works on CHP plant. The profit earned at the end of the first year of the investment was used to determine the percentage decrease in the profit as the business progressed. In this case, the Time Value of Money (TVM) on the investment for each of the terms was considered, and its effect on the profit made was determined based on the NPV.

3 RESULTS AND DISCUSSION

The results obtained from the torrefaction experiment and feedstock characterisation are depicted in Table 1. In this study, the optimum process condition was determined based on the results of the HHV, solid yield, energy yield and the enhancement factor (EF). The order for the optimum process condition are 50:50 (300 ^{O}C at 45 min) > 71:29 (300 ^{O}C at 45 min) > 80:20 (300 ^{O}C at 60 min), while the order for the optimum feedstock are Coal + PSD > Coal + SCB > Coal +CC. Three torrefaction temperature regimes were used for the investigation, but the details of the sever temperature regime employed for the profit evaluation only, was reported as shown in Table I.

Table I: Characterisation and torrefaction experimental results: Sever temperature regime

Feedstock [-]	Temp [^{O}C]	Time [Min]	HHV C+ RB [MJ/kg]	HHV C + TB [MJ/kg]	Solid Yield [%]	Energy Yield [%]	E.F [-]
			Mixing Ratio: 50:50				
Coal + SCB	300	45	18.72	25.83	54.15	74.73	1.38
Coal + CC	300	45	18.01	24.31	56.68	76.52	1.35
Coal + PSD	300	45	20.05	28.27	52.44	73.94	1.41
			Mixing Ratio: 71:29				
Coal + SCB	300	45	18.65	24.991	62.71	84.03	1.34
Coal + CC	300	45	18.36	24.24	65.28	86.17	1.32
Coal + PSD	300	45	19.18	26.08	59.45	80.85	1.36
			Mixing Ratio: 50:50				
Coal + SCB	300	30	18.67	23.52	76.22	96.04	1.26
Coal + CC	300	30	18.26	22.64	78.55	97.4	1.24
Coal + PSD	300	30	19.44	25.47	74.18	97.18	1.31
			Mixing Ratio: 80:20				
Coal + SCB	300	60	18.67	24.46	69.34	90.84	1.31
Coal + CC	300	60	18.26	23.37	73.15	93.63	1.28
Coal + PSD	300	60	19.44	25.86	66.14	87.97	1.33

E.F: Enhancement Factor; SCB: Sugarcane Bagasse; CC: Corn Cob; PSD: Pine Saw- Dust; C: Coal; RB: Raw Biomass; TB: Torrefied Biomass; Temp: Temperature.

The results in Table 1 were used to determine the feed-rate and annual feedstock requirements of the power plant, from which the profit earned in the plant, were assessed using the NPV and PBP model calculations adopted from Ozonoh et al [4].

The PBP was employed to estimate the time taken to recover the costs invested on the project, while the NPV was used to evaluate the value of money with respect to the cash flows for the term under consideration. This determines the actual profit. Table 2 is the profit made from term A to term D using WFC at coal-to-biomass ratio of 50:50. From Table 2, it took around 3 - 4 months for the venture to payback the cost invested in it. Also,

the results of the NPV indicated that the four terms (A – D) studied were viable. Table 3 represents the profit made in the plant for term A to term D using WOFC at coal-to-biomass ratio of 50:50. From Table 3, it can be seen that the capital cost investment for the project was recovered at the first month of each of the evaluation year, as against the WFC that took 3 – 4 months. The results of the NPV equally affirmed the viability of the business for all the terms investigated.

Table II: Profit earning for term A – term D using WFC: 50:50

Feedstock	Investment Cost [USD/Yr.]	Profit Earning [USD/Yr.]	PBP [Yr.]	NPV [USD/Yr.]	Investment Term
Coal + SCB	2241396.554	6707174.875	0.3	4146389.042	
Coal + CC	2368526.508	6580044.921	0.4	3898182.94	1st
Coal + PSD	1894906.501	7053664.928	0.3	4822869.621	
Coal + SCB	2241396.554	6707174.875	0.3	3013850.464	
Coal + CC	2368526.508	6580044.921	0.4	2787110.864	5th
Coal + PSD	1894906.501	7053664.928	0.3	3631824.54	
Coal + SCB	2241396.554	6707174.875	0.3	1876226.996	
Coal + CC	2368526.508	6580044.921	0.4	1671050.278	10th
Coal + PSD	1894906.501	7053664.928	0.3	2435431.885	
Coal + SCB	2241396.554	6707174.875	0.3	984869.2414	
Coal + CC	2368526.508	6580044.921	0.4	796587.605	15th
Coal + PSD	1894906.501	7053664.928	0.3	1498026.934	
Coal + SCB	2241396.554	6707174.875	0.3	286467.1171	
Coal + CC	2368526.508	6580044.921	0.4	111423.2193	20th
Coal + PSD	1894906.501	7053664.928	0.3	763545.6264	

PBP: Payback Period; NPV: Net Present Value; WOFC: Without Feedstock Costing; CC: Corn Cob; SCB: Sugarcane Bagasse; PSD: Pine Sawdust; USD: United State Dollars; USD1.00 = ZAR14.00; ZAR: South African Rand.

Table III: Profit earning for term A – term D using WOFC: 50:50

Feedstock [-]	Investment Cost [USD/Yr.]	Profit Earning [USD/Yr.]	PBP [Yr.]	NPV [USD/Yr.]	Investment Term
Coal + SCB	1011134.62	7937436.81	0.1	6548329.01	
Coal + CC	1063550.30	7885021.14	0.1	6445993.64	1st
Coal + PSD	902582.03	8045989.40	0.1	6760265.02	
Coal + SCB	1011134.62	7937436.81	0.1	5208054.82	
Coal + CC	1063550.30	7885021.14	0.1	5114570.09	5th
Coal + PSD	902582.03	8045989.40	0.1	5401661.20	
Coal + SCB	1011134.62	7937436.81	0.1	3861763.04	
Coal + CC	1063550.30	7885021.14	0.1	3777168.68	10th
Coal + PSD	902582.03	8045989.40	0.1	4036957.50	
Coal + SCB	1011134.62	7937436.81	0.1	2806908.20	
Coal + CC	1063550.30	7885021.14	0.1	2729279.69	15th
Coal + PSD	902582.03	8045989.40	0.1	2967676.44	
Coal + SCB	1011134.62	7937436.81	0.1	1980401.84	
Coal + CC	1063550.30	7885021.14	0.1	1908231.24	20th
Coal + PSD	902582.03	8043170.36	0.1	2129866.75	

PBP: Payback Period; NPV: Net Present Value; WOFC: Without Feedstock Costing; CC: Corn Cob; SCB: Sugarcane Bagasse; PSD: Pine Sawdust; USD: United State Dollars; USD1.00 = ZAR14.00; ZAR: South African Rand.
As evidenced in Table 2, it took a longer time to recover the money invested in the business WFC than WOFC. It was attributed to the logistics cost (e.g. loading & transportation) associated with the WFC estimations. However, the two financial cases (WFC & WOFC) were profitable for the terms studied.
The profits earned at the end of the 20th year of term D using coal-to-biomass blend ratio of 71:29 and 80:20, WFC and WOFC, respectively are presented in Table 4. From Table 4, it took between 4 to 6 months to recover all the money invested in the business, WFC, while only 1-month was taken to recover the investment cost, WOFC. It can be seen from Table 4 as well, that a profit of between USD5, 902,292.46 – USD6, 489,659.30 was earned. That is quite a huge sum of money, but from the future value of money point of view, the entire profit had been eroded as shown in the results of the NPV. The implication is that the project is not worth pursuing. In comparison with the result of profits earned WOFC, the venture is more attractive based on the values of the NPV.

Table IV: Profit evaluation at the end of the 20th Year (Term D): WFC & WOFC

Feedstock [-]	Blend Ratio	Amount of Fuel [Ton/Yr.]	Investment cost [USD/Yr.]	Profit Earning [USD/Yr.]	PBP [Yr.]	NPV [USD/Yr.]
Coal + SCB		32,772.36	2718795.293	6229776.136	0.4	-370858
Coal + CC	71:29*	33,870.67	2664813.056	6283758.372	0.4	-296531
Coal + PSD		30,861.39	2458912.131	6489659.298	0.4	-130278
Coal + SCB		34,775.45	3258807.765	5689763.664	0.6	-234214
Coal + CC	80:20*	35,620.73	3343147.834	5605423.595	0.6	-1230523
		33,267.94	3046278.973	5902292.456	0.5	-821767
Coal + SCB		32,772.36	1114260.366	7834311.064	0.1	1838409
Coal + CC	71:29**	33,870.67	1151602.629	7796968.8	0.1	1786993
Coal + PSD		30,861.39	1049287.269	7899284.157	0.1	1927870
Coal + SCB		34,775.45	1112814.518	7835756.907	0.1	1840400
Coal + CC	80:20**	35,620.73	1139863.306	7808708.121	0.1	1803157
Coal + PSD		33,267.94	1064573.99	7883997.436	0.1	1906822

WFC: With Feedstock Costing; **: WOFC: Without Feedstock Costing; CC: Corn Cob; SCB: Sugarcane Bagasse; PSD: Pine Sawdust. ZAR: South African Rand; PBP: Payback Period; NPV: Net Present Value; USD: United State Dollars; USD1.00 = ZAR14.00; ZAR: South African Rand.
The influence of TVM on profit earning for the four investment terms were carried out using Coal + SCB, Coal + CC and Coal + PSD, but only Coal + PSD and Coal + CC results are reported in this paper because they represented the highest and lowest profits earned in the power plant for the considered investment period, respectively. The profits made from Coal + PSD and Coal + CC decreased with an increase in time (investment period) and it is displayed in percentage basis in Figure 1a and Figure 1b, respectively. The results have shown that the reduction in the profit earned in the plant increased from 1st – 5th (term A) through 15th – 20th (term D) year by around 14.09 - 32.48 % and 16.62 - 75.46 %, respectively. The higher the percentage, the lower the profits based on the NPV. This can be well understood by examining the values of the NPV of each of the terms in Table 1, and not the actual amounts of profits. It has revealed the effect of TVM on the overall investment and profit. Meanwhile, the result could offer substantive information that will assist investors and stake-holders in the area in decision making.

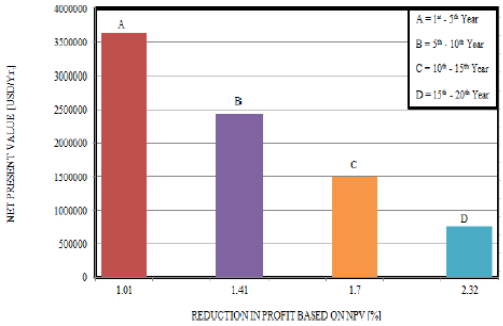


Figure 1a: Profit reduction profile for Coal + PSD: 1st – 5th through 15th – 20th Year

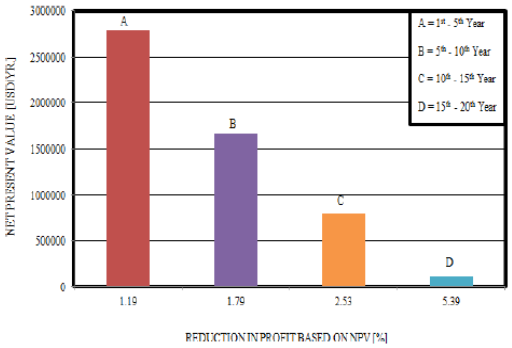


Figure 1b: Profit reduction profile for Coal + CC: 1st –5th through 15th – 20th Year

Effect of blend ratio on the amount of profit earned was evaluated at the 15th year (in term C) using coal-to- biomass ratios of 71:29 and 80:20 are shown in Figure 2a and Figure 2b, respectively. From Figure 2a, all the feedstocks used for the power production were very promising based on the values of the NPV, but the highest profit was made from Coal + PSD. The result is expected considering the heating value and other characteristics of the fuel (Table 1). From Figure 2b, it
can be observed that the NPV of Coal + CC and Coal + PSD were negative. The implication is that the investment costs were not recovered, hence; investors should not consider the blend ratio as a feasible option. A similar trend of result was observed in our previous work where we carried out the techno-economic analysis of blends of coal and un-treated (raw) biomass, and waste-tyre in a 5-MW CHP plant (Ozonoh et al [4].

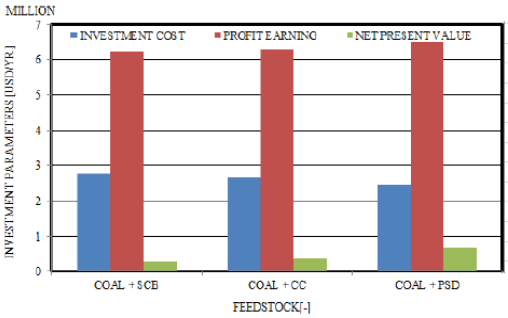


Figure 2a: Influence of blend ratio on profit earning: Blend ratio: [71:29]

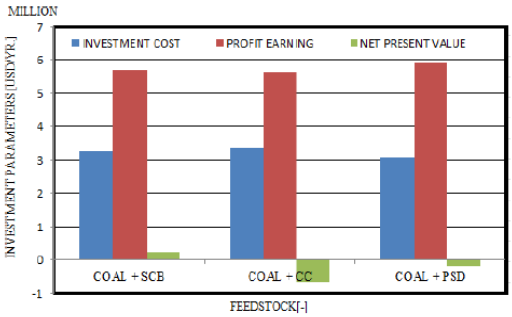


Figure 2b: Influence of blend ratio on profit earning: Blend ratio: [80:20]

The sensitivity analysis of the profit maximization in the plant was carried out using WFC in the 20th year of term D. Table 5a highlights the standard deviation, standard error, and variance of the investment parameters (Annual feedstock Requirement (AFR), Investment Cost (IC), Profit Earning (PE) and Net Present Value (NPV)). Table 5b also, describes the mean and Relative Standard Error (RSE) of the investment parameters. It can be seen that the profits decreased as the mean of the investment cost (IC) increased. This increase equally affected the annual feedstock requirement and the NPV, respectively. The increase in the amount of feedstock increased the investment cost, as well. It is evidenced in the negative values of the NPV for 71:29 and 80:20 coal-to-biomass blend ratios. Similarly, the increase in the blend ratio increased the annual amount of feedstock required and cost of investment in the plant, thus; resulted to reduction in the profits earned. Based on the aforementioned facts, the two most influential parameters affecting the profit are the investment cost (IC) and blend ratio. Following them is the annual feedstock requirement (AFR) that is dependent on the blend ratio, and all these investment parameters determined the NPV.

Table Va: Sensitivity analysis at 20th year, WFC

Annual Feedstock Requirement [Ton/Yr.]			Investment Cost [USD/Yr.]			Ratio
X	$\bar{X}$	$(X-\bar{X})^2$	X	$\bar{X}$	$(X-\bar{X})^2$	
28,889.56*	28,354.92	2.85837E+11	2,241,396.554	2,168,276.52	7.49E+10	
30,387.15**	28,354.92	4.12995E+12	2,368,526.508	2,168,276.52	5.61E+11	
25,788.058***	28,354.92	6.5888E+12	1,894,906.501	2,168,276.52	1.05E+12	
Variance	5.50229E+12		Variance	8.41E+11		
Std. Deviation	2,345,696.61		Std. Deviation	2.45E+05		
Standard Error	1,172,848.31		Standard Error	1.23E+05		
Profit Earning [USD/Yr.]			Net Present Value [USD/Yr.]			
6,707,174.875*	6,780,294.91	7.49E+10	2,864,671.17	387,145.32	1.42E+11	1:1
6,580,044.921**	6,780,294.91	5.61E+11	1,114,232.19	387,145.32	1.06E+12	
7,053,664.928***	6,780,294.91	1.05E+12	763,545.63	387,145.32	1.98E+12	
Variance	8.41E+11		Variance	1.59E+12		
Std. Deviation	2.45E+05		Std. Deviation	3.38E+05		
Standard Error	1.23E+05		Standard Error	1.69E+05		

*: Coal + SCB; **: Coal + CC; ***: Coal + PSD; X: Estimated variable (e.g. Annual feed Requirement, Investment Cost, cash flow, Net Present Value); $\bar{X}$: mean of the variable; Std.: standard; USD: United State Dollars; USD1.00 = ZAR14.00; ZAR: South African Rand.

Table Vb: Mean NPV and RSE of the investment parameters at 20th Year using WFC

Blend	Annual Feed Requirement		Investment Cost		Profit Earning		Net Present Value	
Ratio	Mean AFR [Ton/Yr.]	RSE of AFR [%]	Mean IC [USD/Yr.]	RSE of IC [%]	Mean PE [USD/Yr.]	RSE of PE [%]	Mean NPV [USD/Yr.]	RSE of NPV [%]
50:50	28,354.92	0.04	2,168,277.00	0.06	6,780,294.91	0.02	387,145.30	0.44
79:21	32,501.47	0.02	2,614,173.00	0.03	6,334,397.94	0.01	-226,806.00	-0.42
80:20	34,554.71	0.02	3,258,808.00	0.02	5,732,493.24	0.01	-606,025.00	-0.62

RSE: Relative standard error; AFR: Annual Feedstock Requirement; IC: Investment Cost; PE: Profit Earning; NPV: Net Present Value; USD: United State Dollars; USD1.00 = ZAR14.00; ZAR: South African Rand.

The current work is compared with the literature with respect to the feedstock used, torrefaction process experimental conditions, economic assessment and type of energy plant used. Retizelas & Li [17] investigated the environment emissions and economic benefits of using 100 % biomass (palm kernel shell) and 50:50 coal-to- biomass ratio. The authors found that co-gasification of biomass and coal has marginal profit when compared to 100 % biomass gasification having higher profit because of price of coal. Prando et al [18] used multi-stage modelling technique of a chemical equilibrium model to simulate the energy efficiency due to biomass torrefaction employing a CHP plant, internal combustion engine and gas turbine. The energy efficiency in the plants was enhanced because of torrefaction. Ozonoh et al [4] studied the profits made from a 5-MW CHP plant using mixture of coal and raw biomass, but torrefied biomass was not used to carry out the evaluation as against the current paper. Caputo et al [19] and Bridgwater et al [20] compared the feasibility of power production in power plant with 5-MW capacity using three different energy conversion processes. They assessed the operating efficiency of the plant employing different biomass types, while Malek et al [18] used some selected biomass to investigate the emissions, profits, and the viability of the feedstock for a 10-MW capacity CHP. This paper examined the profits earned from 10-MW CHP plant, percentage reduction in profits earned over investment terms, and effects of blend ratio on the profits for 20-year-investment period. The fuel used in this work was coal mixed with torrefied biomass.

A comparison of this study and literature is presented in Table 6. From Table 6, Starfelt et al [21] stated that integrating a torrefaction unit into an existing CHP plant was attractive and that using torrefied biomass materials and coal as feedstock was profitable, while the techno-economic model result employed by De & Assadi [22] revealed that the electricity cost per unit emission of CO_2 decreased significantly with increasing plant capacity (15 – 50 MW) and that the reduction in CO_2 emission was due to use of torrefied. Selected biomass materials and torrefied biomass mixed with coal were used by Malek et al [16] and Kohl et al [23] to study the profit and emissions and performance efficiency of a CHP plant respectively. Malek and his co-workers affirmed that palm-kernel empty fruit bunch was the most viable feedstock studied and there was reduction in gas emission and higher profit in the plant when compared to the existing energy mix, but the result of the investigation of Kohl and his research group have shown that the amount of heat generated in the plant for district heat supplies increased from 22 – 38 %. Both Ozonoh et al [4)] and

Prando et al [18} studied the profitability and energy conversion efficiency of a 5-MW and 10-MW CHP employing raw coal and biomass as fuels, respectively. It was observed by [4] that Coal + PSD and coal-to-solid waste ratio of 1:1 were the optimum feedstock and blend ratio respectively, and the amount of gases emitted were very low when compared to solitary gasification of coal.

Similarly, there was an enhancement in the energy efficiency of the plant according to Prando et al [18]. Retizelas & Li [17] examined the profitability of a CHP using Coal and biomass as fuel and confirmed that co-gasification of biomass and coal produced marginal profit when compared to 100 % use of biomass as fuel in the plant. Particularly, the difference between this study and the literature discussed above are based on the parameters, feedstock, and investment period studied. The profit earned in a 10-MW CHP with respect to 20- year-investment period that was grouped into 4 investment terms was investigated in this article. Secondly, the profitability of using torrefied biomass in the plant and the percentage increase in profit reduction due to TVM were estimated for each of the terms. Furthermore, a un-certainty analysis was carried out and it revealed that the investment cost and blend ratio were the most sensitive parameter that affected the profit. However, blend of coal and torrefied biomass was used as feedstock.

4 CONCLUSIONS

Investigation of profitability of a co-gasification CHP plant through biomass torrefaction for a 20-year- investment period has been carried out and reported in this article. Blends of Coal + SCB, Coal + CC, and Coal + PSD with coal-to-biomass ratio of 50:50, 71:29, and 80:20, respectively were used in the study. Four investment terms – A (1^{st} – 5^{th}), B (5^{th} – 10^{th}), C (10^{th} – 15^{th}) & D (15^{th} – 20^{th}) and two operational cost models; with feedstock costing (WFC) and without feedstock costing (WOFC) was employed. The following conclusions were reached:

Table VI: Comparison of this work and literature

Feedstock	Plant	Parameters Estimated	Findings	Reference
Coal & torrefied biomass.	CHP	Profitability & Performance efficiency of the plant	Very attractive integrating and using torrefied biomass in an existing CHP for power generation	Starfelt et al., 2015
Coal & raw biomass	CHP electricity	CO_2 Emissions & Cost of	Techno-economic model indicated that electricity cost per unit emission of CO_2 decreased significantly with increasing plant capacity (15 – 50 MW). There was reduction in CO_2 emission due to use of torrefied biomass	De & Assadi, 2009
Coal & torrefied biomass	CHP & Pyrolysis power plant	Plants performance efficiency	A considerable increase in the district heat output as well as number of operating hours (22 – 38 %) of the plant was observed	Kohl et al., 2013
Selected biomass materials	CHP (10-MW)	Profits & Emissions	Palm-kernel empty fruit bunch was the most viable feedstock studied. Gas emission was reduced compared to the existing energy mix. Profitability in the plant was also improved	Malek et al., 2017
Coal & raw biomass	CHP (5-MW)	Profitability: Energy, Economic, & Environmental	Coal + PSD was the most viable feedstock, while Coal-to-solid waste ratio of 1:1 was the optimum ratio in terms of profitability in the plant Emission reduction was enhanced due to the use of blends of raw biomass and coal as against solitary coal gasification.	Ozonoh et al., 2018
Coal & biomass enhanced due to biomass torrefaction	CHP	Energy efficiency	The energy efficiency of the CHP plant was	Prando et al., 2014
Coal & biomass profit when compared to 100 % biomass gasification having higher profit because of price of coal.	CHP	Plant profitability	Co-gasification of biomass and coal has marginal	Retizeler et al., 2016
Coal & torrefied biomass	CHP (10-MW)	Plant profitability, percentage reduction in profit with time	Profitability in the plant was enhanced due to the use of torrefied biomass materials. The percentage reduction in the profit increased with an increase in the investment time because of TVM. Coal+PSD was the most viable feedstock and investment cost and blend ratio were the two most influential variables that affected the profit	This Study

TVM: Time Value of Money; CHP: Combined Heat and Power; PSD: Pine Sawdust.

- At the end of term D (i.e. 20th year), a profit of between USD5,902,292.46 - USD6,489,659.30 and USD7,796,968.80 - USD7,899,284.16 were earned using WFC and WOFC, respectively, but the profits earned from WFC were eroded due TVM, hence; rendered the investment un-attractive.
- The percentage reduction in profits increased from term A through term D by around 1.01 – 2.32 % and 1.19 – 5.39 % using WFC and WOFC. Implying that profitability in the plant is dependent on the future value of money.
- At 15th year (within term C), the NPV of Coal + CC and Coal + PSD were negative for Coal-to-biomass ratio of 80:20, indicating that the business was not lucrative, thus; investors are advised not to consider the blend ratio.
- The investment cost and blend ratio were the two most influential variables that affected the profit

Despite that not all the feedstocks remained profitable for the four investment terms and two operational cost models due to TVM, the fuels are viable for power generation in a co-gasification CHP plant. This study has shown that there is potential in using torrefied biomass for maximization of profit in the CHP plant. Therefore, information documented in this study could be instrumental to guiding decision making by engineers and stakeholders in energy sectors.

5 REFERENCES

[1] I.E.A, IRENA. Biomass Co-firing: Technology Brief. IEA-ETSAP (International Energy Agency – Energy Technology Systems Analysis Program) and IRENA (International Renewable Energy Agency) Technology Brief E21, (2013).

[2] L.J.R., Nunes, J.C.O. Mtias, J.P.S. Catalao. A review on torrefied biomass pellets as a sustainable alternative to coal in power generation, (2014), Pag.153 – 160.

[3] S.O. Bada, E.M.S. Falcon, L.M., C.P. Bergmann. Co-firing potential of raw and thermally treated Phyllo stachys aurea bamboo with coal, (2016), Pag.1345-1354.

[4] M. Ozonoh, T.C. Aniokete, B.O. Oboirien, M.O. Daramola. Techno-economic analysis of electricity and heat production by co-gasification of coal, biomass and waste tyre in South Africa., (2018), Pag.192-206.

[5] N. Kongkeaw, S. Patumsawad. Thermal upgrading of biomass as a fuel by torrefaction, (2011), Pag.38-42.

[6] W.H. Chen, J. Peng, X.Y. Bi. A state-of-the-art review of biomass torrefaction, densification and applications, (2015), Pag.847 – 866.

[7] J.H. Peng, X.T. Bi, S. Sokhansanj, C.J. Lim. Torrefaction and densification of different species of softwood residues, (2013), Pag.411 – 421.

[8] S.W. Park, C.H. Jang, K.R. Baek, J.K. Yang. Torrefaction and low-temperature carbonization of woody biomass: evaluation of fuel characteristics of the products, (2012), Pag.676 – 685.

[9] W.H. Chen, W.Y. Cheng, K.M. Lu, Huang, Y.P. Huang. An evaluation on improvement of pulverized biomass property for solid fuel through torrefaction, (2012), Pag.3636 –3644.

[10] K.M. Lu, W.J. Lee, Chen, W.H, S.H. Liu, T.C. Lin. Torrefaction and low temperature carbonization of oil palm fiber and eucalyptus in nitrogen and air atmospheres, (2012), Pag.98 – 100.

[11] W. Yan, T.C. Acharjee, C.J. Coronella, V.R. Vasquez. Thermal pretreatment of lignocellulosic biomass, (2009), Pag.35 – 40.

[12] B. Arias, C. Pevida, J. Fermoso, M.G. Plaza, F. Rubiera, J.J. Pis. Influence of torrefaction on the grindabilty and reactivity of woody biomass, (2008), Pag.169 – 175.

[13] M. Phanphanich, S. Mani. Impact of torrefaction on the grindabilty and fuel characteristics of forest biomass, (2007), Pag.1246 – 1253.

[14] W.J. Hall. Assessment of carbon dioxide emissions reductions achievable by using torrefaction, (2012), Pag.103 – 113.

[15] B. Batidzirai, A.P. Mignot, W.B. Schakel, H.M. Junginger, A.P. Faaij. Biomass torre-faction technology: techno-economic status and future prospects. Energy, (2013), Pag.196 – 214.

[16] A.A.B.M. Malek, M. Hasanuzzaman, N.S. Rahim, Y.A.A. Turki. Techno-economic analysis and environmental impact assessment of a 10 MW biomass-based power plant in Malaysia, (2017), Pag.502 – 513.

[17] A.A. Rentizelas, J. Li. Techno-economic and carbon emissions analysis of biomass torrefaction downstream in international bioenergy supply chains for co-firing, (2016), Pag.129 – 142.
[18] D. Prando, F. Patuzzi, P. Baggio, M. Baratieri. CHP Gasification Systems Fed by Torrefied Biomass: Assessment of the Energy Performance, (2014), Pag.147 – 155.
[19] A.C. Caputo, M. Palumbo, P.M. Pelaggage, F. Scacchia. Economics of biomass energy utilization in combustion and gasification plants: effects on logistic variables, (2005), Pag.35-51.
[20] A.V. Bridgwater, A.J. Toft, J.G. Brammer. A techno-economic comparison of power production by biomass fast pyrolysis with gasification and combustion, (2002), Pag.181-248.
[21] F. Starfelt, E. T. Aparicio, H. Li, E. Dotzauer. Integration of torrefaction in CHP plant – A case study, (2015), Pag.427-435.
[22] S. De, M. Assadi. Impact of co-firing biomass with coal in power plants: techno-economic assessment, (2009), Pag.283 – 293.
[23] T. Kohl, T. Laukkanen, M. Jarvinen, C.J. Fogelholm Energetic and Environmental Performance of three biomass upgrading processes integrated with a CHP plant, (2013) Pag.124 – 134.

6 ACKNOWLEDGEMENT

Ozonoh acknowledges the financial and moral support of Mr. Nonye Ozonoh & Mrs. Angela Ozonoh in this work.

Chemical Data Collections 25 (2020) 100321

Contents lists available at ScienceDirect

Chemical Data Collections

Data Article

Dataset from estimation of gasification system efficiency using artificial neural network technique

M. Ozonoh [a], B.O. Oboirien [b], A. Higginson [a], M.O. Daramola [a,*]

[a] School of Chemical and Metallurgical Engineering, Faculty of Engineering and the Built Environment, University of the Witwatersrand, Wits 2050, Johannesburg, South Africa
[b] Department of Chemical Engineering, University of Johannesburg, Doornfontein Johannesburg 2028, South Africa

a r t i c l e i n f o

Article history:
Received 12 August 2019
Revised 19 November 2019
Accepted 10 December 2019
Available online 12 December 2019

Keywords:
Artificial neural network
Coal and biomass
Energy conversion
Gasification efficiency
Performance evaluation

a b s t r a c t

The dataset contained in this article supplements the data information contained in the performance evaluation of gasification system efficiency using artificial neural network technique. The dataset was obtained from investigating efficiency of a gasification system using 315 fuel samples containing biomass, coal, and coal-biomass blends via the application of Levenberg–Marquardt (LM) back-propagation and Bayesian Regularization (BR) training algorithms in Artificial Neural Networks (ANN) domain. Input Variables Representation Technique-by-Visual Inspection method (IVRT-VIM) and Output Variables Representation Technique –by-Visual Inspection Method (OVRT-VIM) were developed as well to improve results from the ANN models. Sensitivity analysis on the prediction of the product gas compositions (CO, CO_2, H_2, and CH_4) was carried out using partial derivatives (PaD) method. There was a considerable decrease in the MSE and an increase in the R^2 of around 93 – 96% and 94 – 96% using 10 & 23 number of neurons in the hidden layer and IVRT-VIM technique, respectively. The L-M algorithm offered a better result than the BR algorithm, and with Sulphur as the most important input variable that affected the outputs.

© 2019 Elsevier B.V. All rights reserved.

Specifications Table

Subject area	Gasification Systems and Artificial Intelligence
Compounds	-
Data category	Table, graph, figure
Data acquisition format	Literature: The proximate & ultimate analysis data of the fuel were obtained from biomass, coal and blends of biomass and coal, and different gasifiers (updraft, downdraft, fluidised bed and entrained bed). Thereafter, the dataset was grouped into input and output variables using micro-soft excel (2016), and finally trained the network employing an ANN model under MATLAB environment (2014 Model).
Data type	Raw experimental literature data analyzed & simulated.
Procedure	315 fuel samples obtained from biomass, coal, coal-biomass blends. The dataset is comprised of the compositional analysis (proximate and ultimate analysis) of the fuels, experimental process condition and performance indicators data; input variables. The dataset was used in a Multiple Input-Single Output (MISO) and Multiple Input-Multiple Output (MIMO) feedforward neural network layer of Levenberg Marquardt (LM) and Bayesian regularization (BR) algorithms to predict the outputs (cold gas efficiency (CGE), carbon conversion efficiency (CCE), lower heating value (LHV) and gas composition (e.g. CO, CO_2 , H_2 , and CH_4); output variables [1].
Data accessibility	Data is with this article

* Corresponding author.
E-mail address: michael.daramola@wits.ac.za (M.O. Daramola).

https://doi.org/10.1016/j.cdc.2019.100321
2405-8300/© 2019 Elsevier B.V. All rights reserved.

1. Rationale

Different energy production systems and sources are available around the globe for domestic and industrial purposes. Solid fuels such as biomass and coal are used in this aspect than others, probably because of their availabilities and energy contents [2]. Biomass materials are environmentally friendly, but it may produce some tars during its conversion. Similarly, coal has high energy content when compared to biomass, but it generates huge amount of emissions, while biomass is equally costly [3].

Combustion, gasification and pyrolysis processes can be used to convert the aforementioned solid fuels to energy, but gasification is more attractive than the other two aforementioned methods [4]. Therefore, the problems posed by the solitary utilization of biomass and coal as explained earlier may be addressed by co-gasification.

Importantly, the quality of the fuel is affected by its physio-chemical properties. Secondly, the fuel quality and the experimental process condition determines the product gas quality, yield and efficiency of the gasifier (e.g. cold gas efficiency, carbon conversion efficiency, lower heating value of gas, gas yield and composition (e.g. CO, CO_2, CH_4, H_2) [1].

To ensure that high performance efficiency is achieved in a gasifier, several experiments are required. Gasification experiments are capital intensive and time in-effective, resulting to drawbacks in the energy sector [1]. However, this problem could be overcome by using modelling tools (e.g. Aspen Plus, empirical models, General Algebraic Modelling System (GAMS), Artificial Neural Network). Levenberg Marquardt (LM) and Bayesian Regularization (RB) algorithms are the common methods, and in this case, a Multiple Input-Multiple Out-put (MIMO), Multiple Input-Single Output layer (MISO) network or both are investigated. Reports by a few researchers (e.g. Ref. [5,6]) have shown that an ANN model is a promising approach to evaluating the performance of a gasifier. However, the authors considered a specific type of gasifier and investigated a few experimental process conditions. For example, Baruah et al. [7] predicted major four gas compositions using the results from proximate analysis and experimental process conditions as the input variables. Their findings agreed with the results documented in literature, but the variables used by the authors were limited to only one type of gasifier and biomass. Furthermore, researchers like Puig-Arnavat et al. [8], George et al. [9], and Pandey et al. [10] carried out some experiments to predict gas yield & gas composition; gas composition and syngas yield; LHV of gas & LHV of the gasification products, respectively. In their studies, only MIMO neural network was examined via LM algorithm while the BR MISO layer network was not considered.

Against this background, the study, whose dataset is provided in this article, considered the use of an ANN model to test the efficiency of gasifiers by employing dataset obtained from different gasification systems, fuels (e.g. biomass and coal, and blends of biomass and coal) and experimental process conditions. By so doing, time and cost of experimentation could be saved. In addition, the approach facilitates the prediction of the performance efficiency of a gasifier using different operating conditions and fuels. Consequently, dataset, which will enable stake-holder to design gasifiers that can convert different solid fuels into energy, could be provided and accessible.

2. Procedure

The data used in this study comprised 315 fuel samples obtained from biomass, coal, and blends of coal and biomass. Information regarding their compositional analysis and performance indicators was obtained from the literature [11–42].

For the proximate analysis, the data used were ash content, moisture content (MC), and volatile matter (VM), while the ultimate analysis data include Carbon (C), hydrogen (H), nitrogen (N), oxygen (O), and Sulphur (S), and LHV. The equivalence ratio (ER) and reaction temperature (T) represented the experimental process data, and the gasification performance efficiency parameters were cold gas efficiency (CGE), carbon conversion efficiency (CCE), gas yield, lower heating value (LHV) of gas, and gas composition (e.g. CO, CO_2, CH_4, H_2). The aforementioned dataset was grouped into input and output variables as shown in Table 1 [1], and used in an artificial neural network under MATLAB environment to train a Multiple Input-Multiple Output (MIMO) and Multiple Input- Single Output (MISO) layer networks. The training steps have been described elsewhere [1].

For the estimation of the gasification performance, the cold gas efficiency (CGE), carbon conversion efficiency (CCE), gas yield (η_{Gas}), lower higher heating value of gas (LHV), and product gas composition were employed, and (excluding the gas composition) are used, and are expressed in Eqs. (1)–(5). Eq. (1) [37,38] and Eq. (2) [39,40] adn (3) [41], were employed for

Table 1
R^2 results from predicted gas composition: MISO BR algorithm.

Input variables	Regression co-efficient (R^2)			MSE	Epoch	Output Variable
	Training	Validation	Testing			
C, H, N, S, O, MC, Ash, T, VM, LHV, ER	0.74	0.73	0.65	33.75	4	CO [%]
C, H, N, S, O, MC, Ash, T, VM, LHV, ER	0.74	0.73	0.65	69.86	17	CO_2 [%]
C, H, N, S, O, MC, Ash, T, VM, LHV, ER	0.79	0.77	0.34	7.54	6	CH_4 [%]
C, H, N, S, O, MC, Ash, T, VM, LHV, ER	0.87	0.88	0.89	52.15	134	H_2 [%]

BR: Bayesian Regularization; ER: Equivalence Ratio; T: Reaction Temperature: VM: Volatile Matter; LHV: Lower Heating Value; MC: Moisture Content.

Table 2
R^2 results from predicted gas composition: MISO BR algorithm.

Input Variables	Regression co-efficient (R^2)			MSE	Epoch	Output Variable
	Training	Validation	Testing			
C, VM, T	0.87	0.89	0.90	24.21	6	CO [%]
C, VM, T	0.86	0.90	0.92	32.15	8	CO_2 [%]
C, VM, T	0.89	0.86	0.78	11.29	12	CH_4 [%]
C, VM,T	0.91	0.93	0.90	14.18	9	H_2 [%]

C: Carbon; VM: Volatile matter; T: Reaction temperature; MSE: Mean Square Error.

the calculation of the CGE and CCE, respectively, while Eq. (4) [42] and Eq. (5) [41,42] were used for the determination of the η_{Gas} and LHV of the gas, respectively. Detailed explanation of the gasification indicators is described in details in Ref. [1].

$$CGE = \frac{[Gas\ Yield(\eta_{Gas})]\ X\ LHV_{Syngas}}{[LHV_{Biomass}]} X\ 100 \quad (1)$$

$$CCE = \frac{[CO\% + CH_4 + CO_2\%]}{[22.4\ X\ C\%]} X\ 100 \quad (2)$$

$$CCE = \frac{12\eta_{Gas}[CO\% + CO_2\% + CH_4\%] + 2[C_2H_4\% + C_2H_6\%]}{[22.4\ X\ C\ \%]} X\ 100 \quad (3)$$

$$\eta_{Gas} = \frac{Q_{Syngas}}{M_{Biomass}} \quad (4)$$

$$LHV_{Gas} = 11.76\ X\ [V_{CO} + 11.882]X[V_{H_2} + 37.024]X[V_{CH_4}]X\ -\frac{10}{1000} \quad (5)$$

where, the gases CO, CO_2, CH_4, C_2H_4, and C_2H_6 are in% Vol., and C is in% of carbon in the dry feedstock from the ultimate analysis, and η_{Gas} is the gas yield. Note that Eq. (3) is used when the gas analysis involves C_2H_4, and C_2H_6.

Furthermore, Eqs. (6)–(9) was used for the ANN predictive model and data development (please see ref. [1] for detailed information). Eq. (6) [17, 43] and Eq. (7) [17, 43] describe the mode of operations of the activation functions and Tansigmoid function used in the study, respectively. Eq. (8) [43] and Eq. (9) [44] were used for the output neuron determination and network data minimization, respectively.

$$y_j = f_{Activation} \sum_{i=1} W_{ij}X_i + b_j \quad (6)$$

$$f_{Activation}(X) = \frac{1}{1 + e^{-x}} \quad (7)$$

$$\mu k = f_{Activation} \sum_{j=1} V_{jk}y_f + b_k \quad (8)$$

$$J^tJ + \mu I = J^t x\ E \quad (9)$$

where I is the identity matrix; m is the L-M training algorithm; E is the error vector (e.g. Mean Square Error (MSE)); J is the Jacobian matrix for the network, but the J^tJ can also be referred to as the approximated Hessian. The sensitivity analysis was carried out to determine the most influential input variable on the outputs using Eq. (10) through Eq. (17) as described in Ref. [1].

3. Data

The dataset provided in this article supplements the data contained in the recent publication [1], and it comprises 12 figures and 6 tables. Figs. 1–4 and Figs. 5–8 present the convergence characteristics of CO, CO_2, CH_4, and H_2 predictions and error histogram of CO, CO_2, CH_4, and H_2 predictions, respectively, using Levenberg Marquardt (LM) Multiple Input-Multiple Output (MIMO) layer artificial neural network (ANN). Tables 1 and 2 provide information about the coefficient of determination (R^2) obtained from BR MISO and BR MIMO network layer, respectively, for the gas composition (CO, CO_2, CH_4, and H_2). Tables 3 and 4 are the results of the improvement of the OVRT-VIM model and IVRT-VIM model, respectively, for the BR & LM and LM MIMO algorithms. The results in Table 3 were obtained using all the input variables investigated,

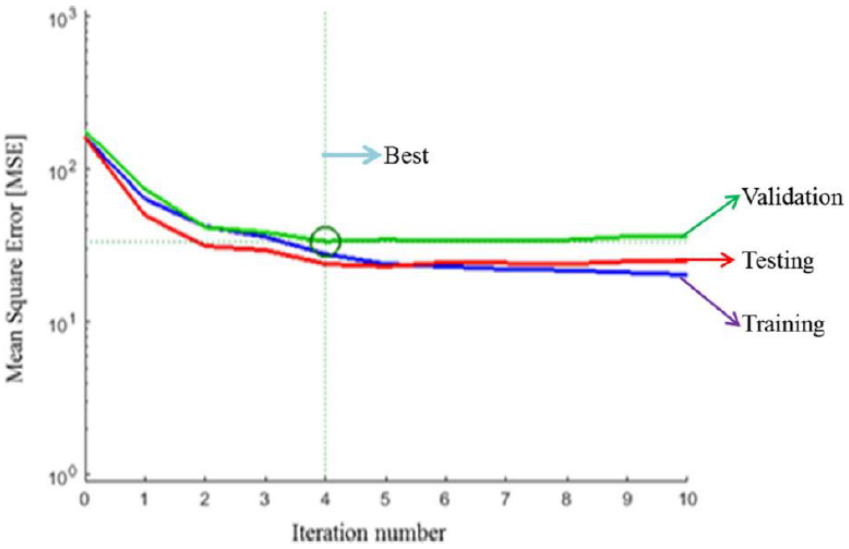


Fig. 1. Convergence characteristics of the MIMO layer network: CO prediction.

Table 3
BR and LM algorithm MIMO network results: OVRT-VIM model improvement.

Algorithm	Number of Neurons	MSE	Epoch	Training	Validation	Testing All*
WCH_4						
BR	10	16.45	6	0.91	–	0.90 0.87
L-M	10	11.27	12	0.93	0.94	0.92 0.93
$WOCH_4$						
BR	10	14.02	9	0.94	–	0.92 0.94
L-M	10	8.51	14	0.97	0.96	0.97 0.95
WCH4						
BR	23	9.24	4.00	0.92	–	0.90 0.88
L-M	23	7.06	7.00	0.95	0.93	0.94 0.93
$WOCH_4$						
BR	23	6.12	11.00	0.94	–	0.93 0.91
L-M	23	3.84	9.00	0.96	0.95	0.97 0.95

WCH_4: With Methane; $WOCH_4$: Without Methane; BR: Bayesian regularization; L–M: Levenberg Marquardt; MSE: Mean Square Error; OVRT-VIM: Output Variables Representation Technique-Visual Inspection Method; All*: All data exploited.

Table 4
Model improvement using IVRT-VIM: MIMO LM algorithm.

Inputs	Algorithm	Coefficient of determination (R^2)					
		Neurons	Training	Validation	Testing	All*	Outputs
C,VM, T	L-M	10	0.96	0.95	0.93	0.93	CO, CO_2 , H_2 , CH_4
		23	0.95	0.94	0.96	0.95	

L-M: Levenberg–Marquardt, C: Carbon; VM: Volatile Matter; T: Reaction Temperature; CO: Carbon monoxide; CO_2: Carbon dioxide; H_2: Hydrogen; CH4: Methane; All*: All data exploited.

while those of Table 4 were developed using C, VM, T input variables, only. Fig. 9–12 show the relative importance of the input variables (C, VM, & T) on the outputs (CO, CO_2, CH_4, and H_2). The code used for the neural network model development is contained in Appendix A1. It is noteworthy to emphasis that in this article, only the prediction of the product gas composition was considered. The evaluation of the other gasification performance indicators (e.g. cold gas efficiency, carbon conversion efficiency, gas yield and lower heating value of the gas) is detailed in Ozonoh et al. [1]. Additional data employed in the study are provided in Tables 5 and 6 in Appendix A and Appendix B.

From Figs. 1–4, the convergence characteristics of MIMO layer network employed for CO, CO_2, CH_4, and H_2 prediction were stable, implying the model offered a better fitting for the variables studied with respect to the dataset provided. In this case, the results for the fitting, validation and testing of the networks are detailed in Tables 1 and 2. From Figs. 5–8, the observed errors could vary based on the input and output variables considered, but the error may reduce significantly

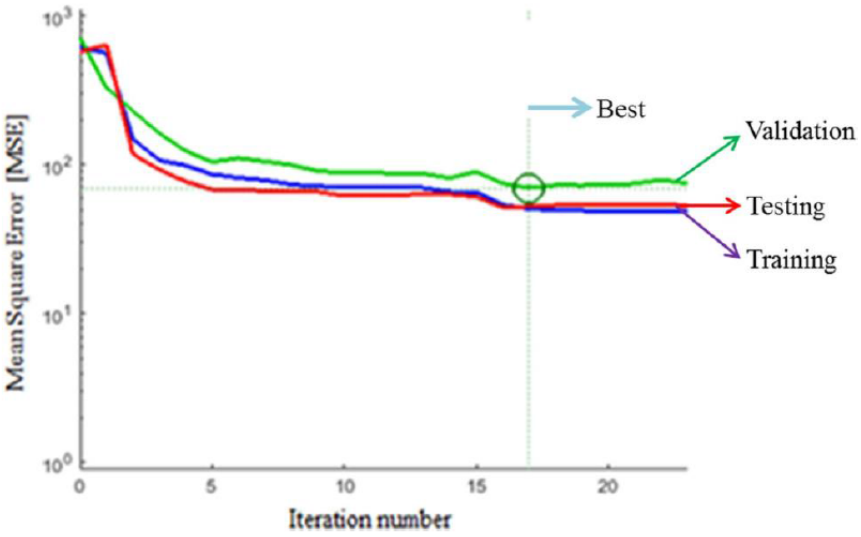


Fig. 2. Convergence characteristics of the MIMO layer network: CO_2 prediction.

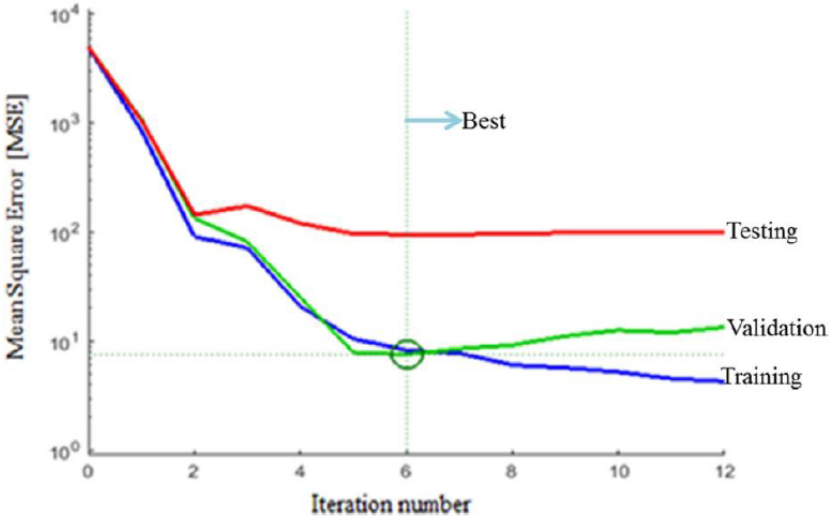


Fig. 3. Convergence characteristics of the MIMO layer network: CH_4 prediction.

by applying the IVRT-VIM and OVRT-VIM techniques as shown in Table 3 (for IVRT-VIM) and Table 4 (for OVRT-VIM). For the model improvement, methane (CH_4) for example (in case of OVRT-VIM) was excluded in some of the training to check model improvement. From Figs. 9–12, Sulphur is the most important input variable affecting the output, besides CH_4 that was mostly influenced by Nitrogen (N). Carbon(C) was expected to be the most important input variable affecting the outputs considering its relevance in the calorific value of fuels in agreement with the trend obtained for other indicators [1], but interestingly Sulphur appears to be the most important variable influencing the outputs. This could be attributed to the emission-producing role of elemental Sulphur in fuels/gas composition or to the nature of the dataset used in the prediction.

4. Data value and validation

41. Prediction of gas composition

Figs. 1–4 display the convergence characteristics of the Multiple Input-Multiple Output (MIMO) layer network for the predicted gas compositions. For the CO prediction (Fig. 1), the neural network learning involved 10 iterations whereby the

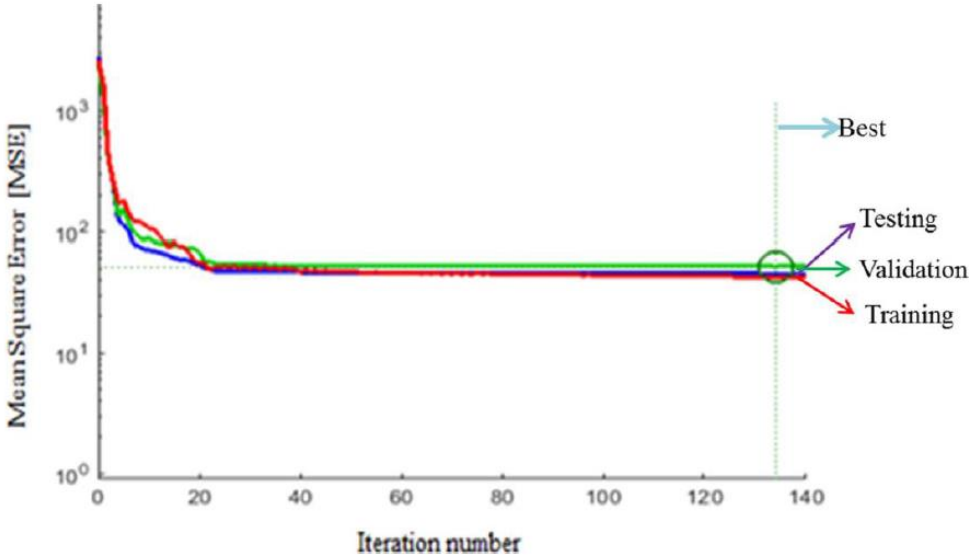


Fig. 4. Convergence characteristics of the MIMO layer network: H_2 prediction.

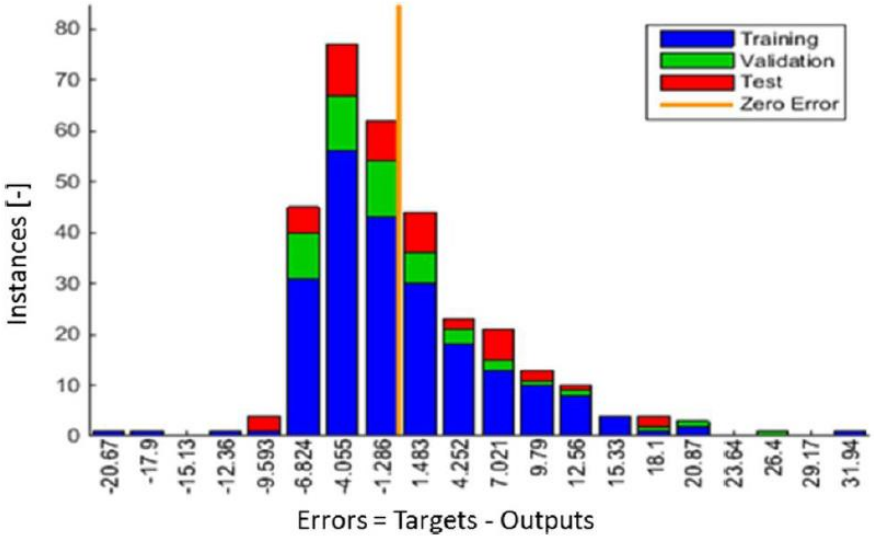


Fig. 5. Error histogram: MISO network layer for CO prediction.

best fitting was obtained at epoch 4. In this case, the convergence curves for the training, testing, and validation were stable, indicating that the model fitted well with dataset studied. Considering the convergence characteristics of the CO_2 estimation shown in Fig. 2, there was a considerable reduction in the MSE with strong stability of the fitting curves at around iteration 20, but the best model performance was achieved at epoch 17.

From Figs. 3 and 4, the MSE obtained are lower than that of Figs. 1 and 2, attributable to the dataset employed in the predictions. Similarly, the stability characteristics of the convergence curves perfect from the origin until around epoch 6 (Fig. 3) for training and validation curves, while the testing curve deviated from the fitting at epoch 2. The implication is that the model at this point, could not describe well the dataset employed for the testing. It can be seen from Fig. 4 that there is a strong stability amongst the fitting curves until epoch 139, indicating that the model describes the dataset very efficiently and it is very reliable for predicting the gas composition.

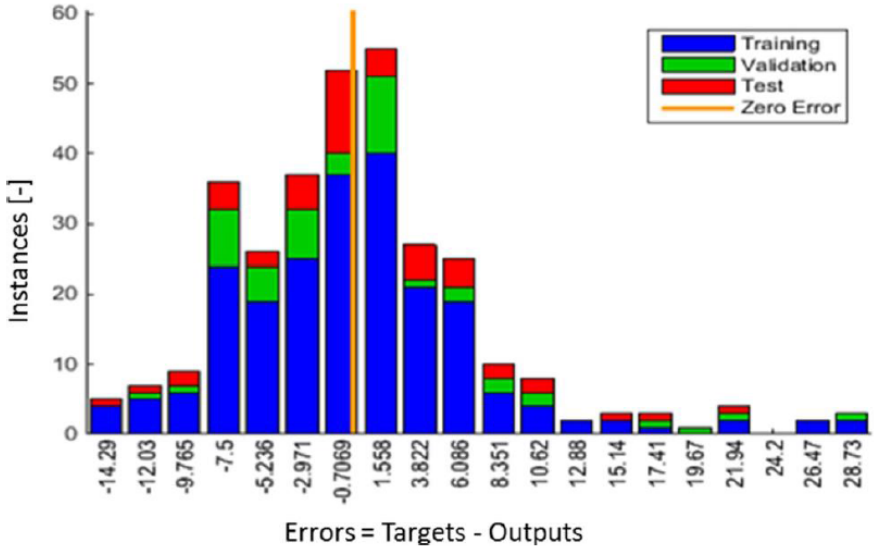


Fig. 6. Error histogram: MISO network layer for CO_2 prediction.

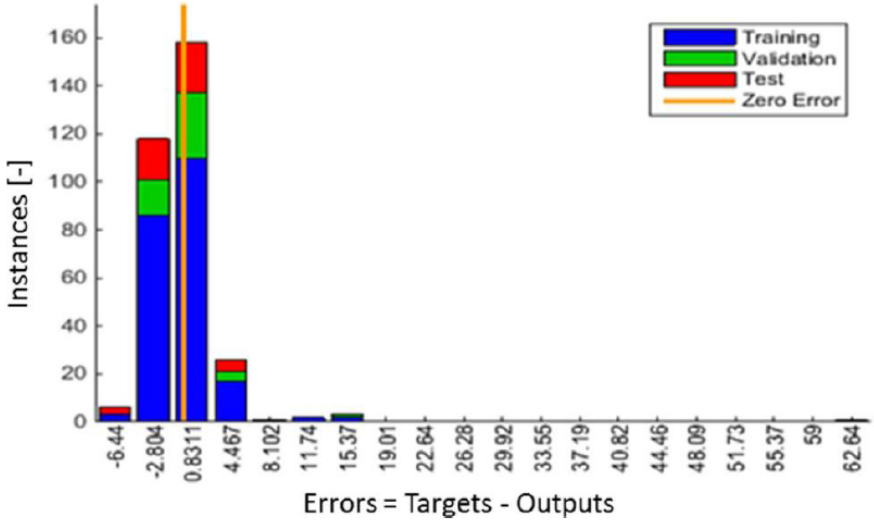


Fig. 7. Error histogram: MISO network layer for CH_4 prediction.

42. Prediction of gas compassion using Bayesian Regularization (BR) Algorithm

Tables 1 and 2 present the MISO layer networks for the Bayesian Regularization (BR) algorithms for the C, H, N, S, O, MC, Ash, T, VM, LHV, ER **and** C, VM, T as the inputs employed for the prediction of the gas compositions (CO, CO_2 , CH_4 , & H_2), respectively. It is very important to note that the MSE reported for Fig. 1 is considerably lower than those reported for Fig. 2. Similarly, the coefficient of determination of the fitting curves (training, validation and testing) reported in Table 2 is higher than that of Table 1.

From Table 3, it can be observed that there is a considerable improvement in the results when the IVRT-VIM was used for the optimization of the model result. A comparison of the Bayesian Regularization (BR) and Levenberg –Marquardt (L-M) was carried out using C, VM & T as the input variables to predict the gas compositions. In this case, two scenarios were considered: (i) with methane (WCH_4) and, (ii) without Methane ($WOCH_4$) using 10 & 23 number of neurons in the hidden layer, respectively. The results obtained from the L-M algorithm ($WOCH_4$ using 23 number of neurons in the hidden layer)

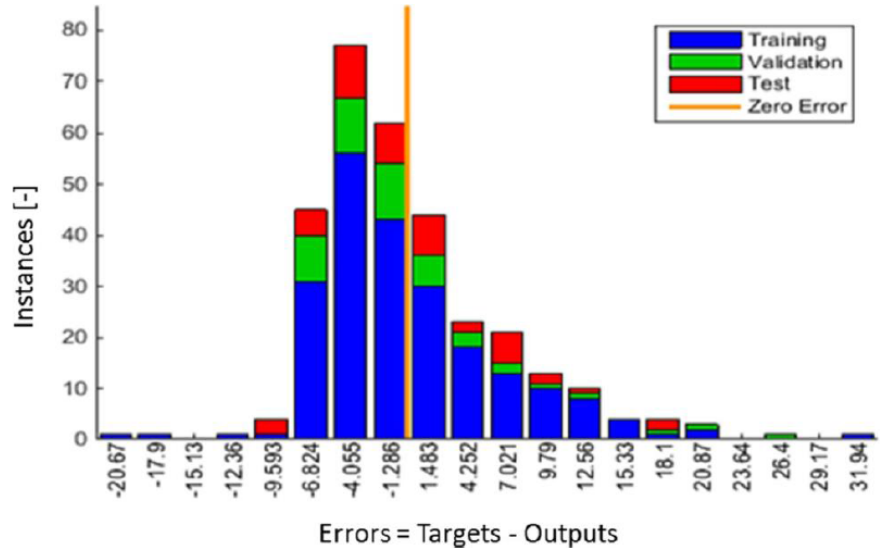


Fig. 8. Error histogram: MISO network layer for H_2 prediction.

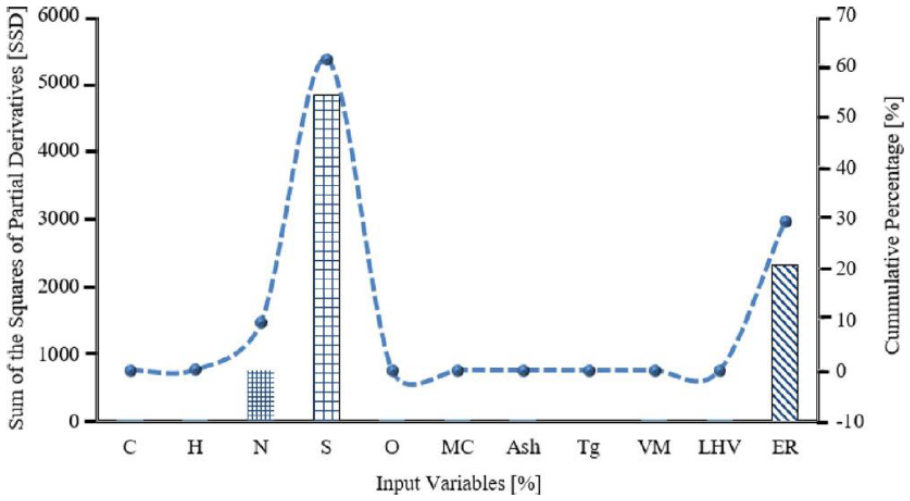


Fig. 9. Relative effect of each input variable on the output variable: CO [%]: MISO layer network: 21 hidden layer neurons.

were better than that of BR algorithm when the R^2 and MSE are considered. The implication is that the L-M algorithm is more reliable than the BR for the prediction of gas composition from coal + biomass materials studied.

43. Prediction of gas compassion using Levenberg–Marquardt (L–M) Algorithm

Table 4 depicts the summary of the results obtained from the L-M network employing 10 and 23 number of neurons in the hidden layer. In this case, the predictive modelling was carried out to evaluate the efficiency of the IVRT-VIM technique in enhancing the model results. The R^2 was in the range of 93 – 96% and 94 – 96% for 10 number of neurons & 23 number of neurons in the hidden layer, respectively. The results from L-M algorithm are better when compared to the results shown in Tables 1 and 2. Therefore, the use of the IVRT-VIM is effective for upgrading the model result.

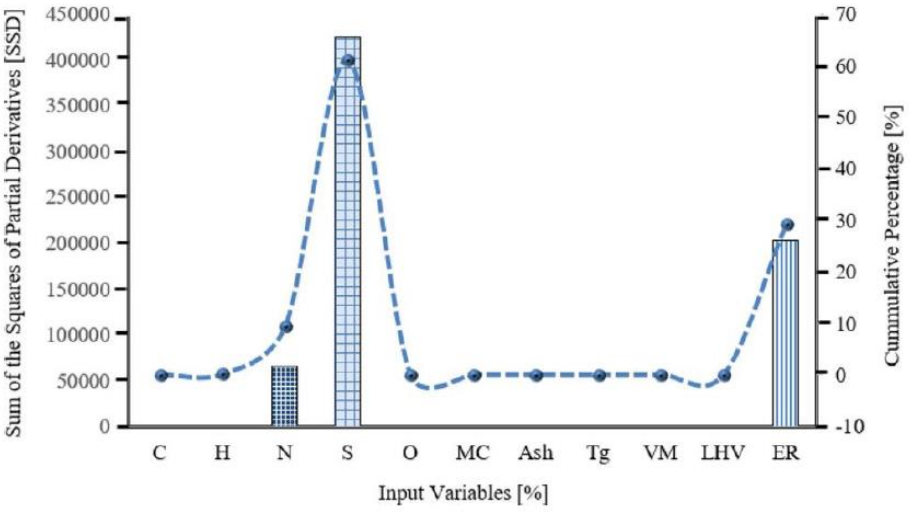


Fig. 10. Relative effect of each input variable on the output variable: CO_2 [%]: MISO layer network: 21 hidden layer neurons.

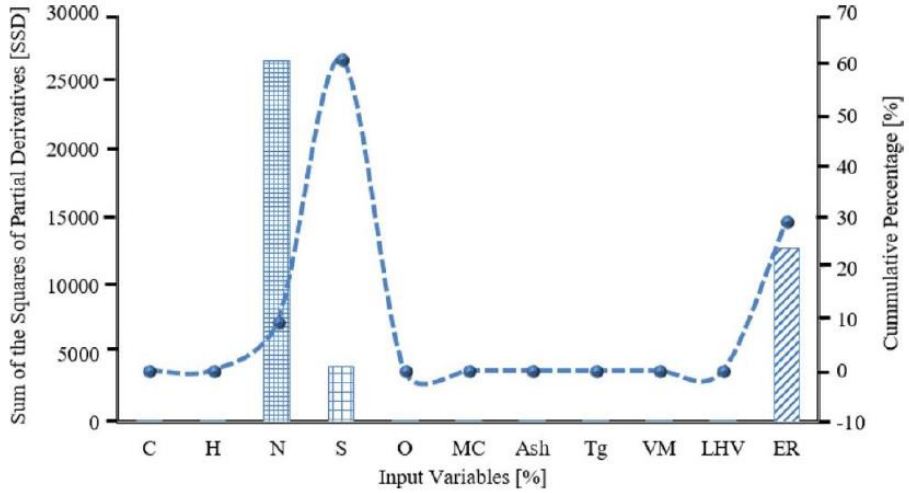


Fig. 11. Relative effect of each input variable on the output variable: CH_4 [%]: MISO layer network: 21 hidden layer neurons.

4.4. Overview of data value and validation

- Gasification experiment is capital intensive and time consuming, especially in evaluating the performance efficiency of the gasifier. Thus the information contained in this data article provides some data that could be instrumental to saving time and cost of experiments.
- A model which is effective for estimating efficiency of gasification units operated at different process conditions and using different fuels such as biomass, coal and their blends is hereby provided.
- Techniques, called Input Variables Representation Technique with Visual Inspection method (IVRT-VIM) and Output Variables Representation Technique with Visual Inspection Method (OVRT-VIM) accounting for the upgrade of the ANN model results, were developed in this data article.
- Data describing the performance efficiency of gasifier in terms of employing different fuels, operating conditions, and gasifiers are not available in the open literature. Therefore, the information contained in this article could assist stakeholders in decision making and creating new window for further R&D in this area.
- The information provided in this data article and in Ozonoh et al. [1] could enable stake-holders to design gasifiers capable of converting different kinds of solid fuels to energy, and could be instrumental to policy-making in thermochemical energy conversion and power generating sectors.

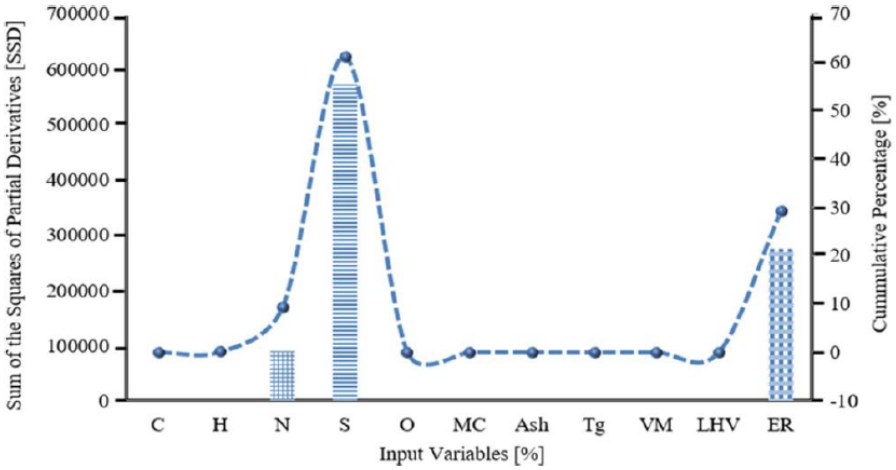


Fig. 12. Relative effect of each input variable on the output variable: H_2 [%]: MISO layer network: 21 hidden layer neurons.

5. Sensitivity analysis

A sensitivity analysis was carried out to determine the most important input variable affecting the output. The results obtained are highlighted in Figs. 9–12 for CO, CO_2, CH_4, & H_2, respectively.

In this study, partial derivatives (PaD) method was used. Details of the method can be found in Ozonoh et al. [1]. From Figs. 9, 10, and 12, Sulphur has the most important influence on the gas composition (CO, CO_2, & H_2), while N was the most important variable affecting the CH_4. For Figs. 9, 10, and 12, the result is expected because of the high concentration of coal used to blend the biomass material. Its presence in the product gas degrades the quality of the gas, while the emission when used as a fuel in energy conversion devise (e.g. internal combustion engines) becomes a huge threat to the environment.

6. Conclusions

In this study, 315 dataset obtained from different gasifiers (e.g. bubbling, circulating, entrained fluidised bed & fixed bed gasifiers) and experimental process conditions using biomass, coal, and their blends were used for the estimation of gasification system efficiency using artificial neural network (ANN) technique. The ANN Bayesian Regularizations (BR) and Levenberg Marquardt (L-M) algorithms with Multiple Input-Multiple Output (MIMO) and Multiple Input-Single Output (MISO) layer networks were considered using C, H, N, S, O, MC, Ash, T, VM, LHV, ER and CO, CO_2, CH_4, & H_2 as the input and output variables, respectively. To optimize the model result, IVRT-VIM which considered two scenarios: With Methane (WCH_4) and without methane ($WOCH_4$) amongst the predicted outputs were studied. The following conclusions were made:

- The MIMO layer network is more efficient than the MISO layer network.
- The results obtained from the L-M algorithm (Without methane ($WOCH_4$)) and using 23 number of neurons in the hidden layer are better than those obtained from BR algorithm when the R^2 and MSE are considered.
- Sulphur is the most important variable that affected the outputs (CO, CO_2, H_2), while nitrogen has the greatest influence on CH_4.

Declaration of Competing Interest

The authors hereby declare no conflict of interest.

Acknowledgments

Ozonoh acknowledges Mr. Nonye Ozonoh and Mrs. Angela Ozonoh for their moral and financial support.

Supplementary materials

Supplementary material associated with this article can be found, in the online version, at doi:10.1016/j.cdc.2019.100321.

Appendix A. Input dataset (Input variables).

C	H	N	S	O	MC	Ash	Tg	VM	LHV	ER	
46.8	5.74	0.66	0.11	41.40	15.00	5.10	750	72.15	15.00	0.25	Yang et al. (2018)
46.8	5.74	0.66	0.11	41.40	15.00	5.10	750	72.15	15.00	0.25	
35.42	4.62	0.47	0.18	31.28	12.2	15.83	800	60.01	16.38	0.32	Pei et al. (2018)
35.42	4.62	0.47	0.18	31.28	12.2	15.83	800	60.01	16.38	0.26	
35.42	4.62	0.47	0.18	31.28	12.2	15.83	800	60.01	16.38	0.25	
35.42	4.62	0.47	0.18	31.28	12.2	15.83	800	60.01	16.38	0.26	
35.42	4.62	0.47	0.18	31.28	12.2	15.83	850	60.01	16.38	0.32	
35.42	4.62	0.47	0.18	31.28	12.2	15.83	850	60.01	16.38	0.26	
35.42	4.62	0.47	0.18	31.28	12.2	15.83	850	60.01	16.38	0.25	
35.42	4.62	0.47	0.18	31.28	12.2	15.83	850	60.01	16.38	0.26	
46.6	5.08	0.04	0.02	47.76	13.74	0.51	900	78.69	18.73	0.30	Villetta et al. (2018)
46.6	5.08	0.04	0.02	47.76	13.74	0.51	900	78.69	18.73	0.30	
46.6	5.08	0.04	0.02	47.76	13.74	0.51	900	78.69	18.73	0.30	
46.6	5.08	0.04	0.02	47.76	13.74	0.51	900	78.69	18.73	0.30	
36.1	3.86	0.56	0.12	20.46	11.17	36.53	900	30.21	14.42	0.75	Rodrigues et al. (2018)
36.1	3.86	0.56	0.12	20.46	11.17	36.53	1000	30.21	14.42	0.75	
36.1	3.86	0.56	0.12	20.46	11.17	36.53	1100	30.21	14.42	0.75	
36.1	3.86	0.56	0.12	20.46	11.17	36.53	1200	30.21	14.42	0.75	
36.1	3.86	0.56	0.12	20.46	11.17	36.53	900	30.21	14.42	0.75	
36.1	3.86	0.56	0.12	20.46	11.17	36.53	1000	30.21	14.42	0.75	
36.1	3.86	0.56	0.12	20.46	11.17	36.53	1100	30.21	14.42	0.75	
36.1	3.86	0.56	0.12	20.46	11.17	36.53	1200	30.21	14.42	0.75	
33.39	3.47	0.61	2.15	16.68	11.06	42.91	1100	20.291	12.85	0.10	Rodrigues et al. (2018)
33.39	3.47	0.61	2.15	16.68	11.06	42.91	1100	20.291	12.85	0.2	
33.39	3.47	0.61	2.15	16.68	11.06	42.91	1100	20.291	12.85	0.60	
33.39	3.47	0.61	2.15	16.68	11.06	42.91	1100	20.291	12.85	0.20	
33.39	3.47	0.61	2.15	16.68	11.06	42.91	1100	20.291	12.85	0.40	
33.39	3.47	0.61	2.15	16.68	11.06	42.91	1100	20.291	12.85	0.60	
33.39	3.47	0.61	2.15	16.68	11.06	42.91	1100	20.291	12.85	0.20	
33.39	3.47	0.61	2.15	16.68	11.06	42.91	1100	20.291	12.85	0.40	
33.39	3.47	0.61	2.15	16.68	11.06	42.91	1100	20.291	12.85	0.60	
33.39	3.47	0.61	2.15	16.68	11.06	42.91	1100	20.291	12.85	0.20	
33.39	3.47	0.61	2.15	16.68	11.06	42.91	1100	20.291	12.85	0.40	
33.39	3.47	0.61	2.15	16.68	11.06	42.91	1100	20.291	12.85	0.60	
51.46	6.10	0.26	0.01	41.85	11.78	0.35	900	86.44	19.31	0.10	Rodrigues et al. (2018)
51.46	6.10	0.26	0.01	41.85	11.78	0.35	900	86.44	19.31	0.20	
51.46	6.10	0.26	0.01	41.85	11.78	0.35	900	86.44	19.31	0.60	
51.46	6.10	0.26	0.01	41.85	11.78	0.35	900	86.44	19.31	0.20	
51.46	6.10	0.26	0.01	41.85	11.78	0.35	900	86.44	19.31	0.40	
51.46	6.10	0.26	0.01	41.85	11.78	0.35	900	86.44	19.31	0.60	
51.46	6.10	0.26	0.01	41.85	11.78	0.35	900	86.44	19.31	0.20	
51.46	6.10	0.26	0.01	41.85	11.78	0.35	900	86.44	19.31	0.40	
51.46	6.10	0.26	0.01	41.85	11.78	0.35	900	86.44	19.31	0.60	
51.46	6.10	0.26	0.01	41.85	11.78	0.35	900	86.44	19.31	0.20	
51.46	6.10	0.26	0.01	41.85	11.78	0.35	900	86.44	19.31	0.40	
51.46	6.10	0.26	0.01	41.85	11.78	0.35	900	86.44	19.31	0.60	
49.00	6.30	0.20	0.10	44.4	8.15	0.79	850	77.86	18.39	0.40	De sales et al. (2017)
49.00	6.30	0.20	0.10	44.4	8.15	0.79	850	77.86	18.39	0.40	
49.00	6.30	0.20	0.10	44.4	8.15	0.79	850	77.86	18.39	0.40	
49.00	6.30	0.20	0.10	44.4	8.15	0.79	850	77.86	18.39	0.40	
49.00	6.30	0.20	0.10	44.4	8.15	0.79	850	77.86	18.39	0.40	
49.00	6.30	0.20	0.10	44.4	8.15	0.79	850	77.86	18.39	0.40	
49.00	6.30	0.20	0.10	44.4	8.15	0.79	850	77.86	18.39	0.40	
49.00	6.30	0.20	0.10	44.4	8.15	0.79	850	77.86	18.39	0.40	
49.00	6.30	0.20	0.10	44.4	8.15	0.79	850	77.86	18.39	0.40	
49.00	6.30	0.20	0.10	44.4	8.15	0.79	850	77.86	18.39	0.40	
49.00	6.30	0.20	0.10	44.4	8.15	0.79	850	77.86	18.39	0.40	
49.00	6.30	0.20	0.10	44.4	8.15	0.79	850	77.86	18.39	0.40	
49.00	6.30	0.20	0.10	44.4	8.15	0.79	850	77.86	18.39	0.40	
99.00	0.00	0.00	0.90	42.51	0.10	10.1	600	5.40	31.5	0.45	Konstantinou and Marsh (2015)
99.00	0.00	0.00	0.90	42.51	0.10	10.1	750	5.40	31.5	0.45	
99.00	0.00	0.00	0.90	42.51	0.10	10.1	800	5.40	31.5	0.45	
99.00	0.00	0.00	0.90	42.51	0.10	10.1	850	5.40	31.5	0.45	
99.00	0.00	0.00	0.90	42.51	0.10	10.1	900	5.40	31.5	0.45	
85.81	13.86	0.12	0.06	0.00	0.02	0.15	700	99.81	38.04	0.30	He et al. (2009)
85.81	13.86	0.12	0.06	0.00	0.02	0.15	900	99.81	38.04	0.30	
85.81	13.86	0.12	0.06	0.00	0.02	0.15	900	99.81	38.04	0.30	

(*continued on next page*)

85.81	13.86	0.12	0.06	0.00	0.02	0.15	900	99.81	38.04	0.30	
85.81	13.86	0.12	0.06	0.00	0.02	0.15	900	99.81	38.04	0.30	
51.81	5.76	0.26	0.36	30.32	0.00	5.98	700	82.28	21.31	0.60	He et al. (2009)
51.81	5.76	0.26	0.36	30.32	0.00	5.98	950	82.28	21.31	0.60	
51.81	5.76	0.26	0.36	30.32	0.00	5.98	950	82.28	21.31	0.60	
51.81	5.76	0.26	0.36	30.32	0.00	5.98	950	82.28	21.31	0.60	
51.81	5.76	0.26	0.36	30.32	0.00	5.98	950	82.28	21.31	0.60	
51.81	5.76	0.26	0.36	30.32	0.00	5.98	950	82.28	21.31	0.60	
50.54	7.08	0.15	0.57	41.11	8.00	0.55	900	82.29	19.15	0.22	
50.54	7.08	0.15	0.57	41.11	8.00	0.55	900	82.29	19.15	0.25	LV et al. (2006)
50.54	7.08	0.15	0.57	41.11	8.00	0.55	900	82.29	19.15	0.24	
50.54	7.08	0.15	0.57	41.11	8.00	0.55	900	82.29	19.15	0.26	
50.54	7.08	0.15	0.57	41.11	8.00	0.55	900	82.29	19.15	0.25	
50.54	7.08	0.15	0.57	41.11	8.00	0.55	900	82.29	19.15	0.25	
50.54	7.08	0.15	0.57	41.11	8.00	0.55	900	82.29	19.15	0.25	
50.54	7.08	0.15	0.57	41.11	8.00	0.55	900	82.29	19.15	0.28	
50.54	7.08	0.15	0.57	41.11	8.00	0.55	900	82.29	19.15	0.27	
50.54	7.08	0.15	0.57	41.11	8.00	0.55	900	82.29	19.15	0.24	
50.54	7.08	0.15	0.57	41.11	8.00	0.55	900	82.29	19.15	0.27	
50.54	7.08	0.15	0.57	41.11	8.00	0.55	900	82.29	19.15	0.27	
50.54	7.08	0.15	0.57	41.11	8.00	0.55	900	82.29	19.15	0.27	
50.54	7.08	0.15	0.57	41.11	8.00	0.55	900	82.29	19.15	0.27	
50.54	7.08	0.15	0.57	41.11	8.00	0.55	900	82.29	19.15	0.27	
51.30	6.10	0.00	0.01	42.6	7.90	1.16	770	79.67	18.35	0.25	
51.30	6.10	0.00	0.01	42.6	7.90	1.16	770	79.67	18.35	0.25	Rapagna et al. (2000)
51.3	6.10	0.00	0.01	42.6	7.90	1.16	770	79.67	18.35	0.25	
43.43	5.95	0.97	0.13	45.01	6.17	5.93	700	75.95	17.75	0.18	
43.43	5.95	0.97	0.13	45.01	6.17	5.93	800	75.95	17.75	0.21	Gai and Dong (2012)
43.43	5.95	0.97	0.13	45.01	6.17	5.93	800	75.95	17.75	0.24	
43.43	5.95	0.97	0.13	45.01	6.17	5.93	800	75.95	17.75	0.28	
43.43	5.95	0.97	0.13	45.01	6.17	5.93	800	75.95	17.75	0.32	
43.43	5.95	0.97	0.13	45.01	6.17	5.93	800	75.95	17.75	0.36	
43.43	5.95	0.97	0.13	45.01	6.17	5.93	800	75.95	17.75	0.41	
52.84	5.37	0.59	0.49	41.01	10.12	5.40	690	84.48	16.88	0.40	
52.84	5.37	0.59	0.49	41.01	10.12	5.40	730	84.48	16.88	0.40	Loha et al. (2011)
52.84	5.37	0.59	0.49	41.01	10.12	5.40	750	84.48	16.88	0.40	
52.84	5.37	0.59	0.49	41.01	10.12	5.40	750	84.48	16.88	0.40	
52.84	5.37	0.59	0.49	41.01	10.12	5.40	750	84.48	16.88	0.40	
52.84	5.37	0.59	0.49	41.01	10.12	5.40	770	84.48	16.88	0.40	
52.84	5.37	0.59	0.49	41.01	10.12	5.40	690	84.48	16.88	0.35	
52.84	5.37	0.59	0.49	41.01	10.12	5.40	730	84.48	16.88	0.35	
52.84	5.37	0.59	0.49	41.01	10.12	5.40	750	84.48	16.88	0.35	
52.84	5.37	0.59	0.49	41.01	10.12	5.40	750	84.48	16.88	0.35	
52.84	5.37	0.59	0.49	41.01	10.12	5.40	750	84.48	16.88	0.35	
52.84	5.37	0.59	0.49	41.01	10.12	5.40	770	84.48	16.88	0.35	
52.84	5.37	0.59	0.49	41.01	10.12	5.40	770	84.48	16.88	0.35	
52.84	5.37	0.59	0.49	41.01	10.12	5.40	770	84.48	16.88	0.35	
52.84	5.37	0.59	0.49	41.01	10.12	5.40	770	84.48	16.88	0.35	
52.84	5.37	0.59	0.49	41.01	10.12	5.40	770	84.48	16.88	0.35	
52.84	5.37	0.59	0.49	41.01	10.12	5.40	770	84.48	16.88	0.35	
36.42	5.40	5.50	1.90	31.5	9.50	29.70	800	51.8	14.86	0.25	Ong et al. (2015)
36.42	5.40	5.50	1.90	31.5	9.50	29.70	800	51.8	14.86	0.25	
44.20	6.10	2.10	1.00	42.5	8.50	6.30	950	42.5	17.63	0.25	
44.20	6.10	2.10	1.00	42.5	8.50	6.30	950	42.5	17.63	0.25	
48.90	5.90	0.57	0.57	33.2	8.69	10.37	700	69.83	16.14	0.20	
48.90	5.90	0.57	0.57	33.2	8.69	10.37	750	69.83	16.14	0.20	Serrano et al. (2016)
48.90	5.90	0.57	0.57	33.2	8.69	10.37	800	69.83	16.14	0.20	
48.90	5.90	0.57	0.57	33.20	8.69	10.37	800	69.83	16.14	0.20	
48.90	5.90	0.57	0.57	33.20	8.69	10.37	800	69.83	16.14	0.20	
44.30	5.90	0.10	0.00	44.40	8.40	0.30	780	74.20	18.30	0.30	
44.30	5.90	0.10	0.00	44.40	8.40	0.30	780	74.20	18.30	0.30	Miccioa et al. (2009)
44.30	5.90	0.10	0.00	44.40	8.40	0.30	780	74.20	18.30	0.30	
44.30	5.90	0.10	0.00	44.40	8.40	0.30	780	74.20	18.30	0.30	
44.30	5.90	0.10	0.00	44.40	8.40	0.30	780	74.20	18.30	0.3	
44.30	5.90	0.10	0.00	44.40	8.40	0.30	780	74.20	18.30	0.30	
35.70	1.90	4.60	0.00	38.20	4.80	19.52	650	69.83	13.20	0.30	
12.10	0.62	2.60	0.00	54.00	1.50	79.86	650	15.64	5.50	0.33	Thakkar et al., 2016

(*continued on next page*)

38.45	2.97	0.49	0.07	36.36	9.95	19.52	650	14.99	14.70	0.25	
38.45	2.97	0.49	0.07	36.36	9.95	19.52	675	14.99	14.70	0.25	Karmakar et al. (2013)
38.45	2.97	0.49	0.07	36.36	9.95	19.52	700	14.99	14.70	0.25	
38.45	2.97	0.49	0.07	36.36	9.95	19.52	725	14.99	14.70	0.25	
38.45	2.97	0.49	0.07	36.36	9.95	19.52	600	14.99	14.70	0.35	
38.45	2.97	0.49	0.07	36.36	9.95	19.52	650	14.99	14.70	0.35	
38.45	2.97	0.49	0.07	36.36	9.95	19.52	700	14.99	14.70	0.35	
38.45	2.97	0.49	0.07	36.36	9.95	19.52	725	14.99	14.70	0.35	
38.45	2.97	0.49	0.07	36.36	9.95	19.52	750	14.99	14.70	0.35	
38.45	2.97	0.49	0.07	36.36	9.95	19.52	600	14.99	14.70	0.45	
38.45	2.97	0.49	0.07	36.36	9.95	19.52	650	14.99	14.70	0.45	
38.45	2.97	0.49	0.07	36.36	9.95	19.52	700	14.99	14.70	0.45	
38.45	2.97	0.49	0.07	36.36	9.95	19.52	725	14.99	14.70	0.45	
38.45	2.97	0.49	0.07	36.36	9.95	19.52	800	14.99	14.70	0.45	
38.45	2.97	0.49	0.07	36.36	9.95	19.52	650	14.99	14.70	0.25	
38.45	2.97	0.49	0.07	36.36	9.95	19.52	675	14.99	14.70	0.25	
38.45	2.97	0.49	0.07	36.36	9.95	19.52	700	14.99	14.7	0.25	
38.45	2.97	0.49	0.07	36.36	9.95	19.52	725	14.99	14.70	0.25	
38.45	2.97	0.49	0.07	36.36	9.95	19.52	600	14.99	14.70	0.35	
38.45	2.97	0.49	0.07	36.36	9.95	19.52	650	14.99	14.70	0.35	
38.45	2.97	0.49	0.07	36.36	9.95	19.52	700	14.99	14.70	0.35	
38.45	2.97	0.49	0.07	36.36	9.95	19.52	725	14.99	14.70	0.35	
38.45	2.97	0.49	0.07	36.36	9.95	19.52	750	14.99	14.70	0.35	
38.45	2.97	0.49	0.07	36.36	9.95	19.52	600	14.99	14.70	0.45	
38.45	2.97	0.49	0.07	36.36	9.95	19.52	650	14.99	14.70	0.45	
38.45	2.97	0.49	0.07	36.36	9.95	19.52	700	14.99	14.70	0.45	
38.45	2.97	0.49	0.07	36.36	9.95	19.52	725	14.99	14.70	0.45	
38.45	2.97	0.49	0.07	36.36	9.95	19.52	800	14.99	14.70	0.45	
38.45	2.97	0.49	0.07	36.36	9.95	19.52	650	55.54	14.70	0.45	
38.45	2.97	0.49	0.07	36.36	9.95	19.52	690	55.54	14.70	0.45	
38.45	2.97	0.49	0.07	36.36	9.95	19.52	730	55.54	14.70	0.45	
38.45	2.97	0.49	0.07	36.36	9.95	19.52	770	55.54	14.70	0.45	
38.45	2.97	0.49	0.07	36.36	9.95	19.52	750	55.54	14.70	0.45	
38.45	2.97	0.49	0.07	36.36	9.95	19.52	750	55.54	14.70	0.45	
38.45	2.97	0.49	0.07	36.36	9.95	19.52	750	55.54	14.70	0.45	
38.45	2.97	0.49	0.07	36.36	9.95	19.52	750	55.54	14.70	0.45	
47.18	3.60	1.01	0.01	48.20	13.63	6.00	880	73.40	16.15	0.30	
47.18	3.60	1.01	0.01	48.20	13.63	6.00	880	73.40	16.15	0.30	Subramanian et al. (2011)
47.18	3.60	1.01	0.01	48.20	13.63	6.00	880	73.40	16.15	0.30	
47.18	3.60	1.01	0.01	48.20	13.63	6.00	880	73.40	16.15	0.30	
47.18	3.60	1.01	0.01	48.20	13.63	6.00	880	73.40	16.15	0.30	
47.18	3.60	1.01	0.01	48.20	13.63	6.00	880	73.40	16.15	0.30	
47.18	3.60	1.01	0.01	48.2	13.63	6.00	880	73.4	16.15	0.30	
47.18	3.60	1.01	0.01	48.2	13.63	6.00	880	73.4	16.15	0.30	
47.18	3.60	1.01	0.01	48.2	13.63	6.00	880	73.4	16.15	0.30	
47.18	3.60	1.01	0.01	48.2	13.63	6.00	880	73.4	16.15	0.30	
47.18	3.60	1.01	0.01	48.2	13.63	6.00	880	73.4	16.15	0.30	
47.18	3.60	1.01	0.01	48.2	13.63	6.00	880	73.4	16.15	0.30	
47.18	3.60	1.01	0.01	48.2	13.63	6.00	880	73.4	16.15	0.30	
47.18	3.60	1.01	0.01	48.2	13.63	6.00	880	73.4	16.15	0.30	
47.18	3.60	1.01	0.01	48.2	13.63	6.00	880	73.4	16.15	0.30	
47.18	3.60	1.01	0.01	48.2	13.63	6.00	880	73.4	16.15	0.30	
47.18	3.60	1.01	0.01	48.2	13.63	6.00	880	73.4	16.15	0.30	
38.92	5.10	2.17	0.12	53.69	8.10	19.33	880	63.8	15.81	0.40	
38.92	5.10	2.17	0.12	53.69	8.10	19.33	880	63.8	15.81	0.40	
38.92	5.10	2.17	0.12	53.69	8.10	19.33	880	63.8	15.81	0.40	Subramanian et al. (2011)
38.92	5.10	2.17	0.12	53.69	8.10	19.33	880	63.8	15.81	0.40	
38.92	5.10	2.17	0.12	53.69	8.10	19.33	880	63.8	15.81	0.40	
38.92	5.10	2.17	0.12	53.69	8.10	19.33	880	63.8	15.81	0.40	
38.92	5.10	2.17	0.12	53.69	8.10	19.33	880	63.8	15.81	0.40	
38.92	5.10	2.17	0.12	53.69	8.10	19.33	880	63.8	15.81	0.40	
38.92	5.10	2.17	0.12	53.69	8.10	19.33	880	63.8	15.81	0.40	
38.92	5.10	2.17	0.12	53.69	8.10	19.33	880	63.8	15.81	0.40	
38.92	5.10	2.17	0.12	53.69	8.10	19.33	880	63.8	15.81	0.40	
38.92	5.10	2.17	0.12	53.69	8.10	19.33	880	63.8	15.81	0.40	
38.92	5.10	2.17	0.12	53.69	8.10	19.33	880	63.8	15.81	0.40	

(*continued on next page*)

38.92	5.10	2.17	0.12	53.69	8.10	19.33	880	63.8	15.81	0.40	
38.92	5.10	2.17	0.12	53.69	8.10	19.33	880	63.8	15.81	0.40	
38.92	5.10	2.17	0.12	53.69	8.10	19.33	880	63.8	15.81	0.40	
38.92	5.10	2.17	0.12	53.69	8.10	19.33	880	63.8	15.81	0.40	
51.33	6.13	0.12	0.02	41.97	9.30	1.80	880	77.76	15.81	0.50	
51.33	6.13	0.12	0.02	41.97	9.30	1.80	880	77.76	17.62	0.50	
51.33	6.13	0.12	0.02	41.97	9.30	1.80	880	77.76	17.62	0.50	Subramanian et al. (2011)
51.33	6.13	0.12	0.02	41.97	9.30	1.80	880	77.76	17.62	0.50	
51.33	6.13	0.12	0.02	41.97	9.30	1.80	880	77.76	17.62	0.50	
51.33	6.13	0.12	0.02	41.97	9.30	1.80	880	77.76	17.62	0.50	
51.33	6.13	0.12	0.02	41.97	9.30	1.80	880	77.76	17.62	0.50	
51.33	6.13	0.12	0.02	41.97	9.30	1.80	880	77.76	17.62	0.50	
51.33	6.13	0.12	0.02	41.97	9.30	1.80	880	77.76	17.62	0.50	
51.33	6.13	0.12	0.02	41.97	9.30	1.80	880	77.76	17.62	0.50	
51.33	6.13	0.12	0.02	41.97	9.30	1.80	880	77.76	17.62	0.50	
51.33	6.13	0.12	0.02	41.97	9.30	1.80	880	77.76	17.62	0.50	
51.33	6.13	0.12	0.02	41.97	9.30	1.80	880	77.76	17.62	0.50	
51.33	6.13	0.12	0.02	41.97	9.30	1.80	880	77.76	17.62	0.50	
51.33	6.13	0.12	0.02	41.97	9.30	1.80	880	77.76	17.62	0.50	
51.33	6.13	0.12	0.02	41.97	9.30	1.80	880	77.76	17.62	0.50	
37.6	5.42	0.38	0.03	36.56	0.00	20.00	665	13.6	14.22	0.25	
37.6	5.42	0.38	0.03	36.56	0.00	20.00	744	13.6	14.22	0.30	
37.6	5.42	0.38	0.03	36.56	0.00	20.00	811	13.6	14.22	0.35	Mansaray et al. (1999)
37.6	5.42	0.38	0.03	36.56	0.00	20.00	670	13.6	14.22	0.25	
37.6	5.42	0.38	0.03	36.56	0.00	20.00	750	13.60	14.22	0.30	
37.6	5.42	0.38	0.03	36.56	0.00	20.00	822	13.60	14.22	0.35	
37.6	5.42	0.38	0.03	36.56	0.00	20.00	700	13.60	14.22	0.25	
37.6	5.42	0.38	0.03	36.56	0.00	20.00	766	13.60	14.22	0.30	
37.6	5.42	0.38	0.03	36.56	0.00	20.00	828	13.60	14.22	0.35	
77.58	4.30	0.22	0.05	17.88	6.20	2.70	975	91.10	15.38	0.25	
77.58	4.30	0.22	0.05	17.88	6.20	2.70	975	91.10	15.38	0.25	
77.58	4.30	0.22	0.05	17.88	6.20	2.70	975	91.10	15.38	0.25	
77.58	4.30	0.22	0.05	17.88	6.20	2.70	975	91.10	15.38	0.25	Salam and Bhattacharya (2006)
77.58	4.30	0.22	0.05	17.88	6.20	2.70	975	91.10	15.38	0.25	
77.58	4.30	0.22	0.05	17.88	6.20	2.70	975	91.10	15.38	0.25	
77.58	4.30	0.22	0.05	17.88	6.20	2.70	975	91.10	15.38	0.25	
77.58	4.30	0.22	0.05	17.88	6.20	2.70	975	91.10	15.38	0.25	
77.58	4.30	0.22	0.05	17.88	6.20	2.70	975	91.10	15.38	0.25	
77.58	4.30	0.22	0.05	17.88	6.20	2.70	975	91.10	15.38	0.25	
77.58	4.30	0.22	0.05	17.88	6.20	2.70	975	91.10	15.38	0.25	
77.58	4.30	0.22	0.05	17.88	6.20	2.70	975	91.10	15.38	0.25	
77.58	4.30	0.22	0.05	17.88	6.20	2.70	975	91.10	15.38	0.25	
77.58	4.30	0.22	0.05	17.88	6.20	2.70	975	91.10	15.38	0.25	
77.58	4.30	0.22	0.05	17.88	6.20	2.70	975	91.10	15.38	0.25	
77.58	4.30	0.22	0.05	17.88	6.20	2.70	975	91.10	15.38	0.25	
45.40	6.50	0.70	0.30	24.20	9.10	20.40	849	0.00	18.60	0.26	
45.40	6.50	0.70	0.30	24.20	9.10	20.40	852	0.00	18.60	0.26	
45.40	6.50	0.70	0.30	24.20	9.10	20.40	869	0.00	18.60	0.27	
45.40	6.50	0.70	0.30	24.2	9.10	20.40	879	0.00	18.00	0.30	Arena and Gregorio (2014)
45.40	6.50	0.70	0.30	24.2	9.10	20.40	898	0.00	18.60	0.32	
45.40	6.50	0.70	0.30	24.2	9.10	20.40	932	0.00	18.60	0.33	
79.34	5.72	1.20	0.66	48.9	9.80	4.50	849	15	14.00	0.20	
37.60	5.42	0.38	0.03	36.56	0.00	20.00	665	66.40	13.55	0.25	
37.60	5.42	0.38	0.03	36.56	0.00	20.00	744	66.40	13.55	0.30	
37.60	5.42	0.38	0.03	36.56	0.00	20.00	811	66.40	13.55	0.35	Lahijani et al. (2011)
37.60	5.42	0.38	0.03	36.56	0.00	20.00	670	66.40	13.55	0.25	Mansaray et al. (1999)
37.60	5.42	0.38	0.03	36.56	0.00	20.00	750	66.40	13.55	0.30	
37.60	5.42	0.38	0.03	36.56	0.00	20.00	822	66.40	13.55	0.35	
37.60	5.42	0.38	0.03	36.56	0.00	20.00	700	66.40	13.55	0.25	
37.60	5.42	0.38	0.03	36.56	0.00	20.00	766	66.40	13.55	0.30	
37.60	5.42	0.38	0.03	36.56	0.00	20.00	828	66.40	13.55	0.35	
44.48	6.49	0.73	0.07	48.23	8.48	1.23	702	75.23	17.88	0.28	
44.48	6.49	0.73	0.07	48.23	8.48	1.23	760	75.23	17.88	0.28	
44.48	6.49	0.73	0.07	48.23	8.48	1.23	846	75.23	17.88	0.28	
49.42	7.82	0.12	0.06	42.49	8.61	1.02	702	76.50	18.21	0.28	Hu et al. (2016)

(*continued on next page*)

49.42	7.82	0.12	0.06	42.49	8.61	1.02	760	76.50	18.21	0.28	
49.42	7.82	0.12	0.06	42.49	8.61	1.02	846	76.50	18.21	0.28	
49.42	7.82	0.12	0.06	42.49	8.61	1.02	846	76.50	18.21	0.28	
49.42	7.82	0.12	0.06	42.49	8.61	1.02	846	76.50	18.21	0.28	
49.42	7.82	0.12	0.06	42.49	8.61	1.02	846	76.50	18.21	0.28	
50.54	6.14	0.96	0.03	42.59	6.30	0.50	755	93.20	17.10	0.20	
50.54	6.14	0.96	0.03	42.59	6.30	0.50	840	93.20	17.10	0.22	
50.54	6.14	0.96	0.03	42.59	6.30	0.50	755	93.20	17.10	0.45	
50.54	6.14	0.96	0.03	42.59	6.30	0.50	840	93.20	17.10	0.23	Campoy et al. (2009)
50.54	6.14	0.96	0.03	42.59	6.30	0.50	755	93.20	17.10	0.42	
50.54	6.14	0.96	0.03	42.59	6.30	0.50	840	93.20	17.10	0.32	
50.54	6.14	0.96	0.03	42.59	6.30	0.50	755	93.20	17.10	0.60	
50.54	6.14	0.96	0.03	42.59	6.30	0.50	840	93.20	17.10	0.31	
50.54	6.14	0.96	0.03	42.59	6.30	0.50	755	93.20	17.10	0.58	
50.54	6.14	0.96	0.03	42.59	6.30	0.50	840	93.20	17.10	0.33	
50.54	6.14	0.96	0.03	42.59	6.30	0.50	755	93.20	17.10	0.56	
50.54	6.14	0.96	0.03	42.59	6.30	0.50	840	93.20	17.10	0.31	
50.54	6.14	0.96	0.03	42.59	6.30	0.50	755	93.20	17.10	0.61	
50.54	6.14	0.96	0.03	42.59	6.30	0.50	840	93.20	17.10	0.10	
50.54	6.14	0.96	0.03	42.59	6.30	0.50	755	93.20	17.10	0.29	
50.54	6.14	0.96	0.03	42.59	6.30	0.50	840	93.20	17.10	0.36	
50.54	6.14	0.96	0.03	42.59	6.30	0.50	755	93.20	17.10	0.54	
50.54	6.14	0.96	0.03	42.59	6.30	0.50	840	93.20	17.10	0.57	
50.54	6.14	0.96	0.03	42.59	6.30	0.50	755	93.20	17.10	0.30	
50.54	6.14	0.96	0.03	42.59	6.30	0.50	840	93.20	17.10	0.56	
41.82	6.07	0.77	0.14	50.3	10.4	7.90	740	64.40	16.36	0.36	
41.82	6.07	0.77	0.14	50.3	10.4	7.90	700	64.40	16.36	0.36	
41.82	6.07	0.77	0.14	50.3	10.4	7.90	740	64.40	16.36	0.36	
41.82	6.07	0.77	0.14	50.30	10.40	7.90	700	64.40	16.36	0.36	George et al. (2018)
41.82	6.07	0.77	0.14	50.30	10.40	7.90	740	64.40	16.36	0.36	
41.82	6.07	0.77	0.14	50.30	10.40	7.90	700	64.40	16.36	0.36	
35.42	4.62	0.47	0.18	31.38	12.20	15.83	620	60.01	16.38	0.18	
35.42	4.62	0.47	0.18	31.38	12.20	15.83	720	60.01	16.38	0.20	
35.42	4.62	0.47	0.18	31.38	12.20	15.83	620	60.01	16.38	0.21	
35.42	4.62	0.47	0.18	31.38	12.20	15.83	720	60.01	16.38	0.20	Pei et al. (2018)
35.42	4.62	0.47	0.18	31.38	12.20	15.83	850	60.01	16.38	0.32	
35.42	4.62	0.47	0.18	31.38	12.20	15.83	850	60.01	16.38	0.26	
35.42	4.62	0.47	0.18	31.38	12.20	15.83	850	60.01	16.38	0.25	
35.42	4.62	0.47	0.18	31.38	12.20	15.83	850	60.01	16.38	0.26	
44.42	3.80	0.89	0.50	13.9	7.80	33.50	800	24.50	17.40	0.00	
42.18	5.70	1.59	0.50	27.54	7.80	33.50	800	24.50	15.70	1.00	Thengane et al., 2019

Appendix B. Output dataset (Output variables)

CO	H_2	CH_4	CO_2	LHV	Gas yield	CGE	CCE	
38.30	36	0.40	23.50	4.00	1.50	81.40	52.11	Yang et al. (2018)
38.30	35.8	0.60	23.50	4.00	1.30	83.10	31.71	
18.50	6.10	5.80	13.7	5.10	1.17	34.99	67.24	Pei et al. (2018)
18.90	5.70	6.80	13.4	5.40	1.29	40.86	76.29	
21.70	6.90	5.40	11.9	5.40	1.44	45.61	84.94	
16.10	6.00	6.30	14.4	4.90	1.24	35.64	69.02	
12.90	11.00	0.60	9.10	3.00	2.75	48.39	94.00	
13.90	12.30	1.20	8.90	3.50	2.62	53.78	95.10	
15.50	13.70	13.70	8.20	3.70	2.7	58.59	152.73	
35.80	19.10	19.10	5.80	6.70	1.90	74.66	174.43	
12.50	11.80	1.00	8.50	3.27	2.22	36.55	56.11	Villetta et al. (2018)
14.10	13.40	1.20	9.50	3.72	2.16	40.56	61.70	
14.200	14.00	1.50	10.40	3.91	2.29	45.12	68.73	
15.10	14.10	1.50	10.20	4.03	2.10	42.67	64.75	
21.50	10.60	0.00	5.51	4.31	0.66	44.00	28.60	Rodrigues et al. (2018)
23.10	12.20	0.00	8.64	6.26	0.96	53.40	42.62	
24.10	13.80	0.00	6.03	9.12	1.34	55.90	44.85	
23.60	14.60	0.00	6.77	9.37	1.44	66.10	45.53	
28.10	13.30	0.00	3.29	13.70	1.76	75.90	45.40	
22.00	14.50	0.00	8.15	7.79	1.27	60.70	46.00	
21.80	14.90	0.00	7.54	8.03	1.32	66.80	44.91	
21.50	13.70	0.00	8.35	6.84	1.12	56.50	38.50	
28.10	22.40	0.03	0.17	3.76	0.59	50.20	26.79	Rodrigues et al. (2018)
31.10	19.00	0.01	0.39	4.85	0.68	58.40	34.37	
11.60	4.920	0.00	10.5	2.85	0.59	24.90	20.92	
27.7	22.8	0.00	3.39	4.33	0.79	75.30	39.41	

(*continued on next page*)

16.9	12.3	0.00	7.83	3.34	0.70	48.40	27.77	
9.16	5.89	0.00	11.30	2.19	0.62	26.50	20.35	
21.10	23.40	0.00	6.47	3.32	0.82	82.90	36.27	
12.80	12.80	0.00	9.42	2.51	0.71	51.50	25.31	
6.81	6.13	0.00	11.9	1.59	0.61	36.70	18.31	
10.8	20.50	0.00	9.41	1.74	0.78	95.40	25.29	
6.26	10.90	0.00	10.60	1.21	0.65	52.70	17.58	
2.74	4.42	0.00	11.70	0.62	0.53	20.80	12.28	
38.7	33.20	0.00	0.12	9.82	1.46	90.50	59.00	Rodrigues et al. (2018)
39.40	27.60	0.00	0.58	11.90	1.63	100.00	67.84	
13.30	7.23	0.00	11.20	6.54	1.27	38.00	32.39	
34.80	28.30	0.00	2.88	10.00	1.67	104.10	65.51	
21.00	15.20	0.00	7.97	7.87	147	68.20	44.33	
11.80	7.59	0.00	11.7	5.45	1.28	39.40	31.31	
29.90	28.1	0.00	5.09	8.24	1.67	105.40	60.83	
18.00	15.20	0.00	9.18	6.39	1.45	67.50	41.03	
9.93	7.01	0.00	12.30	4.31	1.26	37.60	29.15	
19.70	25.70	0.00	8.77	5.01	1.54	97.50	45.64	
11.30	13.40	0.00	11.20	3.63	1.30	56.50	30.45	
15.36	5.73	0.00	13.20	2.09	1.08	25.60	32.11	
17.80	17.00	1.40	4.00	4.61	0.811	18.93	17.01	De sales et al. (2017)
15.40	16.2	1.60	4.00	4.27	0.95	20.49	17.61	
21.00	16.00	1.70	4.00	5.02	1.08	27.44	26.78	
12.20	19.00	1.60	4.00	4.22	0.81	17.33	12.23	
8.70	21.00	1.40	4.00	3.89	0.95	18.67	10.46	
8.30	18.00	1.60	4.00	3.59	1.08	19.62	11.68	
7.20	19.00	1.60	4.00	3.52	0.81	14.45	7.80	
12.80	18.00	1.70	4.00	4.20	0.95	20.15	15.02	
11.10	20.00	1.70	4.00	4.20	1.08	22.96	15.10	
23.20	34.10	3.50	4.00	7.90	0.17	6.81	4.97	
20.80	34.70	3.20	4.00	7.66	0.20	7.71	5.21	
24.30	27.40	5.40	4.00	7.96	0.23	9.15	7.37	
17.80	32.60	3.60	4.00	7.07	0.17	6.10	3.98	
24.80	33.00	4.50	4.00	8.35	0.20	8.40	6.36	
18.00	33.3	3.40	4.00	7.13	0.23	8.20	5.31	
11.80	30.2	0.50	4.00	4.90	3.90	16.00	29.10	Konstantinou and Marsh (2015)
12.30	49.1	1.90	4.00	7.50	7.20	25.10	62.02	
17.40	42.1	2.90	4.00	7.80	7.50	25.20	92.37	
12.90	38.9	2.80	4.00	6.80	6.10	24.40	58.10	
11.90	34.7	3.10	4.00	6.40	5.70	20.60	53.38	
20.33	16.92	21.44	35.28	12.44	1.22	39.9	67.87	He et al. (2009)
21.53	21.31	18.91	32.46	12.15	1.31	41.83	69.00	
22.83	28.94	14.87	27.91	11.67	1.47	45.09	70.22	
25.87	34.96	34.96	21.84	11.36	1.81	54.07	80.68	
27.37	36.98	36.98	20.78	11.31	2.04	60.67	86.54	
9.34	27.01	20.30	35.25	14.44	0.74	49.58	62.05	He et al. (2009)
11.16	34.70	17.89	30.86	13.47	0.85	52.58	62.13	
12.65	40.64	15.57	26.61	12.62	0.98	55.49	64.74	
13.46	45.60	12.24	24.23	11.74	1.12	57.74	68.18	
14.85	48.63	9.62	23.59	10.74	1.28	63.52	72.37	
16.92	53.29	5.76	22.05	9.36	1.48	68.36	74.51	
29.56	31.40	6.23	30.02	5.44	0.91	24.10	63.48	LV et al. (2006)
24.59	28.44	6.50	36.41	5.04	0.88	21.59	62.96	
25.53	28.93	6.82	34.88	4.76	0.82	19.00	58.44	
25.2	29.16	8.21	34.36	5.05	0.85	20.90	61.06	
27.92	35.39	4.36	30.11	5.17	0.94	23.66	62.16	
28.77	31.88	5.54	31.76	4.78	0.91	21.18	63.73	
27.52	31.47	5.70	33.39	4.60	0.88	19.71	62.13	
25.81	31.17	6.01	33.32	4.82	0.86	20.18	59.38	
25.2	29.16	8.21	34.36	5.05	0.85	20.90	61.06	
25.07	27.12	9.02	35.62	5.26	0.78	19.97	57.64	
36.85	26.42	3.52	31.96	9.04	1.50	66.02	115.00	
39.21	30.51	3.29	25.75	9.88	1.62	77.92	117.20	
38.66	28.58	6.01	24.45	11.11	1.42	76.81	104.04	
42.65	29.91	3.58	22.29	10.37	1.24	62.60	90.06	
37.65	27.17	4.78	28.89	9.75	1.32	62.66	99.79	
33.20	43.60	11.5	11.7	13.01	1.10	77.99	64.79	Rapagna et al. (2000)
24.00	55.50	6.40	14.1	10.94	1.90	113.28	88.29	
23.00	52.20	7.90	19.9	11.37	1.70	105.34	90.18	

(continued on next page)

11.35	6.11	1.27	23.93	2.69	1.35	21.17	60.30	Gai and Dong (2012)
13.55	8.23	1.84	20.37	3.32	1.47	28.46	64.24	
16.72	10.92	2.98	16.48	4.43	1.62	41.85	71.62	
18.99	12.78	3.96	13.11	5.30	1.81	55.94	79.76	
14.81	13.51	3.72	11.58	5.39	2.14	67.26	78.74	
17.97	12.26	3.65	13.82	4.99	2.53	73.61	109.57	
15.16	10.58	1.57	18.41	3.69	2.86	61.54	122.81	
14.30	50.50	8.60	26.60	6.80	1.68	90.79	62.60	Loha et al. (2011)
16.30	52.20	7.90	23.50	6.60	1.85	96.34	66.90	
23.70	49.50	5.60	21.20	5.60	1.43	78.84	43.88	
17.75	52.90	7.40	22.25	6.90	2.43	85.65	91.87	
16.40	52.90	7.80	22.9	5.20	2.75	79.44	78.36	
18.00	54.40	7.70	19.40	6.20	2.82	138.85	95.80	
12.99	48.76	7.03	31.21	6.60	1.94	86.42	70.16	
15.45	50.71	5.06	28.74	6.90	1.88	57.53	71.08	
20.59	50.37	4.02	25.01	6.40	1.96	80.59	68.73	
16.64	51.43	4.28	27.65	6.10	1.84	84.66	61.50	
13.50	52.26	4.50	29.74	5.00	2.78	78.72	76.16	
17.72	52.00	3.62	26.66	6.80	2.15	80.56	80.11	
16.26	48.40	6.46	28.88	6.50	2.88	67.21	102.58	
18.94	50.14	4.60	26.33	6.20	2.15	90.15	73.04	
24.22	49.64	3.62	22.52	6.50	1.90	93.66	67.67	
20.15	50.76	3.82	25.22	5.50	1.87	99.87	56.36	
16.78	51.67	4.08	27.47	5.60	1.85	97.61	56.77	
21.28	51.24	3.25	24.25	6.90	2.55	93.55	96.41	
17.10	17.30	11.90	1.70	4.70	2.73	66.9	71.28	Ong et al. (2015)
15.90	17.10	12.20	2.00	4.60	2.52	66.2	64.40	
15.60	16.80	12.70	2.10	4.50	1.83	45.75	45.75	
12.00	13.40	12.50	1.80	3.60	1.96	39.2	39.20	
10.01	13.38	5.33	17.37	5.80	2.54	83.09	83.09	Serrano et al. (2016)
15.05	16.51	4.89	16.77	5.97	2.15	72.39	72.39	
10.68	12.62	4.88	16.98	6.24	2.19	77.08	77.08	
13.89	13.64	5.29	16.83	6.66	2.51	94.28	94.28	
16.71	16.26	4.87	16.56	6.81	2.66	102.17	102.17	
15.2	20.2	4.70	16.4	6.89	1.12	41.71	44.18	Miccioa et al. (2009)
16.4	19.8	4.9	15.9	5.69	1.14	35.06	46.08	
13.8	20.3	4.40	16.9	5.22	1.02	28.78	38.90	
11.7	22.8	4.10	17.7	6.54	1.01	35.70	36.77	
16.7	28.7	2.02	14.5	6.86	1.14	42.27	41.15	
17.60	30.3	1.49	14.3	6.44	1.21	42.12	43.90	
15.20	2.70	3.10	9.30	5.16	1.89	59.0	85.00	Thakkar et al., 2016
14.20	2.50	2.70	10.90	5.22	1.98	57.0	88.00	
26.02	18.71	1.96	13.91	6.38	1.09	49.28	71.51	Karmakar et al. (2013)
27.03	19.18	1.53	13.14	6.44	1.12	51.07	72.44	
27.84	19.49	1.19	12.47	6.46	1.16	53.09	74.07	
28.56	19.69	0.92	11.91	6.50	1.19	54.82	75.82	
16.15	13.82	2.32	18.74	5.13	1.18	42.84	73.43	
18.46	14.78	1.39	16.94	5.19	1.25	46.94	77.77	
20.18	15.18	0.82	15.62	5.24	1.32	48.94	82.68	
20.86	15.24	0.63	15.10	5.26	1.43	53.24	83.91	
21.48	15.22	0.63	14.64	5.28	1.46	54.62	85.43	
10.93	9.89	0.48	21.56	3.53	1.32	33.00	75.46	
12.88	10.47	1.62	20.06	3.61	1.39	35.58	80.20	
14.35	11.10	0.94	18.46	3.69	1.44	37.65	84.17	
14.95	11.54	0.53	17.51	3.77	1.48	39.48	88.57	
16.39	11.14	0.40	16.44	3.86	1.52	41.55	92.83	
24.84	17.22	0.17	40.4	6.38	1.09	49.28	71.51	
25.04	17.93	2.46	40.29	6.44	1.12	51.07	72.44	
25.31	18.12	2.38	40.63	6.46	1.16	53.09	74.07	
26.59	18.49	1.96	40.35	6.50	1.19	54.82	75.82	
17.48	14.13	2.79	45.67	5.13	1.18	42.84	73.43	
20.63	14.22	1.92	45.59	5.19	1.25	46.94	77.77	
20.47	14.63	1.32	44.91	5.24	1.32	48.94	82.68	
22.89	15.88	1.43	46.18	5.26	1.43	53.24	83.91	
22.24	16.08	1.46	46.12	5.28	1.46	54.62	85.43	
11.72	8.92	1.32	54.15	3.53	1.32	33.00	75.46	
13.47	9.32	1.39	53.41	3.61	1.39	35.58	80.20	
15.13	10.15	1.44	52.09	3.69	1.44	37.65	84.17	
16.61	10.27	1.48	51.16	3.77	1.48	39.48	88.57	

(continued on next page)

17.78	10.22	1.52	50.53	3.86	1.52	41.55	92.83	
11.25	42.25	9.60	31.9	11.28	1.03	62.99	84.10	
12.83	50.50	8.16	28.51	11.23	1.12	68.78	85.82	
15.90	52.20	6.25	25.65	11.16	1.16	65.58	85.83	
17.85	53.08	5.17	23.90	11.09	1.21	66.06	87.88	
27.48	47.81	6.62	19.09	12.21	1.05	65.75	86.33	
22.7	48.88	6.22	22.20	11.59	1.09	65.96	86.25	
19.65	51.17	6.03	23.19	11.42	1.16	66.1	87.68	
17.38	51.89	5.92	14.81	11.18	1.21	66.15	90.11	
8.71	8.49	1.52	14.62	2.65	1.98	30.47	55.87	Subramanian et al. (2011)
9.26	7.89	1.36	14.88	2.58	2.02	30.26	58.49	
10.12	9.54	1.89	12.12	3.08	2.26	40.42	61.92	
10.28	10.17	1.53	11.63	3.04	2.18	38.49	58.02	
11.53	10.55	2.67	11.58	3.67	2.21	47.10	64.69	
12.57	10.61	3.82	11.05	4.23	2.32	56.99	72.28	
8.24	7.54	1.08	15.61	2.31	2.24	30.05	63.41	
9.21	8.62	1.59	15.22	2.75	2.12	33.86	62.64	
10.52	8.79	1.32	14.17	2.82	2.24	36.68	66.16	
11.12	9.53	2.54	12.83	3.44	2.68	53.54	80.61	
10.91	10.46	2.50	11.69	3.52	2.52	51.51	71.82	
12.68	10.57	3.60	11.83	4.16	2.69	64.98	85.86	
6.54	5.62	1.91	16.24	2.18	2.73	34.56	76.53	
8.94	6.87	1.21	15.48	2.36	3.14	43.03	91.38	
8.31	7.23	1.86	14.32	2.57	2.83	42.23	78.70	
10.52	9.61	1.33	13.67	2.93	3.24	55.13	93.89	
11.61	9.78	2.42	13.14	3.49	2.9	58.77	89.47	
12.47	9.64	2.91	12.68	4.14	2.84	68.29	90.49	
10.54	6.18	1.04	15.24	2.40	1.86	27.83	68.67	Subramanian et al. (2011)
11.26	7.54	1.25	14.31	2.73	2.14	36.42	79.00	
10.12	6.09	1.49	12.87	2.51	1.79	28.01	60.31	
14.67	7.46	2.88	12.19	3.75	2.18	50.97	89.24	
15.42	8.59	3.21	11.68	4.10	2.25	57.51	93.87	
19.55	8.62	3.24	10.21	4.61	2.31	66.39	104.93	
10.11	5.54	1.08	16.28	2.29	2.23	31.84	84.32	
9.87	6.65	1.27	15.44	2.47	2.37	36.50	86.71	
10.53	6.78	1.66	13.89	2.71	2.31	39.03	82.92	
12.64	6.59	2.26	12.17	3.16	2.49	49.05	92.78	
14.78	7.42	2.01	10.66	3.43	2.56	54.74	96.73	
16.13	7.77	2.78	10.68	3.92	2.57	62.81	104.67	
9.32	5.34	1.03	17.14	2.15	2.18	29.22	82.45	
10.24	5.88	1.19	16.82	2.39	2.35	35.02	91.38	
10.11	6.65	1.57	15.96	2.61	2.42	39.38	92.07	
12.57	7.49	1.62	14.56	3.02	2.57	48.39	101.70	
15.48	7.12	1.71	12.92	3.36	2.68	56.14	111.07	
15.29	7.42	2.06	11.76	3.51	2.81	61.49	112.59	
14.23	6.54	1.02	14.51	2.88	2.42	39.94	75.16	Subramanian et al. (2011)
15.19	7.54	1.81	12.62	3.42	2.51	49.19	77.59	
16.28	7.98	2.04	13.89	3.69	2.43	51.39	81.69	
15.61	8.23	1.60	12.18	3.47	2.52	50.11	77.30	
17.38	9.98	2.45	11.96	4.21	2.71	65.38	89.91	
17.54	10.14	3.21	10.78	4.54	2.64	68.69	86.87	
13.55	5.59	1.06	15.31	2.70	2.84	43.94	88.68	
14.41	6.78	1.17	14.87	2.99	2.92	50.03	92.80	
15.82	7.69	1.24	13.25	3.29	2.89	54.49	91.42	
15.67	7.82	1.8	12.55	3.50	3.01	60.37	94.31	
16.32	8.12	2.14	11.16	3.75	3.15	67.69	97.38	
17.73	9.35	2.62	11.87	4.24	3.21	77.99	107.94	
12.62	5.24	0.98	16.84	2.52	3.01	43.47	95.63	
12.39	5.63	1.25	15.56	2.64	3.41	51.59	103.92	
13.42	6.87	1.62	14.24	3.05	3.61	63.10	110.31	
14.56	7.29	1.24	12.63	3.09	3.57	63.22	105.93	
15.85	7.38	1.82	12.81	3.48	3.64	72.59	115.79	
16.48	8.42	2.18	12.33	3.82	3.70	80.99	119.67	
19.20	4.00	2.90	14.45	5.03	1.50	53.06	76.00	Mansaray et al. (1999)
14.95	3.78	2.27	16.25	3.83	1.73	46.60	78.30	
12.75	3.39	1.98	17.14	3.28	1.98	45.67	81.00	
18.29	3.77	2.36	14.5	4.38	1.49	45.89	70.40	
14.23	3.4	2.00	16.46	3.54	1.71	42.57	72.60	
12.50	3.26	1.85	17.23	3.15	1.97	43.64	78.60	
15.13	3.41	2.00	14.82	3.75	1.30	34.28	55.00	
13.00	3.32	1.91	16.62	3.36	1.50	35.44	66.00	
12.29	3.25	1.84	17.42	3.09	1.70	36.94	67.00	

(continued on next page)

13.96	12.39	0.56	14.08	3.69	2.59	44.23	56.12	Salam and Bhattacharya (2006)
14.44	13.01	0.69	13.66	3.89	2.57	46.34	56.17	
12.31	11.36	0.57	15.42	3.35	2.59	40.07	55.54	
12.79	12.74	0.94	13.9	3.74	2.69	46.6	56.36	
16.02	11.89	0.77	13.62	3.99	2.82	52.04	65.10	
13.79	12.43	0.68	13.9	3.73	2.74	47.22	58.92	
14.77	13.48	0.93	13.86	4.10	2.63	49.78	58.83	
15.64	12.6	0.61	14.75	3.96	2.73	50.11	64.25	
14.49	11.61	0.55	15.08	3.66	2.64	44.63	60.25	
17.65	11.44	0.68	13.58	4.10	2.58	48.98	62.46	
16.58	11.55	0.51	14.22	3.91	2.65	47.95	62.99	
17.19	11.64	0.62	13.41	4.04	2.60	48.53	61.42	
19.76	11.62	0.93	12.39	4.51	2.59	54.05	65.05	
16.00	11.90	0.84	14.41	4.01	2.61	48.36	61.74	
17.68	12.27	0.75	13.14	4.24	2.60	51.11	62.31	
18.42	11.29	0.85	12.87	4.25	2.68	52.72	65.30	
15.5	10.75	0.90	14.19	3.82	2.52	44.6	58.54	
15.32	10.9	0.88	14.05	3.81	2.48	43.58	56.75	
9.74	8.48	4.18	13.36	2.42	1.62	53.00	70.00	
8.98	7.11	4.20	15.68	2.71	1.73	56.00	80.00	Arena and Gregorio (2014)
10.47	8.44	4.51	12.28	2.66	1.72	58.00	75.00	
10.4	8.24	4.51	12.83	2.78	1.91	61.00	81.00	
12.73	7.08	4.35	14.04	2.79	2.04	61.00	92.00	
11.66	7.68	3.33	11.66	2.61	2.00	57.00	79.00	
10.00	6.00	4.00	10.00	4.53	1.76	40.00	71.00	
19.2	4.00	2.9	14.45	5.03	1.50	55.68	76.00	Lahijani et al. (2011)
14.45	3.78	2.37	16.25	3.83	1.73	48.90	78.30	Mansaray et al. (1999)
12.75	3.39	1.98	17.14	3.28	1.98	47.93	81.00	
18.29	3.77	2.36	14.5	4.38	1.49	48.16	70.40	
14.43	3.40	2.00	16.46	3.54	1.71	44.67	72.60	
12.5	3.26	1.85	17.23	3.15	1.97	45.80	78.60	
15.13	3.41	2.00	14.82	3.75	1.30	35.98	55.00	
13.00	3.32	1.91	16.62	3.36	1.50	37.20	60.00	
12.00	3.25	1.84	17.42	3.09	1.70	38.78	67.00	
25.75	33.91	8.14	21.83	14.28	0.93	62.41	78.11	
18.42	40.23	8.11	25.36	12.81	1.12	70.09	83.73	Hu et al. (2016)
26.90	46.31	6.41	16.99	11.61	1.36	72.92	87.14	
13.74	21.31	12.25	33.18	15.31	0.53	33.43	51.61	
17.57	24.73	11.13	29.14	14.94	0.70	43.16	64.82	
22.32	27.14	10.35	25.43	14.51	0.78	48.30	71.30	
17.31	24.42	11.37	31.60	14.8	0.71	45.62	64.47	
22.80	28.92	9.33	25.91	14.57	0.83	51.35	74.47	
25.73	33.91	9.14	21.83	14.28	0.93	56.21	78.11	
15.80	8.70	5.10	1.03	4.76	1.03	59.000	93.00	
15.40	11.90	4.80	1.11	4.95	1.11	62.00	90.00	Campoy et al. (2009)
13.80	13.30	4.60	1.14	4.83	1.14	61.00	92.00	
15.00	140	4.70	0.97	5.09	0.97	54.00	90.00	
11.90	16.20	5.30	1.06	5.15	1.06	57.00	91.00	
18.90	16.40	5.55	1.13	6.12	1.13	64.00	94.00	
15.70	18.30	5.70	1.08	6.00	1.08	60.00	95.00	
20.80	20.00	6.70	0.98	7.18	0.98	61.00	96.00	
15.30	17.50	70.10	20.3	6.88	1.04	60.00	96.00	
20.00	16.60	5.60	16.8	6.14	1.14	66.00	95.00	
17.50	21.80	6.10	18.00	6.00	1.00	60.00	90.00	
23.90	22.40	7.30	12.60	8.06	0.97	64.00	96.00	
19.30	25.10	7.40	16.20	7.81	1.04	65.00	96.00	
27.40	18.30	7.30	16.20	8.06	1.05	67.00	97.00	
25.10	23.10	6.50	13.70	8.00	1.09	69.00	96.00	
23.90	22.30	6.70	14.60	7.83	1.09	69.00	96.00	
20.20	24.50	6.80	16.70	7.67	1.05	64.00	97.00	
19.30	25.7	6.70	17.00	7.62	1.10	66.00	96.00	
28.50	25.7	8.10	9.20	9.28	0.96	68.00	97.00	
23.50	27.5	7.70	14.60	8.70	0.98	63.00	97.00	
9.84	8.74	3.97	7.10	3.61	1.46	35.23	39.00	
9.49	7.68	3.89	7.20	3.42	1.43	32.71	37.70	George et al. (2018)
9.10	6.90	8.10	7.80	4.80	1.69	59.20	54.80	
7.60	5.90	5.40	8.90	3.53	1.55	39.90	40.70	

(continued on next page)

10.70	7.46	5.60	9.20	4.16	1.60	47.57	50.60	
9.84	6.60	4.60	9.05	3.63	1.54	39.75	44.90	
9.10	11.00	0.60	12.92	3.00	2.75	46.98	67.90	
8.90	12.30	1.20	12.30	3.50	2.65	52.82	68.60	Pei et al. (2018)
8.20	13.70	0.90	13.70	3.70	2.70	56.89	72.20	
5.80	19.10	0.40	19.10	6.70	1.90	72.49	87.00	
13.70	6.10	5.80	18.50	5.10	1.17	33.98	48.50	
13.40	5.70	6.80	18.90	5.40	1.29	39.67	54.90	
11.90	6.90	5.40	21.70	5.40	1.44	44.28	61.00	
14.40	6.00	6.30	16.10	4.90	1.24	34.60	49.90	
6.70	7.20	1.20	11.70	2.07	1.94	22.87	45.86	
11.20	8.20	1.40	15.40	2.74	1.98	30.90	70.41	Thengane et al. (2019)

References

[1] M. Ozonoh, B.O. Oboirien, A. Higginson, M.O. Daramola, Performance evaluation of gasification system efficiency using artificial neural network, Renew. Energy 145 (2020) 2253–2270.

[2] I. Narvaez, A. Orio, M.P. Aznar, J. Corella, Biomass gasification with air in an atmospheric bubbling fluidised bed. Effect of six operating variables on the quality of the produced raw gas, Ind. Eng. Chem. Res 35 (1996) 2110–2120.

[3] J. Udomsirichakorn, P.A. Salam, Review of hydrogen-enriched gas production from steam gasification of biomass: the prospect of CaO-based chemical looping gasification, Renew. Sust. Energy Rev. 30 (2014) 565–579.

[4] D.A. Ali, M.A. Gadalla, O.Y. Adelazzi, C.P. Hulleberg, Co-gasification of coal and biomass in an entrained flow gasifier: modelling, simulation and integration opportunities, J. Nat. Gas Sci. Eng. 37 (2017) 126–137.

[5] T.Kessler, E.R. Sacia, A.T. Bell, J.H. Mack, Artificial neural network based predictions of cetane number for furanic biofuel additives, Fuel 206 (2017) 171–179.

[6] S. Azidi, A.K. Jashni, Verifying the performance of artificial neural network and multiple linear regressions in predicting the mean seasonal municipal solid waste generation rate: a case study of Fars province, Iran. Waste Manag. 48 (2016) 14–23.

[7] D. Baruah, D.C. Baruah, M.K. Hazarika, Artificial neural network based modeling of biomass gasification in fixed bed downdraft gasifiers, Biomass Bioenergy 98 (2017) 264–271.

[8] M. Puig-Arnavat, J.A. Hernandez, J.C. Bruno, A. Coronas, Artificial neural network models for biomass gasification in fluidized bed gasifiers, Biomass Bioenergy 49 (2013) 2 7 9-2 8 9.

[9] J. George, P. Arun, C. Muraleedharan, Assessment of producer gas composition in air gasification of biomass using artificial neural network model, Int. J. Hydrog. Energy 43 (2018) 9558–9568.

[10] D.S. Pandey, S. Das, I. Pan, J.J. Leahy, W. Kwapinski, Artificial neural network based modelling approach for municipal solid waste gasification in a fluidized bed reactor, Waste Manag. 58 (2016) 202–213.

[11] S. Yang, B. Li, J. Zheng, R.K. Kankala, Biomass-to-Methanol by dual-stage entrained flow gasification: design and techno-economic analysis based on system modeling, J. Clean Prod. 205 (2018) 364–374.

[12] H. Pei, X. Wang, X. Dai, B. Jin, Y. Huang, A novel two-stage biomass gasification concept: design and operation of a 1.5 MWth demonstration plant, Bioresour. Technol. 267 (2018) 102–109.

[13] M. La Villetta, M. Costa, D. Cirillo, N. Massarotti, L. Vanoli, Performance analysis of a biomass powered micro-cogeneration system based on gasification and syngas conversion in a reciprocating engine, Energy Conv. Manag. 175 (2018) 33–48.

[14] R. Rodriguez, G. Mazza, A. Fernandez, A. Saffe, M. Echegaray, Prediction of the lignocellulosic winery wastes behavior during gasification process in fluidized bed: experimental and theoretical study, J. Environ. Chem. Eng. 6 (2018) 5570–5579.

[15] C.A.V.B. de Sales, D.M.Y. Maya, E.E.S. Lora, R.L. Jaen, A.M.M. Reyes, A.M.M. Gonzalez, R.V. Andrade, J.D. Martínez, Experimental study on biomass (*eucalyptus* spp.) gasification in a two-stage downdraft reactor by using mixtures of air, saturated steam and oxygen as gasifying agents, Energy Conv. Manag. 145 (2017) 314–323.

[16] E. Konstantinou, R. Marsh, Coal char to combustible gas products in the context of underground coal gasification, Fuel 159 (2015) 508–518.

[17] W. He, C.S. Park, J.M. Norbeck, Rheological study of comingled biomass and coal slurries with hydrothermal pretreatment, Energy & Fuels 23 (10) (2009) 4763–4767.

[18] P. Lv, Z. Yuan, C. Wu, L. Ma, Y. Chen, N. Tsubaki, Bio-syngas production from biomass catalytic gasification, Energy Conv. Manag. 48 (2007) 1132–1139.

[19] S. Rapagna, N. Jand, A. Kiennemann, P.U. Foscolo, Steam-gasification of biomass in a fluidised-bed of olivine particles, Biomass Bioenergy 19 (2000) 187–197.

[20] C. Gai, Y. Dong, Experimental study on non-woody biomass gasification in a downdraft gasifier, Int. J. Hydrog. Energy 37 (2012) 4935–4944.

[21] C. Loha, P.K. Chatterjee, H. Chattopadhyay, Performance of fluidized bed steam gasification of biomass – Modeling and experiment, Energy Conv. Manag. 52 (2011) 1583–1588.

[22] Z. Ong, Y. Cheng, T. Maneerung, Z. Yao, Y.W. Tong, C.H. Wang, Y. Dai, Co-gasification of woody biomass and sewage sludge in a fixed-bed downdraft gasifier, AIChE J. 61 (2015) 2508–2521.

[23] D. Serrano, M. Kwapinska, A. Horvat, S. S.Delgado, J. J.Leahy, *Cynara cardunculus* L. gasification in a bubbling fluidized bed: the effect of magnesite and olivine on product gas, tar and gasification performance, Fuel 173 (2016) 247–259.

[24] F. Miccio, B. Piriou, G. Ruoppolo, R. Chirone, Biomass gasification in a catalytic fluidized reactor with beds of different materials, Chem. Eng. J. 154 (2009) 369–374.

[25] M.Thakkar, P.Mohanty J.P.Makwana, M. Shah, V. Singh, In bed catalytic tar reduction in the autothermal fluidized bed gasification of rice husk: extraction of silica, energy and cost analysis, Ind. Crops Prod. 87 (2016) 324–332.

[26] M.K. Karmakar, J. Mandal, S. Haldar, P.K. Chatterjee, Investigation of fuel gas generation in a pilot scale fluidized bed autothermal gasifier using rice husk, Fuel 111 (2013) 584–591.

[27] P. Subramanian, A. Sampathrajan, P. Venkatachalam, Fluidized bed gasification of select granular biomaterials, Bioresour. Technol. 102 (2011) 1914–1920.

[28] K.G. Mansaray, A.E. Ghaly, A.M. Al-Taweel, F. Hamdullahpur, V.I. Ugursa, Air gasification of rice husk in a dual distributor type fluidized bed gasifier, Biomass Bioenergy 17 (1999) 315–332.

[29] P. Abdul Salam, S.C. Bhattacharya, A comparative study of charcoal gasification in two types of spouted bed reactors, Energy 31 (2006) 228–243.

[30] U. Arena, F. Di Gregorio, Energy generation by air gasification of two industrial plastic wastes in a pilot scale fluidized bed reactor, Energy 68 (2014) 735–743.

[31] P. Lahijani, Z.A. Zainal, Gasification of palm empty fruit bunch in a bubbling fluidized bed: a performance and agglomeration study, Bioresour. Technol. 102 (2011) 2068–2076.

[32] J. Hu J. Shao, H. Yang, G. Lin Y. Chen, X. Wang, W. Zhang, H. Chen, Co-gasification of coal and biomass: synergy, characterization and reactivity of the residual char, Bioresour. Technol. 244 (2017) 1–7.

[33]M. Campoy, A. Gomez-Barea, F.B. Vidal P. Ollero, Air–steam gasification of biomass in a fluidised bed: process optimisation by enriched air, Fuel Process. Technol. 90 (2009) 677–685.

[34] J. George, P. Arun, C. Muraleedharan, Assessment of producer gas composition in air gasification of biomass using artificial neural network model, Int. J. Hydrog. 43 (2018) 9558–9568.

[35] H. Pei, X. Wang, X. Dai, B. Jin, Y. Huang, A novel two-stage biomass gasification concept: design and operation of a 1.5 MWth demonstration plant, Bioresour. Technol. 267 (2018) 102–109.

[36] S.K. Thengane, A. Gupta, S.M. Mahajani, Co-gasification of high ash biomass and high ash coal in downdraft gasifier, Bioresour. Technol. 273 (2019) 159–168.

[37] P. Lahijani, Z.A. Zainal, Gasification of palm empty fruit bunches in a fluidised bed; a performance study, Bioresour. Technol. 102 (2011) 2068–2076.
[38] N. Nipattummakul, I.I. Ahmed, S. Kerdsuwan, A.K. Gupta, Hydrogen and syngas production from sewage sludge via steam gasification, Int. J. Hydrog. Energy 35 (2010) 11738–11745.
[39] J. Dascomb, A. Krothapall, in: Hydrogen-Enriched Syngas from Biomass Steam Gasification for Use in Land-Based Gas Turbine Engines Novel Combustion Concept for Sustainable Energy Development, 2014, pp. 89–110.
[40] P.M. Lv, Z.H. Xiong, C.Z. Jang, Y. Wu, J.X. Chen, Z.X. Zhu, An experimental study of biomass air-steam gasification in a fluidized bed, Bioresour. Technol. 95 (2004) 95–101.
[41] F. Guo, Y. Dong, L. Dong, C. Guo, Effect of design and operating parameters on the gasification process of biomass in a downdraft fixed bed: an experimental study, Int. J. Hydrog. Energy 39 (2014) 5625–5633.
[42] L.Q. Wang, Y. Chen, Experimental studies on H_2 -rich gas production by Co-gasification of coal and biomass in an intermittent fluidized bed reactor, Adv. Mater. Res. 201 (2013) 1127–1131.
[43] E. Idoia, B.F. Fábio, T.F. José, A. Roberto, O. Martin, Fitting performance of artificial neural networks and empirical correlations to estimate higher heating values of biomass, Fuel 180 (2016) 377–383.
D.R. Nhuchhen, P.A. Salam, Estimation of higher heating value of biomass from proximate analysis: a new approach, Fuel 99 (2012) 55–63